

High Performance Window Systems and their Effect on Perimeter Space Commercial Building Energy Performance

by

Ivan Yun Tong Lee

A thesis
presented to the University of Waterloo
in fulfillment of the
thesis requirement for the degree of
Master of Applied Science
in
Civil Engineering

Waterloo, Ontario, Canada, 2010

© Ivan Yun Tong Lee 2010

Author's Declaration

I hereby declare that I am the sole author of this thesis. This is a true copy of the thesis, including any required final revisions, as accepted by my examiners.

I understand that my thesis may be made electronically available to the public.

Abstract

In the quest for improving building energy efficiency raising the level of performance of the building enclosure has become critical. As the thermal performance of the building enclosure improves so does the overall energy efficiency of the building. One key component in determining the energy performance of the building enclosure is windows. Windows have an integral role in determining the energy performance of a building by allowing light and heat from the sun to enter into a space. Energy efficient buildings take advantage of this free solar energy to help offset heating energy consumption and electric lighting loads. However, windows are traditionally the least insulating component of the modern building assembly. With excessive use, larger window areas can lead to greater occupant discomfort and energy consumption from greater night-time heat loss, higher peak and total cooling energy demand from unwanted solar gains, and discomfort glare. As a result, windows must be carefully designed to not only minimize heat loss, but also effectively control solar gains to maintain both a thermally and visually comfortable environment for the appropriate climate region and orientation.

In this thesis, a complete analysis of window assemblies for commercial office buildings is presented. The analysis is divided into three sections: the Insulated Glazing Unit (IGU), the Curtain Wall Section (frames), and the overall energy performance of a typical perimeter space in an office building.

The first section investigates the performance characteristics of typical and high performance IGUs, specifically its insulating value (U_{cg}), its solar heat gain properties (Solar Heat Gain Coefficient, SHGC), and its visual transmittance (VT) through one-dimensional heat transfer and solar-optical modeling. Mechanisms of heat transfer across IGUs were investigated giving insight into the parameters that had the most significant effect on improving each performance characteristic. With a thorough understanding of IGU performance, attainable performance limits for each of property were generated from combining of different glazing materials, fill gases, and coatings. Through the right

combination of materials IGU performance can be significantly altered. The U-value performance of IGUs ranges from 2.68 W/m²K (R-2.1) for a double-glazed, clear, air filled IGU to 0.27 W/m²K (R-21) for a quint-glazed, low-E, xenon filled high performance IGU.

The second part of the thesis looks at the thermal performance of curtain wall sections, that hold the IGU, through two-dimensional heat transfer modeling. Similar to the IGUs, heat transfer mechanisms were studied to by substituting different materials to determine which components are crucial to thermal performance. From this analysis improvements were made to typical curtain wall design that significantly reduces the overall heat transfer within the frame section, producing a high-performance curtain wall section. With simple modifications, a high-performance curtain wall section can reduce its U-value by as much as 81% over a typical curtain wall section, going from 13.39 W/m²K to 2.57 W/m²K. Thus significantly reducing the U-value of curtain wall systems, particularly for smaller windows.

The final part of the thesis examines the impact of typical and high-performance windows on the energy performance of perimeter offices in a high-rise commercial building located in Southern Ontario. An hourly simulation model was set up to evaluate both the annual and peak energy consumption of a typical perimeter office space. The office faced the four cardinal directions of north, east, south, and west to evaluate the effect of orientation. The model also included continuous dimming lighting controls to make use of the available daylight. The effect of exterior shading on perimeter space energy performance was also investigated with both dynamic and static exterior shading devices. The results of the simulations revealed that window properties have very little influence on the energy performance of a high internal heat gain office, that is typical of older offices with less energy efficient office equipment and lighting and a higher occupant density. Conversely, window properties, particularly the insulating value of the window, has a greater effect on the energy performance of a mid to low internal heat gain office that is typical of most modern day commercial buildings. The results show windows with lower U-values yet higher SHGC are preferred over windows of similar U-

values but with lower SHGC. The results also indicate that both static and dynamic shading have very little effect on energy performance of mid to low internal heat gain offices. From this analysis optimal window areas in the form of window-to-wall ratios (WWR) are presented for each orientation for mid to low internal heat gain offices. The optimal WWR for south-facing façades are between 0.50 to 0.66, and 0.30 to 0.50 for east-, west-, and north-facing façades, while for high internal heat gain perimeter spaces window areas should be kept to a minimum.

Acknowledgements

I would like to thank my supervisor, Dr. John Straube, for engaging myself in the field of building science during my undergraduate studies and later providing the opportunity to pursue a Masters degree at the University of Waterloo. Dr. Straube's knowledge and guidance throughout my work during my studies was very valuable. His respect for curiosity, doubt, open-mindedness, and attention the broader issues, provided the drive and motivation to carry on this research even at times when progress has seemed to hit the proverbial wall.

Thank you to my fellow team members on the UW Solar Decathlon team, Team North. The experiences that I gained while working on this project not only furthered my research but also my experience in building design and construction.

A special thanks goes to my fellow students in the Building Engineering Group, Rachel, Peter, Nick, Matt, and Rob, for creating an open environment for sharing ideas. Thanks to my friends and family for their love and support and all the great times in between.

Table of Contents

Author's Declaration	ii
Abstract	iii
Acknowledgements	vi
Table of Contents	vii
List of Figures	viii
List of Tables	xvi
CHAPTER 1 Introduction	1
1.1 Need for Building Energy Efficiency	1
1.2 Basic Energy Flows in Commercial Buildings	4
1.3 Objectives	7
1.4 Scope	7
1.5 Approach	7
CHAPTER 2 General Background	9
2.1 Energy Flow through Fenestration Systems	9
2.1.1 Performance Indices	12
2.1.2 Centre-Glass Glazing Analysis	13
2.1.3 Multi-layered Glazing Heat Transfer Analysis	14
2.1.4 Multi-layered Glazing Solar Analysis	19
2.2 Solar Gain Control	22
2.2.1 Shading Devices	23
2.2.2 Dynamic Shading Devices	24
2.2.3 Static Shading Devices	29
2.3 Basics of Daylighting	32
2.3.1 Daylighting Design Concepts	34
2.3.2 Visual Comfort	38
2.3.3 Daylighting Design Strategies	40
2.3.4 Auxiliary Lighting Integration	48
CHAPTER 3 High Performance Insulated Glazing Units	55
3.1 Simulation Parameters and Modeling Objectives	55
3.2 Evaluation of Current and Emerging Glazing Technologies	56
3.2.1 Low-Emissivity Coatings and IGU Heat Transfer	57
3.2.2 Low-Emissivity Coatings and Solar Transmittance and Solar Heat Gain	60
3.2.3 Future Improvements to Low-Emissivity Coatings	63
3.2.4 Substitute Fill Gases and IGU Heat Transfer	66
3.2.5 Optimal Cavity Spacing for Minimizing IGU Cavity Heat Transfer	69
3.2.6 Plastic Films and IGU Performance	70
3.3 Evaluation of Multi-layered IGUs	71
3.3.1 U-value of Multi-layered IGUs	71
3.3.2 SHGC and VT of Multi-layered IGUs	82
3.4 Survey of Multi-layered IGU Performance Thresholds	84
3.5 High Performance Multi-layered IGUs	87

CHAPTER 4 High Performance Window Assemblies	90
4.1 Review of the Basic Functions of Window Assemblies.....	90
4.1.1 Anatomy of Commercial Window Assemblies.....	93
4.1.2 Pressure Plate Curtain Wall.....	95
4.1.3 Edge Spacer Construction	99
4.2 Heat Transfer Analysis of Edge and Frame Regions	101
4.2.1 Computer Simulation Software	101
4.2.2 Cap Screw Conductivity Analysis.....	103
4.3 Evaluation of the Thermal Performance of Commercial Curtain Walls	105
4.3.1 Thermal Performance of Edge Spacers.....	107
4.3.2 Thermal Performance of Aluminum Curtain Wall Sections.....	109
4.3.3 Thermal Performance of High Performance Aluminum Curtain Wall Sections	120
4.3.4 Thermal Performance of High Performance Timber Curtain Wall Sections...	124
4.4 Evaluation of Overall Window Assembly Thermal Performance.....	131
CHAPTER 5 Energy Performance of Perimeter Spaces and Window Systems	139
5.1 Previous Research – Technical Review.....	139
5.1.1 Window Design for Offices in Cold Climates	141
5.2 Modeling Objectives and Parameters.....	148
5.2.1 Modeling Objectives.....	148
5.2.2 EnergyPlus Description.....	148
5.2.3 Model Description	150
5.3 Window Properties and Perimeter Space Energy Consumption.....	161
5.3.1 Energy Load and Energy Consumption.....	162
5.3.2 Effect of Internal Heat Sources (Gains) on Energy Consumption	164
5.3.3 Window Properties: U-value and Solar Heat Gain Coefficient.....	173
5.4 Optimal Window Design for High-performance Façades	177
5.4.1 South-Facing Perimeter Zones	177
5.4.2 East-Facing Perimeter Zones.....	181
5.4.3 West-Facing Perimeter Zones	184
5.4.4 North-Facing Perimeter Zones	187
5.5 Optimal Window Design for High-performance Facades with Solar Control.....	192
5.5.1 South-facing Perimeter Zones with Solar Control.....	192
5.5.2 East-Facing Perimeter Zones with Solar Control.....	196
5.5.3 West-Facing Perimeter Zones with Solar Control.....	200
5.5.4 North-Facing Perimeter Zones with Solar Control.....	204
CHAPTER 6 Conclusions and Recommendations	210
References.....	215
Appendix A Solar Calculations	220
Appendix B IGU Performance Characteristics And Specifications.....	231
Appendix C1 Typical Aluminum Curtain Wall Frame Performance Characteristics ...	235
Appendix C2 High Performance Aluminum and Timber Curtain Wall Frame Performance Characteristics	256
Appendix C3 Window Assembly U-values	261
Appendix D1 EnergyPlus Model Parameters.....	266

Appendix D2	Comparison of Energy Performance of High and Low Internal Heat Gain Offices.....	274
Appendix D3	Comparison of Window U-value and Solar Heat Gain Coefficient on Energy Performance.....	283
Appendix D4	Energy Performance of Unshaded and Shaded Offices	290

List of Figures

Figure 1.1.1	Commercial / Institutional building secondary energy consumption end use – Canada (NRCan, 2010).....	2
Figure 1.1.2	Commercial / Institutional building secondary energy consumption distribution – Canada (top). 2007 Canadian Commercial / Institutional building secondary energy consumption by end use (bottom). (NRCan, 2010).....	3
Figure 1.2.1	Energy flow in typical commercial building (adapted from MIT, 2009).....	5
Figure 1.2.2	Balance of internal heat gain (artificial lighting etc.) on space heating and cooling demand.....	6
Figure 2.1.1	Fenestration system regions.....	10
Figure 2.1.2	Buildings with punched windows and curtain-wall systems (Lstiburek and Straube, 2008).....	11
Figure 2.1.3	Centre-glass nomenclature for heat transfer analysis (Hollands et al., 2001).....	15
Figure 2.1.4	Correlation for natural convection heat transfer across tall vertical cavity (Wright, 1996).....	18
Figure 2.1.5	Solar flux distribution in multi-layered glazing system (Wright, 1998).....	20
Figure 2.2.1	Photographs of electrochromatic IGU (left) and tinted glazing (right).....	24
Figure 2.2.2	Interior venetian blinds.....	25
Figure 2.2.3	In-between blinds from SurPlus Home, Team Germany 2009 Solar Decathlon. Top: exterior view, bottom: interior view.....	26
Figure 2.2.4	Solar Heat Gain of a typical window with and without interior and exterior shading (Straube and Burnett, 2005).....	27
Figure 2.2.5	Exterior venetian blinds and interior roller blinds of North House.....	28
Figure 2.2.6	Overhang design.....	30
Figure 2.2.7	Shaded area of south-facing window with static shading devices in November afternoon.....	31
Figure 2.3.1	Daylight Autonomy of a fully glazed south-facing facade in a rectangular office in New York City with a minimum illuminance of 500 lux from 8 am to 5 pm (Reinhart, 2005).....	36
Figure 2.3.2	Sky exposure angle (Enermodal, 2002).....	37
Figure 2.3.3	Typical building perimeter and core zones for daylighting (Enermodal, 2002).....	41
Figure 2.3.4	Daylight distribution of north- and south-facing facades (Enermodal, 2002).....	42
Figure 2.3.5	Predictions of daylight penetration depth from various rules of thumb relating window head height (Reinhart, 2005).....	43
Figure 2.3.6	Frequency distribution of daylight depths with 50% daylight autonomy of various North American cities (Reinhart, 2005).....	44

Figure 2.3.7	Frequency distribution of predicted daylit zone depth with blinds for a) varying minimum illuminances (Reinhart, 2005), b) varying visible transmittances (Reinhart, 2005)	45
Figure 2.3.8	Frequency distribution of daylit zone depth with various facade arrangements below the work plane height (Reinhart, 2005).....	46
Figure 2.3.9	Frequency distribution of predicted daylit zone depths of varying latitudes (Reinhart, 2005).....	46
Figure 2.3.10	Frequency distribution curves of predicted daylit zone with blinds for North, East, South, and West orientations (Reinhart, 2005)	47
Figure 2.3.11	Daylit zone depth and daylight distribution of facades with light shelves (Enermodal, 2002).....	48
Figure 2.3.12	Direct/Indirect illumination distribution (Enermodal, 2002).....	50
Figure 2.3.13	Illumination levels with staged controls (Enermodal, 2002).....	51
Figure 2.3.14	Efficacy of CFL and LED sources (Canlyte, 2009)	52
Figure 2.3.15	Visual comparison of light sources with different correlated colour temperatures (Canlyte, 2009).....	53
Figure 2.3.16	Spectral distribution of different light sources (Canlyte, 2009).....	53
Figure 3.2.1	Reflectance, transmittance, and absorptance of glass (Straube and Burnett, 2005).....	57
Figure 3.2.2	Heat flux across a double-glazed air filled IGU (results determined by VISION (Ferguson et. al, 1984))	58
Figure 3.2.3	Application process of 'hard' and 'soft' coat low-E coatings (Hollands et al., 2001).....	60
Figure 3.2.4	Resulting visible transmittance and solar heat gain of double-glazed IGUs with and without low-E coatings as determined by Window5 (LBNL, 2003)	61
Figure 3.2.5	Mechanics of SHGC and low-E coating location (adapted from LBNL, 2003).....	62
Figure 3.2.6	Winter night-time centre-glass U-value dependence on emissivity of surface 3 of an air filled double-glazed IGU as determined by using VISION (Ferguson et al., 1984) (adapted from Hollands et al., 2001).....	63
Figure 3.2.7	SHGC and solar transmittance of current low-E coatings (adapted from Hollands et al, 2001).....	65
Figure 3.2.8	Cavity heat transfer h_{cav} and U_{cg} at varying cavity spacing for various fill gases in a double-glazed low-e coated IGU at winter night-time conditions (Hollands et al., 2001).....	68
Figure 3.3.1	Relationship between cavity space and U_{cg} for double-glazed IGUs	73
Figure 3.3.2	Relationship between cavity space and U_{cg} for triple-glazed IGUs.....	73
Figure 3.3.3	Relationship between cavity space and U_{cg} for quad-glazed IGUs	74
Figure 3.3.4	Relationship between cavity space and U_{cg} for quint-glazed IGUs.....	74
Figure 3.3.5	Infrared emissivity and solar transmission of glazing products as listed in Window5 database (LBNL, 2003).....	83
Figure 3.3.6	Proposed IGU performance characteristic matrix.....	84
Figure 3.4.1	Possible IGU performance range as determined by Window5 (LBNL, 2003) simulations.....	85

Figure 4.1.1	Buildings with curtain wall system (Left: Adam Joseph Lewis Center for Environmental Studies, Oberlin College, Right: Art Gallery of Ontario)	93
Figure 4.1.2	Curtain wall types (left: pressure plate, right: structural silicone) (Lstiburek and Straube, 2008)	94
Figure 4.1.3	Thermally broken aluminum curtain wall sections (Left: Kawneer 1600 curtain wall section, Right: Kawneer 7550 curtain wall section)....	97
Figure 4.1.4	Edge spacer construction (adapted from Carmody, 2007).....	100
Figure 4.3.1	Typical and high-performance curtain wall sections.....	106
Figure 4.3.2	Comparison of typical edge spacer with THERM model.....	108
Figure 4.3.3	Frame and edge U-values with various edge spacers for double-glazed IGU (2G-2s) with a typical thermally non-broken aluminum curtain wall	109
Figure 4.3.4	THERM6 (LBNL, 2008) model of aluminum curtain wall section	111
Figure 4.3.5	Evaluation of individual components on thermal performance of aluminum curtain walls with aluminum spacers for double-glazed IGUs.....	112
Figure 4.3.6	Evaluation of individual components on thermal performance of aluminum curtain walls with PVC spacers for double-glazed IGUs	112
Figure 4.3.7	Frame and edge thermal performance with cumulative modifications of a standard aluminum curtain wall for a double-glazed IGU.....	117
Figure 4.3.8	Frame and edge thermal performance with cumulative modifications of a standard aluminum curtain wall for a triple-glazed IGU	117
Figure 4.3.9	Frame and edge thermal performance with cumulative modifications of a standard aluminum curtain wall for a quad-glazed IGU.....	118
Figure 4.3.10	Frame and edge thermal performance with cumulative modifications of a standard aluminum curtain wall for a quint-glazed IGU	118
Figure 4.3.11	Photograph of RAICO THERM+ A-I series (Raico, 2010).....	121
Figure 4.3.12	Proposed design of a high-performance aluminum curtain wall section	121
Figure 4.3.13	Temperature profile of the proposed high-performance aluminum curtain wall section, evaluated using THERM6 (LBNL, 2008).....	123
Figure 4.3.14	Left: Commercially available Raico THERM+ H-I / H-V timber curtain wall (Raico, 2010). Right: custom timber curtain wall from North House (North House, 2009).....	125
Figure 4.3.15	Proposed high-performance timber curtain wall section	126
Figure 4.3.16	Comparison between typical aluminum, proposed high-performance aluminum, and proposed high-performance timber curtain wall sections.....	127
Figure 4.3.17	Temperature profile of the proposed ultra-low U-value high-performance timber curtain wall section, evaluated using THERM6 (LBNL, 2008)	128
Figure 4.3.18	Evaluation of spacer types on thermal performance in timber curtain walls	129

Figure 4.3.19	Evaluation of individual components on thermal performance of ultra-low U-value timber curtain walls with PVC spacers for double-glazed IGUs	130
Figure 4.4.1	Overall thermal performance of curtain wall systems of varying sizes with aluminum frames.....	132
Figure 4.4.2	Overall thermal performance of proposed ultra-low U-value high-performance timber curtain walls of varying sizes.....	134
Figure 4.4.3	Proposed curtain wall system performance rating system	136
Figure 5.1.1	Window and exterior shading arrangement (Carmody et al., 2004).....	143
Figure 5.1.2	Annual energy consumption of various window types for all orientations in a northern climate (Carmody et al., 2004)	146
Figure 5.1.3	Peak energy consumption of various window types for all orientations in a northern climate (Carmody et al., 2004)	147
Figure 5.2.1	Layout of theoretical building used in building simulation	151
Figure 5.2.2	Opaque building enclosure.....	151
Figure 5.2.3	Model window arrangement.....	155
Figure 5.2.4	Total annual energy use of EnergyPlus Model using Window B from Carmody et al. (2004) for Chicago, IL.....	158
Figure 5.2.5	Comparison of EnergyPlus model with 2007 Canadian commercial/institutional building energy consumption by end use (NRCan, 2007) (upper right: WWR 0.20, lower right: WWR 0.40, lower left: WWR 0.60)	161
Figure 5.3.1	Comparison of average energy load, average energy consumption, and average source energy consumption for a double-glazed, clear, air-filled, aluminum window.....	163
Figure 5.3.2	Average annual energy consumption of a high internal heat gain office with double-glazed (2G-2s) and quint-glazed (5G-2s) high solar gain wood window	166
Figure 5.3.3	Average peak energy consumption for a high internal loads office with double-glazed (2G-2s) and quint-glazed (5G-2s) high solar heat gain wood windows	167
Figure 5.3.4	Average annual energy consumption of a high internal heat gain office with a high (2G-2s) and low (2G-4uv) solar gain double-glazed wood window	168
Figure 5.3.5	Average peak energy consumption of a high internal heat gain office with a high (2G-2s) and low (2G-4uv) solar gain double-glazed wood window	169
Figure 5.3.6	Averaged annual energy consumption of a low internal heat gain office with a double-glazed (2G-2s) and quint-glazed (5G-2s) high solar gain wood window	170
Figure 5.3.7	Averaged peak energy consumption of a low internal heat gain office with a double-glazed (2G-2s) and quint-glazed (5G-2s) high solar gain wood window.....	171
Figure 5.3.8	Average annual energy consumption of a low internal gain office with high (2G-2s) and low (2G-4uv) solar gain double-glazed wood window	172

Figure 5.3.9	Average peak energy consumption of a low internal gain office with high (2G-2s) and low (2G-4uv) solar gain double-glazed wood window.....	173
Figure 5.3.10	Average annual energy consumption of double-glazed windows of different properties.....	175
Figure 5.3.11	Average peak energy consumption of double-glazed windows of different properties.....	176
Figure 5.4.1	Annual energy consumption of offices in south-facing perimeter zones with multi-layered low solar gain, low and ultra-low U-value wood windows.....	178
Figure 5.4.2	Peak energy consumption of south-facing, multi-layered low solar gain, low and ultra-low U-value wood windows.....	180
Figure 5.4.3	Annual energy consumption of offices in east-facing perimeter zones with multi-layered low solar gain, low and ultra-low U-value wood windows.....	181
Figure 5.4.4	Peak energy consumption of offices in east-facing perimeter zones with multi-layered low solar gain, low and ultra-low U-value wood windows.....	183
Figure 5.4.5	Annual energy consumption of offices in west-facing perimeter zone with multi-layered low solar gain, low and ultra-low U-value wood windows.....	184
Figure 5.4.6	Peak energy consumption of offices in west-facing perimeter zones with multi-layered low solar gain, low and ultra-low U-value wood windows.....	186
Figure 5.4.7	Annual energy consumption of offices in north-facing perimeter zone with multi-layered low solar gain low and ultra-low U-value wood windows.....	187
Figure 5.4.8	Annual energy consumption of offices in the north-facing perimeter zone with multi-layered low solar gain, low and ultra low U-value wood windows.....	189
Figure 5.4.9	Optimal WWR for an un-shaded building with low U-value double-glazed windows.....	190
Figure 5.4.10	Optimal WWR for an un-shaded building with triple-glazed ultra-low U-value windows.....	191
Figure 5.4.11	Rendering of optimal WWR for an un-shaded building with quad- or quint-glazed ultra-low U-value windows.....	191
Figure 5.5.1	Annual energy consumption of an office space in the south-facing perimeter zone with low U-value double-glazed windows with fixed and dynamic solar control.....	194
Figure 5.5.2	Annual energy consumption of an office space in the south-facing perimeter zone with ultra-low U-value triple-glazed windows with fixed and dynamic solar control.....	195
Figure 5.5.3	Annual energy consumption of an office space in the south-facing perimeter zone with ultra-low U-value quad-glazed windows with fixed and dynamic solar control.....	195

Figure 5.5.4	Annual energy consumption of an office space in the south-facing perimeter zone with ultra-low U-value quint-glazed windows with fixed and dynamic solar control.....	196
Figure 5.5.5	Annual energy consumption of an office in east-facing perimeter zone with double-glazed windows and fixed and dynamic solar control.....	198
Figure 5.5.6	Annual energy consumption of an office in east-facing perimeter zone with triple-glazed windows and fixed and dynamic solar control.....	199
Figure 5.5.7	Annual energy consumption of an office in east-facing perimeter zone with quad-glazed windows and fixed and dynamic solar control.....	199
Figure 5.5.8	Annual energy consumption of an office in east-facing perimeter zone with quint-glazed windows and fixed and dynamic solar control.....	200
Figure 5.5.9	Annual energy consumption of an office in west-facing perimeter zone with double-glazed windows and fixed and dynamic solar control.....	202
Figure 5.5.10	Annual energy consumption of an office in west-facing perimeter zone with triple-glazed windows and fixed and dynamic solar control.....	203
Figure 5.5.11	Annual energy consumption of an office in west-facing perimeter zone with quad-glazed windows and fixed and dynamic solar control.....	203
Figure 5.5.12	Annual energy consumption of an office in west-facing perimeter zone with quint-glazed windows and fixed and dynamic solar control.....	204
Figure 5.5.13	Annual energy consumption of an office in north-facing perimeter zone with double-glazed windows and fixed and dynamic solar control.....	206
Figure 5.5.14	Annual energy consumption of an office in north-facing perimeter zone with triple-glazed windows and fixed and dynamic solar control.....	207
Figure 5.5.15	Annual energy consumption of an office in north-facing perimeter zone with quad-glazed windows and fixed and dynamic solar control.....	207
Figure 5.5.16	Annual energy consumption of an office in north-facing perimeter zone with quint-glazed windows and fixed and dynamic solar control.....	208

List of Tables

Table 3.1.1	NFRC standard simulation conditions in Window5 (LBNL, 2003).....	56
Table 3.2.1	Optical properties for clear and low-E coated glass (LBNL, 2003)	60
Table 3.2.2	Approximate price of fill gases (ChemiCool, 2009).....	69
Table 3.3.1	Optical properties of glazing layers used in Window5 simulations to generate results (LBNL, 2003)	72
Table 3.3.2	Resulting performance indices of investigated high performance IGUs (results generated from Window5 (LBNL, 2003) simulations)	77
Table 3.3.3	Resulting range of reductions in U _{cg} , cavity width, L, and overall IGU width, t for different fill gases and multi-layered IGU configurations (double to quint).....	81
Table 3.4.1	Upper and lower limits of performance of IGUs investigated as analyzed by Window5 (LBNL, 2003).....	86
Table 3.5.1	High performance IGU properties as generated by Window5 (LBNL, 2003)	88
Table 4.1.1	Properties of common curtain wall materials	98
Table 4.2.1	NFRC Standard Simulation Conditions in THERM6 (LBNL, 2008).....	103
Table 4.3.1	Spacer material properties (LBNL, 2008)	107
Table 4.3.2	Aluminum curtain wall component study conclusions	113
Table 4.3.3	Base and modified aluminum curtain wall thermal transmittance.....	120
Table 4.3.4	Proposed high-performance aluminum curtain wall thermal transmittance values	123
Table 4.3.5	Proposed ultra-low U-value high-performance timber curtain wall thermal performance	127
Table 4.4.1	Typical curtain wall glazed panel opening dimensions.....	133
Table 4.4.2	Comparison of curtain wall system U-values at maximum IGU dimension.....	135
Table 5.1.1	Properties of windows analyzed (Carmody et al., 2004)	142
Table 5.2.1	Office occupancy schedule	152
Table 5.2.3	Office lighting schedule	152
Table 5.2.4	Supply air temperature and humidity	154
Table 5.2.5	Thermostatic set points.....	155
Table 5.2.6	Modeled Window Assembly Properties.....	156
Table 5.3.1	Source-site ratios (Energy Star, 2009)	164
Table 5.3.2	Window properties tested for internal gain study	165
Table 5.3.3	Double-glazed window properties	174
Table 5.3.4	Window U-value of double-glazed windows investigated.....	174
Table 5.4.1	Annual energy consumption of offices in south-facing perimeter zones.....	179
Table 5.4.2	Optimal WWR for offices in south-facing perimeter zones.....	180
Table 5.4.3	Annual energy consumption of offices in east-facing perimeter zones.....	182
Table 5.4.4	Optimal WWR for offices in east-facing perimeter zones	183
Table 5.4.5	Annual energy consumption of offices in west-facing perimeter zones.....	185

Table 5.4.6	Optimal WWR for offices in west-facing perimeter zones	186
Table 5.4.7	Annual energy consumption of offices in north-facing perimeter zones	188
Table 5.4.8	Optimal WWR for offices in north-facing perimeter zones	189
Table 5.5.1	Effect of static and dynamic shading on energy consumption of offices located in south-facing perimeter zones.....	193
Table 5.5.2	Effect of static and dynamic shading on energy consumption of offices located in east-facing perimeter zones.....	197
Table 5.5.3	Effect of static and dynamic shading on energy consumption of offices located in west-facing perimeter zones.....	201
Table 5.5.4	Effect of static and dynamic shading on energy consumption of offices located in north-facing perimeter zones.....	205

CHAPTER 1

Introduction

1.1 Need for Building Energy Efficiency

With concerns of climate change and the depletion of nonrenewable energy resources, there is an emerging trend towards sustainability and energy efficiency. This trend is not only exclusive to heavy industries and transportation sectors but also to the built environment, particularly in buildings with the “green” architecture movement. A recent study from the U.S. Energy Information Association (EIA) indicates that U.S. buildings are responsible for approximately 48% of all energy consumed, including a 76% share of all electricity produced used to operate buildings (U.S. Energy Information Administration, 2009). These statistics found in the U.S. are consistent with most developed nations around the world. It is clear that buildings represent a significant portion of the energy consumed in our society, particularly in operational energy, since most buildings operate well beyond 20-30 years. Many environmental agencies including the Intergovernmental Panel on Climate Change (IPCC) estimates the building sector could generate 29% in reductions in its energy consumption by 2020 without large costs (IPCC, 2007). This is the greatest potential reduction of all sectors including transportation, industry, energy generation, agriculture and forestry. Not only would reduction in building energy consumption help reduce greenhouse gas emissions (GHG) and alleviate energy concerns, but it also represents significant financial savings. In 2006 the U.S. Department of Energy (DOE) reported that the building sector spent a total of U.S. \$392.2 B on energy, including U.S. \$123.1 B spent on electricity alone (DOE, 2009). The DOE forecasts total U.S. building expenditures will raise to US \$501.6 B by the year 2030.

With these concerns in mind, many building designers are taking the initiative to design more energy efficient buildings. Organizations such as Architecture 2030 have set up the

‘2030 Challenge’ aimed at reducing operational GHG emissions by 60% for all new buildings, developments, and major renovations by 2010 and incrementally decreasing allowable emission standards until achieving carbon neutrality by the year 2030 (Architecture2030, 2009). While this goal seems lofty, it is certainly not unattainable. To achieve these goals the energy consumption of all buildings must be significantly reduced such that the appropriate deployment of on-site renewable energy can be used to meet the building's remaining energy needs. Designers are already striving for this by designing and operating Net-Zero buildings, buildings which achieve an annual net-zero energy balance, and with competition such as the U.S. and European Solar Decathlon, challenging students all over the world to design, construct, and operate an energy efficient home that is capable of meeting all of its energy needs through solar power alone.

While significant energy efficiency improvements have been made in residential buildings, energy efficiency in commercial buildings seems to be lagging, particularly in Canada. A detailed look into commercial and institutional building energy consumption from 1990 to 2007 reveals a growing trend in total energy consumption. This trend is likely to continue with increased building construction.

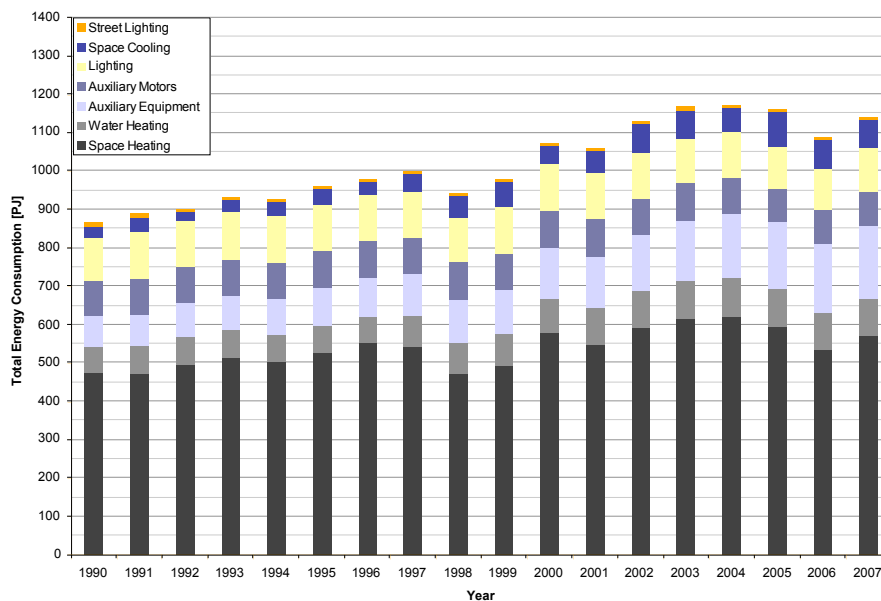


Figure 1.1.1 Commercial / Institutional building secondary energy consumption end use – Canada (NRCan, 2010)

A closer look into this data reveals that a significant portion of the total consumption is dominated by space heating, auxiliary equipment and motors, lighting, and space cooling.

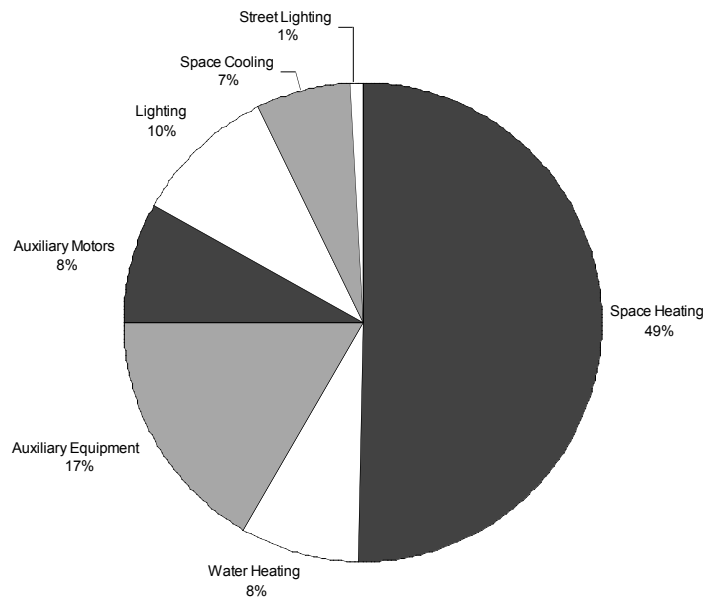
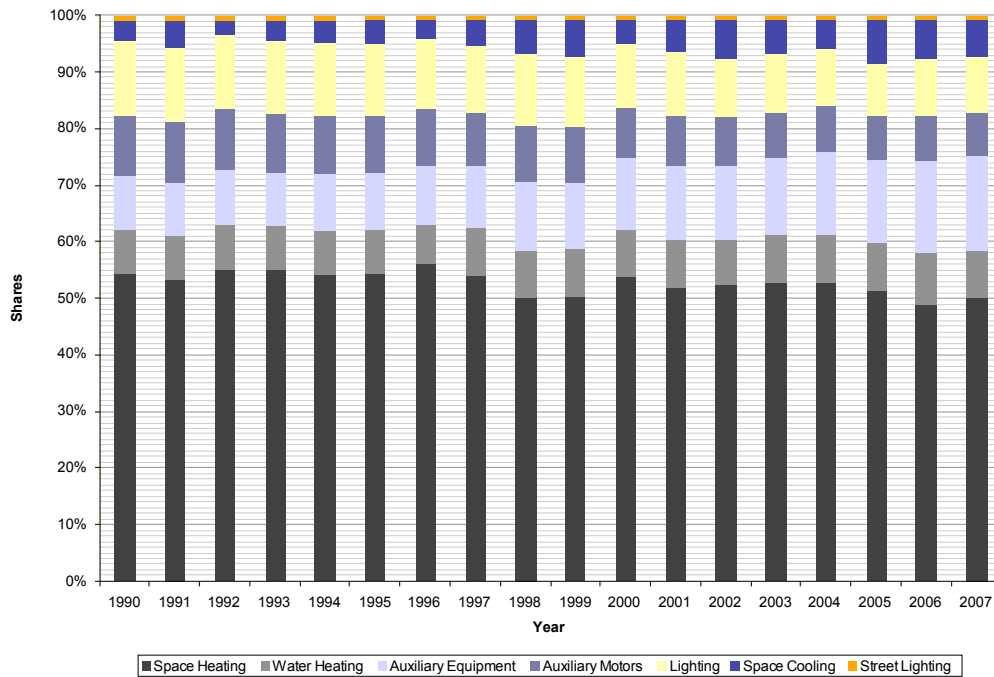


Figure 1.1.2 Commercial / Institutional building secondary energy consumption distribution – Canada (top). 2007 Canadian Commercial / Institutional building secondary energy consumption by end use (bottom). (NRCan, 2010).

Most of the major energy end use loads such as space heating, cooling, and lighting are, largely attributed to the building envelope, in particular to windows due to the highly glazed façades of typical commercial and institutional buildings.

1.2 Basic Energy Flows in Commercial Buildings

To effectively reduce the energy consumption of most commercial buildings the energy flow through the system must be understood to make proper changes that have the highest impact.

The energy flow of typical commercial buildings can be complex as energy used in buildings can be in multiple forms and is heavily dependent on a number of factors including occupancy, climate, orientation, and mechanical systems. With regards to building energy performance however, the primary energy of concern is heat. Aside from providing structure and shelter, buildings are also responsible for providing thermal and visual comfort, which are largely related to energy. Thermal comfort is achieved by controlling the interior temperature of the space and often requires the injection (space heating) and extraction (space cooling) of heat, while visual comfort is achieved by providing adequate lighting for the intended task. In order to maintain both thermal and visual comfort a balance between heat gained or injected, and heat loss or extracted must be achieved within an appropriate range, while lighting levels must be maintained at an equilibrium level. Unfortunately there are multiple sources of heat gains and sinks within a commercial building that can easily offset this balance. Figure 1.2.1 shows typical heat flows in a commercial building along with sources which are commonly referred to as internal gains. In most commercial buildings, such as offices, internal gains are mostly attributed to electrical devices such as computers, artificial lighting, and people.

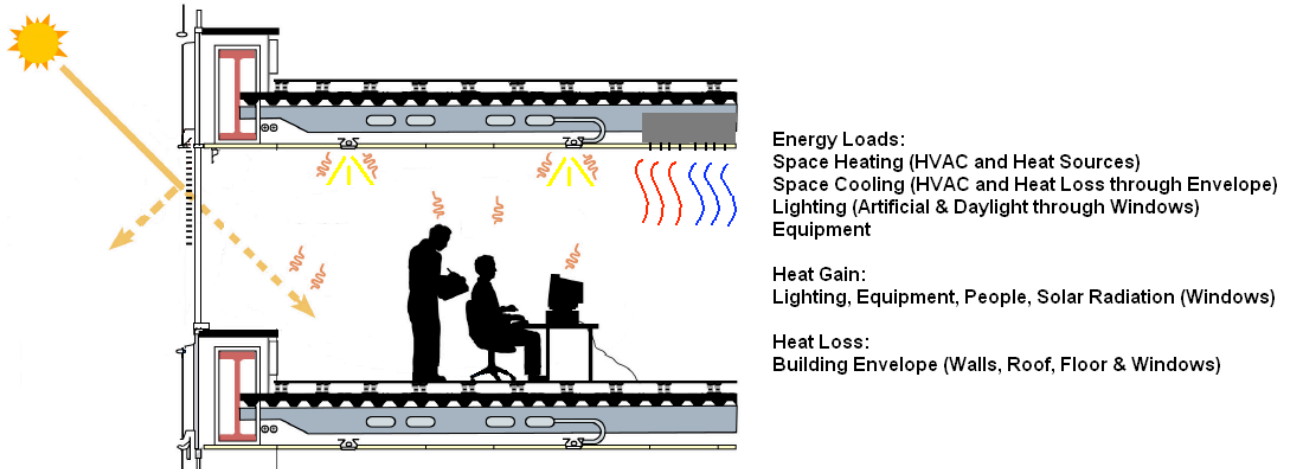


Figure 1.2.1 Energy flow in typical commercial building (adapted from MIT, 2009)

In addition to internal gains, sources of heat gain in a typical commercial building include solar gains through the window(s) and Heating, Ventilation, and Air-Conditioning (HVAC) equipment, while sources of heat loss include the building enclosure and also the HVAC system, which is primarily used to offset any additional heat loss or gain to help maintain thermal comfort. Similarly, daylight is provided by window(s) and skylights in the building envelope. For most buildings the building enclosure plays an important role in the energy consumption, as a heavily insulated building enclosure can effectively decrease both space heating and cooling loads by thermally isolating the interior space from environmental changes that could upset the temperature balance inside the building. In addition, penetrations within the building enclosure can provide daylight to help offset the energy required for artificial lighting. Having a properly designed building enclosure can significantly improve the energy efficiency of the building.

An important element of the building enclosure is windows. While windows provide the same functions as the rest of the building envelope such as insulation, windows also provide daylight and solar heat gains, which can help offset lighting and space heating loads. Despite these benefits however, windows are typically the least insulating part of the building enclosure and are subjected to unwanted solar heat gain during warm periods where, heat from the sun adds to the building's cooling demand. Therefore windows

have a significant impact on the building's space heating, space cooling, and lighting loads. The factors that influence the size of these loads include:

- Window Area
- Orientation / Solar Exposure
- Window Assembly Insulating Value
- Window Solar Heat Gain

Generally, buildings with large window areas and good solar exposure will tend to have higher total and peak heating and cooling loads due to the poor insulating properties of windows and the excessive solar gains. However, these buildings will tend to have a smaller lighting load, which can have a secondary benefit on heating and cooling demand since lighting loads are a source of internal heat gain. All of this translates into a delicate balancing act between internal heat gain and space heating and cooling loads.

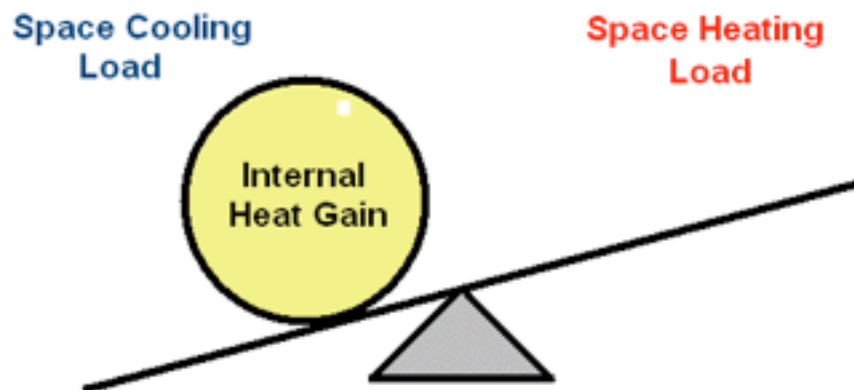


Figure 1.2.2 Balance of internal heat gain (artificial lighting etc.) on space heating and cooling demand

Due to the intricacy and importance of energy flows in the building, precise control of both light and heat flow across windows is imperative in creating a high performance building enclosure for an energy efficient building.

1.3 Objectives

The objective of this research is outlined by the two following statements:

- Investigate levels of overall window performance that are achievable with current and developing technologies
- Determine the ultimate impacts on energy building energy consumption with these high performance window assemblies

This thesis reviews the background science and previous research, as well as documents the research findings and results.

1.4 Scope

The scope of this project includes a series of computer simulations to assess the performance of Insulated Glazing Units (IGUs), frame construction, and window area. A detailed survey of the properties of commercially available glazing products was undertaken to assess a range of possible IGU performance of materials of different construction. Two-dimensional heat transfer analysis was also performed to determine the thermal performance of both conventional and high performance curtain wall sections. Curtain walls were chosen for analysis due to their popularity within the commercial building industry. The designs used in the analysis are based on similar designs found on the market. Finally, the overall performance of the window assembly was assessed with an hourly building simulation of a typical perimeter office in a high-rise building to determine the changes in overall and peak heating, cooling and lighting loads for various orientations and window areas in a mixed climate.

1.5 Approach

The thesis begins with an overview of how window assemblies can affect space heating, cooling, and lighting loads through a review of window heat transfer mechanisms and overall performance analysis of window assemblies, as well as design considerations for daylighting. Previous work on assessing how window properties affect space heating, cooling, and lighting loads are further discussed in Chapter 2. The discussion continues

with a detailed assessment of current IGU performance of various construction in Chapter 3, while Chapter 4 discuss the important of frame thermal performance on overall window assemblies, specifically curtain wall systems. Finally, a description and results of an hourly building model simulation are presented and discussed in Chapter 5, regarding the impact of various window assemblies on energy consumption in a typical commercial building located in a mixed climate zone. Conclusions and recommendations for industry are presented in Chapter 6.

CHAPTER 2

General Background

As transparent sections of the building enclosure, windows have a significant influence on the energy performance of most commercial buildings, particularly in the building's heating, cooling, and lighting energy demand. However, before a full analysis can be done to assess the impact of glazed surfaces on building energy performance, technical background information is required on how building performance is measured. Windows are actually a subset of architectural elements known as fenestration, which include all openings in the building enclosure, such as windows, curtain walls, window walls, doors, and associated shading devices. In this chapter, background information is presented on quantifying the performance of common commercial glazed fenestration systems and requirements for daylighting as it relates to fixed fenestration assemblies.

2.1 Energy Flow through Fenestration Systems

The energy flow through common window or fenestration systems is quite complex due to their transparent/translucent property as building enclosure elements. To fully assess the overall performance of window systems a thorough understanding of both heat transfer and solar-optics is required. For simplicity, the energy flow paths through fenestration systems can be divided into three sections, as illustrated in Figure 2.1.1:

- Centre-glass, *cg*
- Edge-glass, *eg*
- Frame, *fr*

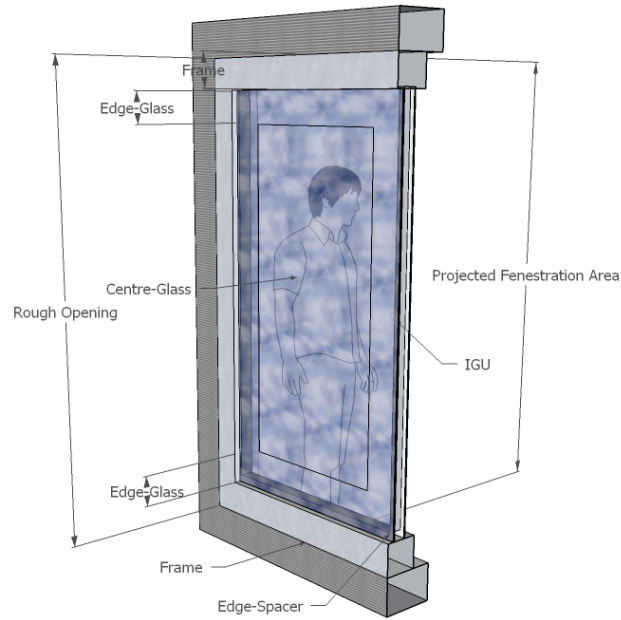


Figure 2.1.1 Fenestration system regions

The centre-glass region, denoted by cg , refers to the centre region of the insulated glazing unit (IGU). Since it is transparent to certain wavelengths of solar radiation, the energy performance of the centre-glass region is determined by a one-dimensional simulation of energy transfer that includes both heat transfer and solar-optical analysis (Wright, 1998). The edge-glass region, denoted by eg , refers to a smaller area around the perimeter of the IGU that is 63.5 mm (2 ½ in.) wide from the visible edge of the frame, as determined by national standards from the National Fenestration Research Council (NFRC) (LBNL, 2003). The frame region, fr , refers to the two-dimensional projected elevation area of the frame. The heat transfer of both edge and frame regions are often dependent on the thermal characteristics of the frame and edge spacer material and are modeled together as a two-dimensional heat transfer analysis (LBNL, 2003).

There are two types of fenestration systems in commercial buildings: punched windows and curtain walls. Punched windows are typically smaller windows and are commonly found in smaller residential buildings. These windows fit into a rough opening within the building enclosure and is typically surrounded by opaque walls. Curtain walls,

however, are typically found in mid- to large-sized commercial buildings, in which the entire façade is clad with a glazed surface. Curtain wall systems hold both IGUs and opaque spandrel panels that are filled with insulation across multiple floors (Carmody, 2007). This offers greater transparency and larger window areas allowing for views and daylight quantity. A hybrid system of punched windows and curtain walls is the window wall system which is made up of curtain wall sections that are fitted into an opaque wall. Window wall systems do not span across multiple floors and are typically anchored to the floor and roof of most commercial store fronts to provide added strength. Although there are various glazed fenestration systems, the performance metrics are the same and the same analysis can be applied for all windows. The following sections describe the analysis used to characterize the performance of typical glazed fenestration systems.



Figure 2.1.2 Buildings with punched windows and curtain-wall systems (Lstiburek and Straube, 2008)

2.1.1 Performance Indices

The energy performance of windows assemblies as it relates to building energy consumption is determined by the heat transfer through the unit, the amount of solar heat gained through the glazing system, and the amount of visible light that passes through the IGU. All three of these characteristics are quantified by the following coefficients:

- The overall thermal transmission coefficient, U
- The solar heat gain coefficient, SHGC
- The visible transmittance, τ_{vis} , or VT

where the U-value describes the heat transferred through either the entire window assembly or the IGU. SHGC describes the fraction of solar heat that enters an interior space from the sun. It is calculated as a ratio of inward flowing heat from the sun that passes through the window assembly to the total amount of solar radiation that is exposed to the window surface (Hollands *et al.*, 2001). VT describes the ratio of visible light that passes through the window assembly to the total incident solar radiation that falls on the window. Since IGUs are the only transparent/translucent part of the window system, VT and SHGC are generally applied to the entire aperture area of the window and the values reported of the centre-glass region, while U-value can be applied to both the aperture, or IGU, and window assembly.

Standard environmental conditions are imposed for comparison of these indices since both the U-value and SHGC are highly sensitive to outdoor/indoor temperature difference and solar irradiation. In North America the standard conditions are set by the NFRC, where U-values of IGUs, edge-glass, and frames are reported under standard winter conditions, while SHGC is reported under standard summer conditions (LBNL, 2003).

All three of these indices have a significant influence on building energy performance. In a mixed climate, windows with higher U-values are expected to have higher heating loads due to greater heat loss in the winter. They will typically have more problems with condensation and thermal comfort complaints from falling cold air and a lower mean

radiant temperature. With lower U-values there is a smaller range of conditions which condensation can occur (LBNL, 2003). Conversely, windows with higher solar heat gain are expected to have lower heating loads during the winter from free solar gains, yet a higher cooling load in the summer since SHGC is the most significant factor in determining the air-conditioning load (LBNL, 2003). The amount of visible light that is transmitted through the IGU determines the amount and quality of daylight that enters the building. Windows with higher VT tend to be clearer and allow more light in. However, large window areas of high VT can lead to glare problems (Enermodal, 2002).

2.1.2 Centre-Glass Glazing Analysis

Considerable research on the topic of glazing has been conducted over the past 50 years leading to the development of very reliable models to describe centre-glass glazing performance. In the centre-glass region all three performance indices, U-value, SHGC, and VT are evaluated with one-dimensional models. The flow of solar energy through glazing systems in a building enclosure is non-trivial due to the coupling of the three modes of heat transfer. Solar flux incident on a window is reflected, absorbed, and transmitted at each layer, resulting in many inter-reflections of solar rays in the glazing array. Fortunately, glazing system analysis takes advantage of the fact that there is no appreciable overlap in wavelength between solar (short-wave, avg. $\lambda = 0.5 \mu\text{m}$) and thermal (long-wave, avg. $\lambda = 10 \mu\text{m}$) radiation. The analysis can be carried out in two steps: a solar analysis to determine the transmitted, reflected, and absorbed solar fluxes at each glazing layer, and a heat transfer analysis that uses the absorbed quantities as source terms to establish an energy balance at each layer considering convection and long-wave radiation exchange (Wright, 1998). Both analyses will yield values for U_{cg} and $SHGC_{cg}$. The total heat flux of the centre-glass region of a glazing system is given by

$$q_{net} = U_{cg}(T_{out} - T_{in}) + SHGC_{cg}G_s$$

Equation 2.1.1

(Hollands *et al.*, 2001)

Where: q_{net} = Net energy flow per unit area of the centre-glass region referenced from exterior to interior

U_{cg} = Centre-glass U-value

T_{out} = Outdoor temperature
 T_{in} = Indoor temperature
 $SHGC_{cg}$ = Centre-glass Solar Heat Gain Coefficient
 G_s = Solar irradiance

2.1.3 Multi-layered Glazing Heat Transfer Analysis

The centre-glass U-value, U_{cg} , describes the overall heat transfer through the centre-glass region of the window system per unit area. All three modes of heat transfer are present however, the dominant mode of heat transfer across IGU is radiation (Hollands *et al.*, 2001), followed by convection, and conduction. While the overall heat flux, and in turn U-value, is dependent on the absorbed solar radiation, the U-values that are generally reported are calculated under standard winter night time conditions without the presence of the sun. Thus solar heat source terms are eliminated from the model. Without solar gains, the centre-glass U-value can be simply calculated as

$$U_{cg} = \frac{q_{cg}}{\Delta T}$$

Equation 2.1.2

(Hollands *et al.*, 2001)

Where: U_{cg} = Overall centre-glass heat transfer coefficient

q_{cg} = Overall heat flux

ΔT = Temperature gradient between the exterior and interior environment

The overall heat flux, q_{cg} , describes the net energy flow through the centre-glass region, which changes depending on the interior and exterior temperature and the amount of incident solar radiation. Detailed heat transfer models used to evaluate the centre-glass heat flux, which includes coupled conductive, convective, and radiation heat transfer analysis, have been developed extensively from previous research by Hollands *et al.* (2001) and Wright (1998). Although there are various versions of this model, the model generally assumes that each glazing layer possesses 'grey' or wavelength-independent long-wave properties. This model also allows for diathermanous layers or glazing layers that are capable of passing long-wave thermal radiation in the analysis. While glass is opaque to long-wave thermal radiation, plastic films may partially transmit long-wave

radiation at very low thicknesses. Figure 2.1.3 shows the long-wave energy flows for the i^{th} glazing layer in a multi-layered glazing system.

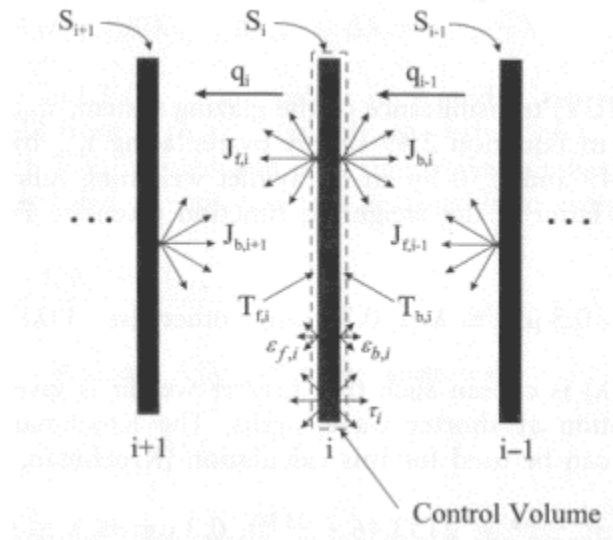


Figure 2.1.3 Centre-glass nomenclature for heat transfer analysis (Hollands *et al.*, 2001)

The heat flux at each layer, q_i , is calculated using Equation 2.1.3 from Hollands *et al.* (2001).

$$q_i = h_i [T_{f,i} - T_{b,i+1}] + J_{f,i} - J_{b,i+1}$$

Equation 2.1.3

Where:

q_i = heat flux across layer i

h_i = convective heat transfer coefficient at layer i

$T_{f,i}$ = temperature of outdoor-facing (front) surface at layer i

$T_{b,i}$ = temperature of indoor-facing (back) surface at layer i

$J_{f,i}$ = radiosity of outdoor-facing (front) surface at layer i

$J_{b,i}$ = long-wave radiosity of indoor-facing (back) surface at layer i

While convective heat transfer is described by the convective heat transfer coefficient, h_i , radiant heat exchange is described by finding the difference in long-wave radiosity between two surfaces facing a gap (Hollands *et al.*, 2001). Radiosity essentially describes the radiant flux leaving the surface; it is calculated by finding the sum of the three radiant fluxes at each layer, which includes the emitted, transmitted, and reflected

long-wave radiant flux. Equation 2.1.4 and Equation 2.1.5 show how radiosities are calculated.

$$J_{f,i} = \epsilon_{f,i}\sigma T_{f,i}^4 + \tau_i J_{f,i-1} + \rho_{f,i} J_{b,i+1}$$

Equation 2.1.4
(Hollands *et al.*, 2001)

$$J_{b,i} = \epsilon_{b,i}\sigma T_{f,i}^4 + \tau_i J_{b,i+1} + \rho_{b,i} J_{f,i-1}$$

Equation 2.1.5
(Hollands *et al.*, 2001)

Where: $\epsilon_{b,i}$ = back surface emissivity of layer i
 $\epsilon_{f,i}$ = front surface emissivity of layer i
 τ_i = transmissance of layer i
 $\rho_{b,i}$ = reflectivity of layer i
 $\rho_{f,i}$ = reflectivity of layer i
 σ = Stefan-Boltzmann constant

In addition to the previous equations, Equation 2.1.6 is required to account for the temperature difference across each glazing layer. Although glazing layers are assumed to be isothermal, the temperature across the front and back surface can change particularly from absorbed solar energy that is not reflected or transmitted.

$$T_{b,i} - T_{f,i} = \frac{t_{gl,i}}{2k_{gl,i}} [2q_{i-1} + S_i]$$

Equation 2.1.6
(Hollands *et al.*, 2001)

Where: $t_{gl,i}$ = thickness of layer i
 $k_{gl,i}$ = thermal conductivity of layer i
 S_i = absorbed solar energy

Finally, using Equation 2.1.3, Equation 2.1.4, and Equation 2.1.5, an energy balance can be imposed on the surfaces of the control volume, layer i , in the form of Equation 2.1.7. By solving for this energy balance at each glazing surface, the heat flux for the entire

glazing system will be generated. Solving the energy balance at each layer of the system requires numerous iterations since both the convective and radiative heat flux are sensitive to the layer temperature. An iterative procedure is required to solve for the layer temperatures until the fluxes at each layer are balanced. This type of task is best suited for computer applications.

$$h_i[T_{f,i} - T_{b,i+1}] + J_{f,i} - J_{b,i+1} = S_i + h_{i-1}[T_{f,i-1} - T_{b,i}] + J_{f,i-1} - J_{b,i}$$

Equation 2.1.7
(Hollands *et al.*, 2001)

It is worth noting that the convective heat transfer coefficient, h_i , is based on natural convection in the cavity between two tall vertical isothermal surfaces, which equations from correlating experimental data are used. For this model, the convective coefficient, h_i , is calculated from the Nusselt number using Equation 2.1.8.

$$h_i = Nu \frac{k}{L}$$

Equation 2.1.8
(Hollands *et al.*, 2001)

Where: Nu = Nusselt number
 k = thermal conductivity of the fill gas
 L = thickness of the cavity

The Nusselt number is determined using a correlation from the Rayleigh number, Ra , which is calculated from Equation 2.1.9.

$$Ra = \frac{\rho_g^2 L^3 g \beta \Delta T}{\mu k}$$

Equation 2.1.9
(Hollands *et al.*, 2001)

Where: ρ_g = density of the fill gas
 β = volumetric thermal expansion coefficient

μ = viscosity

ΔT = temperature difference across the cavity

A correlation between the Nusselt number and Rayleigh number is presented in Figure 2.1.4. This relationship is based on the correlation developed by Wright (1996), which is based on experiments by El Sherbiny *et al.* (1982) and Shewen *et al.* (1996) and is valid for cavities with aspect ratios H/L greater than 20, where H is the vertical height of the glazing and L is the cavity gap. The correlation can be described mathematically by

$$Nu = \left[1 + \left[\frac{0.0665 Ra^{1/3}}{1 + (9000/Ra)^{1.4}} \right]^2 \right]^{1/2}$$

Equation 2.1.10
(Wright, 1996)

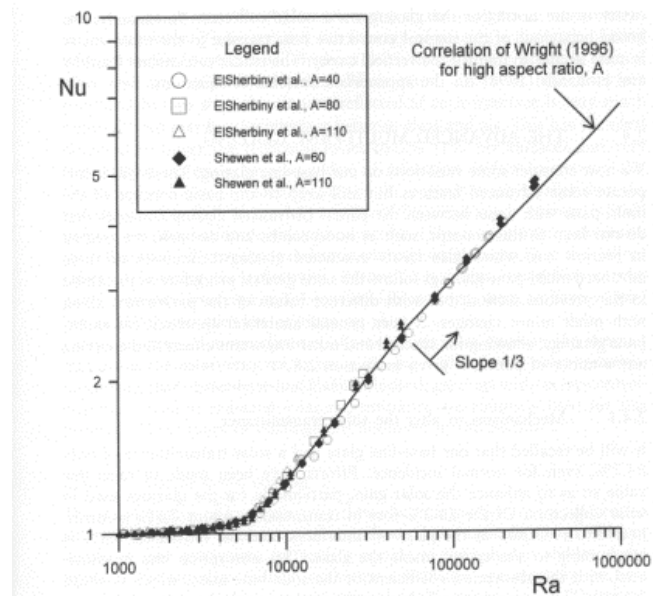


Figure 2.1.4 Correlation for natural convection heat transfer across tall vertical cavity (Wright, 1996)

From the heat transfer analysis it is clear that the IGU U-value is significantly affected by the number of glazing layers, the emissivities of surfaces, the type of fill gas, and the

sealed cavity width(s). The effect of all of these factors on typical commercial IGUs will be discussed in Chapter 3.

2.1.4 Multi-layered Glazing Solar Analysis

Solar analysis is required in order to calculate the SHGC of an IGU. Since SHGC describes the inward flow of heat from the sun, it comprises of both a short-wave and long-wave radiation component and can be written as

$$SHGC_{cg} = \tau_{cg} + \sum_{i=1}^n N_i A_i$$

Equation 2.1.11

(Wright and McGowan, 1999)

Where: $SHGC_{cg}$ = Centre-glass Solar Heat Gain Coefficient
 τ_{cg} = Centre-glass solar transmittance
 N_i = Inward flowing fraction of glazing layer i
 A_i = Solar absorptance of glazing layer i
 n = Total number of glazing layers

The inward flowing fraction, N_i , is dependent on the thermal resistance of each layer and system and can be determined by

$$N_i = \frac{R_i}{R_{tot}}$$

Equation 2.1.12

(Wright and McGowan, 1999)

Where: N_i = Inward flowing fraction of glazing layer i
 R_i = Thermal resistance from layer i to the indoors
 R_{tot} = total resistance across the glazing system

The summation of resistances from outdoors to indoors requires a uniform temperature to be used on each of the outdoor and indoor sides for convective and long-wave radiation.

To account for the difference in radiant and ambient air temperatures, the radiant resistance can be adjusted such that the resultant heat flux is equivalent to the long-wave exchange between the mean radiant temperature of the surroundings (Hollands *et al.*, 2001).

In order to find both τ_{cg} and A_i the net-radiation method for multi-layered glazing analysis must be carried out to find the distribution of solar fluxes (Wright, 1998) as shown in Figure 2.1.5. For this analysis three solar-averaged properties are needed to describe the i^{th} glazing. Each should be specified as a function of the wavelength of the incident solar radiation (Hollands *et al.*, 2001). The three solar-averaged properties include:

- Front (outdoor side) reflectance, $\rho_{f,i}(\lambda)$
- Back (indoor side) reflectance, $\rho_{b,i}(\lambda)$
- Transmittance, $\tau_i(\lambda)$

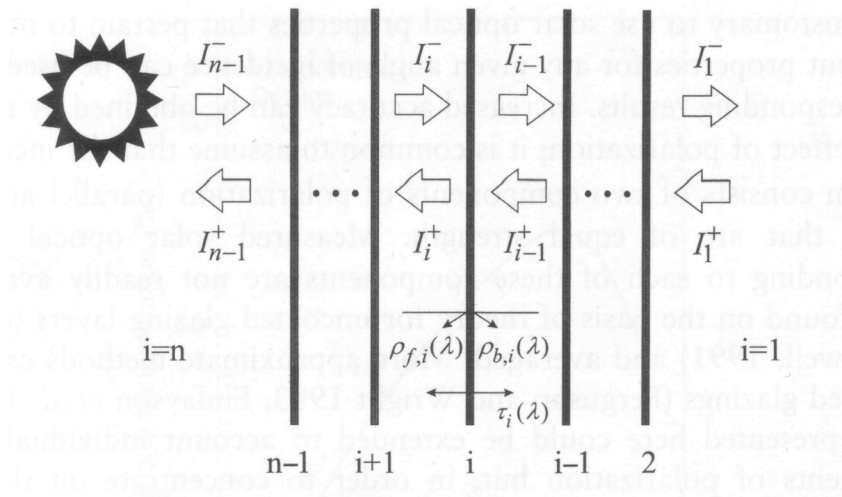


Figure 2.1.5 Solar flux distribution in multi-layered glazing system (Wright, 1998)

To find the rate of absorbed solar radiation of a give wavelength in the interior space and at each glazing layer, radiant energy fluxes between the i^{th} and $(i + 1)^{th}$ glazings, referred to as $I_i^+(\lambda)$ and $I_i^-(\lambda)$, respectively, must be calculated by using Equation 2.1.13 and Equation 2.1.14 .

$$I_i^+ = \tau_i(\lambda)I_{i-1}^+(\lambda) + \rho_{f,i}(\lambda)I_i^-(\lambda) \quad i = 1 \text{ to } n-1$$

Equation 2.1.13
(Hollands *et al.*, 2001)

$$I_i^- = \tau_{i+1}(\lambda)I_{i+1}^-(\lambda) + \rho_{b,i+1}(\lambda)I_i^+(\lambda) \quad i = 1 \text{ to } n-2$$

Equation 2.1.14
(Hollands *et al.*, 2001)

The formulation of these equations can be found in numerous sources (ie. Edwards, 1977, van Dijk and Goulding, 1996, Sielgel, 1973, Shurcliff, 1974, Walton, 1986, Wijesundera, 1975).

The system of equations can be solved the setting the transmittance and reflectance of indoor surfaces to zero, $\tau_i(\lambda) = 0$, and $\rho_{f,i}(\lambda) = 0$, respectively. Having all of the values of $I_i^+(\lambda)$ and $I_i^-(\lambda)$ calculated, the solar absorptance of the i^{th} glazing layer for a given wavelength λ , $A_i(\lambda)$, is calculated from

$$A_i(\lambda) = \frac{I_i^-(\lambda) - I_i^+(\lambda) + I_{i-1}^+(\lambda) - I_{i-1}^-(\lambda)}{I_{n-1}^-(\lambda)}$$

Equation 2.1.15
(Hollands *et al.*, 2001)

Similarly the overall transmittance of the entire glazing system at a given wavelength, λ , is calculated by

$$\tau_{cg}(\lambda) = \frac{I_1^-(\lambda)}{I_{n-1}^-(\lambda)}$$

Equation 2.1.16
(Hollands *et al.*, 2001)

and the spectral overall reflectance at a given wavelength is

$$\rho_{cg}(\lambda) = \frac{I_{n-1}^+(\lambda)}{I_{n-1}^-(\lambda)}$$

Equation 2.1.17
(Hollands *et al.*, 2001)

The visible transmittance, VT, is calculated simply from Equation 2.1.16 as a weighted average over the wavelengths within the visible spectrum (0.4 to 0.8 μm).

2.2 Solar Gain Control

As with all things building science, controlling energy and mass flows will often lead to better, more durable, and energy efficient buildings, this is the same for windows. Given the current architectural trend towards highly glazed facades in commercial buildings, managing solar gains has become increasingly important in the design and operation of energy efficient buildings (Carmody *et al.*, 2004).

Solar heat gain through windows is one of the most variable and largest energy gains in a building and often leads to higher peak and total cooling loads that can offset any benefit of a thermally benign enclosure. A common problem with increased cooling loads from solar gains are oversized HVAC systems that are designed to meet peak cooling demand rather than the average environmental conditions since cooling and air-conditioning systems are significantly affected by solar gains (LBNL, 2003). On hot summer days the demand for air-conditioning causes a spike in electrical load simultaneously across large geographic areas straining the electrical power grid causing an increased risk of rolling brownouts that can cost the economy billions of dollars annually from lost productivity. In addition, oversized cooling systems can lead to part-load humidity problems. Because air-conditioners not only cool but also dehumidify the air, running the cooling system intermittently during non-peak cooling conditions leads to a build up of humidity inside the building. This may lead to moisture problems within the building enclosure and occupant comfort problems such as clamminess and even odours. In order to remove the excess humidity, the air-conditioner must be kept running which can overcool the

building. By decreasing the peak cooling load to match that of the average cooling demand, the cooling system can be properly sized such that it can simultaneously meet both the sensible and latent cooling load.

Another common problem with highly glazed building without appropriate solar control is asymmetric solar gains. Zones within buildings often experience uneven heating due to the sun during the course of a day. For example, a building with a highly glazed façade during winter is likely to experience overheating on its east side due to the low angle sun and excessive heat loss on the west side due to the absence of the direct sun. Under these conditions the building must provide heating and cooling at the same time (Straube, 2008). With the appropriate solar control strategy and an insulating building enclosure the effect of asymmetric heating can be reduced, leading to lower energy consumption and peak demands. With all of these concerns there is a real case for design and implantation of shading devices to control solar heat gains.

2.2.1 Shading Devices

Various technologies have been used to reduce solar gains. In the mid 1980s to the mid 1990s the popular choice of solar control for most commercial buildings was to use tinted windows. Although solar gains were reduced, the tinted windows also reduced visibility and dramatically altered the quality of daylight entering through the window. With the physiological comfort and energy conservation that daylight provides, tinted windows soon fell out of favour. Newer products such as electrochromatics, thermochromatics, and photochromatic glazings can reduce solar gains by altering its opacity with an electrical current, temperature, and solar irradiation, respectively (Fernandez, 2009). However, such technologies are still in development and are still far away from the commercial market. By far, the most effective form of solar gain control is shading devices.

Shading devices comes in all forms from operable slat-type louver blinds, such as venetian blinds, to roller blinds, drapes, overhangs, fins, and retractable awnings, yet their effectiveness varies often depending on the location of the device and shading coverage.



Figure 2.2.1 Photographs of electrochromatic IGU (left) and tinted glazing (right)

2.2.2 Dynamic Shading Devices

Dynamic shading devices are typically characterized by its operability. They can be deployed either manually or automatically and may be adjusted, particularly in the case of venetian and slat-louvers which can alter daylighting levels by adjusting its angles. Dynamic shading devices are available in three types dictated by its location with respect to the window:

- Interior blinds
- In-between blinds
- Exterior blinds

Interior blinds such as venetian blinds, roller blinds, and drapes are great at controlling glare; however, they are not very effective at controlling solar gains (Carmody *et al.*, 2004). Consider that the SHGC is made up of both a solar transmission and an inward flowing fraction that is largely caused by the absorption of solar radiation. When blinds are deployed on the interior side of the window, the blind is able to block off most of the transmitted solar gains, depending on its opacity. However, the blind now acts as an additional layer in the fenestration system and any non-transmitted solar radiation is subjected to be reflected or absorbed by the blind. A non-reflective blind will absorb the majority of the solar radiation causing the blind to heat up (Straube and Burnett, 2005). Since the blind is placed behind an insulated window, heat from the blind will flow into the interior space either through radiation or convection. Similarly, a reflective blind will reflect most of the radiation onto the interior pane of glass causing it to heat up.

However, since the IGU is designed to limit heat transfer to the exterior, most of the heat will also be transferred into the room.



Figure 2.2.2 Interior venetian blinds

Placing the blind in between glazings inside the IGU will improve the solar control performance over interior blinds since most of the solar gains do not enter the building envelope. However, research has shown that the presence of the blinds increases the window U-value (Collins *et al.*, 2009). This may be attributed to the increase in heat transfer rate by conduction due to the presence of the blind, since U-values increased when the blinds were in the fully opened position (Collins *et al.*, 2009). One advantage that in-between blinds hold is that they are able to provide good solar control while being protected from both the interior and exterior environment, making them a good candidate for high rise buildings in the future.



Figure 2.2.3 In-between blinds from SurPlus Home, Team Germany 2009 Solar Decathlon. Top: exterior view, bottom: interior view

By far the most effective way of controlling solar gains is to place the blind on the exterior side of the window. At this position most of the solar radiation is blocked before it penetrates the building enclosure. Any heat build up in the external blind is likely to be radiated and convected away to the external environment and thus significantly reducing the inward flowing heat (Straube and Burnett, 2005). Figure 2.2.4 illustrates the significant difference in solar gains between interior and exterior blinds for a typical IGU.

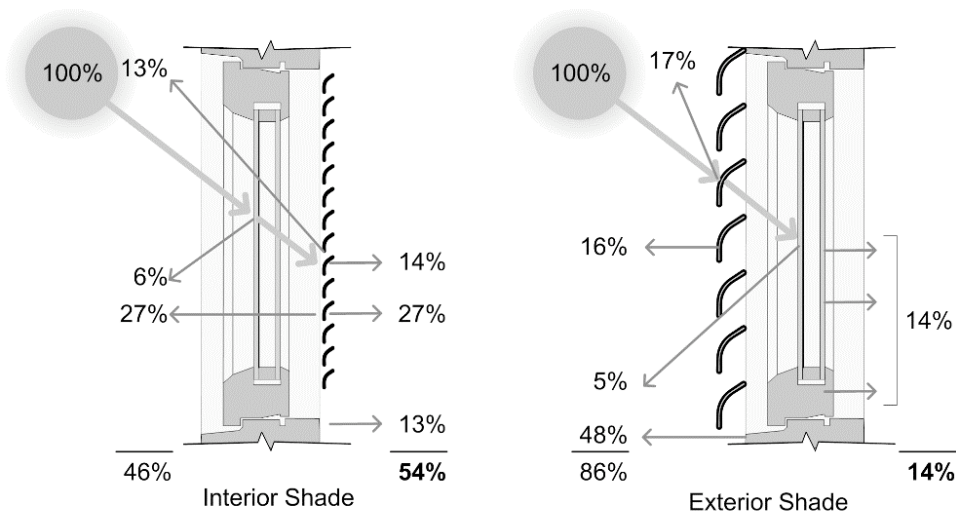
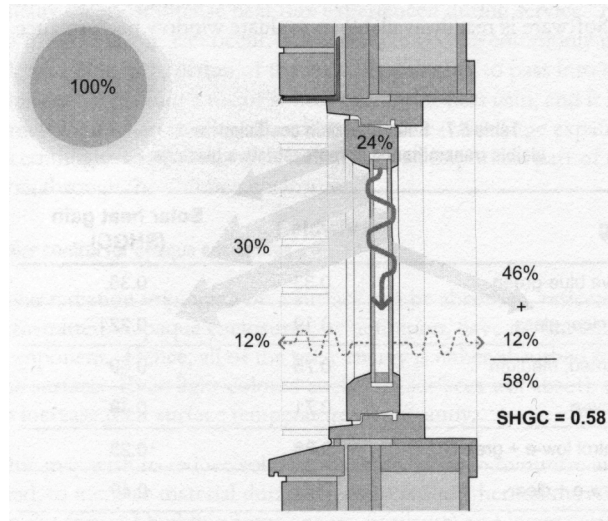


Figure 2.2.4 Solar Heat Gain of a typical window with and without interior and exterior shading (Straube and Burnett, 2005)

Although exterior blinds are effective at controlling solar heat gains they are subjected to harsh weather conditions and can be easily damaged. To limit damage, exterior blinds must be protected during inclement weather events through proper control strategies. For example, exterior venetian blinds may be retracted during periods of high winds while external louver slats are switched offline during the winter to avoid operational issues due to ice build up (North House, 2009).



Figure 2.2.5 Exterior venetian blinds and interior roller blinds of North House

For most commercial buildings both exterior and interior blinds should be employed to limit solar heat gain and control glare. Perhaps the best way to use shading devices to control both solar gains and visual glare is to separate them by using a combination of exterior slatted blinds that can be adjusted to block direct solar radiation and white light diffusing roller blinds in the interior for glare control. For optimum performance the

exterior blinds should be controlled in concert with the HVAC system such that instances of overheating and free heating from solar gains can be finely controlled without using excess energy from mechanical systems (North House, 2009). This can be considered as a responsive building enclosure that actively controls passive energy loads. Such systems are rare due to its cost; however, with the maturity of building automation systems, creating an automated shading system that is responsive to the building's interior conditions is fast becoming a market viable reality.

2.2.3 Static Shading Devices

Static shading devices are extremely popular with older buildings as it is an effective and inexpensive form of shading that can be easily incorporated into the architecture of the building. Static shading devices typically refer to fixed overhangs above window openings and fins parallel to windows and are designed primarily to block direct solar radiation. Therefore, proper design of overhangs and fins must take into account the location of the building (latitude and longitude) as well as the orientation of the window. This type of information is key in determining the sun angle for a particular time and location from which the shaded area can be calculated by geometry (McQuiston *et al.*, 2005). Overhangs are often designed to provide a specified shaded area at a specific time of day for specific days, depending on its orientation. For example, a great use of overhangs is to provide shading on south-facing façades during the summer and no shading during the winter. In this instance, the overhang can be designed such that the entire window is shaded during the longest day of the year, the summer solstice, and unshaded during the shortest day of the year, the winter solstice, by taking advantage of the high solar altitude during the summer and low solar altitude during the winter as illustrated in Figure 2.2.6. With this type of shading unwanted solar gains are rejected during warmer seasons while solar gains are unobstructed during cooler seasons.

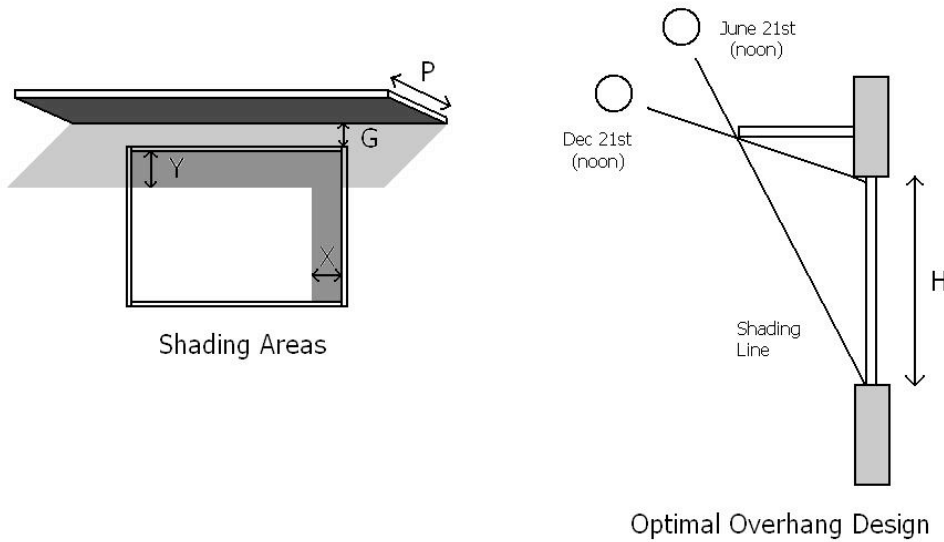


Figure 2.2.6 Overhang design

Similarly, fins provide shading on either side of the window and are most particularly useful at providing shade as the sun is traversing across the sky in the mornings and afternoons. They are also designed to provide shading at a specified time of day at specific dates (McQuiston *et al.*, 2005). Fins and overhangs can be designed using simple geometry after the solar position is calculated, equations for calculating the shaded widths as shown in Figure 2.2.7 in relation to the solar position are

$$y = P \left(\frac{\tan \alpha}{\cos \gamma} \right)$$

Equation 2.2.1
(McQuiston *et al.*, 2005)

$$x = B \tan \gamma$$

Equation 2.2.2
(McQuiston *et al.*, 2005)

Where: y = overhang shaded width
 x = fin shaded width
 P = Overhang width

B = Fin width

α = Solar altitude

γ = Wall solar azimuth angle

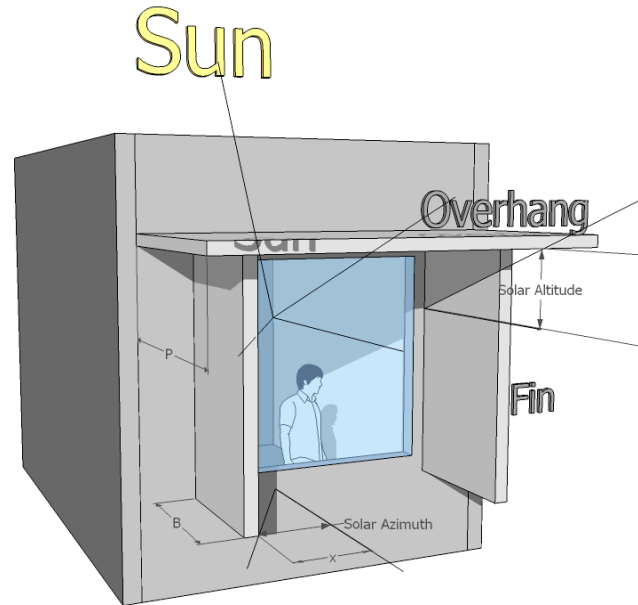


Figure 2.2.7 Shaded area of south-facing window with static shading devices in November afternoon

Due to its design static shading devices are orientated such that it blocks direct solar gains while still allowing for diffuse solar radiation for daylighting (McQuiston *et al.*, 2005). Despite its simplicity and relatively low cost, static shading devices has one significant disadvantage: it lacks precise control of solar gains. For example, in a building with a highly insulated enclosure with high internal heat gain, solar gains may not be desired during the winter due to the risk of overheating. With static shading devices unwanted solar gains are still present since the shading device was designed to allow sunlight in during those periods. Static shading devices also do not offer a lot of protection against low angle sun (Carmody *et al.*, 2004). For east- and west-facing façades, static shading devices can do little to shade it from unwanted solar gains since the sun will at some point be normal to the façade. In addition, with larger windows, overhangs and fins will have to grow in size, often to dimensions that are impractical to meet the desired shaded coverage area. Because static shading devices are placed around windows, they can potentially block views by reducing the effective aperture (Carmody

et al., 2004). Therefore the design of static shading devices must be carefully considered, particularly relating to construction constraints due to the size of the shading device and views.

2.3 Basics of Daylighting

Lighting is one of the most important aspects in commercial building design since visual comfort is essential to carrying out tasks. Increasingly daylighting has been incorporated in many lighting design schemes as a measure to help reduce electrical lighting demand. The case of supplying daylight into buildings is substantial with benefits including:

- **Improved lighting quality:**

Daylight imparts the same spectral distribution as sunlight, with the same mix of colours, while electric lights can only provide a limited spectral range that is typically concentrated in the blue/green or yellow/green range. This allows daylight to provide improved lighting quality by enhancing colour discrimination and rendering, making it better suited to human vision (Enermodal, 2002).

- **Better occupant comfort and health:**

Studies have shown the physiological benefits of daylight on the human body, suggesting that working by daylight results in less stress and discomfort (Rusak *et al.*, 1995). Conversely, a lack of daylight can lead to Seasonal Affective Disorder (SAD) and can affect the secretion of melatonin which can affect sleep, body temperature, and promote tumor development (Rusak *et al.*, 1995). Occupants also tend to feel an improved sense of well being through greater exposure to exterior surroundings through the use of windows by providing a view to the outside. Views are particularly important as the quality of the view is determined by its "information content" and is maximized when three view elements are included: the skyline, upright middle ground objects (ie. trees, buildings etc.), and horizontal foreground objects (ie. streets etc.).

- **Increased productivity:**

People exposed to daylight are often found to be more efficient and productive, and tend to miss less work due to illness. The benefits of this are substantial considering a company's personnel costs clearly outweigh all other costs of the building including the capital cost of the building (Enermodal, 2002).
- **Reduced auxiliary lighting load:**

Daylighting can significantly reduce a building's overall energy consumption since interior lighting accounts for approximately 30-40% of the electricity consumption for most commercial buildings (Enermodal, 2002). With proper daylighting design and lighting controls, the auxiliary lighting load can be reduced by up to 66%.
- **Reduced cooling load:**

Compared to electrical lighting, daylight delivers more of its energy as visible light rather than heat. Therefore, daylighting has the potential to reduce cooling loads. However, the relationship between daylighting and excessive solar gains are quite complex and careful consideration must be taken in balancing thermal losses with solar gains. Proper daylighting design that reduces cooling loads will employ both interior and exterior shading along with the appropriate IGU selection that will limit unwanted solar gains and reduce thermal losses through the fenestration system (Enermodal, 2002).
- **Reduced peak electricity demand:**

By utilizing daylighting as a light source, both the cooling and lighting loads reduced, thus reducing electricity demand. Commercial buildings are perfectly suited for daylighting since most buildings are occupied during hours when daylight is available (Enermodal, 2002).

The ultimate goal of good daylighting design is to minimize energy use and maximize occupant comfort. A well daylit building should be able to adequately lit with daylight while using electrical lighting as an auxiliary backup when daylight is not available.

Unfortunately daylighting design is relatively new field of study in building design and many practitioners do not fully understand its principles. As a result, many designers chose to build façades with higher window areas (WWR) with the belief that this will bring more daylight into the building and reduce energy load of both. Unfortunately this is not the case since highly glazed facades will lead to higher cooling loads and excess glare problems. In this section the basic design principles of daylighting are presented along with appropriate daylighting design strategies that provide visual comfort and can ultimately help reduce the overall energy consumption of commercial buildings.

2.3.1 Daylighting Design Concepts

Daylighting performance in a typical building is often evaluated by a few select parameters that measures the amount of light that enters the room and how deep it goes, the brightness of the room, and when is it available. All of these qualities are typically measured by the following parameters:

- **Illuminance:**

The density of luminous flux incident on a surface (usually a working plane, approximately 0.8 m above the finished floor). It is typically measured in lux (lumens/m^2) (SI) or footcandles (lumens/ft^2) (Imp) (Enermodal, 2002)

- **Luminance:**

The physical measure of the stimulus that produces a sensation of luminosity or brightness in terms of intensity of light emitted in a given direction by a unit surface area that is emitting, transmitting, or reflecting light. It is measured by the luminous intensity of the light emitted or reflected in a given direction from a surface element divided by the area of element in the same direction, in units of units of candela per square meter (cd/m^2) or footlambert (fL) (Enermodal, 2002)

- **Daylight Factor:**

Ratio of inside illuminance, at a single point or an average of points, to outside illuminance, expressed as a percentage. The daylight factor is used as a common means of predicting whether the amount of daylight is sufficient. A higher daylight factor translates into greater availability of natural light. Daylight factors are usually determined for overcast sky conditions. In general a room with an average daylight factor of 5% will appear well lit and will only require electric lighting during mainly non-daylight hours, while a room with an average daylight factor of 2% will appear under lit and will require electrical lighting near the back of the room (Enermodal, 2002). Daylight Factors are calculated using the following equation:

$$DF_{avg} = \frac{V_T A_{Glazing} \theta}{A_s (1 - R^2)}$$

Equation 2.3.1

(Enermodal, 2002)

Where: V_T = visual transmittance of the IGU
 $A_{Glazing}$ = net glazing area
 θ = sky exposure angle, the portion of the sky visible from the centre of the window, in degrees
 A_s = total area of interior surfaces (ie. sum of total surface area of walls, windows, ceiling and floor)
 R = area weighted average reflectance of interior surfaces

- **Daylight Penetration:**

The depth of the daylit area within a room that has a certain acceptable level of illuminance. In most commercial buildings and offices, 500 lux is the minimum illuminance on a working surface for detailed work such as writing. However, some studies of shown that illuminance of 300 lux is adequate for most office work, particularly in offices where most of the work is done on computers (Reinhart & Voss, 2003).

- **Daylight Autonomy:**

A prediction of the percentage of occupied times when a required illuminance level can be maintained by daylight alone. It is commonly used in daylighting simulations to predict how useful the daylight is in terms of electrical energy savings (Reinhart, 2005). Daylight autonomy has been proposed as a parameter in measuring daylight performance in commercial buildings since it takes into other considerations such as climate, façade orientation, and window size into account through its simulations in programs such as DaySim, developed by the National Research Council of Canada (NRC) (Reinhart, 2006). An example of daylight autonomy is shown in Figure 2.3.1 for a south-facing rectangular office in New York City, with a fully glazed façade above the work plane, and an IGU with a VT of 35%. The minimum illuminance is 500 lux and office hours are Monday to Friday from 8:00 am to 5:00 pm.

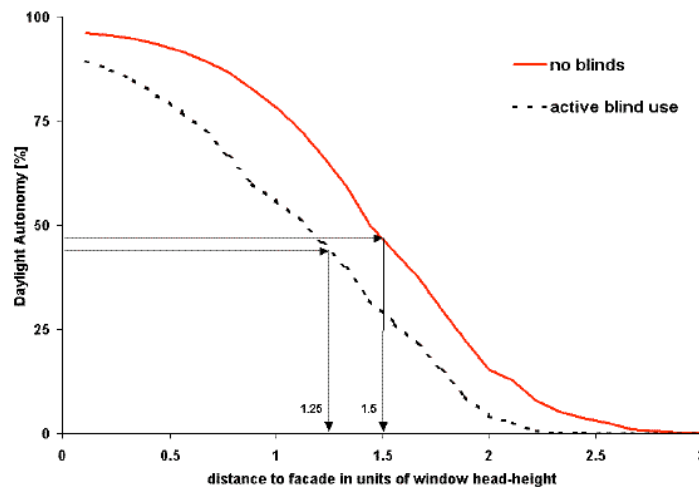


Figure 2.3.1 Daylight Autonomy of a fully glazed south-facing facade in a rectangular office in New York City with a minimum illuminance of 500 lux from 8 am to 5 pm (Reinhart, 2005)

Another important concept in daylighting design is daylight availability. Daylight availability is dependent on various factors including sky illumination and its

surroundings (ie. sky exposure). Sky exposure angles are measured from the centre of the window between the vertical and lowest sight line to the sky as shown in Figure 2.3.2.

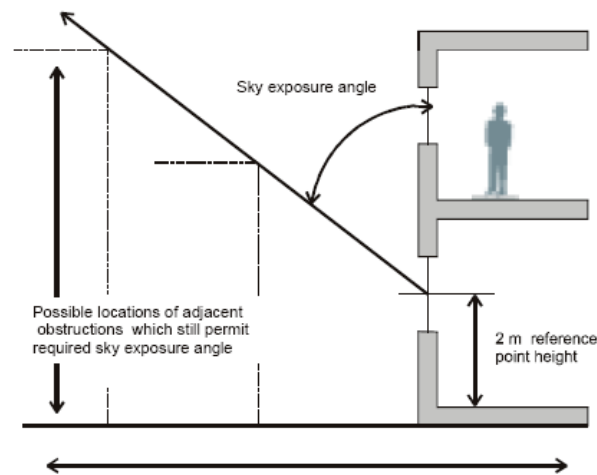


Figure 2.3.2 Sky exposure angle (Enermodal, 2002)

Recommended sky exposure angles are dependent on the location of the building, however, many daylighting guides, such as the Daylighting Guide for Canadian Commercial Buildings (Enermodal, 2002), provides sky exposure angles for most Canadian cities. In general, providing daylighting for buildings in urban areas is more difficult than in rural areas due to shading from neighbouring buildings. Daylighting on floors closer to the ground is particularly challenging.

Sky illumination, is also important in assessing daylight availability and it is dependent on weather conditions. Even though Canada is located far from the equator, Canada still has access to sufficient daylight to light commercial buildings. In fact, the average illumination under overcast skies at a latitude of 46° , which is where the majority of the nation's population lives, is 7500 lux, almost 15 times more than the illumination required to perform average indoor tasks (Reinhart, 2005). Contrary to popular belief, overcast skies provide better conditions for daylighting than clear skies, since an overcast sky acts as a bright, diffuse light source that is a lot easier to control than direct sunlight. Direct sunlight is often too intense and can easily cause glare and heat gain problems; in fact incident sunlight falling on a small aperture within a room is sufficient to provide adequate daylight levels in large interior spaces (Reinhart, 2005). Therefore,

understanding the local climate and environmental conditions can have a significant impact on the daylighting performance of a building.

2.3.2 Visual Comfort

Visual comfort is one of the most important aspects of daylighting design as occupants are very sensitive to visually uncomfortable environments. It encompasses many aspects including lighting quality, views, and glare. Both lighting quality and view are related to the visible transmittance of the IGU. IGUs that are tinted will significantly affect the quality of light entering the room as certain wavelengths of visible light are filtered. This in turn dramatically alters the colour rendering quality of the light and can be a source of visual discomfort. Similarly, the clarity of the IGU affects the quality of the view out of the window. As previously mentioned most occupants desire a view to the exterior, a window that is dark and some-what translucent will reduce the clarity of the view, making it less appealing. Both of these visual qualities are related to the visible transmittance, VT, of the IGU. In fact, the VT is directly correlated to the average daylight factor from Equation 2.3.1 (Enermodal, 2002). An IGU with a higher VT will tend to be clear and allow a greater portion of the visible spectrum to pass through the IGU. For most IGUs the minimum VT which views and daylight quality is affected is around 0.4, which is also the minimum point for all IGUs considered in this project.

Avoiding excessive glare is a major design challenge in daylighting design. Glare is often produced by large contrasts between the light source and its surrounding area which is highly dependent on the by the intensity and brightness of the source. In most buildings, discomfort glare is a result of the contrast between the window and the adjacent wall and ceiling, typically from direct sunlight. One of the design issues that compounds the problem of glare, is that most window sizes are designed to provide sufficient daylight during overcast conditions rather than sunny conditions (Enermodal, 2002). This leads to excess light and solar gains entering the room and requires the use of shading devices to control the amount of direct sunlight during sunny periods.

Although discomfort glare is subjective, since it is perceived by occupants, attempts have been made to quantify which conditions cause discomfort glare. Glare studies have been performed since the second half of the 20th century, first with basic studies by Luckiesh and Guth, and Petherbridge and Hopkinson (Boubekri *et al.*, 1992) which developed a formula that describes discomfort glare for small light sources, while studies at the Building Research Station in England and Cornell University investigated glare from larger sources and predicted the formula known as the 'Cornell formula'. Most of these and many other studies have largely rested on subjective appraisals based on how groups of people responded to different levels in brightness and contrasts in brightness. These studies later led to the establishment of glare criteria based on the glare index. The glare criteria divided the glare index into multiple groups, ranging from 'just imperceptible', with a glare index less than and equal to 10, to 'just intolerable' with a glare index greater than and equal to 28. The accepted glare index value is in between these limits and is largely dependent on the room and task at hand (Boubekri *et al.*, 1992). For most commercial buildings a glare index greater than 22 is considered intolerable, therefore that is the threshold which most designers are set to (Boubekri *et al.*, 1992).

Since discomfort glare is caused by direct sunlight, the glare index can be substantially reduced by managing and avoiding direct sunlight in the room. Some strategies include (Enermodal, 2002):

- Avoid reflective interior finishes: matte finishes help diffuse direct sunlight reducing its brightness and intensity
- Avoid positioning computer monitors near direct sunlight: computer screens are best-positioned perpendicular to windows and away from direct sunlight
- Use appropriate exterior and interior shading devices to block or diffuse direct sunlight.

While avoiding reflective interior finishes and positioning to minimize discomfort glare may be relatively simple, choosing the appropriate shading strategy may be more difficult due to the wide variety of choices and their different effects on shading. Similar to

controlling solar gains, both exterior and interior shading devices can be used. However, the goal of shading devices for daylighting is to only block direct sunlight while allowing diffuse light to enter the building. In this case, static exterior shading devices such as awnings and overhangs works particularly well for south-facing facades, while fins are appropriate for facades facing east and west. As a general rule of thumb, fins should be designed such that the projection from the building is equal to the spacing between fins or window width (Enermodal, 2002). For buildings with greater window area, fin projection can be scaled back by reducing the spacing and adding more fins. Other architectural shading techniques such as recessing windows deeper into walls can provide additional shading against direct sunlight. Even vegetation, such as deciduous trees, can provide seasonal shading by blocking direct sunlight in the summer months and allowing solar gains in the winter for free heating, particularly against the low angle sun for east- and west-facing façades. Perhaps the most effective shading strategy for controlling glare are interior shading devices that can be manually adjusted by the occupant such that conditions for visual comfort can be finely tuned. Shading devices such as venetian blinds can block direct sunlight by setting the slats perpendicular to the sun and still allow diffuse light to pass through. Roller blinds and screens are also very effective at reducing glare since they not only block direct sunlight, but they also provide a diffuse light source by diffusing sunlight. These blinds can be mounted either as pull-down or pull-up shades to allow for refined control of blind positioning while still allowing diffuse sunlight to pass through the window. The blinds should be light colour to help diffuse direct sunlight and should have a visible transmittance no greater than 0.1 (Enermodal, 2002).

2.3.3 Daylighting Design Strategies

Daylight design can be affected by numerous factors in and around the building. As a result, a good daylighting design will require inputs from a multidisciplinary team including owners, architects, electrical and mechanical engineers and contractors. Daylighting can come in many forms as well, depending on the location inside the building. Daylighting strategies for providing perimeter zones generally rely on windows whereas daylighting in the core uses skylights, atriums, and solar tubes to bring daylight

into the building. Perimeter zones are generally considered to be approximately 5 m (16'-5") deep as shown in Figure 2.3.3.

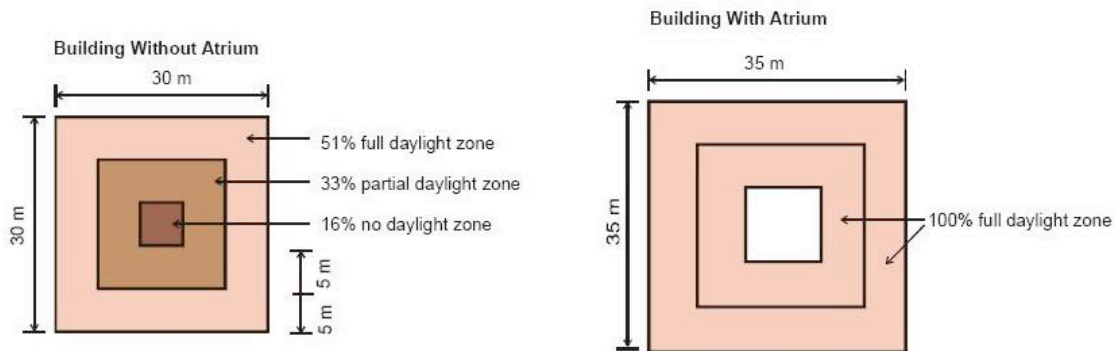


Figure 2.3.3 Typical building perimeter and core zones for daylighting (Enermodal, 2002)

Since most commercial and high rise buildings do not have atriums, only daylighting in the perimeter zone is discussed in this project. In this case rooms within the perimeter zone are side-lit, since daylight generally comes from windows in the walls.

The variables taken into consideration for providing daylight in perimeter zones are:

- Building orientation and form
- Window area (WWR)
- Window head height
- IGU visible transmittance (VT) and performance characteristics

Building orientation and form are important as the building should be designed for maximum daylight exposure in perimeter zones while minimizing unwanted solar gains. As a result, most buildings tend to be elongated along the east-west axis to maximize sunlight exposure along the north and south facades while minimizing solar gains on the east and west facades. This is particularly beneficial since south-facing facades has the most daylight access and best control of excess solar gain in the summer making it the most suitable facade for daylighting, while north-facing facades has a near-constant availability of diffuse skylight that is uniform, allowing for larger glazing areas to minimize electric light use and making it the second most suitable orientation for daylight design (Enermodal, 2002).

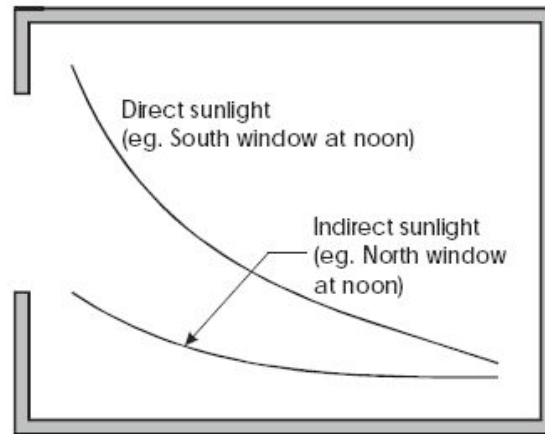


Figure 2.3.4 Daylight distribution of north- and south-facing facades (Enermodal, 2002)

Conversely, east- and west-facing facades are very difficult to design for daylighting since there is a high degree of variability in availability and intensity, with half-day exposures and low angle sun, making it difficult to control daylight penetration and discomfort glare. Placing work areas in these parts of the building should be avoided along with work areas in the building core where daylight is absent. Instead room depths and offices should be designed to correspond with the daylighting zone to make the most use of daylight penetration and reduce the need for auxiliary lighting. Windows should also be placed on two walls if possible to provide bilateral lighting in side-lit rooms. This helps eliminate problems with glare by reducing lighting contrast in the room (Enermodal, 2002).

Window size and area is another important factor in daylight design since it can determine the amount of daylight that enters the building. There are various ways to determine the appropriate window size for providing daylight from computer simulations that calculates daylight autonomy to simplified general equations that are based on correlations and rules of thumb. One such equation presented in the Daylighting Guide for Canadian Commercial Buildings (Enermodal, 2002) relates daylight factor and interior reflectances through a room geometry factor, visual transmittance of the IGU and sky exposure angle to window area expressed as the WWR, as shown in Equation 2.3.2.

$$WWR = \frac{RoomGeometryFactor}{V_T \theta}$$

Equation 2.3.2

(Enermodal, 2002)

Where: WWR = Window-to-Wall Ratio, window area
 Room Geometry Factor = values listed in the Daylighting Design Guide for Canadian Commercial Buildings for rooms of various widths and depths with varying wall colour for a specified daylight factor
 VT = visible transmittance of the IGU selected
 θ = sky exposure angle

The equation suggests that IGUs with lower VT and exposure to the sky will require larger WWRs. For typical commercial buildings with a daylight factor of 3%, the recommended WWR is approximately 30% (Enermodal, 2002), suggesting that adequate daylighting can be achieved with minimal window area. It is also noted that any window area below the working plane or desk height, should not be counted for daylighting purposes since it provides no useful daylight in the room.

Contrary to popular belief daylight penetration is unrelated to window area; instead daylight penetration is dependent on the window head height (Reinhart, 2005). Many designers are somewhat aware of this from many forms of empirical rules of thumb that suggests the maximum daylight depth of 1.5 to 2 times the window head height as shown in Figure 2.3.5.

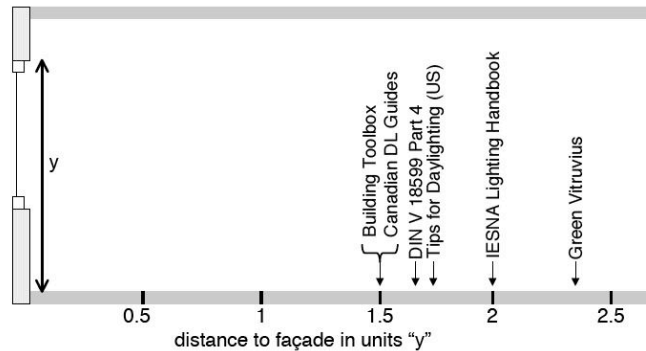


Figure 2.3.5 Predictions of daylight penetration depth from various rules of thumb relating window head height (Reinhart, 2005)

While all of these predictions are relatively easy to follow it does not take into account the location or orientation of the building, let alone the minimum illuminance level or visible transmittance of the glazing and lacks any analytical evidence. To determine the proper daylight penetration depth that is related to the window head height a series of computer simulations were performed by Reinhart (2005) to calculate the daylight autonomy of different rooms at different orientations. The width of the rooms were 1.6 times the head height of the window, and it had ceiling, wall, and floor reflectances of 80%, 50%, and 20%, respectively. All of the rooms followed a regular occupancy schedule in which it was occupied during weekdays from 8 am to 5 pm with intermittent breaks (Reinhart, 2004). For most populous North American cities, the daylit zone depth which achieves 50% daylight autonomy ranges from 0.5 to 3.3 times the window-head-height with over 85% of the predicted zone depth falling in between 1 and 1.5 times the window-head-height without shading. With the implementation of interior shades that are deployed when direct sunlight irradiance on the work plane is greater than 50 W/m^2 , the daylit zone depth decreases with 85% of all predictions lying between 0.8 and 2 times the window-head-height (Reinhart, 2005) as shown in Figure 2.3.6.

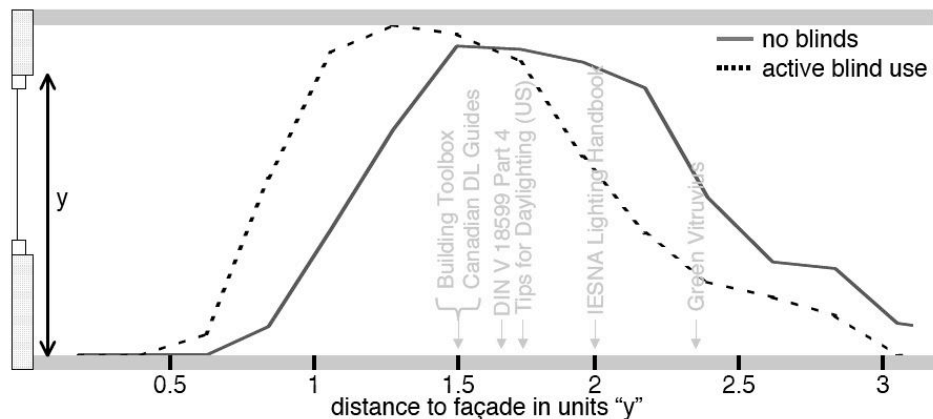


Figure 2.3.6 Frequency distribution of daylight depths with 50% daylight autonomy of various North American cities (Reinhart, 2005)

The study also indicates the daylit zone depth changes with different minimum illuminance levels and glazing visible transmittance (Reinhart, 2005). Figure 2.3.7 shows the distribution curves of daylight depths of a room with a minimum illuminance of 300 and 500 lux, as well as IGUs with VTs of 35% and 75%. These graphs shows by

reducing the minimum illuminance level from 500 lux to 300 lux, the daylight zone depth increases from 1 to 1.5 times the window-head-height. Similarly, by increasing the IGU's VT from 35% to 75% the peak frequency distribution is increased from 1 to 1.8 times the window-head-height (Reinhart, 2005). Given that many human factor studies suggests that most office workers work below desktop illuminances of 300 lux (Reinhart and Voss, 2003), lighting standards should be shifted from 500 lux to accommodate the realities of the workplace. This in turn will translate into greater flexibility for daylighting design and allow for IGUs with lower VTs that are often more insulating and have lower SHGC to be used while still meeting daylighting requirements.

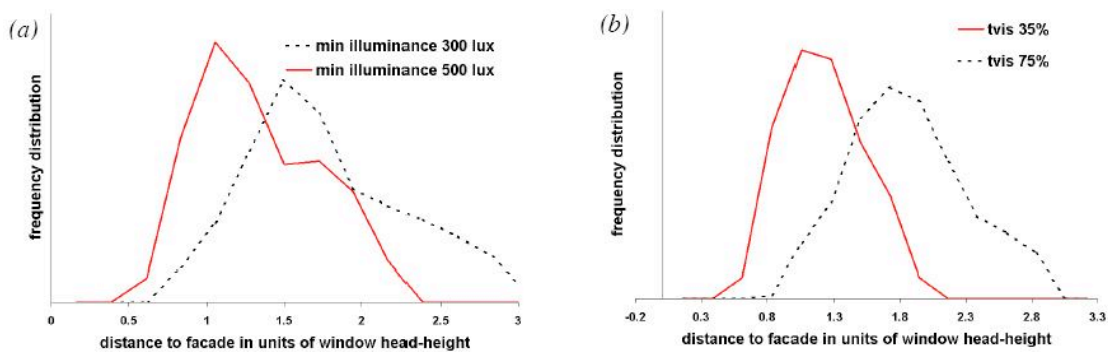


Figure 2.3.7 Frequency distribution of predicted daylight zone depth with blinds for a) varying minimum illuminances (Reinhart, 2005), b) varying visible transmittances (Reinhart, 2005)

The study showed, however, that window area below the work plane had very little effect on the daylight zone depth by varying the size of the glazed portion of the wall below the working plane with obstructions such as balustrades and window-sills (Reinhart, 2005). These results confirms the common notion that façade openings below the work plane height do not contribute to the amount of daylight in a space and it is the window-head-height, not the ceiling-height that determines the size of the daylight zone depth (Reinhart, 2005).

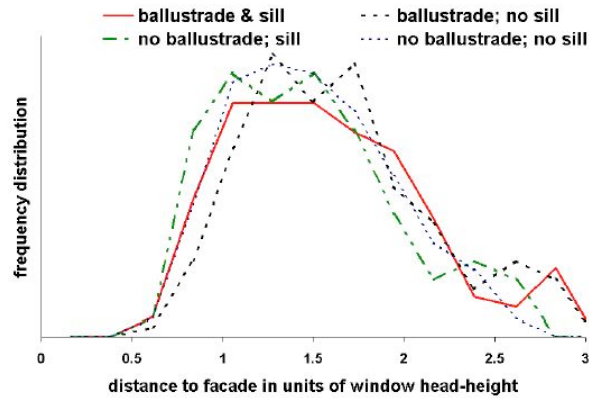


Figure 2.3.8 Frequency distribution of daylit zone depth with various facade arrangements below the work plane height (Reinhart, 2005)

The location of the building also has an important role in the predicted daylit zone depth. As shown in Figure 2.3.9, the shape frequency curves of the predicted daylit zone depth are the same, however, the daylit zones tend to decrease with increasing latitude (Reinhart, 2005) due to the daylight availability and increasing summer sun angles.

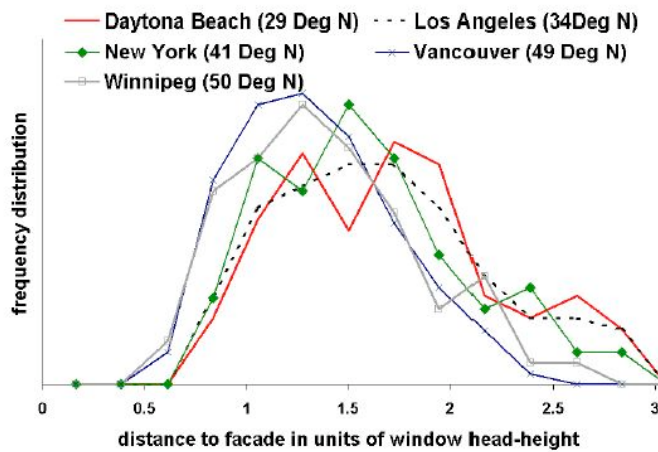


Figure 2.3.9 Frequency distribution of predicted daylit zone depths of varying latitudes (Reinhart, 2005)

Finally, the most important aspect in daylit zone depth is the room orientation. This study suggests that the peak frequency distribution lies within 1.25 to 1.75 times the window-head-height for the North, South, and West façades, while the peak is closer to 1 for the east façade (Reinhart, 2005). The frequency distribution curves shown in Figure

2.3.10 indicates that, with the exception of the east façade, all of the curves are similar in shape. The predicted daylit zone depth is much shallower in the east since under this blind control algorithm, the blinds are deployed in first thing in the morning and do not retract until the sun passes after noon.

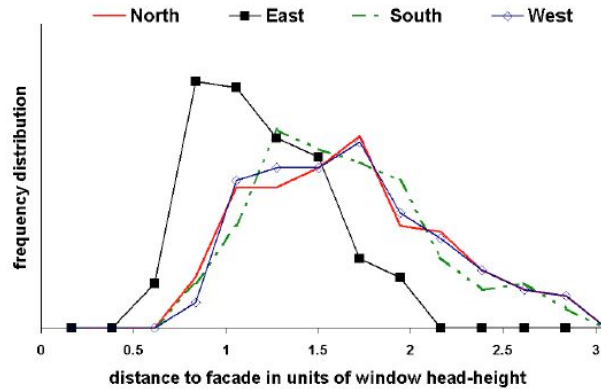


Figure 2.3.10 Frequency distribution curves of predicted daylit zone with blinds for North, East, South, and West orientations (Reinhart, 2005)

Overall, the results of this study suggests that daylit zone depth depends heavily on the window-head-height as oppose to the window area. The daylit zone depth for most North American cities around 1 to 1.5 times the window-head-height, and changes from 0.8 to 2 times the head-height depending the shading algorithm (Reinhart, 2005). The only factors that significantly alter the daylit zone depth are minimum illuminance levels and visible transmittance of the IGU. Reducing the minimum illuminance level increases the daylit zone depth as does increasing the visible transmittance of the glazing unit. Of course, these are general results, for offices with special orientations, geometries, and shading obstructions detailed simulations may be required. Other factors that can change the daylit zone penetration include light shelves which are believed to increase daylight penetration to as much as 2.5 times the window-head-height (Enermodal, 2002).

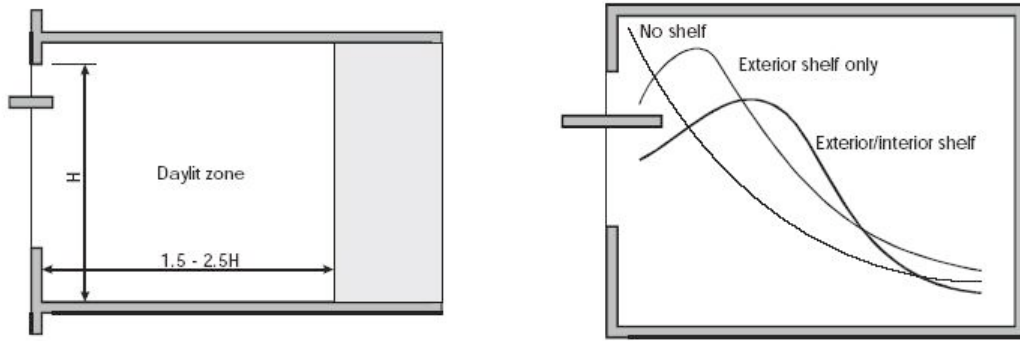


Figure 2.3.11 Daylit zone depth and daylight distribution of facades with light shelves (Enermodal, 2002)

2.3.4 Auxiliary Lighting Integration

Any daylighting design efforts can be considered useless without the proper auxiliary lighting control. If the auxiliary lights are unable to be dimmed or turned off under the presence of daylight then all potential energy savings associated with daylighting are nullified. There are many strategies and technological solutions to integrate auxiliary lighting with daylighting, however, they can only be effective if they meet the occupants' needs. The following guidelines have been recommended by the Daylighting Guide for Canadian Commercial Buildings (Enermodal, 2002) for designers to follow:

- Do not compromise lighting quality for energy efficiency. Each area must be lit according to the tasks performed for user comfort, skill, and safety
- Ensure all lighting control systems meets user needs and is operating properly. Unpredictable or poorly functioning controls are a major source of occupant frustration.
- Provide opportunities for manual override and place manual controls in convenient and visible locations such that occupants can maintain a degree of control over their work space.

In addition to the above guidelines, lighting should also provide the following functions, listed in order of importance (Enermodal, 2002):

1. Scheduling

Lights should be turned on and off according to the day/night and holiday occupancy schedule. This can be easily implemented with a building automation system, and/or occupancy sensors for each zone.

2. Daylighting

Auxiliary lights are dimmed or shut off in response to interior daylight levels

3. Tuning

Lighting levels are fine-tuned to the desired illumination by the occupant

4. Lumen Maintenance

Using the same hardware for daylight dimming, new lamps can be dimmed until their light output meets the required design level. As lamps age or become dirty, power input increases to maintain the desired illumination, thus routine maintenance is required.

There are numerous ways to effectively integrate an auxiliary lighting system with daylighting to provide energy savings. Some of which include selecting the appropriate:

- Lighting fixture (luminaire) location(s)
- Dimming strategy
- Lighting technology

Lighting fixture, or luminaire, location is important to visual comfort. If well planned, electric lighting can be used to augment the daylight that is present in building spaces. In this scheme daylight would be considered as the prime source of light with artificial light used as a backup. An effective way to make use of interpreting this rule is to use daylighting for ambient lighting, while task-specific lighting can be provided by user control auxiliary luminaires for fine detailed work (Enermodal, 2002). Another consideration is to keep exposed bulbs out of view to limit distractions and glare. A good

solution to this while still providing sufficient artificial light is to use direct/indirect luminaires such as the ones shown in Figure 2.3.12, since indirect light does not produce lamp reflectance on computer screens (Enermodal, 2002).

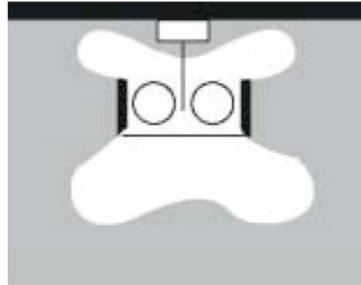


Figure 2.3.12 Direct/Indirect illumination distribution (Enermodal, 2002)

Choosing the right dimming strategy is another important consideration in integrating auxiliary lighting with daylighting. There are three commonly used dimming controls used in daylit buildings (Enermodal, 2002):

1. On/off control:

Lights turned on or off in response to indoor illumination level. This offers the simplest level of control, but it also has greatest fluctuation in lighting level, therefore it is only appropriate for areas where large variation in lighting levels are acceptable, such as entrances, atria, and cafeterias.

2. Staged or switching controls:

This type of control switches off successive rows of lamps or fixtures using relay switches as daylight level increases. This type of control best suited to corridors and rooms where fine work not being done.

3. Continuous dimming controls:

Under this arrangement lamps are continuously dimmed as daylight increases. This type of control system is typically more expensive and requires special lamps, ballasts, and more elaborate controls. However, increased energy savings achieved with a well-designed set up, especially with the right sensor placement,

hardware quality and commissioning practices. This type of control is best suited to offices.

Dimming control systems typically require either an occupancy or daylight sensor that determines when the auxiliary lights should be turned on and at which levels. The sensors should be placed in a location that is appropriate to the task. For a room with only one task area, a ceiling-mounted sensor should be placed above task, while for a room with multiple task areas, the most representative location should be chosen (Enermodal, 2002). For most commercial buildings, the daylight sensor should be placed approximately 2/3 into the depth of the daylit control zone since this is where daylight penetration drops off. In addition, the daylighting controls should have some sort of hysteresis in the form of a deadband or dual-setpoints such that frequently varying daylight conditions do not trigger auxiliary lights to be continuously switched on and off causing a visual disturbance to the occupant(s).

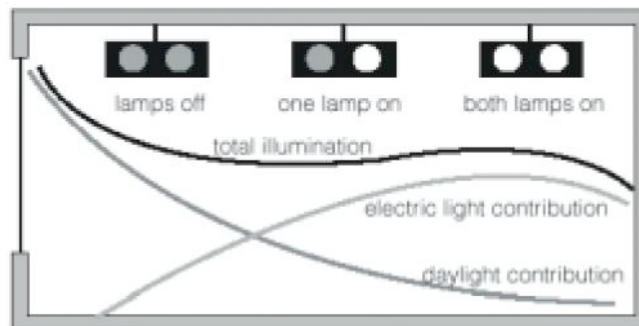


Figure 2.3.13 Illumination levels with staged controls (Enermodal, 2002)

Finally, lighting technology can affect the overall lighting load. With emerging lighting technologies tending towards greater efficiencies, the energy savings from daylighting may be reduced; however, there are other benefits of daylighting besides providing light. With that in mind, energy efficient lighting technologies are still important in reducing overall building energy consumption since auxiliary lighting must be provided with or without daylighting in the building. Some of the emerging lighting technologies include energy efficient fluorescent tubes such as T8s and T5s. The energy consumption of these lights are approximately 32 W and 14-28 W, respectively (Canlyte, 2009) depending on

the length of the tube, whereas traditional T12s are 34 W and provides less lumens and do not dim reliably. Other lighting technologies include Light Emitting Diodes (LEDs), which are in the order of 10-20 W and can be easily dimmed (Canlyte, 2009). Aside from the reduced wattage specifications that lighting designers should be aware of include lighting efficacy, Correlated Colour Temperature (CCT) and the Colour Rendering Index (CRI). Lighting efficacy describes the energy efficiency of the luminaire, it is measured in lumens per watt. Although fluorescent lighting is much more energy efficient than traditional incandescent lighting, the efficacy is unmatched by LED sources. Figure 2.3.14 compares the difference in system efficacy between Compact Fluorescent Light (CFL) and LED sources.

CFL Source		LED Source	
8021CCLW with 612632BG120 (26W TTT)		C420LEDDL30KCCLW with C420LED1	
Total Input Watts	31W	Total Input Watts	20W
Ballast Efficiency	84%		
Source Wattage	26W		
Source Lumens	1800		
Reflector Efficiency	48%		
Total Fixture Lumens	865	Total Fixture Lumens	1000
Lumens per Watt	27.9	Lumens per Watt	50.0

Figure 2.3.14 Efficacy of CFL and LED sources (Canlyte, 2009)

CCT and CRI describes the 'colour' of the light and the its ability to reveal colours of objects it shines on, respectively. In order to match daylight, luminaires with higher CCTs and CRIs should be selected, since higher CCTs will produce a 'whiter' light while luminaires with higher CRIs will reveal different shades of colour on objects more effectively, both of these qualities closely match that of natural daylight which comes from a high temperature source and contains all of the colours in the visible spectrum (Canlyte, 2009). The CRI is dependent on the spectral distribution of the light source. The recommended CCTs should be approximately 4000 K and CRIs should be greater than 80 (Canlyte, 2009). A comparison of different CCTs and spectral distribution of CFL and LED light sources are shown in Figure 2.3.15 and Figure 2.3.16, respectively.

It is important for the designers to make the best use of various lighting technologies that delivers a visually comfortable environment.



Figure 2.3.15 Visual comparison of light sources with different correlated colour temperatures (Canlyte, 2009)

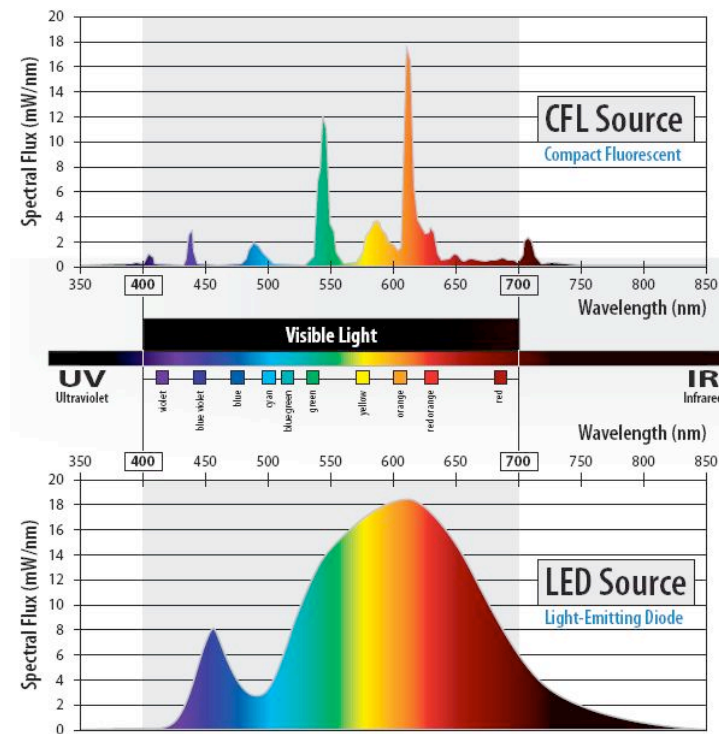


Figure 2.3.16 Spectral distribution of different light sources (Canlyte, 2009)

From this perspective windows play an important role in the performance of perimeter spaces, since it can potentially affect both thermal and visual comfort. The following chapters of this thesis examine the technical advances of window technology along with a detailed evaluation of their performance from a component to overall system level.

CHAPTER 3

High Performance Insulated Glazing Units

With advances in both research and manufacturing, the performance of Insulated Glazing Units (IGUs) continues to improve. This chapter evaluates the performance of high-performance IGUs by first examining the properties of state-of-the-art glazing components in the first section. The design characteristics of each separate component such as low-emissivity (low-E) coatings, plastic films, and exotic fill gases are evaluated through a series of one-dimensional energy transfer simulations in both Window5 (LBNL, 2003) and VISION (Ferguson *et al.*, 1984). The results presented from this analysis are intended to provide greater understanding of how these components and properties affect IGU energy transfer and to provide designers some background in IGU design. The implications of these advanced glazing properties to IGU performance are then evaluated in great detail in the second section through a set of multi-layered IGUs that are also evaluated using Window5 (LBNL, 2003). The objective of this activity is to determine and document the technological limits of performance that can be achieved with advanced and conventional glazing materials. This survey of IGU performance allows designers to determine how to best construct IGUs to meet their desired properties. It also provides a ‘road map’ to creating a set of high-performance IGUs that are suitable for cool and moderate climates. By modifying the glazing properties of the upper and lower bound IGUs a set of high-performance IGUs was specially designed and presented in this chapter.

3.1 Simulation Parameters and Modeling Objectives

All of the IGU evaluation performed in this thesis was conducted using Window5 (LBNL, 2003) and VISION (Ferguson, *et al.*, 1984). Both of these programs simulate IGUs by a one-dimensional energy transfer analysis that is similar to the evaluation method outlined in Chapter 2. All IGUs are evaluated under standard NFRC conditions, which include winter night-time conditions for U-value and summer day-time conditions for SHGC. The NFRC standard conditions are summarized in Table 3.1.1.

Table 3.1.1 NFRC standard simulation conditions in Window5 (LBNL, 2003)

Standard	Interior Air Temperature [°C]	Exterior Air Temperature [°C]	Solar Irradiation [W/m ²]	Exterior Convective Coefficient [W/m ² K]	Exterior Wind Speed [m/s]
NFRC 100-2001 Winter	21	-18	0	26	5.5
NFRC 100-2001 Summer	24	32	783	15	2.75

The objectives of the simulations for each section are listed below:

For glazing technologies:

- Investigate the mechanisms of to how different properties of each type of glazing component, such as low-E coatings, fill gases, and plastic films affect both the thermal (U-value) and solar performance (Visible Transmittance, VT, and Solar Heat Gain Coefficient, SHGC) of IGUs. Most of the simulations performed are for simple double-glazed IGUs.
- Indicate future areas of improvement for each of these glazing components.

For multi-layered IGUs:

- Investigate the combined effect of the different properties of glazing components on IGU thermal and solar performance. This analysis includes double-, triple-, quadruple-, and quintuple-glazed IGUs.
- Provide a survey of upper and lower performance thresholds of multi-layered IGU performance with the products that are currently available on the market
- Create and evaluate a set of high performance IGUs guided by the performance thresholds found in the IGU survey.

3.2 Evaluation of Current and Emerging Glazing Technologies

Over the past 40 years the performance of IGUs have steadily improved due to new and emerging technologies. In the past, advances in glazing construction led to the rise of the double-glazed IGU in the 1970s, while research into metallic coatings and natural convection in tall vertical cavities led to the development and commercialization of low

emissivity (low-E) coatings and exotic fill gases in the 1990s. Development continued in the late 1990s and early 2000s with the introduction of transparent plastic films as glazing layers in multi-layered IGUs, leading to the rise of high-performance, highly insulated triple-, quadruple-, and even quintuple-glazed IGUs that has a similar thickness and weight of a traditional double-glazed IGU. This section examines such technological advances in glazing materials.

3.2.1 Low-Emissivity Coatings and IGU Heat Transfer

The development of low-E coatings has been the single most significant innovation in improving the energy performance of IGUs. Low-E coatings work by reducing the long-wave infrared radiation (IR) exchange across the glazing cavity through increasing the long-wave reflectance of the glazing surface. Recall, from Figure 3.2.1, that radiation can either be absorbed, reflected, or transmitted once it strikes a surface, including glass.

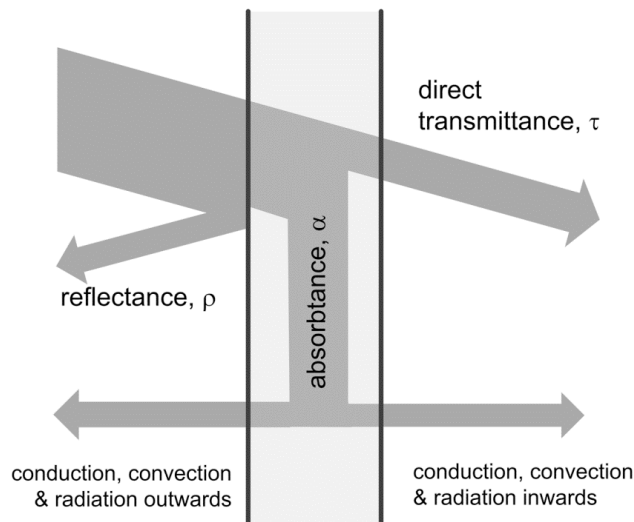


Figure 3.2.1 Reflectance, transmittance, and absorbance of glass (Straube and Burnett, 2005)

The absorbance, α , can be substituted for the emissivity, ϵ , according to Kirchoff's Law. Since most glazing materials are opaque to long-wave radiation, low-E coatings can only increase the reflectivity of the surface at this wavelength. This wavelength independence also allows for low-E coatings to be applied with little effect on the solar properties of the IGU (Wright, 1998).

The effect of reducing the overall heat flow through the IGU with low-E coatings is significant. A simple evaluation of heat transfer mechanisms of a conventional double-glazed air-filled IGU with clear glass ($\epsilon = 0.84$) using VISION (Ferguson *et al.*, 1984) shows that radiation accounts for approximately 61% of the heat flow across the cavity. From this analysis, it appears that the percentage increases with heavier fill gases and can be as high as 73% for xenon. Figure 3.2.2 illustrates the results of this analysis by comparing the radiative and convective heat flux that occurs through a double-glazed air-filled IGU for both clear glass ($\epsilon = 0.84$) and low-E coated glass ($\epsilon = 0.10$).

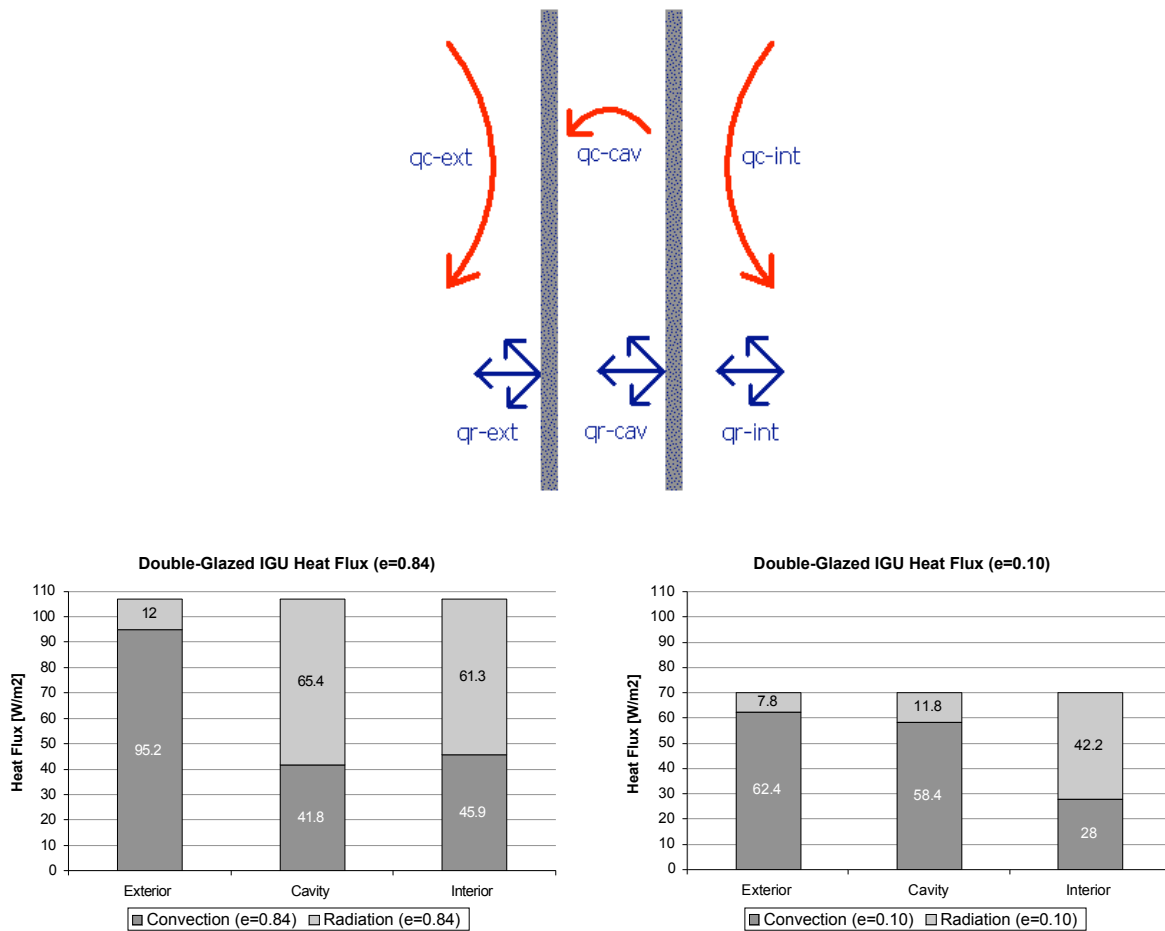


Figure 3.2.2 Heat flux across a double-glazed air filled IGU (results determined by VISION (Ferguson *et al.*, 1984))

From Figure 3.2.2, the radiative heat flux can be reduced by approximately 82% just from reducing the emissivity from 0.84 to 0.1. This significant reduction in radiative heat

flux in turn reduces the total heat flux across the IGU system, thus improving the thermal resistance of the glazing unit.

To reduce the long-wave surface emissivity, low-E coatings are composed of metals such as copper, silver, and gold (Smith *et al.*, 1986). These metallic coatings are applied in such thin layers such that they are transparent to short-wave radiation yet still reflect the majority of long-wave radiation. There are two main methods of preparing the coatings, pyrolytic 'hard coats' and multi-layer sputtered 'soft coats'. Pyrolytic coatings are applied through a process called spray pyrolysis, in which a solution containing metal chloride or acetylacetonate is directly sprayed as an aerosol onto a heated sheet of glass. The aerosol vaporizes before reaching the glass and the metallic compounds are deposited as vapours on the surface. The resulting metallic oxide that forms on the surface of the hot glass becomes the low-E coating (Hollands *et al.*, 2001). These coatings typically can reach emissivities as low as 0.15 (Hollands *et al.*, 2001). Alternatively, multi-layered sputtered low-E coatings are applied inside a vacuum chamber with an inert gas at an approximate pressure of 1 Pa. The metallic compounds that make up the coating are deposited through sputter cathodes, which uses a self-sustained plasma to dislodge atoms from a plate that is made of the raw coating material. The atoms are then transferred from the metallic plate onto the glass at very high speeds and sticks to the glass. Multiple layers can be applied by passing the glass under several cathodes. Because of this process, 'soft coat' low-E coatings hold several advantages over 'hard coats'. One of which is 'soft coat' coatings can be applied to dielectric thin films since the substrate does not have to be heated. 'Soft coats' generally can achieve lower emissivities than 'hard coats' since the coating can be applied in multiple layers. The emissivities of 'soft coat' low-E coatings are typically around 0.1 or less (Hollands *et al.*, 2001). One significant disadvantage with a 'soft coat' is its durability, particularly its resistance to scratches. 'Hard coats' are generally tougher than 'soft coats' and can even be applied to the exterior-facing surfaces of IGUs, while 'soft coats' must be placed in a benign environment such as the interior cavity space in between glazing layers. Figure 3.2.3 shows schematically the application process for both 'hard coat' and 'soft coat' low-E coatings.

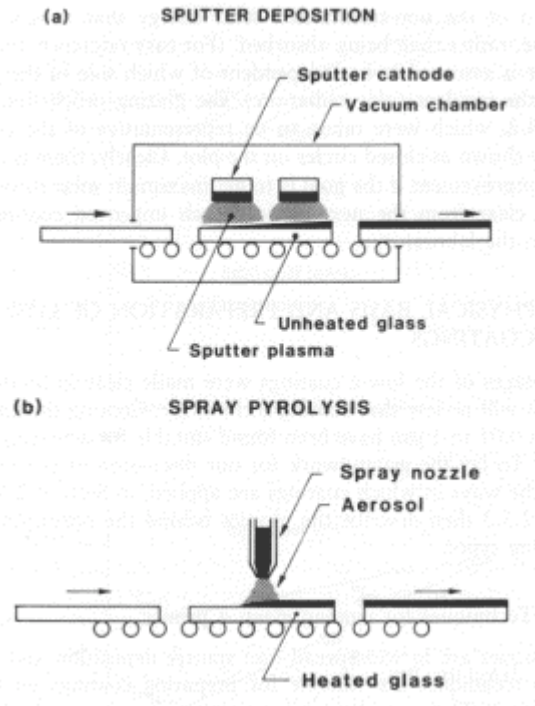


Figure 3.2.3 Application process of 'hard' and 'soft' coat low-E coatings (Hollands *et al.*, 2001)

3.2.2 Low-Emissivity Coatings and Solar Transmittance and Solar Heat Gain

While low-E coatings are transparent to short wave radiation, the solar transmittance of the glazing with low-E coatings are reduced, particularly as the long-wave emissivity decreases. Table 3.2.1 shows the optical properties for both clear and low-E coated glass. The values presented are from the Window5 database (LBNL, 2003), for a 5.613 mm thick glass sheet manufactured by Guardian Industries.

Table 3.2.1 Optical properties for clear and low-E coated glass (LBNL, 2003)

Type	ϵ	τ_{sol}	ρ_{sol}	α_{sol}	τ_{vis}	ρ_{vis}
Float Glass	0.84	0.804	0.073	0.123	0.892	0.082
Pyrolytic Low-E	0.168	0.506	0.191	0.303	0.738	0.051
Sputter Low-E	0.036	0.36	0.465	0.175	0.757	0.053

By applying a multi-layer 'soft coat' low-E coating on clear glass ($\epsilon = 0.036$) the incident solar transmittance is reduced by approximately 55%, similarly applying a 'hard coat'

low-E coating ($\epsilon = 0.168$) on clear glass reduces the solar transmission by 37%. It is important to note that while the solar transmittance is significantly reduced with low-E coatings, the visible transmittance is reduced as well but to a lesser degree. The visible transmittance only decreases by 15% with a multi-layer 'soft coat' low-E coating and 17% with a 'hard coat' low-E coating. Although the reduction in visible transmission for each layer is relatively small, the overall solar and visible transmittance for a multi-layered IGU with several low-E coatings can be significantly reduced. For this reason IGUs with multiple low-E coatings tend to appear darker than clear double-glazed IGUs.

In addition to reducing both the solar and visible transmittance of IGUs, low-E coatings can also reduce the solar heat gain. Figure 3.2.4, illustrates the changes in SHGC and visible transmittance, VT, for a double-glazed IGUs constructed out of the same glazing as the ones listed in Table 3.2.1 as evaluated in Window5 (LBNL, 2003). All IGUs have a 12.7 mm gap (1/2 in.) air gap between glazings.

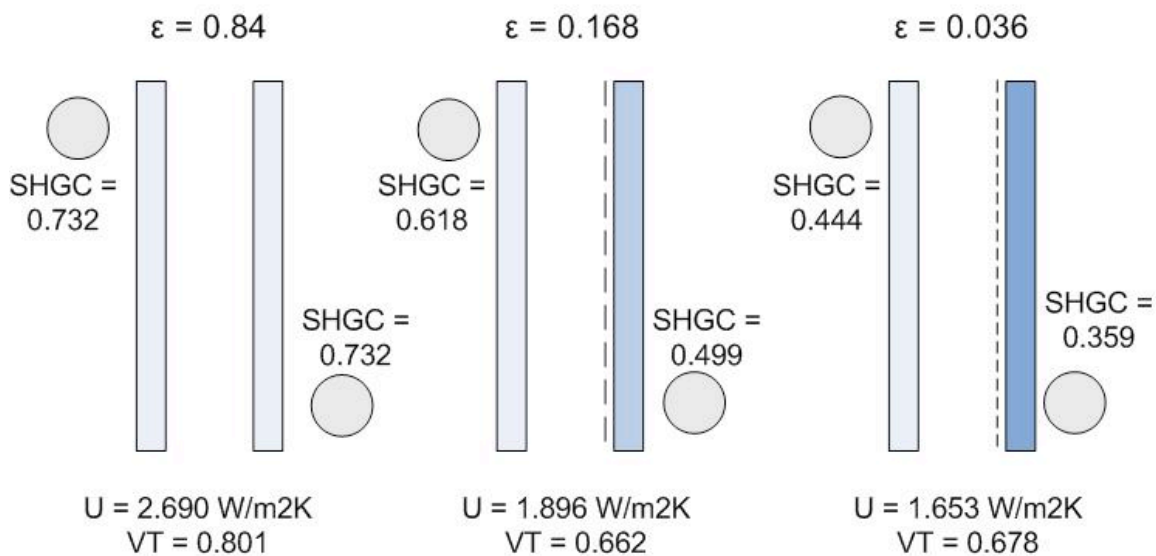


Figure 3.2.4 Resulting visible transmittance and solar heat gain of double-glazed IGUs with and without low-E coatings as determined by Window5 (LBNL, 2003)

Since the SHGC is composed of both the direct solar transmittance through the IGU and inward heat flow fraction from absorbed solar radiation and the environment, the SHGC is dependent on both the emissivity and location of the coating. As shown in Figure

3.2.4, glazings with lower emissivities, generally have lower solar transmittances, which in turn reduces the solar transmittance component of the SHGC. The location of the coating is also important. From Figure 3.2.4, IGUs with a low-E coating on the exterior side of the cavity will have a lower SHGC than IGUs with a low-E coating on the opposite side of the cavity. Because low-E coatings increase the solar reflectance, ρ_{sol} , on both surfaces of the glazing, the reflected solar radiation may be trapped inside the IGU if the coating is placed on the interior side of the cavity. As illustrated in Figure 3.2.5, some of the reflected solar radiation will be absorbed by the exterior glazing, which re-emits a portion of this radiation as infrared radiation across the cavity and through the IGU. By placing the low-E coating on the exterior side of the cavity, most of the solar radiation is reflected to the environment and is not trapped inside the glazing unit.

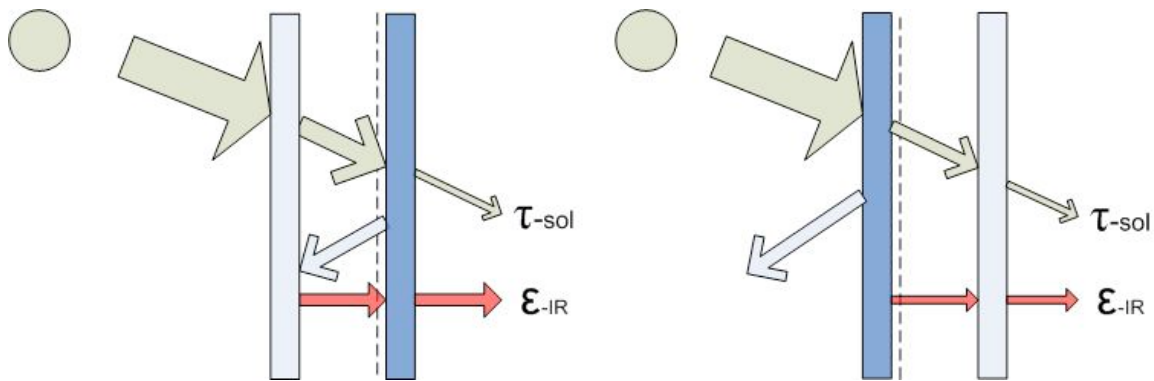


Figure 3.2.5 Mechanics of SHGC and low-E coating location (adapted from LBNL, 2003)

This feature is noteworthy because the increased solar reflectance from low-E coatings can result in very high temperatures inside the cavity space(s) of multi-layered IGUs depending on the environmental conditions and location of the low-E coatings. Since the heat from the absorbed solar radiation can be trapped inside the IGU the temperatures can easily rise, particularly in the centre-glass region. This can pose potential problems for durability, particularly for IGUs with low-E coated plastic films, and problems with temperature gradients across centre-glass and edge regions, which are typically cooler.

3.2.3 Future Improvements to Low-Emissivity Coatings

Although low-E coatings have revolutionized the IGU industry through significantly improving its thermal performance, there are still areas of development that can further improve IGUs. Most of these improvements include increasing the solar transmittance while lowering or maintaining a low long-wave emissivity of the coating. Figure 3.2.6 demonstrates how the winter night-time centre-glass U-value changes with the emissivity of surface 3 (cavity facing surface of the inner glazing) for a double-glazed IGU with various fill gases at 12.7 mm (1/2 in.) spacing. This plot is based on figure from Hollands *et al.* (2001), which showed similar trends for a double-glazed air-filled and argon-filled IGU. All four curves in the figure were determined by simulations from VISION (Ferguson *et al.*, 1984).

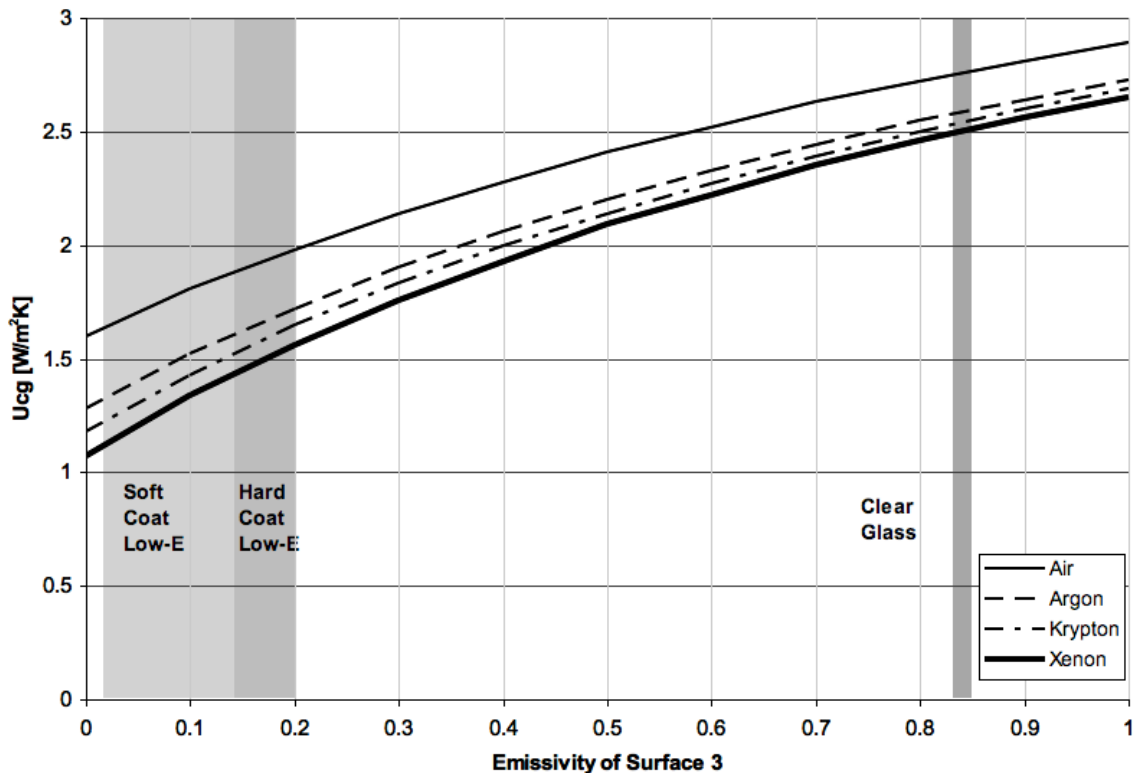


Figure 3.2.6 Winter night-time centre-glass U-value dependence on emissivity of surface 3 of an air filled double-glazed IGU as determined by using VISION (Ferguson *et al.*, 1984) (adapted from Hollands *et al.*, 2001)

The figure shows that reducing the emissivity by half from 0.8 (clear glass) to 0.4 (modest coating) will reduce the U-value by approximately 16%, but reducing the

emissivity by the same factor from 0.2 to 0.1 will only reduce the U-value by less than 9% for an air filled cavity. This shows any additional gains in thermal resistance increases at a diminishing rate with lower emissivities. Since most current coatings have relatively low emissivities, it is clear that future improvements to low-E coatings should be focused on improving the optical properties of these coatings, not lowering their emissivities.

One of the observed problems with low-E coatings is its effect on reducing solar transmission of the glazing. This poses two potential problems:

- 1. Reduced SHGC**

As the surface emissivity is reduced the solar transmission also decreases which in turn decreases the SHGC since τ_{sol} makes up a significant component of the SHGC. Buildings that require lower emissivities are typically in heating-dominated climates, which can often benefit from a higher SHGC through passive heating.

- 2. Increased glazing temperatures**

As the solar transmission decreases, the solar reflectance and absorptance increases. Depending on the ratio of reflectance and absorptance the temperature of the glazing layer can substantially increase particularly if the solar absorptance is high. This can lead to potential problems with premature failure of the glazing due to thermal stress from daily temperature swings.

Figure 3.2.7 compares optical performance of some glazings with relatively low emissivity low-E coatings. The graph plots the solar transmission of the coated glazing against the centre-glass SHGC for the same IGU as in Figure 3.2.6 but for an air filled gap. The conditions have been switched to summer day-time in order to get a representative SHGC. This graph is also based on a similar plot from Hollands *et al.* (2001), however, the optical performance of the coatings have been updated to reflect

that of the coatings that are currently available. The low-E coatings are plotted along with four lines at various values of β , which is fraction of non-transmitted solar energy that is reflected by the coating and can be calculated as:

$$\beta = \frac{\rho}{(1 - \tau)}$$

Equation 3.2.1

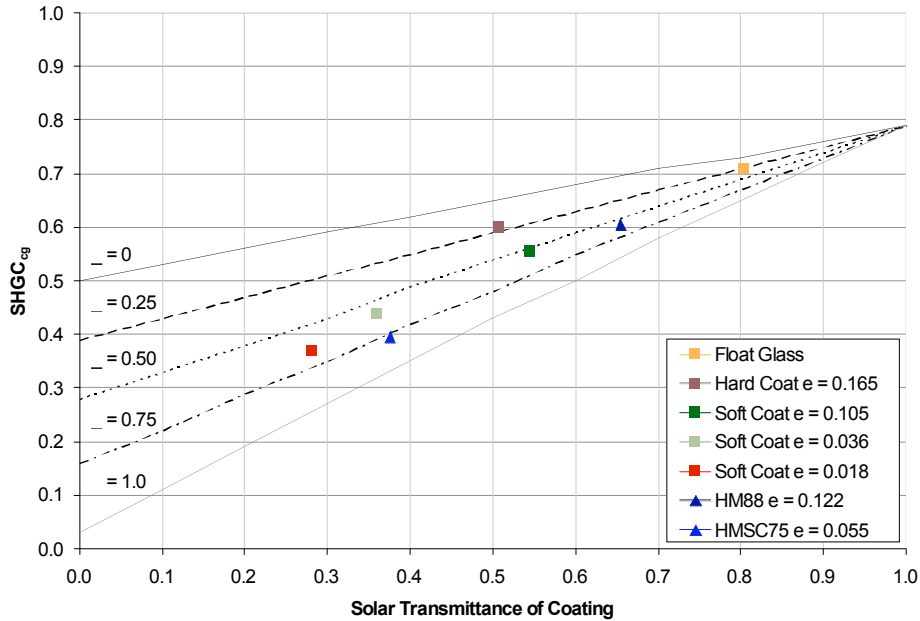


Figure 3.2.7 SHGC and solar transmittance of current low-E coatings (adapted from Hollands et al, 2001)

Glazings that lie closer to lines with lower β have a higher absorptance than glazings with a lower β . From Figure 3.2.7, most low emissivity low-E coatings, such as soft coats, tend to have lower solar transmission and SHGC than higher emissivity coatings. Most low-E coatings are very far from having a high SHGC; consequently, improvements to low-E coatings should strive for higher solar transmissions with a reasonably high β value. One potential technological solution is to use plastic films, which are shown on Figure 3.2.7 as triangles. Relative to glass, plastic films tend to have a higher solar transmission due to its very small thickness. As a result, plastic films can have relatively low emissivity coatings while still providing high solar transmission. Plastic films also absorb less solar radiation than glass, thus temperatures do not build as quickly with these

films as glass. This makes plastic films suitable for multi-layered IGUs since multiple low-E coatings can be applied while still maintaining a reasonable SHGC.

3.2.4 Substitute Fill Gases and IGU Heat Transfer

While low-E coatings significantly reduce the radiation exchange across the glazing cavity, the next dominant mode of heat transfer is natural convection. To reduce the convective heat transfer across the cavity in between glazing layers one could:

1. Evacuate or reduce the pressure of the cavity
2. Replace the air inside the cavity with another gas at approximately atmospheric pressure that reduces the convective heat transfer

Of the two options, evacuating or reducing the pressure of the cavity poses significant technical challenges. The seals around the cavity must be reliably air tight to withstand the differences in atmospheric pressure and the glazing layers must be mechanically supported throughout the cavity with pillars in order to avoid bowing from the unbalanced atmospheric pressure (Eames, 2008). However, if these challenges can be overcome, vacuum insulated glazings (VIGs) can offer highly insulated IGUs that are comparable to multi-layered IGUs yet at less than a quarter of the thickness and with higher SHGCs and VTs since they do not require multiple layers.

The alternative option to evacuating or reducing the pressure of the cavity is to replace the air with another gas that reduces the convective heat transfer across the cavity. This also poses some technical challenges, in particular to the seals, however, they are considered relatively minor compared to VIGs and have been mostly resolved by IGU manufacturers. Since the IGU must be perfectly sealed to trap the replacement gas, the pressure in the cavity can vary due to variations in temperatures. For most IGUs the change in temperature can be in order of 0.1 ATM over the seasons. Pressures variations at this magnitude can easily break the glass or destroy the seal if not for the flex of the glass panes in response to the pressure difference. As the glass flexes, the volume of the cavity increases large enough to reduce the overall pressure exerted on the glazings and

seals to a tolerable level. However, for IGUs with cavity spacing that are greater than 25 mm, the change in volume from the flexing glazings can be too small to reduce the pressure exerted on the glazing and the IGU can fail (Hollands *et al.*, 2001).

To reduce the convective heat transfer across the cavity, the candidate gas must have a lower h_{cav} , as calculated by Equation 2.1.8, in Chapter 2, which is determined by numerous parameters. It is important to note that while natural convection is the dominant mode of heat transfer in the cavity, gaseous conduction is the next most significant mode. Therefore, it is important to consider the thermal conductivity, k , of the candidate gas. Gases that have a larger molecule and molar mass typically have a lower thermal conductivity (Bird *et al.*, 1960). However, these gases also have greater densities, which enhances the buoyant effect of the gas (ie. raises the Rayleigh number) for natural convection. Therefore, while a larger molecule minimizes gaseous conduction, a smaller molecule is often used to minimize convection and the overall heat transfer across the cavity. Additional factors that must be considered when choosing a gas to reduce the h_{cav} , are its viscosity (viscous forces suppress fluid motion) and specific heat (heat is transferred by mass flow).

When all these factors are considered, it is evident that the desired molecule should be as simple as possible and as massive as possible, which makes mono-atomic gases such as helium, neon, argon, krypton, and xenon, suitable. Lighter gases such as helium and neon are too light to offer any advantages over air, yet heavier gases, such as argon, krypton, and xenon can reduce the convective heat transfer significantly over air and are preferred. Figure 3.2.8 shows the total heat transfer within the cavity, h_{cav} , and U-value of a double glazed IGU with various fill gases for different cavity widths under winter conditions, with fixed interior and exterior heat transfer coefficients and a low-E coating of 0.083 (Hollands *et al.*, 2001).

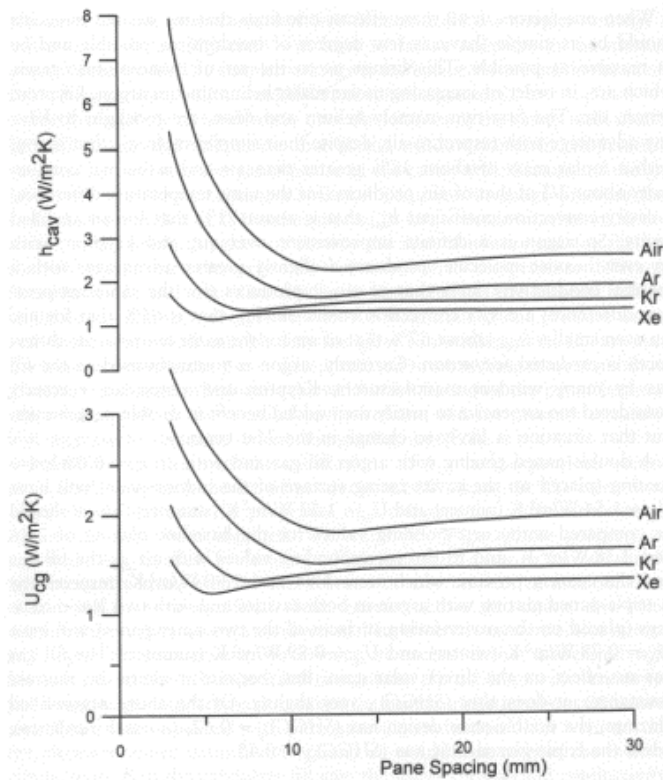


Figure 3.2.8 Cavity heat transfer h_{cav} and U_{cg} at varying cavity spacing for various fill gases in a double-glazed low-e coated IGU at winter night-time conditions (Hollands *et al.*, 2001)

It is clear that heavier fill gases offer a significant advantage over air, as all three gases decrease both h_{cav} and U_{cg} . While h_{cav} and U_{cg} decreases with gases with increasing molecular mass, the improvements are relatively small, as shown in

Figure 3.2.8. A cavity filled with argon has a h_{cav} that is approximately 71% that of air, while the same cavity with krypton has a h_{cav} approximately 65% of air, and a cavity with xenon has a h_{cav} that is about 57% of air (Hollands *et al.*, 2001). Currently argon is by far the most commonly used fill gas since it offers the most significant reduction in U_{cg} at a very reasonable price. Heavier gases such as krypton are becoming more popular for energy-efficient buildings in particular, while xenon is still considered to be too expensive to be economically feasible in the building industry. Table 3.2.2 lists the approximate price of each fill gas; the price of these gases is mainly driven by their abundance and ease of production.

Table 3.2.2 Approximate price of fill gases (ChemiCool, 2009)

Gas	Approximate Price [\$US /100g]	Price at Optimum Width for Double- glazed IGU [\$US / m ²]
Air	\$0.00	\$0.00
Argon	\$0.50	\$0.20
Krypton	\$33.00	\$23.28
Xenon	\$120.00	\$117.98

3.2.5 Optimal Cavity Spacing for Minimizing IGU Cavity Heat Transfer

Since both gaseous conduction and natural convection are two modes of heat transfer that must be balanced within the IGU cavity, the overall heat transfer across the cavity, h_{cav} , varies according to the cavity width. This means that there is an optimum cavity spacing for each gas which minimizes the overall heat transfer across the glazing cavity.

Figure 3.2.8, illustrates the relationships between h_{cav} and U_{cg} and the cavity width (Hollands *et al.*, 2001). For all gases, the h_{cav} and U_{cg} drops significantly as the cavity width grows since the increased cavity width decreases the effectiveness of heat transfer through gases conduction. The curve continues to decline with increasing cavity width to a minimum and increases again as natural convection takes over as the dominant mode of heat transfer. The minimum for each curve represents the optimal cavity spacing that provides the greatest thermal resistance for the IGU. This minimum width varies with different fill gases since each gas has different properties in thermal conductivity, molecular sizes, viscosity, and specific heat.

In addition to different gas properties, the optimum spacing also varies depending on the IGU. Since natural convection is highly sensitive to temperature, the optimum cavity gap size will change depending on the number of glazing layers, the location of the low-E coatings and both the exterior and interior boundary conditions, including the air temperature and wind speed. Consequently, there could potentially be a unique optimal gap at different temperatures. However there is only one accepted optimal cavity width, since most IGUs are rated against standard winter night time conditions set by the NFRC

which are 21°C interior air temperature, -18°C exterior air temperature, and an exterior convective coefficient of 26 W/m²K, with no solar radiation. The optimal gap spacing and its effect on IGU indices will be discussed in later sections for different configurations of multi-layered IGUs.

3.2.6 Plastic Films and IGU Performance

Another significant innovation in the development of high performance IGUs is application of suspended thin plastic films in multi-layered IGUs. Suspended films are typically placed in between two sheets of glass as the inner layers of a triple-, quadruple-, or quintuple-layered IGU. These films serve as vertical convection dividers to allow for more gas to be used for insulating purposes without creating large convection loops and additional surfaces for low-E coatings. These features can provide significant improvements to the overall thermal performance of the IGU.

The films are well protected by the glass inside the glazing cavity from scratching, mechanical abuse, corrosion, weathering, and visual distortions from wind pressure. They are suspended along the perimeter at the edge spacer and are heat shrunk to ensure they remain flat under all conditions. These films are typically made of polyester and are specially treated to resist UV degradation (Carmody, 2007).

Plastic films hold many advantages to glass in multi-layered IGU construction, particularly in weight. The plastic films used in multi-layered IGUs are less than 1 mm thick such as Southwall Technologies' HM88 (LBNL, 2003), and weigh significantly less than glass. Weight has been a drawback that limited the popularity of multi-layered glass IGUs, since those glazing units were very heavy and bulky from the thicker glass; making it difficult to handle and mount. Another advantage of plastic films is its high solar and visible transmittance compared to glass. Since the films are significantly thinner, both the visible and solar transmission is higher; this leads to higher visible transmittance and solar heat gain for multi-layered IGUs using suspended plastic films. Like glass, low-E coatings can be applied to plastic films. However, since the films cannot tolerate high temperatures, soft-coat low-E coatings are applied, which generally

have lower emissivities and further decreases the U-value of the IGU. In some applications, the low-E coating on the plastic film is low enough that low-E coatings are not required on the glass surface.

3.3 Evaluation of Multi-layered IGUs

With the demand for high performance IGUs rising, multi-layered IGUs are gaining popularity within the building industry. As seen in the previous section, advances in the properties of each of the glazing components can significantly alter the performance of a simple double-glazed IGU. In this section, the combined effect of various advances in glazing technologies are examined for different types of multi-layered IGUs, specifically, double-, triple-, quad-, and quint-glazed IGUs.

3.3.1 U-value of Multi-layered IGUs

One of the major advantages in adding multiple layers to an IGU is the significant reduction in U-values they offer. The reduction to U-values can be significant due to two major effects:

- 1. Providing additional surfaces for low-E coatings**

Since the dominant mode of heat transfer across glazing surfaces is by radiation, multiple low-E coatings can significantly reduce the centre-glass U-value of the IGU.

- 2. Providing additional cavity spaces**

The second most dominant mode of heat transfer across IGUs is convection across the glazing layer cavities. By using multiple layers, the overall convective heat transfer between inner most and outer most glazing is significantly reduced. The heat transfer rate between the glass panes can be reduced by the large gas filled cavity, while the intermediate glazing layers limits the heat transfer from the convective loop(s).

From simulations performed in Window5 (LBNL, 2003), these two effects alone can reduce the centre-glass U-value by approximately 84% when comparing a double-glazed

clear IGU to a quintuple-glazed low-E unit. While this reduction in U-value is significant, additional gains in thermal resistance can be achieved by choosing the appropriate fill gas. Additional simulations in Window5 (LBNL, 2003) have shown that the appropriate fill gas can reduce the U_{cg} by another 6% for a quintuple-glazed low-E xenon-filled IGU, resulting in an overall reduction in U_{cg} by approximately 90% when compared to a double-glazed clear air-filled IGU. Choosing the appropriate fill gas in multi-layered IGUs becomes very important beyond double-glazed systems. Recall from previous sections, each type of fill gas has a unique characteristic cavity width, L , that minimizes U_{cg} . This optimum cavity width decreases with heavier fill gases, thus heavier fill gases have the added benefit of not only decreasing the centre-glass U-value, but also reduces the additional overall thickness, t . The optimal cavity width, L , is not only unique to each type of fill gas. Simulations in Window5 (LBNL, 2003) show that the optimum cavity width, L , changes with the number of layers in the IGU and the emissivity of the glazed surfaces. The resulting relationship between U_{cg} and cavity width, L for double-, triple-, quad-, and quint-glazed clear and Low-E IGUs are plotted in Figure 3.3.1 to Figure 3.3.4. The plots are generated from IGU centre-glass simulations in Window5 (LBNL, 2003) using glazing layers found within the Window5 library, which are listed in Table 3.3.1.

Table 3.3.1 Optical properties of glazing layers used in Window5 simulations to generate results (LBNL, 2003)

Materials	Trade Name	Thickness [mm]	τ_{sol}	ρ_{sol1}	ρ_{sol2}	τ_{vis}	ρ_{vis1}	ρ_{vis2}	τ_{ir}	ϵ_1	ϵ_2
Clear Glass	Generic Clear Glass	5.715	0.771	0.07	0.07	0.884	0.08	0.08	0	0.84	0.84
Low-E Glass	PPG - Solarban 70XL on Starphire	5.664	0.281	0.513	0.562	0.72	0.077	0.059	0	0.841	0.018
Single Coat Plastic Film	Southwall - Heat Mirror 88 Suspended Film	0.076	0.654	0.231	0.212	0.878	0.061	0.065	0	0.122	0.755

The IGUs simulated in Figure 3.3.1 to Figure 3.3.4 are representative of the best passive solar IGU that is currently available in the market, which minimizes U_{cg} while maximizing the SHGC.

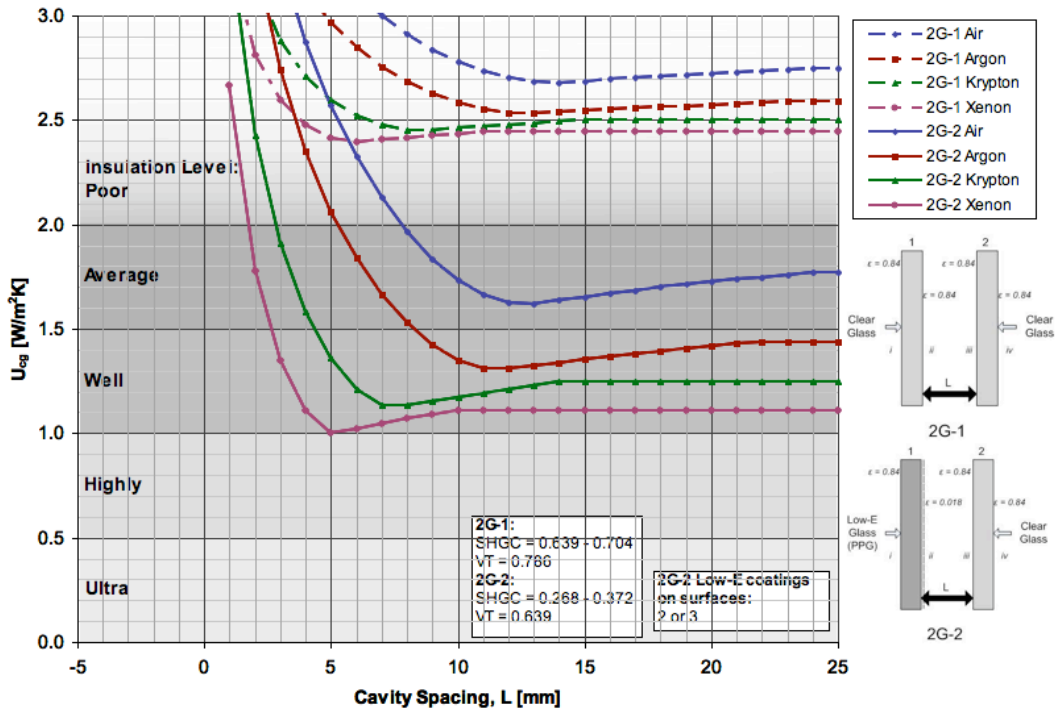


Figure 3.3.1 Relationship between cavity space and U_{cg} for double-glazed IGUs

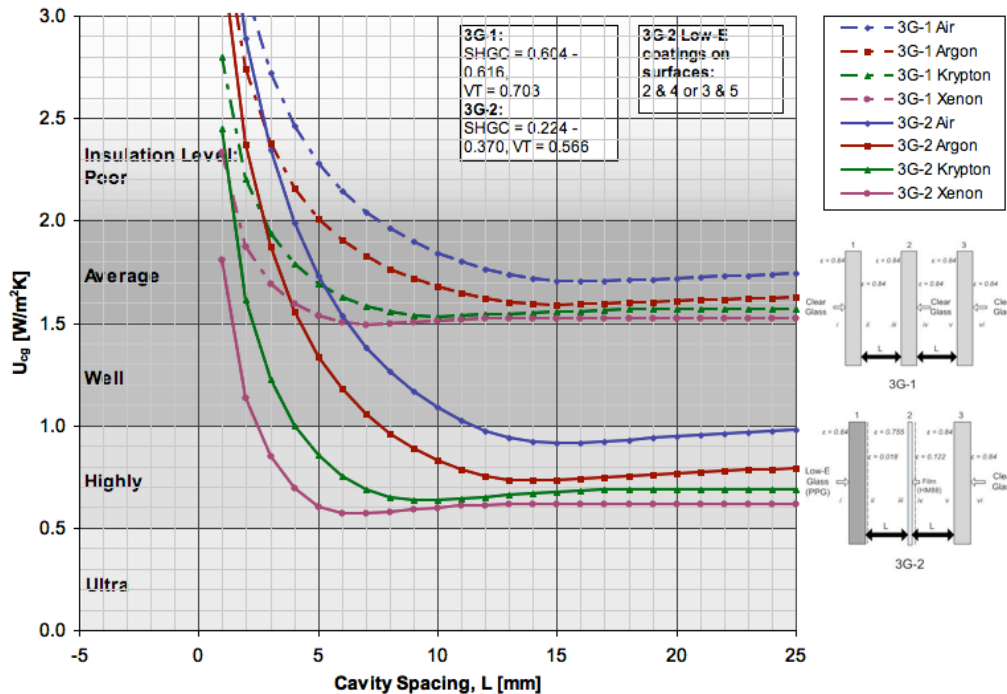


Figure 3.3.2 Relationship between cavity space and U_{cg} for triple-glazed IGUs

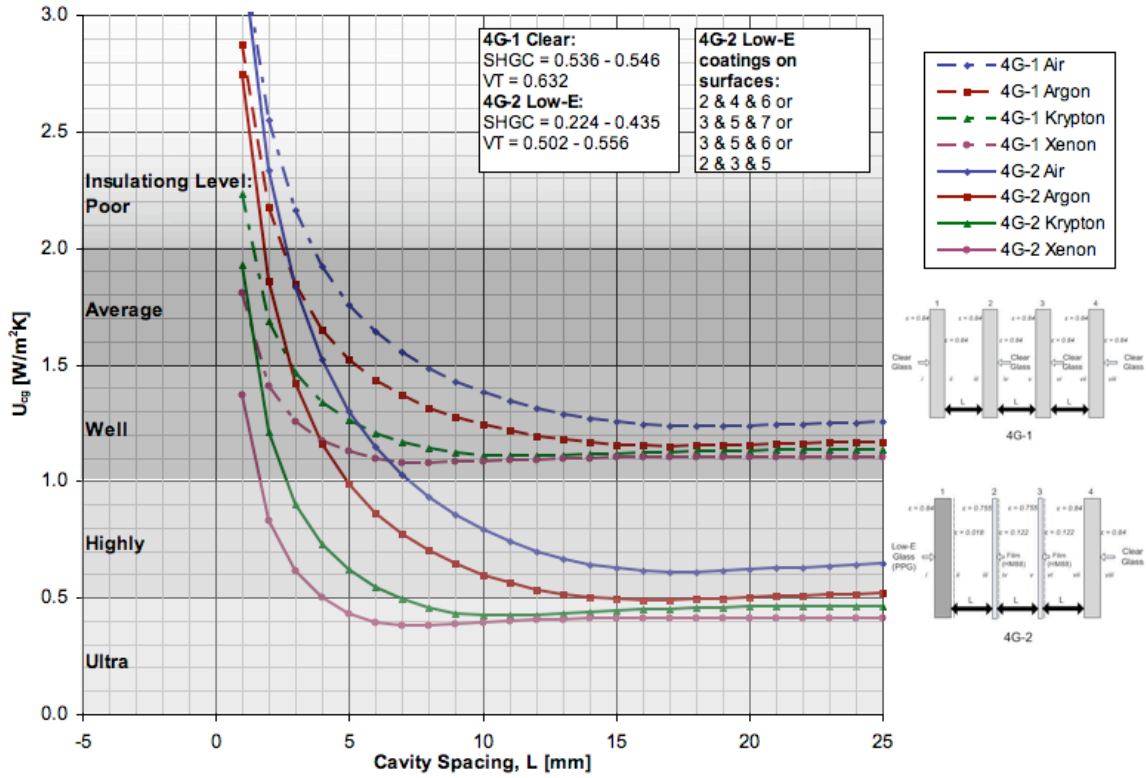


Figure 3.3.3 Relationship between cavity space and U_{cg} for quad-glazed IGUs

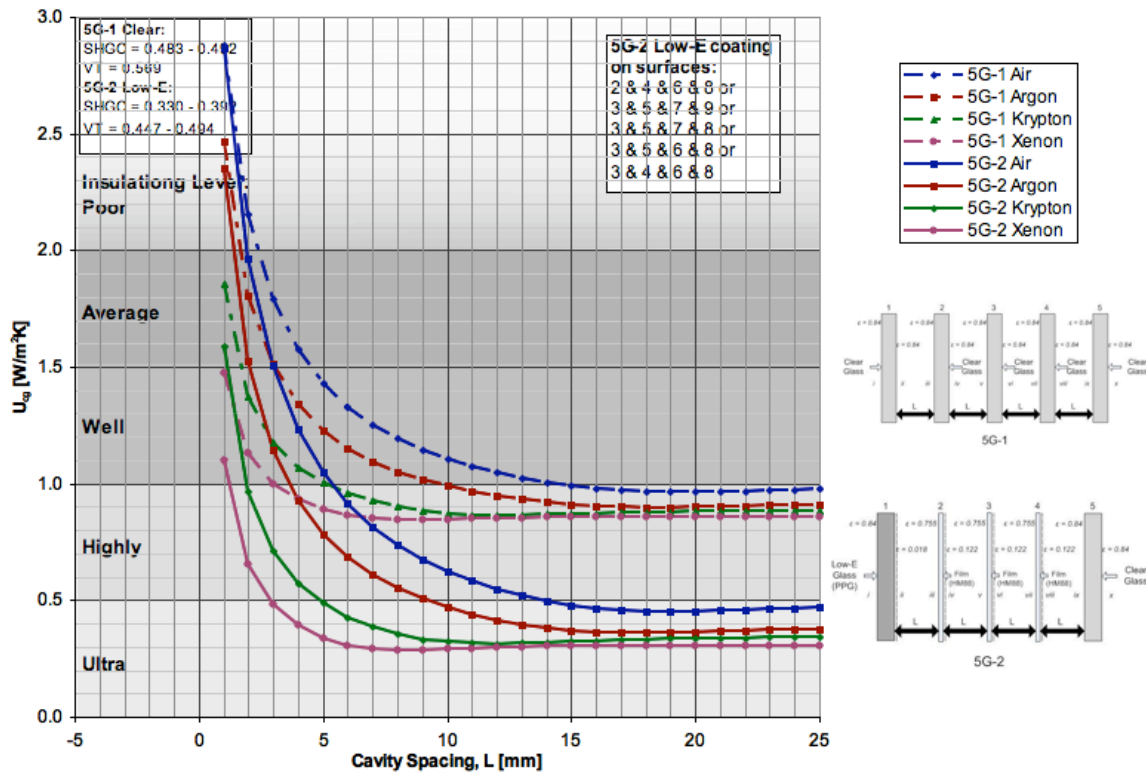


Figure 3.3.4 Relationship between cavity space and U_{cg} for quint-glazed IGUs

Despite the differences in U_{cg} and cavity widths, all of the graphs share similar trends. All U -values start off relatively high and decrease sharply over the first 5 mm to 10 mm of cavity width to reach a minimum before becoming asymptotic to some value at greater cavity widths. This occurs because at smaller cavity widths, heat is primarily transferred via gaseous conduction. As the cavity width increases, more space is available for bulk fluid motion to develop for natural convection to occur. Over large cavity widths, convective heat transfer dominates over conduction. The minimum or ‘dip’ in the U_{cg} -cavity width curve represents the point where neither enough space is available for natural convection to occur and the cavity is wide enough to minimize heat transfer across the cavity through conduction.

The optimal cavity width for minimizing heat transfer is primarily dependent on the type of fill gases because it influences natural convection across the glazing layers. However, since the convective heat transfer is heavily dependent on the surface temperature of the glazing, any changes that affect the overall heat transfer of the IGU system and cause changes in glazing surface temperatures, such as the glazing surface emissivity, can alter natural convection in the cavity and thus the optimal width. Consequently, the optimal gap width changes with not only the glazing surface emissivity but also with environmental conditions, including the interior and exterior air temperature, the amount of incoming solar radiation, and the interior and exterior convective heat transfer depending on windy or calm conditions. This is shown in all of the figures, as the optimal cavity width is very different for both the clear IGU and low-E IGU. In fact, the ‘dips’ in the low-E U_{cg} -cavity width curves are much more pronounced than for the clear IGUs. Therefore, even under standard NFRC rating conditions the optimal cavity width is specific to the optical properties of the glazing layers and fill gas and can vary depending on the surface IR emissivity. However, the variation is very small, thus the optimal cavity widths from Figure 3.3.1 to Figure 3.3.4 are within similar range of most IGUs.

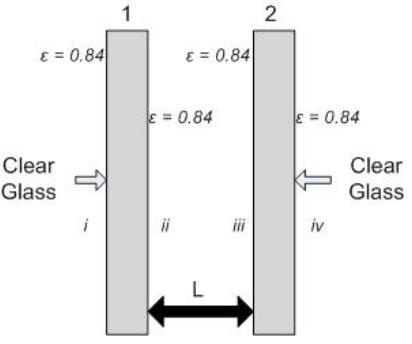
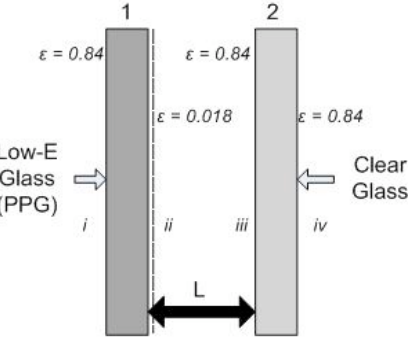
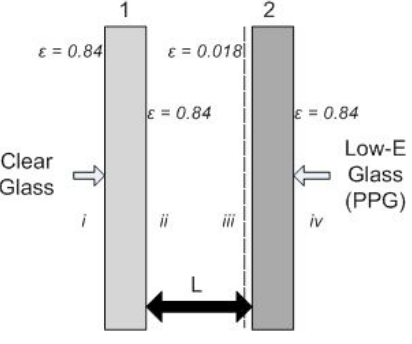
Several trends can be noted from Figure 3.3.1 to Figure 3.3.4. The optimal gap widths and U_{cg} decrease with heavier fill gases. This is mainly due to the thermal conductivity

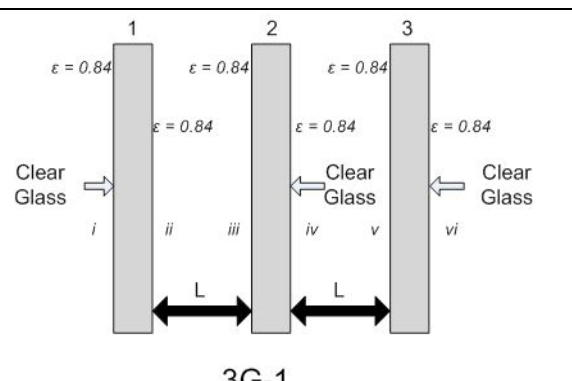
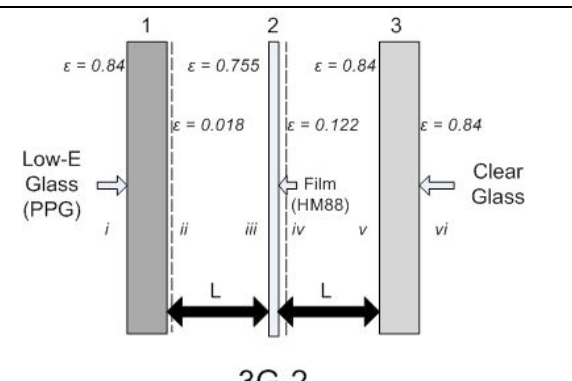
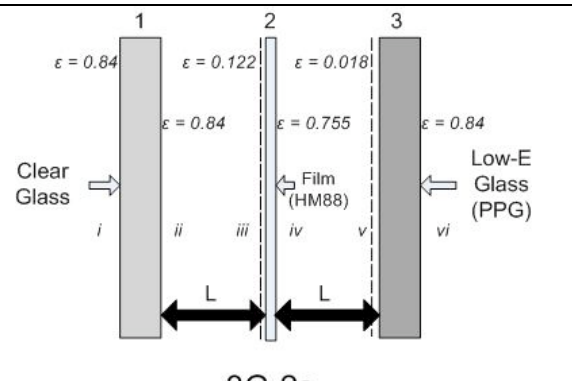
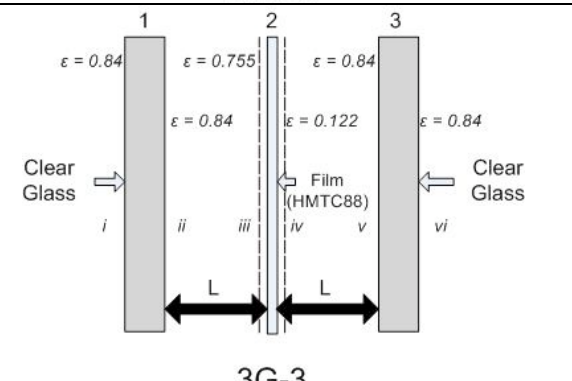
and viscosity of the gas. Heavier gases tend to have lower thermal conductivities and are more viscous which tend to develop natural convective flows at smaller channel widths.

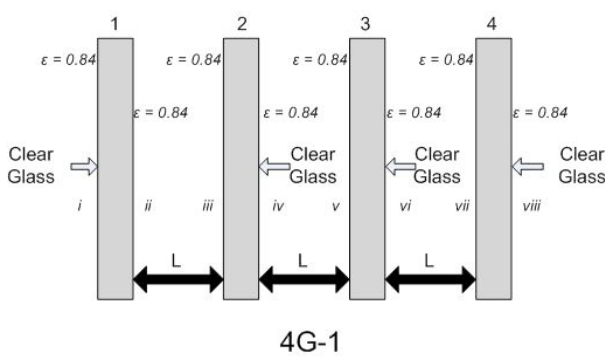
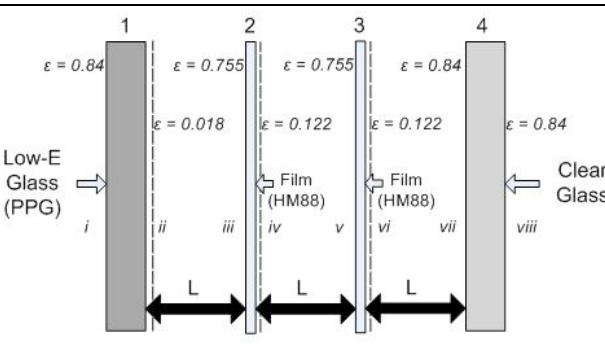
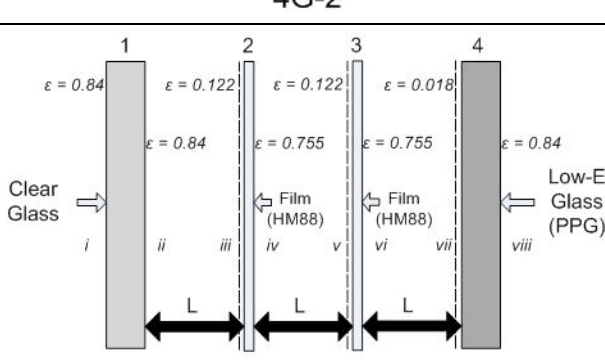
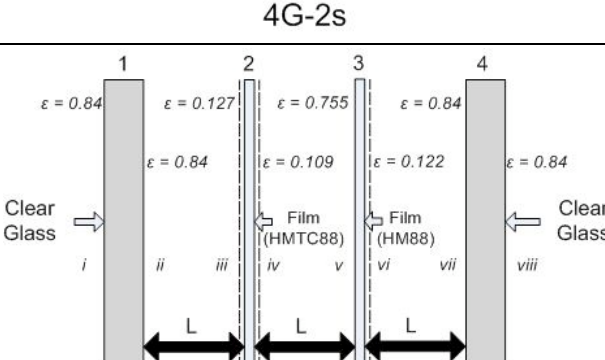
- The U_{cg} and optimal gap width are reduced just by decreasing the surface IR emissivity of the glass from 0.84 to 0.018 on either of the cavity facing surfaces. This is because reducing the surface emissivity significantly reduces the radiation heat flux across the IGU, which is responsible for a significant amount of the overall heat flow. The low-E coatings also alter the temperature of the glazing surface since the amount of thermal radiation that it can absorb and emit is significantly reduced. This change in surface temperature alters the cavity temperature and the natural convection across the cavity.
- The cavity width, L , decreases with heavier gases. Since heavier gases are more viscous, the optimal cavity width is usually smaller than for lighter gases. This is very beneficial to multi-layered IGUs where overall thickness is of a concern.

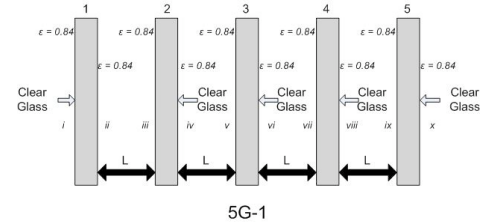
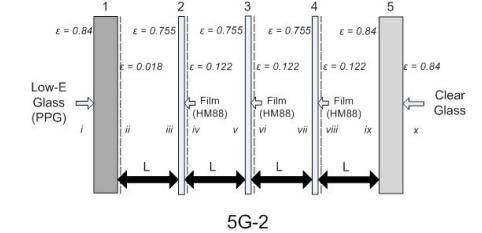
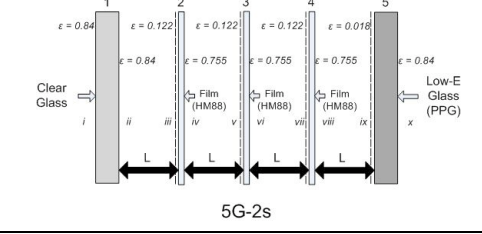
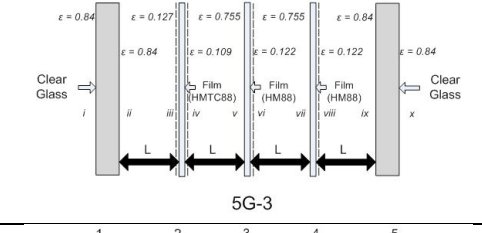
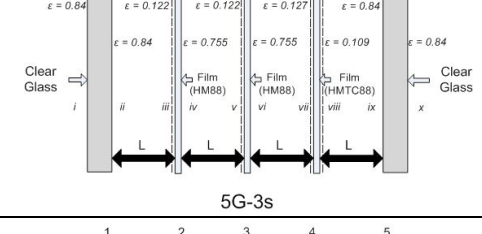
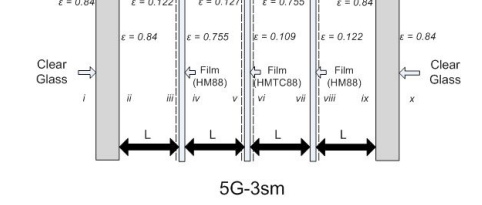
To illustrate the variations in IGU design and thermal performance, the thermal and optical properties of a set of IGUs evaluated in Window5 (LBNL, 2003) as part of this thesis are listed in Table 3.3.2 along with the optimum cavity widths for thermal performance and overall IGU thickness.

Table 3.3.2 Resulting performance indices of investigated high performance IGUs
(results generated from Window5 (LBNL, 2003) simulations)

IGU	Fill Gas	U_{cg} [W/m ² K]	SHGC	VT	Overall t [mm]	Cavity L [mm]
 <p>2G-1</p>	Air	2.680	0.702	0.786	25.1	13.6
	Argon	2.531	0.702	0.786	24.1	12.6
	Krypton	2.449	0.703	0.786	19.7	8.2
	Xenon	2.395	0.703	0.786	17.2	5.7
 <p>2G-2</p>	Air	1.617	0.275	0.639	24.0	12.5
	Argon	1.305	0.272	0.639	22.9	11.4
	Krypton	1.125	0.271	0.639	18.9	7.4
	Xenon	1.000	0.270	0.639	16.7	5.2
 <p>2G-2s</p>	Air	1.618	0.369	0.639	23.9	12.4
	Argon	1.305	0.370	0.639	22.9	11.4
	Krypton	1.125	0.371	0.639	18.9	7.4
	Xenon	1.000	0.371	0.639	16.7	5.2

IGU	Fill Gas	U_{cg} [W/m ² K]	SHGC	VT	Overall t [mm]	Cavity L [mm]
 <p>3G-1</p>	Air	1.702	0.615	0.703	48.7	15.8
	Argon	1.590	0.615	0.703	46.3	14.6
	Krypton	1.531	0.616	0.703	37.1	10.0
	Xenon	1.492	0.616	0.703	31.1	7.0
 <p>3G-2</p>	Air	0.912	0.246	0.566	41.9	15.2
	Argon	0.730	0.245	0.566	39.9	14.2
	Krypton	0.631	0.245	0.566	30.1	9.3
	Xenon	0.566	0.244	0.566	24.1	6.3
 <p>3G-2s</p>	Air	0.891	0.369	0.566	41.1	14.8
	Argon	0.706	0.367	0.566	39.1	13.8
	Krypton	0.607	0.366	0.566	29.5	9.0
	Xenon	0.541	0.364	0.566	24.1	6.3
 <p>3G-3</p>	Air	0.975	0.481	0.628	41.7	15.1
	Argon	0.800	0.481	0.628	39.3	13.9
	Krypton	0.707	0.481	0.628	29.5	9.0
	Xenon	0.645	0.481	0.628	24.3	6.4

IGU	Fill Gas	U_{cg} [W/m ² K]	SHGC	VT	Overall t [mm]	Cavity L [mm]
 <p>4G-1</p>	Air	1.235	0.545	0.632	76.0	17.7
	Argon	1.151	0.546	0.632	71.5	16.2
	Krypton	1.107	0.546	0.632	55.3	10.8
	Xenon	1.079	0.546	0.632	45.1	7.4
 <p>4G-2</p>	Air	0.611	0.224	0.502	63.4	17.3
	Argon	0.488	0.224	0.502	59.8	16.1
	Krypton	0.424	0.224	0.502	42.4	10.3
	Xenon	0.381	0.224	0.502	34.0	7.5
 <p>4G-2s</p>	Air	0.596	0.355	0.502	61.3	16.6
	Argon	0.472	0.353	0.502	57.7	15.4
	Krypton	0.406	0.351	0.502	42.4	10.3
	Xenon	0.364	0.350	0.502	32.5	7.0
 <p>4G-3</p>	Air	0.644	0.410	0.556	62.9	17.1
	Argon	0.524	0.409	0.556	59.6	16.0
	Krypton	0.462	0.409	0.556	42.2	10.2
	Xenon	0.421	0.409	0.556	33.5	7.3

IGU	Fill Gas	U_{cg} [W/m ² K]	SHGC	VT	Overall t [mm]	Cavity L [mm]
 <p>5G-1</p>	Air	0.964	0.489	0.569	104.6	19.0
	Argon	0.898	0.489	0.569	99.4	17.7
	Krypton	0.864	0.489	0.569	75.4	11.7
	Xenon	0.843	0.489	0.569	60.2	7.9
 <p>5G-2</p>	Air	0.451	0.207	0.447	86.8	18.8
	Argon	0.361	0.207	0.447	80.4	17.2
	Krypton	0.314	0.207	0.447	57.2	11.4
	Xenon	0.284	0.207	0.447	42.8	7.8
 <p>5G-2s</p>	Air	0.440	0.335	0.447	84.4	18.5
	Argon	0.349	0.333	0.447	79.2	16.9
	Krypton	0.302	0.332	0.447	55.6	11.3
	Xenon	0.271	0.330	0.447	42.8	7.7
 <p>5G-3</p>	Air	0.471	0.359	0.494	85.7	18.1
	Argon	0.383	0.359	0.494	79.3	17.2
	Krypton	0.337	0.358	0.494	56.9	11.0
	Xenon	0.308	0.359	0.494	42.5	7.9
 <p>5G-3s</p>	Air	0.471	0.392	0.494	84.1	18.4
	Argon	0.382	0.391	0.494	80.5	17.3
	Krypton	0.337	0.391	0.494	55.7	11.1
	Xenon	0.307	0.391	0.494	43.3	8.0
 <p>5G-3sm</p>	Air	0.471	0.379	0.493	85.3	18.2
	Argon	0.382	0.378	0.493	80.9	17.1
	Krypton	0.337	0.378	0.493	56.1	11.1
	Xenon	0.307	0.378	0.493	43.7	8.0

The trends seen in Figure 3.3.1 to Figure 3.3.4 are clearly laid out in Table 3.3.2. For each IGU, both the U_{cg} and cavity widths are reduced with heavier fill gases, while the SHGC and VT remain largely constant. This is because both SHGC and VT are governed the solar-transmission of the glazing layers. The SHGC and VT only decrease with greater numbers of glazing layers, since the overall solar transmission of the IGU is reduced as the light passes through multiple layers. The greater the number of layers, the greater the amount of light is filtered.

One noticeable trend for all multi-layered IGUs is the significant reduction in U_{cg} and cavity width between IGUs with and without low-E coatings. IGUs with low-E coatings tend to benefit from using heavier gases more than clear IGUs by showing a greater reduction in U_{cg} and cavity width. This reduction is actually very similar across all IGU types when only the fill gas is varied. The reduction in U_{cg} , cavity width, and overall width from using different fill gases are summarized in Table 3.3.3.

Table 3.3.3 Resulting range of reductions in U_{cg} , cavity width, L, and overall IGU width, t for different fill gases and multi-layered IGU configurations (double to quint)

U-value Reduction

Fill Gas	Clear	Low-E
Ar	6-7%	19-22%
Kr	9-11%	27-34%
Xe	11-13%	34-42%

Cavity Width, L, Reduction

Fill Gas	Clear	Low-E
Ar	6-8%	5-9%
Kr	37-40%	37-40%
Xe	56-58%	56-59%

Overall Width, t, Reduction

Fill Gas	Clear	Low-E
Ar	3-6%	4-7%
Kr	21-33%	21-34%
Xe	31-50%	30-51%

From Table 3.3.3 it is shown that the reduction in U-value from the use of heavier fill gases is greatly increased with low-E coatings. This is due to the significant reduction in long-wave radiative heat flux, which is the dominant mode of heat transfer across the centre-glass regions of all IGUs followed by convection. Thus, when the radiative heat flux is reduced, changes that reduce the convection in the cavity become more effective. From the trends observed in these simulations in Window5 (LBNL, 2003), it leads to the conclusion that any IGU that is designed for low U_{cg} should:

1. Apply low-E coating to glazing layer(s)
2. Use fill gases:
 - a. Argon or Krypton for double- or triple-glazed IGUs
 - b. Krypton or Xenon for quad- or quint-glazed IGUs

These conclusions are largely driven by the desire to reduce U_{cg} while keeping the overall thickness of the IGU to a suitable dimension that can be received by most frames. For example, quint-glazed low-E xenon filled IGUs achieve an optimal U-value at a thickness of approximately 42 – 44 mm, which is almost twice the size of a double-glazed low-E argon filled IGU that is typically used today. The added size of the IGU can pose significant problems not only for frame design, but also for spatial considerations, which will be discussed in the Chapter 4.

3.3.2 SHGC and VT of Multi-layered IGUs

Aside from designing IGUs for low U_{cg} and cavity widths, IGUs can also be optimized for its solar performance in terms of SHGC and VT. This is easily achievable for most multi-layered IGUs, particularly for IGUs with a greater amount of layers, since different kinds of glazing can be combined to finely tune the IGU.

In most commercial buildings, IGUs with low SHGC are required due to the high internal heat gains in the building and the large window area. This requirement for low solar heat gain IGUs however, is balanced by the desired to have good daylighting and visual quality, which is govern by the VT. Unfortunately both of these performance indices are

governed largely by the same property: solar transmission, τ_{sol} . VT is merely a subset of the solar transmission, for which only the transmittance of the visible portion of the solar spectrum is measured. Therefore, as previously mentioned, glazing layers with lower τ_{sol} tend to also have lower VT. To strike a balance between SHGC and VT, IGUs with a VT lower than 0.4 have been excluded from this analysis due to its effect on visibility and daylight. IGUs with VTs lower than 0.4 tend to be darker compromising visual quality. Another factor that can affect visual quality is the colour of the visible light transmitted, usually from tinted glazings. This can alter the quality of the light entering the room. While this can dramatically affect the daylight quality, this was not considered in this study.

When selecting glazing for IGUs with specific optical and thermal performance, it is important to consider its surface IR emissivity and solar transmission τ_{sol} . Figure 3.3.5 shows a plot of glazings found in the Window5 database (LBNL, 2003) that have a VT greater than 0.4.

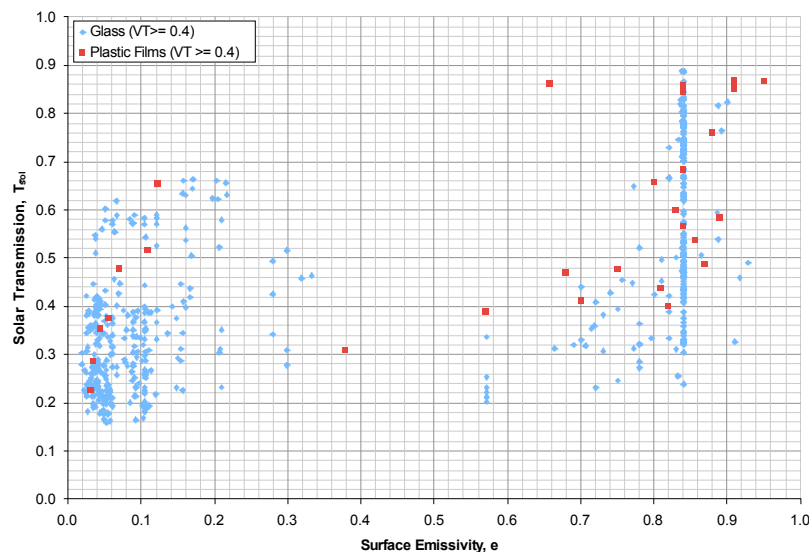


Figure 3.3.5 Infrared emissivity and solar transmission of glazing products as listed in Window5 database (LBNL, 2003)

This figure shows the spread of glazing products that are current available. Notice that despite a relatively large spread amongst the solar transmission, there is an absolute minimum that is approximately 0.15. There are also two distinct clusters of glazing

products around clear and low-E coated glazings. The solar transmission of the low-E coated products are lower than the clear products. The two emissivity clusters and solar transmission minimum hints that there are limitations to both SHGC and U_{cg} given the constraint of designing IGUs with VT greater than 0.4.

From the performance levels achieved in Table 3.3.2, it appears that most IGUs fall into one of four categories as summarized in Figure 3.3.6. Each of these categories are expected to be well suited for a different climate as described in the figure due to their thermal and solar properties.

<p>IGUs with low U_{cg} and high SHGC Appropriate for most passively heated buildings with low to moderate WWR in cold climates, which solar gains are maximized while heat loss minimized.</p> <p>$(1.5 > U_{cg} > 0 \text{ W/m}^2\text{K})$ $(0.8 > \text{SHGC} > 0.4)$</p>	<p>IGUs with high U_{cg} and high SHGC Most common IGU used in North America, typical of most double-glazed IGUs. This type of IGU is typically not considered to be high performance due to its poor control of solar gain and heat loss.</p> <p>$(3.0 > U_{cg} > 1.5 \text{ W/m}^2\text{K})$ $(0.8 > \text{SHGC} > 0.4)$</p>
<p>IGUs with low U_{cg} and low SHGC Appropriate for most commercial buildings with moderate to high WWR in cold climates, which most of the heating load during the day is met by high internal gains and solar gains are minimized during the day to avoid overheating.</p> <p>$(1.5 > U_{cg} > 0 \text{ W/m}^2\text{K})$ $(0.4 > \text{SHGC} > 0)$</p>	<p>IGUs with high U_{cg} and low SHGC Appropriate for most commercial buildings with moderate to high WWR in warm climates, where cooling load dominates over heating load. Reducing solar gains can significantly risk of overheating as well as annual and peak cooling loads.</p> <p>$(3.0 > U_{cg} > 1.5 \text{ W/m}^2\text{K})$ $(0.4 > \text{SHGC} > 0)$</p>

Figure 3.3.6 Proposed IGU performance characteristic matrix

3.4 Survey of Multi-layered IGU Performance Thresholds

Choosing the appropriate IGU to minimize the energy consumption in buildings is ultimately dependent on the exterior climate, façade orientation, window-to-wall ratio (WWR), building internal heat gains, and building occupancy. With a wide array of

glazing products available and various glazing configurations and arrangements a seemingly endless combination of IGUs can be designed and evaluated to suite almost any condition. However, since the glazing properties of many components are limited by current technology IGU performance is also limited by achievable upper and lower bounds. Through a series of one-dimensional energy transfer simulations using Window5 (LBNL, 2003) a complete survey of IGU performance thresholds was completed. The performance limitations are categorized by the type of IGU and have a lower VT limit. Since IGUs with a VT lower than 0.4 are generally perceived to be 'dark' and more difficult to see through, the VT of all IGUs considered in this project are equal or greater than 0.4. All of the glazing specifications and performance are listed in Appendix B. The performance limitations of each type of multi-layered IGU is shown in Figure 3.4.1 which overlays the performance characteristics that define the other high performance IGU types. This figure is particularly useful in helping designers chose the proper IGU construction given the desired IGU properties as determined during preliminary design or with simple energy simulation models.

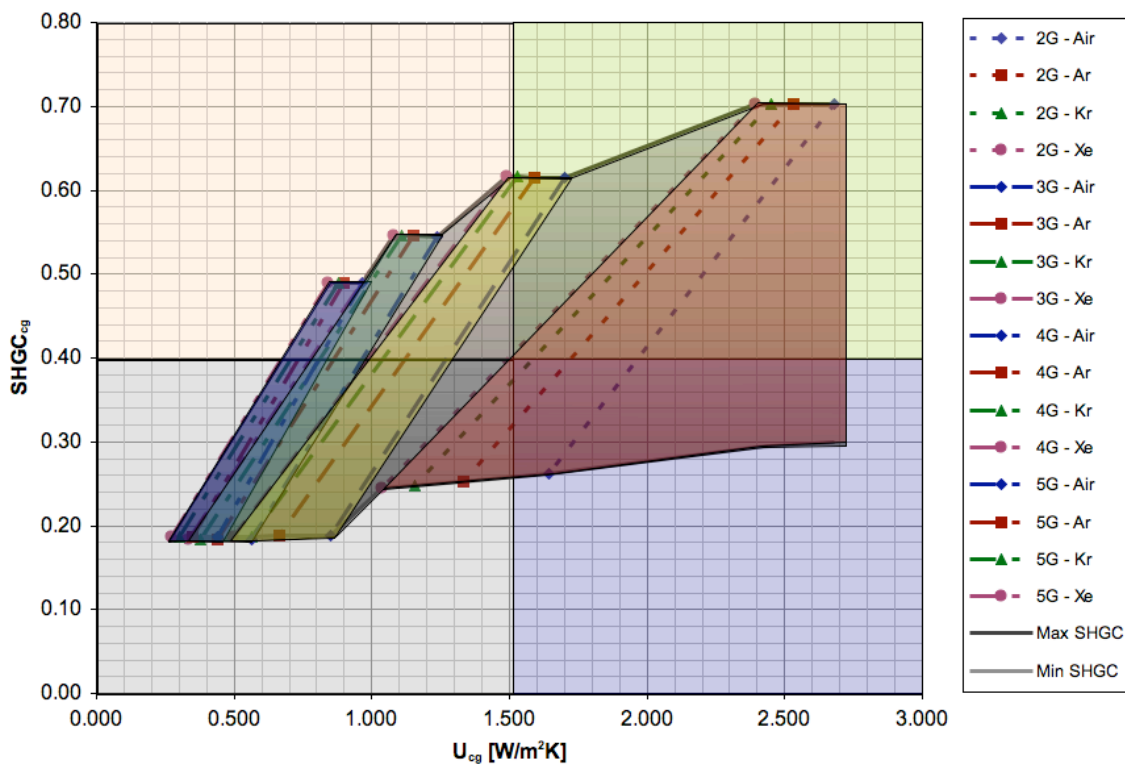


Figure 3.4.1 Possible IGU performance range as determined by Window5 (LBNL, 2003) simulations

The dark shaded regions in Figure 3.4.1 that are bound by the dotted lines show the possible performance range that can be achieved with current glazing technology. This figure allows designers to assess how IGUs can be assembled to meet the desired characteristics. The dotted lines join the performance of each IGU type with different fill gases, which largely affects the U-value of the IGU. Although the performance range for multi-layered IGUs with additional layers diminishes, the resolution within the range increases. This is largely due to the greater number of possible glazing combinations. From Figure 3.4.1 it can be seen that the upper limit of SHGC is significantly affected by the number of glazing layers in the IGU, while the lower limit severely affected by the number of glazing layers beyond a double-glazed IGU, since VT is limited to greater than 0.4. Thus, if thermal performance is not a significant concern, a low SHGC IGU can be easily designed from a triple-glazed system. The performance indices of these IGUs that represent the upper and lower range of performance in Figure 3.4.1 are listed in Table 3.4.1.

Table 3.4.1 Upper and lower limits of performance of IGUs investigated as analyzed by Window5 (LBNL, 2003)

IGU	Fill Gas	U_{cg} [W/m²K]	SHGC	VT	Overall t [mm]	Cavity L [mm]
2G-1 (high U and SHGC)	Air	2.680	0.702	0.786	25.1	13.6
	Argon	2.531	0.702	0.786	24.1	12.6
	Krypton	2.449	0.703	0.786	19.7	8.2
	Xenon	2.395	0.703	0.786	17.2	5.7
2G-4uv (low U and SHGC)	Air	1.642	0.262	0.413	23.9	12.5
	Argon	1.334	0.253	0.413	22.9	11.5
	Krypton	1.157	0.248	0.413	18.9	7.5
	Xenon	1.035	0.244	0.413	16.6	5.2

IGU	Fill Gas	U_{cg} [W/m ² K]	SHGC	VT	Overall t [mm]	Cavity L [mm]
3G-1 (high U and SHGC)	Air	1.702	0.615	0.703	48.7	15.8
	Argon	1.590	0.615	0.703	46.3	14.6
	Krypton	1.531	0.616	0.703	37.1	10.0
	Xenon	1.492	0.616	0.703	31.1	7.0
3G-5uv (low U and SHGC)	Air	0.850	0.189	0.431	40.9	14.7
	Argon	0.663	0.188	0.431	39.1	13.8
	Krypton	0.562	0.187	0.431	30.1	9.3
	Xenon	0.496	0.187	0.431	24.5	6.5
4G-1 (high U and SHGC)	Air	1.235	0.545	0.632	76.0	17.7
	Argon	1.151	0.546	0.632	71.5	16.2
	Krypton	1.107	0.546	0.632	55.3	10.8
	Xenon	1.079	0.546	0.632	45.1	7.4
4G-5uv (low U and SHGC)	Air	0.566	0.184	0.397	61.9	16.8
	Argon	0.441	0.184	0.397	58.3	15.6
	Krypton	0.376	0.184	0.397	42.1	10.2
	Xenon	0.333	0.184	0.397	33.1	7.2
5G-1 (high U and SHGC)	Air	0.964	0.489	0.569	104.6	19.0
	Argon	0.898	0.489	0.569	99.4	17.7
	Krypton	0.864	0.489	0.569	75.4	11.7
	Xenon	0.843	0.489	0.569	60.2	7.9
5G-4uv (low U and SHGC)	Air	0.441	0.187	0.406	84.4	18.2
	Argon	0.350	0.187	0.406	80.0	17.1
	Krypton	0.303	0.187	0.406	56.0	11.1
	Xenon	0.272	0.187	0.406	43.6	8.0

3.5 High Performance Multi-layered IGUs

From the performance thresholds established by the IGUs listed in Table 3.4.1, a set of high-performance IGUs can be derived by carefully modifying the glazing properties of the different components. Since the major technological challenge seems to be the

development of low U-value IGUs, the aim of all high-performance IGUs is to have a low centre-glass U-value. By substituting different glazing products a set of low and ultra-low U-value high-performance IGUs were created and evaluated using Window5 (LBNL, 2003) and are listed in Table 3.5.1. These IGUs have been classified by the number of glazing layers and SHGC. It is important to note that even though all of these units can be categorized as low U-value and low SHGC IGUs by the performance matrix in Figure 3.3.6, both low and ultra-low SHGC IGU types are listed, since there are slight variations in SHGCs. This is a good example of how low U-values often compromise SHGCs, however, as seen in later chapters the low absolute value of the SHGC do not significantly compromise energy performance of perimeter spaces in high-rise commercial and institutional buildings.

Table 3.5.1 High performance IGU properties as generated by Window5 (LBNL, 2003)

IGU	Fill Gas	U_{cg} [W/m²K]	SHGC	VT	Overall t [mm]	Cavity L [mm]
2G-2s (low U and low SHGC)	Argon	1.305	0.37	0.64	22.9	11.4
2G-4uv (low U and low SHGC)	Argon	1.334	0.25	0.41	22.9	11.5
3G-2s (ultra-low U and low SHGC)	Krypton	0.670	0.37	0.57	29.5	9.0
3G-5uv (ultra-low U and ultra-low SHGC)	Krypton	0.562	0.19	0.43	30.1	9.3
4G-2s (ultra-low U and low SHGC)	Krypton	0.406	0.35	0.50	42.4	10.3
4G-5uv (ultra-low U and ultra-low SHGC)	Krypton	0.461	0.43	0.56	42.7	10.4
5G-2s (ultra-low U and low SHGC)	Xenon	0.271	0.33	0.45	42.8	7.8
5G-4uv (ultra-low U and ultra-low SHGC)	Xenon	0.272	0.19	0.41	43.6	8.0

From the one-dimensional energy transfer analysis of multi-layered IGUs under standard NFRC conditions using Window5 (LBNL, 2003) in this chapter it is shown that performance indices such as U-value, SHGC, and VT can be significantly altered by the material properties of the glazing components. Simulations with double-glazed IGUs showed that significant reductions in U-values, of up to 60%, can be achieved with the application of low-E coatings on the cavity-facing surface of the IGU. By incorporating additional low-E coatings on glazed surfaces through adding more glazing layers, the centre-glass U-value can be further reduced. Further reductions in U-values can be achieved with the substitution of air for heavier fill gases such as argon, krypton, and xenon. Since each of these gases has an unique set of thermal conductance and natural convective properties, the optimum cavity widths varies with the type of gas. As observed in the results of Window5 (LBNL, 2003) simulations, heavier fill gases tend to reduce the cavity width, making it ideal for multi-layered IGUs with many layers. A comparison of a clear air-filled double-glazed IGU with a low-E xenon-filled quint-glazed IGU shows a reduction in U-value of up to 90%. With an extensive selection of glazing materials that are available in the market and the different variations in glazing construction that is possible, there is a seemingly endless combination of glazing construction and performance. In order to identify true high-performance IGU characteristics, a survey of possible IGU performance was required. The results of this survey are presented in Table 3.4.1. From these IGUs a set of high-performance IGUs were investigated. The high-performance IGUs are derived from the low U-value IGUs from the survey, taking into account practicality and solar heat gain performance. The resulting high-performance IGUs push the envelop in terms of low U-value and high and low SHGC without compromising VT to lower than 0.4. This set of high-performance IGUs is presented in Table 3.5.1 and are considered to be on the leading edge of IGU performance. As such, they form the bases of analysis in upcoming chapters of this thesis.

CHAPTER 4

High Performance Window Assemblies

While the performance of the Insulated Glazing Unit (IGU) plays an important role in the overall window performance, other elements such as the edge spacer and window frame can significantly alter the thermal performance of window assemblies as well. In this chapter the thermal performance of both edge spacers and window frames are evaluated in four separate sections. First, the basic functions and structure of edge spacers and curtain wall window frames are introduced as part of a technical review; second, the heat transfer characteristics of edge spacers and curtain walls are investigated and discussed with different material properties. Similar to the survey of IGU properties, the results of this investigation are used to develop a design of low and ultra-low U-value high-performance curtain wall sections, which are presented in the third part of the chapter. In the last section, the effect the edge spacer and curtain wall heat transfer characteristics on overall window U-values are examined. Factors that can affect the U-value of the overall window assembly such as edge spacer and frame insulating values and dimensions are explored for conventional and high-performance edge and frame systems coupled with low and ultra-low high-performance IGUs from the pervious chapter.

4.1 Review of the Basic Functions of Window Assemblies

Although glazing properties have an important role in window performance, the overall performance of the window assembly is dependent on the window frame and edge spacer construction. Just as technical innovations in IGUs have significantly improved IGU performance, frame and edge spacer technology have improved over the same period, however, their progress is relatively slow and have lagged behind IGUs. In order to design and build a truly insulating high-performance window one must consider frame and edge spacer performance.

Similar to IGUs, a window frame serves multiple functions including (Carmody *et al.*, 2004):

1. Provide Adequate Thermal Insulation

To get the most out of the thermal performance of an IGU, window frames and edge spacers must be insulated to minimize thermal bridging to prevent short-circuiting of heat flow around the highly insulated IGU. Since the major mode of heat transfer across edge spacers and window frames is conduction, material selection is critical since various materials have different thermal conductivities.

2. Provide Structural Support

Although window systems do not carry any dead load from the structure, all window assemblies must be able to resist lateral loads from wind. Since glass is a very stiff material, it can efficiently collect and transfer all wind loads from the IGU to the window frame, where it is again then collected and transferred directly to the structure. Consequently, window frames must be designed to withstand wind loads predetermined by local building codes and they must be within tolerable deflection limits such that they will not break the IGU that it is carrying. To provide adequate lateral support both the geometry and selection of materials, with appropriate structural properties, is paramount.

3. Provide Sealed Interface between IGU and Building Enclosure

Apart from providing thermal insulation and structural support, window assemblies play a significant role in the overall building enclosure. Just like any other part of the building enclosure, window assemblies must control heat, air, and moisture. The frame and edge spacer material provides control of heat, the control of air and moisture is done by gaskets and seals around the window, between the IGU and frame, as well as between the window frame and building enclosure. A well sealed window assembly will stop unwanted air and water

leakage, thus improving on the thermal performance of the window assembly and its durability.

4. Provide a Mechanism for Operability

Operable windows have subtle performance differences between them and fixed windows. Operable windows typically have wider and thicker frames to provide structural support for the operating mechanism and IGU; therefore, they typically have higher U-values, since a greater portion of the opening is occupied by the less insulating frame. In addition, operable windows are typically prone to air and water leakage, depending on the operating mechanism and the quality of gaskets and seals. While operable windows provide natural ventilation and are required by local building codes to meet fire egress requirements in residential buildings, this is not the case for most commercial buildings. Operable windows are much less popular in most commercial buildings due to risks of falling through the window opening and strong winds at great heights. In fact, most operable windows for commercial windows are limited to open no more than 102 mm (4 in.) to reduce the risk of falling through. Instead fixed window systems are much more common. Since this thesis is focused on how windows affect energy loads in commercial buildings, only fixed windows are investigated.

From the list of functions, providing both adequate thermal insulation and structural support are the two dominate requirements in window frame design. Both of these functions are significantly affected by the properties of the materials used. To provide structural support a stiffer material that is able to withstand high wind loads without resulting in significant deflections is desired, while materials with low thermal conductivities are desired to provide thermal insulation to the window frame. Unfortunately, there are very few materials that have both qualities; in fact for most materials these are contradictory. Stiffer materials tend to be dense and are highly thermally conductive, while thermally insulating materials tend to be soft and are easily deformable. The main challenge to high performance window construction is to design

an assembly that can serve both functions through means of creative geometries and arrangements that takes advantage of different material properties.

4.1.1 Anatomy of Commercial Window Assemblies

Many typical commercial buildings glazed facades are curtain wall systems rather than window assemblies. Curtain walls are external, non-load bearing wall that typically compose the entire outer skin of the building. It may consist of both vision glazing as well as opaque spandrel panel, which are typically glass to form an exterior envelope of glass and framing materials (Carmody *et al.*, 2004). Curtain walls can either be hung over several storeys and anchored periodically along ceiling and floors or installed in between floor and ceilings, where they are referred to as window walls. Window walls are frequently used in storefronts for their strength (CMHC, 2004).



Figure 4.1.1 Buildings with curtain wall system (Left: Adam Joseph Lewis Center for Environmental Studies, Oberlin College, Right: Art Gallery of Ontario)

Curtain walls are typically either prefabricated (unitized), where whole sections of glazing and frame are delivered as one for on-site for assembly, or assembled from extrusions (CMHC, 2004). In either case, most frame-to-glazing connections come in one of two forms, the exterior batten in the form of a pressure plate and structural adhesion through silicone. Figure 4.1.2 shows typical sections of both types of connections. In addition, there is a less popular third type is interior glazed, which is mechanically captured via a removable clamping piece on the interior.

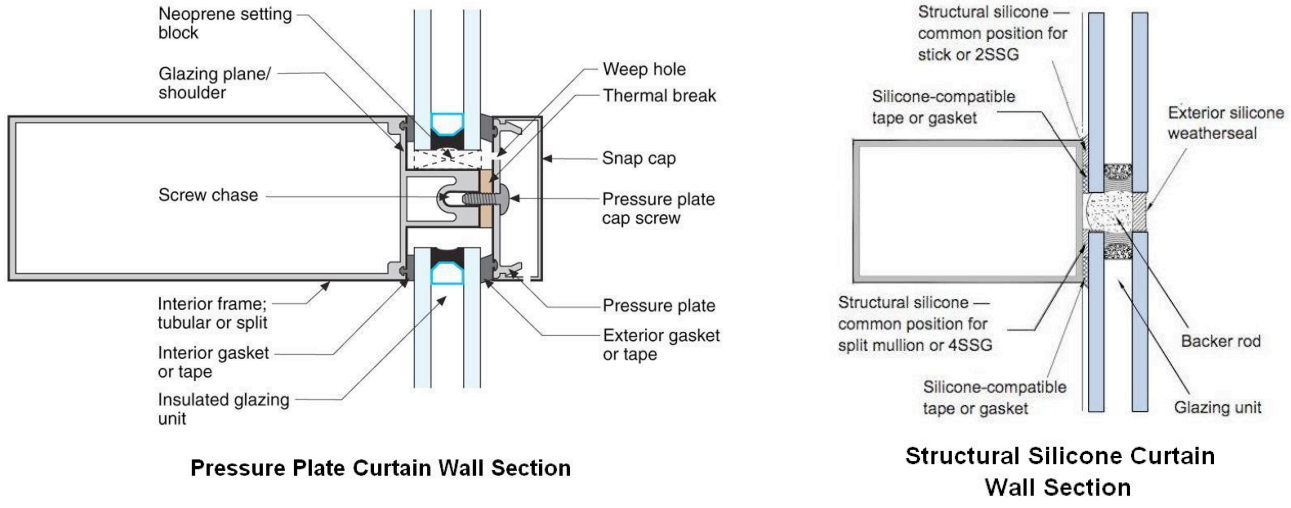


Figure 4.1.2 Curtain wall types (left: pressure plate, right: structural silicone) (Lstiburek and Straube, 2008)

Traditionally most curtain walls have a pressure plate connection, in which IGUs or spandrel panels are placed within the glazing rabbet, between the interior frame and the exterior pressure plate. The pressure plate is attached to the interior frame with a cap screw, which enables the plate to apply pressure on the IGU or spandrel panel to hold it in place. An air- and water-tight connection can be easily created through simple compression from the pressure plate. This type of curtain wall is commonly referred to as the ‘Exterior Batten’ or ‘Pressure Plate’ curtain wall since the outside of each IGU is captured with a pressure plate (CMHC, 2004). Pressure Plate curtain walls have the advantage of reliability since the strength provided by the plate is through mechanical means, making it less susceptible to deterioration due to weathering. However, since the pressure plate is attached with a cap screw, this creates a thermal bridge, which can diminish the thermal performance of the frame section. One variant of the pressure plate curtain wall that minimizes thermal bridging is to replace the pressure plate and snap cap with a synthetic rubber profile. This arrangement does not provide as much strength as the pressure plate, rather it provides a means for unwanted water and air leakage, and is often used in conjunction with pressure plate connections at the head and sill of the frame to secure the IGU or spandrel panel in place.

Another popular curtain wall type is Structural Silicone Glazing (SSG), where the IGU or spandrel panels are directly adhered to the interior frame (CMHC, 2004). This eliminates any thermal bridging from screws and bolts and offers a smooth exterior aesthetic finish. One of the drawbacks of this system is the eventual deterioration of the structural silicone. Since the silicone is directly exposed to the exterior it is more susceptible to weathering. SSG systems typically are available as either two or four-sided. A two-sided SSG curtain wall has silicone along two parallel sides of the IGU, while the other sides have pressure plate connections (CMHC, 2004). Because pressure plate connections are more common, they have been chosen as the subject of investigation to improve its thermal performance.

4.1.2 Pressure Plate Curtain Wall

The main components of the Pressure Plate curtain walls are the interior frame, pressure plate, cap screw, thermal break, and snap cap, as shown in pressure plate curtain section in Figure 4.1.2. The functions of each are as follows:

1. Interior Frame

The interior frame provides structural support to the curtain wall and is the main element that resists lateral deflections due to wind loads. Since most curtain walls are connected to the superstructure at floors and ceilings, interior frames can be designed as a simply supported beam. The minimal dimensions of window frame section are dependent on the wind load and strength of the material used. In general, deeper interior frame sections tend to have larger moment of inertia and thus are better able to resist wind loads. However, larger sections will have higher U-values since there is more frame area. This is particularly the case for highly thermally conductive materials such as aluminum frames, which heat transfer is dominated by its surface area rather than the frame width. The interior frame can be made out of extruded aluminum, steel, fiberglass, or wood.

2. Pressure Plate

The pressure plate secures the IGU or spandrel panel to the interior frame by applying mechanical pressure through the cap screw. It is typically made out of the same material as the interior frame (CMHC, 2004); however, for improved thermal performance materials with lower thermal conductivities such as fiberglass can be used. Because of its location to the exterior in relation to the exterior of the glazing, the pressure plate can have a significant affect on the thermal performance of the window assembly. A less thermally conductive pressure plate can significantly improve curtain wall thermal performance. Pressure plates also include ventilation and drainage openings to allow for water to drain away from the IGU or spandrel panel (CHMC, 2004).

3. Cap Screw

The cap screw links the pressure plate with the interior frame and applies pressure to the pressure plate to hold the IGU or spandrel panel. The cap screw is installed over regularly spaced intervals that can vary depending on the expected wind load and stiffness of the pressure plate material. Most commercial curtain wall systems have cap screws installed at spacings of 230 mm (9 in.) on centre, which is an industry standard (Griffith *et al.*, 1998).

4. Thermal Break

Thermal breaks are typically used in metal window frames to help improve its thermal performance. By splitting the frame components into exterior and interior pieces with a less thermally conductive material, it is able to interrupt heat flow enough to reduce the heat loss of the frame. The location of the thermal break is dependent on both the potential heat flow paths and structural capacity of the frame. For pressure plate curtain walls, thermal breaks are usually placed between the main interior frame and the pressure plate inline with the IGU. Thermal breaks are typically constructed out of rubber or plastics such as PVC, polyurethane, or polyamide (nylon) for their low conductivity and high stiffness.

Depending on their length thermal breaks can reduce the frame U-value by 28-48%. Figure 4.1.3 shows thermal breaks for two typical types of curtain walls.



Figure 4.1.3 Thermally broken aluminum curtain wall sections (Left: Kawneer 1600 curtain wall section, Right: Kawneer 7550 curtain wall section)

5. Snap Cap

Aside from serving as a decorative cover, the snap cap acts as a baffle to the drainage openings in the horizontal pressure plate (CMHC, 2004). It also The main function of snap caps is to provide protection for the pressure plate and cap screw from weathering and is drained with weep holes to allow for water to flow out if it gets between the glazing and pressure plate. Snap caps are typically made of extruded aluminum or the same type of alloy as the interior frame (CMHC, 2004).

Most commercial curtain walls are made of extruded anodized or painted aluminum, for its lightweight, strength, durability, non-corrosive properties, and its ability to be extruded to accommodate special shapes within the frame. However, one major drawback of aluminum is its thermal conductivity. Aluminum has a very high thermal conductivity and can significantly reduce the thermal resistance of the overall window

assembly even if it is assembled with a low U-value IGU. In order to improve the U-value of window assemblies thermal breaks are introduced or alternate materials are sought. Table 4.1.1 lists thermal and mechanical properties of common materials used in curtain walls and window frames.

Table 4.1.1 Properties of common curtain wall materials¹

Material	Thermal Conductivity, k [W/m.K]	Modulus of Elasticity [MPa]	Durability	Areas of Use
Aluminum	237	69 000	Very durable against weathering, will not corrode.	Ideal for all parts of pressure cap curtain wall, particularly interior frame and snap cap for its strength and durability.
Stainless Steel	17	200 000	Very durable against weathering, will not corrode.	Ideal for all parts of curtain wall for its strength and durability
Vinyl (PVC)	0.14	2 600	High impact and moisture resistance. However, it is not very durable against sunlight and hot and cold temperatures.	Ideal for thermal breaks and interior frames.
Wood (Fir)	0.14	13 000	Not as durable as aluminum or vinyl, it is susceptible to rot.	Ideal for interior frames where it is protected from weathering.

¹ From various sources, including: LBNL, 2008; Engineering Toolbox, 2010; Lstiburek and Straube, 2008

Fiberglass	0.231	45 000	Very stable to weathering.	Ideal for pressure plates. Can be used for frames if heavier extrusions are employed.
Polyurethane	0.024	n/a	Not stable to weathering.	Ideal for insulating cavities in frames.
Polyamide (nylon)	0.25	n/a	Very stable to weathering.	Ideal for thermal breaks and rubber profiles.

The potential effect of these materials on the frame and edge U-value is examined through two-dimensional heat transfer analysis summarized in section 4.3 in this chapter.

4.1.3 Edge Spacer Construction

Aside from the frame, another major component of heat transfer across window assemblies is at the edge spacer. The edge spacer is located along the edge of the IGU and provides structural support to the sheets of glazing within the IGU. Depending on the spacer material, warm edge spacers can improve the edge U-value by 2-10% (based on simulations presented later). In addition to improving the edge of glass thermal performance and keep the glazing separated, edge spacers also serve multiple functions including:

1. Accommodate stresses from thermal expansion, pressure differences, and self weight of IGU.
2. Provide moisture resistance that prevents water or water vapour from passing into the IGU to fog the unit. Many spacers are packed with a silicone desiccant to reduce the risk of fog within the glazing cavity.
3. Create a gas-tight seal that prevents leakage of exotic fill gases within the cavity.

There are typically two types of edge spacers: shell and foam. A shell spacer is typically constructed out an aluminum, stainless steel, or vinyl (PVC) shell and is filled with a silicone desiccant, while a foam spacer is made of silicone foam surrounded by polyester

foil along the sides (Carmody, 2007). The spacer shells are very versatile due to their strength, whereas the foam spacers provide less support. In multi-layered IGUs, shell and foam spacers are used together, often with stiffer shell spacers located in the outer cavities, while the middle cavities use foam spacers as thermal breaks.

The spacers are sealed to the glazing with a polyisobutadien primary sealant that provides a tight moisture and gas seal, while a secondary silicone or urethane sealant is placed behind the spacer to additional structural strength and moisture protection (Carmody, 2007). Figure 4.1.4 illustrates how typical shell and soft spacers are arranged within the IGU.

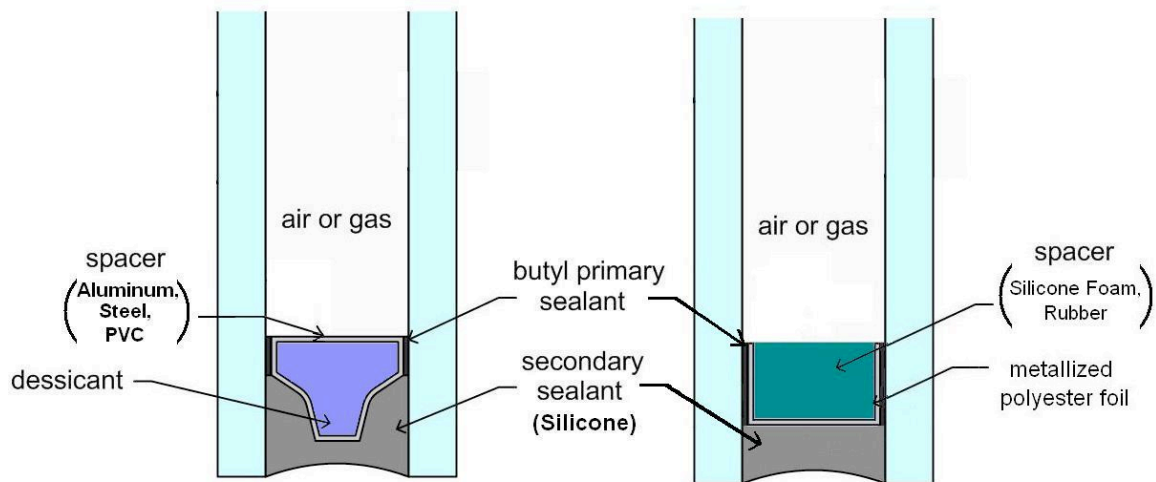


Figure 4.1.4 Edge spacer construction (adapted from Carmody, 2007)

Edge spacers are most commonly constructed out of aluminum shells. However, since aluminum is an excellent thermal conductor, this creates a thermal 'short circuit' to increase the heat transfer at the edge of the IGU and reduce the thermal performance of the window system. Thermally conductive spacers and frames are also more prone to condensation. As centre-of-glass U-values improve with high performance glazing, the edge loss becomes more pronounced and the demand for a more thermally insulating spacer becomes more important.

4.2 Heat Transfer Analysis of Edge and Frame Regions

Similar to IGUs, all three heat transfer modes of conduction, convection, and radiation, exists at edge and frame regions of curtain walls. However, unlike IGUs, the dominant mode of heat transfer is typically conduction through solid materials due to the materials used and the geometry of the section. Convection and radiation does occur within the frame, however, only at a limited capacity typically within hollow air cavities in the section. Another significant difference from IGU heat transfer is the heat flows across frame and edge regions can be one-, two-, and sometimes three-dimensional. Conduction can occur in one to three dimensions, while radiation and convection occurs in two and three dimensions through hollow cavities within the frame typically found in extruded aluminum, vinyl and fiberglass sections (Gustavsen *et al.*, 2008). This implies an effective high performance curtain wall system must be designed with thermally insulating materials placed at areas of higher heat flows to minimize total heat loss across the section.

4.2.1 Computer Simulation Software

U-values for frames and edge regions can be evaluated either with laboratory testing or with two-dimensional heat transfer analysis with computer simulations. Today, computer simulations are by far the most popular and cost effective way at analyzing two-dimensional heat transfer across edge and frame regions. Software programs such as THERM6 (LBNL, 2008), uses Finite Element Method (FEM) to model two-dimensional heat transfer. FEM models work particularly well for one- and two-dimensional conduction for solid materials, while hollow frame cavities are given an effective conductivity derived from convection correlations and view-factor-based radiation models in accordance to the ISO standards ISO 15099 and ISO 10077-2. Both of these standards are algorithms based on well-documented heat transfer correlations derived from laboratory tests. Comparison between laboratory tests and computer simulations show these algorithms are relatively accurate to within 10% for most typical energy-efficient window frames which are considered to be frames with U-values of around 2 W/m²K (Gustavsen *et al.*, 2008). These correlations have also been shown to provide accurate solutions for most traditional highly conductive window frames, such as curtain

walls as well. Comparisons between lab mock-up tests and simulations have shown a mean temperature difference of 2.6°C using National Fenestration Research Council (NFRC) test standards (No *et al.*, 2007). The NFRC test conditions specify both a wintertime and summertime exterior temperatures of -18°C and 82°C, respectively, while the interior side of the curtain wall was kept at 24°C.

However, as window frames are constructed out of less thermally conductive materials, convective and radiation heat transfer becomes more and more significant. For high performance window frames a more sophisticated convection and radiation model using Computational Fluid Dynamics (CFD) and ray-tracing methods may be required. A recent study comparing simulation results between window frame sections analyzed with CFD and ray-tracing methods, and ISO 15099 convective correlations and view-factor-radiation-modeling, showed U-value differences no greater than 2.9% for aluminum and vinyl sections (Gustavsen *et al.*, 2007). This study verified that ISO 15099 procedures when combined with view-factor-radiation modeling as found in THERM can provide reasonably accurate results.

Unfortunately one factor that can significantly alter the heat transfer characteristics of the frame that cannot be simulated is unwanted air leakage from improperly installed frames or leaky gaskets. Depending on the outdoor and indoor temperatures and pressure difference, the effective thermal transmittance can significantly increase, rendering all previous analysis virtually useless. Therefore, two-dimensional heat transfer simulations are useful tools to help guide the designer in making appropriate decisions to reduce heat transfer. However, designers should also consider other factors that cannot be simulated and can alter the performance of the window assembly, such as constructability and water and air leakage.

As standard procedure, the boundary conditions set in THERM6 (LBNL, 2008) follow NFRC Winter night time conditions as summarized in Table 4.2.1. These conditions are the same boundary conditions used to evaluate centre-of-glass U-values for IGUs, making it easier to calculate the overall U-value of the window assembly.

Table 4.2.1 NRFC Standard Simulation Conditions in THERM6 (LBNL, 2008)

Standard	Interior Air Temperature [°C]	Exterior Air Temperature [°C]	Solar Irradiation [W/m ²]	Exterior Convective Coefficient [W/m ² K]	Exterior Wind Speed [m/s]	Interior Convective Coefficient [W/m ² K]
NFRC 100-2001 Winter	21	-18	0	26	5.5	3.29

4.2.2 Cap Screw Conductivity Analysis

When calculating frame and edge region U-values of pressure plate curtain walls, the thermal bridge created by the cap screw can present a significant problem since THERM6 (LBNL, 2008) performs calculations for unique 2-D sections whereas cap screws are intermittently spaced along the length of each section. Two methods that are commonly used to account for this thermal bridging issue are the 'parallel path' method and the 'isothermal planes' method. The 'parallel path' method has been used extensively when analyzing thermal transmittances of composite wall sections with significant thermal bridging, such as stud walls. This method requires analysis of both clear and screw sections, and the actual thermal transmittance is approximated as an area weighted average of the U-values across both sections. However, given the relatively high thermal conductivities of the stainless steel cap screw, this method may not be very accurate. Instead an alternative method which assumes 'isothermal planes' has been proposed. Rather than finding the area-weighted average of both sections, the 'isothermal planes' method finds the effective conductivity, k_{eff} , through an area-weighted method of "screw-space". First the effective conductivity of the non-screw "screw-space" is calculated as the inverse of the sum of the thermal resistances of the material occupying the space in the non-screw case, divided by the total length of the screw. This effective conductivity is then combined with the screw's conductivity as follows:

$$k_{eff} = F_s \cdot k_s + F_n \cdot k_n$$

Equation 4.2.1

Where: k_{eff} = effective conductivity of the 'screw space' incorporating both screw and non-screw sections
 F_s = cap screw area fraction (screw head diameter/ nominal screw spacing)
 F_n = fraction of non-screw area ($1 - F_s$)
 k_s = thermal conductivity of screw
 k_n = effective thermal conductivity of materials occupying screw case in non-screw sections

A study comparing the two methods to experimental results by Griffith *et al.*(1998) on aluminum curtain wall sections, showed the 'isothermal planes' method consistently yielded conservative results while the 'parallel path' method underestimated the total thermal transmittance. The study compared warm side average temperatures of both simulation methods with recorded temperatures with different screw spacings. The 'isothermal panes' predicted lower temperatures that were 84% to 95% of the measured temperature, while the 'parallel path' method had over predicted the surface temperatures by 103% to 110% (Griffith *et al.*, 1998). The accuracy of the temperatures varied with the screw spacing, larger spacings tend to yield more accurate predictions. Predicting lower temperatures translated into a higher U-value, while predicting higher temperatures corresponded to a lower U-value, hence the 'isothermal plane' method yielded conservative results (Griffith *et al.*, 1998). Given these results, the 'isothermal planes' method is used for all two-dimensional frame heat transfer analysis throughout this thesis.

Other findings of this study included:

- The 'parallel path' method yielded better results for non-metal spacers, since it predicted conservative temperatures that are within 3-5% of the measured temperature.

- The thermal bridging from screws is not extremely detrimental for standard materials and spacing. For stainless steel screws at 229 mm apart, the frame U-value is only increased by 18%, which is still considered significant.
- The screw's head governs the screw's effect on thermal bridging since it acts as a fin when connected to the aluminum frame.

4.3 Evaluation of the Thermal Performance of Commercial Curtain Walls

Most high performance commercial window assemblies have a lower frame and edge U-value to produce a more insulating window assembly. As centre-glass IGU U-values continue to decrease with improving technologies, window frames are rapidly becoming the weakest link in window energy performance. Poorly insulated frames and spacers quickly diminish any improvements in thermal performance from the IGU, particularly for smaller windows. Ideally, window assemblies should match or exceed the centre-glass U-values to produce a thermally uniform building envelope. However, given the multiple functions that window assemblies serve and the properties of suitable materials, window assemblies still significantly lag in energy performance. Improvements in thermal performance can still be achieved through the substitution of materials of certain components. Figure 4.3.1 shows typical and high-performance curtain wall sections and their performance numbers. These sections are based on curtain walls that are typically found in many commercial buildings and are representative of the Alumicor 2500 series and the high-performance RAICO THERM⁺ aluminum and timber series.

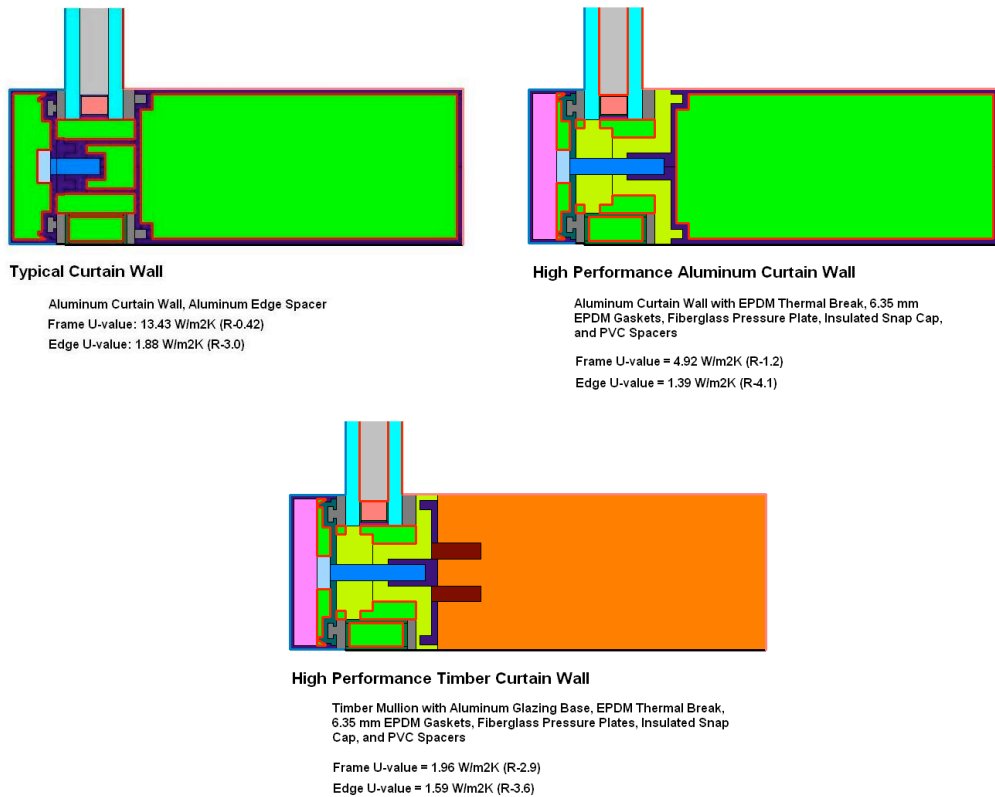


Figure 4.3.1 Typical and high-performance curtain wall sections

In this section the thermal performance of commercial curtain wall sections, including the edge spacer construction are evaluated. All of the results originate from two-dimensional heat transfer models created in THERM6 (LBNL, 2008). As such, the majority of the material properties used in these models were taken from the THERM6 materials database (LBNL, 2008). All of the results of the simulations are listed in Appendix C.

The objectives of this study include:

- Determining how different materials used in the edge spacer construction can affect heat transfer of the edge and frame regions.
- Determining the effect of IGU construction can affect edge and frame thermal performance.
- Determining the heat transfer mechanisms of a typical curtain wall section. This is achieved by calculating the U-value of the edge and frame section in which materials of different heat transfer properties individually substituted. The result

of this exercise will reveal which components are most effective at improving the thermal performance of the edge and frame design.

- Determining the combined effect of various materials can affect edge and frame heat transfer. Components that were previously individually evaluated are combined to see if there is an improvement in thermal performance.
- Design and evaluate low and ultra-low U-value high-performance curtain wall sections that are suitable for high-performance IGUs presented in chapter 3. The design of these sections is guided by the findings of the component study.

4.3.1 Thermal Performance of Edge Spacers

The performance of the edge-glass region of windows and curtain wall assembly is largely dependent on the spacer material. Since edge spacers primarily hold the glazing layers apart within an IGU, the dominant mode of heat transfer is primarily conduction. As a result, more insulating materials with lower thermal conductivities are sought to reduce the effect of thermal bridging across the spacer. Table 4.3.1 lists materials that are typically used in edge spacers along with their thermal conductivities.

Table 4.3.1 Spacer material properties (LBNL, 2008)

Spacer Material	Thermal Conductivity, k [W/mK]
Aluminum	237
Stainless Steel	17
Silicone Foam	0.17
Rubber (EcoSpacer™)	0.18
Vinyl (PVC)	0.14

To illustrate the effects these materials on overall thermal performance of a curtain wall, a simple study comparing different types of edge spacers was done. The analysis was performed in THERM6 (LBNL, 2008) with a double-glazed low-e argon-filled IGU with a cavity width of 11.6 mm in a non-thermally broken aluminum curtain wall frame as shown as the typical curtain wall section in Figure 4.3.1. All of the edge spacers were

approximated as rectangular sections to simplify the geometry as shown in Figure 4.3.2. This provides a more conservative analysis since most spacers are shaped with a thinner bottom section.

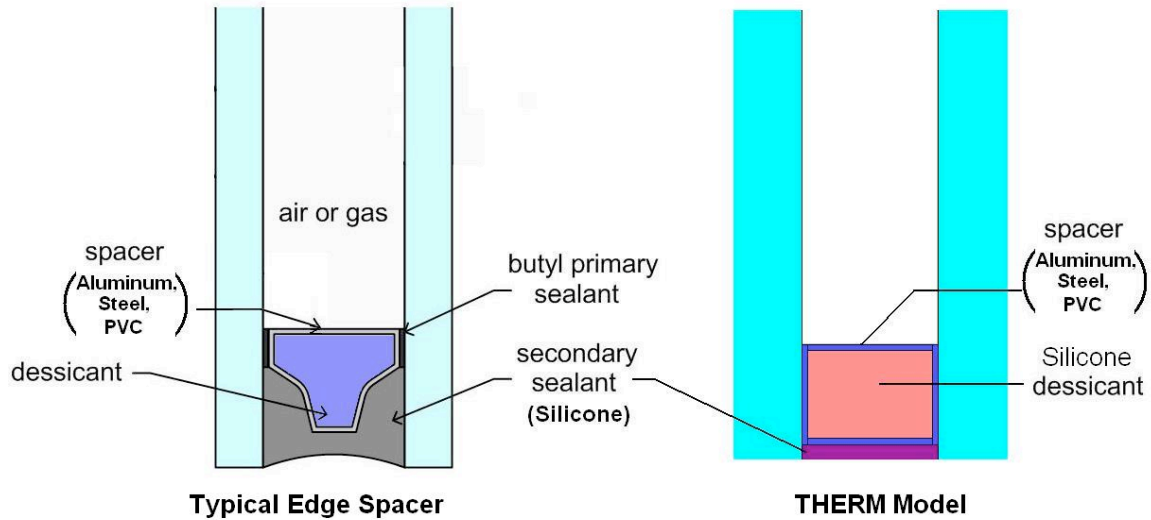


Figure 4.3.2 Comparison of typical edge spacer with THERM model

Shell spacers such as the aluminum, stainless steel, and PVC, were assumed to have a thickness of 0.50 mm and were filled with a silicone desiccant, which is representative of typical spacers of the same type, and silicone foam and EcoSpacer™ spacers filled the void completely without any desiccant, similar to that of Figure 4.1.4. The results of the THERM6 (LBNL, 2008) models are shown in Figure 4.3.3. Although the U-values of the frame do not vary significantly from approximately 13.4 W/m²K, the U-value of the edge-glass region shows reductions up to 10%, improving from 1.86 W/m²K with an aluminum spacer to 1.66 W/m²K with a PVC spacer.

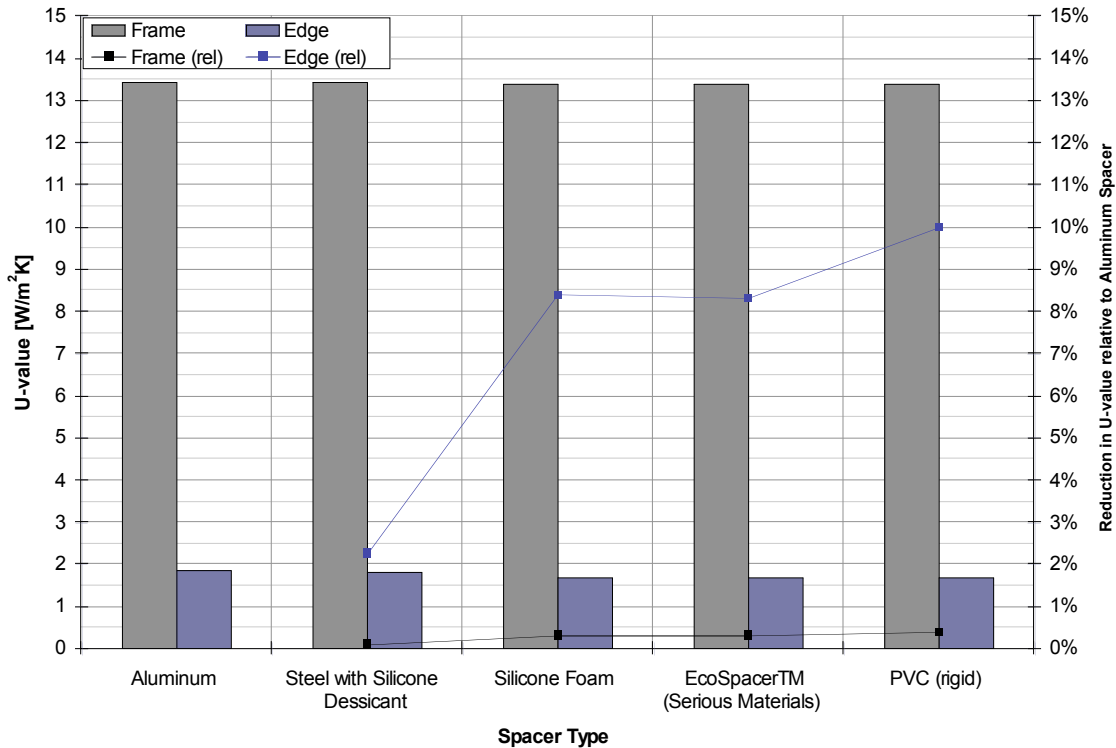


Figure 4.3.3 Frame and edge U-values with various edge spacers for double-glazed IGU (2G-2s) with a typical thermally non-broken aluminum curtain wall

It is clear from the results that the PVC edge spacer yields the greatest improvement in edge performance. This is followed by both the silicone foam and EcoSpacer™ spacer with an 8% reduction. The stainless steel spacer showed the least improvement at 2%. While the edge U-value reductions are not particularly significant, the results do suggest edge spacer construction can have some effect on the overall window assembly thermal performance.

4.3.2 Thermal Performance of Aluminum Curtain Wall Sections

Aluminum is the most popular material in curtain wall construction due to its strength, weight, and its dimensional stability for close tolerances. However, one of the major drawbacks of aluminum is its high thermal conductivity, which raises the overall U-value of the curtain wall system. Unlike other curtain walls, the thermal resistance of the aluminum frame is determined by the surface area of the frame rather than its thickness or projected area (Carmody *et. al.*, 2004). Therefore, simple compact sections will perform better than complex and larger sections. However, larger and deeper sections

can span taller heights and reduces the frame to vision glass area, providing additional benefits to sight lines and strength.

Since the dominant mode of heat transfer across aluminum curtain walls is through solid conduction, one of the most effective ways to improve its thermal performance is to replace critical components with less conductive material to act as a thermal break and interrupt heat flow. This way the thermal resistance can be improved without sacrificing any of the desired strength provided by the aluminum interior frame section. To fully understand the heat flow paths across a curtain wall section, a component study was conducted on a typical section of an aluminum curtain wall. A base model was created and individual components were changed for each case. The results of the study help determine which components are critical to improving the overall curtain wall thermal performance and for the design of a high-performance curtain wall. The sections were analyzed with THERM6 (LBNL, 2008) and Figure 4.3.4 shows a layout of the model. For comparison purposes only components were altered with no changes were made to the overall design of the curtain wall section. The components that were analyzed included:

- Insulated snap cap with Spaceloft™ insulation
- Insulated interior frame section with polyurethane spray foam
- PVC thermal break, which varied in width relative to the IGU size to maintain consistency thermally broken frames for thicker IGUs
- Fiberglass pressure plate

All of the results are summarized in this section and also listed in Appendix C1.

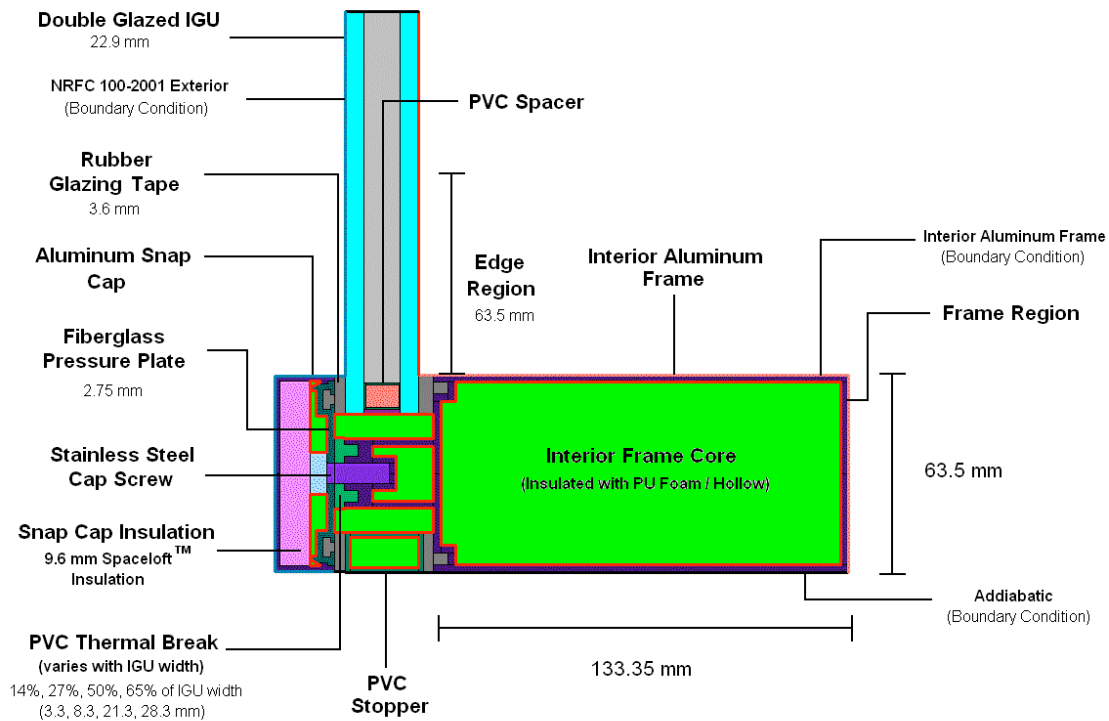


Figure 4.3.4 THERM6 (LBNL, 2008) model of aluminum curtain wall section

The impact of each individual component for each case has been plotted in Figure 4.3.5 and Figure 4.3.6. Although U-values of different sections of the frame, such as the jamb, sill, and head can differ, the variance is small; therefore, all simulation values presented in this project are from jamb sections of the frame.

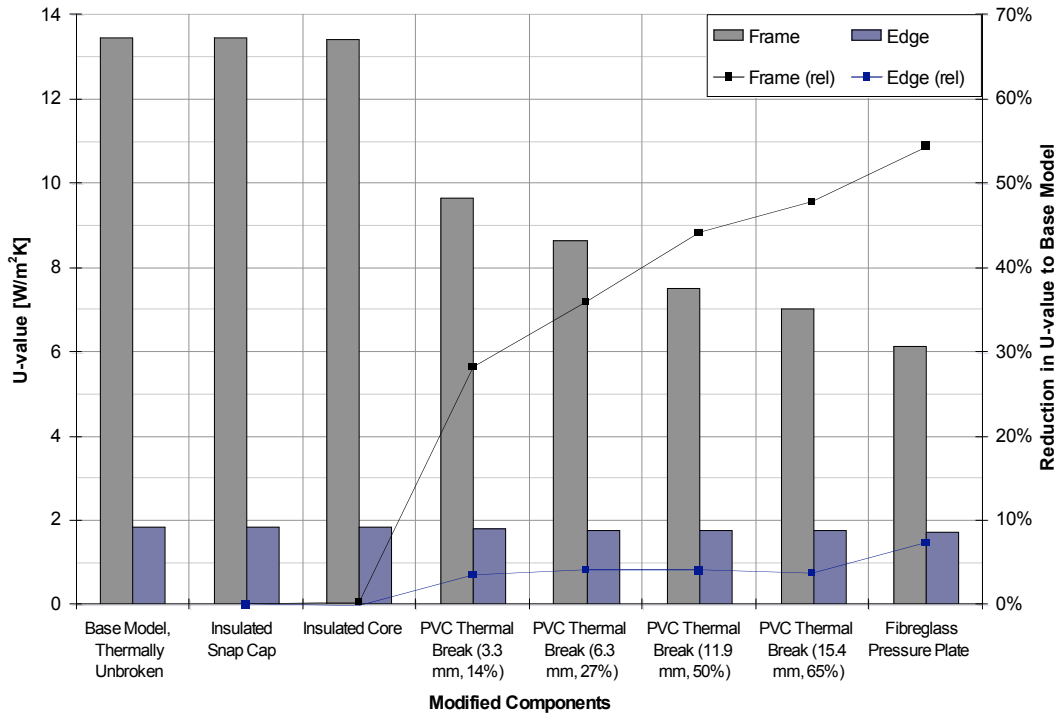


Figure 4.3.5 Evaluation of individual components on thermal performance of aluminum curtain walls with aluminum spacers for double-glazed IGUs

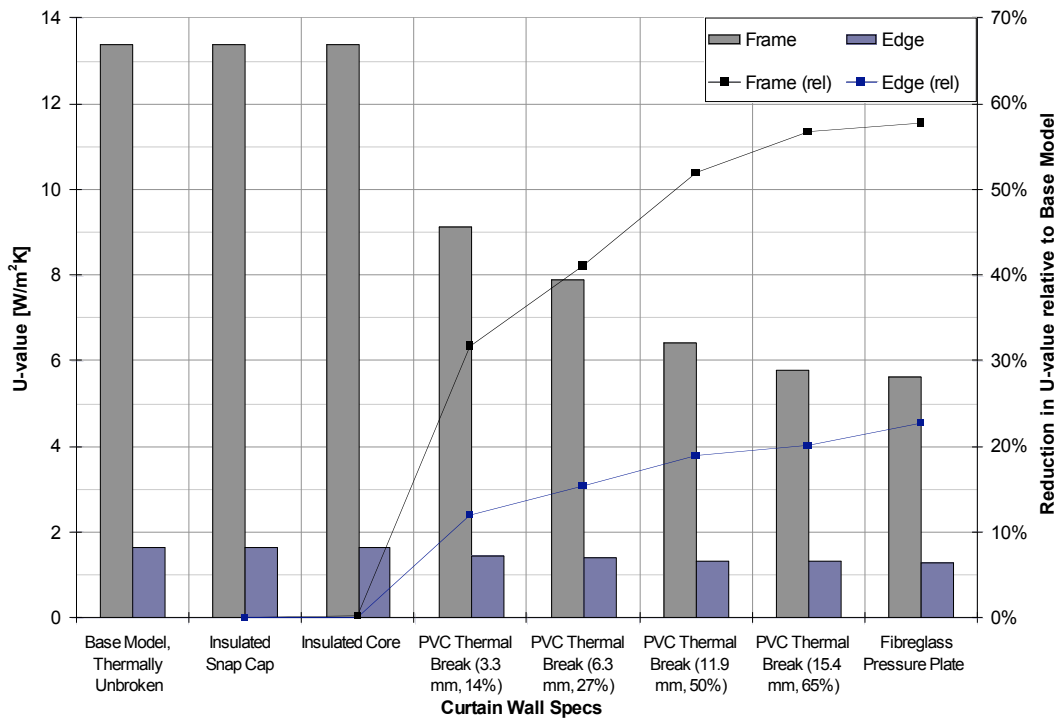
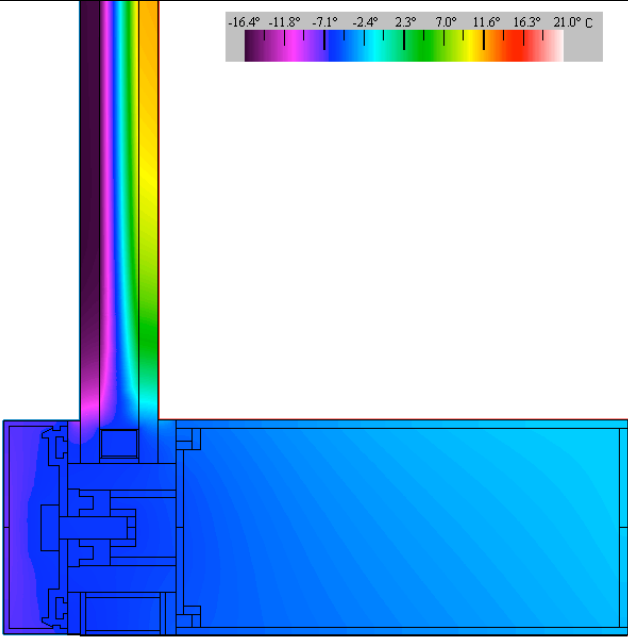
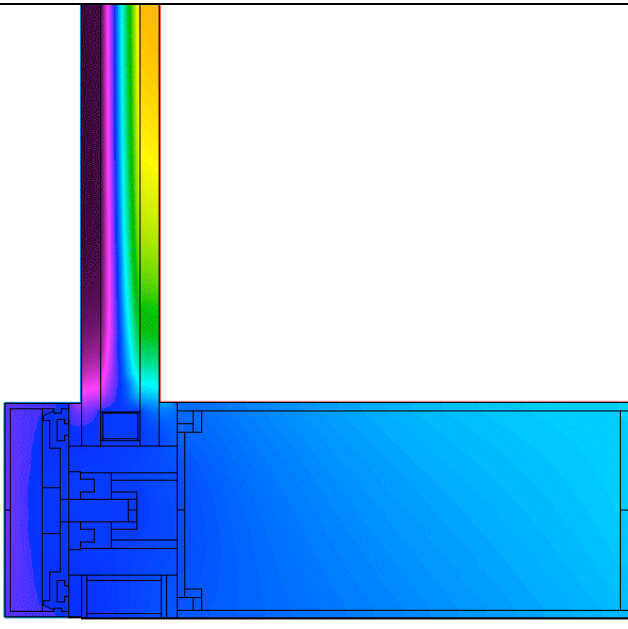
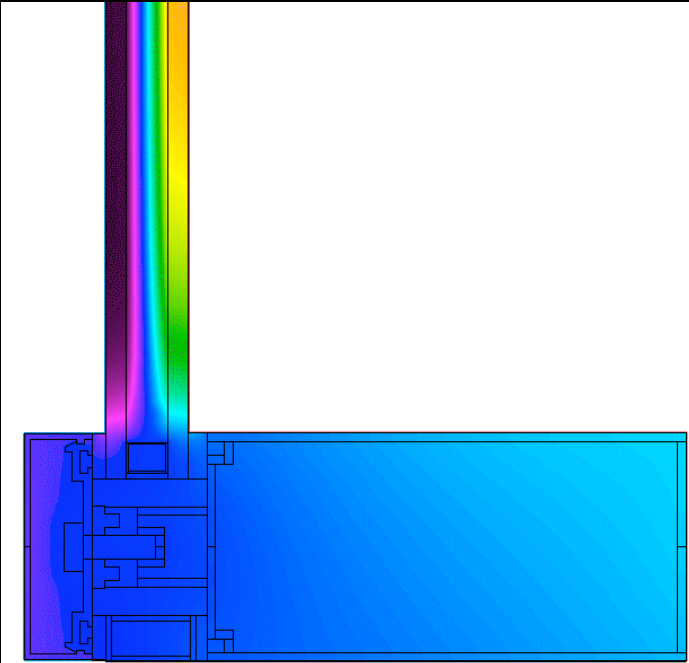


Figure 4.3.6 Evaluation of individual components on thermal performance of aluminum curtain walls with PVC spacers for double-glazed IGUs

From the component study, the following conclusions were made about each of the modifications to the frame section in regards to thermal performance and are listed in Table 4.3.2.

Table 4.3.2 Aluminum curtain wall component study conclusions

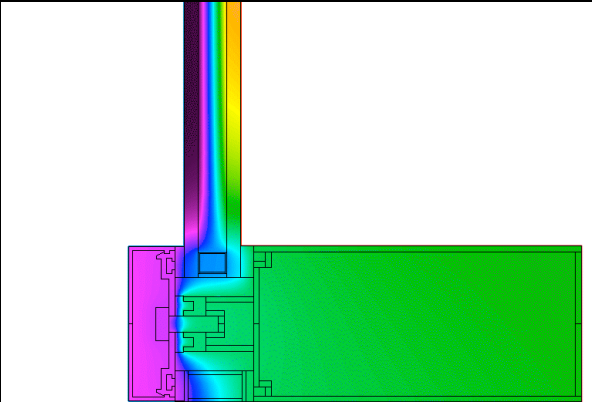
 <p>Base Model - Thermally Unbroken</p>	<p><i>Base Model, Thermally Unbroken</i></p> <p>Heat transfer through an unmodified aluminum curtain wall is pretty simple. Since there are no thermal breaks or insulating material, heat is easily conducted through the section. This can be easily seen in the temperature profile, as the section remains cool since it is able to conduct heat away easily.</p>
 <p>Insulated Cap - Thermally Unbroken</p>	<p><i>Insulated Snap Cap</i></p> <p>Providing insulation inside the snap cap insulates the pressure plate and screw head. From the results of the component study shown in Figure 4.3.5 and Figure 4.3.6, the changes in frame thermal performance are nominal. This is due to a thermal bridge between the aluminum pressure plate and snap cap, which acts as a thermal short circuit that bypasses the snap cap insulation. From the temperature profile the section resembles that of the base model.</p>



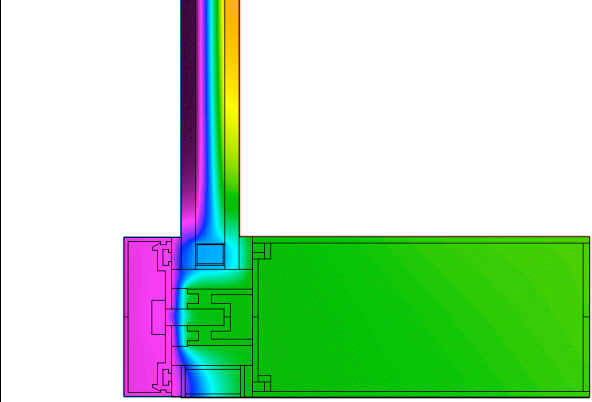
Insulated Interior Frame - Thermally Unbroken

Insulated Interior Frame (Core)

Insulating the hollow frame section with polyurethane insulation provided virtually no improvement to thermal performance, since aluminum is such a great thermal conductor it easily carries heat to the exterior. The temperature distribution of the section suggests very little change from the base model. The only potential benefit of insulating the frame section is to minimize convection cells within the frame. However, since the frame is so thermally conductive changing the convective heat transfer rate would not significantly alter its thermal performance.



PVC Thermal Break (14% of rabbet)

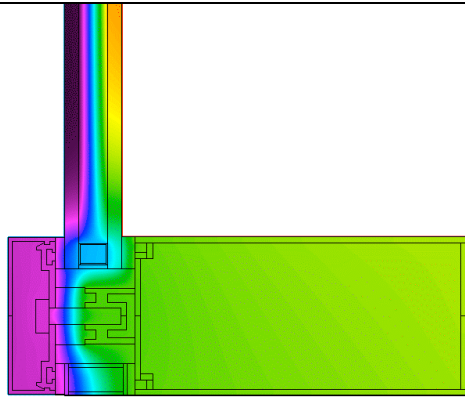


PVC Thermal Break (27% of rabbet)

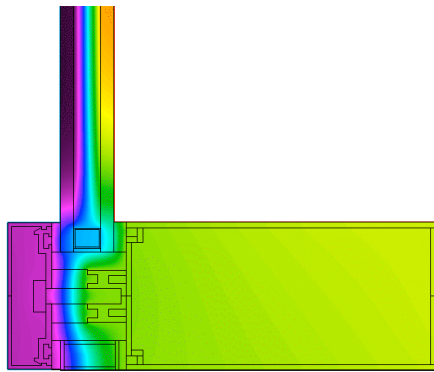
PVC Thermal Break between the Interior Frame and Pressure Plate

Thermal breaks are very important to enhancing the thermal performance of all window frames, including curtain walls. Adding a 3.26 mm thermal break, which spans 14% of the glazing rabbet, reduced the frame U-value by 28% for aluminum spacers and 32% for PVC spacers, while adding a 6.35 mm (27%), 11.9 mm (50%), 15.4 mm (65%) reduced the frame U-value by 36-41%, 44-52%, and 48-57%, respectively. The percentages of thermal breakage were determined by ratios likely used for double-, triple-, quadruple-, and quintuple-glazed IGUs.

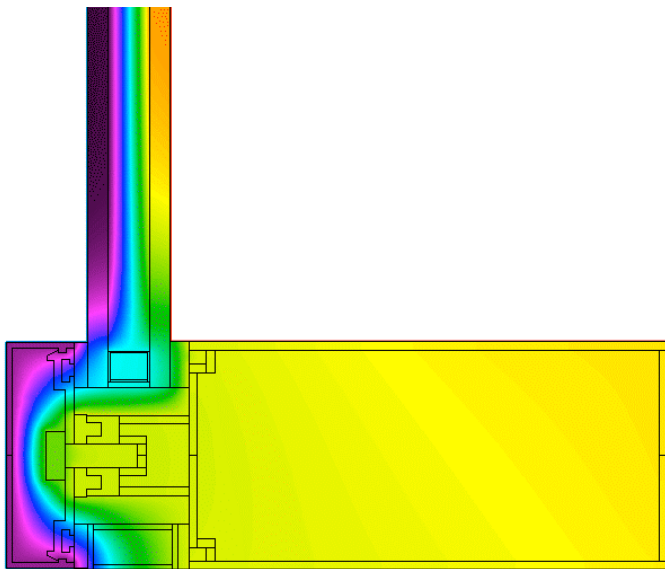
Inserting a thermal break to significantly reduce heat flow across the curtain wall section and



PVC Thermal Break (50% of rabbet)



PVC Thermal Break (65% of rabbet)



Fibreglass Pressure Plate - Thermally Unbroken

is a very effective modification. This is clearly shown by the temperature profiles as the increased in thermal break size causes warmer temperatures at the interior frame. However, the images also show there is a significant amount of heat loss across the section particularly at the edge spacer despite larger thermal breaks. Therefore, while thermal breaks significantly decrease heat flow across the glazing head, other heat flow paths still exist at the edge spacer.

Fiberglass Pressure Plate

The pressure plate is a critical component in the heat transfer of curtain wall sections, since it is in contact with the interior frame, exterior face of the glazing, and snap cap. It is part of a thermal bridge that allows heat to flow through the glazing rabbet or through the spacer itself. By switching to a less thermally conductive material such as fiberglass the overall thermal transmittance of the section can be improved by 54% with aluminum edge spacers and 58% with PVC spacers. From the temperature profile, the curtain wall section is significantly warmer as is the air cavity at the glazing rabbet.

Another significant component that has a secondary effect on performance is the edge spacer. A comparison of the relative frame and edge U-value reductions from Figure 4.3.5 and Figure 4.3.6 suggests more insulating spacers, such as PVC, yields greater reductions in U-value than less insulating spacers for the same component modifications. The PVC spacer had a +4 to +9% differential, in frame U-values, over the aluminum spacer with modifications to the thermal break, while it only held a +4% improvement with the fiberglass pressure plate. The edge U-values vary significantly with different spacers by as much as 16%. This is because the edge spacer acts as a thermal bridge over the window assembly. With only a thermal break in the glazing rabbet, heat easily flows through the spacer, thus a more insulating spacer will show greater reductions in heat flux. The performance benefit is less with fiberglass pressure plates since the insulation is placed outboard of the IGU and frame assembly which effectively blocks off most heat flow. Generally, insulating spacers will yield greater performance benefits than with highly conducting spacers and should be used in all high-performance window assemblies.

To construct a more insulating curtain wall a combination of most of these modifications will be needed. The cumulative effects of most of these modifications for double-, triple-, quadruple-, and quintuple-layered IGUs are shown in Figure 4.3.7 to Figure 4.3.10.

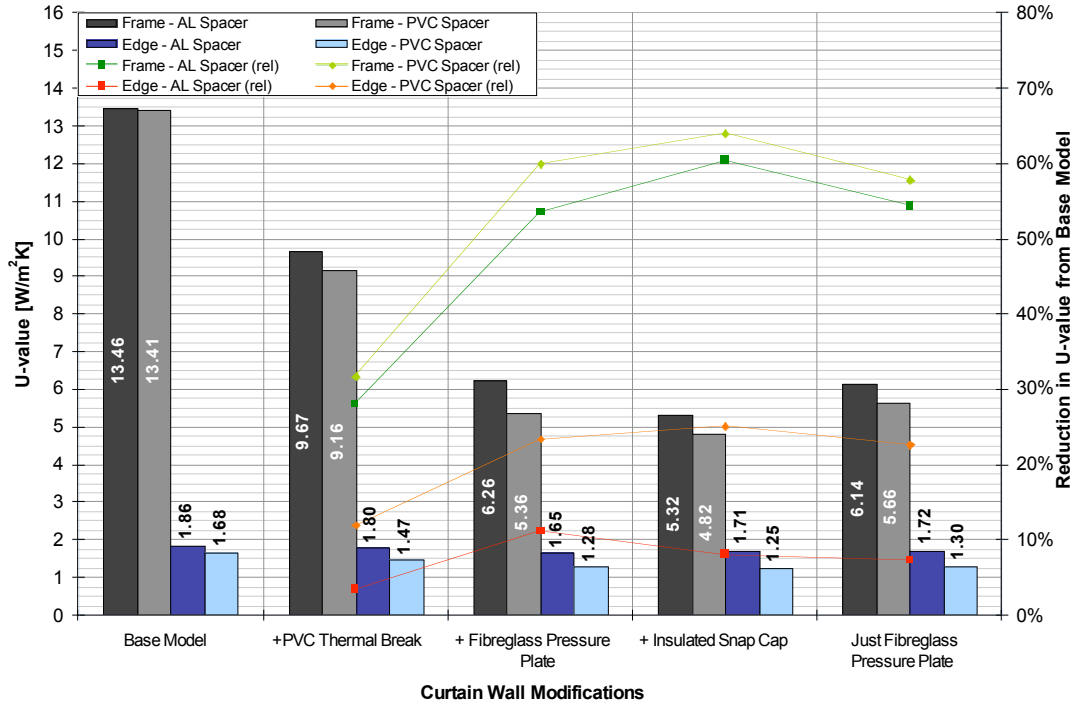


Figure 4.3.7 Frame and edge thermal performance with cumulative modifications of a standard aluminum curtain wall for a double-glazed IGU

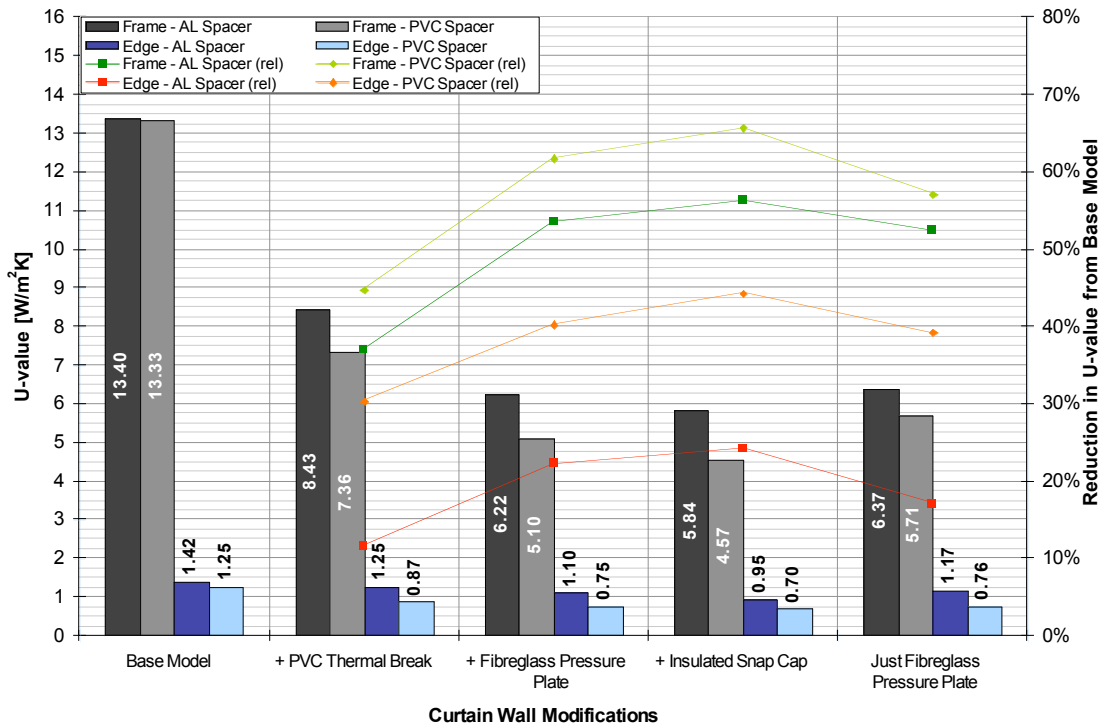


Figure 4.3.8 Frame and edge thermal performance with cumulative modifications of a standard aluminum curtain wall for a triple-glazed IGU

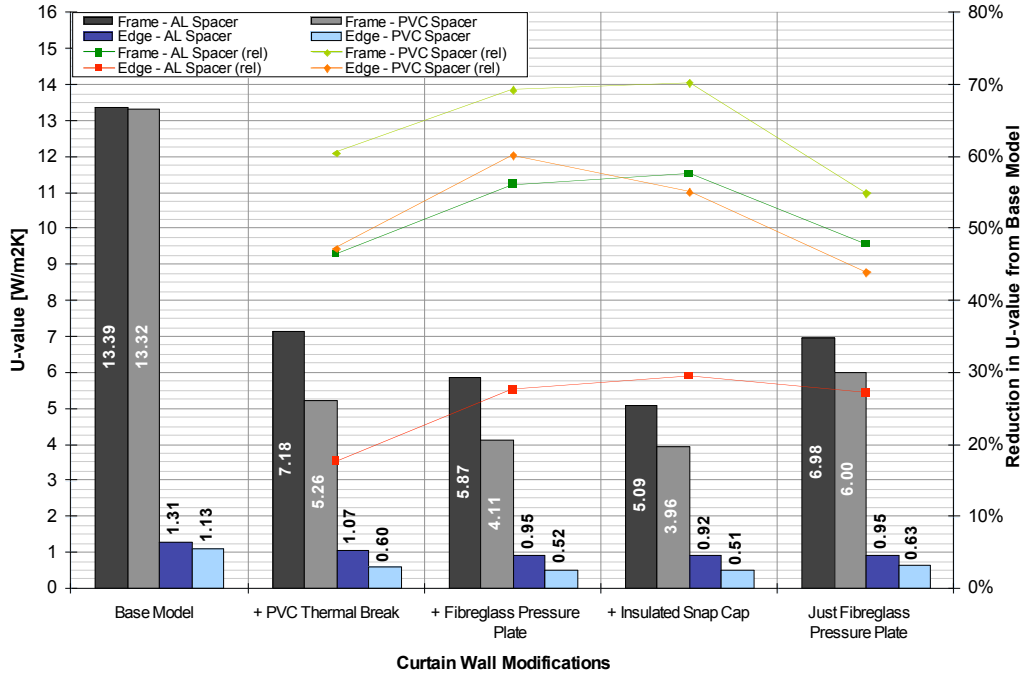


Figure 4.3.9 Frame and edge thermal performance with cumulative modifications of a standard aluminum curtain wall for a quad-glazed IGU

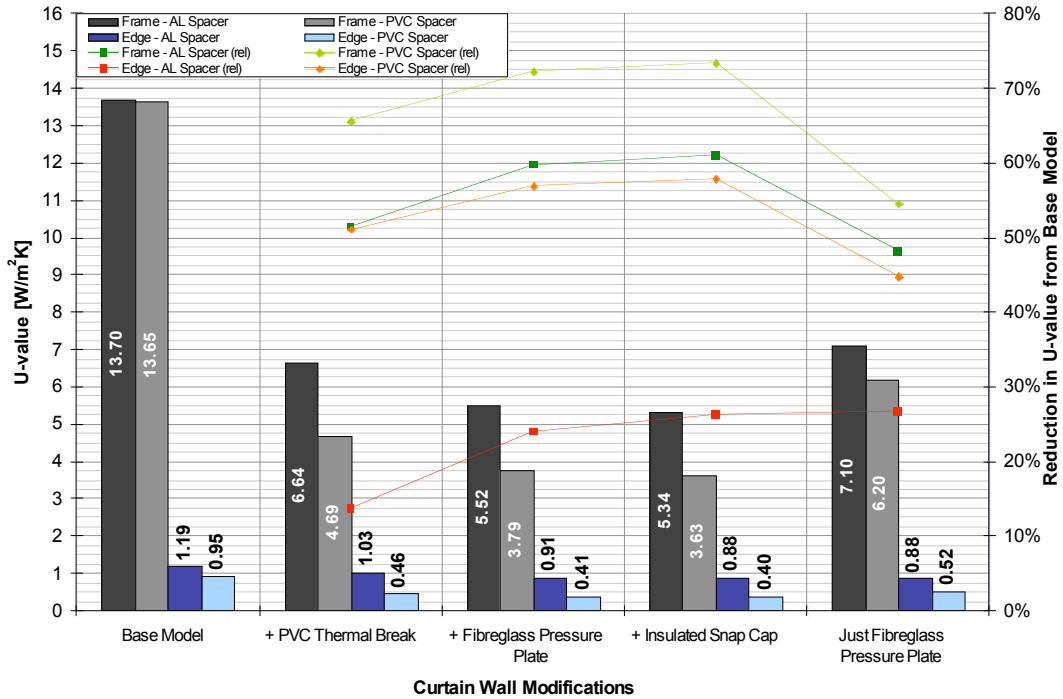


Figure 4.3.10 Frame and edge thermal performance with cumulative modifications of a standard aluminum curtain wall for a quint-glazed IGU

From Figure 4.3.7, Figure 4.3.8, Figure 4.3.9, and Figure 4.3.10 the improvements in thermal performance with each modification diminishes as more changes are made to the section. This is consistent with most insulated assemblies, as the benefit diminishes exponentially with greater levels of insulation. While the U-value continually decreases with each modification, it does so at a diminishing rate. The graphs also compare the performance of the cumulative modifications to that of switching the pressure plate from aluminum to fiberglass. The component study for a double-glazed aluminum curtain wall showed the pressure plate has the greatest performance improvement. This is true only in cases where the thermal break is relatively small, in the order of less than 3 mm or 14% of the IGU width, as with the double-glazed aluminum curtain wall section. Curtain walls that can accommodate larger thermal breaks are more effective at reducing overall heat flow. This is why most commercially available aluminum curtain wall sections have wider thermal breaks to improve its performance. Thermal breaks are particularly effective if they occupy approximately 50% of the overall IGU width within the glazing rabbet, as in the case of most triple-, quad-, and quint-glazed IGUs. However, for thinner IGUs that require smaller glazing rabbet, switching to an insulating pressure plate is more effective at improving thermal performance. The graphs also show PVC spacers tend to yield greater benefits in performance with each modification than its aluminum counterpart. This is consistent with the trends observed in the individual component study.

From the two-dimensional heat transfer study of typical aluminum curtain wall sections, a high-performance aluminum curtain wall should have the following:

- Large insulating thermal break
- Fiberglass pressure plate
- Insulated snap cap
- PVC edge spacers

These modifications will improve performance significantly. The frame and edge U-values of both typical and modified aluminum curtain walls are listed in Table 4.3.3.

However, relative to the IGU U-value, both the frame and edge U-values still remain high.

Table 4.3.3 Base and modified aluminum curtain wall thermal transmittance

IGU Type	IGU U-value [W/m ² K]	Base Model U-value [W/m ² K]		Modified Model U-value [W/m ² K]	
		Frame (Thermally Unbroken)	Edge (Aluminum Spacer)	Frame (Thermally broken)	Edge (PVC Spacer)
Double-glazed (2G-2s)	1.305 (R-4.3)	13.46 (R-0.4)	1.86 (R-3.1)	4.82 (R-1.2)	1.25 (R-4.5)
Triple-glazed (3G-5uv)	0.562 (R-10.1)	13.40 (R-0.4)	1.42 (R-4.0)	4.57 (R-1.2)	0.70 (R-8.1)
Quad-glazed (4G-5uv)	0.376 (R-15.1)	13.39 (R-0.4)	1.31 (R-4.3)	3.96 (R-1.4)	0.51 (R-11.1)
Quint-glazed (5G-2s)	0.271 (R-21.0)	13.70 (R-0.4)	1.19 (R-4.8)	3.63 (R-1.6)	0.40 (R-13.2)

4.3.3 Thermal Performance of High Performance Aluminum Curtain Wall Sections

Although a modified typical curtain wall section can significantly improve the thermal performance of aluminum curtain walls, a low U-value high-performance curtain wall should be redesigned to alter heat flow paths by substituting critical components with more insulating materials. Based on examples of low U-value aluminum curtain wall sections such as the RAICO THERM⁺ A-I series, shown in Figure 4.3.11, a high-performance curtain wall design was proposed and analyzed in THERM6 (LBNL, 2008) as part of this investigation. This newly designed section, as shown in Figure 4.3.12, is very similar to a typical aluminum curtain wall; some of its distinguishable features include a larger thermal break (from 3.3 mm to 14.8 mm) and thicker (6.35 mm) EPDM gaskets to help isolate the IGU from the aluminum frame. Given the relative performance levels achieved by curtain wall sections, any section with a frame U-value less than 5.0 W/m²K (R-1.1) is considered to be a high-performance frame in this thesis.

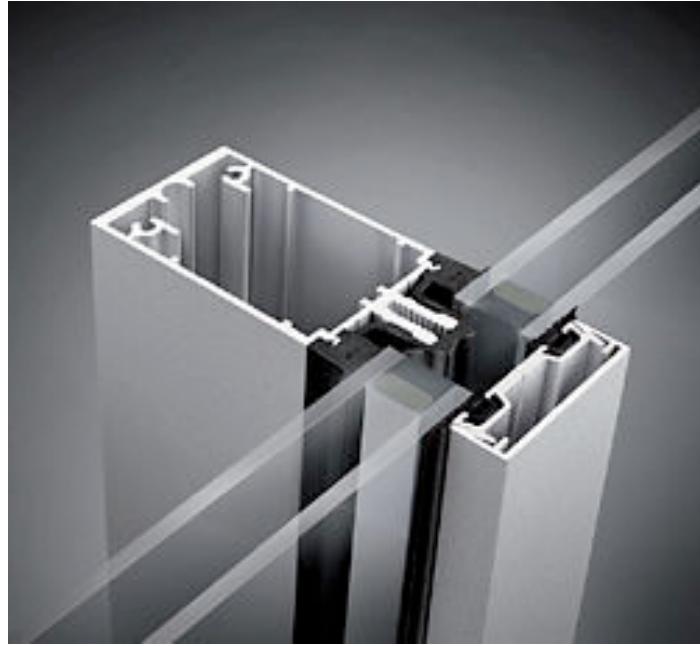


Figure 4.3.11 Photograph of RAICO THERM⁺ A-I series (Raico, 2010)

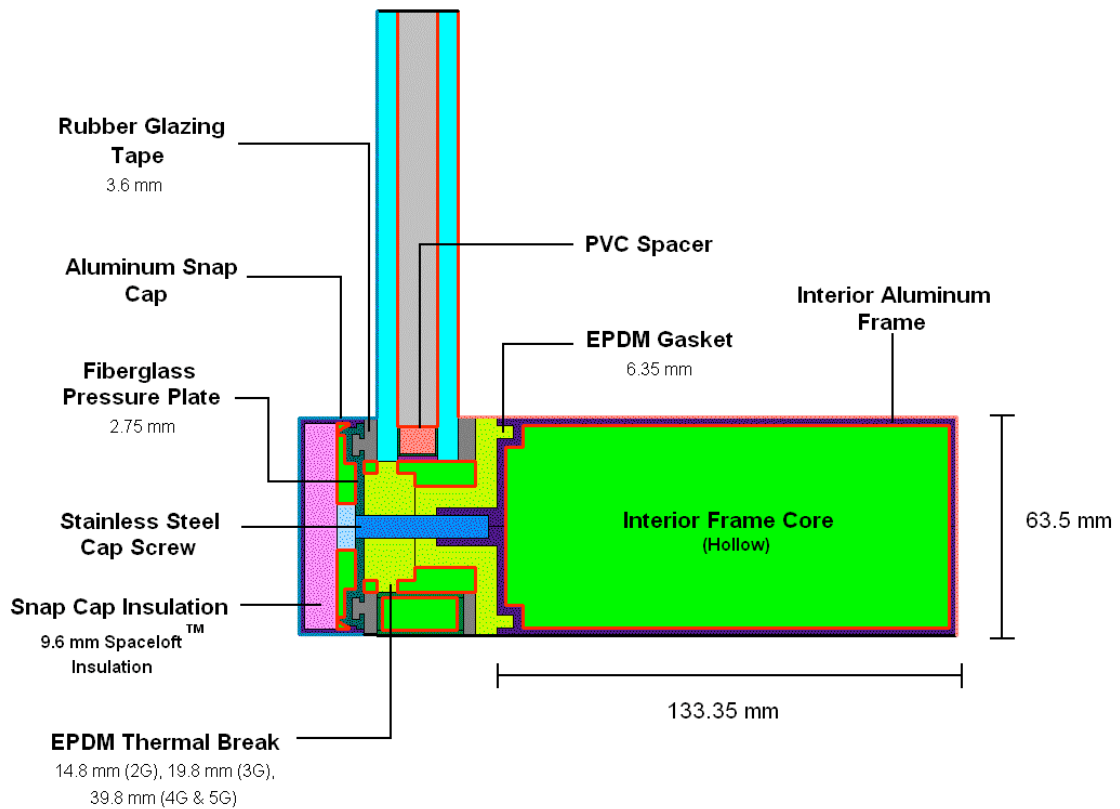


Figure 4.3.12 Proposed design of a high-performance aluminum curtain wall section

Compared to the modified aluminum curtain wall section, the proposed high-performance sections show a general improvement of 1-35% in thermal performance over its modified aluminum curtain wall counterpart, particularly when combined with thicker IGUs. This is largely attributed to the larger thermal break in the high-performance frame, which limits heat flow across the aluminum curtain wall section. Conversely, the larger thermal break did not improve the thermal performance of the double-glazed aluminum curtain wall section since the majority of heat flow is through the IGU, thus both sections showed similar performance. The edge performance values generally declined with the proposed high-performance curtain wall section since a greater amount of heat now flows through the edge region and spacer due to the limited heat flow through the thermal break. Although the edge region U-values are higher, the reductions in frame U-values are greater than the increases in edge U-value, and thus the thermal performance of the overall curtain wall system is still significantly improved with high performance frames. Similar to previous curtain wall sections, the thermal performance of this section was also evaluated by a two-dimensional heat transfer analysis program with THERM6 (LBNL, 2008) and the heat transfer characteristics can be assessed through the temperature profile the sections in Figure 4.3.13, while the insulating value of this frame is listed in Table 4.3.4. The results of simulations of high-performance curtain wall sections are also listed in Appendix C2.

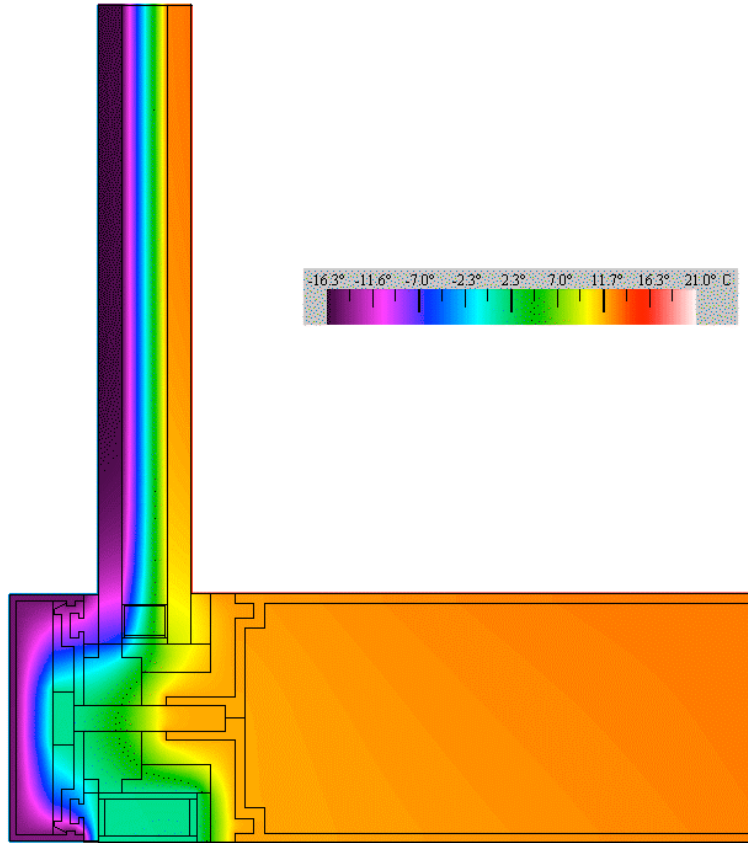


Figure 4.3.13 Temperature profile of the proposed high-performance aluminum curtain wall section, evaluated using THERM6 (LBNL, 2008)

Table 4.3.4 Proposed high-performance aluminum curtain wall thermal transmittance values

IGU Type	IGU U-value [W/m ² K]	U-value [W/m ² K]		U-value Reduction over Modified Section	
		Frame	Edge	Frame	Edge
Double-glazed (2G-2s)	1.305 (R-4.3)	4.79 (R-1.2)	1.31 (R-4.3)	1%	-4%
Triple-glazed (3G-5uv)	0.562 (R-10.1)	3.43 (R-1.7)	0.67 (R-8.5)	25%	3%
Quad-glazed (4G-5uv)	0.376 (R-15.1)	2.57 (R-2.2)	0.50 (R-11.3)	35%	1%
Quint-glazed (5G-2s)	0.271 (R-21.0)	2.81 (R-2.0)	0.44 (R-12.9)	22%	-10%

Despite the improvement in thermal performance, the U-values of the proposed low U-value high-performance aluminum curtain wall section is still relatively high, especially when compared to the low and ultra-low IGU centre-glass U-values. Therefore, to truly design a ultra-low U-value high-performance curtain wall frame another material that has better insulating properties must be sought to produce a curtain wall section that may ultimately match the U-value of high-performance IGUs.

4.3.4 Thermal Performance of High Performance Timber Curtain Wall Sections

Wood is an alternate building material that is suitable for curtain walls. Wood has been traditionally used for window frames in the past due to its highly insulating properties, strength, similar thermal expansion coefficient as glass, and workability into complex shapes required for windows. The disadvantage of wood, however, is its relatively high cost and susceptibility to rot; yet with the right design a well-built and maintained frame can be very durable.

Traditionally timber is not commonly used as a curtain wall material; instead curtain wall sections are mostly dominated by aluminum. However, with a lower thermal conductivity, timber curtain wall systems can significantly reduce the U-value of the overall façade. Because of its strength and lower thermal conductivity timber is the perfect material to provide structural support and insulation as the interior mullion. By keeping the timber mullion in the interior space of the building enclosure it is sheltered from extreme temperature swings and weathering, making it almost immune to damage. Accordingly timber mullions have been designed to withstand a standard wind load of 1 kPa (OBC, 2009) with a rated deflection of less than $L/120$. The structural analysis was done by simplifying the mullion to a simply supported beam since it will be supported at both ends by the opaque wall.

Since timber curtain walls are still a relatively new product, most exist as custom built products, there are only a few companies that have a commercially available line of timber curtain wall products. Companies such as RAICO are manufacturing timber curtain walls that have U-values as low as $0.7 \text{ W/m}^2\text{K}$ (R-8.1), which easily allows

designers to meet the Passive House standard for overall window assemblies of U-values no greater than $0.8 \text{ W/m}^2\text{K}$ (PassivHaus Institut, 2010). Figure 4.3.14 shows sections of both commercially available timber curtain wall sections from Raico and custom built sections from the North House competition house (North House, 2009). Unlike aluminum curtain wall sections, the interior mullion of a timber curtain wall is solid to provide strength against wind loads and insulation. The interior mullion can be either made of a single solid piece of wood or by combining several smaller pieces such as glue-laminated (glulam) timber, which allows for scrap wood to be used thereby making the most of timber waste products (North House, 2009). The glazing rabbet that holds the pressure plate can be milled out of wood, but in most cases is attached as a separate piece of aluminum. As with traditional curtain walls, the pressure plate can be either aluminum or fiberglass for added insulation and the snap cap can also be insulated. Since timber curtain walls can provide significantly better thermal performance than aluminum curtain walls, most of its design is a derivative of high performance aluminum sections to maximize its full performance potential. Figure 4.3.15 shows a layout of a proposed ultra-low U-value high-performance timber curtain wall section that was designed for this thesis. It was developed from similar modifications from the proposed low U-value high-performance aluminum curtain wall section.

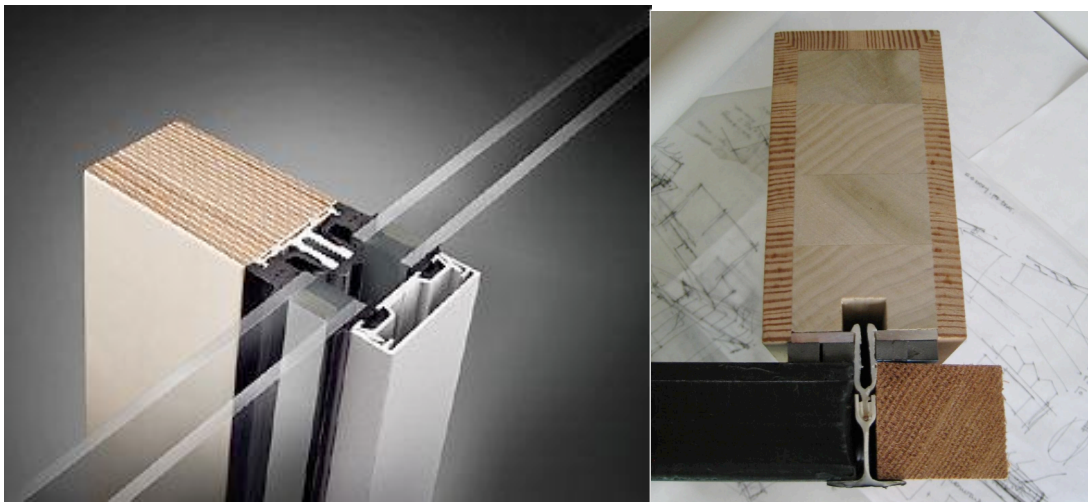


Figure 4.3.14 Left: Commercially available Raico THERM⁺ H-I / H-V timber curtain wall (Raico, 2010). Right: custom timber curtain wall from North House (North House, 2009)

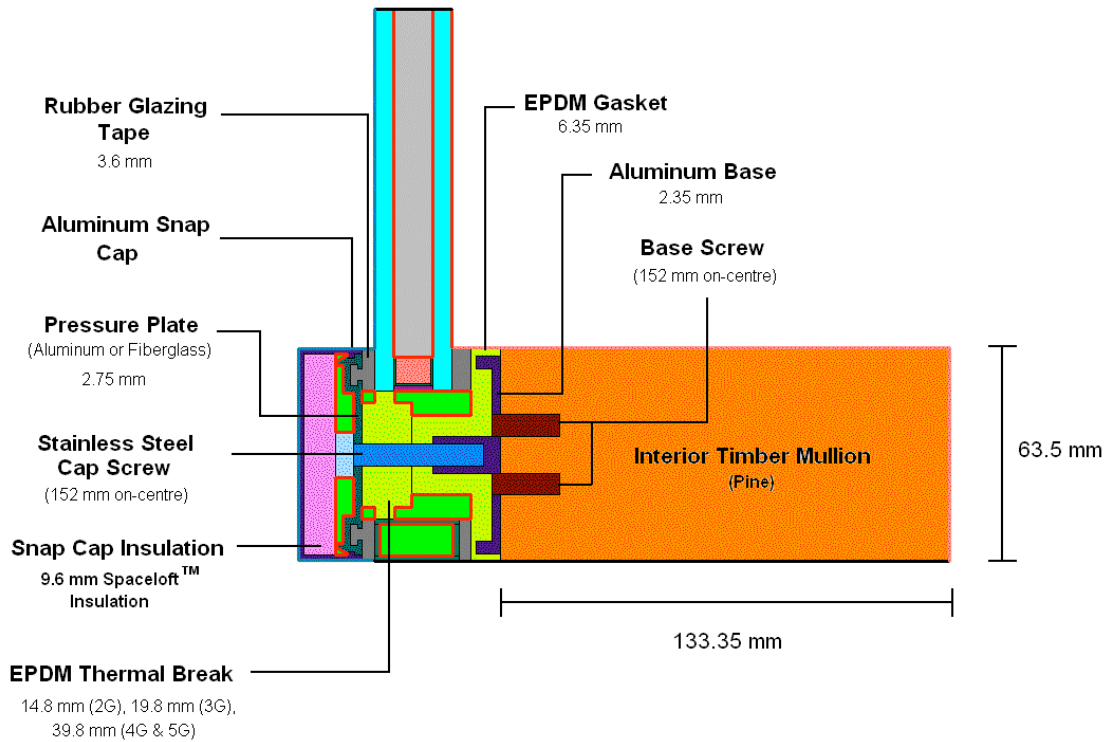


Figure 4.3.15 Proposed high-performance timber curtain wall section

A comparison between a typical aluminum, low U-value high-performance aluminum, and ultra-low U-value high-performance timber curtain wall sections is shown in Figure 4.3.16 while Table 4.3.5 compares the performance between both proposed high-performance timber and aluminum curtain wall sections across different IGU types. The advantage in performance of timber curtain wall sections is demonstrated in this figure; despite the close resemblance of the proposed timber and aluminum high-performance curtain wall sections. The improved performance is mainly due to the high insulating value of the solid pine interior frame. The temperature profile generated from the THERM6 (LBNL, 2008) model, presented in Figure 4.3.17, shows how the interior frame can affect the overall thermal performance of the frame and alternate heat flow paths. Results of the simulation are also listed in Appendix C2.

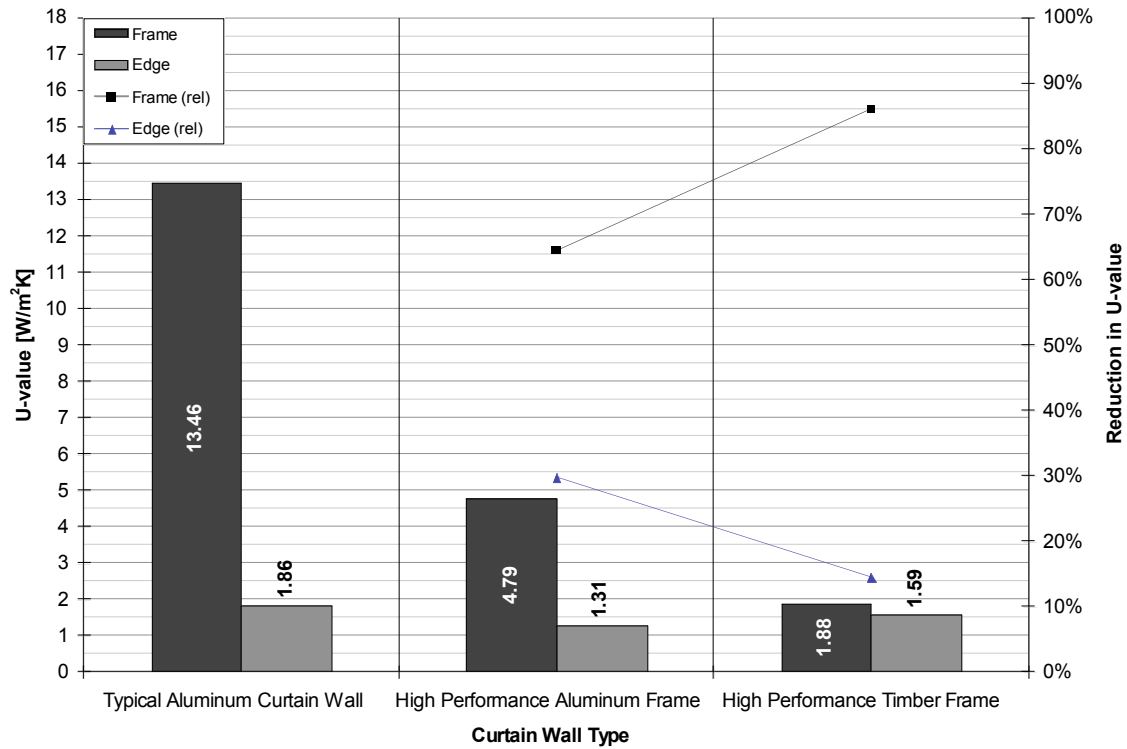


Figure 4.3.16 Comparison between typical aluminum, proposed high-performance aluminum, and proposed high-performance timber curtain wall sections

Table 4.3.5 Proposed ultra-low U-value high-performance timber curtain wall thermal performance

IGU Type	IGU U-value [W/m²K]	U-value [W/m²K]		U-value Reduction over Proposed High Performance Aluminum Section	
		Frame	Edge	Frame	Edge
Double-glazed (2G-2s)	1.305 (R-4.3)	1.88 (R-3.0)	1.59 (R-3.6)	61%	-22%
Triple-glazed (3G-5uv)	0.562 (R-10.1)	1.71 (R-3.3)	1.02 (R-5.6)	50%	-52%
Quad-glazed (4G-5uv)	0.376 (R-15.1)	1.63 (R-3.5)	0.79 (R-7.2)	37%	-56%
Quint-glazed (5G-2s)	0.271 (R-21.0)	1.62 (R-3.5)	0.70 (R-8.1)	42%	-60%

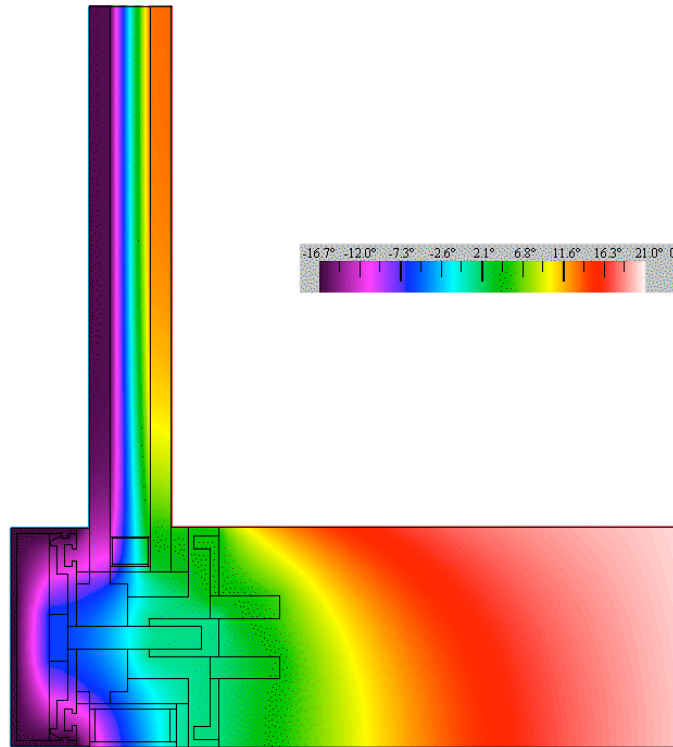


Figure 4.3.17 Temperature profile of the proposed ultra-low U-value high-performance timber curtain wall section, evaluated using THERM6 (LBNL, 2008)

Compared to aluminum curtain walls, the interior frame of the timber curtain wall is much warmer, in fact areas close to the interior are close to the interior room temperature of 21°C suggesting very little heat loss. Areas of greater temperature change and heat loss occur near the glazing plane, where the thermal break and metallic hardware is located. From the THERM analysis, the cap and base screws plays a significant role in the thermal performance of the section. The base screws extend regions of lower temperatures into the mullion, thereby allowing for greater heat flow at the glazing plane and edge regions, while the cap screw effectively conducts heat from the glazing rabbet to the insulated snap cap, thereby warming the pressure plate beyond the exterior plane of the IGU. All of this happens despite the relatively large thermal break located in-line with the IGU. The performance of this curtain wall can be improved by substituting EPDM with another alternate material that has a lower thermal conductivity, yet is stiff enough to provide adequate structural support as the thermal break.

Another area of significant influence in thermal performance is the edge spacer. A comparison of edge-glass U-values in Table 4.3.5 indicates an increase in U-value in the edge region for ultra-low U-value high-performance timber curtain walls. This is due to the highly insulating nature of the curtain wall frame, making the edge spacer the most thermally conductive part of the curtain wall system. A study of how edge spacer materials affect the overall curtain wall performance was performed in THERM6 (LBNL, 2008) and the results are summarized in Figure 4.3.18.

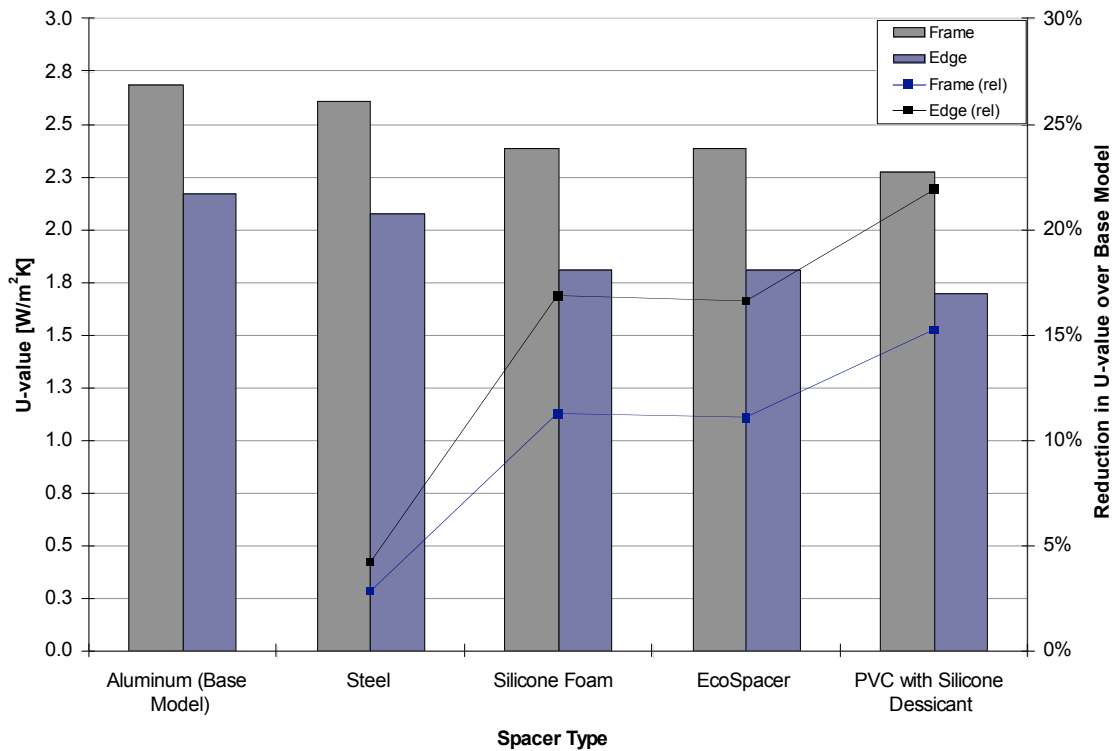


Figure 4.3.18 Evaluation of spacer types on thermal performance in timber curtain walls

Similar to aluminum curtain walls, the type of warm-edge spacers has an effect on the edge region thermal performance. However, its effect is much more significant due to the highly insulating properties of the curtain wall material. By switching to an insulating spacer, significant reductions in edge region U-values can be achieved. Consequently, as with most high-performance curtain walls, timber curtain walls should be used with highly insulating edge spacers such as PVC. From Figure 4.3.18 high performance edge spacers can improve the overall edge and frame U-values by as much as 15 to 22%.

Other components that are important to the performance of the timber curtain wall include the snap cap and pressure plate. Similar to the aluminum curtain wall, a component study was performed in THERM6 (LBNL, 2008) to assess the impact of each component. The results of that study are presented in Figure 4.3.19.

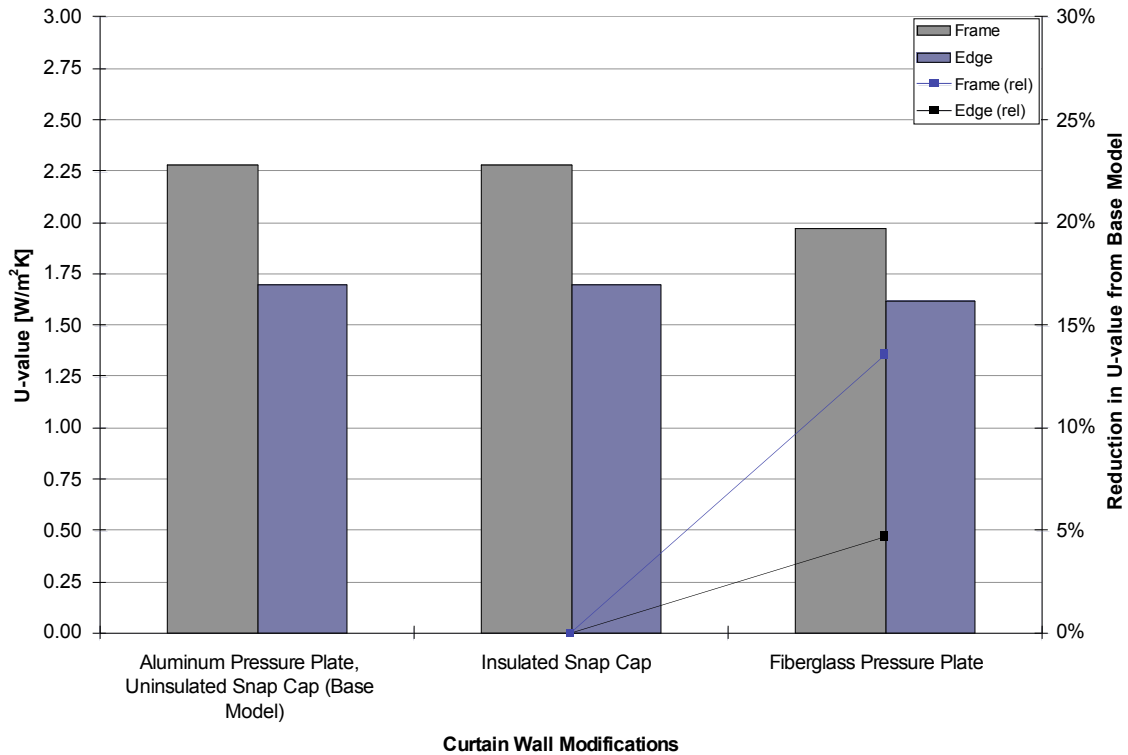


Figure 4.3.19 Evaluation of individual components on thermal performance of ultra-low U-value timber curtain walls with PVC spacers for double-glazed IGUs

From the component study, the most significant reduction in frame U-value, at approximately 14%, comes from using a fiberglass pressure plate instead of aluminum. This suggests the area of most heat transfer for this design is beyond the IGU, particularly since the frame already has a large thermal break. Adding insulation in the snap cap, however, provides very little improvement in overall thermal performance, but may protect the pressure plate from large temperature swings that can result in thermal stresses.

The results of both the component and edge spacer studies leads to the conclusion that a ultra-low U-value high-performance timber curtain wall section should have the following properties:

- Highly insulated thermal break
- Thermal (warm) edge spacers
- Fiberglass pressure plates
- Insulated snap cap

Compared to the proposed low U-value high-performance aluminum curtain wall section the proposed ultra-low U-value timber curtain wall has significantly improved thermal performance, with U-value reductions of between 37 to 61%, depending on the IGU type. However, this has lead to an increase in edge region U-values since that section of the window assembly has become the weakest point in limiting heat flow. Despite the relative performance losses in the edge region, the absolute performance gains in frame U-value still makes this design better than the best aluminum curtain wall section. Unfortunately, even with a highly insulating interior mullion, the timber curtain wall U-values do not approach the IGU U-values. As discussed in the next section, building a curtain wall system that closely matches the IGU, edge, and frame U-values is still very difficult.

4.4 Evaluation of Overall Window Assembly Thermal Performance

The overall thermal performance of the entire curtain wall system is dependent on the U-values of the frame, edge-glass, and centre-glass regions. To determine the curtain wall system U-value, the thermal transmittance of all of these components is combined as an area-weighted average, as outlined in Equation 4.4.1 (ASHRAE, 2001).

$$U_o = \frac{U_{cg} A_{cg} + U_{eg} A_{eg} + U_f A_f}{A_{pf}}$$

Equation 4.4.1

- Where:
- U_o = Overall thermal transmittance of curtain wall
 - U_{cg} = Thermal transmittance through the centre-glass (IGU)
 - U_{eg} = Thermal transmittance through the edge-glass
 - U_f = Thermal transmittance through the frame
 - A_{cg} = Total area of centre-glass region in the curtain wall
 - A_{eg} = Total area of edge-glass region, approximately 63.5 mm (2.5") from very edge of glass
 - A_f = Total area of the frame in the curtain wall system
 - A_{pf} = Area of the window assembly from frame edge to frame edge

Therefore, the thermal performance of an entire curtain wall assembly is largely dependent on its geometry. Larger glazed openings that is dominated by centre-glass area will have a lower U-value than a smaller panels that is dominated mostly by frame and edge areas since the centre-glass region typically has better performance than the edge and frame. A critical measure that can be used to help predict the performance of curtain wall systems is the centre-glass to window opening ratio (area of window measured from outer edge of frame). As shown in Figure 4.4.1, a curtain wall opening with less centre-glass to frame and edge area has a higher thermal transmittance.

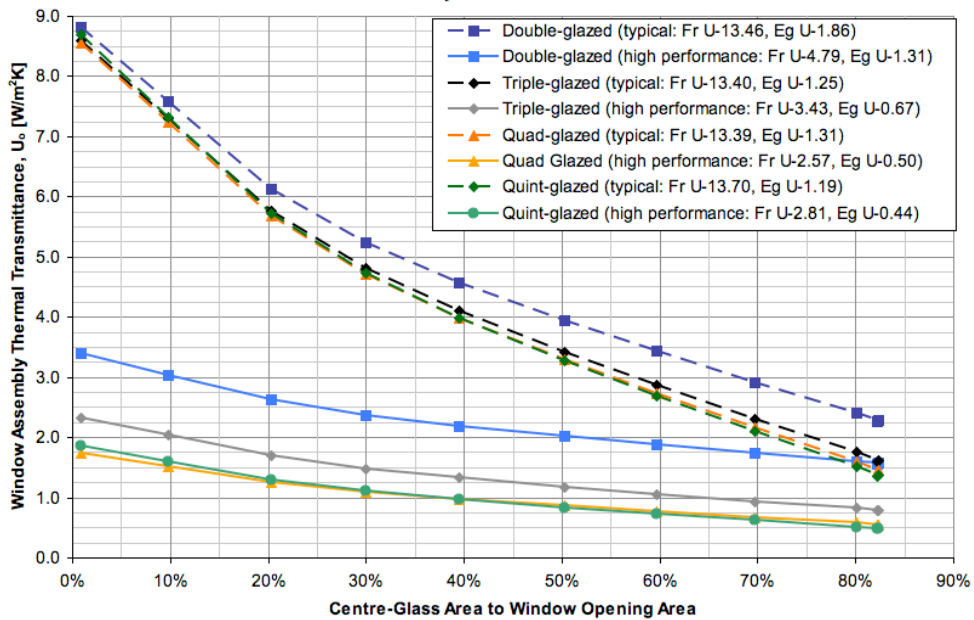


Figure 4.4.1 Overall thermal performance of curtain wall systems of varying sizes with aluminum frames

Figure 4.4.1, shows the performance of both a typical and the proposed high performance aluminum curtain wall sections for double-, triple-, quadruple-, and quintuple-glazed IGUs. As previously mentioned, all curtain wall assembly U-values decreases with increasing centre-glass area, particularly for typical aluminum curtain wall sections. The U-values are plotted against centre-glass to overall glazed panel opening area because it is a more generalized measure that is inline with thermal performance. Glazed panels can have the same opening area, yet different aspect ratios leading to differing frame and edge areas resulting in different U-values. The window opening dimensions that correspond to the centre-glass to opening ratios used in Figure 4.4.1 for a typical 63.5 mm (2.5") wide by 133.35 mm (5.25") deep curtain wall section are listed in Table 4.4.1.

Table 4.4.1 Typical curtain wall glazed panel opening dimensions

Centre-Glass : Opening	Height [mm]	Width [mm]
0.01 : 1	300	200
0.1 : 1	310	400
0.2 : 1	610	290
0.3 : 1	900	325
0.4 : 1	1200	380
0.5 : 1	1500	480
0.6 : 1	1800	620
0.7 : 1	2100	910
0.8 : 1	2400	1800
0.82 : 1	2360	2360

It is of note that the maximum opening area is 5.57 m² (60 sq ft.) due to the limiting design wind load. At this area, the centre-glass can only make up a maximum of 82% of the opening area.

With more insulating frames, the U-value curves in Figure 4.4.1 tend to flatten out, since the differences in U-values between the edge, frame, and centre-glass significantly

decreases. This is evident in the overall curtain wall assembly thermal transmittance plots for high performance timber curtain wall sections in Figure 4.4.2.

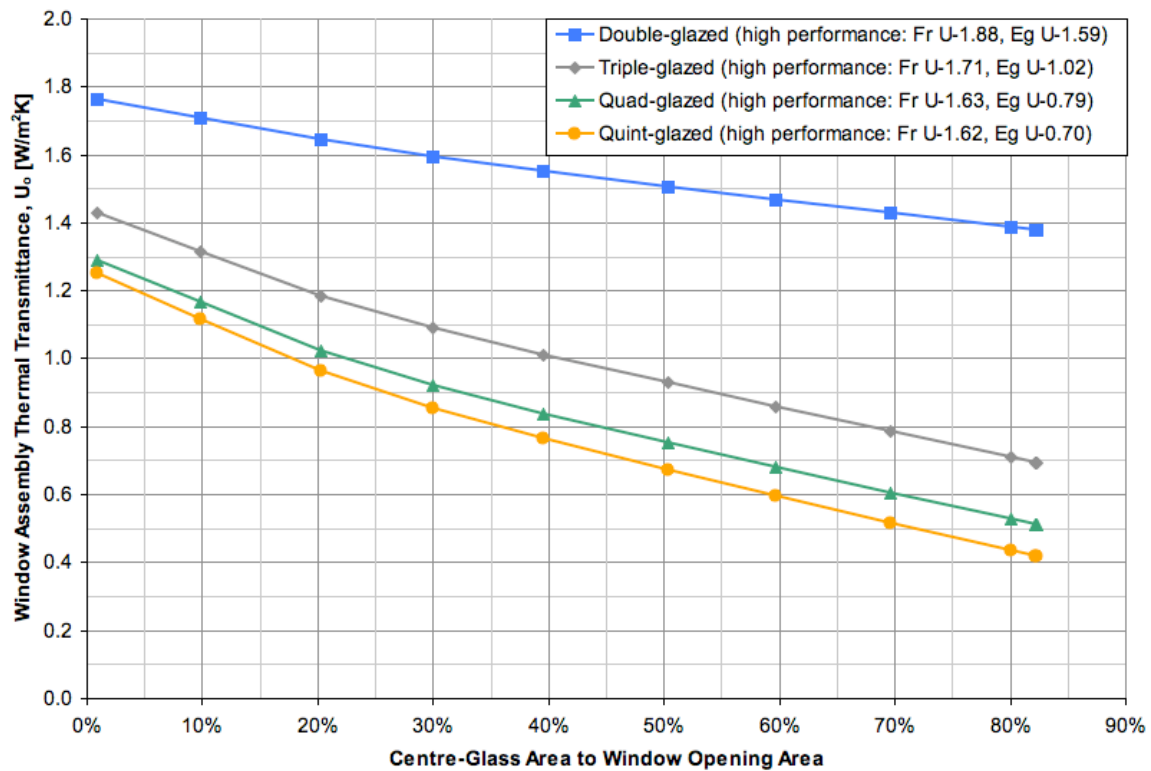


Figure 4.4.2 Overall thermal performance of proposed ultra-low U-value high-performance timber curtain walls of varying sizes

A comparison of the overall window U-values between Figure 4.4.1 and Figure 4.4.2 indicates that high-performance timber curtain wall assemblies significantly outperforms high-performance aluminum curtain wall for all glazing types. This indicates there are cases where one can design a more insulating glazed façade by pairing a less insulating IGU with a more insulating curtain wall section than combing a low or ultra low U-value high-performance IGU with a poorly insulating frame. For example, a quint-glazed IGU coupled with a non-thermally broken aluminum frame has a U-value of 3.27 W/m²K (R-1.5) at 50% centre-glass to opening ratio, while a double-glazed IGU fitted into a high performance timber curtain wall with the same dimensions has a U-value of 1.51 W/m²K (R-3.7). This is an extreme scenario, as low and ultra-low U-value high-performance IGUs should be paired with low and ultra-low U-value high-performance frames. However, in cases where it is important to balance solar gains with U-value, pairing a

less insulating IGU that has a higher SHGC with a more insulating high-performance frame may be desirable. This way the overall façade has a higher SHGC while still retaining a similar U-value. The plots also suggest that highly insulating frames and spacers are better suited for smaller windows, where frame and edge area tend to dominate. For example, in Figure 4.4.2 the high performance timber-frame double-glazed curtain wall system out performs all other regular curtain walls with non-thermally broken aluminum frames with centre-glass to opening ratio from 1% to approximate 80%.

From this analysis, it is clearly shown to design a high-performance curtain wall system that is able to match the insulating value of the IGU that it is holding is difficult, particularly for highly insulating IGUs. Even for large glazed areas and with highly insulating materials, curtain wall frames reduce the thermal performance of IGUs. Table 4.4.2 lists the centre-glass U-values with the overall curtain wall system U-values for assemblies with a maximum practical centre-glass to opening ratio of 82% (2.36 m x 2.36 m).

Table 4.4.2 Comparison of curtain wall system U-values at maximum IGU dimension

IGU Type	IGU [W/m²K]	SHGC	VT	Aluminum Curtain Wall [W/m²K]	Low U-value High- Performance Aluminum Curtain Wall [W/m²K]	Ultra-low U- value High Performance Timber Curtain Wall [W/m²K]
Double-glazed (2G-2s)	1.305 (R-4.4)	0.37	0.64	2.26 (R-2.5)	1.60 (R-3.5)	1.38 (R-4.1)
Triple-glazed (3G-5uv)	0.562 (R-10.1)	0.19	0.43	1.60 (R-3.6)	0.79 (R-7.2)	0.69 (R-8.1)
Quad-glazed (4G-5uv)	0.376 (R-15.1)	0.18	0.40	1.44 (R-4.0)	0.55 (R-10.3)	0.51 (R-11.1)
Quint-glazed (5G-2s)	0.271 (R-21.0)	0.33	0.45	1.36 (R-4.2)	0.48 (R-11.9)	0.42 (R-13.6)

With this complete analysis curtain wall systems can now be classified just as IGUs are. By incorporating the performance metrics in the IGU classification system outlined in Figure 3.2.1 a new curtain wall performance classification system can be created as shown in Figure 4.4.3.

<p>Curtain Walls with low U_o and high SHGC</p> <p>Appropriate for most solar heated buildings with low to moderate WWR in cool climates, for which solar gains are maximized while heat loss is minimized.</p> <p>($U_o < 2.0 \text{ W/m}^2\text{K}$) ($0.8 > \text{SHGC} > 0.4$)</p>	<p>Curtain Walls with high U_o and high SHGC</p> <p>Most common window type used in North America, typical of most double-glazed IGUs. This type of window is not considered to be high performance due to its poor control of solar gain and heat loss.</p> <p>($U_o > 2.0 \text{ W/m}^2\text{K}$) ($0.8 > \text{SHGC} > 0.4$)</p>
<p>Curtain Walls with low U_o and low SHGC</p> <p>Appropriate for most commercial buildings with moderate to high WWR in moderate to cool climates, for which most of the heating load during the day is met by high internal gains and solar gains are minimized during the day to avoid overheating.</p> <p>($U_o < 2.0 \text{ W/m}^2\text{K}$) ($0.4 > \text{SHGC} > 0$)</p>	<p>Curtain Walls with high U_o and low SHGC</p> <p>Appropriate for most commercial buildings with moderate to high WWR in moderate to warm climates, where the cooling load dominates over the heating load. Reducing solar gains can significantly reduce the risk of overheating as well as the annual and peak cooling loads.</p> <p>($U_o > 2.0 \text{ W/m}^2\text{K}$) ($0.4 > \text{SHGC} > 0$)</p>

Figure 4.4.3 Proposed curtain wall system performance rating system

Under this rating system most low and ultra-low U-value IGUs coupled with low and ultra-low high-performance curtain walls are rated as low U-value curtain wall systems even with smaller glazed openings, while typical curtain wall sections only achieve this rating near the maximum glazed opening. Almost all of the high-performance windows considered in this thesis are classified as low U-value and low SHGC window assemblies due to the low SHGC of the IGUs.

From this investigation, it can be concluded that the thermal performance of the edge region can be significantly improved with the use of warm-edge spacers such as PVC

spacers. Similarly, heat transfer through a typical aluminum curtain wall section can be significantly reduced with the introduction of a thermal break at the glazing rabbet and the use of a fiberglass pressure plate. In fact, the individual component study showed that the fiberglass pressure plate provide greater reductions in the edge and frame U-values than the thermal break for thinner glazing units such as double-glazed IGUs. The results from this investigation also showed there was no significant improvement in thermal performance with the use of more thermally insulating components. These findings from the typical curtain wall study have led to the design of high performance curtain wall sections made of aluminum and timber. Evaluation of both of these sections in THERM6 (LBNL, 2008) has shown that the frame U-value can be significantly reduced by more than 12 times that of a conventional non-thermally broken aluminum curtain wall. While edge and frame U-values can be significantly reduced with high-performance curtain wall sections, these U-values are still higher than that of most IGUs. The results also show that there is a definite trade off between edge and frame thermal performance. As the frame U-value decreases the edge U-value either increased or remained the same, since the edge spacer became a more and more conductive thermal bridge within the IGU as the frame became more and more thermally insulating. This suggests that the insulating value of edge spacers must be improved with the use of high performance curtain wall sections. Finally, the overall U-value of the window assembly was evaluated with the different types of IGU, frame, and edge spacer construction. This part of the study showed that the size of the window, specifically the size of the centre-glass area, plays a significant role in determining the U-value of the window assembly. Since frame and edge U-values are higher than IGU U-values, larger windows tend to have better thermal performance than smaller windows with larger edge and frame areas. However, the difference in overall U-value between larger and smaller windows are diminished as the frame, edge, and IGU U-values converge with high-performance curtain wall sections and edge spacer construction.

Despite the current technological advances, both the frame and edge regions are still the least insulating part of the overall curtain wall assembly and will diminish the thermal performance of the overall glazed façade. More research into new materials and systems

is required to help improve the thermal performance of frames and edge spacers. The results presented in this chapter regarding the typical and high-performance curtain wall section frame and edge U-values forms the basis of analysis in the next chapter, which investigates the impact of window properties on the energy performance of perimeter spaces of commercial and institutional high-rise buildings.

CHAPTER 5

Energy Performance of Perimeter Spaces and Window Systems

The energy performance of the perimeter space of most buildings is heavily dependent on the window properties. In this chapter, the effect of window properties on the energy performance of perimeter spaces of commercial and institutional buildings is examined. This discussion is divided into four sections; first as an introduction, previous research is examined to determine what are the critical properties that affect energy performance. Second, the modeling objectives and model description of an hourly based computer model in EnergyPlus (Crawley *et al.*, 2005) is introduced. The model will incorporate the findings from the previous two chapters to determine how conventional and high-performance windows affect energy performance of perimeter spaces. Finally, the simulation results of both conventional and high-performance windows are presented and discussed in two separate sections. The first section examines the effect of both U-value and Solar Heat Gain Coefficient (SHGC) on energy consumption of perimeter spaces for typical double-glazed windows to better understand which properties are critical in window design. The second section examines how the high-performance windows developed throughout the previous two chapters alters energy performance from a typical double-glazed window. The last section of the chapter then discusses how the energy performance of perimeter spaces change with solar control through external shading. All of the models presented were simulated in EnergyPlus (Crawley *et al.*, 2005).

5.1 Previous Research – Technical Review

The effect of window design on building energy performance can be very complex since energy transfer in buildings occurs in multiple ways. As a result, it is very difficult to definitively select an optimal window for a low-energy building. Much of the building energy performance that is related to windows systems depends on the following parameters:

- The local building climate
- Orientation of the façade
- The window area (window-to-wall ratio, WWR)
- Surface to floor area ratio
- The equipment operated in the building and its associated internal heat gain
- The insulation value of the opaque building enclosure (walls, roofs, floors)
- The mechanical heating ventilation and air conditioning system (HVAC)

Without detailed analysis it is very difficult for building designers to specify the optimal window system U-value and SHGC. One way of specifying these performance parameters is to evaluate energy demand through whole-building computer models, which simulate the energy consumption of a building during specified time periods and weather conditions. Although computer models do not equivocally account for all of the complex interactions of energy transfer within a building system, they do provide results that can help designers make better decisions. Computer simulations are also able to provide inexpensive and quick results that allow designers and researchers to easily make changes to the building and compare the relative differences in performance, making it a suitable tool for design and research. While full field tests may provide better results, they are often very expensive and time intensive. Many of these building simulation programs are developed with validation from laboratory measurements. With the advance of computer technology and further understanding of energy transfer in buildings, building simulation programs continue to evolve and improve with greater accuracy, making them ideal for such applications. In the past designers and researchers have used computer programs such as DOE2.0, BLAST, DaySIM, ESP-r, and EnergyPlus.

Past research has been done in assessing the impact of various window systems on building energy performance in both North America and Europe. For commercial buildings, these experiments focused on changes in annual space heating, cooling, and electrical lighting energy demand in perimeter zones. Many of these projects simulated a

typical office room located in the perimeter of a commercial building with five adiabatic sides and exterior facing wall. The orientation of the room is varied from the four cardinal directions, north, east, south, and west, all the while the WWR is being changed; shading was also included in some cases. The results of these simulations suggests what the optimal window area is for each type of window system investigated for each of the four main orientations. This information can be used to help designers in selecting the right window properties for a low-energy building.

Such simulations were performed by Carmody *et al.* (2004) for both hot and cold North American climates with a 3.0 m (10 ft) by 4.6 m (15 ft) deep second floor private office from a representative three-storey office building. The building has a floor-to-floor height of 3.7 m (12 ft) and includes a 0.9 m (3 ft) high unconditioned plenum. This model was derived from a representative office building that was developed by the Lawrence Berkley National Laboratory (LBNL) for the study of building energy consumption and the development of energy standards such as ASHRAE 90.1 (ASHRAE, 1999). The insulation values of the building enclosure was chosen from the maximum U-values in ASHRAE 90.1-1999 (ASHRAE, 1999), which varied depending on the climatic zone which the building was analyzed for. For cold climates such as Chicago and Minneapolis, ASHRAE 90.1-1999 (ASHRAE, 1999) stipulates a maximum wall U-value of $0.477 \text{ W/m}^2\text{K}$ which is approximately R-12. Although simulations were performed for both hot and cold climates, the results of the cold climate models are of particular interest to this research and are presented.

5.1.1 Window Design for Offices in Cold Climates

As part of Carmody's analysis, a set of eight window systems were evaluated for office buildings in both cold and hot climates. Since the cold climate is representative of most Canadian cities, the results of the cold climate analysis are presented. The locations used by Carmody *et al.* (2004) for cold climates are from Chicago and Minneapolis. Of the eight window systems evaluated, two represented older construction, such as single glazed windows, and were not presented in the final results. The other six window systems tested ranged from double-glazed clear windows to high-performance spectrally

selective double-glazed to triple-glazed low-E windows. All window systems were installed in a thermally-broken aluminum frame and aluminum spacers. Properties of the window systems tested are listed in Table 5.1.1; the window overall U-values are based from a 1.2 m by 1.8 m (4 x 6 ft) window.

Table 5.1.1 Properties of windows analyzed (Carmody *et al.*, 2004)

Window	IGU Type	IGU [W/m ² K]	SHGC	VT	Frame [W/m ² K]	1.2 m x 1.8 m Window [W/m ² K]
B	Double glazed, clear, air filled	2.73 (R-2.1)	0.70	0.78	5.68 (R-1.0)	3.41 (R-1.7)
D	Double glazed, with reflective coating, air filled	2.27 (R-2.5)	0.17	0.13	5.68 (R-1.0)	3.07 (R-1.8)
E	Double glazed, low-E, bronze tint, air filled	1.87 (R-3.0)	0.44	0.44	5.68 (R-1.0)	2.78 (R-2.0)
F	Double glazed, spectrally selective low-E and tint, air filled	1.65 (R-3.4)	0.29	0.53	5.68 (R-1.0)	2.62 (R-2.2)
G	Double glazed, spectrally selective low-E clear, air filled	1.65 (R-3.4)	0.38	0.71	5.68 (R-1.0)	2.61 (R-2.2)
H	Triple glazed, low- E, clear, air filled	0.85 (R-6.7)	0.26	0.46	1.99 (R-2.9)	1.14 (R-5.0)

These windows were tested at five window sizes, specifically 0.0, 0.15, 0.30, 0.45, and 0.60 WWR, with the window head height set at 2.74 m (9ft) flush with the finished ceiling for all WWRs, except for 0.15 WWR. Exterior shading in the form of both overhangs and fins were also included in some cases. The depth and width of the overhangs and fins were designed to provide complete shading during the cooling season and were constrained to depths deemed acceptable by standard practice for a south-facing

window (Carmody *et al.*, 2004). The arrangement of the window and exterior shading are shown in Figure 5.1.1.

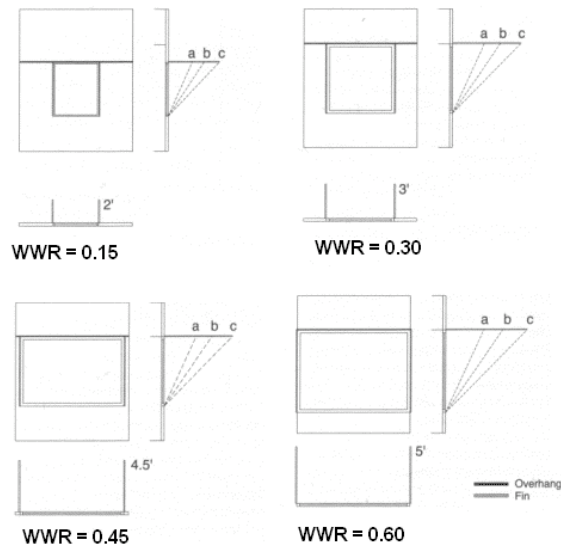


Figure 5.1.1 Window and exterior shading arrangement (Carmody *et al.*, 2004)

Interior shading was also included in the model along with dimmable auxiliary lighting. The interior shades were deployed once the glare index exceeded 22, beyond the "just uncomfortable" rating recommended for general office work, while the electrical lighting system was modeled with recessed fluorescent lighting and had a lighting density of 13 W/m² (1.2 W/ft²), as stipulated by ASHRAE 90.1-1999 (ASHRAE, 1999). Daylighting controls were set to continuously dim the lights in order to maintain an illuminance level of 538 lux (50 foot-candles) at the 0.762 m (2.5 ft) work plane height. The interior temperature was set at a heating set point of 21.1°C (70°F) and a cooling set point of 23.9°C (75°F) during occupied hours, with nighttime set backs of 12.8°C (55°F) for heating, and 37.2°C (99°F) for cooling. The results of the analysis were reported in terms of total annual energy load and peak power demand per square foot of perimeter floor area, along with other performance metrics that are relevant to the other performance criteria.

Results of the annual energy analysis indicate for most windows and most orientations the optimal WWR is between 0.15 and 0.30 is consistent with most other studies such as

Poirazis *et al.* (2007), Yu *et al.* (2008), and ASHRAE (2004). These results are summarized in Figure 5.1.2 and suggest the following:

- The optimal WWR for east- and west-facing orientations is 0.15 unless a window with a low overall U-value and SHGC, such as Window H is used, in which case optimal WWR is expanded to 0.30. Windows with lower SHGC such as Windows D and H tend to have better annual energy performance.
- Exterior shading has the greatest affect on the energy consumption of east-, west-, and south-facing windows. For east- and west-facing façades, shading significantly lowers the energy consumption at the optimal WWR, while for south-facing façades, exterior shading can not only reduce the annual energy consumption but also alter the optimal WWR. Windows of moderate to low U-values, such as Windows E through H, can increase the WWR by 0.15 with the addition of exterior shading. Shading has little to no effect for north-facing windows.
- The north-facing façade seems to be the most benign, as energy consumption does not vary significantly with increasing WWR, particularly with well-insulated windows such as Window H.
- The annual energy consumption of windows with different SHGC, but of the same U-value, such as Windows F and G, varies slightly. With SHGCs of 0.27 and 0.34 for Windows F and G, respectively, the annual energy consumption of Window F is only slightly less than Window G, due to the high internal gains of a typical office. Both windows showed similar trends with increasing WWR at all four orientations.
- Windows with low SHGC, yet high U-values such as Window D do not have an optimal WWR in which the overall energy consumption is lower than the base

0.0 WWR case. However, when compared to other windows the energy consumption is reduced for larger WWRs, particularly for WWR 0.45 or greater.

- The best performing window for all orientations is Window H, which has a low U-value and low SHGC. The energy consumption of the office with windows is less than the base case of WWR 0.0 for all window areas tested. This is a case in which high-performance window enhances the energy performance of buildings.

The results also suggest that U-value has a greater influence on annual energy performance than the SHGC for commercial buildings in northern climates. A comparison of the energy performance between windows with different SHGC and the same U-value, such as Windows F and G, showed minimal differences in energy consumption, while comparing windows with similar SHGC yet different U-values, such as Windows D and H, show significant differences in energy performance. With a longer heating season in northern climates and the very low thermal insulation value of most windows, heat loss is still a significant problem. Lower U-values alone, can alter the optimal WWR, while lower SHGC reduces energy consumption at the same optimal WWR. Only when the U-values between windows are similar, does the SHGC affect the annual energy consumption.

For peak energy consumption however, the trends are significantly different. While small WWRs are preferable, the optimal WWR varies between 0.0, 0.15, and 0.30 depending on the SHGC. Windows with lower SHGC only show a significant increase in peak energy demand for larger WWRs, of 0.45 and greater, for north- and south-facing façades and 0.30 for east- and west-facing façades. The effect of U-value on peak energy performance is minimal, since conditions of peak energy demand only occur during high solar periods from unwanted solar gains driving up peak cooling demand. Exterior shading is very effective at reducing peak energy demand for all windows and all WWRs for all orientations. The peak energy loads for commercial buildings in northern climate are summarized in Figure 5.1.3. The results from Figure 5.1.2 and Figure 5.1.3 suggest that a high-performance façade for a commercial building located in a northern climate

will likely require a highly insulated window of moderate window area of approximately WWR 0.30, and exterior shading.

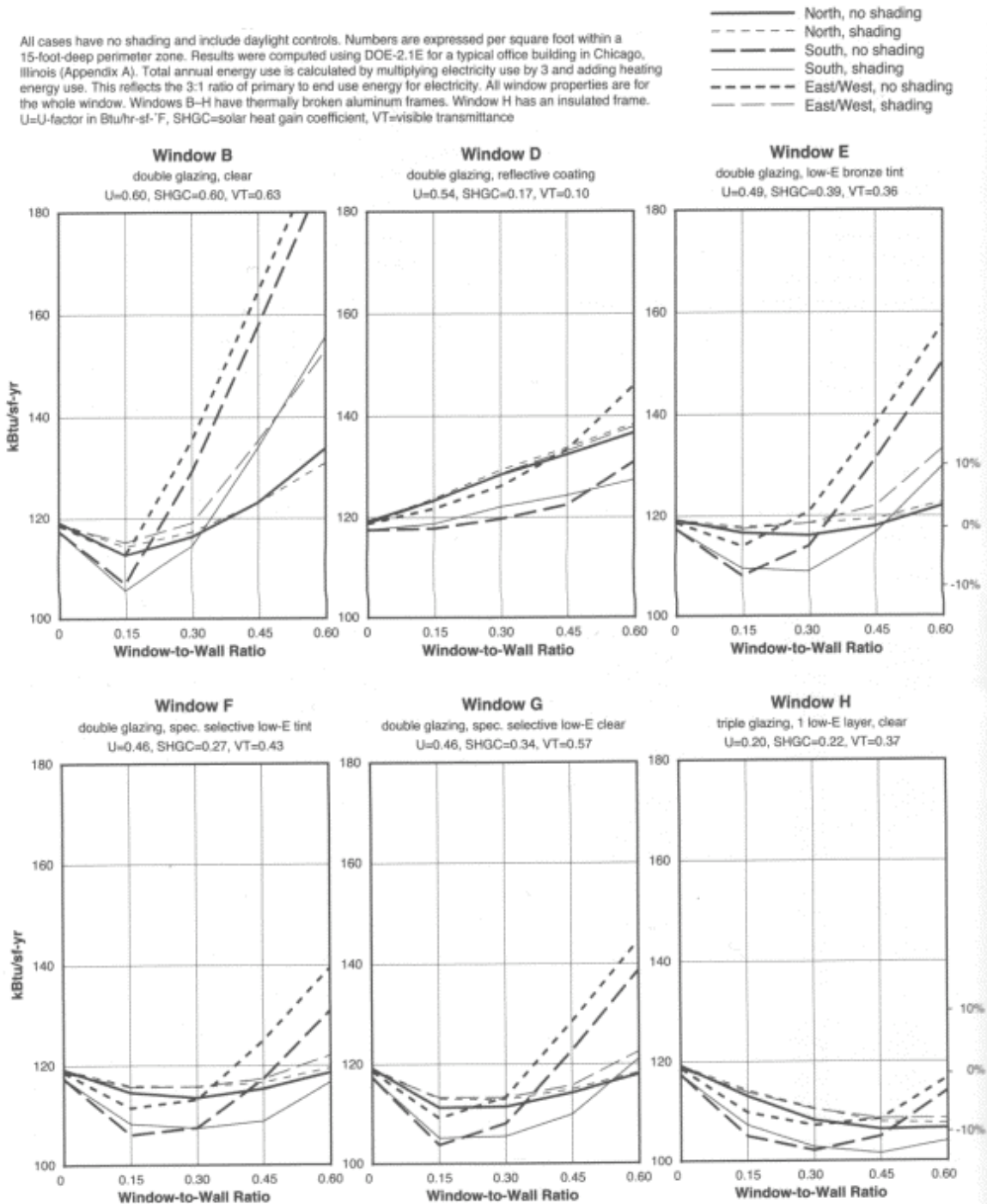


Figure 5.1.2 Annual energy consumption of various window types for all orientations in a northern climate (Carmody *et al.*, 2004)

All cases have no shading and include daylight controls. Numbers are expressed in Watts per square foot within a 15-foot-deep perimeter zone. Results were computed using DOE-2.1E for a typical office building in Chicago, Illinois (Appendix A). All window properties are for the whole window. Windows B-H have thermally broken aluminum frames. Window H has an insulated frame. U=U-factor in Btu/hr-sf-F, SHGC=solar heat gain coefficient, VT=visible transmittance

- North, no shading
- - - North, shading
- South, no shading
- - - South, shading
- - - East/West, no shading
- - - East/West, shading

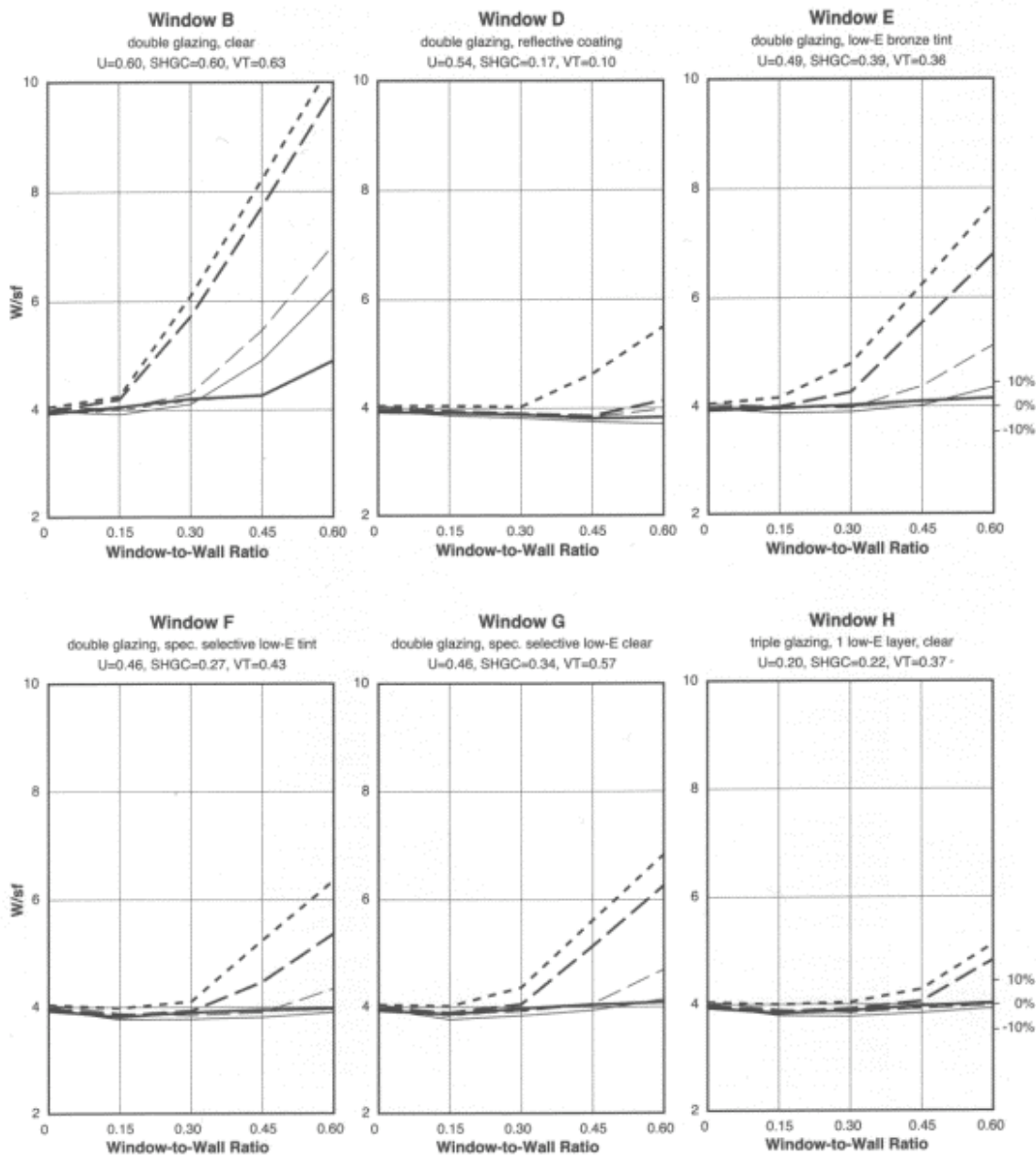


Figure 5.1.3 Peak energy consumption of various window types for all orientations in a northern climate (Carmody *et al.*, 2004)

5.2 Modeling Objectives and Parameters

5.2.1 Modeling Objectives

In order to fully assess the impact of high-performance windows on energy consumption in a typical commercial building, building simulation models were developed and their results were analyzed. The primary objective of the building simulations is to quantify and understand the effect of window performance indices on peak and annual building energy performance specifically space heating, sensible space cooling, and electrical lighting demand. The effect of these different window performance indices was evaluated for different orientations and window areas. In addition, secondary effects that can alter building energy performance such as static and dynamic shading were also evaluated. The results of these simulations should provide reference to designers in for creating an energy-efficient building enclosure for commercial buildings in a mixed northern climate such as southern Ontario. These results are meant to be used for comparison only between different window types analyzed in this thesis, since the actual overall and peak energy consumption will greatly depend on the insulation value of the actual building enclosure and the mechanical system in the building along with the different occupancy schedules and set-points.

The results of the analysis aim to specifically determine:

- The importance of overall window U-value and SHGC to building energy performance
- The effect of internal loads on total and peak energy consumption
- The effect of window area and orientation on building energy performance
- The effects of both static and dynamic shading on building performance

5.2.2 EnergyPlus Description

Similar to previous studies such as Carmody *et al.* (2004), the assessment of various window systems on space heating, sensible cooling, and lighting energy, is done using computer simulations of a typical office. All of the energy simulations are done annually for a typical office located in Toronto, Ontario, using EnergyPlus.

EnergyPlus (Crawley *et al.*, 2005) is a modular, structured software tool based on the popular features of BLAST¹ (Building Systems Laboratory, 1999) and DOE-2.1E² (Winkelmann *et al.*, 1993). It is a simulation engine, designed to provide integrated simulations for accurate temperature and comfort predictions by calculating loads via a heat balance engine at a user-specified time step, which is then passed to the building systems simulation module to determine the heating and cooling system and plant and electrical system response. Both modules can run on different time steps, allowing for a more detailed analysis. Using this approach, EnergyPlus (Crawley *et al.*, 2004) is able to come up with more accurate space temperature predictions, which may be important for system and plant sizing, occupant comfort and health calculations. This integrated simulation also allows users to better evaluate realistic system controls, as well as better hygrothermal analysis of building elements including moisture adsorption and desorption and advanced HVAC systems such as radiant heating and cooling and interzone air flow (Crawley *et al.*, 2005).

All of the thermal analysis of EnergyPlus (Crawley *et al.*, 2004), specifically, the heat and mass balance calculations are based on IBLAST, which is a research version of BLAST (Building Systems Laboratory, 1999) that is capable of performing integrated HVAC systems and building load simulations. Heat balance calculations are performed by the heat balance module, which manages both the surface and air heat balance submodules and acts as an interface to the building simulation manager. The surface heat balance module simulates inside and outside surface heat balances, including boundary conditions, conduction, convection, radiation, and mass transfer effects, while the air mass balance module simulates the effects of mass streams, specifically ventilation and exhaust air and infiltration, accounting for zone air thermal mass and direct convective heat gains (Crawley *et al.*, 2005). Similarly, all of the window and daylighting models are inherited from DOE-2.1E (Winkelmann *et al.*, 1993), where fenestration performance is based on WINDOW5 (LBNL, 2003) calculations and daylighting analysis is based on

¹ BLAST is a popular energy simulation program that is used to investigate the energy performance of new or retrofit building designs by determining energy loads and matching it with a Central Plant system.

² DOE-2.1E is suitable at predicting hourly energy use and cost of a building using hourly weather information, building geometry, HVAC description, and the utility rate structure. It is one of the most popular simulation engines to date and is used for a wide variety of programs.

the split-flux interreflection model and anisotropic sky models. This detailed daylighting model allows EnergyPlus to accurately predict interior daylight illuminance, glare from windows, glare control, and electric lighting controls, such as on/off, stepped, and continuous dimming, and determine the electric lighting reduction for the heat balance module (Crawley *et al.*, 2005). The combination of these modules makes EnergyPlus (Crawley *et al.*, 2004) an ideal tool for analyzing the effect of heat balance and daylighting of various window systems.

5.2.3 Model Description

The model created in EnergyPlus (Crawley *et al.*, 2004) is representative of a typical office building that is similar to the building used by Carmody *et al.* (2004). The building is located in Toronto, Ontario, and uses weather data of the same location from CWEC, which contains hourly weather observations representing an artificial one-year period specifically designed for building energy calculations. Toronto was chosen as a suitable climate zone since it features equally long heating and cooling season, with temperatures ranging from approximately -25°C to $+35^{\circ}\text{C}$. This range of temperature fluctuation for a sustained period of time is unmatched by most climates in Canada. In addition, the southern Ontario area is one of the most densely populated regions in Canada, thus research relevant to this area can have the greatest impact on future building design. The following is a brief description of the model, further the details can be found in Appendix D1.

Rather than consider an entire building, this study, like Carmody *et al.* (2004), focuses on a single representative office that may be repeated many times through a building. The office is 2.75 m (9 ft) wide by 4.65 (15.3 ft) deep, with a floor-to-floor height 3.75 m (12.3 ft) and a 1 m (3.3 ft) tall unconditioned plenum, leaving a floor-to-ceiling height of 2.75 m (9 ft). It is intended for a single occupant and is representative of a typical office located in the perimeter zone of a commercial building as shown in Figure 5.2.1. The model is also characteristic of an intermediate-level office that can be located on any floor other than the ground and top floor, with five adiabatic sides and one exterior-facing wall.

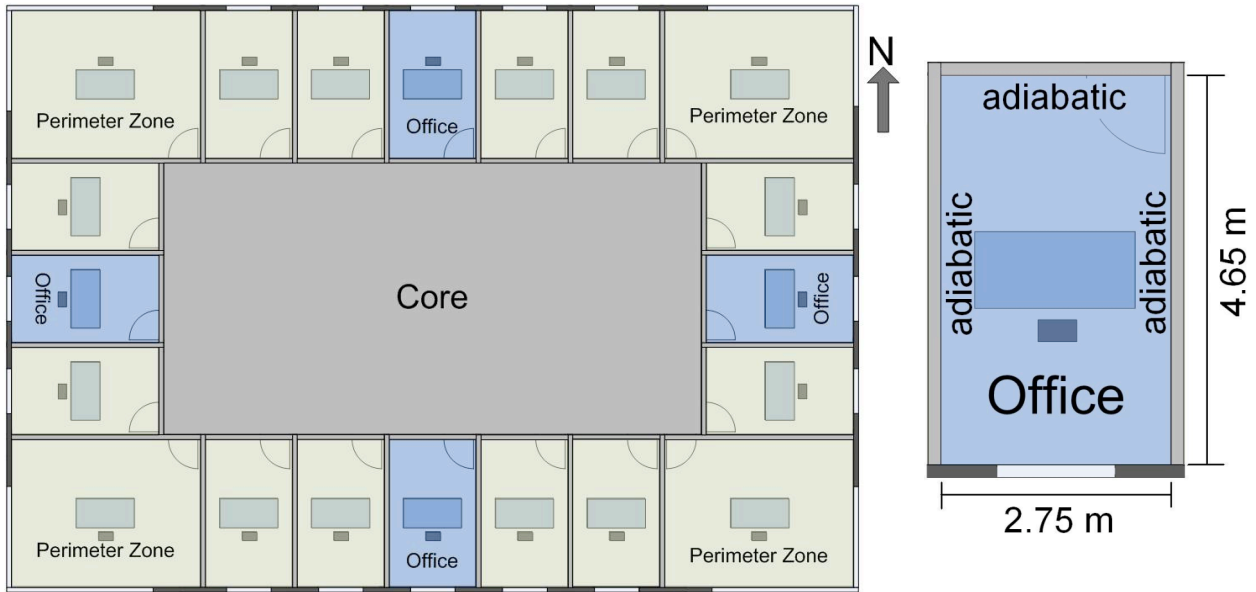


Figure 5.2.1 Layout of theoretical building used in building simulation

The building enclosure is constructed out of heavy construction with concrete block, polyisocyanurate insulation, and brick cladding, as shown in Figure 5.2.2, and has an overall U-value of $0.407 \text{ W/m}^2\text{K}$ (R-14). While this type of construction is not popular amongst most commercial buildings, it is not rare to find concrete block institutional building enclosures. Furthermore, the insulating value of R-14 is very common for most newly constructed buildings as it complies with the building enclosure requirements of ASHRAE Standard 90.1-2007 (ASHRAE, 2007).

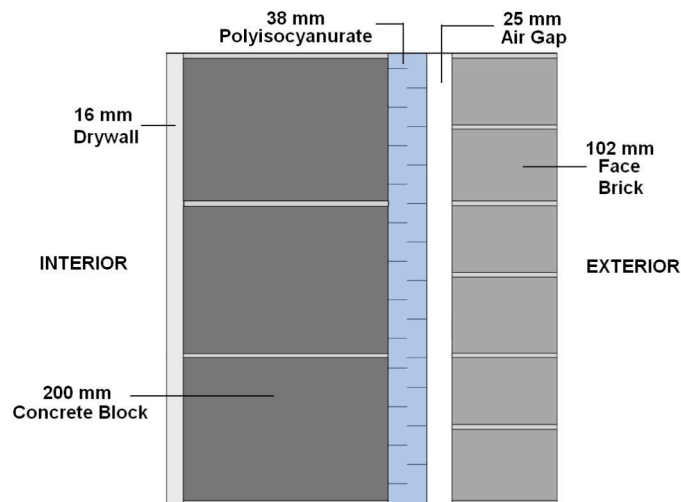


Figure 5.2.2 Opaque building enclosure

The office has only one primary occupant along with a desktop computer and associated workplace electronics. The internal heat gains from the occupant and computer are 125 W and 225 W, respectively, and are based on design parameters from the ASHRAE Handbook of Fundamentals (ASHRAE, 2001). The occupancy schedule is listed in Table 5.2.1.

Table 5.2.1 Office occupancy schedule

Start [hour]	End [hour]	Number of Occupants	Fraction of Electronics On	Consumed Electrical Power [W]
0	8	0	0.1	22.5
8	18	1	1	225
18	24	0	0.1	22.5

Auxiliary lighting is provided by six 28W T5 fluorescent tubes, and one 16 W desk lamp with a total load of 184 W and a lighting power density of 14.4 W/m². This is compliant with ASHRAE Standard 90.1-1999 (ASHRAE, 1999), which requires a minimum lighting density of 14 W/m² and is consistent with the standards used by Carmody *et al.* (2004). All of the lighting is set to operate on the following lighting schedule.

Table 5.2.2 Office lighting schedule

Start [hour]	End [hour]	Lighting Power [W]
0	8	28
8	18	184
18	24	28

This combination of electronic equipment and lighting load produces a moderate internal heat gain level that is comparable to most modern mid occupancy density offices. Offices with higher internal heat gain levels are typically older offices that uses older less energy efficient equipment and luminaries, or high-density offices which up to four occupants would occupy the same space in the office considered. In both cases the

energy consumption intensity is much higher. As technology improves and commercial buildings expand, the energy consumption intensity is expected to decrease with more efficient office equipment and lighting, this equates to smaller internal heat gains.

Daylighting controls are also incorporated into model, and are capable of continuously dimming the auxiliary lighting to maintain an illuminance level of 500 lux at the centre of the room at a work plane height of 0.762 m (2.5 ft), similar to that of Carmody *et al.* (2004). Discomfort glare is also controlled with interior roller blinds, which are deployed once a glare index rating of 22 is reached. The glare index is calculated from the centre of the room, at a 90° angle from the window, facing one of the side walls. This arrangement is representative of an ideal office placement, which glare is minimized by placing computers along the side wall in a side-lit office as recommended by the Canadian Daylighting Design Guide (Enermodal, 2002).

The office is also set to provide ventilation at a rate of 6.5 L/s (13.8 cfm) to satisfy the requirements of ASHRAE Standard 62.1-2004 (ASHRAE, 2004). The standard specifies that the minimum ventilation rate based on the expected number of occupants and floor area, calculated as:

$$V_{bz} = R_p P_z + R_a A_z$$

Equation 5.2.1

Where:

- V_{bz} = Minimum ventilation rate in zone [L/s]
- R_p = Ventilation rate per person, (2.5 [L/(s person)]) in an office setting)
- P_z = Number of occupants per zone
- R_a = Ventilation rate per floor area, (0.3 [L/(s m²)] in an office setting)
- A_z = Floor area of zone

Thus, for the office considered, the ventilation rate would be 2.5 L + (12.8 m²)*0.3 L/(s m²) = 6.3 L/s (13.4 cfm) rounded up to 6.5 L/s (13.8 cfm).

The air leakage of the building enclosure is estimated at 0.5 ACH, which is considered a relatively air-tight and potentially energy efficient building. Older office buildings may have air infiltration rates of 1 to 2 ACH. For the office analyzed, the rate is 0.5 ACH * (35.2 m³) = 17.6 m³/hr or 28.4 L/min/m² of enclosure at operating conditions.

Since space heating and sensible space cooling loads are sought in this analysis, a complete HVAC system is not included in this model. Instead, the space conditioning loads are calculated from the amount of heat required to be added to or removed from the return air stream of a forced air system needed to keep the air temperature within each zone between its cooling and heating set points. With this arrangement only the space conditioning loads are reported and the results of this analysis can be interpreted by building and HVAC designers in selecting an appropriate HVAC system. This type of analysis however, does not include dehumidification, as a result, only the sensible cooling load is calculated. EnergyPlus, however, does specify the supply air temperature and humidity ratio, which is listed in Table 5.2.3. In most new commercial buildings, however, it is becoming increasingly common to provide all ventilation air via a Dedicated Outdoor Air System (DOAS), which dehumidifies the outdoor air, with the energy provided centrally at the main plant. Each zone then provides only sensible heating and cooling locally.

Table 5.2.3 Supply air temperature and humidity

	Supply Air Temperature [C]	Supply Air Humidity Ratio [kg_{water}/kg_{air}]	Supply Air Relative Humidity
Heating	24	0.06445	35%
Cooling	20	0.007955	55%

Similar to the occupancy and lighting schedules, the thermostat is also operated on a schedule, with nighttime setbacks for both heating and cooling set points, which is similar to Carmody *et al.* (2004). The thermostatic set point schedule is listed in Table 5.2.4.

Table 5.2.4 Thermostatic set points

Start [hour]	End [hour]	Heating Set Point [C]	Cooling Set Point [C]
0	6	15	30
6	20	20	24
20	24	15	30

The window area tested ranges from 0 to 0.66 WWR at increments of 0.10. All windows are placed flush with the finished ceiling to maximize daylight penetration and have aspect ratios that are approximate to 1. Because the WWR is calculated as the overall wall area (from floor-to-floor height), 0.66 WWR was chosen as the maximum practical window area and stretched the window area from the floor to ceiling. Elevations of the window arrangement are shown in Figure 5.2.3.

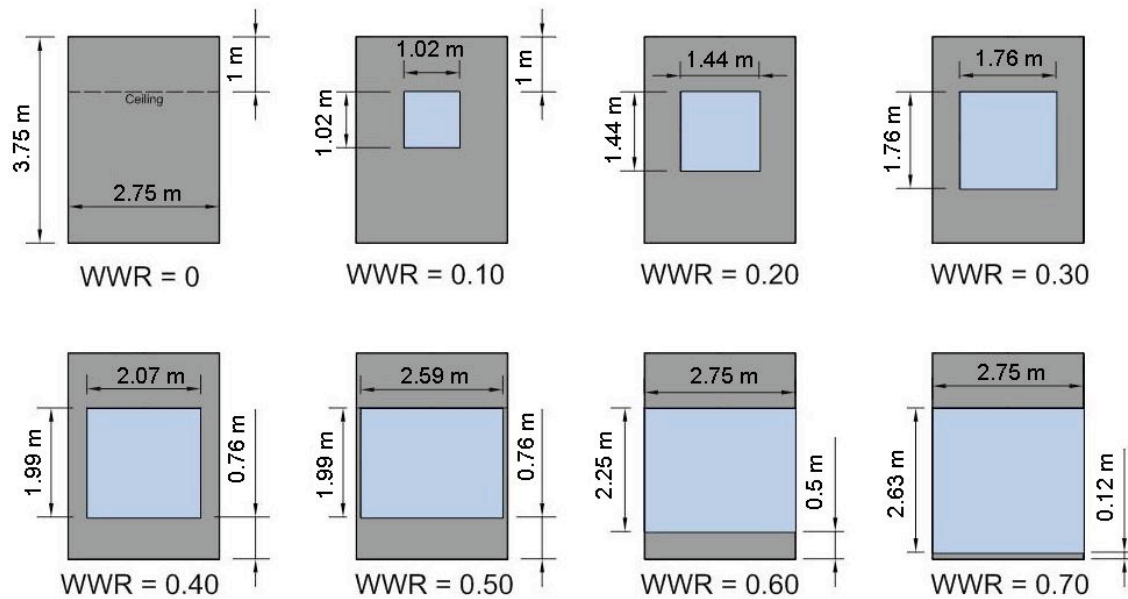


Figure 5.2.3 Model window arrangement

A total of 10 window assemblies were considered, including a set of high and low U-value double-glazed windows to high-performance low U-value windows. This provides a range of results that represents current conventional and state-of-the-art window technology, with any variations in the window assembly design falling between these performance levels. A list of the tested window assemblies is provided in

Table 5.2.5, the windows are named after the IGUs from Chapter 3. All of the window properties tested can also be found in Appendix D1.

Table 5.2.5 Modeled Window Assembly Properties

Type	IGU [W/m ² K]	SHGC	VT	Edge [W/m ² K]	Frame [W/m ² K]	Notes
2G-1 (air, typ. AL frame)	2.680 (R-2.1)	0.702	0.786	1.861 (R-3.1)	13.463 (R-0.4)	High U and high SHGC (Base case)
2G-2s (Ar, High-performance Timber frame)	1.305 (R-4.4)	0.37	0.639	1.592 (R-3.6)	1.883 (R-3.0)	Low U and low SHGC
2G-4uv (Ar, High-performance Timber frame)	1.334 (R-4.3)	0.253	0.413	1.592 (R-3.6)	1.883 (R-3.0)	Low U and ultra-low SHGC
2G-3v (air, typ. AL frame)	2.679 (R-2.1)	0.299	0.416	1.861 (R-3.1)	13.463 (R-0.4)	High U and ultra-low SHGC
3G-2s (Kr, High-performance Timber frame)	0.607 (R-9.4)	0.366	0.566	1.021 (R-5.6)	1.705 (R-3.3)	Ultra-low U and low SHGC
3G-5uv (Kr, High-performance Timber frame)	0.562 (R-10.1)	0.187	0.431	1.021 (R-5.6)	1.705 (R-3.3)	Ultra-low U and ultra-low SHGC
4G-2s (Kr, High-performance Timber frame)	0.406 (R-14.0)	0.351	0.502	0.786 (R-7.2)	1.634 (R-3.5)	Ultra-low U and low SHGC
4G-5uv (Kr, High-performance Timber frame)	0.376 (R-15.1)	0.184	0.397	0.786 (R-7.2)	1.634 (R-3.5)	Ultra-low U and ultra-low SHGC
5G-2s (Xe, High-performance Timber frame)	0.271 (R-21.0)	0.33	0.447	0.705 (R-8.1)	1.620 (R-3.5)	Ultra-low U and low SHGC

5G-4uv (Xe, High- performance Timber frame)	0.272 (R-20.9)	0.187	0.406	0.705 (R-8.1)	1.620 (R-3.5)	Ultra-low U and ultra-low SHGC
--	-------------------	-------	-------	------------------	------------------	-----------------------------------

Exterior shading is designed to keep the sun away from the window. Two types of exterior shading are evaluated, including static and dynamic shading. Static shading took the form of overhangs for the south-façade and fins on both the east- and west-façades. South-facing overhangs were designed to completely shade the window during the summer solstice, while leaving the window exposed to the low angle sun during the winter solstice. The overhangs were designed with the aid of solar positioning equations (listed in Appendix A). The projecting depth of the fins was designed to be the same as the width of the window, following the recommendations of the Canadian Daylighting Guide (Enermodal, 2002) and should provide effective shading against the low angle sun. However, since the width of the windows is quite large ranging from 1.02 m to 2.75 m, having such a large fin can be not practical. Instead, for the office considered, the fin-projected depth is limited to the width of the smallest window at 1.02 m. Typically deeper fin projections would require some alteration of the architecture of the building. Details of the static shading elements can be found in Appendix D1.

Dynamic exterior shading is in the form of exterior mounted louvers, and has been programmed to block incident solar radiation when the interior air temperature reached 23°C, 1°C less than the cooling set point. This type of shading strategy was intended to use the exterior louvers would help cool the office before activating the HVAC system. Such shading algorithm can be considered as part of an active-passive cooling strategy, in which it actively responds to changing interior conditions by deploying a passive cooling mechanism. While systems like these are rare, they have been deployed in projects such as the North House for the 2009 U.S. DOE Solar Decathlon (North House, 2009). The effectiveness of this type of shading algorithm remains to be seen, however, as performance data from long term monitoring programs of these systems have not yet been completed. The results of this type of shading algorithm are presented later in this chapter.

A comparison of this model and the model used by Carmody *et al.* (2004) was done to verify and characterize the EnergyPlus model. Conditions used in the Carmody *et al.* (2004) model were replicated in EnergyPlus (Crawley *et al.*, 2004) using a window with the exact properties, window placement, and window area, along with a similar Chicago weather file. The results from the EnergyPlus model are corrected for the same HVAC efficiencies, such as a fixed heating efficiency factor (HEF) of 0.8 and a fixed coefficient of performance of 3.0 for the cooling system. In addition, all electricity used is multiplied by 3 to reflect the 3:1 ratio of primary to end use energy efficiency. The results are plotted in Figure 5.2.4 and are comparable to the total annual energy use for Window B in Figure 5.1.2.

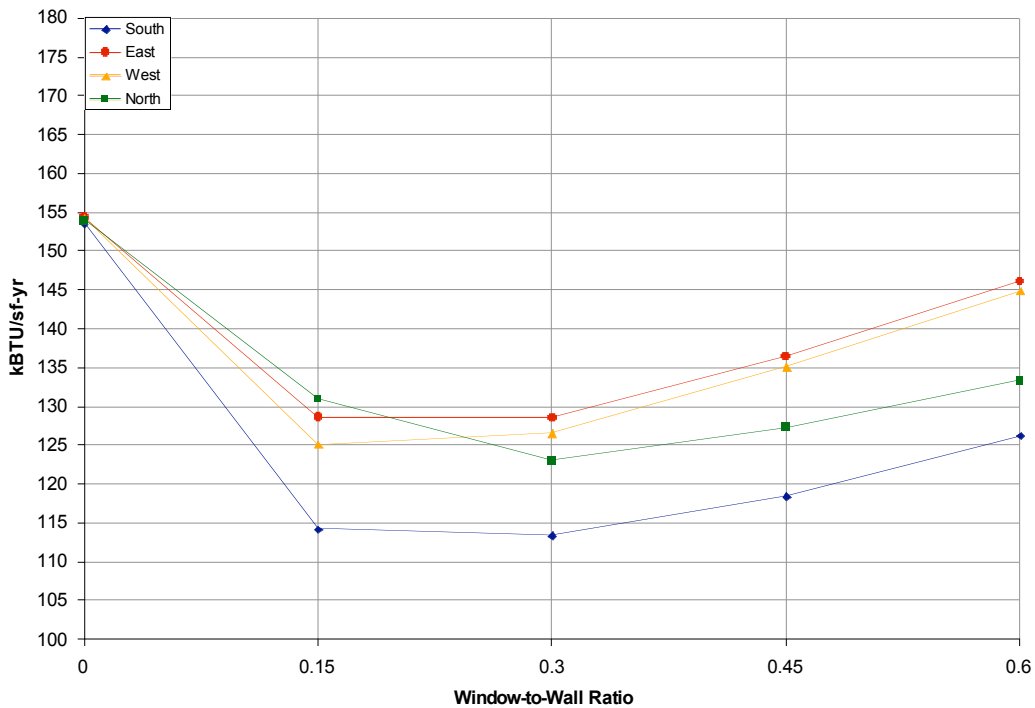


Figure 5.2.4 Total annual energy use of EnergyPlus Model using Window B from Carmody *et al.* (2004) for Chicago, IL

Although results from the two models show broadly similar trends (a U-shaped plot with a minimum between 0.15 and 0.30 WWR), the values of the office considered are approximately 30% higher. In addition, the impact of higher WWR is muted since all orientations show a decrease in energy consumption relative to the windowless case,

while results from Carmody *et al.* (2004) show a significant increase in energy consumption that is much higher than the windowless office. The EnergyPlus model is less sensitive to variations to window areas than the Carmody. This may be due to several significant differences between the two models:

- **Location of the daylight illuminance sensor:** The daylighting sensor in the EnergyPlus model is set at 50% depth of the room, whereas the Carmody model has set the daylight sensor at 67% depth of the room. By setting the daylight sensor deeper into the room more lighting energy is used which could affect both the space heating and cooling load.
- **Temperature Night Time Setbacks:** In the EnergyPlus model the heating setpoint is set to 20°C during occupied hours and 15°C during unoccupied hours, while the cooling setpoint is set to 24°C and 30°C for occupied and unoccupied hours, respectively. Conversely, in Carmody's model the heating setpoint is set to 21°C during occupied hours and 13°C during unoccupied hours and the cooling setpoint is set to 24°C during occupied hours and 37°C during unoccupied hours. Using a wider temperature deadband during unoccupied hours results in greater energy consumption and higher peak loads for buildings with greater window area since the insulating value of the building enclosure is minimized and the building has a greater temperature range to maintain. This could result in lower energy use for buildings with small window areas and higher energy usage for buildings with larger window areas.
- **Scheduling:** All of the lighting, electrical equipment, and temperature setpoints run on a schedule. Specific details regarding the lighting energy use, electrical equipment use schedules, and occupancy schedules were not provided from Carmody *et al.* (2004). As a result, the internal heat gain cannot be properly identified, which can have a significant effect on the results. Higher internal heat gains typically results in lower heating loads and higher cooling loads. Since the

- results between the two models are so different for various window areas, it is likely that the internal gains and schedules are very different.
- **Simulation Method:** In the EnergyPlus model, each individual office is considered to be an isolated zone with 5 adiabatic sides and one exterior wall. This results in a thermally benign environment in which there is only one source of heat gain and loss, the exterior wall. This setup is representative of a multi-storey high rise building in which offices are closely packed and are far from both the roof and floor. Conversely, the Carmody model simulates all three floors of the building for offices facing a particular direction and considers all three floors to be one zone. In this arrangement each zone has three non-adiabatic sides, including a foundation and roof in addition to an exterior wall. Added to that, the floor and wall facing the core zone are also non-adiabatic. This makes the model more sensitive to exterior conditions, in particular with larger window areas. While the Carmody model may be considered to be more complete building model, it is specific only to a three-storey commercial office building. Some of the results presented may not be as applicable to a multi-storey high rise, where the majority of the offices are far away from the floor and roof of the building and most sides of the building may be approximated as adiabatic.

Despite the differences in simulation results, the parameters set for the EnergyPlus model seem to be reasonable for most new buildings constructed at this time. In addition, the end-use energy consumption break down is similar to that of the 2007 average Canadian commercial/institutional building energy consumption as shown in Figure 5.2.5. This data was from Natural Resources Canada (NRCan) and represents the average energy consumption of Canadian commercial/institutional buildings. While the average building energy consumption data includes both core and perimeter zones, the simulations in this chapter are exclusively limited to offices in the perimeter zone. However, despite this difference the energy consumption breakdown by end use are still very similar. This suggests that the results from the EnergyPlus analysis do reflect that of most buildings in Canada.

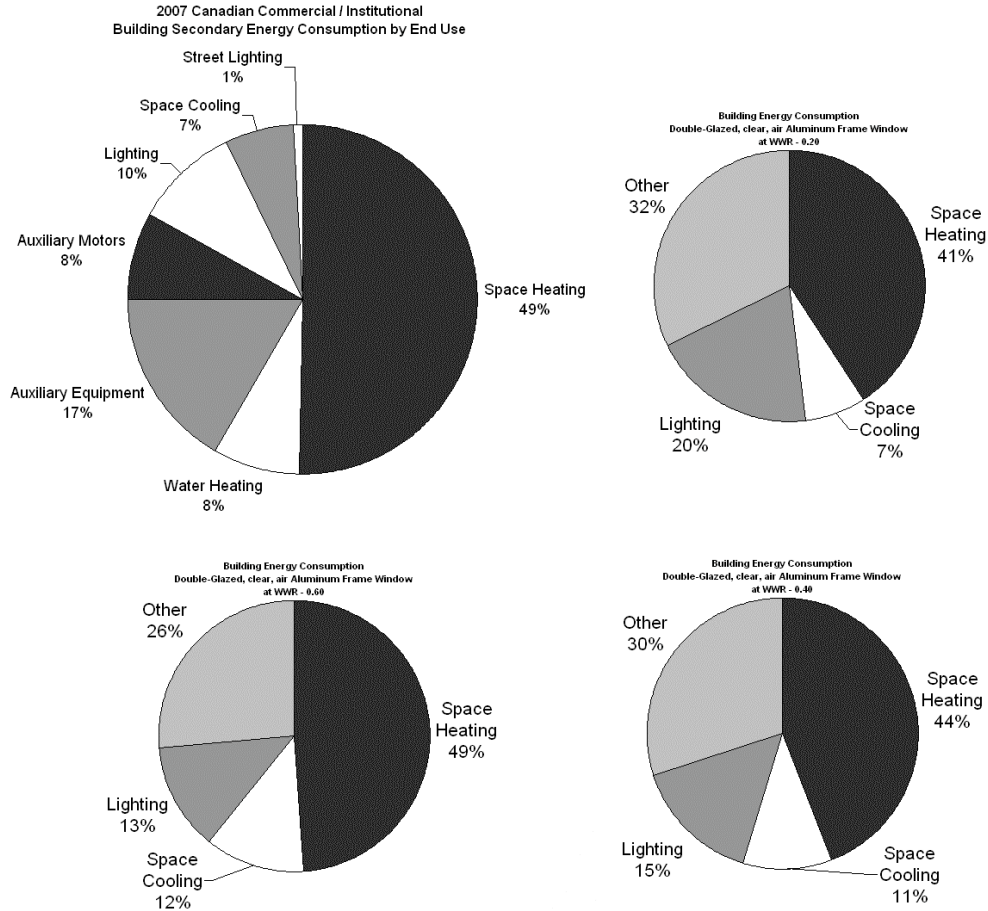


Figure 5.2.5 Comparison of EnergyPlus model with 2007 Canadian commercial/institutional building energy consumption by end use (NRCan, 2007) (upper right: WWR 0.20, lower right: WWR 0.40, lower left: WWR 0.60)

5.3 Window Properties and Perimeter Space Energy Consumption

In this section the effect of window properties on perimeter zone energy consumption of commercial office buildings is discussed. This section investigates how window properties such as window U-value and SHGC can affect average annual and peak energy consumption in perimeter zone offices for different scenarios such as a high and low internal gain office. The influence of the SHGC on energy performance is also analyzed by comparing a set of double-glazed windows with similar U-values but different SHGCs. However, in order to quantify the energy performance of perimeter zone offices, energy consumption metrics must be discussed first.

5.3.1 Energy Load and Energy Consumption

The amount of energy used by a building may be expressed as either an energy load or energy consumed. While both of these measures share the same units, the calculation of both values may be very different. Energy load refers to the energy demand that is required to keep the building zone within its desired setting. In the EnergyPlus model, energy loads are simply the amount of heat added or removed from the zone as well as the amount of electricity used in that zone to power the auxiliary lighting and electrical equipment. This value excludes all efficiencies of various building systems. Energy consumed however, refers to the amount of energy that was "spent" or passed through a utility meter to maintain the zone at its desired setting. This includes efficiency factors of each building system, particularly for HVAC systems. For example, most commercial buildings are heated by a natural gas boiler with a typical system efficiency of 80%. That is of all the energy used to provide heat to the zone or building, only 80% of it is delivered as heat, the rest is lost due to energy conversion and transmission losses, such as losses up the chimney, pumping energy, fan energy, air leakage out of the duct work. Similarly, most commercial buildings are cooled by electricity-driven, compression-based cooling systems with a system Coefficient of Performance, COP, of 2 to 3. That is the desired cooling can be met by using only 1/2 or 1/3 as much electricity as the cooling load, the system is essentially 200% to 300% efficient. While modern chillers can have COP's of over 5 (500% "efficient"), the fans and pumps used to move heat transfer fluids through the building will usually reduce the system COP to 3 or even lower.

The efficiencies of both the heating and cooling systems vary significantly depending on the type of system and the technologies employed. For example, a hydronic system using a series of heat pumps combined with a radiant distribution system can be approximately 3 to 4 times more efficient than a forced air electric coil system. Given the range of these factors, selecting the appropriate HVAC system can greatly affect the overall annual energy and peak energy consumption.

The EnergyPlus (Crawley *et al.*, 2004) model uses a forced air delivery system due to its popularity in most commercial buildings. However, since the model is representative of

most new buildings, the efficiencies of the HVAC system are set to a higher level: 90% for the heating system and a COP of 3 for the cooling system. The significance of these factors becomes apparent when calculating the total overall energy consumption, particularly when looking for methods to reduce energy consumption. Since heating energy numbers are inflated and the cooling energy numbers are significantly reduced, this makes space heating the major energy end use category as measured at the building meter. As a result, the total energy consumption numbers are more biased towards space heating savings since it accounts for the majority of the energy use. The difference between energy load and energy use is shown in Figure 5.3.1 for an office with a double-glazed clear window located in Toronto.

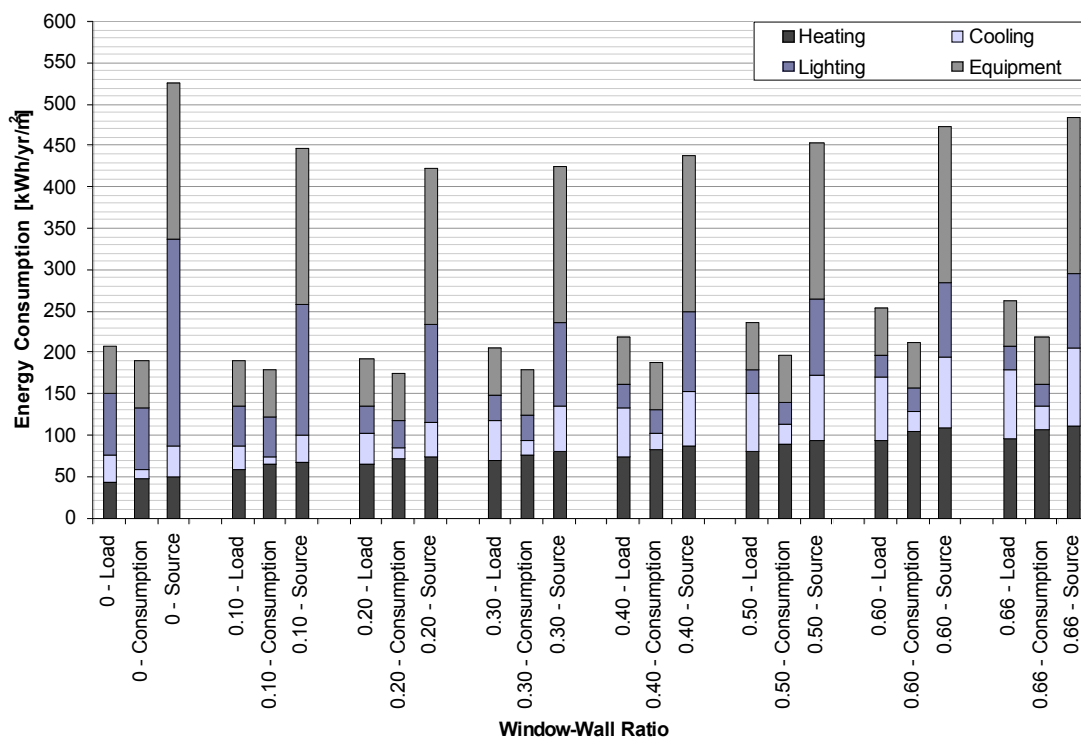


Figure 5.3.1 Comparison of average energy load, average energy consumption, and average source energy consumption for a double-glazed, clear, air-filled, aluminum window

In addition to the energy load and energy consumption, Figure 5.3.1 also includes a comparison for source energy, which better captures resource use, operating cost, and pollution. Source energy refers to the amount of energy required to deliver energy to the building site for domestic consumption. It is particularly important for fossil fuel based

electric plants in which the source energy refers to the energy in the raw fuel that is burned to generate electricity (Energy Star, 2009). Source energy also includes the energy required in extraction and delivery. In order to fully normalize all energy consumption from a resource perspective, secondary energy end use, such as heating and cooling energy consumption is converted to source energy with source-site ratio, which accounts for both conversion and distribution losses. However, with various methods of electric power generation, the source-site ratio is dependent on the efficiency of the generation method as well as the mix of generation. Sources from renewable energy are typically cheaper and have lower source-site ratios than power from non-renewable sources. Furthermore, on-site power generation is considered to have a source-site ratio of 1. For most locations within North America, national source-site averages such as the ones listed in Table 5.3.1 are used from Energy Star (2009).

Table 5.3.1 Source-site ratios (Energy Star, 2009)

Fuel Type	Source-Site Ratio
Grid Purchase Electricity	3.340
On-site Solar or Wind Generated Electricity	1
Natural Gas	1.047
Fuel Oil (1, 2, 4, 5, 6, Diesel, Kerosene)	1.01
Propane & Liquid Propane	1.01
Steam	1.45
Hot Water	1.35
Chilled Water	1.05
Wood	1.0
Coal/Coke	1.0
Other	1.0

5.3.2 Effect of Internal Heat Sources (Gains) on Energy Consumption

Internal heat sources, commonly referred to as internal heat gains, have a significant effect on the energy consumption of office buildings. This effect is not limited to the amount of electricity consumed for equipment and lighting but also to the space heating and cooling demand. Because most commercial and institutional buildings are typically large buildings that have a large volume compared to its surface area, internal heat sources typically dictate its thermal behaviour. For most conventional large commercial

and institutional buildings, much of its energy consumption make up is lighting and equipment, followed by space cooling rather than heating. In fact for most commercial buildings cooling is needed even on the coldest days of the year due to the high internal heat gains. In most of these buildings, the high internal heat gain comes from a large array of desktop computers and servers that remain on through the year, as well as non-dimmable lighting that are constantly left on. The amount of internal heat gain can have a significant effect on the energy consumption of the building, so much so that it can even alter how the building interacts with different configurations in the building enclosure.

A comparative study was conducted in which the electric equipment and lighting demand of the EnergyPlus model was modified to show the effects of internal heat gains on annual and peak energy consumption. A high internal gain model was developed in which all office equipment and lighting remained on full power throughout the year: lighting power and equipment power density were set to 14.4 W/m² and 17.6 W/m² respectively. A relatively low internal gain model was also developed in which the electrical equipment and lighting power density is reduced to 8.2 W/m² and 8.7 W/m², respectively. These models were fitted with two types of double-glazed windows and one type of quint-glazed window, to show how energy performance are affected by U-value and SHGC for high and low internal gain perimeter zones. The properties of the windows tested are listed in Table 5.3.2, while the results of these simulations are listed in Appendix D2.

Table 5.3.2 Window properties tested for internal gain study

Window	SHGC	VT	U-value [W/m ² K]						
			WWR 0.1	WWR 0.2	WWR 0.3	WWR 0.4	WWR 0.5	WWR 0.6	WWR 0.66
2G-2s	0.37	0.64	1.50	1.45	1.42	1.41	1.40	1.41	1.41
2G-4uv	0.25	0.41	1.51	1.47	1.44	1.43	1.42	1.43	1.43
5G-2s	0.33	0.41	0.67	0.56	0.51	0.48	0.46	0.49	0.48

In offices with higher internal heat gains, window U-value had very little effect on the overall energy consumption for all window areas. Figure 5.3.2 shows the results of the

simulations from the high internal heat gain model fitted with a double- and a quint-glazed window that significantly differ in U-value. The results from this case indicates that the window U-value has very little affect in altering the annual energy consumption of a high internal gain perimeter zone. Much of the energy savings from the ultra-low U-value quint-glazed window is offset by the higher cooling energy consumption, which is evident in the peak energy consumption between the two windows shown in Figure 5.3.3. As expected, the peak heating values are much less for the ultra-low U-value quint-glazed window, while the peak cooling values are very similar since both of these windows have similar SHGCs. It is also noted that the annual energy consumption increases slightly with greater area for both window types.

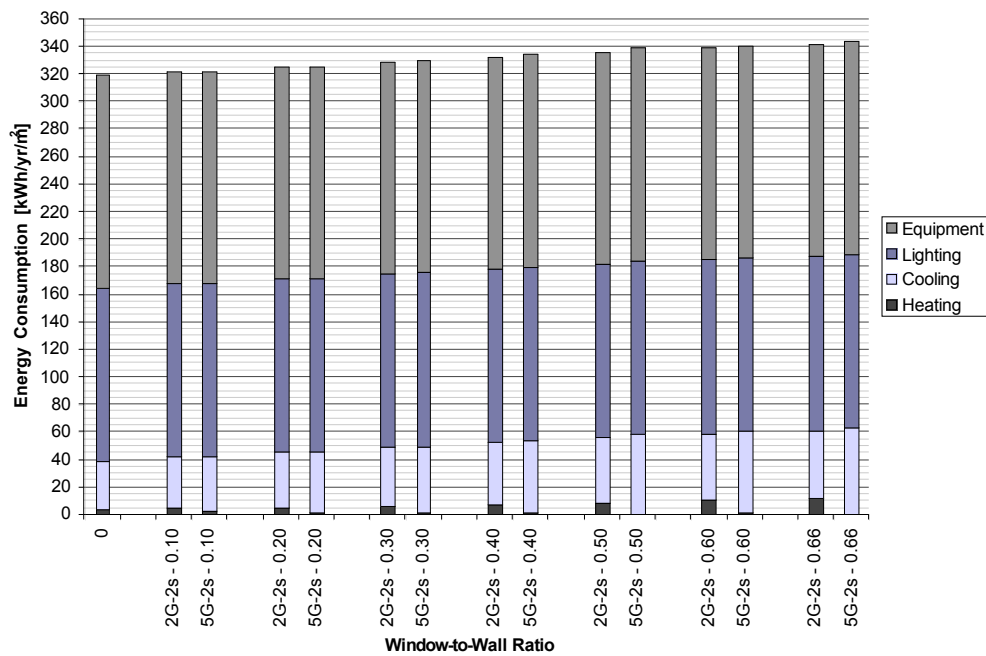


Figure 5.3.2 Average annual energy consumption of a high internal heat gain office with double-glazed (2G-2s) and quint-glazed (5G-2s) high solar gain wood window

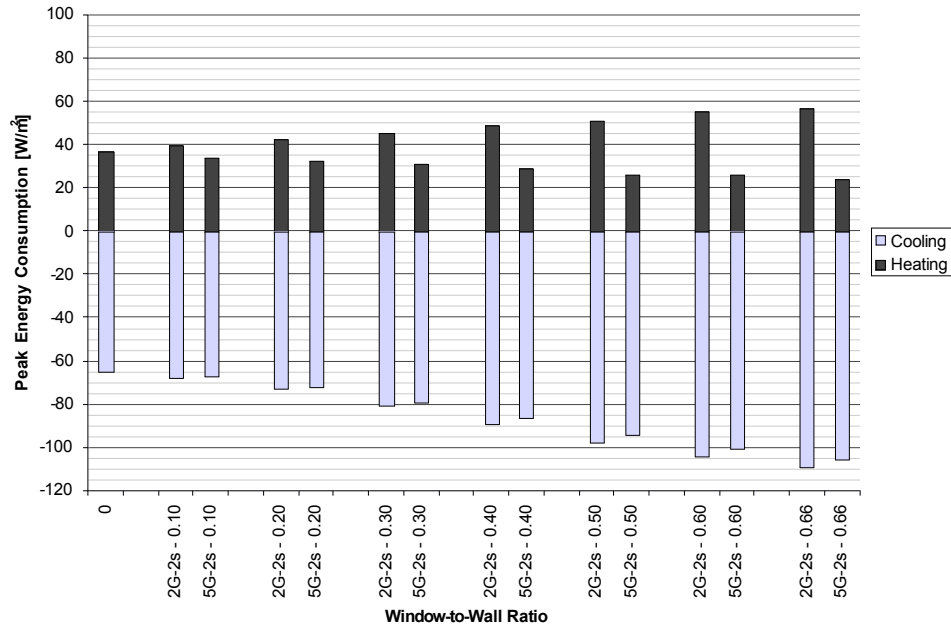


Figure 5.3.3 Average peak energy consumption for a high internal loads office with double-glazed (2G-2s) and quint-glazed (5G-2s) high solar heat gain wood windows

With higher internal heat gain, it is reasonable to expect that effects of reducing the cooling demand such as windows with lower SHGCs will reduce the annual energy consumption. While it is true, the effect of a significant reduction in solar heat gain is not as great as expected. A comparison of a high and ultra-low solar gain double-glazed window (2G-2s and 2G-4uv) in Figure 5.3.4 shows that a 32% reduction in the SHGC only yields 0.2% to 1.2% in annual energy consumption. It appears the savings in cooling demand is offset by an increase in the heating load from the low solar gain windows. Since the COP of the cooling system reduces the proportion of cooling energy in the overall energy make up, significant reductions in the cooling demand are not reflected in the overall energy consumption.

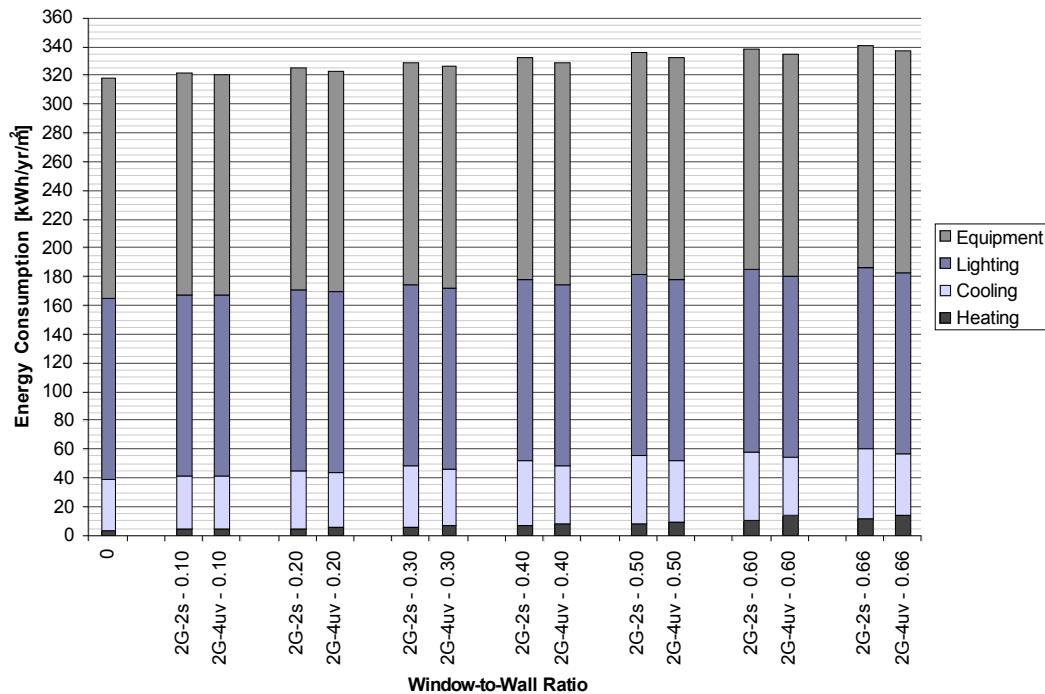


Figure 5.3.4 Average annual energy consumption of a high internal heat gain office with a high (2G-2s) and low (2G-4uv) solar gain double-glazed wood window

Evidence of a reduced cooling load is only shown in the peak heating and cooling energy consumption in Figure 5.3.5, which the peak cooling energy is less for the low solar gain window, while the peak heating energy is higher. It is also worth noting that differences in peak energy consumption only occur for mid- to large-window areas beyond WWR 0.30 while the total energy consumption continues to increase with larger window areas. This suggests that the benefits of a low to ultra-low solar gain window are most significant for buildings with large window areas; however, since energy consumption increases with larger windows, the savings are quickly diminished. As the results in Figure 5.3.4 and Figure 5.3.5 shows, the ideal design strategy for reduced peak and annual energy consumption is to keep window areas to a minimum, as the windowless office had the lowest energy consumption.

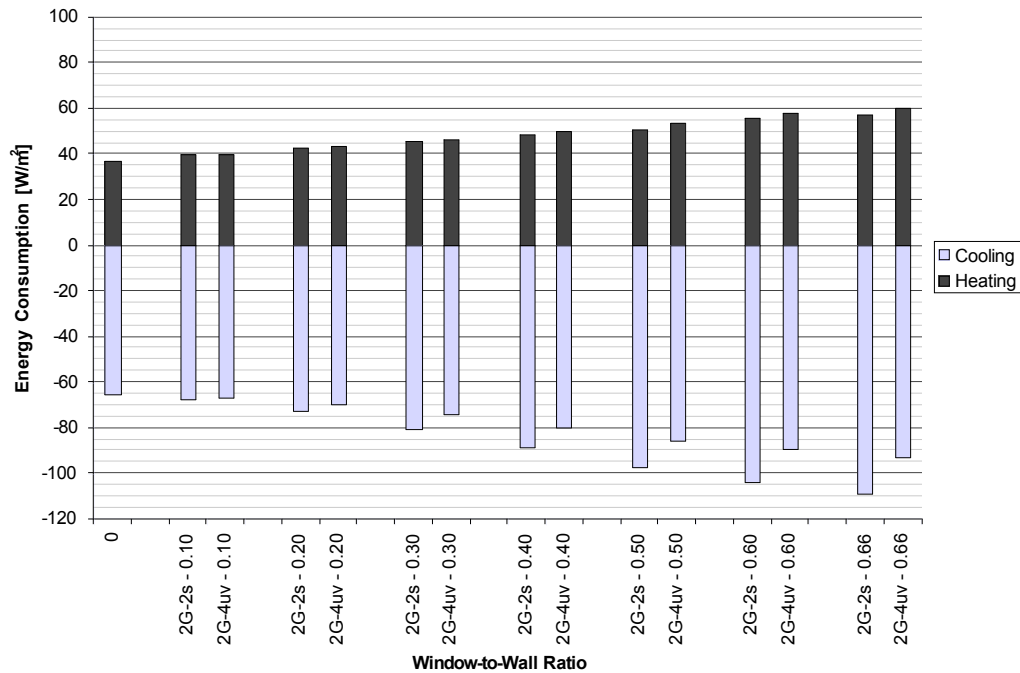


Figure 5.3.5 Average peak energy consumption of a high internal heat gain office with a high (2G-2s) and low (2G-4uv) solar gain double-glazed wood window

As technology advances and becomes more and more energy efficient, it is changing the energy density of the workplace. With energy efficient computers and office equipment as well as high efficiency lighting, the internal heat gain of office buildings is progressively reducing. For buildings with moderate to low internal heat gains, particularly with daylighting controls, the thermal behaviour of the building is very different. In these buildings the end use that dominates the total annual and peak energy consumption is space heating. When combined with daylighting controls, windowless offices are no longer the least energy intensive designs, instead savings in annual energy consumption are observed even at large window areas. This is shown in Figure 5.3.6 which compares the annual energy consumption of a low internal heat gain office with a double-glazed (2G-2s) and quint-glazed (5G-2s) wood window. This low internal load office has a reduced electrical equipment power density at 8.2 W/m^2 and a lighting power density of 8.7 W/m^2 with nighttime setbacks and daylighting controls.

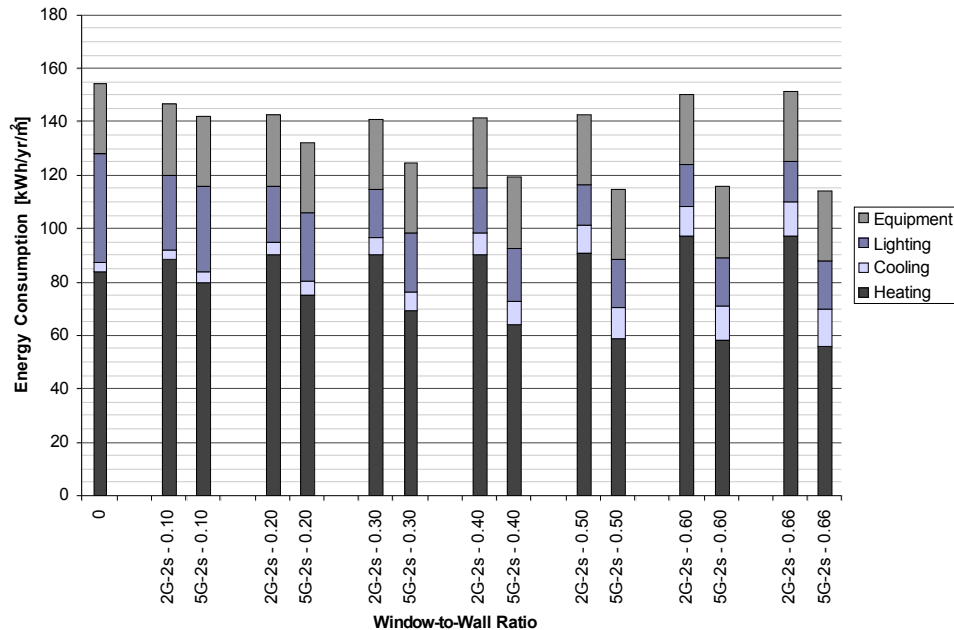


Figure 5.3.6 Averaged annual energy consumption of a low internal heat gain office with a double-glazed (2G-2s) and quint-glazed (5G-2s) high solar gain wood window

Since space heating makes up a significant portion of the total energy consumption, the office benefits from windows with lower U-values, such as 5G-2s. Even at larger window areas, the total energy consumption declines as the larger window area allows for greater solar gains, which are kept inside the office due to the highly insulated window. Conversely, space heating energy consumption actually increases with larger window area for the double-glazed, 2G-2s, window since the added solar gain is offset by a less insulating value. This opposing trend in space heating energy demand is clear when comparing the peak energy consumption for space heating and cooling in Figure 5.3.7, as the peak heating energy consumption decreases with increasing window area for the 5G-2s window and increases for the 2G-2s window. The peak cooling energy consumption increases with increasing window area for both windows, and is particularly large for large window areas, almost equaling that of the peak heating energy consumption. Despite the relatively low annual energy consumption for cooling, larger windows do lead to larger peak energy consumption for cooling which can significantly affect occupant comfort and the capital cost of the HVAC system. Even with low internal heat

gains and high-performance windows, buildings with large window areas still consume more energy.

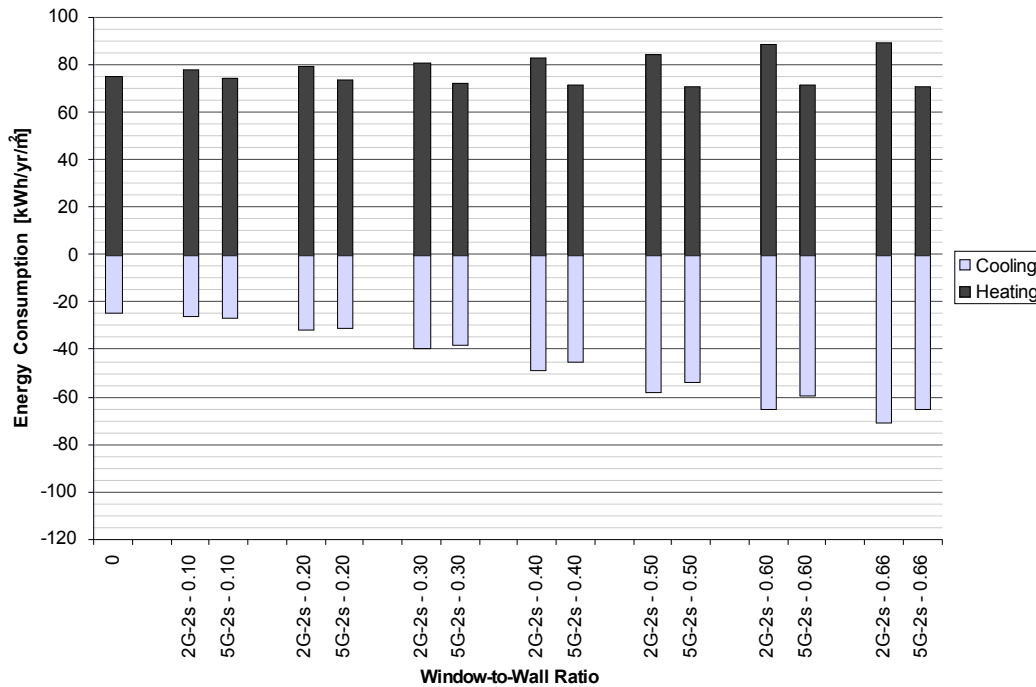


Figure 5.3.7 Averaged peak energy consumption of a low internal heat gain office with a double-glazed (2G-2s) and quint-glazed (5G-2s) high solar gain wood window

Since offices with low internal heat gains are dominated by heating, reducing the solar heat gain of the offices increases the total annual energy consumption, however, similar to high internal gain offices, the difference is not as significant as expected. In a comparison of a low and an ultra-low solar gain double-glazed wood window, 2G-2s and 2G-4uv, respectively, reducing the SHGC by 32% increases the energy consumption by 3% to 6%, depending on the window area. The results of this study are shown in Figure 5.3.8.

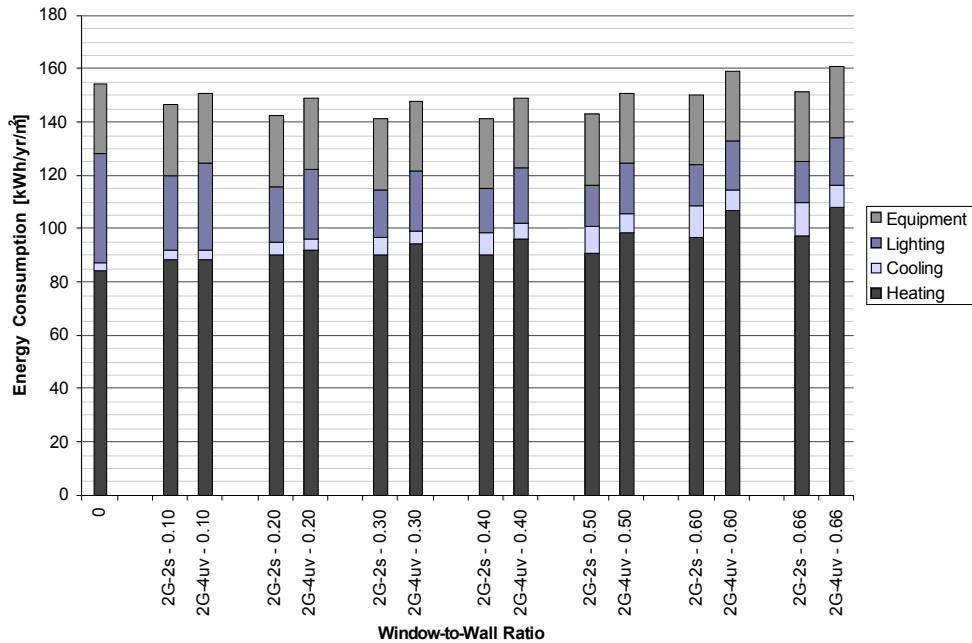


Figure 5.3.8 Average annual energy consumption of a low internal gain office with high (2G-2s) and low (2G-4uv) solar gain double-glazed wood window

While differences in total annual energy consumption are not significant between these two windows, there is a significant difference in peak cooling energy consumption. A comparison of the peak heating and cooling energy consumption in Figure 5.3.9 shows a significant difference in peak cooling energy beyond a WWR of 30%, in which the peak cooling energy is reduced by 15% to 24% depending on the window area. These results indicate that while reducing the SHGC may not have a significant effect on the annual energy consumption, it can reduce the peak cooling energy consumption.

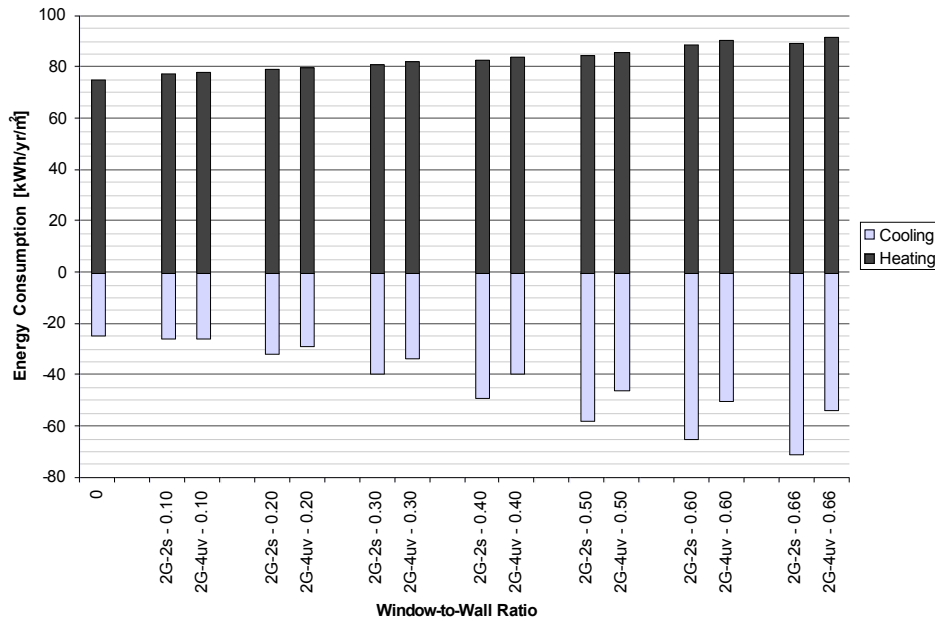


Figure 5.3.9 Average peak energy consumption of a low internal gain office with high (2G-2s) and low (2G-4uv) solar gain double-glazed wood window

5.3.3 Window Properties: U-value and Solar Heat Gain Coefficient

Window properties can play a significant role in the overall energy consumption of a commercial and institutional office building. Properties such as window U-value and SHGC can often affect the overall annual and peak energy consumption. When designing a building it is important to note which of the two properties are significant. In this section, the effect of the window U-value and SHGC are examined with a set of double-glazed windows, varying in both U-value and SHGC. The results of this study can be found in Appendix D3.

In order to determine the effect of the window U-value and SHGC on the energy performance of perimeter spaces, a set of four double-glazed windows of various properties were tested. Each window is from the curtain wall system performance rating system in Figure 4.5.3. The properties of the double-glazed windows are listed in Table 5.3.3 and Table 5.3.4.

Table 5.3.3 Double-glazed window properties

Type	IGU [W/m ² K]	SHGC	VT	Edge [W/m ² K]	Frame [W/m ² K]	Notes
2G-1 (air, unbroken AL frame)	2.680 (R-2.1)	0.702	0.786	1.861 (R-3.1)	13.463 (R-0.4)	high U and high SHGC
2G-2s (Ar, High- performance Wood frame)	1.305 (R-4.4)	0.37	0.639	1.592 (R-3.6)	1.883 (R-3.0)	low U and low SHGC
2G-4uv (Ar, High- performance Wood frame)	1.334 (R-4.3)	0.253	0.413	1.592 (R-3.6)	1.883 (R-3.0)	low U and ultra low SHGC
2G-3v (air, unbroken AL frame)	2.679 (R-2.1)	0.299	0.416	1.861 (R-3.1)	13.463 (R-0.4)	high U and ultra low SHGC

Table 5.3.4 Window U-value of double-glazed windows investigated

Window	SHGC	VT	Window U-value [W/m ² K]						
			WWR 0.1	WWR 0.2	WWR 0.3	WWR 0.4	WWR 0.5	WWR 0.6	WWR 0.66
2G-1	0.70	0.79	5.01	4.35	4.06	3.88	3.76	4.11	3.82
2G-2s	0.37	0.64	1.50	1.45	1.42	1.41	1.40	1.41	1.41
2G-4uv	0.25	0.41	1.51	1.47	1.44	1.43	1.42	1.43	1.43
2G-3v	0.30	0.42	4.93	4.25	3.95	3.76	3.65	3.76	3.71

The results of this study are plotted in Figure 5.3.10 and Figure 5.3.11, which are the total annual energy consumption and the peak energy consumption, respectively. From Figure 5.3.10 it is evident that windows with lower U-value results in energy savings for all window areas, particularly for highly glazed facades, while reducing the SHGC tends to increase the energy consumption. These trends can be explained by both the internal gains and clarity of the window. With a somewhat reduced internal gain from daylighting control and off-hour setbacks to office equipment, the space heating once again makes up a significant portion of the overall energy consumption. As seen, in previous case studies, increasing the overall window U-value also increases the space heating energy consumption, which in turn increases the overall energy consumption.

Therefore, windows with high U-values such as 2G-1 and 2G-3v, will consume more energy. Similarly, windows with lower SHGCs, such as ultra-low SHGC windows, will also consume more energy than their high solar gain counterparts, since the reduced SHGC limits the amount of solar heat gain to help offset the space heating demand. Reduced SHGC also increases the lighting load since less light enters the office space. The combined effect of these trends is clearly seen in the energy performance of the 2G-3v window, which also has the worse energy performance, since its high U-value increases heat loss, yet its ultra-low SHGC makes it difficult to offset the increased heating demand with free solar gains during the day.

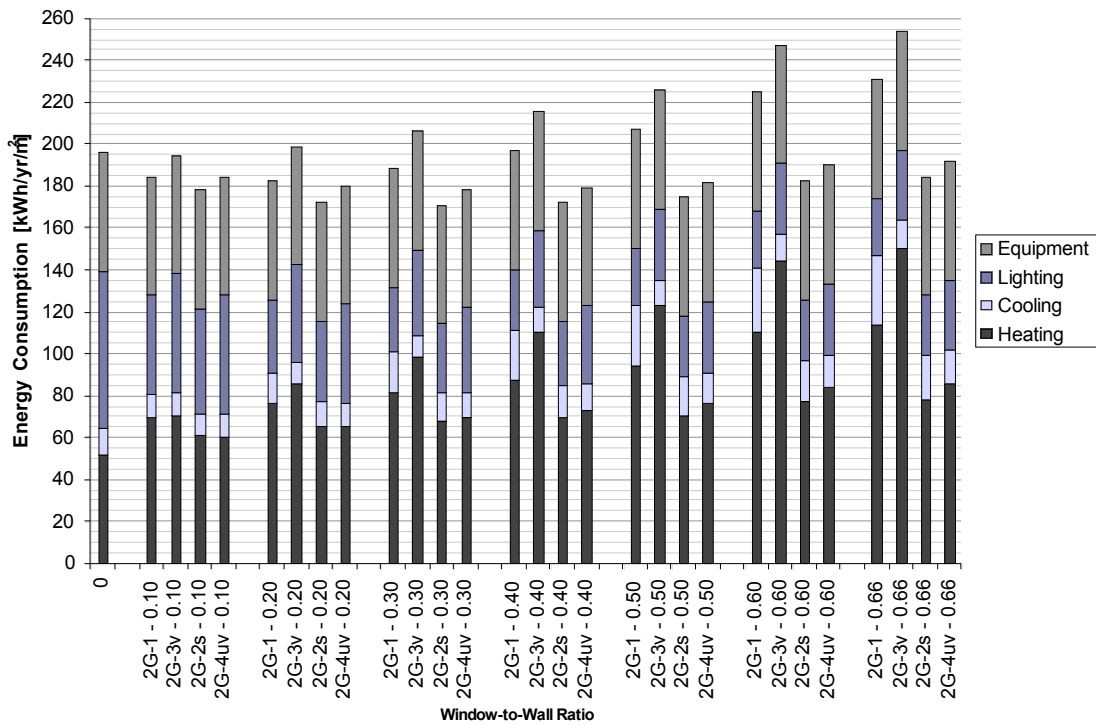


Figure 5.3.10 Average annual energy consumption of double-glazed windows of different properties

Similar to previous studies, windows with lower SHGCs are best used for reducing the peak cooling energy consumption, as shown in Figure 5.3.11. From the results of this study, it is clearly shown that windows of lower U-value have better energy performance on an annual basis, particularly high-performance windows with low SHGC, while windows with ultra-low SHGC, such as are ideal for limiting the peak cooling energy consumption. The choice between low and ultra-low SHGC high-performance low U-

value windows depends on the designer's preference to reduce operating costs through savings in annual energy consumption or from reduced capital costs with smaller peak cooling loads since the heating loads for both these windows are very similar.

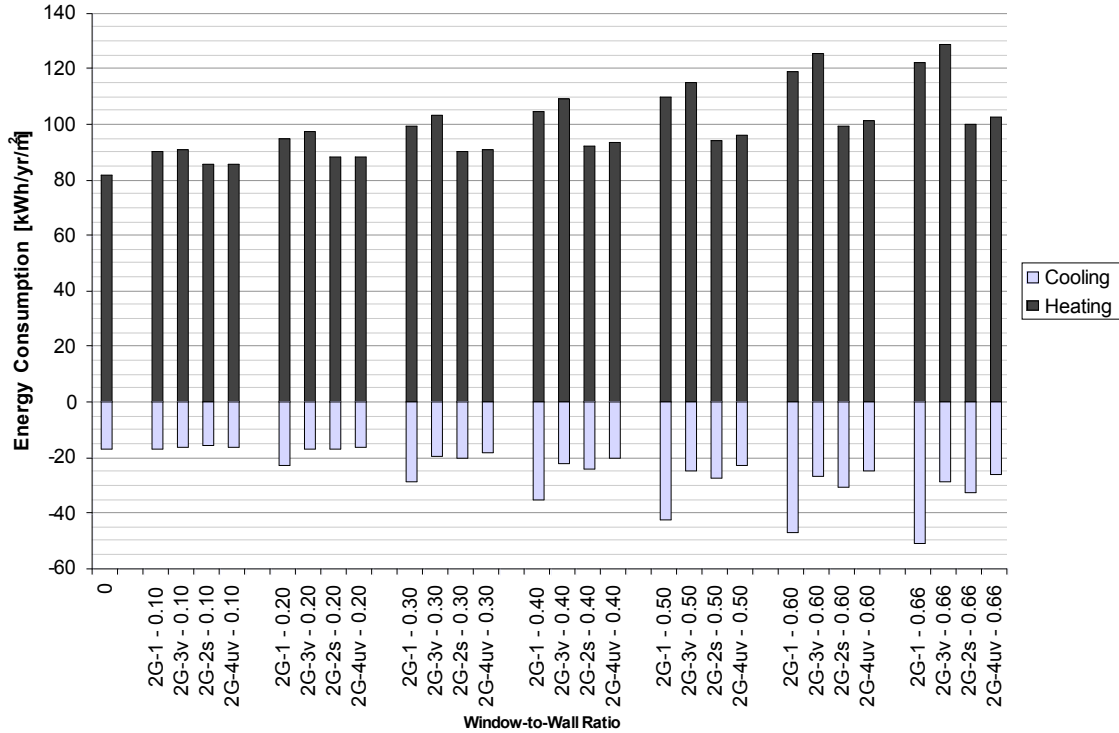


Figure 5.3.11 Average peak energy consumption of double-glazed windows of different properties

The various results from this study, gave valuable insight as to the interaction between window properties and the energy performance of offices in the perimeter zone. In particular, the results showed that for low internal gain offices the window U-value, specifically the IGU U-value, has a significant effect in reducing energy consumption in a mixed climate such as Toronto, Ontario. As a result, the high performance window facades investigated in the next section will feature low and ultra-low U-value high performance window assemblies developed in Chapters 3 and 4.

5.4 Optimal Window Design for High-performance Façades

While important conclusions were drawn from previous case studies regarding the effect of internal heat gain, window U-value, and SHGC, the results largely have been reported from energy consumption averaged over the four cardinal facing façades. Since each façade faces different environmental conditions, the orientation of the façade has a significant effect on the overall and peak energy consumption, leading to different optimal window designs. In order to completely minimize the energy efficiency of an entire building, perimeter zones of each orientation must be considered separately. As part of this study a set of eight multi-layered ultra-low U-value high-performance timber framed windows were tested in offices in each of the perimeter zones. The set of windows includes low and ultra low U-value and SHGC windows that are currently available in the market. The properties of the windows tested are listed earlier in

Table 5.2.5. These windows can help determine whether the optimum window properties for various window areas at different orientations for the Toronto climate. Results of the simulations are summarized in this section, while detailed calculations can be found in Appendix D4.

5.4.1 South-Facing Perimeter Zones

South-facing façades have the advantage of ample solar gains during the winter combined with lower solar gains in the summer due to the variation in sun angles. With this seasonal variation in solar positioning, south-facing perimeter zones can take advantage of free solar gains in the winter to offset heating demand, while receiving moderate amounts of solar gains in the summer to avoid overheating conditions. Therefore, bigger window areas are typically favoured for south-facing façades. This trend is seen from the annual overall energy consumption plot for low solar gain windows for offices in south-facing perimeter zones in Figure 5.4.1.

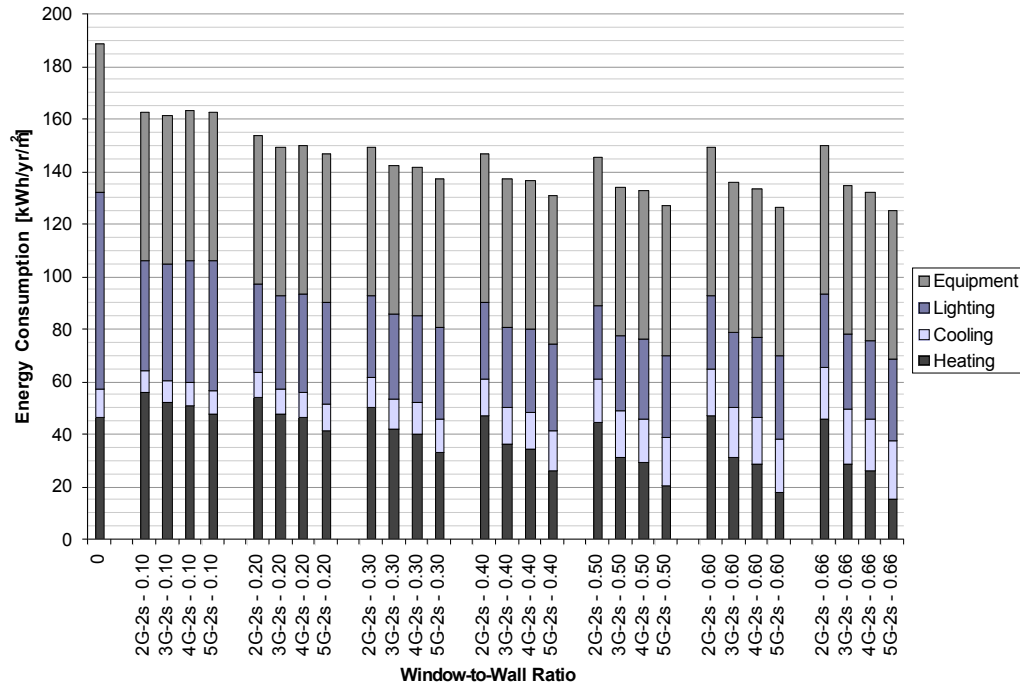


Figure 5.4.1 Annual energy consumption of offices in south-facing perimeter zones with multi-layered low solar gain, low and ultra-low U-value wood windows

With the lowest annual energy consumption of all other orientations at 6% to 15% less than the average of all zones, the south-facing perimeter zones benefit from greater window area as annual energy consumption decreases with larger windows, particularly with windows of ultra-low U-values. This is mainly due to a significant decrease in space heating energy. Since Figure 5.4.1 shows the 'metered' energy use, the annual energy consumption is biased towards space heating energy due to efficiencies in the HVAC system. As a result, measures to reduce heating energy demand, such as larger window areas and windows of ultra-low U-values will decrease the annual energy consumption.

Decreasing the SHGC of windows in offices in the south-facing perimeter zone increases the overall energy consumption, since it increases both the space heating and lighting loads, which offsets any savings in cooling energy. The differences in energy consumption between low and ultra-low solar gain windows for all window types are summarized in Table 5.4.1.

Table 5.4.1 Annual energy consumption of offices in south-facing perimeter zones

WWR	Window Type	Total Energy Consumption [kWh/yr/m ²] (Percentage savings from double-glaze window)			
		Double-glaze	Triple-glaze	Quad-glaze	Quint-glaze
0	-	189.1	189.1	189.1	189.1
0.10	Low Solar	162.8	161.8 (1%)	163.2 (0%)	162.7 (0%)
	Ultra-Low Solar	171.0	168.6 (1%)	169.8 (1%)	167.4 (2%)
0.20	Low Solar	154.0	149.6 (3%)	149.9 (3%)	147.0 (5%)
	Ultra-Low Solar	162.3	158.3 (2%)	158.8 (2%)	154.3 (5%)
0.30	Low Solar	149.4	142.4 (5%)	142.1 (5%)	137.5 (8%)
	Ultra-Low Solar	158.7	152.9 (4%)	152.8 (4%)	146.5 (8%)
0.40	Low Solar	146.9	137.7 (6%)	136.7 (7%)	131.3 (11%)
	Ultra-Low Solar	157.0	149.1 (5%)	148.4 (6%)	140.7 (10%)
0.50	Low Solar	145.9	134.6 (8%)	132.8 (9%)	127.0 (13%)
	Ultra-Low Solar	156.4	145.9 (7%)	144.6 (8%)	135.6 (13%)
0.60	Low Solar	149.8	135.9 (9%)	133.4 (11%)	126.5 (16%)
	Ultra-Low Solar	161.6	148.0 (8%)	146.2 (10%)	135.2 (16%)
0.66	Low Solar	149.9	135.2 (10%)	132.4 (12%)	125.4 (16%)
	Ultra-Low Solar	161.7	146.7 (9%)	144.7 (11%)	133.0 (18%)

Although the annual energy consumption decreases with increasing window area, this does not mean larger windows will result in smaller heating systems have little impact on the cooling system. As shown in Figure 5.4.2, depending on the window U-value, increasing the window area may also increase the peak heating demand. However, increasing the window area certainly increases the peak cooling demand, regardless of

the window type. With ultra-low solar gain windows, the peak cooling demand is slightly reduced.

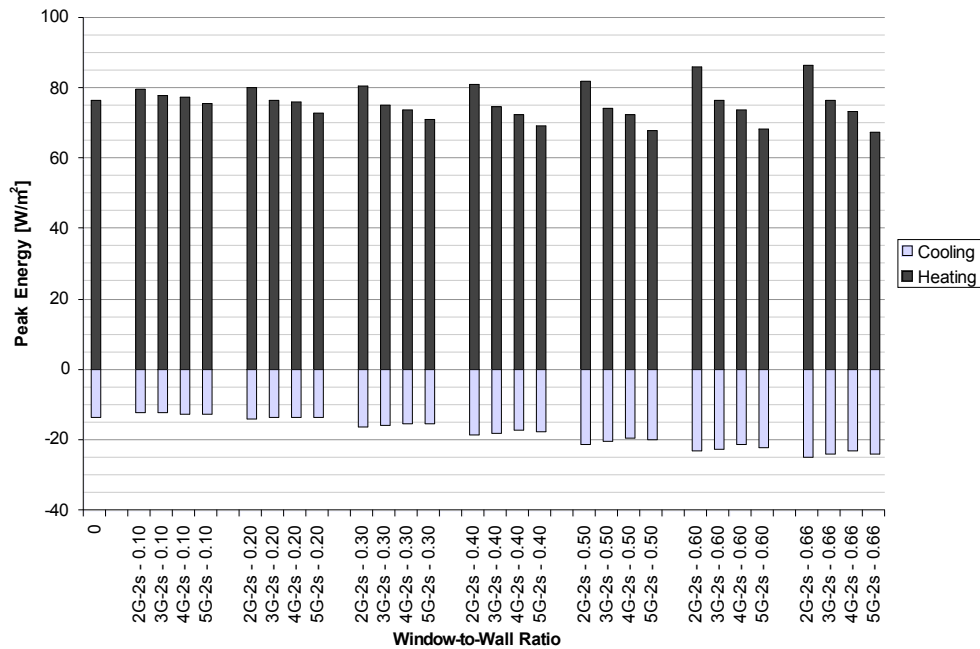


Figure 5.4.2 Peak energy consumption of south-facing, multi-layered low solar gain, low and ultra-low U-value wood windows

The optimal window area for moderate heat gain offices in the south-facing perimeter zone is listed in Table 5.4.2 for different window types.

Table 5.4.2 Optimal WWR for offices in south-facing perimeter zones

Orientation	Window Type	Total Energy Consumption	Peak Heating Consumption	Peak Cooling Consumption
South	Double-Glaze (2G-2s)	0.50	0.10	0.10
	Triple-Glaze (3G-2s)	0.50	0.50	0.10
	Quad-Glaze (4G-2s)	0.66	0.50	0.10
	Quint-Glaze (5G-2s)	0.66	0.66	0.10

5.4.2 East-Facing Perimeter Zones

Unlike south-facing façades east-facing façades receive direct sunlight daily during the morning and no direct sunlight in the afternoon. This imbalance in direct solar irradiation can lead to higher heating and cooling loads, making windows an energy liability rather than a benefit like for south-facing perimeter zones. The preference for smaller window areas is seen in Figure 5.4.3, as annual energy consumption increases with increasing window area. However, low WWRs are not preferred since space heating is still the dominant energy end use, making up 30%-40% of the total energy consumption. As a result, moderate WWRs are desired to help offset the heating load, while larger WWRs leads to higher cooling loads and higher heating loads due to night time heat loss. As with offices in the south-facing perimeter zone, decreasing the window U-value also decreases the annual energy consumption. Greater WWRs however, do reduce the lighting load which in turn leads to less internal gains and increases the space heating energy demand while reducing cooling energy demand.

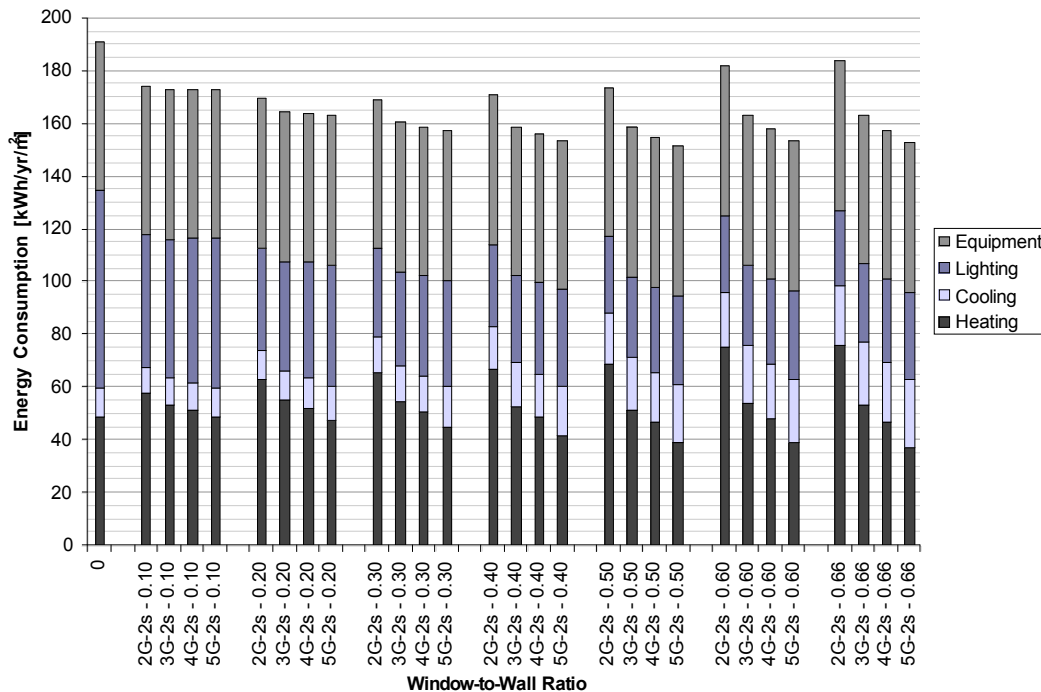


Figure 5.4.3 Annual energy consumption of offices in east-facing perimeter zones with multi-layered low solar gain, low and ultra-low U-value wood windows

Decreasing the SHGC leads to some energy savings, however, since the dominant energy use is space heating, it does not have as significant of an effect as decreasing the window

U-value. The difference in energy performance for offices in east-facing perimeter zones fitted with low and ultra-low solar gain windows are summarized in Table 5.4.3.

Table 5.4.3 Annual energy consumption of offices in east-facing perimeter zones

WWR	Window Type	Total Energy Consumption [kWh/yr/m ²] (Percentage savings from double-glaze window)			
		Double-glaze	Triple-glaze	Quad-glaze	Quint-glaze
0	-	191.4	191.4	191.4	191.4
0.10	Low Solar	174.5	172.8 (1%)	173.3 (1%)	173.2 (1%)
	Ultra-Low Solar	180.3	176.3 (2%)	176.5 (2%)	175.2 (3%)
0.20	Low Solar	169.7	164.5 (3%)	164.2 (3%)	163.3 (4%)
	Ultra-Low Solar	176.6	169.1 (4%)	168.5 (5%)	166.1 (6%)
0.30	Low Solar	169.2	160.5 (5%)	159.0 (6%)	157.3 (7%)
	Ultra-Low Solar	176.1	165.0 (6%)	163.6 (7%)	160.3 (9%)
0.40	Low Solar	171.0	159.0 (7%)	156.3 (9%)	153.9 (10%)
	Ultra-Low Solar	177.5	162.9 (6%)	160.2 (10%)	156.5 (12%)
0.50	Low Solar	173.8	158.6 (9%)	154.6 (19%)	151.4 (13%)
	Ultra-Low Solar	179.7	161.4 (10%)	157.6 (12%)	153.3 (15%)
0.60	Low Solar	181.7	163.0 (10%)	157.9 (13%)	153.4 (16%)
	Ultra-Low Solar	188.3	165.6 (12%)	160.7 (15%)	155.2 (18%)
0.66	Low Solar	184.0	163.6 (11%)	157.7 (14%)	152.8 (17%)
	Ultra-Low Solar	190.3	165.5 (13%)	160.0 (16%)	154.2 (19%)

Similarly, higher WWRs also lead to greater peak heating and cooling demands. Since the east façade only receives direct sunlight for approximately 25% of the day, the peak heating load increases with increasing WWR due to greater heat loss. Without thermal storage in the form of thermal mass or Phase Change Materials (PCMs), the solar heat

gained during the morning is offset by heat loss during the afternoon and night. In addition, due to the intense period of direct solar radiation, increasing the WWR also increases the cooling load. These trends are shown in Figure 5.4.4.

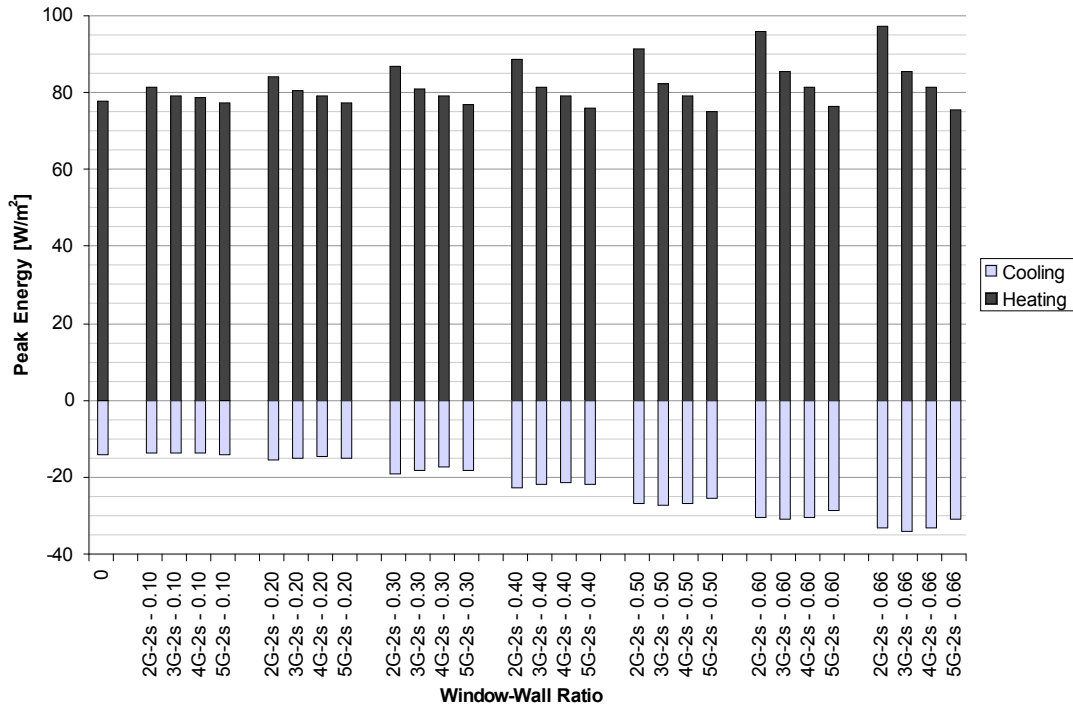


Figure 5.4.4 Peak energy consumption of offices in east-facing perimeter zones with multi-layered low solar gain, low and ultra-low U-value wood windows

From the simulation results the optimal window areas for offices in east-facing perimeter zones are listed Table 5.4.4.

Table 5.4.4 Optimal WWR for offices in east-facing perimeter zones

Orientation	Window Type	Total Energy Consumption	Peak Heating Consumption	Peak Cooling Consumption
East	Double-Glaze (2G-2s)	0.30	0.10	0.10
	Triple-Glaze (3G-2s)	0.50	0.10	0.10
	Quad-Glaze (4G-2s)	0.50	0.10	0.10
	Quint-Glaze (5G-2s)	0.50	0.50	0.10

5.4.3 West-Facing Perimeter Zones

Like east-facing façades, west-facing facades also experience an imbalance of direct sunlight from the low angle sun during the afternoon. As a result, offices in both east- and west-facing perimeter zones have the same energy performance and the preference for lower window areas. In fact, offices in both perimeter zones uses approximately 1%-5% more energy than the average of all zones. The results of the simulations are shown in Figure 5.4.5, which indicates that windows with moderate WWRs are preferred since they have the least annual energy consumption.

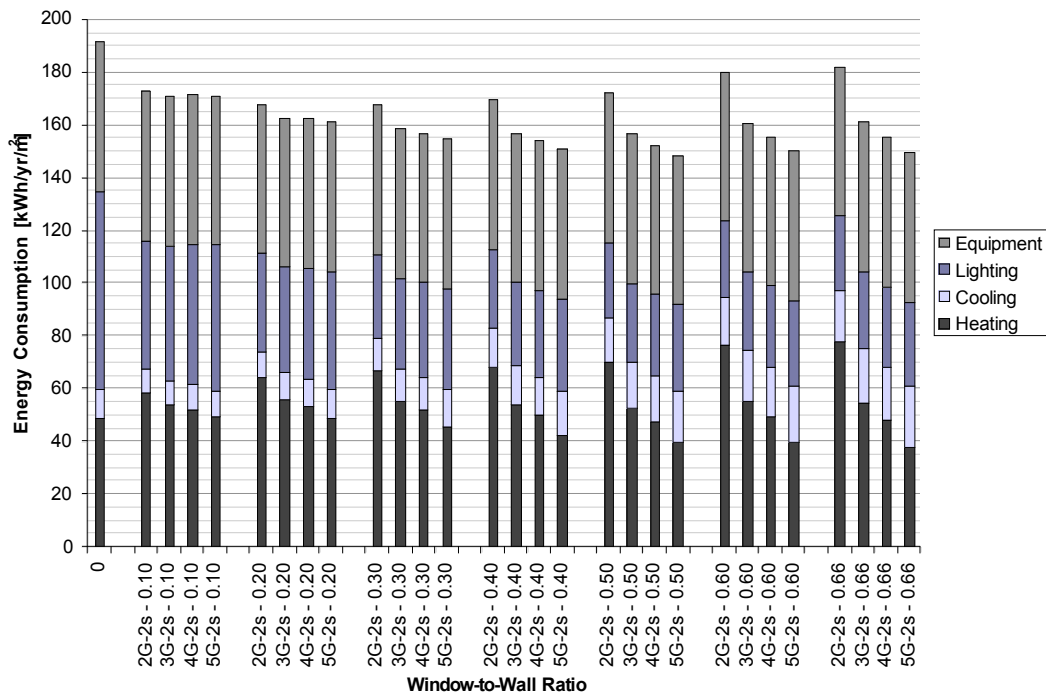


Figure 5.4.5 Annual energy consumption of offices in west-facing perimeter zone with multi-layered low solar gain, low and ultra-low U-value wood windows

As expected, the effect of reducing the SHGC increases the annual energy consumption due to higher heating and lighting energy demand. The increase in overall energy use however, is slight and does not significantly affect the energy performance of the office. The energy consumption for offices with high and low solar gain windows are listed in Table 5.4.5.

Table 5.4.5 Annual energy consumption of offices in west-facing perimeter zones

WWR	Window Type	Total Energy Consumption [kWh/yr/m ²] (Percentage savings from double-glaze window)			
		Double-glaze	Triple-glaze	Quad-glaze	Quint-glaze
0	-	191.5	191.5	191.5	191.5
0.10	Low Solar	172.8	170.9 (1%)	171.4 (1%)	171.3 (1%)
	Ultra-Low Solar	178.7	174.6 (2%)	174.8 (2%)	173.4 (3%)
0.20	Low Solar	168.1	162.7 (3%)	162.4 (3%)	161.1 (4%)
	Ultra-Low Solar	175.1	167.4 (4%)	166.8 (5%)	164.2 (6%)
0.30	Low Solar	167.7	158.6 (5%)	157.0 (6%)	154.7 (8%)
	Ultra-Low Solar	174.7	163.4 (6%)	162.0 (10%)	158.5 (9%)
0.40	Low Solar	169.5	157.0 (7%)	154.2 (9%)	151.0 (11%)
	Ultra-Low Solar	176.0	161.4 (8%)	158.6 (10%)	154.6 (12%)
0.50	Low Solar	172.3	156.7 (9%)	152.6 (11%)	148.5 (14%)
	Ultra-Low Solar	178.4	160.0 (10%)	156.1 (12%)	151.5 (15%)
0.60	Low Solar	180.2	160.9 (11%)	155.7 (14%)	150.3 (17%)
	Ultra-Low Solar	187.2	164.2 (12%)	159.3 (15%)	153.2 (18%)
0.66	Low Solar	182.3	161.3 (11%)	155.5 (15%)	149.6 (18%)
	Ultra-Low Solar	189.2	164.1 (13%)	158.6 (16%)	152.1 (20%)

The peak heating and cooling consumption are also similar to that of the offices in east-facing perimeter zones. Without adequate thermal storage, increasing the window area increases both the peak heating and cooling energy consumption.

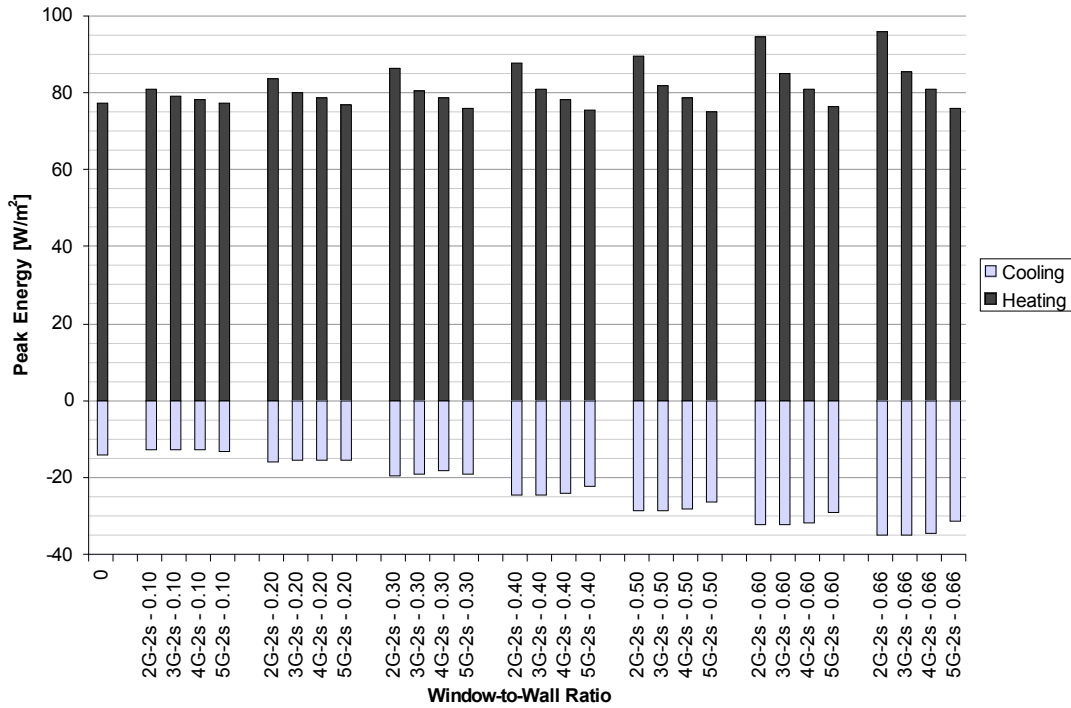


Figure 5.4.6 Peak energy consumption of offices in west-facing perimeter zones with multi-layered low solar gain, low and ultra-low U-value wood windows

From the simulation results the optimal window areas for offices in west-facing perimeter zones are listed Table 5.4.6.

Table 5.4.6 Optimal WWR for offices in west-facing perimeter zones

Orientation	Window Type	Total Energy Consumption	Peak Heating Consumption	Peak Cooling Consumption
West	Double-Glaze (2G-2s)	0.30	0.10	0.10
	Triple-Glaze (3G-2s)	0.50	0.10	0.10
	Quad-Glaze (4G-2s)	0.50	0.10	0.10
	Quint-Glaze (5G-2s)	0.50	0.10	0.10

5.4.4 North-Facing Perimeter Zones

North-facing façades do not receive a lot of direct solar radiation due to solar positioning. As a result, north-facing perimeter zones are characterized by higher heating loads over cooling loads. In fact, offices in north-perimeter zones use the most energy out of all orientations, at approximately 6%-8% more than the average consumption of all perimeter zones. Since space heating is critical to the energy performance of north-facing perimeter zones, energy consumption significantly decreases with decreasing window U-value. In addition, smaller window areas are preferred over large window areas. The energy performance of an office in north-facing perimeter zone is shown in Figure 5.4.7 for various window types. The plot shows that for most windows the annual energy consumption dips to a minimum at around WWR 0.30-0.40, due to savings in lighting energy.

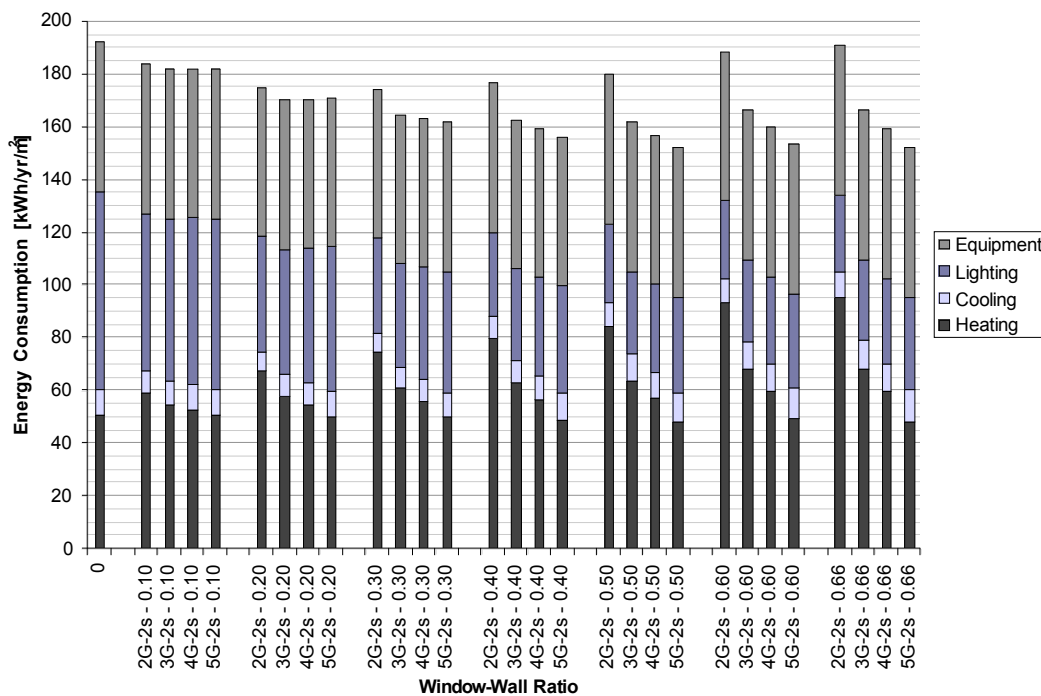


Figure 5.4.7 Annual energy consumption of offices in north-facing perimeter zone with multi-layered low solar gain low and ultra-low U-value wood windows

Similar to all other perimeter zones, decreasing the SHGC of north-facing windows only increase the annual energy consumption. Since cooling demand is not significant, decreasing the SHGC only increases the space heating and light energy demand, which raises the overall annual energy consumption. The annual energy consumption for

offices in north-facing perimeter zones with low and ultra-low solar gain windows are summarized in Table 5.4.7.

Table 5.4.7 Annual energy consumption of offices in north-facing perimeter zones

WWR	Window Type	Total Energy Consumption [kWh/yr/m ²] (Percentage savings from double-glaze window)			
		Double-glaze	Triple-glaze	Quad-glaze	Quint-glaze
0	-	192.2	192.2	192.2	192.2
0.10	Low Solar	183.8	181.8 (1%)	182.1 (1%)	181.8 (1%)
	Ultra-Low Solar	189.0	184.6 (2%)	184.4 (2%)	183.1 (3%)
0.20	Low Solar	175.2	170.2 (3%)	170.7 (3%)	171.1 (2%)
	Ultra-Low Solar	185.6	176.5 (5%)	176.5 (5%)	174.2 (6%)
0.30	Low Solar	174.5	164.8 (6%)	163.3 (6%)	161.8 (7%)
	Ultra-Low Solar	182.9	169.8 (7%)	168.6 (8%)	165.3 (10%)
0.40	Low Solar	176.9	162.7 (8%)	159.5 (10%)	156.4 (12%)
	Ultra-Low Solar	183.8	166.7 (9%)	164.2 (11%)	160.0 (13%)
0.50	Low Solar	179.8	161.8 (10%)	156.9 (13%)	152.2 (15%)
	Ultra-Low Solar	185.8	164.9 (11%)	160.6 (14%)	155.8 (16%)
0.60	Low Solar	188.7	166.3 (12%)	160.0 (15%)	153.6 (19%)
	Ultra-Low Solar	195.4	169.6 (13%)	164.1 (16%)	157.6 (19%)
0.66	Low Solar	191.0	166.4 (13%)	159.4 (17%)	152.2 (20%)
	Ultra-Low Solar	197.8	169.6 (14%)	163.3 (17%)	156.3 (21%)

Since north-facing façades do not receive any direct sun, increasing the window area only increases the peak heating energy consumption, while it does not change the peak cooling

load. These trends are shown in Figure 5.4.8, which plots the peak heating and cooling energy consumption of an office in the north-facing perimeter zone.

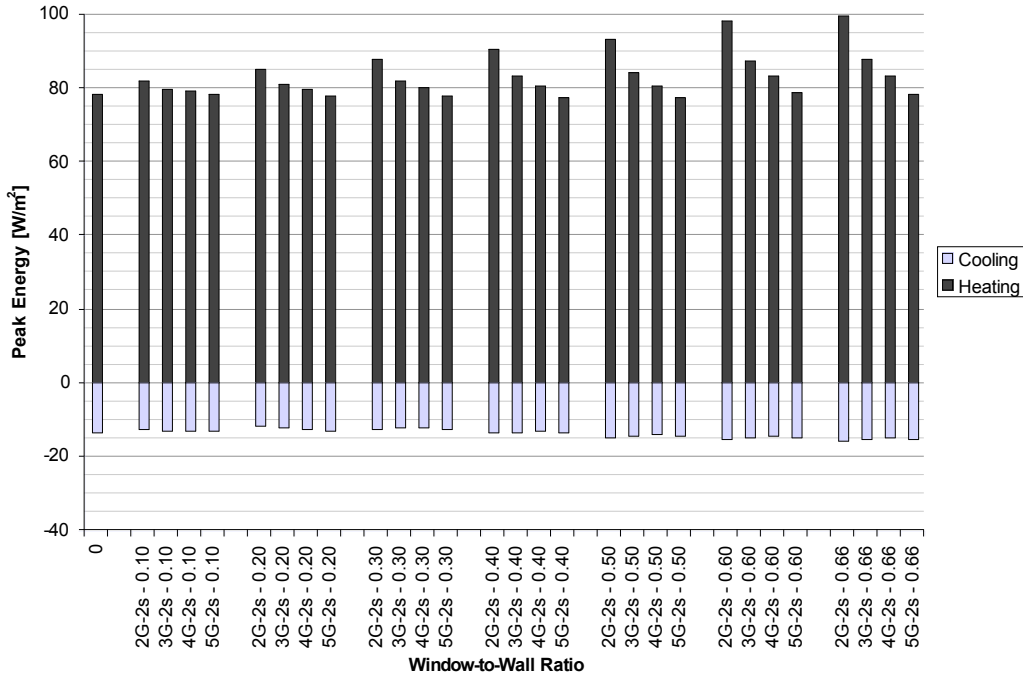


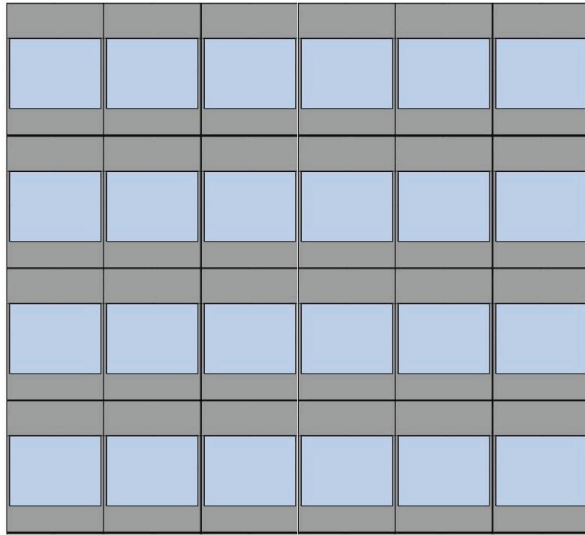
Figure 5.4.8 Annual energy consumption of offices in the north-facing perimeter zone with multi-layered low solar gain, low and ultra low U-value wood windows

From these results it is evident that smaller WWRs are preferred to limit heat loss and keep heating loads to a minimum. Table 5.4.8 lists the optimal WWRs for various window types for an office located in the north-facing perimeter zone.

Table 5.4.8 Optimal WWR for offices in north-facing perimeter zones

Orientation	Window Type	Total Energy Consumption	Peak Heating Consumption	Peak Cooling Consumption
North	Double-Glaze (2G-2s)	0.30	0.10	0.20
	Triple-Glaze (3G-2s)	0.50	0.10	0.20
	Quad-Glaze (4G-2s)	0.50	0.10	0.30
	Quint-Glaze (5G-2s)	0.50	0.50	0.30

With these optimal window areas, an energy efficient building would look like something similar to Figure 5.4.9 with double-glazed low U-value windows and Figure 5.4.10 for triple-glazed ultra-low U-value windows, while for buildings with quad- and quint-glazed ultra-low U-value windows the facades would appear to be similar to Figure 5.4.11.

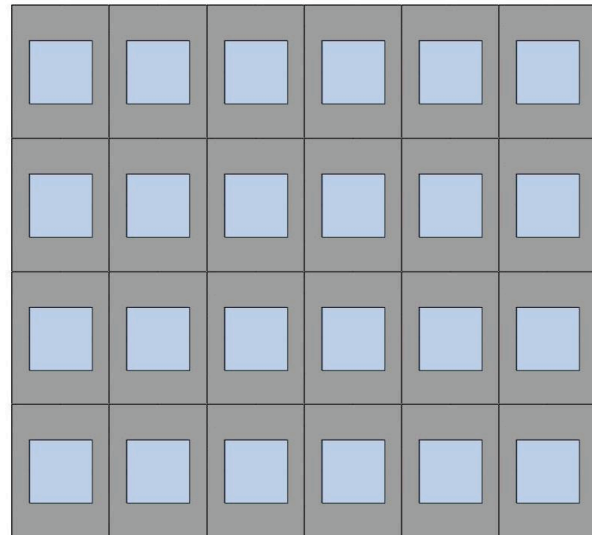


WWR = 0.50

$$1.40 \text{ W/m}^2\text{K} < U < 1.42 \text{ W/m}^2\text{K}$$

$$0.25 < \text{SHGC} < 0.37$$

South Façade



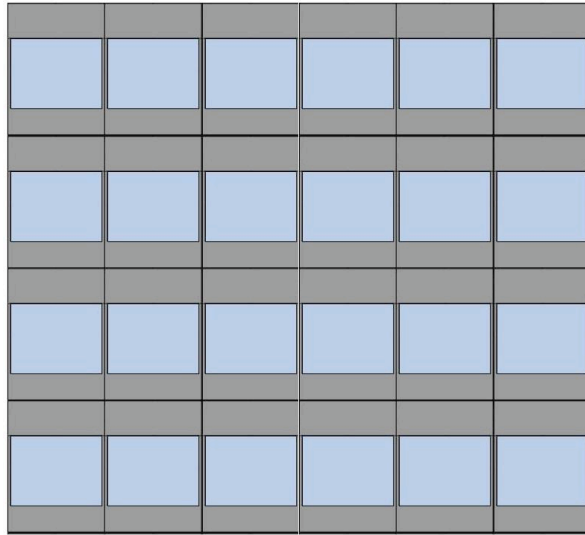
WWR = 0.30

$$1.42 \text{ W/m}^2\text{K} < U < 1.44 \text{ W/m}^2\text{K}$$

$$0.25 < \text{SHGC} < 0.37$$

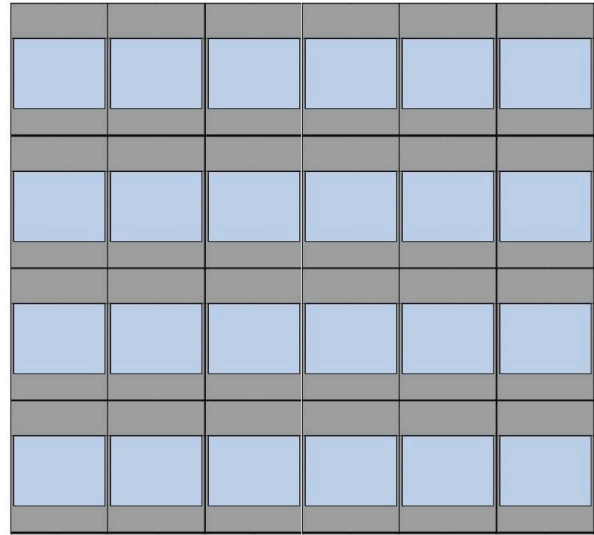
East, West, North Façade

Figure 5.4.9 Optimal WWR for an un-shaded building with low U-value double-glazed windows



WWR = 0.50

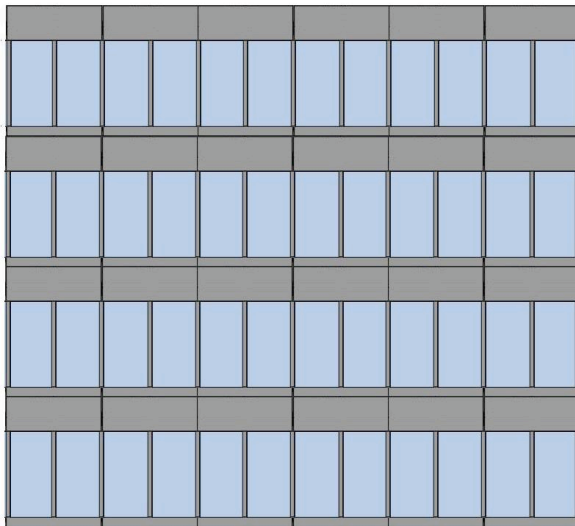
$0.73 \text{ W/m}^2\text{K} < U < 0.77 \text{ W/m}^2\text{K}$
 $0.19 < \text{SHGC} < 0.37$
 South Façade



WWR = 0.50

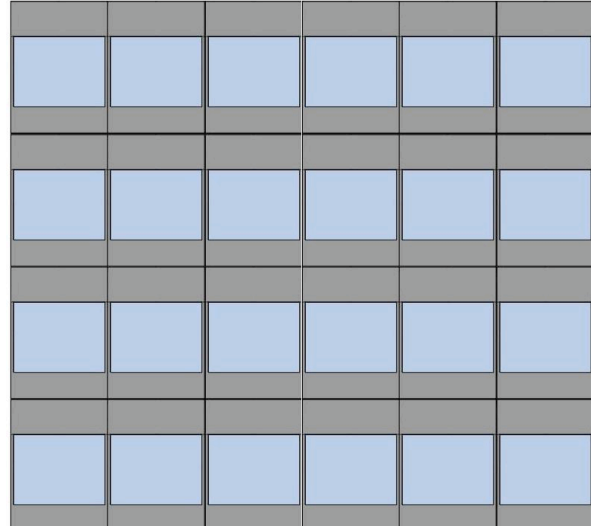
$0.73 \text{ W/m}^2\text{K} < U < 0.77 \text{ W/m}^2\text{K}$
 $0.19 < \text{SHGC} < 0.37$
 East, West, North Façade

Figure 5.4.10 Optimal WWR for an un-shaded building with triple-glazed ultra-low U-value windows



WWR = 0.66

$0.48 \text{ W/m}^2\text{K} < U < 0.60 \text{ W/m}^2\text{K}$
 $0.18 < \text{SHGC} < 0.35$
 South Façade



WWR = 0.50

$0.46 \text{ W/m}^2\text{K} < U < 0.58 \text{ W/m}^2\text{K}$
 $0.18 < \text{SHGC} < 0.35$
 East, West, North Façade

Figure 5.4.11 Rendering of optimal WWR for an un-shaded building with quad- or quint-glazed ultra-low U-value windows

5.5 Optimal Window Design for High-performance Facades with Solar Control

With the addition of exterior shading, the amount of solar gain at the façade is reduced. This reduction can not only change the annual and peak energy consumption for space heating, cooling, and lighting, but if the changes are significant enough it may also alter the optimal window area. As with un-shaded façades, the optimal window design will change depending on the shading strategy and orientation. In this section the impact of both static and dynamic exterior shading devices on the energy performance of the office considered is examined for all four orientations through a series of simulations. The results of these simulations are summarized in this section and can be found in Appendix D4.

5.5.1 South-facing Perimeter Zones with Solar Control

The addition of solar control in the form of overhangs and adjustable louvers increased the annual energy consumption of offices located in south-facing perimeter zones. These solar control devices reduced solar gains, which led to lower cooling loads, but also higher heating and lighting loads, both of which offset any energy savings from a smaller cooling load. The degree of variation in annual energy consumption as well as peak energy consumption varied depending on the window type, window area, and shading device. The effect of both static and dynamic shading devices on both annual and peak energy consumption are summarized in Table 5.5.1.

Table 5.5.1 Effect of static and dynamic shading on energy consumption of offices located in south-facing perimeter zones

Energy Consumption by type	Static Shading (Overhang)	Dynamic Shading (Adjustable Louvers)
Space Heating	<p>Increases annual heating energy consumption with increasing window area and decreasing window U-value.</p> <p>For double-glazed windows the increase in heating energy consumption is approximately 4%-6% at low WWRs (WWR 0.10-0.20), 11%-16% at moderate WWRs (WWR 0.30-0.50), and 17%-19% for high WWRs (WWR 0.60-0.66). Conversely, for quint-glazed windows the annual heating energy consumption is increased by 32%-55% at low WWRs, 75%-173% at moderate WWRs, and 229%-287% at high WWRs.</p>	<p>Increases annual heating energy consumption by 1%-7% for low to moderate window areas (WWR 0.10-0.50) and by 11%-19% for large window areas (WWR 0.60-0.66). For highly insulated quint-glazed windows the increase in heating energy is as high as 30% at WWR 0.66</p>
Sensible Cooling	<p>Decreases annual cooling energy consumption with increasing window area and decreasing window U-value.</p> <p>At lower window areas of around WWR 0.10-0.20, the cooling energy consumption is decreased by 12%-33%, while at moderate window areas (WWR 0.30-0.50), the cooling energy consumption is decreased by 28%-43%, and by 35%-48% at larger window areas (WWR 0.60-0.66).</p>	<p>Increase annual cooling energy consumption by 5%-22% at low WWRs (WWR 0.10-0.20), with the greatest increase at WWR 0.10. However, at moderate window areas (WWR 0.30-0.50) dynamic shading decreases annual cooling energy by 7%-31% and by as much as 40% for large window areas.</p> <p>Increase in cooling energy caused by an increase in lighting load.</p>
Lighting	<p>Increases annual lighting energy consumption for less insulating windows with greater clarity. However, as the window's VT decreases with U-value, lighting energy consumption is equal to</p>	<p>Increases annual lighting energy consumption by 20%-35% for all windows and window areas. This increase in lighting energy causes an increase in</p>

	that of an un-shaded façade.	cooling load at smaller window areas.
Peak Heating	Increases peak heating loads by as much as 17% and increases with increasing window area.	Unchanged by shading device.
Peak Cooling	Reduces peak cooling loads by 4%-25% depending on the window type and window area.	Reduces peak cooling loads, particularly at larger window areas. The peak cooling load can be reduced by 3%-25% for low to moderate window areas (WWR 0.10-0.50), and up to 30% for large window areas (WWR 0.60-0.66).

The results of the simulations are also plotted in Figure 5.5.1 to Figure 5.5.4 for double-, triple-, quad-, and quint-glazed high-performance timber windows.

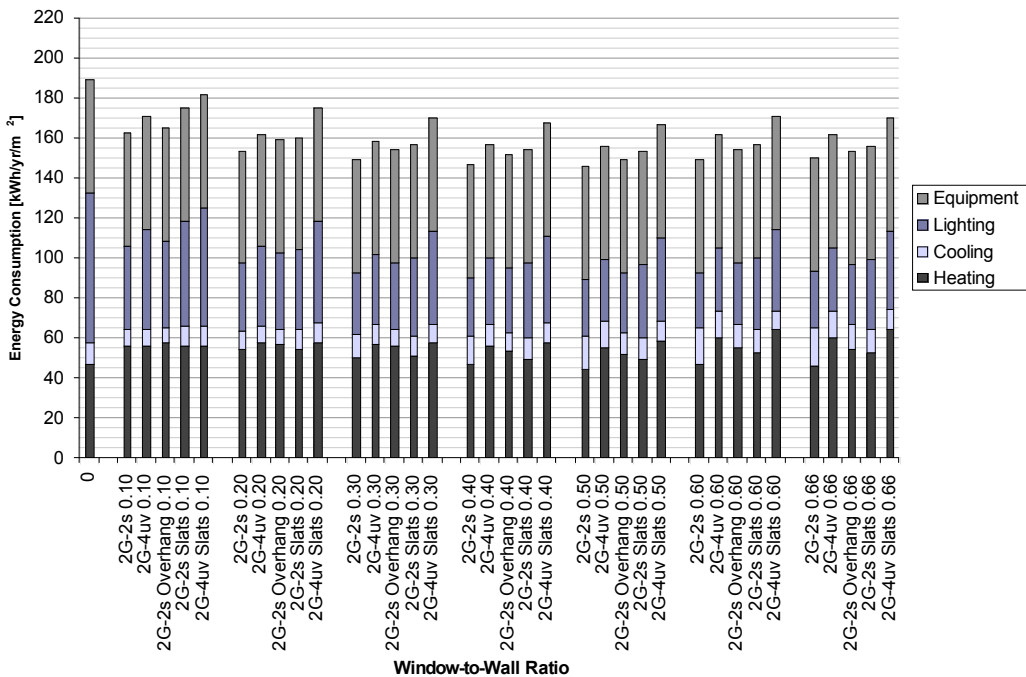


Figure 5.5.1 Annual energy consumption of an office space in the south-facing perimeter zone with low U-value double-glazed windows with fixed and dynamic solar control

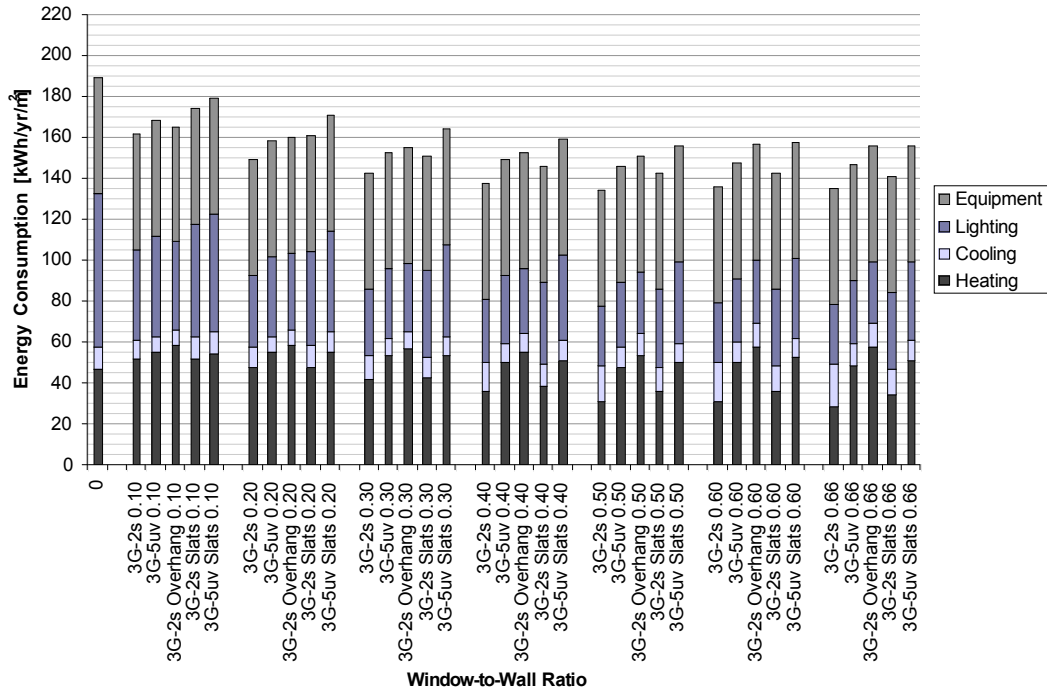


Figure 5.5.2 Annual energy consumption of an office space in the south-facing perimeter zone with ultra-low U-value triple-glazed windows with fixed and dynamic solar control

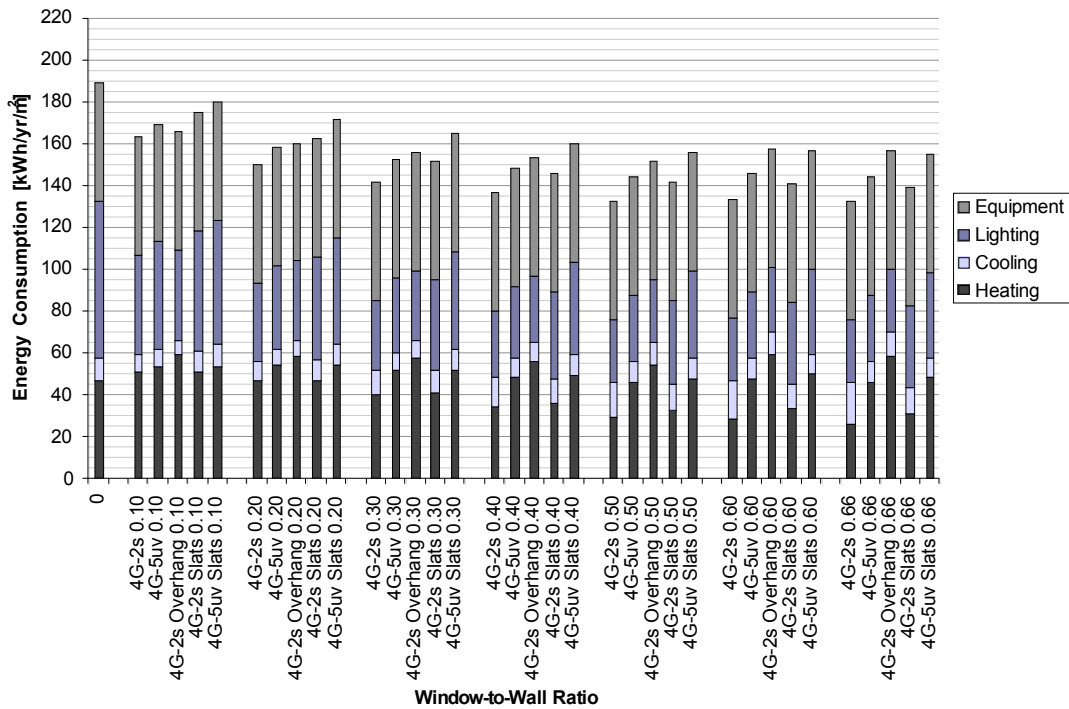


Figure 5.5.3 Annual energy consumption of an office space in the south-facing perimeter zone with ultra-low U-value quad-glazed windows with fixed and dynamic solar control

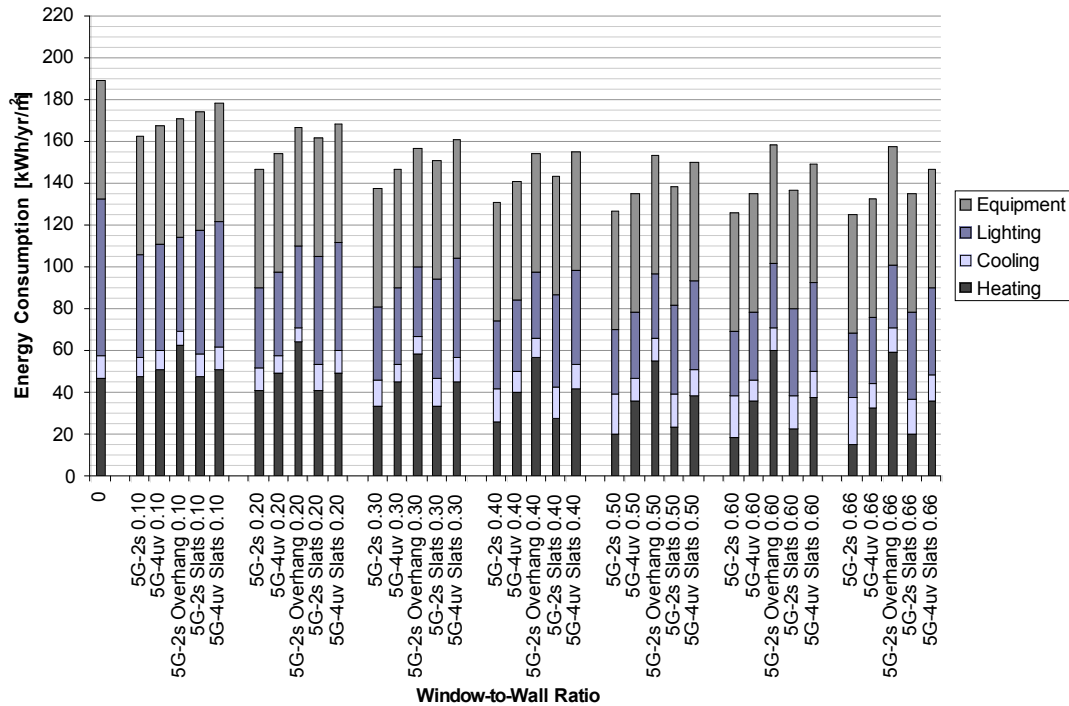


Figure 5.5.4 Annual energy consumption of an office space in the south-facing perimeter zone with ultra-low U-value quint-glazed windows with fixed and dynamic solar control

From these results it is clear that fixed shading devices do not provide any benefit to moderate internal gain offices located in south-facing perimeter zones other than for a reduction in peak cooling energy. Since the increase in annual total energy consumption is similar across all window areas, the optimal window areas remains the same as for facades without solar control at WWR 0.50 for low U-value double- and ultra-low U-value triple-glazed facades and WWR 0.66 for all other window types.

5.5.2 East-Facing Perimeter Zones with Solar Control

Similar to south-facing perimeter zones, adding solar control in the form of fins and adjustable louvers to east-facing façades, increased the annual energy consumption of offices located in east-facing perimeter zones. Although peak cooling loads were reduced with less solar gains, peak and annual heating energy consumption was increased, along with lighting energy consumption. In some cases the annual cooling energy consumption was also increased due to higher internal heat gain from higher lighting loads. As with offices in the south-facing perimeter zone, the degree variation in

annual energy consumption as well as peak energy consumption changed depending on the window type, window area, and shading device. The effect of both static and dynamic shading devices on both annual and peak energy consumption are summarized in Table 5.5.2.

Table 5.5.2 Effect of static and dynamic shading on energy consumption of offices located in east-facing perimeter zones

Energy Consumption by type	Static Shading (Overhang)	Dynamic Shading (Adjustable Louvers)
Space Heating	<p>Increases heating loads with increasing window area and decreasing window U-values.</p> <p>For double-glazed windows, the increase in heating load is by 14%-60% from WWR 0.10-0.66, for triple-glazed windows the increase is 14%-60%, for quad-glazed windows the increase is 18%-84%, and for quint-glazed windows the increase is 30%-137%.</p>	<p>Does not affect annual heating energy consumption for low to moderately glazed façades (WWR 0.10-0.30).</p> <p>It only increases the heating load at higher WWRs by at most 5%.</p>
Sensible Cooling	<p>Decreases cooling loads with increasing window area and decreasing window U-values.</p> <p>For double-glazed windows, the cooling load is reduced by 10%-15%, 13%-19% for triple-glazed windows, 15%-17% for quad-glazed windows, and 24%-28% for quint-glazed windows.</p>	<p>Increases annual cooling energy consumption by approximately 10% at very low WWRs (WWR 0.10).</p> <p>However it reduces cooling loads by 12%-35% at moderate window areas (WWR 0.30-0.50) and by 31%-44% at higher window areas (WWR 0.60-0.66).</p>
Lighting	<p>Increases lighting loads for most window types with a peak jump of 25% at WWR 0.40.</p> <p>However, the increase is reduced with larger window areas.</p>	<p>Increases lighting loads by 15%-30% at low WWRs (WWR 0.10-0.20), 33%-45% at moderate WWRs (WWR 0.30-0.50), and 42%-45% at high WWRs (WWR 0.60-0.66).</p>

Peak Heating	Increases peak heating loads by as much as 33% with increasing window area.	Unchanged by shading device.
Peak Cooling	Reduces peak cooling loads by 2%-11% depending on the window type and window area, which is not as significant as the south façade.	Reduces peak cooling loads, particularly at larger window areas. With dynamic shading, peak cooling loads can be reduced by 2%-43% for low to moderate window areas.

The results of the simulations are also plotted in Figure 5.5.5 to Figure 5.5.8 for double-, triple-, quad-, and quint-glazed high-performance wood windows.

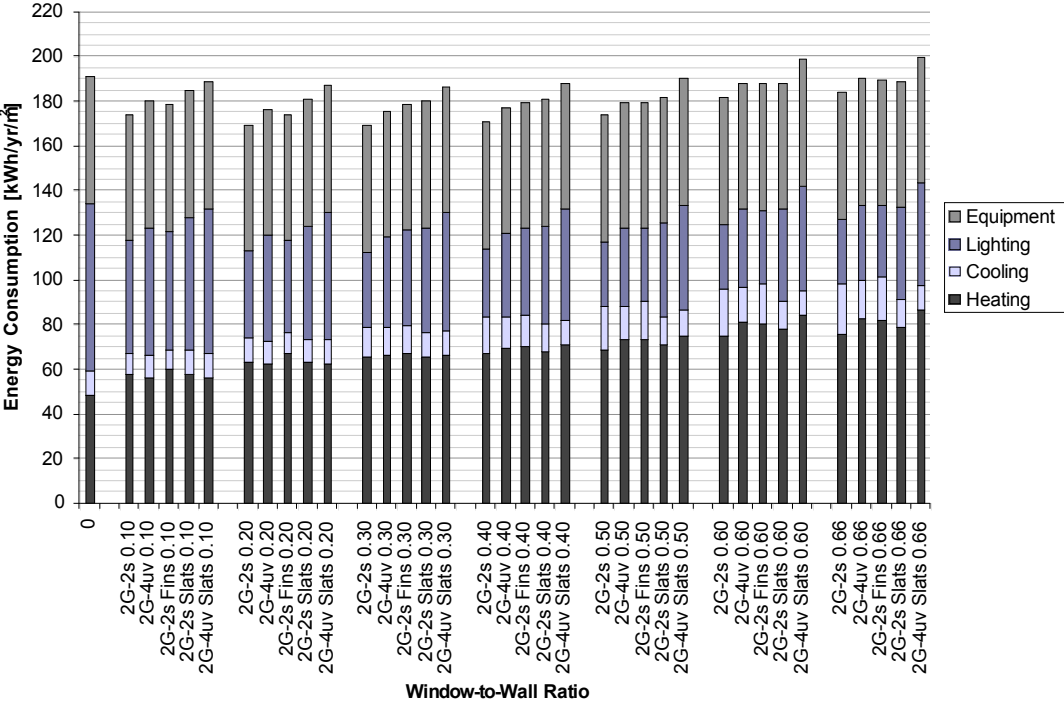


Figure 5.5.5 Annual energy consumption of an office in east-facing perimeter zone with double-glazed windows and fixed and dynamic solar control

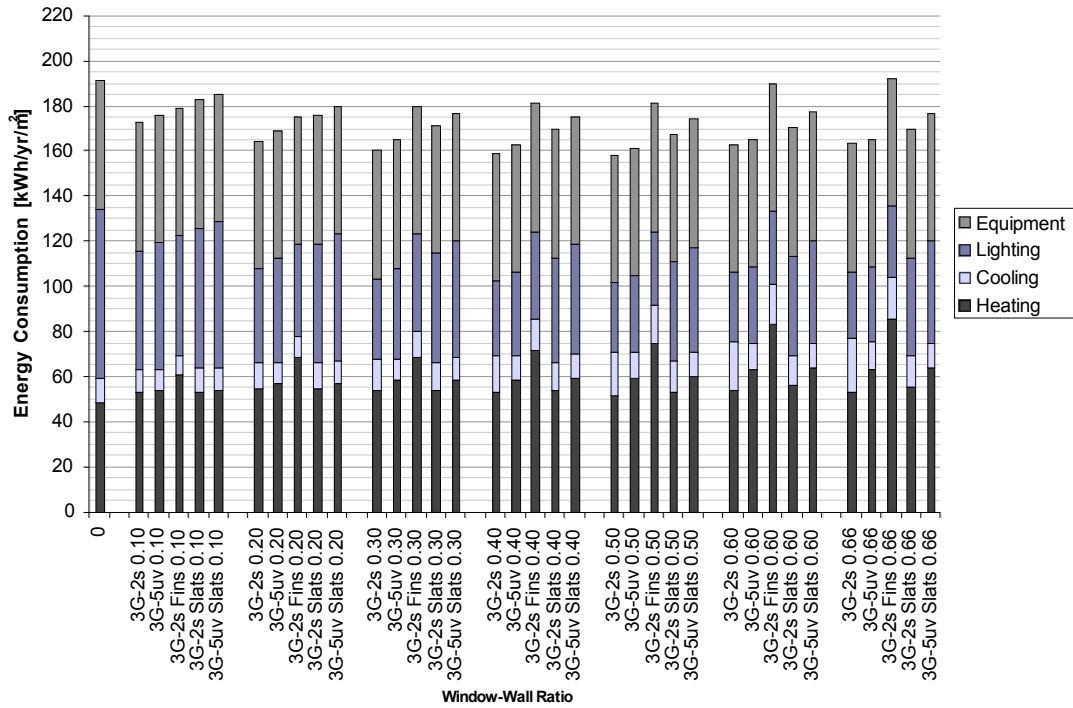


Figure 5.5.6 Annual energy consumption of an office in east-facing perimeter zone with triple-glazed windows and fixed and dynamic solar control

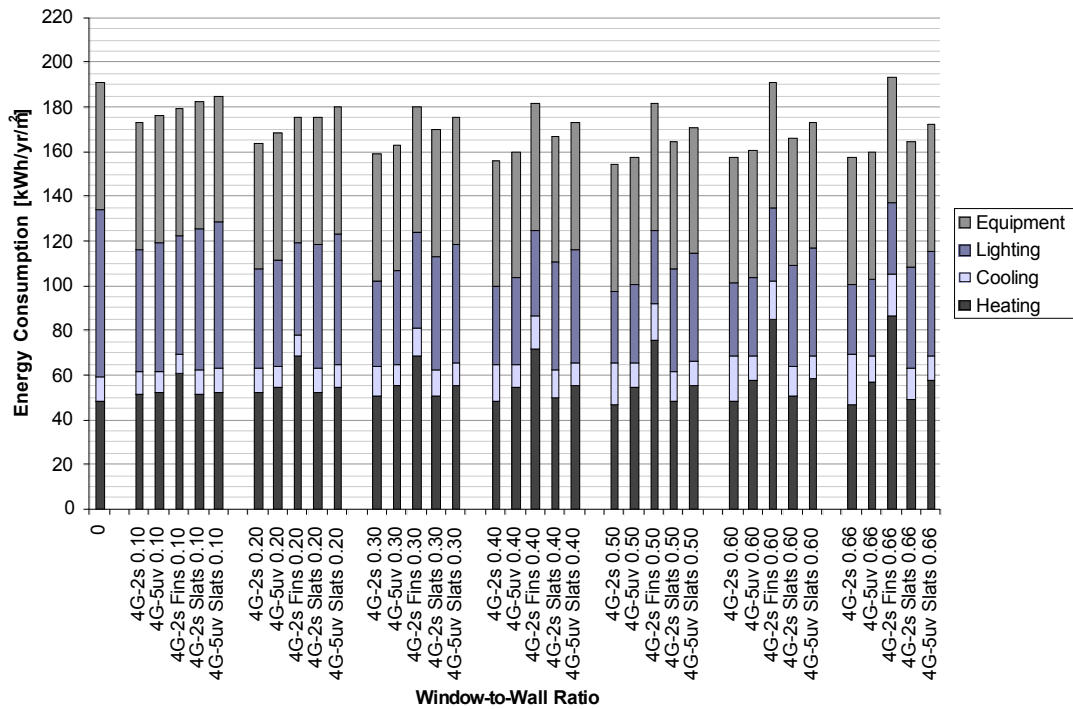


Figure 5.5.7 Annual energy consumption of an office in east-facing perimeter zone with quad-glazed windows and fixed and dynamic solar control

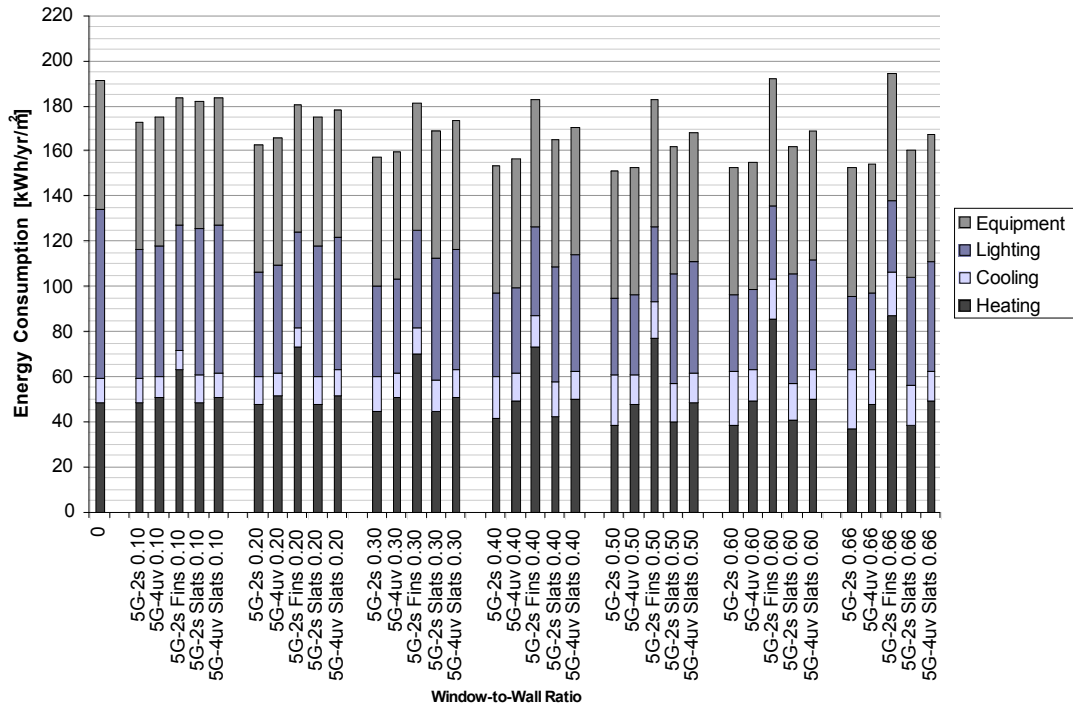


Figure 5.5.8 Annual energy consumption of an office in east-facing perimeter zone with quint-glazed windows and fixed and dynamic solar control

Similar to the south-facing perimeter zone, exterior shading provides very little benefit to energy consumption other than reducing peak cooling loads for a moderate internal gain office. Like the south façade, the cooling load savings were offset by an increase in both the heating and lighting loads, resulting in higher annual energy consumption. Since exterior shading added to the energy consumption by similar amounts across all window areas, the optimal WWR remains the same as for the un-shaded façade at WWR 0.30 for double-glazed façade and WWR 0.50 for all other window types.

5.5.3 West-Facing Perimeter Zones with Solar Control

Since the west-facing perimeter zone behaves very similar to the east-facing perimeter zone, adding exterior shading to the west façade provided similar results as the east façade. The addition of both static and dynamic shading increased the annual energy consumption, particularly in both heating and lighting loads. This increase in both loads effectively offset any energy savings from a reduced cooling load. However, exterior shading is effective at reducing the peak cooling load, which can provide savings during construction when selecting an appropriate cooling system. As with offices in the east-

facing perimeter zone, the degree variation in annual and peak energy consumption changes depending on the window type, window area, and shading device. The effect of both static and dynamic shading devices on both annual and peak energy consumption are summarized in Table 5.5.3.

Table 5.5.3 Effect of static and dynamic shading on energy consumption of offices located in west-facing perimeter zones

Energy Consumption by type	Static Shading (Overhang)	Dynamic Shading (Adjustable Louvers)
Space Heating	<p>Increases heating loads with increasing window area and decreasing window U-values.</p> <p>For double-glazed windows, the increase in heating load is by 4%-8% from WWR 0.10-0.66, for triple-glazed windows the increase is 14%-60%, for quad-glazed windows the increase is 19%-84%, and for quint-glazed windows the increase is 33%-136%.</p>	<p>Does not affect annual heating energy consumption for low to moderately glazed façades (WWR 0.10-0.30). It only increases the heating load at higher WWRs by at most 5%.</p>
Sensible Cooling	<p>Reduces cooling loads with increasing window area and decreasing window U-values.</p> <p>For double-glazed windows, the cooling load is reduced by 10%-16%, 13%-21% for triple-glazed windows, 15%-19% for quad-glazed windows, and 24%-30% for quint-glazed windows.</p>	<p>Increases annual cooling energy consumption approximately 20% at very low WWRs (WWR 0.10).</p> <p>However it reduces cooling loads by 6%-34% at moderate window areas (WWR 0.30-0.50) and by 27%-43% at higher window areas (WWR 0.60-0.66) with decreasing savings from decreasing U-values.</p>
Lighting	<p>Increases lighting loads for most window types with a peak jump of 28% at WWR 0.30.</p> <p>However, the increase is reduced with larger window areas.</p>	<p>Increases lighting loads by 18%-30% at low WWRs (WWR 0.10-0.20), 35%-49% at moderate WWRs (WWR 0.30-0.50), and 33%-44% at high WWRs (WWR 0.60-0.66).</p>

Peak Heating	Increases peak heating loads by as much as 31% with increasing window area.	Unchanged by shading device.
Peak Cooling	Reduces peak cooling loads by 4%-65% depending on the window type and window area, which is much greater than the east façade.	Reduces peak cooling loads by 6%-44% for low to moderate window areas (WWR 0.10-0.50), and up to 51% for large window areas (WWR 0.60-0.66).

The results of the simulations are also plotted in Figure 5.5.9 to Figure 5.5.12 for double-, triple-, quad-, and quint-glazed high-performance wood windows.

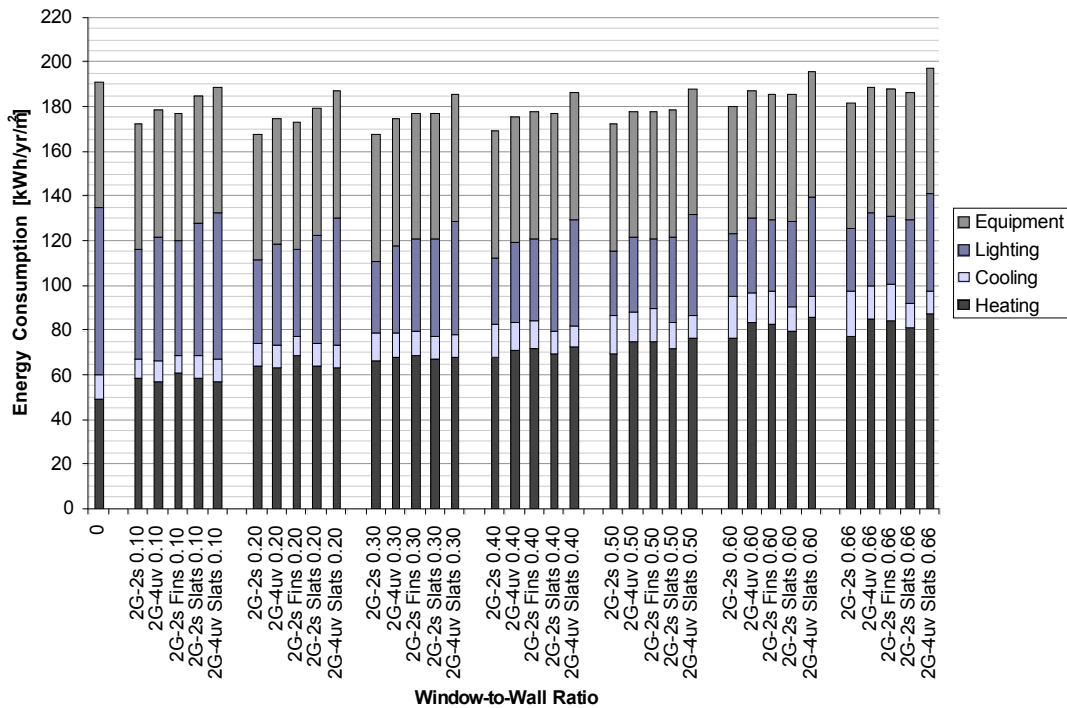


Figure 5.5.9 Annual energy consumption of an office in west-facing perimeter zone with double-glazed windows and fixed and dynamic solar control

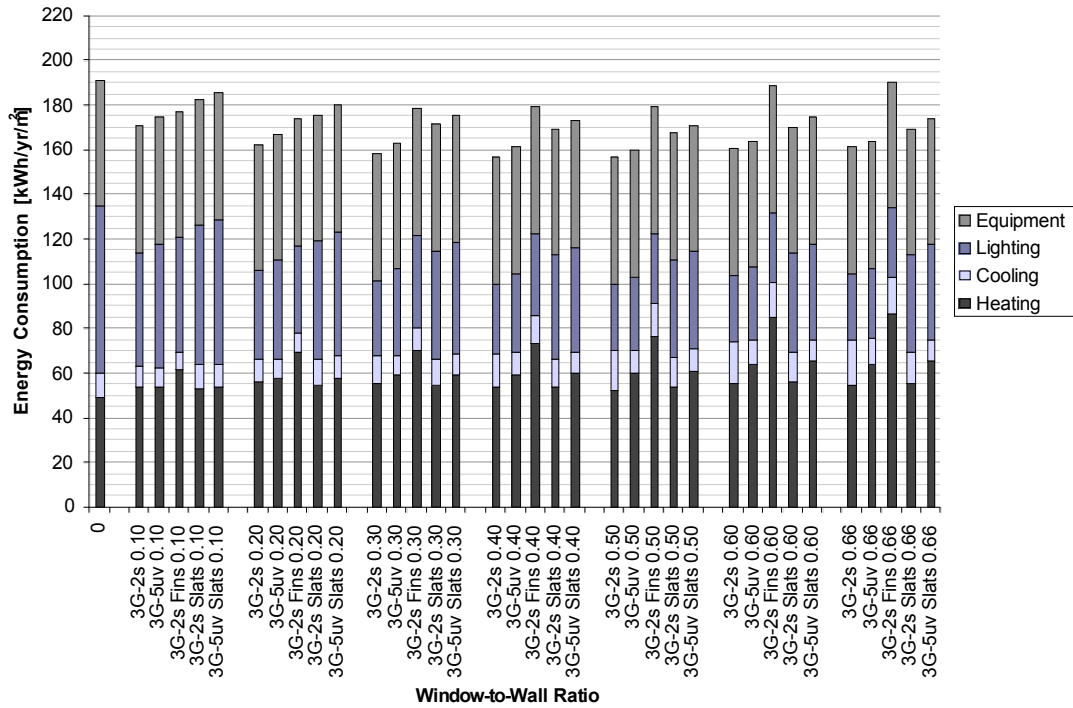


Figure 5.5.10 Annual energy consumption of an office in west-facing perimeter zone with triple-glazed windows and fixed and dynamic solar control

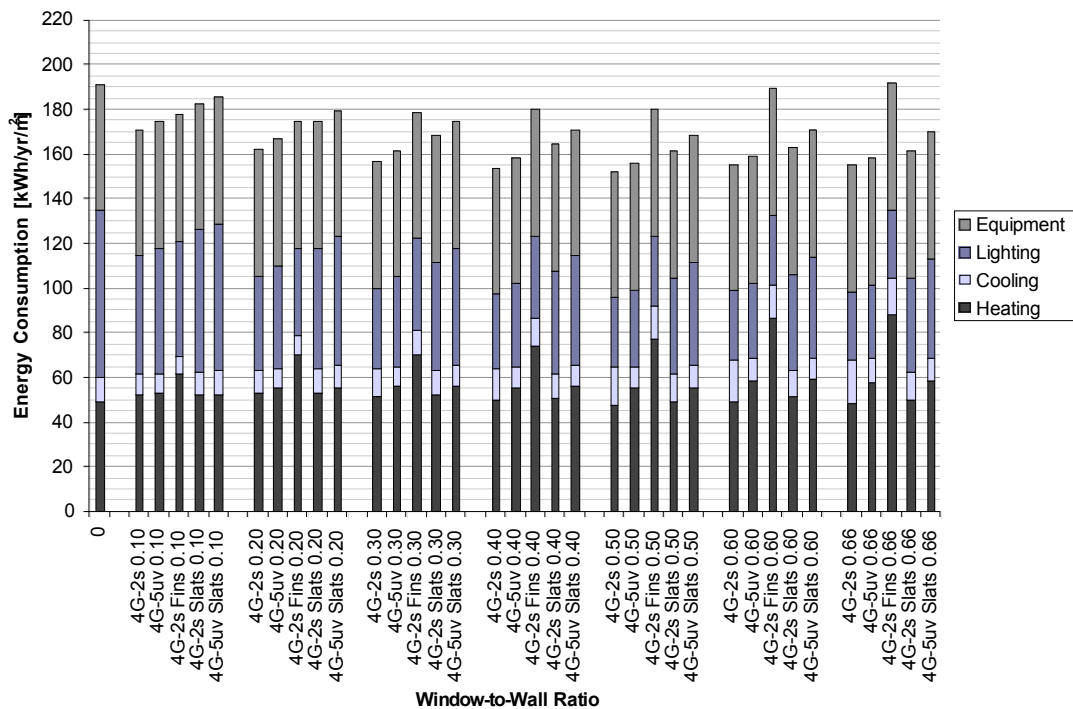


Figure 5.5.11 Annual energy consumption of an office in west-facing perimeter zone with quad-glazed windows and fixed and dynamic solar control

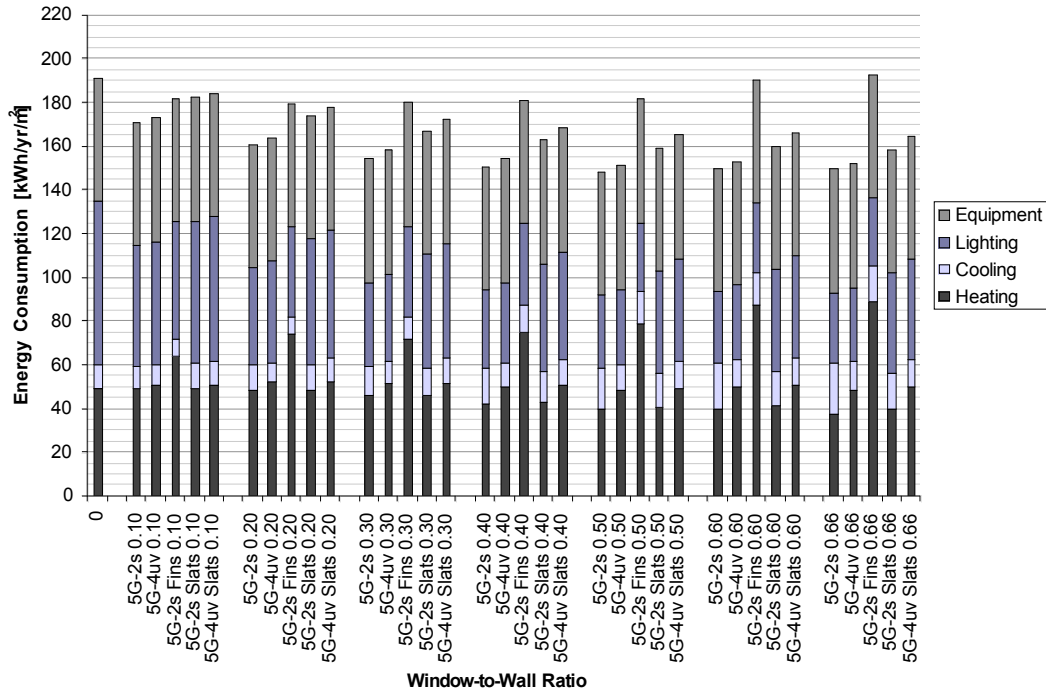


Figure 5.5.12 Annual energy consumption of an office in west-facing perimeter zone with quint-glazed windows and fixed and dynamic solar control

Just as for the south- and east-facing façade, exterior shading does not provide any benefit in terms of energy consumption other than at reducing the peak cooling rate. In most cases the addition of exterior shading devices only increases the heating and lighting loads, which effectively offset any energy savings from a reduced cooling load. Because exterior shading added to the energy consumption by similar amounts for all window areas, optimal WWR remains the same as an un-shaded façade at WWR 0.30 for double-glazed façade and WWR 0.50 for all other window types.

5.5.4 North-Facing Perimeter Zones with Solar Control

Like all other orientations, the addition of solar control on the north façade resulted in an increase in annual energy consumption. This is expected since the north façade receives very little direct sunlight. Exterior shading may provide some energy savings by reducing cooling loads, however, since the cooling energy consumption is relatively small from the moderate internal heat gain, providing exterior shading only increases the heating and lighting loads. As a result the annual energy consumption is increased. In addition, since the north façade does not receive a lot of direct solar gain, peak cooling

energy largely remains unchanged, particularly with dynamic shading, while peak heating loads are altered. The changes in heating, cooling, and lighting loads for an office located in the north-facing perimeter zone are summarized in Table 5.5.4.

Table 5.5.4 Effect of static and dynamic shading on energy consumption of offices located in north-facing perimeter zones

Energy Consumption by type	Static Shading (Overhang)	Dynamic Shading (Adjustable Louvers)
Space Heating	Reduces heating demand by at most 2%, especially for large window areas.	Does not decrease heating loads compared to unshaded façades
Sensible Cooling	<p>Does very little to decrease the cooling load at WWR 0.10.</p> <p>However, at WWR 0.20 and 0.30 the cooling load increases due to higher lighting loads. This trend in increasing cooling load continues for higher window areas with decreasing window U-value.</p> <p>For lesser insulating windows, static shading is very effective at reducing the cooling load at larger window areas. Static shading is not effective for quad- and quint-glazed windows due to an increase in lighting load.</p>	<p>Increases cooling load with at low to moderate WWRs between 0.10 and 0.30 by approximately 15%-33%.</p> <p>However, the increase in cooling load is reduced with larger WWRs and dynamic shading results in cooling energy savings at large WWRs of 0.60 and 0.66.</p>
Lighting	Increases the lighting load by 11%-18% with the greatest change in lighting load at moderate window areas (WWR 0.30-0.50).	<p>Increases lighting energy use by 10%-30% for low WWRs of 0.10 and 0.20 and by 40%-52% for moderate to large WWRs.</p> <p>This in turn adds to the cooling load via an increase in internal heat gain</p>
Peak Heating	Does not increase peak heating loads.	Unchanged by shading device.
Peak Cooling	Reduces peak cooling loads by 2%-5% depending on the	Increases peak cooling load for low to moderate WWRs

	<p>window type and window area, which is much greater than any other façades.</p>	<p>(WWR 0.10-0.30) by 6%-15%.</p> <p>Peak cooling loads only decrease at higher WWRs (WWR 0.60-0.66) by 3%-12%.</p>
--	---	---

The results of the simulations are also plotted in Figure 5.5.13 to Figure 5.5.16 for double-, triple-, quad-, and quint-glazed high-performance wood windows.

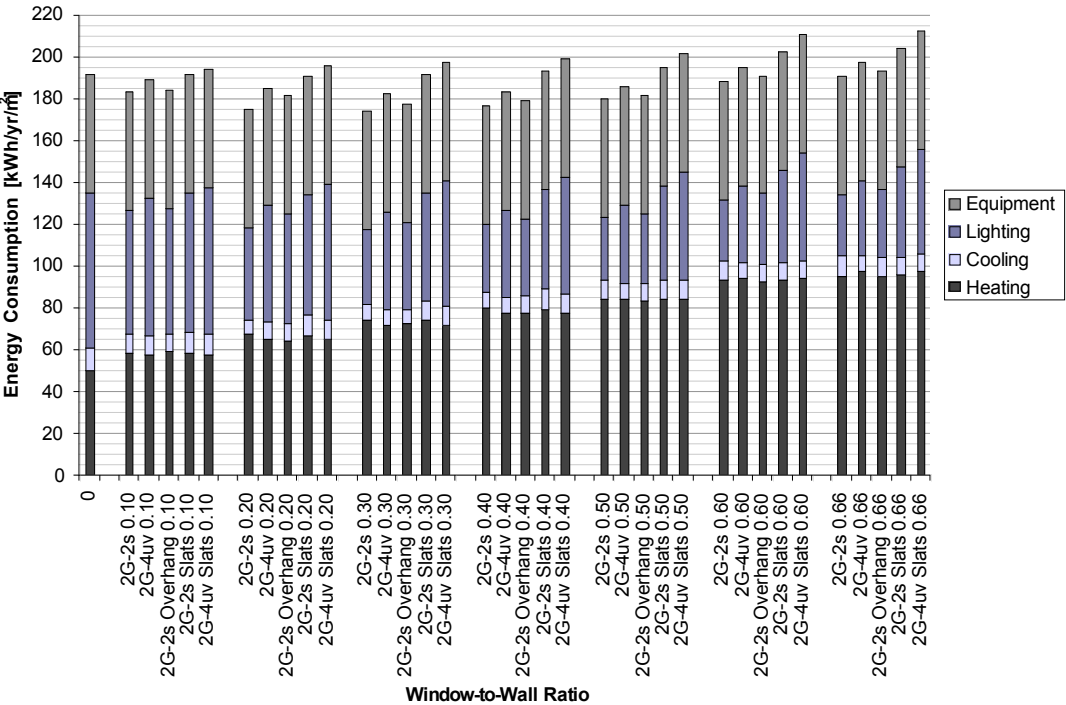


Figure 5.5.13 Annual energy consumption of an office in north-facing perimeter zone with double-glazed windows and fixed and dynamic solar control

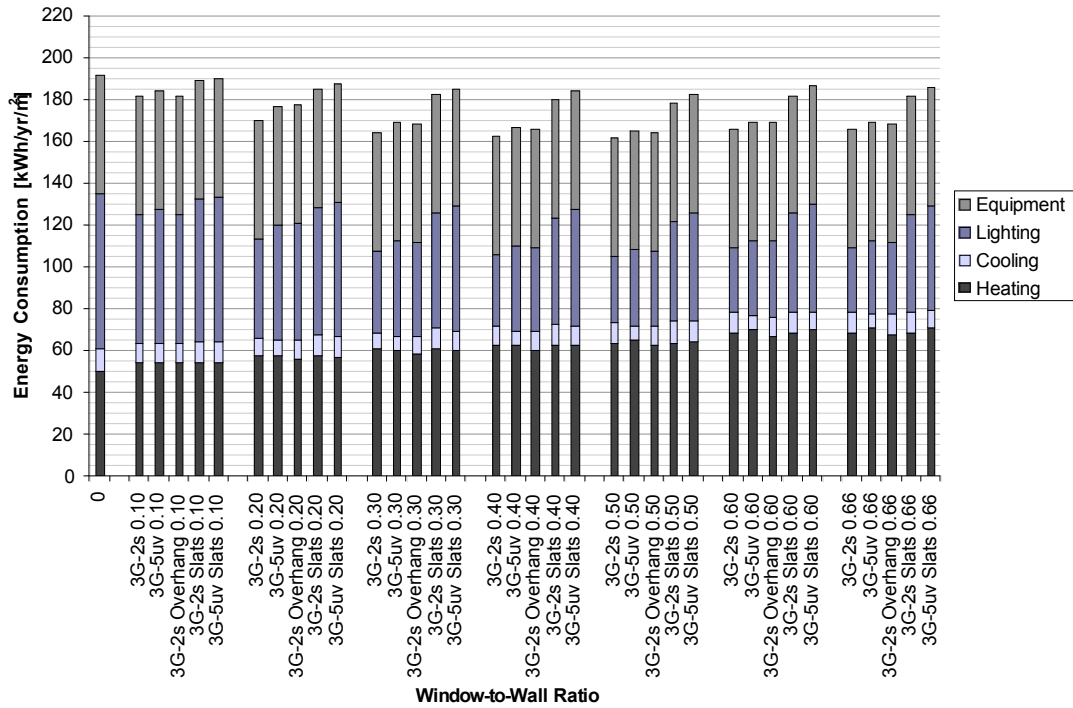


Figure 5.5.14 Annual energy consumption of an office in north-facing perimeter zone with triple-glazed windows and fixed and dynamic solar control

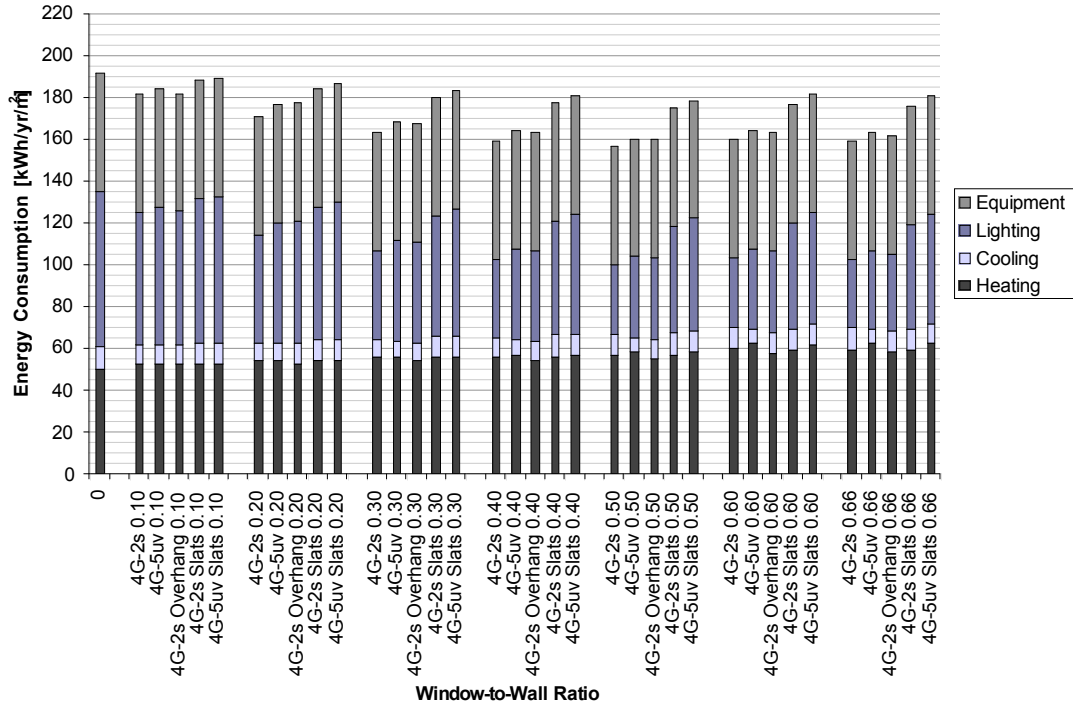


Figure 5.5.15 Annual energy consumption of an office in north-facing perimeter zone with quad-glazed windows and fixed and dynamic solar control

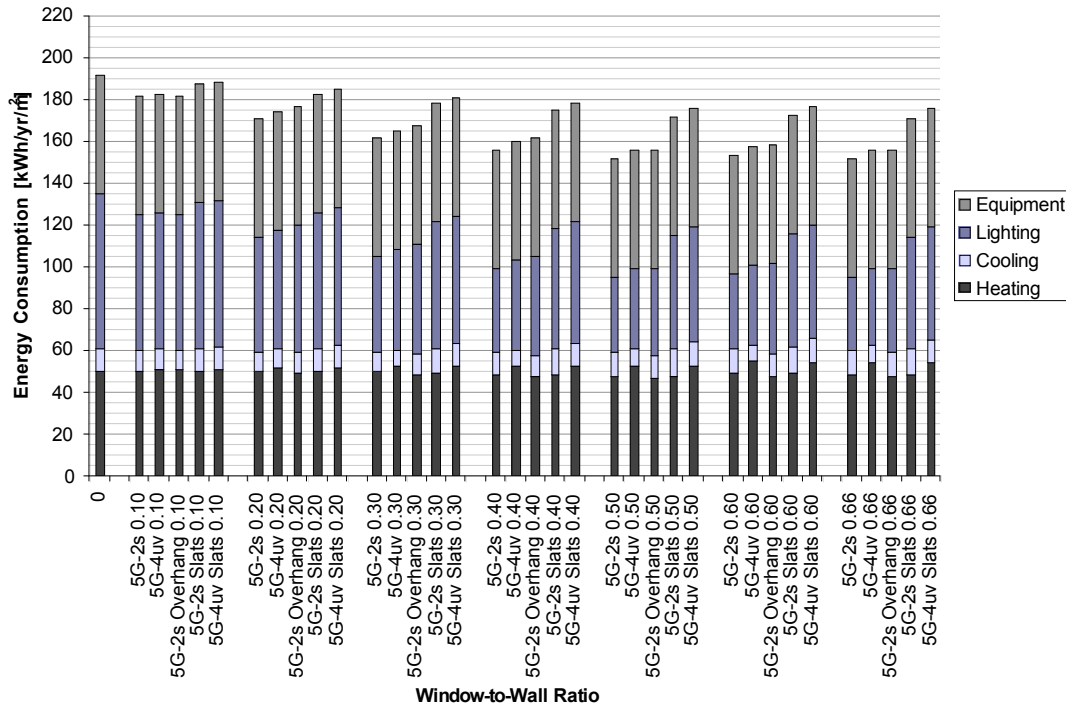


Figure 5.5.16 Annual energy consumption of an office in north-facing perimeter zone with quint-glazed windows and fixed and dynamic solar control

Similar to all other facades, exterior shading brings very little benefit to reducing energy consumption of offices in north-facing perimeter zones with moderate internal heat gain. Instead, it increases annual energy consumption by increasing the annual energy consumption for heating and lighting, while producing little to no savings in cooling energy. Because exterior shading adds to the existing energy consumption, the optimal WWR remains the same as for the un-shaded façade at WWR 0.30 for double-glazed façade and WWR 0.50 for all other window types.

From the results of this analysis, the dynamic shading algorithm used did not reduce the total energy consumption of low internal gain perimeter zone offices. In most cases, the exterior louvers often interfered with the daylighting controls by prematurely blocking off useful daylight, resulting in higher lighting loads that required more space cooling energy. In other words this dynamic shading algorithm had no net benefit in total energy consumption as the trade off between the reduced cooling load and increased lighting load was even. However, dynamic shading did reduce the peak cooling load, by as much

as 44%, depending on the window size and orientation. Larger windows facing east and west had the greatest reductions in peak cooling energy. In order to reduce the total energy consumption, the dynamic shading algorithm must be refined such that it only blocks direct sunlight to prevent overheating while still allowing daylight to enter the office. Since this is beyond the scope of this thesis, an investigation of a refined dynamic shading algorithm will have to be done at a later time. Similarly, fixed exterior shading also did not provide much energy consumption reduction in perimeter zones as it also blocked the direct sun at times when it was needed. This resulted in higher space heating, cooling, and lighting loads.

CHAPTER 6

Conclusions and Recommendations

From the results of this research it is clear that high performance window assemblies for commercial buildings can be constructed and implemented for today's high performance buildings. Even with current technology, IGU performance has reached uncharted levels, from traditional double-glazed IGUs with a U-value of $2.68 \text{ W/m}^2\text{K}$ (R-2.1) to U-values as low as $0.271 \text{ W/m}^2\text{K}$ (R-21). Such high performance levels were reached with the help of advanced coatings, glazing material, and fill gases. However, even with such high performance levels, IGU design is made no easier by the wealth of materials available. In order to select the appropriate IGU it is important to determine the desired performance indices that reduce energy consumption. Although the insulating value of an IGU may be important, other indices such as the SHGC and VT can also affect energy consumption and thermal and visual comfort. From the analysis in this thesis, it is shown that IGU performance can be altered by:

- Adding multiple layers of glazing. Adding multiple layers not only limits the convective cells within the IGU, but also provides additional surfaces to apply Low-E coatings which limit heat transfer through radiation, the most dominant mode of heat transfer in an IGU.
- Substituting air for heavier noble gases within the IGU cavity. Heavier fill gases such as Argon, Krypton, and Xenon, not only reduce convective heat transfer across the glazing cavity, they also reduce the optimal cavity width, allowing multi-layered IGUs to be even thinner.
- Emissivity and location of the Low-E coatings. Typically glazings with lower emissivities will have lower U-values at the cost of a lower SHGC. However, by placing the glazing such that the coated surface(s) are closer to the interior of the building, higher SHGC can be achieved.

By determining the appropriate IGU properties, detailed analysis of IGUs can be performed to determine how to construct the appropriate IGU with the desired properties.

Aside from IGU performance, the insulating value of the frame plays a critical role in determining the overall U-value of the window. For most commercial buildings, the frame material of choice is aluminum because of its cost and ability to span over several storeys, making it ideal for buildings with large window areas. Although aluminum is a great material for strength and precision, which is required to accommodate most IGUs, aluminum has very high thermal conductivity, making it a poor thermally insulating material. Non-thermally-broken aluminum curtain wall frames combined with aluminum spacers that have been designed in the past have frame U-values as high as $13.4 \text{ W/m}^2\text{K}$ (R-0.4) and edge U-values as high as $1.86 \text{ W/m}^2\text{K}$ (R-3.1) for a double-glazed IGU. However, with a few minor modifications the frame and edge U-values can be reduced to $4.82 \text{ W/m}^2\text{K}$ (R-1.2) and $1.25 \text{ W/m}^2\text{K}$ (R-4.5), respectively. From the results of the research in this thesis, frame and edge U-values are affected by:

- Size of the thermal break within the frame. Adding a polymeric at the glazing rabbet will significant reduce the frame U-value. However, the improvement in performance will depend on the size of the thermal-break. The high-performance aluminum curtain wall section investigated in this thesis was specially designed with an over-sized thermal-break yet it could only produce frame and edge U-values of $4.79 \text{ W/m}^2\text{K}$ (R-1.2) and $1.31 \text{ W/m}^2\text{K}$ (R-4.3), respectively, for a double-glazed IGU. The U-value further decreases with thicker higher order multi-layered IGUs, such as quint-glazed windows which has a frame U-value as low as $2.81 \text{ W/m}^2\text{K}$ (R-2.0).
- Substituting aluminum for fiberglass as pressure plate material. Since the pressure plate lies on the outside of the IGU, selecting a more insulating material for the pressure plate significantly reduces the frame U-value by decreasing the heat transfer rate of the frame and IGU. For smaller curtain wall frames designed for thinner IGUs, using fiberglass pressure plates provides the greatest impact in reducing the frame U-value. For a double-glazed IGU, using a

fiberglass pressure plate reduces the frame U-value by as much as 60% while adding a small thermal break reduces the frame U-value by only 35%.

- Substituting the frame material. Materials such as timber can be substituted in place of aluminum to reduce the frame U-value. Since wood is strong yet insulating, it is an ideal material for the interior frame. By substituting wood for aluminum in a high-performance curtain wall frame, the frame U-value can be reduced by 61% for a double-glazed frame resulting in a frame U-value of 1.88 W/m²K (R-3.0).
- Substituting edge spacer material. Aside from changing materials within the frame, the window U-value can also be improved by reducing the heat transfer at the edge of the glass region. Substituting the edge spacer material from aluminum to PVC can reduce the edge U-value by 10%.
- Increasing the ratio of the centre-glass region to edge and frame regions. Since the overall U-value of a window is dependent on the area of the IGU, frame, and edge regions, maximizing the area of the IGU will result in a lower window U-value since IGUs are much more insulating. Therefore, larger windows with aspect ratios close to 1 are desired to keep frame and edge areas to a minimum.

Even with such technological advances, the thermal performance of frames and edge spacers still lag significantly behind IGUs. Thus, it is important curtain walls be properly designed to best match that of the IGU and interior environment. While a highly insulating IGU combined with a curtain wall of moderate performance may have the same overall U-value as a lower performing IGU with a better performing frame, the more insulating frame may provide better thermal comfort as its interior surface temperature will be higher, resulting in less chance of condensation on the frame and radiative heat transfer to the occupant. Windows of the same areas may not have the same thermal performance as well, it is the centre-glass to gross window area that ultimately determines the window U-value. Since the thermal performance of curtain wall sections still sorely lags behind that of IGUs, it is recommended that further research into new materials and systems be undertaken to help reduce the heat transfer of both frames and edge spacers.

Through a series of annual building energy simulations of offices located within the perimeter zones of different orientations, it is clear that window area, window U-value, and SHGC play a significant role in energy performance. From the analysis for the Toronto climate, it is concluded that:

- Internal heat gain is the most significant factor related to the energy performance of offices located in the perimeter zone of commercial and institutional buildings. Offices with high internal heat gain sources respond negatively to larger window areas.
- Windows with lower U-values provided the greatest energy savings over less insulating windows for moderate and low internal heat gain offices. This is particularly true for high-performance windows with ultra low U-values. Window U-values and SHGC were less significant to offices with higher internal heat gains as different window properties had similar total annual and peak energy consumption even with ultra low SHGCs.
- Windows with ultra low SHGCs ($0.19 < \text{SHGC} < 0.25$), like those of high-performance windows, increased the total annual energy consumption over moderate and low internal heat gain offices with higher SHGC, yet it decreased the peak cooling load.
- The optimal window area increased from WWR 0.30 to over WWR 0.50 with lower U-value windows ($U_{\text{cg}} < 0.41 \text{ W/m}^2\text{K}$).
- Solar control for moderate internal gain offices, in the form of static shading such as overhangs and fins and dynamic shading with adjustable louvers, resulted in an increase in total energy consumption and peak heating loads, while reducing the peak cooling load. Of the two types of solar control, static shading performed the worse as it significantly raised the heating and lighting energy consumption by limiting solar gains. Due to the complexity of the energy flow within a moderate internal gain office, the control strategy and exterior shading design must be reconsidered to better reduce energy consumption.

From these results, it is clear that moderate to low internal heat gain offices with daylighting control and highly efficient equipment can significantly benefit from high-performance, ultra low U-value windows and window areas of WWR 0.50 to 0.60. Following the trend of advanced technologies in high efficiency lighting and office equipment, and an increase in building surface area to volume ratio with offices that have larger perimeter zones, the results of this research are becoming more and more relevant. Although window performance did affect the energy consumption of offices in perimeter zones, the energy consumption may be altered by other factors, such as building use and occupant behaviour. It is recommended that these effects and others such as external shading from surrounding buildings be further studied, and that some of these simulations be verified with a set of field measurements of real buildings.

References

- Architecture 2030 (2009).** Retrieved 2009 from www.Architecture2030.org
- ASHRAE, (1999).** *ASHRAE/IESNA Standard 90.1-1999 ASHRAE Standard Energy Standard for Buildings Except Low-Rise Residential Buildings*, American Society of Heating, Refrigerating and Air Conditioning Engineers, Inc.
- ASHRAE (2001).** *ASHRAE Handbook – Fundamentals*, American Society of Heating, Refrigerating and Air Conditioning Engineers, Inc.
- ASHRAE, (2004).** *Advanced Energy Design Guide for Small Office Buildings Achieving 30% Energy Savings Over ANSI/ASHRAE/IESNA Standard 90.1-1999*, American Society of Heating, Refrigerating and Air Conditioning Engineers, Inc.
- ASHRAE, (2004).** *ANSI/ASHRAE Standard 62.2-2004 ASHRAE Standard Ventilation and Acceptable Indoor Air Quality in Low-Rise Residential Buildings*, American Society of Heating, Refrigerating and Air Conditioning Engineers, Inc.
- ASHRAE, (2007).** *ASHRAE/IESNA Standard 90.1-2007 ASHRAE Standard Energy Standard for Buildings Except Low-Rise Residential Buildings*, American Society of Heating, Refrigerating and Air Conditioning Engineers, Inc.
- Bird, R. B., Stewart, W. E., Lightfoot, E. N. (1996).** *Transport Phenomena*, Wiley Sons, New York, pp. 243-264
- Boubekrit, M., Boyer, L. L. (1992).** 'Effect of Window Size and Sunlight Presence on Glare', *Lighting Research and Technology*, Vol. 24 (2), pp. 69-74
- Building Systems Laboratory, (1999).** *BLAST 3.0 Users Manual*, Urbana-Champaign, Illinois: Building Systems Laboratory, Department of Mechanical and Industrial Engineering, University of Illinois.
- Canada Mortgage and Housing Corporation (CMHC), (2004).** *Glass and Metal Curtain Walls Best Practice Guide Building Technology*, CMHC, Ottawa, Ontario
- Canlyte. (2009).** *Solid-State Downlighting*, retrieved 2009, from www.canlyte.com
- Carmody, J., (2007).** *Residential Windows: a Guide to New Technologies and Energy Performance*, W.W. Norton, New York
- Carmody, J., Selkowitz, S., Lee, E. S., Arasteh, D., Willmert, T. (2004).** *Window Systems for High-Performance Building*, W. W. Norton & Company, New York

- ChemiCool (2009).** Retrieved 2009, from <http://chemicool.com/>
- Collins, M., Tasnim, S., Wright, J., (2009).** ‘Numerical analysis of convective heat transfer in fenestration with between-the-glass louvered shades’, *Building and Environment*, Vol. 44 , pp. 2185-2192
- Crawley, D. B., Hand, J. W., Kummert, M., Griffith, B. T., (2005).** *Contrasting the Capabilities of Building Energy Performance Simulation Programs*, U.S. Department of Energy
- Crawley, D. B., Lawrie, L. K., Pedersen, C. O., Winkelmann, F. C., Witte, M. J., Strand, R. K., Liesen, R. J., Buhl, W. F., Huang, Y. J., Henninger, R. H., Glazer, J., Fisher, D. E., Shirey, D. B., Griffith, B. T., Ellis, P. G., Gu, L., (2004).** ‘EnergyPlus: New Capable and Linked’, *Proceedings of the SimBuild 2004 Conference*
- D&R International, Ltd. (2009).** *2009 Buildings Energy Data Book*, Prepared for the Buildings Technologies Program Energy Efficiency and Renewable Energy U.S. Department of Energy
- Edwards, D. K. (1977).** ‘Solar Absorption by Each Element in an Absorber-Coverglass Array’, *Solar Energy*, Vol. 19, pp. 401-402
- El Sherbiny, S. M., Raithby, G. D., Hollands, K. G. T. (1982).** ‘Heat Transfer by Natural Convection Across Vertical and Inclined Air Layers’, *Journal of Heat Transfer*, Vol. 204, pp. 96-102
- Eames, C., P., (2008).** ‘Vacuum glazing: Current performance and future prospects’, *Vacuum Surface Engineering, Surface Instrumentation & Vacuum Technology*, Vol. 82, pp. 717-722
- Energy Star (2009).** *Methodology for Incorporating Source Energy Use*, retrieved 2010, from www.energystar.gov/ia/business/evaluate_performance/site_source.pdf
- Enermodal Engineering Ltd. (2002).** *Daylighting Guide for Canadian Commercial Buildings*, Public Works and Government Services Canada
- Ferguson, J.E., Wright, J. L. (1984).** *VISION: A Computer Program to Evaluate the Thermal Performance of Super Windows*, National Research Council of Canada, Division of Energy, Ottawa, Ontario
- Fernandez, J., E., (2009).** ‘Windows and Facades’, *MIT: Department of Architecture: Building Technology Program*, Retrieved 2009 from <http://architecture.mit.edu/>
- Griffith, B., Finlayson, E., Yazdani, M., Arasteh, D. K. (1998).** ‘The Significance of

- Bolts in the Thermal Performance of Curtain-Wall Frames for Glazed Facades' *ASHRAE Transactions*, Vol. 104 (1B), pp. 1063-1069
- Gustavsen, A., Arasteh, D., Jelle, B., Curcija, C., Kohler, C. (2008).** 'Developing Low-conductance Window Frames: Capabilities and Limitations of Current Window Heat Transfer Design Tools – State-of-the-Art Review', *Journal of Building Physics*, Vol. 32 (2), pp. 131-153
- Gustavsen, A., Arasteh, D., Kohler, C., Dalehaug A. (2007).** 'Two-Dimensional CFD and Conduction Simulations of Heat Transfer in Horizontal Window Frames with Internal Cavities', *ASHRAE Transactions*, Vo. 113 (1), pp. 165-175
- Hollands, K. G. T, Wright, J. L., Granqvist, C. G. (2001).** 'Glazings and Coatings', *Solar Energy the State of the Art: ISES Position Papers*, pp. 29-107
- Intergovernmental Panel on Climate Change. (2007).** *Climate Change 2007: Mitigation Contribution of Working Group III to the Fourth Assessment Report of the Intergovernmental Panel on Climate Change*, Cambridge University Press, New York
- Lawrence Berkeley National Laboratory (2003).** *Window5/ Therm5 NFRC Simulation Manual*, University of California, Berkeley, California
- Lawrence Berkeley National Laboratory (2008).** *Window 6.2/ Therm 6.2 Research Version User Manual*, University of California, Berkeley, California
- Lstiburek, J., Straube, J., (2008).** 'Windows and Curtainwalls', *Building Science 2008*, Retrieved 2009 from www.buildingscience.com
- McQuiston, F., Parker, J., Spitler, J., (2005).** *Heating, Ventilating, and Air Conditioning Analysis and Design*, John Wiley and Sons, Inc., Hoboken, NJ
- Natural Resources Canada. (2009).** *Office of Energy Efficiency*, retrieved 2010, from http://www.oeo.nrcan.gc.ca/corporate/statistics/neud/dpa/trends_com_ca.cfm.
- No, S.T., Kim, K.S., Jung, J.S. (2008).** 'Simulation and Mock-up Tests of Thermal Performance of Curtain Walls', *Energy and Buildings*, Vol. 40, pp. 1135-1144
- North House (2009).** Retrieved 2009, from <http://www.team-north.com/>
- PassivHaus Institut (2010).** retrieved 2010 from <http://www.passiv.de/>
- Poirazis, H., Blomsterberg, A., Wall, M., (2007).** 'Energy Simulations for Glazed Office Buildings in Sweden', *Energy and Buildings*, Vol. 40, pp. 1161-1170
- Province of Ontario (2009).** *Ontario Regulation 349/09 made under the Building Code*

ACT, 1992, Toronto, Ontario

- Raico (2010).** retrieved 2010 from <http://raico.de/index.php?4843d9b1c62b8>
- Reinhart, C. F. (2005).** ‘A Simulation-Based Review of the Ubiquitous Window-Head-Height to Daylit Zone Depth Rule-of-Thumb’, *Institute for Research in Construction*, National Research Council Canada, Ottawa, Ontario
- Reinhart, C. F. (2004).** ‘Lightswitch 2002: A Model for Manual Control of Electric Lighting and Blinds’, *Solar Energy*, Vol. 77 (1), pp. 15-28
- Reinhart, C. F., (2006).** *DaySim*, National Research Council of Canada, Ottawa, Ontario
- Reinhart, C. F., Voss, K. (2003).** ‘Monitoring Manual Control of Electric Lighting and Blinds’, *Lighting Research & Technology*, Vol. 35 (3), pp. 243-260
- Rusak, B., Eskes, G. A., Shaw, S. R. (1995).** *Lighting and Human Health – A Review of the Literature*. Canada Mortgage and Housing Corporation – Technical Policy & Research Division, Ottawa, Ontario
- Shewen, E., Hollands, K. G. T., Raithby, G. D. (1996).** ‘Heat Transfer by Natural Convection Across a Vertical Air Cavity of Large Aspect Ratio’, *Journal of Heat Transfer*, Vol. 118, pp. 993-995
- Shurcliff, W. A. (1974).** ‘Transmittance and Reflection Loss of Multi-plate Window of a Solar Radiation Collector: Formulas and Tabulations of Results for the Case of $n = 1.5$ ’, *Solar Energy*, Vol. 16, pp. 149-154
- Siegel, R. (1973).** ‘Net Radiation Method for Transmission through Partially Transparent Plates’, *Solar Energy*, Vol. 15, pp. 273-276
- Smith, G. B., Niklasson, G. A., Svensson, J. S. E. M., Granqvist, C. G. (1986).** ‘Nobel-metal-based Transparent Infrared Reflectors: Experiments and Theoretical Analyses for Very Thin Gold Films’, *Journal of Applied Physics*, Vol. 59, pp. 571-581
- Straube, J., (2008).** ‘Insight: Can Highly Glazed Building Façades be Green?’, *Building Science 2008*, Retrieved 2009 from www.buildingscience.com
- Straube, J., Burnett, E., (2005).** *Building Science for Building Enclosures*, Building Science Press, Westford MA
- The Engineering Toolbox, (2010).** Retrieved 2010 from www.engineeringtoolbox.com
- U.S. Energy Information Administration (2009).** Retrieved 2009 from <http://www.eia.doe.gov/>

- Van Dijk, H. A. L., Goulding J. (1996).** ‘WIS Reference Manual (updated draft)’, *TNO Building and Construction Research*, TNO, Delft.
- Walton, G. N. (1986).** ‘Modelling Window Optics for Building Energy Analysis’, *Report NBSIR 86-3426*, prepared for Solar Buildings Technology Division, Office of Solar Heat Technologies, U.S. Department of Energy, Washington, D.C.
- Wijesundera, N. E. (1975).** ‘A Net Radiation Method for the Transmittance and Absorptivity of a Series of Parallel Regions’, *Solar Energy*, Vo. 17, pp. 75-77
- Winkelmann, F. C., Birdsall, B. E., Buhl, W. F., Ellington, K. L., Erdem, A. E., Hirsch, J. J., Gates, S., (1993).** *DOE-2 Supplement, Version 2.1E*, LBL-34947, Lawrence Berkeley National Laboratory. Springfield: National Technical Information Service
- Wright, J. L., McGowan, A. (1999).** ‘Calculating the Solar Heat Gain of Window Frames’, *ASHRAE Transactions*, Vol.105 (2), pp. 1011-1021
- Wright, J. L. (1998).** ‘Calculating Centre-Glass Performance Indices of Windows’, *ASHRAE Transactions*, Vol. 104 (1B), pp. 1230-1241
- Wright, J. L. (1996).** ‘A Correlation to Quantify Convective Heat Transfer Between Vertical Window Glazings’, *ASHRAE Transactions*, Vol. 102 (1), pp. 940-946
- Yu, J., Yang, C., Tian, Li, (2008).** ‘Low-Energy Envelope Design of Residential Building in hot summer and cold winter zone in China’, *Energy and Buildings*, Vol. 40, pp. 1536-1546

Appendix A
Solar Calculations

Static shading devices, such as overhangs and fins, are properly designed to minimize unwanted solar gain at specific time of day and year. In order to properly design static shading devices the angle of the sun must be determined.

SOLAR ANGLES

$$\delta = \delta_m \sin [2\pi (284 + n) / 365] \quad \text{Equation A}$$

$$\omega = \varpi t \quad \text{Equation B}$$

Where:

- δ = declination in radians
- $\delta_m = 0.4093$ rad
- n = day number in the year (where January 1st is $n=1$)
- ω = hour angle in radians (note all morning hours are negative)
- ϖ = angular velocity of the sun, 2π rad/day
- t = time of day in hours

The Solar Zenith, θ_z , is the angle between the incoming solar radiation and the normal to the earth's surface. It is calculated using Equation C.

$$\cos\theta_z = \cos\phi \cos\delta \cos\omega + \sin\phi \sin\delta \quad \text{Equation C}$$

Where:

- θ_z = the solar zenith
- ϕ = the local latitude

The Solar Altitude, α_s , is the angle between the incoming solar radiation and the earth's surface. It is calculated using Equation D.

$$\alpha_s = \pi/2 - \theta_z \quad \text{Equation D}$$

The Solar Azimuth, γ_s , is the angle between due south and the sun on a horizontal plane. All angles west of due south are positive, while angles east of due south are negative. It is calculated using Equation E.

$$\cos\gamma_s = (\sin\alpha_s \sin\phi - \sin\delta) / (\cos\alpha_s \cos\phi) \quad \text{Equation E}$$

The Wall Solar Azimuth, $\gamma_s - \gamma$, is the angle between the wall and solar azimuth on a horizontal plane. γ is the wall azimuth or the direction of the wall with respect of south. For a south facing wall at solar noon, the wall solar azimuth is zero.

With these solar angles, the shaded areas of specific overhang and fin designs can be calculated. The shaded lengths and widths are determined using Equations F and G.

$$X = B \tan (\gamma_s - \gamma) \quad \text{Equation F}$$

$$Y = \frac{P \cdot \tan(\alpha_s)}{\cos(\gamma_s - \gamma)} \quad \text{Equation G}$$

- Where:
- X = horizontal shaded width
 - Y = vertical shaded width
 - B = setback depth at the jambs
 - P = overhang width
 - $\gamma_s - \gamma$ = wall solar azimuth
 - α_s = solar altitude

The wall solar azimuth, $\gamma_s - \gamma$, is the angle between the direction in which the wall is facing and the sun on a horizontal plane. Similarly, the solar altitude, α_s , is the angle between the sun and the earth's surface on a vertical plane measured from the ground up. Diagrams of these solar angles are presented in Figure A.

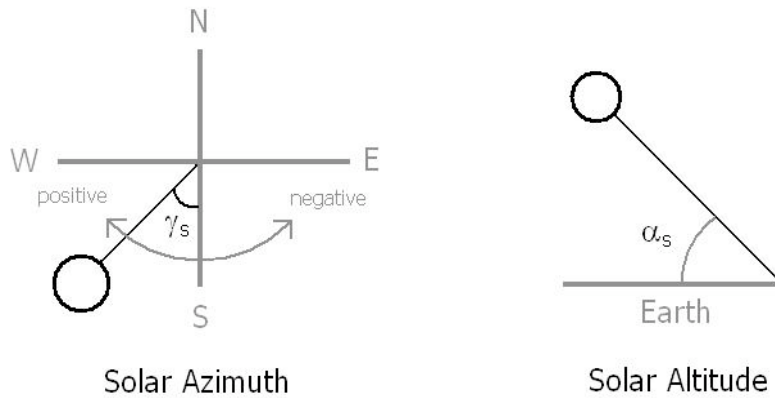


Figure A Solar Angles

An optimal overhang design is one which is able to fully shade the window on the longest day of the year, the summer solstice (June 21st), and allow full exposure to the sun during the shortest day of the year, the winter solstice (December 21st) at solar noon when sun is at its highest point of the day. This design strategy is illustrated in Figure B and the overhang depth and shaded coverage are listed in the following:

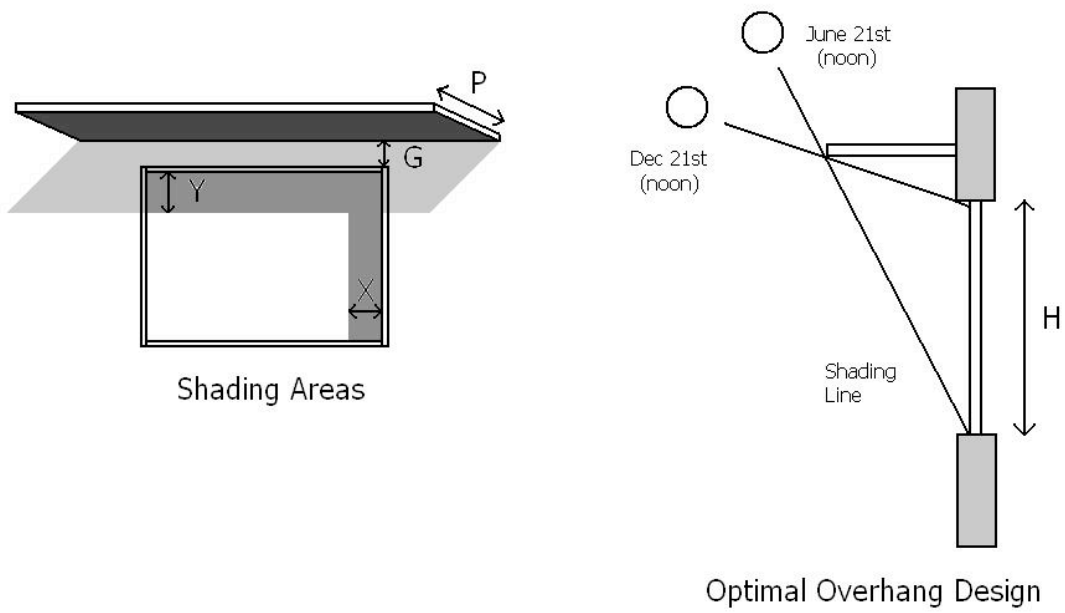


Figure B **Optimal Shading Layout**

WWR 0.10

Shading Performance of Overhang Throughout the year at Solar Noon for South Facing Wall

Latitude	Toronto	43.68 [deg]	Shade Coverage		
P	0.4 m	Overhang Width	21-Mar	11.1%	
G	0.3 m	Freeboard	21-Jun	77.3%	
H	1.016 m	Window Height	21-Sep	11.4%	
W	1.016 m	Window Width	21-Dec	0.0%	
B	0.05 m	Setback			
A	1.032256m2	Window Area			

Month	Day	Jan	Feb	March	April	May	June	July	August	September	October	November	December
	1	0.00%	0.00%	1.26%	17.95%	42.14%	69.69%	75.43%	52.03%	24.74%	6.05%	0.00%	0.00%
	2	0.00%	0.00%	1.68%	18.63%	43.07%	70.38%	75.03%	51.08%	23.99%	5.56%	0.00%	0.00%
	3	0.00%	0.00%	2.11%	19.31%	44.00%	71.04%	74.61%	50.13%	23.24%	5.07%	0.00%	0.00%
	4	0.00%	0.00%	2.54%	20.00%	44.93%	71.67%	74.14%	49.18%	22.51%	4.59%	0.00%	0.00%
	5	0.00%	0.00%	2.99%	20.71%	45.87%	72.27%	73.65%	48.23%	21.78%	4.13%	0.00%	0.00%
	6	0.00%	0.00%	3.44%	21.42%	46.82%	72.84%	73.12%	47.29%	21.06%	3.66%	0.00%	0.00%
	7	0.00%	0.00%	3.89%	22.14%	47.76%	73.39%	72.56%	46.34%	20.36%	3.21%	0.00%	0.00%
	8	0.00%	0.00%	4.36%	22.87%	48.71%	73.90%	71.97%	45.40%	19.66%	2.76%	0.00%	0.00%
	9	0.00%	0.00%	4.83%	23.61%	49.65%	74.38%	71.36%	44.47%	18.97%	2.32%	0.00%	0.00%
	10	0.00%	0.00%	5.31%	24.37%	50.60%	74.82%	70.71%	43.53%	18.29%	1.89%	0.00%	0.00%
	11	0.00%	0.00%	5.80%	25.12%	51.55%	75.24%	70.04%	42.60%	17.62%	1.47%	0.00%	0.00%
	12	0.00%	0.00%	6.30%	25.89%	52.50%	75.61%	69.34%	41.68%	16.95%	1.05%	0.00%	0.00%
	13	0.00%	0.00%	6.80%	26.67%	53.44%	75.95%	68.62%	40.76%	16.30%	0.64%	0.00%	0.00%
	14	0.00%	0.00%	7.31%	27.46%	54.39%	76.25%	67.88%	39.85%	15.66%	0.23%	0.00%	0.00%
	15	0.00%	0.00%	7.83%	28.26%	55.32%	76.52%	67.11%	38.94%	15.02%	0.00%	0.00%	0.00%
	16	0.00%	0.00%	8.36%	29.06%	56.26%	76.74%	66.33%	38.04%	14.40%	0.00%	0.00%	0.00%
	17	0.00%	0.00%	8.89%	29.88%	57.19%	76.93%	65.53%	37.15%	13.78%	0.00%	0.00%	0.00%
	18	0.00%	0.00%	9.44%	30.70%	58.11%	77.08%	64.71%	36.26%	13.18%	0.00%	0.00%	0.00%
	19	0.00%	0.00%	9.99%	31.53%	59.02%	77.19%	63.87%	35.39%	12.58%	0.00%	0.00%	0.00%
	20	0.00%	0.00%	10.55%	32.37%	59.93%	77.26%	63.02%	34.51%	11.99%	0.00%	0.00%	0.00%
	21	0.00%	0.00%	11.12%	33.22%	60.83%	77.29%	62.15%	33.65%	11.41%	0.00%	0.00%	0.00%
	22	0.00%	0.00%	11.69%	34.08%	61.71%	77.28%	61.27%	32.80%	10.83%	0.00%	0.00%	0.00%
	23	0.00%	0.00%	12.28%	34.95%	62.58%	77.23%	60.38%	31.95%	10.27%	0.00%	0.00%	0.00%
	24	0.00%	0.00%	12.88%	35.82%	63.44%	77.14%	59.48%	31.12%	9.71%	0.00%	0.00%	0.00%
	25	0.00%	0.00%	13.48%	36.71%	64.29%	77.01%	58.57%	30.29%	9.16%	0.00%	0.00%	0.00%
	26	0.00%	0.03%	14.09%	37.59%	65.12%	76.84%	57.65%	29.47%	8.62%	0.00%	0.00%	0.00%
	27	0.00%	0.43%	14.71%	38.49%	65.93%	76.64%	56.72%	28.66%	8.09%	0.00%	0.00%	0.00%
	28	0.00%	0.84%	15.34%	39.39%	66.73%	76.39%	55.79%	27.86%	7.57%	0.00%	0.00%	0.00%
	29	0.00%		15.98%	40.30%	67.50%	76.11%	54.86%	27.06%	7.05%	0.00%	0.00%	0.00%
	30	0.00%		16.63%	41.22%	68.25%	75.79%	53.92%	26.28%	6.55%	0.00%	0.00%	0.00%
	31	0.00%		17.28%		68.99%		52.97%	25.51%	0.00%			0.00%

WWR 0.20

Shading Performance of Overhang Throughout the year at Solar Noon for South Facing Wall

Latitude	Toronto	43.68 [deg]	Shade Coverage	
P	0.55 m	Overhang Width	21-Mar	18.6%
G	0.3 m	Freeboard	21-Jun	83.0%
H	1.436 m	Window Height	21-Sep	18.9%
W	1.436 m	Window Width	21-Dec	0.0%
B	0.05 m	Setback		
A	2.062096m2	Window Area		

Month	Jan	Feb	March	April	May	June	July	August	September	October	November	December
Day 1	0.00%	0.16%	9.06%	25.30%	48.83%	75.64%	81.21%	58.45%	31.91%	13.72%	2.08%	0.00%
2	0.00%	0.40%	9.47%	25.95%	49.73%	76.30%	80.83%	57.52%	31.17%	13.24%	1.80%	0.00%
3	0.00%	0.64%	9.88%	26.62%	50.64%	76.94%	80.41%	56.60%	30.45%	12.77%	1.54%	0.00%
4	0.00%	0.89%	10.31%	27.30%	51.55%	77.56%	79.96%	55.68%	29.73%	12.30%	1.27%	0.00%
5	0.00%	1.14%	10.74%	27.98%	52.46%	78.14%	79.48%	54.76%	29.02%	11.85%	1.02%	0.00%
6	0.00%	1.40%	11.18%	28.67%	53.38%	78.70%	78.97%	53.84%	28.33%	11.40%	0.77%	0.00%
7	0.00%	1.67%	11.62%	29.38%	54.30%	79.23%	78.43%	52.92%	27.64%	10.96%	0.52%	0.00%
8	0.00%	1.94%	12.08%	30.09%	55.22%	79.73%	77.85%	52.00%	26.96%	10.52%	0.28%	0.00%
9	0.00%	2.22%	12.54%	30.81%	56.14%	80.19%	77.25%	51.09%	26.29%	10.10%	0.05%	0.00%
10	0.00%	2.50%	13.00%	31.54%	57.06%	80.63%	76.62%	50.18%	25.62%	9.67%	0.00%	0.00%
11	0.00%	2.79%	13.48%	32.28%	57.99%	81.03%	75.97%	49.28%	24.97%	9.26%	0.00%	0.00%
12	0.00%	3.09%	13.96%	33.02%	58.91%	81.39%	75.29%	48.38%	24.33%	8.85%	0.00%	0.00%
13	0.00%	3.39%	14.45%	33.78%	59.83%	81.72%	74.59%	47.49%	23.69%	8.45%	0.00%	0.00%
14	0.00%	3.69%	14.95%	34.55%	60.74%	82.02%	73.87%	46.60%	23.07%	8.06%	0.00%	0.00%
15	0.00%	4.01%	15.45%	35.32%	61.66%	82.27%	73.13%	45.72%	22.45%	7.67%	0.00%	0.00%
16	0.00%	4.33%	15.96%	36.11%	62.57%	82.49%	72.36%	44.84%	21.84%	7.29%	0.00%	0.00%
17	0.00%	4.65%	16.49%	36.90%	63.47%	82.68%	71.58%	43.97%	21.24%	6.92%	0.00%	0.00%
18	0.00%	4.98%	17.01%	37.70%	64.37%	82.82%	70.78%	43.11%	20.65%	6.55%	0.00%	0.00%
19	0.00%	5.32%	17.55%	38.51%	65.26%	82.93%	69.97%	42.26%	20.07%	6.19%	0.00%	0.00%
20	0.00%	5.67%	18.10%	39.33%	66.14%	83.00%	69.14%	41.41%	19.50%	5.84%	0.00%	0.00%
21	0.00%	6.02%	18.65%	40.16%	67.01%	83.03%	68.30%	40.57%	18.93%	5.49%	0.00%	0.00%
22	0.00%	6.37%	19.21%	40.99%	67.87%	83.02%	67.44%	39.74%	18.37%	5.15%	0.00%	0.00%
23	0.00%	6.74%	19.78%	41.83%	68.72%	82.97%	66.57%	38.92%	17.82%	4.82%	0.00%	0.00%
24	0.00%	7.11%	20.36%	42.68%	69.56%	82.88%	65.70%	38.11%	17.28%	4.49%	0.00%	0.00%
25	0.00%	7.48%	20.95%	43.54%	70.38%	82.75%	64.81%	37.30%	16.75%	4.17%	0.00%	0.00%
26	0.00%	7.87%	21.54%	44.41%	71.18%	82.59%	63.92%	36.50%	16.22%	3.85%	0.00%	0.00%
27	0.00%	8.26%	22.15%	45.28%	71.97%	82.39%	63.02%	35.71%	15.71%	3.54%	0.00%	0.00%
28	0.00%	8.65%	22.76%	46.16%	72.75%	82.15%	62.11%	34.93%	15.20%	3.24%	0.00%	0.00%
29	0.00%		23.38%	47.04%	73.50%	81.87%	61.20%	34.16%	14.70%	2.94%	0.00%	0.00%
30	0.00%		24.01%	47.93%	74.23%	81.56%	60.29%	33.40%	14.20%	2.65%	0.00%	0.00%
31	0.05%		24.65%		74.95%		59.37%	32.65%		2.36%		0.00%

WWR 0.30

Shading Performance of Overhang Throughout the year at Solar Noon for South Facing Wall

Latitude	Toronto	43.68 [deg]	Shade Coverage	
P	0.67 m	Overhang Width	21-Mar	22.3%
G	0.3 m	Freeboard	21-Jun	86.3%
H	1.759 m	Window Height	21-Sep	22.5%
W	1.759 m	Window Width	21-Dec	0.0%
B	0.05 m	Setback		
A	3.094081m2	Window Area		

Month	Jan	Feb	March	April	May	June	July	August	September	October	November	December
Day												
1	0.00%	3.88%	12.73%	28.88%	52.28%	78.94%	84.49%	61.85%	35.45%	17.36%	5.79%	0.02%
2	0.00%	4.12%	13.14%	29.53%	53.18%	79.60%	84.11%	60.93%	34.72%	16.89%	5.52%	0.00%
3	0.00%	4.36%	13.55%	30.19%	54.08%	80.24%	83.69%	60.01%	34.00%	16.42%	5.25%	0.00%
4	0.00%	4.61%	13.97%	30.87%	54.98%	80.85%	83.24%	59.09%	33.29%	15.96%	4.99%	0.00%
5	0.00%	4.86%	14.40%	31.55%	55.89%	81.43%	82.77%	58.18%	32.58%	15.50%	4.73%	0.00%
6	0.00%	5.12%	14.84%	32.24%	56.81%	81.99%	82.25%	57.26%	31.89%	15.06%	4.48%	0.00%
7	0.00%	5.38%	15.28%	32.93%	57.72%	82.51%	81.71%	56.35%	31.21%	14.62%	4.24%	0.00%
8	0.00%	5.65%	15.73%	33.64%	58.64%	83.01%	81.14%	55.44%	30.53%	14.19%	4.00%	0.00%
9	0.07%	5.93%	16.19%	34.36%	59.55%	83.47%	80.55%	54.53%	29.86%	13.76%	3.77%	0.00%
10	0.18%	6.21%	16.65%	35.08%	60.47%	83.90%	79.92%	53.63%	29.20%	13.34%	3.54%	0.00%
11	0.30%	6.50%	17.12%	35.82%	61.39%	84.30%	79.27%	52.73%	28.56%	12.93%	3.32%	0.00%
12	0.42%	6.79%	17.60%	36.56%	62.30%	84.66%	78.60%	51.84%	27.92%	12.53%	3.11%	0.00%
13	0.54%	7.09%	18.09%	37.32%	63.22%	84.99%	77.90%	50.95%	27.28%	12.13%	2.90%	0.00%
14	0.68%	7.39%	18.59%	38.08%	64.13%	85.29%	77.18%	50.06%	26.66%	11.74%	2.69%	0.00%
15	0.81%	7.71%	19.09%	38.85%	65.04%	85.54%	76.44%	49.19%	26.05%	11.35%	2.49%	0.00%
16	0.96%	8.02%	19.60%	39.63%	65.94%	85.76%	75.69%	48.32%	25.44%	10.98%	2.30%	0.00%
17	1.11%	8.35%	20.12%	40.42%	66.84%	85.94%	74.91%	47.45%	24.85%	10.60%	2.11%	0.00%
18	1.26%	8.68%	20.64%	41.21%	67.73%	86.09%	74.11%	46.60%	24.26%	10.24%	1.93%	0.00%
19	1.42%	9.01%	21.18%	42.02%	68.62%	86.19%	73.30%	45.75%	23.68%	9.88%	1.75%	0.00%
20	1.58%	9.36%	21.72%	42.83%	69.49%	86.26%	72.48%	44.90%	23.11%	9.53%	1.58%	0.00%
21	1.75%	9.70%	22.27%	43.66%	70.36%	86.29%	71.64%	44.07%	22.55%	9.18%	1.42%	0.00%
22	1.93%	10.06%	22.83%	44.49%	71.22%	86.28%	70.79%	43.24%	21.99%	8.84%	1.26%	0.00%
23	2.11%	10.42%	23.39%	45.32%	72.06%	86.23%	69.93%	42.43%	21.45%	8.51%	1.11%	0.00%
24	2.30%	10.79%	23.97%	46.17%	72.89%	86.15%	69.06%	41.62%	20.91%	8.18%	0.96%	0.00%
25	2.49%	11.16%	24.55%	47.02%	73.71%	86.02%	68.18%	40.82%	20.38%	7.86%	0.81%	0.00%
26	2.69%	11.54%	25.14%	47.88%	74.51%	85.86%	67.29%	40.02%	19.86%	7.55%	0.68%	0.00%
27	2.90%	11.93%	25.75%	48.75%	75.30%	85.66%	66.39%	39.24%	19.34%	7.24%	0.54%	0.00%
28	3.11%	12.33%	26.35%	49.63%	76.07%	85.42%	65.49%	38.46%	18.84%	6.94%	0.42%	0.00%
29	3.32%		26.97%	50.51%	76.82%	85.14%	64.58%	37.70%	18.34%	6.64%	0.30%	0.00%
30	3.54%		27.60%	51.39%	77.55%	84.83%	63.67%	36.94%	17.85%	6.35%	0.18%	0.00%
31	3.77%		28.23%		78.25%		62.76%	36.19%		6.07%		0.00%

WWR 0.40

Shading Performance of Overhang Throughout the year at Solar Noon for South Facing Wall

Latitude	Toronto	43.68 [deg]	Shade Coverage	
P	0.75 m	Overhang Width	21-Mar	23.9%
G	0.3 m	Freeboard	21-Jun	87.3%
H	1.988 m	Window Height	21-Sep	24.1%
W	2.075 m	Window Width	21-Dec	0.2%
B	0.05 m	Setback		
A	4.1251m2	Window Area		

Month	Day	Jan	Feb	March	April	May	June	July	August	September	October	November	December
	1	1.19%	5.65%	14.41%	30.41%	53.59%	79.99%	85.48%	63.06%	36.91%	19.00%	7.54%	0.45%
	2	1.26%	5.88%	14.81%	31.05%	54.47%	80.64%	85.11%	62.15%	36.19%	18.53%	7.27%	0.43%
	3	1.33%	6.12%	15.22%	31.71%	55.37%	81.28%	84.70%	61.24%	35.48%	18.06%	7.00%	0.40%
	4	1.41%	6.36%	15.64%	32.37%	56.26%	81.88%	84.25%	60.33%	34.77%	17.61%	6.74%	0.38%
	5	1.49%	6.61%	16.07%	33.05%	57.16%	82.46%	83.78%	59.42%	34.08%	17.16%	6.49%	0.36%
	6	1.58%	6.87%	16.50%	33.73%	58.06%	83.01%	83.27%	58.52%	33.39%	16.72%	6.24%	0.34%
	7	1.67%	7.13%	16.94%	34.42%	58.97%	83.53%	82.74%	57.61%	32.71%	16.28%	6.00%	0.32%
	8	1.77%	7.40%	17.38%	35.12%	59.88%	84.02%	82.17%	56.71%	32.04%	15.85%	5.76%	0.30%
	9	1.87%	7.67%	17.83%	35.83%	60.79%	84.48%	81.58%	55.81%	31.38%	15.43%	5.53%	0.29%
	10	1.98%	7.95%	18.29%	36.55%	61.69%	84.90%	80.96%	54.92%	30.73%	15.02%	5.31%	0.27%
	11	2.09%	8.24%	18.76%	37.28%	62.60%	85.30%	80.32%	54.03%	30.09%	14.61%	5.09%	0.26%
	12	2.21%	8.53%	19.24%	38.02%	63.51%	85.66%	79.65%	53.14%	29.45%	14.21%	4.88%	0.25%
	13	2.34%	8.82%	19.72%	38.76%	64.42%	85.98%	78.96%	52.26%	28.83%	13.82%	4.67%	0.24%
	14	2.47%	9.13%	20.21%	39.52%	65.32%	86.27%	78.25%	51.39%	28.21%	13.43%	4.47%	0.23%
	15	2.61%	9.43%	20.71%	40.28%	66.22%	86.53%	77.52%	50.52%	27.60%	13.05%	4.27%	0.22%
	16	2.75%	9.75%	21.21%	41.05%	67.11%	86.74%	76.77%	49.66%	27.00%	12.67%	4.08%	0.21%
	17	2.90%	10.07%	21.73%	41.83%	68.00%	86.92%	76.00%	48.80%	26.41%	12.31%	3.89%	0.21%
	18	3.05%	10.40%	22.25%	42.62%	68.89%	87.07%	75.21%	47.95%	25.83%	11.94%	3.71%	0.20%
	19	3.21%	10.73%	22.78%	43.42%	69.76%	87.17%	74.41%	47.11%	25.26%	11.59%	3.54%	0.20%
	20	3.37%	11.07%	23.31%	44.23%	70.63%	87.24%	73.59%	46.28%	24.69%	11.24%	3.37%	0.20%
	21	3.54%	11.41%	23.86%	45.04%	71.49%	87.27%	72.76%	45.45%	24.13%	10.90%	3.21%	0.20%
	22	3.71%	11.77%	24.41%	45.86%	72.34%	87.26%	71.92%	44.63%	23.58%	10.56%	3.05%	0.20%
	23	3.89%	12.12%	24.97%	46.69%	73.18%	87.21%	71.06%	43.82%	23.04%	10.23%	2.90%	0.20%
	24	4.08%	12.49%	25.54%	47.53%	74.00%	87.12%	70.20%	43.02%	22.51%	9.91%	2.75%	0.21%
	25	4.27%	12.86%	26.12%	48.38%	74.81%	87.00%	69.33%	42.23%	21.99%	9.59%	2.61%	0.21%
	26	4.47%	13.24%	26.71%	49.23%	75.60%	86.84%	68.45%	41.44%	21.47%	9.28%	2.47%	0.22%
	27	4.67%	13.62%	27.30%	50.09%	76.38%	86.64%	67.56%	40.67%	20.96%	8.97%	2.34%	0.22%
	28	4.88%	14.01%	27.90%	50.95%	77.14%	86.41%	66.67%	39.90%	20.46%	8.67%	2.21%	0.23%
	29	5.09%		28.52%	51.83%	77.89%	86.13%	65.77%	39.14%	19.96%	8.38%	2.09%	0.24%
	30	5.31%		29.14%	52.70%	78.61%	85.83%	64.87%	38.39%	19.48%	8.09%	1.98%	0.25%
	31	5.53%		29.77%		79.31%		63.96%	37.65%		7.81%		0.27%

WWR 0.50

Shading Performance of Overhang Throughout the year at Solar Noon for South Facing Wall

Latitude	Toronto	43.68 [deg]		Shade Coverage	
P	0.75 m	Overhang Width		21-Mar	23.9%
G	0.3 m	Freeboard		21-Jun	87.3%
H	1.988 m	Window Height		21-Sep	24.1%
W	2.594 m	Window Width		21-Dec	0.2%
B	0.05 m	Setback			
A	5.156872m2	Window Area			

Month	Day	Jan	Feb	March	April	May	June	July	August	September	October	November	December
	1	1.19%	5.65%	14.41%	30.41%	53.59%	79.99%	85.48%	63.06%	36.91%	19.00%	7.54%	0.36%
	2	1.26%	5.88%	14.81%	31.05%	54.47%	80.64%	85.11%	62.15%	36.19%	18.53%	7.27%	0.34%
	3	1.33%	6.12%	15.22%	31.71%	55.37%	81.28%	84.70%	61.24%	35.48%	18.06%	7.00%	0.32%
	4	1.41%	6.36%	15.64%	32.37%	56.26%	81.88%	84.25%	60.33%	34.77%	17.61%	6.74%	0.31%
	5	1.49%	6.61%	16.07%	33.05%	57.16%	82.46%	83.78%	59.42%	34.08%	17.16%	6.49%	0.29%
	6	1.58%	6.87%	16.50%	33.73%	58.06%	83.01%	83.27%	58.52%	33.39%	16.72%	6.24%	0.27%
	7	1.67%	7.13%	16.94%	34.42%	58.97%	83.53%	82.74%	57.61%	32.71%	16.28%	6.00%	0.26%
	8	1.77%	7.40%	17.38%	35.12%	59.88%	84.02%	82.17%	56.71%	32.04%	15.85%	5.76%	0.24%
	9	1.87%	7.67%	17.83%	35.83%	60.79%	84.48%	81.58%	55.81%	31.38%	15.43%	5.53%	0.23%
	10	1.98%	7.95%	18.29%	36.55%	61.69%	84.90%	80.96%	54.92%	30.73%	15.02%	5.31%	0.22%
	11	2.09%	8.24%	18.76%	37.28%	62.60%	85.30%	80.32%	54.03%	30.09%	14.61%	5.09%	0.21%
	12	2.21%	8.53%	19.24%	38.02%	63.51%	85.66%	79.65%	53.14%	29.45%	14.21%	4.88%	0.20%
	13	2.34%	8.82%	19.72%	38.76%	64.42%	85.98%	78.96%	52.26%	28.83%	13.82%	4.67%	0.19%
	14	2.47%	9.13%	20.21%	39.52%	65.32%	86.27%	78.25%	51.39%	28.21%	13.43%	4.47%	0.18%
	15	2.61%	9.43%	20.71%	40.28%	66.22%	86.53%	77.52%	50.52%	27.60%	13.05%	4.27%	0.18%
	16	2.75%	9.75%	21.21%	41.05%	67.11%	86.74%	76.77%	49.66%	27.00%	12.67%	4.08%	0.17%
	17	2.90%	10.07%	21.73%	41.83%	68.00%	86.92%	76.00%	48.80%	26.41%	12.31%	3.89%	0.17%
	18	3.05%	10.40%	22.25%	42.62%	68.89%	87.07%	75.21%	47.95%	25.83%	11.94%	3.71%	0.16%
	19	3.21%	10.73%	22.78%	43.42%	69.76%	87.17%	74.41%	47.11%	25.26%	11.59%	3.54%	0.16%
	20	3.37%	11.07%	23.31%	44.23%	70.63%	87.24%	73.59%	46.28%	24.69%	11.24%	3.37%	0.16%
	21	3.54%	11.41%	23.86%	45.04%	71.49%	87.27%	72.76%	45.45%	24.13%	10.90%	3.21%	0.16%
	22	3.71%	11.77%	24.41%	45.86%	72.34%	87.26%	71.92%	44.63%	23.58%	10.56%	3.05%	0.16%
	23	3.89%	12.12%	24.97%	46.69%	73.18%	87.21%	71.06%	43.82%	23.04%	10.23%	2.90%	0.16%
	24	4.08%	12.49%	25.54%	47.53%	74.00%	87.12%	70.20%	43.02%	22.51%	9.91%	2.75%	0.16%
	25	4.27%	12.86%	26.12%	48.38%	74.81%	87.00%	69.33%	42.23%	21.99%	9.59%	2.61%	0.17%
	26	4.47%	13.24%	26.71%	49.23%	75.60%	86.84%	68.45%	41.44%	21.47%	9.28%	2.47%	0.17%
	27	4.67%	13.62%	27.30%	50.09%	76.38%	86.64%	67.56%	40.67%	20.96%	8.97%	2.34%	0.18%
	28	4.88%	14.01%	27.90%	50.95%	77.14%	86.41%	66.67%	39.90%	20.46%	8.67%	2.21%	0.19%
	29	5.09%		28.52%	51.83%	77.89%	86.13%	65.77%	39.14%	19.96%	8.38%	2.09%	0.19%
	30	5.31%		29.14%	52.70%	78.61%	85.83%	64.87%	38.39%	19.48%	8.09%	1.98%	0.20%
	31	5.53%		29.77%		79.31%		63.96%	37.65%		7.81%		0.21%

WWR 0.60

Shading Performance of Overhang Throughout the year at Solar Noon for South Facing Wall

Latitude	Toronto	43.68 [deg]	Shade Coverage	
P	0.85 m	Overhang Width	21-Mar	25.7%
G	0.3 m	Freeboard	21-Jun	89.2%
H	2.25 m	Window Height	21-Sep	25.9%
W	2.75 m	Window Width	21-Dec	0.4%
B	0.05 m	Setback		
A	6.1875m2	Window Area		

Month	Day	Jan	Feb	March	April	May	June	July	August	September	October	November	December
	1	2.97%	7.43%	16.21%	32.22%	55.44%	81.88%	87.38%	64.92%	38.74%	20.80%	9.32%	0.59%
	2	3.04%	7.67%	16.61%	32.87%	56.33%	82.53%	87.00%	64.01%	38.02%	20.33%	9.05%	0.57%
	3	3.11%	7.91%	17.02%	33.53%	57.22%	83.16%	86.59%	63.10%	37.30%	19.87%	8.79%	0.56%
	4	3.19%	8.15%	17.44%	34.20%	58.12%	83.77%	86.14%	62.19%	36.60%	19.41%	8.53%	0.54%
	5	3.27%	8.40%	17.87%	34.87%	59.02%	84.35%	85.67%	61.28%	35.90%	18.96%	8.28%	0.53%
	6	3.36%	8.66%	18.30%	35.55%	59.92%	84.90%	85.16%	60.37%	35.21%	18.52%	8.03%	0.51%
	7	3.45%	8.92%	18.74%	36.25%	60.83%	85.42%	84.63%	59.47%	34.53%	18.08%	7.79%	0.50%
	8	3.55%	9.19%	19.18%	36.95%	61.74%	85.91%	84.06%	58.57%	33.86%	17.65%	7.55%	0.49%
	9	3.65%	9.46%	19.64%	37.66%	62.65%	86.37%	83.47%	57.67%	33.20%	17.23%	7.32%	0.48%
	10	3.76%	9.74%	20.10%	38.38%	63.56%	86.80%	82.85%	56.77%	32.55%	16.82%	7.10%	0.47%
	11	3.88%	10.03%	20.57%	39.11%	64.47%	87.19%	82.21%	55.88%	31.90%	16.41%	6.88%	0.46%
	12	4.00%	10.32%	21.04%	39.85%	65.38%	87.55%	81.54%	54.99%	31.27%	16.01%	6.66%	0.45%
	13	4.12%	10.61%	21.52%	40.59%	66.28%	87.88%	80.85%	54.11%	30.64%	15.61%	6.45%	0.45%
	14	4.25%	10.92%	22.02%	41.35%	67.19%	88.17%	80.13%	53.24%	30.03%	15.22%	6.25%	0.44%
	15	4.39%	11.23%	22.51%	42.11%	68.09%	88.42%	79.40%	52.37%	29.42%	14.84%	6.06%	0.43%
	16	4.53%	11.54%	23.02%	42.89%	68.98%	88.64%	78.65%	51.50%	28.82%	14.47%	5.86%	0.43%
	17	4.68%	11.86%	23.53%	43.67%	69.87%	88.82%	77.88%	50.65%	28.23%	14.10%	5.68%	0.43%
	18	4.83%	12.19%	24.06%	44.46%	70.76%	88.96%	77.09%	49.80%	27.64%	13.74%	5.50%	0.42%
	19	4.99%	12.52%	24.58%	45.26%	71.64%	89.07%	76.29%	48.95%	27.07%	13.38%	5.32%	0.42%
	20	5.15%	12.86%	25.12%	46.07%	72.51%	89.14%	75.47%	48.12%	26.50%	13.03%	5.15%	0.42%
	21	5.32%	13.21%	25.67%	46.88%	73.37%	89.16%	74.64%	47.29%	25.94%	12.69%	4.99%	0.42%
	22	5.50%	13.56%	26.22%	47.70%	74.22%	89.16%	73.79%	46.47%	25.39%	12.35%	4.83%	0.42%
	23	5.68%	13.92%	26.78%	48.54%	75.05%	89.11%	72.94%	45.66%	24.85%	12.02%	4.68%	0.42%
	24	5.86%	14.28%	27.35%	49.37%	75.88%	89.02%	72.07%	44.86%	24.32%	11.70%	4.53%	0.42%
	25	6.06%	14.65%	27.93%	50.22%	76.69%	88.90%	71.20%	44.06%	23.79%	11.38%	4.39%	0.43%
	26	6.25%	15.03%	28.52%	51.07%	77.48%	88.74%	70.32%	43.28%	23.28%	11.07%	4.25%	0.43%
	27	6.45%	15.42%	29.12%	51.93%	78.26%	88.54%	69.43%	42.50%	22.77%	10.76%	4.12%	0.44%
	28	6.66%	15.81%	29.72%	52.80%	79.03%	88.30%	68.54%	41.73%	22.26%	10.46%	4.00%	0.44%
	29	6.88%		30.33%	53.67%	79.77%	88.03%	67.64%	40.97%	21.77%	10.17%	3.88%	0.45%
	30	7.10%		30.96%	54.55%	80.49%	87.72%	66.73%	40.22%	21.28%	9.88%	3.76%	0.46%
	31	7.32%		31.59%		81.20%		65.83%	39.48%		9.60%		0.47%

WWR 0.66

Shading Performance of Overhang Throughout the year at Solar Noon for South Facing Wall

Latitude	Toronto	43.68 [deg]	Shade Coverage	
P	0.93 m	Overhang Width	21-Mar	26.7%
G	0.3 m	Freeboard	21-Jun	89.8%
H	2.475 m	Window Height	21-Sep	26.9%
W	2.75 m	Window Width	21-Dec	0.5%
B	0.05 m	Setback		
A	6.80625m2	Window Area		

Month	Jan	Feb	March	April	May	June	July	August	September	October	November	December
Day 1	4.10%	8.54%	17.26%	33.19%	56.28%	82.58%	88.05%	65.71%	39.68%	21.83%	10.41%	0.70%
2	4.16%	8.77%	17.66%	33.84%	57.16%	83.23%	87.68%	64.81%	38.96%	21.36%	10.15%	0.69%
3	4.23%	9.01%	18.07%	34.49%	58.05%	83.86%	87.27%	63.90%	38.24%	20.90%	9.88%	0.67%
4	4.31%	9.25%	18.49%	35.15%	58.95%	84.46%	86.82%	63.00%	37.54%	20.45%	9.62%	0.66%
5	4.39%	9.50%	18.91%	35.82%	59.84%	85.04%	86.35%	62.10%	36.85%	20.00%	9.37%	0.65%
6	4.48%	9.75%	19.34%	36.50%	60.74%	85.59%	85.85%	61.19%	36.16%	19.56%	9.13%	0.63%
7	4.57%	10.01%	19.78%	37.19%	61.64%	86.10%	85.32%	60.29%	35.49%	19.12%	8.89%	0.62%
8	4.67%	10.28%	20.22%	37.89%	62.55%	86.59%	84.75%	59.39%	34.82%	18.70%	8.65%	0.61%
9	4.77%	10.55%	20.67%	38.60%	63.45%	87.05%	84.16%	58.50%	34.16%	18.28%	8.42%	0.60%
10	4.88%	10.83%	21.13%	39.32%	64.36%	87.47%	83.55%	57.61%	33.51%	17.87%	8.20%	0.59%
11	5.00%	11.11%	21.60%	40.04%	65.26%	87.87%	82.91%	56.72%	32.87%	17.46%	7.98%	0.58%
12	5.11%	11.40%	22.07%	40.77%	66.17%	88.23%	82.24%	55.84%	32.24%	17.06%	7.77%	0.58%
13	5.24%	11.70%	22.55%	41.52%	67.07%	88.55%	81.56%	54.96%	31.62%	16.67%	7.56%	0.57%
14	5.37%	12.00%	23.04%	42.27%	67.97%	88.84%	80.85%	54.09%	31.01%	16.28%	7.36%	0.57%
15	5.51%	12.31%	23.53%	43.03%	68.86%	89.09%	80.12%	53.23%	30.40%	15.90%	7.16%	0.56%
16	5.65%	12.62%	24.04%	43.80%	69.76%	89.31%	79.37%	52.37%	29.80%	15.53%	6.97%	0.56%
17	5.79%	12.94%	24.55%	44.58%	70.64%	89.49%	78.60%	51.52%	29.22%	15.17%	6.79%	0.55%
18	5.95%	13.26%	25.07%	45.36%	71.52%	89.63%	77.82%	50.67%	28.64%	14.81%	6.61%	0.55%
19	6.10%	13.60%	25.59%	46.16%	72.39%	89.73%	77.02%	49.83%	28.06%	14.45%	6.44%	0.55%
20	6.27%	13.93%	26.13%	46.96%	73.26%	89.80%	76.20%	49.00%	27.50%	14.10%	6.27%	0.55%
21	6.44%	14.28%	26.67%	47.77%	74.11%	89.83%	75.38%	48.18%	26.95%	13.76%	6.10%	0.55%
22	6.61%	14.63%	27.22%	48.59%	74.96%	89.82%	74.54%	47.36%	26.40%	13.43%	5.95%	0.55%
23	6.79%	14.98%	27.78%	49.42%	75.79%	89.77%	73.69%	46.56%	25.86%	13.10%	5.79%	0.55%
24	6.97%	15.35%	28.35%	50.25%	76.61%	89.69%	72.83%	45.76%	25.33%	12.78%	5.65%	0.55%
25	7.16%	15.72%	28.92%	51.09%	77.42%	89.56%	71.96%	44.97%	24.81%	12.46%	5.51%	0.55%
26	7.36%	16.09%	29.51%	51.94%	78.21%	89.40%	71.08%	44.19%	24.29%	12.15%	5.37%	0.56%
27	7.56%	16.48%	30.10%	52.80%	78.99%	89.20%	70.20%	43.41%	23.78%	11.85%	5.24%	0.56%
28	7.77%	16.86%	30.70%	53.66%	79.74%	88.97%	69.31%	42.65%	23.29%	11.55%	5.11%	0.57%
29	7.98%		31.31%	54.53%	80.48%	88.70%	68.42%	41.89%	22.79%	11.26%	5.00%	0.57%
30	8.20%		31.93%	55.40%	81.20%	88.39%	67.52%	41.14%	22.31%	10.97%	4.88%	0.58%
31	8.42%		32.56%		81.90%		66.62%	40.41%		10.69%		0.59%

Appendix B

IGU Performance Characteristics

And Specifications

OPTIMAL IGU CONSTRUCTION

IGU	Gas	U _{cg} [W/m ² K]	SHGC	VT	Overall t [mm]	Cavity L [mm]	Reduction in U _{ca}	Reduction in Overall Width, t	Reduction in Cavity Width, L
2G-1 Standard IGU	Air	2.680	0.702	0.786	25.1	13.6			
	Argon	2.531	0.702	0.786	24.1	12.6	6%	4%	7%
	Krypton	2.449	0.703	0.786	19.7	8.2	9%	21%	40%
	Xenon	2.395	0.703	0.786	17.2	5.7	11%	31%	58%
2G-2 Low U Mid SHGC	Air	1.617	0.275	0.639	24.0	12.5			
	Argon	1.305	0.272	0.639	22.9	11.4	19%	5%	9%
	Krypton	1.125	0.271	0.639	18.9	7.4	30%	21%	41%
	Xenon	1.000	0.270	0.639	16.7	5.2	38%	30%	58%
2G-2s Low U Low SHGC	Air	1.618	0.369	0.639	23.9	12.4			
	Argon	1.305	0.370	0.639	22.9	11.4	19%	4%	8%
	Krypton	1.125	0.371	0.639	18.9	7.4	30%	21%	40%
	Xenon	1.000	0.371	0.639	16.7	5.2	38%	30%	58%
2G-3v High U Low VT	Air	2.679	0.30	0.42	25.1	13.5			
	Argon	2.530	0.30	0.42	24.1	12.5	6%	4%	7%
	Krypton	2.448	0.30	0.42	19.8	8.2	9%	21%	39%
	Xenon	2.394	0.29	0.42	17.3	5.7	11%	31%	58%
2G-4uv Low U Ultra Low SHGC	Air	1.642	0.26	0.41	23.9	12.5			
	Argon	1.334	0.25	0.41	22.9	11.5	19%	4%	8%
	Krypton	1.157	0.25	0.41	18.9	7.5	30%	21%	40%
	Xenon	1.035	0.24	0.41	16.6	5.2	37%	31%	58%
3G-1 Standard IGU	Air	1.702	0.615	0.703	48.7	15.8			
	Argon	1.590	0.615	0.703	46.3	14.6	7%	5%	8%
	Krypton	1.531	0.616	0.703	37.1	10.0	10%	24%	37%
	Xenon	1.492	0.616	0.703	31.1	7.0	12%	36%	56%
3G-2 Low U Mid SHGC	Air	0.912	0.246	0.566	41.9	15.2			
	Argon	0.730	0.245	0.566	39.9	14.2	20%	5%	7%
	Krypton	0.631	0.245	0.566	30.1	9.3	31%	28%	39%
	Xenon	0.566	0.244	0.566	24.1	6.3	38%	43%	59%
3G-2s Ultra Low U Low SHGC	Air	0.891	0.369	0.566	41.1	14.8			
	Argon	0.706	0.367	0.566	39.1	13.8	21%	5%	7%
	Krypton	0.607	0.366	0.566	29.5	9.0	32%	28%	39%
	Xenon	0.541	0.364	0.566	24.1	6.3	39%	41%	57%
3G-3 Mid U Mid SHGC	Air	0.975	0.481	0.628	41.7	15.1			
	Argon	0.800	0.481	0.628	39.3	13.9	18%	6%	8%
	Krypton	0.707	0.481	0.628	29.5	9.0	27%	29%	40%
	Xenon	0.645	0.481	0.628	24.3	6.4	34%	42%	58%
3G-4v High U Low VT	Air	1.719	0.44	0.40	42.7	15.5			
	Argon	1.604	0.44	0.40	40.88	14.6	7%	4%	6%
	Krypton	1.544	0.44	0.40	30.7	9.5	10%	28%	39%
	Xenon	1.505	0.44	0.40	24.9	6.6	12%	42%	57%
3G-5uv Ultra Low U Ultra Low SHGC	Air	0.850	0.19	0.43	40.9	14.7			
	Argon	0.663	0.19	0.43	39.1	13.8	22%	4%	6%
	Krypton	0.562	0.19	0.43	30.1	9.3	34%	26%	37%
	Xenon	0.496	0.19	0.43	24.5	6.5	42%	40%	56%

4G-1 Standard IGU	Air	1.235	0.545	0.632	76.0	17.7			
	Argon	1.151	0.546	0.632	71.5	16.2	7%	6%	8%
	Krypton	1.107	0.546	0.632	55.3	10.8	10%	27%	39%
	Xenon	1.079	0.546	0.632	45.1	7.4	13%	41%	58%
4G-2 Ultra Low U Mid SHGC	Air	0.611	0.224	0.502	63.4	17.3			
	Argon	0.488	0.224	0.502	59.8	16.1	20%	6%	7%
	Krypton	0.424	0.224	0.502	42.4	10.3	31%	33%	40%
4G-2s Ultra Low U Low SHGC	Xenon	0.381	0.224	0.502	34.0	7.5	38%	46%	57%
	Air	0.596	0.355	0.502	61.3	16.6			
	Argon	0.472	0.353	0.502	57.7	15.4	21%	6%	7%
	Krypton	0.406	0.351	0.502	42.4	10.3	32%	31%	38%
4G-3 Ultra Low U Low SHGC	Xenon	0.364	0.350	0.502	32.5	7.0	39%	47%	58%
	Air	0.644	0.410	0.556	62.9	17.1			
	Argon	0.524	0.409	0.556	59.6	16.0	19%	5%	6%
	Krypton	0.462	0.409	0.556	42.2	10.2	28%	33%	40%
4G-3s Ultra U Low SHGC	Xenon	0.421	0.409	0.556	33.5	7.3	35%	47%	57%
	Air	0.643	0.435	0.556	62.8	17.1			
	Argon	0.523	0.434	0.556	59.5	16.0	19%	5%	6%
	Krypton	0.461	0.434	0.556	42.7	10.4	28%	32%	39%
4G-4v Low U Ultra Low VT	Xenon	0.420	0.434	0.556	33.7	7.4	35%	46%	57%
	Air	1.257	0.444	0.427	63.8	17.2			
	Argon	1.170	0.443	0.427	61.7	16.5	7%	3%	4%
	Krypton	1.126	0.443	0.427	43.7	10.5	10%	32%	39%
4G-5uv Ultra Low U Ultra Low SHGC	Xenon	1.097	0.443	0.427	34.4	7.4	13%	46%	57%
	Air	0.566	0.184	0.397	61.9	16.8			
	Argon	0.441	0.184	0.397	58.3	15.6	22%	6%	7%
	Krypton	0.376	0.184	0.397	42.1	10.2	34%	32%	39%
5G-1 Standard IGU	Xenon	0.333	0.184	0.397	33.1	7.2	41%	47%	57%
	Air	0.964	0.489	0.569	104.6	19.0			
	Argon	0.898	0.489	0.569	99.4	17.7	7%	5%	7%
	Krypton	0.864	0.489	0.569	75.4	11.7	10%	28%	38%
5G-2 Ultra Low U Ultra Low SHGC	Xenon	0.843	0.489	0.569	60.2	7.9	13%	42%	58%
	Air	0.451	0.207	0.447	86.8	18.8			
	Argon	0.361	0.207	0.447	80.4	17.2	20%	7%	9%
	Krypton	0.314	0.207	0.447	57.2	11.4	30%	34%	39%
5G-2s Ultra Low U Low SHGC	Xenon	0.284	0.207	0.447	42.8	7.8	37%	51%	59%
	Air	0.440	0.335	0.447	84.4	18.2			
	Argon	0.349	0.333	0.447	79.2	16.9	21%	6%	7%
	Krypton	0.302	0.332	0.447	55.6	11.0	31%	34%	40%
5G-3 Ultra Low U Low SHGC	Xenon	0.271	0.330	0.447	42.8	7.8	38%	49%	57%
	Air	0.471	0.359	0.494	85.7	18.5			
	Argon	0.383	0.359	0.494	79.3	16.9	19%	7%	9%
	Krypton	0.337	0.358	0.494	56.9	11.3	28%	34%	39%
5G-3s Ultra Low U Low SHGC	Xenon	0.308	0.359	0.494	42.5	7.7	35%	50%	58%
	Air	0.471	0.392	0.494	84.1	18.1			
	Argon	0.382	0.391	0.494	80.5	17.2	19%	4%	5%
	Krypton	0.337	0.391	0.494	55.7	11.0	28%	34%	39%
5G-3sm Ultra Low U Low SHGC	Xenon	0.307	0.391	0.494	43.3	7.9	35%	49%	56%
	Air	0.471	0.379	0.493	85.3	18.4			
	Argon	0.382	0.378	0.493	80.9	17.3	19%	5%	6%
	Krypton	0.337	0.378	0.493	56.1	11.1	28%	34%	40%
5G-4v Low U Low VT	Xenon	0.307	0.378	0.493	43.7	8.0	35%	49%	57%
	Air	0.981	0.267	0.417	86.4	18.7			
	Argon	0.912	0.265	0.417	82.0	17.6	7%	5%	6%
	Krypton	0.877	0.264	0.417	57.6	11.5	11%	33%	39%
5G-4uv Ultra Low U Ultra Low SHGC	Xenon	0.855	0.263	0.417	43.2	7.9	13%	50%	58%
	Air	0.441	0.187	0.406	84.4	18.2			
	Argon	0.350	0.187	0.406	80.0	17.1	21%	5%	6%
	Krypton	0.303	0.187	0.406	56.0	11.1	31%	34%	39%
5G-4uv Ultra Low SHGC	Xenon	0.272	0.187	0.406	43.6	8.0	38%	48%	56%

HIGH PERFORMANCE IGU CONSTRUCTION

IGU	Layer	Product Name	Window5 ID	Emissivity Front	Emissivity Back	Thickness [mm]	R _{sol}		T _{vis}		R _{vis}		T _{IR}
							Front	Back	Front	Back	Front	Back	
2G-2s	Layer 1	Generic Clear Glass	103	0.84		5.715	0.771	0.07	0.07	0.884	0.08	0.08	0
	Layer 2	PPG - Solarban 70XL Starphire	5439	0.018	0.841	5.664	0.281	0.513	0.56	0.72	0.077	0.06	0
2G-4uv	Layer 1	AFG - Comfort Ti-R Low E	938	0.84		5.664	0.228	0.44	0.14	0.467	0.023	0.05	0
	Layer 2	Generic Clear Glass	103	0.84	0.84	5.715	0.771	0.07	0.07	0.884	0.08	0.08	0
3G-2s	Layer 1	Generic Clear Glass	103	0.84		5.715	0.771	0.07	0.07	0.884	0.08	0.08	0
	Layer 2	Heat Mirror 88	1506	0.122	0.755	0.076	0.654	0.231	0.21	0.878	0.061	0.07	0
	Layer 3	PPG - Solarban 70XL Starphire	5439	0.018	0.841	5.664	0.281	0.513	0.56	0.72	0.077	0.06	0
3G-5uv	Layer 1	PPG - Solarban 70XL Starphire	5439	0.84	0.018	5.664	0.281	0.513	0.56	0.72	0.077	0.06	0
	Layer 2	Heat Mirror 66	1504	0.755	0.043	0.076	0.354	0.552	0.52	0.65	0.261	0.28	0
	Layer 3	Generic Clear Glass	103	0.84	0.84	5.715	0.771	0.07	0.07	0.884	0.08	0.08	0
4G-2s	Layer 1	Generic Clear Glass	103	0.84		5.715	0.771	0.07	0.07	0.884	0.08	0.08	0
	Layer 2	Heat Mirror 88	1506	0.122	0.755	0.076	0.654	0.231	0.21	0.878	0.061	0.07	0
	Layer 3	Heat Mirror 88	1506	0.122	0.755	0.076	0.654	0.231	0.21	0.878	0.061	0.07	0
	Layer 4	PPG - Solarban 70XL Starphire	5000	0.018	0.84	5.664	0.281	0.513	0.56	0.72	0.077	0.06	0
4G-5uv	Layer 1	PPG - Solarban 70XL Starphire	5439	0.84	0.018	5.664	0.281	0.513	0.56	0.72	0.077	0.06	0
	Layer 2	Solar Control 75	1510	0.755	0.055	0.076	0.375	0.46	0.46	0.756	0.128	0.11	0
	Layer 3	Heat Mirror 77	1505	0.755	0.07	0.076	0.478	0.41	0.39	0.786	0.128	0.15	0
	Layer 4	Generic Clear Glass	103	0.84	0.84	5.715	0.771	0.07	0.07	0.884	0.08	0.08	0
5G-2s	Layer 1	Generic Clear Glass	103	0.84		5.715	0.771	0.07	0.07	0.884	0.08	0.08	0
	Layer 2	Heat Mirror 88	1506	0.122	0.755	0.076	0.654	0.231	0.21	0.878	0.061	0.07	0
	Layer 3	Heat Mirror 88	1506	0.122	0.755	0.076	0.654	0.231	0.21	0.878	0.061	0.07	0
	Layer 4	Heat Mirror 88	1506	0.122	0.755	0.076	0.654	0.231	0.21	0.878	0.061	0.07	0
	Layer 5	PPG - Solarban 70XL Starphire	5439	0.018	0.84	5.664	0.281	0.513	0.56	0.72	0.077	0.06	0
5G-4uv	Layer 1	PPG - Solarban 70XL Starphire	5439	0.84	0.018	5.664	0.281	0.513	0.56	0.72	0.077	0.06	0
	Layer 2	Heat Mirror 77	1505	0.755	0.07	0.076	0.478	0.41	0.39	0.786	0.128	0.15	0
	Layer 3	Heat Mirror 88	1506	0.755	0.122	0.076	0.654	0.231	0.21	0.878	0.061	0.07	0
	Layer 4	Heat Mirror 88	1506	0.755	0.122	0.076	0.654	0.231	0.21	0.878	0.061	0.07	0
	Layer 5	Generic Clear Glass	103	0.84	0.84	5.715	0.771	0.07	0.07	0.884	0.08	0.08	0

Appendix C1

Typical Aluminum Curtain Wall Frame

Performance Characteristics

PRESSURE PLATE CURTAIN WALL

Jamb-End Sections

Double-Glazed Spacer Study

Spacer Material	Pressure Cap Material	Thermal Break	IGU			Edge		Frame		Window (10' x 4')	
			Type	U [W/m2K]	R [ft2Fh/BTU]	U [W/m2K]	R [ft2Fh/BTU]	U [W/m2K]	R [ft2Fh/BTU]	U [W/m2K]	R [ft2Fh/BTU]
Aluminum with Silicone	Aluminum (anodized)	None	2G-2s	1.305	4.35	1.8608	3.05	13.4626	0.42	2.480	2.29
Steel with Silicone Dessicant	Aluminum (anodized)	None	2G-2s	1.305	4.35	1.819	3.12	13.4492	0.42	2.473	2.30
Silicone Foam EcoSpacerTM	Aluminum (anodized)	None	2G-2s	1.305	4.35	1.7048	3.33	13.4204	0.42	2.455	2.31
(Serious Materials)	Aluminum (anodized)	None	2G-2s	1.305	4.35	1.7065	3.33	13.4212	0.42	2.455	2.31
PVC (rigid)	Aluminum (anodized)	None	2G-2s	1.305	4.35	1.6752	3.39	13.4123	0.42	2.450	2.32

Conclusions

Spacer type has minimal effect on R-value

PVC spacer is most insulating, next to Silicone foam and EcoSpacer, but not by much

Best overall window R-value is 49% of CoG

**Double-Glazed Aluminum Curtain Wall Component Study
Thermal Break Sizes**

Window	IGU Width [mm]	TB Length [mm]	TB/IGU	Eq TB Length [mm]
2G	23.6	3.26	14%	3.26
3G	30.7	8.26	27%	6.36
4G	42.1	21.26	50%	11.91
5G	43.4	28.26	65%	15.36

With Aluminum Spacer

Spacer Material	Pressure Cap Material	Thermal Break	IGU			Edge		Frame		Window (10' x 4')	
			Type	U [W/m2K]	R [ft2Fh/BTU]	U [W/m2K]	R [ft2Fh/BTU]	U [W/m2K]	R [ft2Fh/BTU]	U [W/m2K]	R [ft2Fh/BTU]
Aluminum with Silicone Dessicant	Aluminum (anodized)	None	2G-s	1.305	4.35	1.8608	3.05	13.4626	0.42	2.480	2.29
Aluminum with Silicone Dessicant	Aluminum (anodized)	None	2G-2s	1.305	4.35	1.7244	3.29	6.1405	0.92	1.799	3.16
Aluminum with Silicone Dessicant	Aluminum (anodized)	PVC (3.3 mm, 14%)	2G-2s	1.305	4.35	1.7958	3.16	9.6725	0.59	2.128	2.67
Aluminum with Silicone Dessicant	Aluminum (anodized)	PVC (6.3 mm, 27%)	2G-2s	1.305	4.35	1.784	3.18	8.6382	0.66	2.033	2.79
Aluminum with Silicone Dessicant	Aluminum (anodized)	PVC (11.9 mm, 50%)	2G-2s	1.305	4.35	1.7857	3.18	7.5103	0.76	1.931	2.94
Aluminum with Silicone Dessicant	Aluminum (anodized)	PVC (15.4 mm, 65%)	2G-2s	1.305	4.35	1.792	3.17	7.0198	0.81	1.888	3.01
Aluminum with Silicone Dessicant	Insulated Snap Cap, Aluminum	None	2G-2s	1.305	4.35	1.8607	3.05	13.46	0.42	2.479	2.29
Aluminum with Silicone Dessicant	Aluminum (anodized)	Insulated Core	2G-2s	1.305	4.35	1.8618	3.05	13.4304	0.42	2.477	2.29

Conclusion

Non Thermally Broken:	Window R-value is 48% of CoG
Fibreglass Pressure Plate:	Fibreglass Cap adds approximately +R-0.91 to base model Reduction in U-value to base model is: 31% Window R-value is 69% of CoG
PVC Thermal Break (14%):	PVC thermal break at typical double glazed length (14% of IGU) adds approximately +R-0.39 to base model Reduction in U-value to base model is: 16% Window R-value is 57% of CoG
PVC Thermal Break (27%):	PVC thermal break at 27% of IGU adds approximately +R-0.51 to base model Reduction in U-value to base model is: 20%, better than typical thermal break, but still not as great as FGpress Window R-value is 59% of CoG
PVC Thermal Break (50%):	PVC thermal break at 50% of IGU adds approximately +R-0.65 to base model Reduction in U-value to base model is: 24%, not as effective as FGpress Window R-value is 63% of CoG
PVC Thermal Break (65%):	PVC thermal break at 65% of IGU adds approximately +R-0.71 to base model Reduction in U-value to base model is: 26%, not as effective as Fgpress Window R-value is 64% of CoG
Insulated Snap Cap:	Aerogel Snap Cap adds approximately nothing to base model Reduction in U-value to base model is: 0% Window R-value is 48% of CoG
Insulated Core:	It does nothing Window R-value is 48% of CoG

With PVC Spacer

Spacer Material	Pressure Cap Material	Thermal Break	IGU			Edge		Frame		Window (10' x 4')	
			Type	U [W/m2K]	R [ft2Fh/BTU]	U [W/m2K]	R [ft2Fh/BTU]	U [W/m2K]	R [ft2Fh/BTU]	U [W/m2K]	R [ft2Fh/BTU]
PVC with Silicone Dessicant	Aluminum (anodized)	None	2G-2s	1.305	4.35	1.6752	3.39	13.4123	0.42	2.450	2.32
PVC with Silicone Dessicant	Aluminum (anodized)	None	2G-2s	1.305	4.35	1.295	4.38	5.6569	1.00	1.697	3.35
PVC with Silicone Dessicant	Aluminum (anodized)	PVC (3.3 mm, 14%)	2G-2s	1.305	4.35	1.4744	3.85	9.1552	0.62	2.038	2.79
PVC with Silicone Dessicant	Aluminum (anodized)	PVC (6.3 mm, 27%)	2G-2s	1.305	4.35	1.4177	4.01	7.9011	0.72	1.917	2.96
PVC with Silicone Dessicant	Aluminum (anodized)	PVC (11.9 mm, 50%)	2G-2s	1.305	4.35	1.358	4.18	6.4366	0.88	1.776	3.20
PVC with Silicone Dessicant	Aluminum (anodized)	PVC (15.4 mm, 65%)	2G-2s	1.305	4.35	1.3385	4.24	5.7963	0.98	1.716	3.31
PVC with Silicone Dessicant	Aluminum (anodized)	Insulated Snap Cap, None, Insulated Core	2G-2s	1.305	4.35	1.6749	3.39	13.4097	0.42	2.450	2.32
Aluminum with Silicone Dessicant	Aluminum (anodized)	Insulated Core	2G-2s	1.305	4.35	1.6758	3.39	13.3797	0.42	2.447	2.32

Conclusion

Non-Thermally Broken:	Window R-value is 48% of CoG
Fibreglass Pressure Plate:	Fibreglass Cap adds approximately +R-1.11 to base model Reduction in U-value to base model is: 35% Window R-value is 69% of CoG
PVC Thermal Break (14%):	PVC thermal break at typical double glazed length (14% of IGU) adds approximately +R-0.51 to base model Reduction in U-value to base model is: 19%, not as good as FGpress, but better than relative comparison with Al spacers Window R-value is 60% of CoG
PVC Thermal Break (27%):	PVC thermal break at 27% of IGU adds approximately +R-0.69 to base model Reduction in U-value to base model is: 25%, better than typical thermal break, but still not as great as FGpress, better than Al spacers by relative comparison Window R-value is 64% of CoG
PVC Thermal Break (50%):	PVC thermal break at 50% of IGU adds approximately +R-0.65 to base model Reduction in U-value to base model is: 24%, not as effective as FGpress Window R-value is 63% of CoG
PVC Thermal Break (65%):	PVC thermal break at 65% of IGU adds approximately +R-1.07 to base model Reduction in U-value to base model is: 34%, close to FGpress Window R-value is 73% of CoG
Insulated Snap Cap:	Aerogel Snap Cap adds approximately nothing to base model Reduction in U-value to base model is: 0% Window R-value is 48% of CoG

**Aluminum Curtain Wall Cumulative Study
Double Glazed (2G-2s)**

Spacer Material	Pressure Cap Material	Thermal Break	IGU			Edge		Frame		Window (10' x 4')	
			Type	U [W/m2K]	R [ft2Fh/BTU]	U [W/m2K]	R [ft2Fh/BTU]	U [W/m2K]	R [ft2Fh/BTU]	U [W/m2K]	R [ft2Fh/BTU]
Aluminum with Silicone Dessicant	Aluminum (anodized)	None	2G-2s	1.305	4.35	1.8608	3.05	13.4626	0.42	2.480	2.29
Steel with Silicone Dessicant	Aluminum (anodized)	None	2G-2s	1.305	4.35	1.819	3.12	13.4492	0.42	2.473	2.30
Silicone Foam EcoSpacerTM	Aluminum (anodized)	None	2G-2s	1.305	4.35	1.7048	3.33	13.4204	0.42	2.455	2.31
(Serious Materials)	Aluminum (anodized)	None	2G-2s	1.305	4.35	1.7065	3.33	13.4212	0.42	2.455	2.31
PVC with Silicone Dessicant	Aluminum (anodized)	None	2G-2s	1.305	4.35	1.6752	3.39	13.4123	0.42	2.450	2.32
Aluminum with Silicone Dessicant	Aluminum (anodized)	PVC (3.3 mm)	2G-2s	1.305	4.35	1.7958	3.16	9.6725	0.59	2.128	2.67
Steel with Silicone Dessicant	Aluminum (anodized)	PVC (3.3 mm)	2G-2s	1.305	4.35	1.7431	3.26	9.8828	0.57	2.140	2.65
Silicone Foam EcoSpacerTM	Aluminum (anodized)	PVC (3.3 mm)	2G-2s	1.305	4.35	1.5553	3.65	9.6073	0.59	2.090	2.72
(Serious Materials)	Aluminum (anodized)	PVC (3.3 mm)	2G-2s	1.305	4.35	1.5581	3.64	9.6118	0.59	2.090	2.72
PVC with Silicone Dessicant	Aluminum (anodized)	PVC (3.3 mm)	2G-2s	1.305	4.35	1.4744	3.85	9.1552	0.62	2.038	2.79
Aluminum with Silicone Dessicant	Fiberglass (reinforced Nylon)	PVC (3.3 mm)	2G-2s	1.305	4.35	1.6523	3.44	6.2577	0.91	1.800	3.15
Steel with Silicone Dessicant	Fiberglass (reinforced Nylon)	PVC (3.3 mm)	2G-2s	1.305	4.35	1.5771	3.60	6.1262	0.93	1.778	3.19

Silicone Foam	Fiberglass (reinforced Nylon)	PVC (3.3 mm)	2G-2s	1.305	4.35	1.3485	4.21	5.5989	1.01	1.699	3.34
EcoSpacerTM (Serious Materials)	Fiberglass (reinforced Nylon)	PVC (3.3 mm)	2G-2s	1.305	4.35	1.3521	4.20	5.6077	1.01	1.700	3.34
PVC with Silicone Dessicant	Fiberglass (reinforced Nylon)	PVC (3.3 mm)	2G-2s	1.305	4.35	1.283	4.43	5.3633	1.06	1.669	3.40
Aluminum with Silicone Dessicant	Fiberglass (reinforced Nylon)	None	2G-2s	1.305	4.35	1.7244	3.29	6.1405	0.92	1.799	3.16
PVC with Silicone Dessicant	Fiberglass (reinforced Nylon)	None	2G-2s	1.305	4.35	1.295	4.38	5.6569	1.00	1.697	3.35
Aluminum with Silicone Dessicant	Insulated Snap Cap, Fiberglass	PVC (3.3 mm)	2G-2s	1.305	4.35	1.7101	3.32	5.316	1.07	1.722	3.30
Steel with Silicone Dessicant	Insulated Snap Cap, Fiberglass	PVC (3.3 mm)	2G-2s	1.305	4.35	1.5477	3.67	5.589	1.02	1.725	3.29
Silicone Foam	Insulated Snap Cap, Fiberglass	PVC (3.3 mm)	2G-2s	1.305	4.35	1.3166	4.31	5.0437	1.13	1.645	3.45
EcoSpacerTM (Serious Materials)	Insulated Snap Cap, Fiberglass	PVC (3.3 mm)	2G-2s	1.305	4.35	1.3203	4.30	5.0532	1.12	1.646	3.45
PVC with Silicone Dessicant	Insulated Snap Cap, Fiberglass	PVC (3.3 mm)	2G-2s	1.305	4.35	1.2545	4.53	4.8245	1.18	1.616	3.51

Conclusions

Non-thermally broken Aluminum Curtain Wall:	Spacer type has minimal effect on R-value PVC spacer is most insulating, next to Silicone foam and EcoSpacer, but not by much Best overall window R-value is 49% of CoG
+PVC Thermal Break:	Minor improvements from without thermal break PVC thermal break is one of the most effective materials (very low k) yet still stiff enough Improvement is +R-0.48 to +R-0.67, warm edge spacers, ie. PVC has greater benefit from thermal break Best overall window R-value is 64% of CoG, good but hoping for better
+ Fibreglass Pressure Plate:	Fibreglass pressure plates with PVC thermal breaks can significantly improve the R-value of the overall window (frame and edge) very little difference between EcoSpacer and Silicone Foam spacer (mostly due to construction) +R-0.41 to +R-0.56, addition of FG pressure plate does not significantly improve window R-value Warm edge spacers, ie. PVC benefit greater from FG pressure plate PVC spacer is warmest Best window R-value is 77% of CoG, that's really good so far! Inching towards a better window!
Just Fibreglass Pressure Plate (AL Spacer):	Fibreglass Cap adds approximately +R-0.91 to base model Reduction in U-value to base model is: 31% Window R-value is 69% of CoG
Just Fibreglass Pressure Plate (PVC Spacer):	Fibreglass Cap adds approximately +R-1.11 to base model Reduction in U-value to base model is: 35% Window R-value is 69% of CoG
+ Insulated Snap Cap:	Adding aerogel insulation only decreases U-value slightly, not most effective use of material adding aerogel to cap only improves window R-value by +R-0.09 to +R-0.12 PVC spacer is most insulating warm edge spacers tend to benefit most from aerogel insulation Best window R-value is 80% of CoG, its good, but slightly better than without AG cap

**Aluminum Curtain Wall Cumulative Study
Triple Glazed (3G-5uv)**

Spacer Material	Pressure Cap Material	Thermal Break	IGU			Edge		Frame		Window (10' x 4')	
			Type	U [W/m2K]	R [ft2Fh/BTU]	U [W/m2K]	R [ft2Fh/BTU]	U [W/m2K]	R [ft2Fh/BTU]	U [W/m2K]	R [ft2Fh/BTU]
Steel with Silicone Dessicant	Aluminum (anodized)	None	3G-5uv	0.562	10.10	1.3882	4.09	13.3341	0.43	1.829	3.11
Aluminum with Silicone Dessicant	Aluminum (anodized)	None	3G-5uv	0.562	10.10	1.4162	4.01	13.3962	0.42	1.838	3.09
PVC with Silicone Dessicant	Aluminum (anodized)	None	3G-5uv	0.562	10.10	1.2497	4.54	13.3257	0.43	1.809	3.14
Silicone Foam and Steel	Aluminum (anodized)	None	3G-5uv	0.562	10.10	1.3374	4.25	13.2909	0.43	1.818	3.12
Silicone Foam and PVC	Aluminum (anodized)	None	3G-5uv	0.562	10.10	1.2857	4.42	13.2913	0.43	1.811	3.14
EcoSpacer and Steel	Aluminum (anodized)	None	3G-5uv	0.562	10.10	1.3382	4.24	13.2918	0.43	1.818	3.12
EcoSpacer and PVC	Aluminum (anodized)	None	3G-5uv	0.562	10.10	1.2859	4.42	13.2918	0.43	1.811	3.14
Steel with Silicone Dessicant	Aluminum (anodized)	PVC (8.3 mm)	3G-5uv	0.562	10.10	1.1561	4.91	8.5893	0.66	1.368	4.15
Aluminum with Silicone Dessicant	Aluminum (anodized)	PVC (8.3 mm)	3G-5uv	0.562	10.10	1.2523	4.53	8.4303	0.67	1.367	4.15
PVC with Silicone Dessicant	Aluminum (anodized)	PVC (8.3 mm)	3G-5uv	0.562	10.10	0.8707	6.52	7.3608	0.77	1.219	4.66
Silicone Foam and Steel	Aluminum (anodized)	PVC (8.3 mm)	3G-5uv	0.562	10.10	1.008	5.63	7.9718	0.71	1.292	4.39
Silicone Foam and PVC	Aluminum (anodized)	PVC (8.3 mm)	3G-5uv	0.562	10.10	0.9276	6.12	7.8774	0.72	1.273	4.46
EcoSpacer and Steel	Aluminum (anodized)	PVC (8.3 mm)	3G-5uv	0.562	10.10	1.0107	5.62	7.9808	0.71	1.294	4.39

EcoSpacer and PVC	Aluminum (anodized)	PVC (8.3 mm)	3G-5uv	0.562	10.10	0.9283	6.12	7.8817	0.72	1.273	4.46
Steel with Silicone Dessicant	Fiberglass (reinforced Nylon)	PVC (8.3 mm)	3G-5uv	0.562	10.10	0.986	5.76	5.9872	0.95	1.110	5.12
Aluminum with Silicone Dessicant	Fiberglass (reinforced Nylon)	PVC (8.3 mm)	3G-5uv	0.562	10.10	1.1012	5.16	6.223	0.91	1.147	4.95
PVC with Silicone Dessicant	Fiberglass (reinforced Nylon)	PVC (8.3 mm)	3G-5uv	0.562	10.10	0.7466	7.61	5.0997	1.11	0.997	5.69
Silicone Foam and Steel	Fiberglass (reinforced Nylon)	PVC (8.3 mm)	3G-5uv	0.562	10.10	0.8274	6.86	5.3239	1.07	1.028	5.52
Silicone Foam and PVC	Fiberglass (reinforced Nylon)	PVC (8.3 mm)	3G-5uv	0.562	10.10	0.7481	7.59	5.2059	1.09	1.007	5.64
EcoSpacer and Steel	Fiberglass (reinforced Nylon)	PVC (8.3 mm)	3G-5uv	0.562	10.10	0.8303	6.84	5.3353	1.06	1.030	5.51
EcoSpacer and PVC	Fiberglass (reinforced Nylon)	PVC (8.3 mm)	3G-5uv	0.562	10.10	0.7489	7.58	5.2126	1.09	1.008	5.63
Steel with Silicone Dessicant	Fiberglass (reinforced Nylon)	None	3G-5uv	0.562	10.10	1.0483	5.42	6.0885	0.93	1.127	5.04
Aluminum with Silicone Dessicant	Fiberglass (reinforced Nylon)	None	3G-5uv	0.562	10.10	1.1745	4.83	6.3663	0.89	1.170	4.85
PVC with Silicone Dessicant	Fiberglass (reinforced Nylon)	None	3G-5uv	0.562	10.10	0.7597	7.47	5.7136	0.99	1.055	5.38

Silicone Foam and Steel	Fiberglass (reinforced Nylon)	None	3G-5uv	0.562	10.10	0.8604	6.60	5.9446	0.96	1.089	5.21
Silicone Foam and PVC	Fiberglass (reinforced Nylon)	None	3G-5uv	0.562	10.10	0.7873	7.21	5.8549	0.97	1.071	5.30
EcoSpacer and Steel	Fiberglass (reinforced Nylon)	None	3G-5uv	0.562	10.10	0.8631	6.58	5.9541	0.95	1.090	5.21
EcoSpacer and PVC	Fiberglass (reinforced Nylon)	None	3G-5uv	0.562	10.10	0.788	7.21	5.86	0.97	1.072	5.30
Steel with Silicone Dessicant	Insulated Snap Cap, Fiberglass	PVC (8.3 mm)	3G-5uv	0.562	10.10	0.9547	5.95	5.5535	1.02	1.066	5.32
Aluminum with Silicone Dessicant	Insulated Snap Cap, Fiberglass	PVC (8.3 mm)	3G-5uv	0.562	10.10	1.0732	5.29	5.8393	0.97	1.108	5.12
PVC with Silicone Dessicant	Insulated Snap Cap, Fiberglass	PVC (8.3 mm)	3G-5uv	0.562	10.10	0.696	8.16	4.567	1.24	0.942	6.03
Silicone Foam and Steel	Insulated Snap Cap, Fiberglass	PVC (8.3 mm)	3G-5uv	0.562	10.10	0.7947	7.14	4.8733	1.17	0.983	5.77
Silicone Foam and PVC	Insulated Snap Cap, Fiberglass	PVC (8.3 mm)	3G-5uv	0.562	10.10	0.7173	7.92	4.7572	1.19	0.962	5.90
EcoSpacer and Steel	Insulated Snap Cap, Fiberglass	PVC (8.3 mm)	3G-5uv	0.562	10.10	0.7977	7.12	4.8855	1.16	0.985	5.77
EcoSpacer and PVC	Insulated Snap Cap, Fiberglass	PVC (8.3 mm)	3G-5uv	0.562	10.10	0.7182	7.91	4.764	1.19	0.963	5.90

Conclusion

Base Model:	PVC spacer is best, but very similar to SiFoam and EcoSpacer with PVC, with Steel it's a little worse Best overall window R-value is 28% of CoG
+ PVC Thermal Break:	PVC spacer is most insulating EcoSpacer and Silicone foam spacer are have close performance characteristics +R-1.60 to +R-0.99 depending on insulating value of spacer, spacers that are more insulating benefit from PVC thermal break more best window R-value is 44% of CoG, meh
+ Fibreglass Pressure Plate:	PVC spacer is most insulating followed closely by Si foam and EcoSpacer with PVC EcoSpacer and Silicone foam spacer have close performance characteristics PVC spacer benefited most from Fibreglass pressure plate, warm edge spacers showed greater improvement in insulation value than colder space +R-0.82 to +R-1.42 depending on insulating value of spacer, spacers that are more insulating have greater benefit of PVC thermal break and fibreglass pressure plate Best window R-value is about 58% that of CoG R-value, better but still not great
Just Fibreglass Pressure Plate:	PVC spacer is most insulating followed closely by Si foam and EcoSpacer with PVC EcoSpacer and Silicone foam spacer have close performance characteristics PVC spacer benefited most from Fibreglass pressure plate, warm edge spacers showed greater improvement in insulation value than colder space +R-0.82 to +R-1.42 depending on insulating value of spacer, spacers that are more insulating have greater benefit of PVC thermal break and fibreglass pressure plate Best window R-value is about 58% that of CoG R-value, better but still not great
+ Insulated Snap Cap:	PVC spacer is best, followed closely by Silicone foam and EcoSpacer with PVC Warm edge spacers show greater benefit from adding Aerogel insulated cap, however benefit is still very minimal HOWEVER, PVC spacer shows little difference in R (+R-0.01) with addition of insulated pressure plate, weird +R-0.01 to +R-0.26 Best window R-value is 58% that of CoG, better but not great

**Aluminum Curtain Wall Cumulative Study
Quad Glazed (4G-5uv)**

Spacer Material	Pressure Cap Material	Thermal Break	IGU			Edge		Frame		Window (10' x 4')	
			Type	U [W/m2K]	R [ft2Fh/BTU]	U [W/m2K]	R [ft2Fh/BTU]	U [W/m2K]	R [ft2Fh/BTU]	U [W/m2K]	R [ft2Fh/BTU]
Steel with Silicone Dessicant	Aluminum (anodized)	None	4G-5uv	0.376	15.10	1.2367	4.59	13.3598	0.43	1.666	3.41
Aluminum with Silicone Dessicant	Aluminum (anodized)	None	4G-5uv	0.376	15.10	1.3059	4.35	13.3913	0.42	1.679	3.38
PVC with Silicone Dessicant	Aluminum (anodized)	None	4G-5uv	0.376	15.10	1.1322	5.02	13.3231	0.43	1.649	3.44
Silicone foam with Steel	Aluminum (anodized)	None	4G-5uv	0.376	15.10	1.1978	4.74	13.3473	0.43	1.660	3.42
EcoSpacer with Steel	Aluminum (anodized)	None	4G-5uv	0.376	15.10	1.1985	4.74	13.3474	0.43	1.660	3.42
Silicone foam with PVC	Aluminum (anodized)	None	4G-5uv	0.376	15.10	1.134	5.01	13.323	0.43	1.649	3.44
EcoSpacer with PVC	Aluminum (anodized)	None	4G-5uv	0.376	15.10	1.134	5.01	13.323	0.43	1.649	3.44
Steel with Silicone Dessicant	Aluminum (anodized)	PVC (21.26 mm)	4G-5uv	0.376	15.10	0.8839	6.42	6.7114	0.85	1.018	5.58
Aluminum with Silicone Dessicant	Aluminum (anodized)	PVC (21.26 mm)	4G-5uv	0.376	15.10	1.0746	5.28	7.1754	0.79	1.085	5.23
PVC with Silicone Dessicant	Aluminum (anodized)	PVC (21.26 mm)	4G-5uv	0.376	15.10	0.5972	9.51	5.2559	1.08	0.847	6.70
Silicone foam with Steel	Aluminum (anodized)	PVC (21.26 mm)	4G-5uv	0.376	15.10	0.7487	7.58	6.2261	0.91	0.955	5.94
EcoSpacer with Steel	Aluminum (anodized)	PVC (21.26 mm)	4G-5uv	0.376	15.10	0.7511	7.56	6.2327	0.91	0.956	5.94
Silicone foam with PVC	Aluminum (anodized)	PVC (21.26 mm)	4G-5uv	0.376	15.10	0.6229	9.12	5.6336	1.01	0.885	6.42

EcoSpacer with PVC	Aluminum (anodized)	PVC (21.26 mm)	4G-5uv	0.376	15.10	0.6229	9.12	5.6336	1.01	0.885	6.42
Steel with Silicone Dessicant	Fibreglass (rigid)	PVC (21.26 mm)	4G-5uv	0.376	15.10	0.773	7.35	5.3389	1.06	0.878	6.46
Aluminum with Silicone Dessicant	Fibreglass (rigid)	PVC (21.26 mm)	4G-5uv	0.376	15.10	0.9456	6.00	5.8709	0.97	0.950	5.98
PVC with Silicone Dessicant	Fibreglass (rigid)	PVC (21.26 mm)	4G-5uv	0.376	15.10	0.5196	10.93	4.1136	1.38	0.733	7.74
Silicone foam with Steel	Fibreglass (rigid)	PVC (21.26 mm)	4G-5uv	0.376	15.10	0.6505	8.73	4.9111	1.16	0.823	6.90
EcoSpacer with Steel	Fibreglass (rigid)	PVC (21.26 mm)	4G-5uv	0.376	15.10	0.6528	8.70	4.9174	1.15	0.824	6.89
Silicone foam with PVC	Fibreglass (rigid)	PVC (21.26 mm)	4G-5uv	0.376	15.10	0.5302	10.71	4.2726	1.33	0.749	7.58
EcoSpacer with PVC	Fibreglass (rigid)	PVC (21.26 mm)	4G-5uv	0.376	15.10	0.5302	10.71	4.2726	1.33	0.749	7.58
Steel with Silicone Dessicant	Fibreglass (rigid)	None	4G-5uv	0.376	15.10	0.8153	6.96	6.656	0.85	1.003	5.66
Aluminum with Silicone Dessicant	Fibreglass (rigid)	None	4G-5uv	0.376	15.10	0.9514	5.97	6.9836	0.81	1.051	5.40
PVC with Silicone Dessicant	Fibreglass (rigid)	None	4G-5uv	0.376	15.10	0.6345	8.95	5.9997	0.95	0.919	6.18
Silicone foam with Steel	Fibreglass (rigid)	None	4G-5uv	0.376	15.10	0.7318	7.76	6.4808	0.88	0.976	5.82
EcoSpacer with Steel	Fibreglass (rigid)	None	4G-5uv	0.376	15.10	0.7332	7.74	6.4818	0.88	0.976	5.82
Silicone foam with PVC	Fibreglass (rigid)	None	4G-5uv	0.376	15.10	0.636	8.93	6.0226	0.94	0.922	6.16
EcoSpacer with PVC	Fibreglass (rigid)	None	4G-5uv	0.376	15.10	0.636	8.93	6.0226	0.94	0.922	6.16
Steel with Silicone Dessicant	Insulated Snap Cap, Fibreglass	PVC (21.26 mm)	4G-5uv	0.376	15.10	0.7495	7.58	5.0871	1.12	0.852	6.66

Aluminum with Silicone Dessicant	Insulated Snap Cap, Fibreglass	PVC (21.26 mm)	4G-5uv	0.376	15.10	0.9201	6.17	5.6771	1.00	0.929	6.11
PVC with Silicone Dessicant	Insulated Snap Cap, Fibreglass	PVC (21.26 mm)	4G-5uv	0.376	15.10	0.5084	11.17	3.9602	1.43	0.718	7.91
Silicone foam with Steel	Insulated Snap Cap, Fibreglass	PVC (21.26 mm)	4G-5uv	0.376	15.10	0.6304	9.01	4.6672	1.22	0.798	7.11
EcoSpacer with Steel	Insulated Snap Cap, Fibreglass	PVC (21.26 mm)	4G-5uv	0.376	15.10	0.6327	8.97	4.6752	1.21	0.799	7.10
Silicone foam with PVC	Insulated Snap Cap, Fibreglass	PVC (21.26 mm)	4G-5uv	0.376	15.10	0.5124	11.08	4.0157	1.41	0.724	7.85
EcoSpacer with PVC	Insulated Snap Cap, Fibreglass	PVC (21.26 mm)	4G-5uv	0.376	15.10	0.5124	11.08	4.0157	1.41	0.724	7.85

Conclusion

Base Model:	Aluminum pressure plate reduces R-value significantly PVC spacer has greatest effect, it is the most insulating changing from stainless steel to PVC structural spacers for EcoSpacer and Silicone foam spacer has little effect PVC spacer is the BEST Best overall window R-value is 21% that of CoG
+ PVC Thermal Break:	Adding thermal break provides significant increase in R-value Benefit of thermal break is more significant for highly insulating warm-edge spacers (ie. PVC, Si Foam with PVC, and EcoSpacer with PVC) +R-1.55 to +R-3.31 (best seen by PVC spacer) PVC spacer vs Si foam with PVC and EcoSpacer with PVC differ slightly +R-0.05 Best overall window R-value is 43% of CoG R-value, better but still not great
+ Fibreglass Pressure Plate:	Somewhat significant improvements to window R-value by switching from Al to Fibreglass pressure plates indicates Fibreglass pressure plates is just as important, if not more than thermal breaks +R-0.69 to +R-1.11 more insulating spacers benefited more from FG pressure plates PVC spacer still has the best window R-value Best window R-value is 50% that of CoG R-value, good but not great, kind of disappointing
Just Fibreglass Pressure Plate:	Somewhat significant improvements to window R-value by switching from Al to Fibreglass pressure plates indicates Fibreglass pressure plates is just as important, if not more than thermal breaks +R-0.69 to +R-1.11 more insulating spacers benefited more from FG pressure plates PVC spacer still has the best window R-value Best window R-value is 50% that of CoG R-value, good but not great, kind of disappointing
+ Insulated Snap Cap:	Insignificant improvement to overall window R-value with addition of aerogel to snap cap +R-0.14 to +R-0.29 more insulating spacers benefit more from aerogel insulated snap cap PVC spacer has best overall window R-value Best overall window R-value is 52% of CoG R-value, an improvement, but still very poor overall

**Aluminum Curtain Wall Cumulative Study
Quint Glazed (5G-2s)**

Spacer Material	Pressure Cap Material	Thermal Break	IGU			Edge		Frame		Window (10' x 4')	
			Type	U [W/m2K]	R [ft2Fh/BTU]	U [W/m2K]	R [ft2Fh/BTU]	U [W/m2K]	R [ft2Fh/BTU]	U [W/m2K]	R [ft2Fh/BTU]
Steel with Silicone Dessicant	Aluminum (anodized)	None	5G-2s	0.271	20.95	1.1078	5.13	13.676	0.42	1.596	3.56
Aluminum with Silicone Dessicant	Aluminum (anodized)	None	5G-2s	0.271	20.95	1.1943	4.75	13.7004	0.41	1.610	3.53
PVC with Silicone Dessicant	Aluminum (anodized)	None	5G-2s	0.271	20.95	0.9488	5.98	13.6463	0.42	1.572	3.61
Silicone foam with Steel	Aluminum (anodized)	None	5G-2s	0.271	20.95	1.0418	5.45	13.664	0.42	1.586	3.58
EcoSpacer with Steel	Aluminum (anodized)	None	5G-2s	0.271	20.95	1.0428	5.44	13.6642	0.42	1.586	3.58
Silicone foam with PVC	Aluminum (anodized)	None	5G-2s	0.271	20.95	0.9538	5.95	13.6511	0.42	1.573	3.61
EcoSpacer with PVC	Aluminum (anodized)	None	5G-2s	0.271	20.95	0.9539	5.95	13.6511	0.42	1.573	3.61
Steel with Silicone Dessicant	Aluminum (anodized)	PVC (28.26 mm)	5G-2s	0.271	20.95	0.8112	7.00	6.1546	0.92	0.876	6.48
Aluminum with Silicone Dessicant	Aluminum (anodized)	PVC (28.26 mm)	5G-2s	0.271	20.95	1.0311	5.51	6.6429	0.85	0.950	5.98
PVC with Silicone Dessicant	Aluminum (anodized)	PVC (28.26 mm)	5G-2s	0.271	20.95	0.4635	12.25	4.6897	1.21	0.697	8.15
Silicone foam with Steel	Aluminum (anodized)	PVC (28.26 mm)	5G-2s	0.271	20.95	0.612	9.28	5.4677	1.04	0.787	7.21
EcoSpacer with Steel	Aluminum (anodized)	PVC (28.26 mm)	5G-2s	0.271	20.95	0.6151	9.23	5.4784	1.04	0.788	7.20
Silicone foam with PVC	Aluminum (anodized)	PVC (28.26 mm)	5G-2s	0.271	20.95	0.4915	11.55	5.0787	1.12	0.736	7.72

EcoSpacer with PVC	Aluminum (anodized)	PVC (28.26 mm)	5G-2s	0.271	20.95	0.4919	11.54	5.0811	1.12	0.736	7.72
Steel with Silicone Dessicant	Fiberglass (reinforced Nylon)	PVC (28.26 mm)	5G-2s	0.271	20.95	0.7138	7.95	5.0135	1.13	0.760	7.47
Aluminum with Silicone Dessicant	Fiberglass (reinforced Nylon)	PVC (28.26 mm)	5G-2s	0.271	20.95	0.907	6.26	5.5158	1.03	0.831	6.83
PVC with Silicone Dessicant	Fiberglass (reinforced Nylon)	PVC (28.26 mm)	5G-2s	0.271	20.95	0.4087	13.89	3.7866	1.50	0.608	9.35
Silicone foam with Steel	Fiberglass (reinforced Nylon)	PVC (28.26 mm)	5G-2s	0.271	20.95	0.5378	10.56	4.4277	1.28	0.683	8.31
EcoSpacer with Steel	Fiberglass (reinforced Nylon)	PVC (28.26 mm)	5G-2s	0.271	20.95	0.5406	10.50	4.4373	1.28	0.684	8.30
Silicone foam with PVC	Fiberglass (reinforced Nylon)	PVC (28.26 mm)	5G-2s	0.271	20.95	0.4251	13.36	3.992	1.42	0.628	9.04
EcoSpacer with PVC	Fiberglass (reinforced Nylon)	PVC (28.26 mm)	5G-2s	0.271	20.95	0.4254	13.35	3.9941	1.42	0.629	9.03
Steel with Silicone Dessicant	Fiberglass (reinforced Nylon)	None	5G-2s	0.271	20.95	0.7317	7.76	6.8279	0.83	0.926	6.13
Aluminum with Silicone Dessicant	Fiberglass (reinforced Nylon)	None	5G-2s	0.271	20.95	0.8756	6.48	7.0964	0.80	0.970	5.85
PVC with Silicone Dessicant	Fiberglass (reinforced Nylon)	None	5G-2s	0.271	20.95	0.5239	10.84	6.2028	0.92	0.842	6.75

Silicone foam with Steel	Fiberglass (reinforced Nylon)	None	5G-2s	0.271	20.95	0.6196	9.16	6.6317	0.86	0.893	6.36
EcoSpacer with Steel	Fiberglass (reinforced Nylon)	None	5G-2s	0.271	20.95	0.6212	9.14	6.6349	0.86	0.894	6.35
Silicone foam with PVC	Fiberglass (reinforced Nylon)	None	5G-2s	0.271	20.95	0.528	10.75	6.2327	0.91	0.845	6.72
EcoSpacer with PVC	Fiberglass (reinforced Nylon)	None	5G-2s	0.271	20.95	0.5281	10.75	6.2332	0.91	0.845	6.72
Steel with Silicone Dessicant	Insulated Snap Cap, Fiberglass	PVC (28.26 mm)	5G-2s	0.271	20.95	0.6915	8.21	4.8098	1.18	0.738	7.69
Aluminum with Silicone Dessicant	Insulated Snap Cap, Fiberglass	PVC (28.26 mm)	5G-2s	0.271	20.95	0.8811	6.44	5.3381	1.06	0.812	7.00
PVC with Silicone Dessicant	Insulated Snap Cap, Fiberglass	PVC (28.26 mm)	5G-2s	0.271	20.95	0.3989	14.23	3.6257	1.57	0.592	9.60
Silicone foam with Steel	Insulated Snap Cap, Fiberglass	PVC (28.26 mm)	5G-2s	0.271	20.95	0.5224	10.87	4.2407	1.34	0.664	8.55
EcoSpacer with Steel	Insulated Snap Cap, Fiberglass	PVC (28.26 mm)	5G-2s	0.271	20.95	0.5251	10.81	4.2501	1.34	0.665	8.54
Silicone foam with PVC	Insulated Snap Cap, Fiberglass	PVC (28.26 mm)	5G-2s	0.271	20.95	0.4125	13.76	3.7906	1.50	0.608	9.33
EcoSpacer with PVC	Insulated Snap Cap, Fiberglass	PVC (28.26 mm)	5G-2s	0.271	20.95	0.4128	13.75	3.7926	1.50	0.609	9.33

Conclusion

Base Model:	<p>EcoSpacer with PVC is most insulating</p> <p>PVC spacer is better than EcoSpacer or SiFoam spacer with stainless</p> <p>changing from stainless steel to PVC structural spacers for EcoSpacer and Silicone foam spacer has SIGNIFICANT effect</p> <p>Best overall window R-value is 19% that of CoG, horrid</p>
+ PVC Thermal Break:	<p>PVC spacer is most insulating</p> <p>Aluminum and Steel spacers are horrible</p> <p>PVC spacer is better than EcoSpacer or SiFoam spacer with stainless, Si Foam and EcoSpacer with PVC is same, with Stainless Si Foam is better +R-2.05 to +R-4.66, PVC thermal break most beneficial for warm edge spacers, ie. PVC, Si Foam with PVC, EcoSpacer with PVC</p> <p>Adding PVC thermal break significantly improves overall R-value of window, since thermal break is large in curtain wall section</p> <p>Best overall window R-value is 38% that of CoG, good but not great</p>
+ Fibreglass Pressure Plate:	<p>PVC spacer is most insulating</p> <p>Aluminum and Steel spacers are horrible</p> <p>PVC spacer is better than EcoSpacer or SiFoam spacer with stainless, Si Foam and EcoSpacer with PVC is same, with Stainless Si Foam is better +R-0.76 to +R-1.23, Fiberglass pressure plate most beneficial for warm edge spacers, ie. PVC, Si Foam with PVC, EcoSpacer with PVC</p> <p>Adding Fibreglass pressure plate improves overall R-value of window, but not by too much with an overall improvement of about +R-1.0</p> <p>Best overall window R-value is 44% that of CoG, better but still not great</p>
Just Fibreglass Pressure Plate:	<p>PVC spacer is most insulating</p> <p>Aluminum and Steel spacers are horrible</p> <p>PVC spacer is better than EcoSpacer or SiFoam spacer with stainless, Si Foam and EcoSpacer with PVC is same, with Stainless Si Foam is better +R-0.76 to +R-1.23, Fiberglass pressure plate most beneficial for warm edge spacers, ie. PVC, Si Foam with PVC, EcoSpacer with PVC</p> <p>Adding Fibreglass pressure plate improves overall R-value of window, but not by too much with an overall improvement of about +R-1.0</p> <p>Best overall window R-value is 44% that of CoG, better but still not great</p>
+ Insulated Snap Cap:	<p>PVC spacer is most insulating</p> <p>Aluminum and Steel spacers are horrible</p> <p>PVC spacer is better than EcoSpacer or SiFoam spacer with stainless, Si Foam and EcoSpacer with PVC is same, with Stainless Si Foam is better +R-0.19 to +R-0.30, Spaceloft Aerogel insulation most beneficial for warm edge spacers, ie. PVC, Si Foam with PVC, EcoSpacer with PVC</p> <p>Adding Spaceloft Aerogel insulation improves overall R-value of window, but only marginally, less than R-1, not useful</p> <p>Best overall window R-value is 46% that of CoG, still pretty bad</p>

Appendix C2

High Performance Aluminum and Timber Curtain Wall Frame Performance Characteristics

HIGH PERFORMANCE ALUMINUM AND TIMBER CURTAIN WALL SECTIONS

High Performance Aluminum Curtain Wall

Spacer Material	Pressure Cap Material	Thermal Break	IGU			Edge		Frame		Window (10' x 4')	
			Type	U [W/m2K]	R [ft2Fh/BTU]	U [W/m2K]	R [ft2Fh/BTU]	U [W/m2K]	R [ft2Fh/BTU]	U [W/m2K]	R [ft2Fh/BTU]
PVC with Silicone Dessicant	Insulated Snap Cap, Fiberglass (reinforced Nylon)	EPDM	2G-2s	1.305	4.35	1.3088	4.34	4.7881	1.19	1.621	3.50
PVC with Silicone Dessicant	Insulated Snap Cap, Fiberglass (reinforced Nylon)	EPDM	3G-5uv	0.562	10.10	0.6722	8.45	3.4345	1.65	0.837	6.79
PVC with Silicone Dessicant	Insulated Snap Cap, Fiberglass (reinforced Nylon)	EPDM	4G-5uv	0.376	15.10	0.5048	11.25	2.5727	2.21	0.592	9.59
PVC with Silicone Dessicant	Insulated Snap Cap, Fiberglass (reinforced Nylon)	EPDM	5G-2s	0.272	20.88	0.4393	12.93	2.8123	2.02	0.524	10.83

High Performance Timber Curtain Wall

Spacer Material	Pressure Cap Material	Thermal Break	IGU			Edge		Frame		Window (10' x 4')	
			Type	U [W/m2K]	R [ft2Fh/BTU]	U [W/m2K]	R [ft2Fh/BTU]	U [W/m2K]	R [ft2Fh/BTU]	U [W/m2K]	R [ft2Fh/BTU]
PVC with Silicone Dessicant	Insulated Snap Cap, Fiberglass (reinforced Nylon)	EPDM	2G-2s	1.305	4.35	1.5916	3.57	1.8827	3.02	1.396	4.07
PVC with Silicone Dessicant	Insulated Snap Cap, Fiberglass (reinforced Nylon)	EPDM	3G-5uv	0.562	10.10	1.0209	5.56	1.7051	3.33	0.727	7.81
PVC with Silicone Dessicant	Insulated Snap Cap, Fiberglass (reinforced Nylon)	EPDM	4G-5uv	0.376	15.10	0.7862	7.22	1.6336	3.48	0.545	10.42
PVC with Silicone Dessicant	Insulated Snap Cap, Fiberglass (reinforced Nylon)	EPDM	5G-2s	0.272	20.88	0.7047	8.06	1.62	3.50	0.452	12.55

**High Performance Timber Curtain Wall
Spacer Study**

Spacer Material	Pressure Cap Material	Thermal Break	IGU			Edge		Frame		Window (10' x 4')	
			Type	U [W/m2K]	R [ft2Fh/BTU]	U [W/m2K]	R [ft2Fh/BTU]	U [W/m2K]	R [ft2Fh/BTU]	U [W/m2K]	R [ft2Fh/BTU]
Aluminum with Silicone Dessicant	Insulated Snap Cap, Fiberglass (reinforced Nylon)	EPDM	2G-2s	1.305	4.35	2.1727	2.61	2.6897	2.11	1.547	3.67
Steel with Silicone Dessicant	Insulated Snap Cap, Fiberglass (reinforced Nylon)	EPDM	2G-2s	1.305	4.35	2.0815	2.73	2.6133	2.17	1.528	3.72
Silicone Foam	Insulated Snap Cap, Fiberglass (reinforced Nylon)	EPDM	2G-2s	1.305	4.35	1.807	3.14	2.3877	2.38	1.471	3.86
EcoSpacer	Insulated Snap Cap, Fiberglass (reinforced Nylon)	EPDM	2G-2s	1.305	4.35	1.8118	3.13	2.3919	2.37	1.472	3.86
PVC with Silicone Dessicant	Insulated Snap Cap, Fiberglass (reinforced Nylon)	EPDM	2G-2s	1.305	4.35	1.5916	3.57	1.8827	3.02	1.396	4.07

**High Performance Timber Curtain Wall
Component Study**

Spacer Material	Pressure Cap Material	Thermal Break	IGU			Edge		Frame		Window (10' x 4')	
			Type	U [W/m2K]	R [ft2Fh/BTU]	U [W/m2K]	R [ft2Fh/BTU]	U [W/m2K]	R [ft2Fh/BTU]	U [W/m2K]	R [ft2Fh/BTU]
PVC with Silicone Dessicant	Aluminum (anodized) Insulated Snap Cap,	EPDM	2G-2s	1.305	4.35	1.697	3.35	2.2797	2.49	1.446	3.93
PVC with Silicone Dessicant	Aluminum (anodized) Fiberglass	EPDM	2G-2s	1.305	4.35	1.697	3.35	2.2797	2.49	1.446	3.93
PVC with Silicone Dessicant	(reinforced Nylon)	EPDM	2G-2s	1.305	4.35	1.697	3.35	2.2797	2.49	1.446	3.93

Appendix C3

Window Assembly U-values

OVERALL TRANSPARENT CURTAIN WALL U-VALUE

Double-Glazed Curtain Wall (2G-2s)

Frame Type	IGU		Edge		Frame	Window		CoG: Opening	Raw Opening				
	Type	U [W/m2K]	U [W/m2K]	U [W/m2K]	U [W/m2K]	U [W/m2K]	R [ft2Fh/BTU]		Height [ft]	Width [ft]	Height [mm]	Width [mm]	Area [m2]
Non-Thermally Broken Aluminum	2G-2s	1.305	1.8608	13.4626	8.82	0.64	1%	0.984	0.656	300	200	0.06	
					7.58	0.75	10%	1.017	1.312	310	400	0.12	
					6.13	0.93	20%	2.001	0.951	610	290	0.18	
					5.24	1.08	30%	2.953	1.066	900	325	0.29	
					4.57	1.24	40%	3.937	1.247	1200	380	0.46	
					3.94	1.44	50%	4.921	1.575	1500	480	0.72	
					3.43	1.66	60%	5.906	2.034	1800	620	1.12	
					2.92	1.95	70%	6.890	2.986	2100	910	1.91	
					2.40	2.36	80%	7.874	5.906	2400	1800	4.32	
					2.28	2.49	82%	8.858	6.726	2700	2050	5.54	
				2.26	2.51	82%	10	6	3048	1829	5.57		
High Performance Aluminum	2G-2s	1.305	1.3088	4.7881	3.40	1.67	1%	0.984	0.656	300	200	0.06	
					3.04	1.87	10%	1.017	1.312	310	400	0.12	
					2.62	2.17	20%	2.001	0.951	610	290	0.18	
					2.37	2.40	30%	2.953	1.066	900	325	0.29	
					2.18	2.60	40%	3.937	1.247	1200	380	0.46	
					2.01	2.82	50%	4.921	1.575	1500	480	0.72	
					1.88	3.03	60%	5.906	2.034	1800	620	1.12	
					1.74	3.26	70%	6.890	2.986	2100	910	1.91	
					1.60	3.54	80%	7.874	5.906	2400	1800	4.32	
					1.57	3.62	82%	8.858	6.726	2700	2050	5.54	
				1.56	3.63	82%	10	6	3048	1829	5.57		
High Performance Timber Curtain Wall	2G-2s	1.305	1.5916	1.8827	1.76	3.22	1%	0.984	0.656	300	200	0.06	
					1.71	3.32	10%	1.017	1.312	310	400	0.12	
					1.64	3.46	20%	2.001	0.951	610	290	0.18	
					1.59	3.56	30%	2.953	1.066	900	325	0.29	
					1.55	3.66	40%	3.937	1.247	1200	380	0.46	
					1.51	3.77	50%	4.921	1.575	1500	480	0.72	
					1.47	3.87	60%	5.906	2.034	1800	620	1.12	
					1.43	3.98	70%	6.890	2.986	2100	910	1.91	
					1.39	4.09	80%	7.874	5.906	2400	1800	4.32	
					1.38	4.12	82%	8.858	6.726	2700	2050	5.54	
				1.38	4.12	82%	10	6	3048	1829	5.57		

Triple-Glazed Curtain Wall (3G-5uv)

Frame Type	IGU		Edge		Frame	Window		CoG: Opening	Raw Opening				
	Type	U [W/m2K]	U [W/m2K]	U [W/m2K]	U [W/m2K]	U [W/m2K]	R [ft2Fh/BTU]		Height [ft]	Width [ft]	Height [mm]	Width [mm]	Area [m2]
Non-Thermally Broken Aluminum	3G-5uv	0.562	1.4162	13.3962	8.60	0.66	1%	0.984	0.656	300	200	0.06	
					7.30	0.78	10%	1.017	1.312	310	400	0.12	
					5.76	0.99	20%	2.001	0.951	610	290	0.18	
					4.82	1.18	30%	2.953	1.066	900	325	0.29	
					4.10	1.38	40%	3.937	1.247	1200	380	0.46	
					3.42	1.66	50%	4.921	1.575	1500	480	0.72	
					2.87	1.98	60%	5.906	2.034	1800	620	1.12	
					2.31	2.46	70%	6.890	2.986	2100	910	1.91	
					1.75	3.24	80%	7.874	5.906	2400	1800	4.32	
					1.62	3.51	82%	8.858	6.726	2700	2050	5.54	
				1.60	3.55	82%	10	6	3048	1829	5.57		
High Performance Aluminum	3G-5uv	0.562	0.6722	3.4345	2.33	2.44	1%	0.984	0.656	300	200	0.06	
					2.04	2.79	10%	1.017	1.312	310	400	0.12	
					1.69	3.36	20%	2.001	0.951	610	290	0.18	
					1.48	3.83	30%	2.953	1.066	900	325	0.29	
					1.33	4.28	40%	3.937	1.247	1200	380	0.46	
					1.18	4.82	50%	4.921	1.575	1500	480	0.72	
					1.06	5.36	60%	5.906	2.034	1800	620	1.12	
					0.94	6.04	70%	6.890	2.986	2100	910	1.91	
					0.82	6.93	80%	7.874	5.906	2400	1800	4.32	
					0.79	7.18	82%	8.858	6.726	2700	2050	5.54	
				0.79	7.22	82%	10	6	3048	1829	5.57		
High Performance Timber Curtain Wall	3G-5uv	0.562	1.0209	1.7051	1.43	3.98	1%	0.984	0.656	300	200	0.06	
					1.32	4.31	10%	1.017	1.312	310	400	0.12	
					1.19	4.79	20%	2.001	0.951	610	290	0.18	
					1.09	5.20	30%	2.953	1.066	900	325	0.29	
					1.01	5.61	40%	3.937	1.247	1200	380	0.46	
					0.93	6.11	50%	4.921	1.575	1500	480	0.72	
					0.86	6.61	60%	5.906	2.034	1800	620	1.12	
					0.79	7.22	70%	6.890	2.986	2100	910	1.91	
					0.71	7.98	80%	7.874	5.906	2400	1800	4.32	
					0.70	8.17	82%	8.858	6.726	2700	2050	5.54	
				0.69	8.18	82%	10	6	3048	1829	5.57		

Quad-Glazed Curtain Wall (4G-5uv)

Frame Type	IGU		Edge		Frame	Window		CoG: Opening	Raw Opening				
	Type	U [W/m2K]	U [W/m2K]	U [W/m2K]	U [W/m2K]	U [W/m2K]	R [ft2Fh/BTU]		Height [ft]	Width [ft]	Height [mm]	Width [mm]	Area [m2]
Non-Thermally Broken Aluminum	4G-5uv	0.376	1.3059	13.3913	8.55	0.66	1%	0.984	0.656	300	200	0.06	
					7.23	0.79	10%	1.017	1.312	310	400	0.12	
					5.68	1.00	20%	2.001	0.951	610	290	0.18	
					4.72	1.20	30%	2.953	1.066	900	325	0.29	
					3.99	1.42	40%	3.937	1.247	1200	380	0.46	
					3.29	1.72	50%	4.921	1.575	1500	480	0.72	
					2.73	2.08	60%	5.906	2.034	1800	620	1.12	
					2.16	2.63	70%	6.890	2.986	2100	910	1.91	
					1.59	3.57	80%	7.874	5.906	2400	1800	4.32	
					1.45	3.90	82%	8.858	6.726	2700	2050	5.54	
				1.44	3.95	82%	10	6	3048	1829	5.57		
High Performance Aluminum	4G-5uv	0.376	0.5048	2.5727	1.75	3.25	1%	0.984	0.656	300	200	0.06	
					1.52	3.73	10%	1.017	1.312	310	400	0.12	
					1.26	4.51	20%	2.001	0.951	610	290	0.18	
					1.10	5.17	30%	2.953	1.066	900	325	0.29	
					0.98	5.82	40%	3.937	1.247	1200	380	0.46	
					0.86	6.60	50%	4.921	1.575	1500	480	0.72	
					0.77	7.41	60%	5.906	2.034	1800	620	1.12	
					0.67	8.44	70%	6.890	2.986	2100	910	1.91	
					0.58	9.82	80%	7.874	5.906	2400	1800	4.32	
					0.56	10.23	82%	8.858	6.726	2700	2050	5.54	
				0.55	10.29	82%	10	6	3048	1829	5.57		
High Performance Timber Curtain Wall	4G-5uv	0.376	0.7862	1.6336	1.29	4.40	1%	0.984	0.656	300	200	0.06	
					1.17	4.86	10%	1.017	1.312	310	400	0.12	
					1.02	5.55	20%	2.001	0.951	610	290	0.18	
					0.92	6.16	30%	2.953	1.066	900	325	0.29	
					0.84	6.78	40%	3.937	1.247	1200	380	0.46	
					0.75	7.55	50%	4.921	1.575	1500	480	0.72	
					0.68	8.35	60%	5.906	2.034	1800	620	1.12	
					0.61	9.37	70%	6.890	2.986	2100	910	1.91	
					0.53	10.71	80%	7.874	5.906	2400	1800	4.32	
					0.51	11.07	82%	8.858	6.726	2700	2050	5.54	
				0.51	11.10	82%	10	6	3048	1829	5.57		

Quint-Glazed Curtain Wall (5G-2s)

Frame Type	IGU		Edge		Frame	Window		CoG: Opening	Raw Opening				
	Type	U [W/m2K]	U [W/m2K]	U [W/m2K]	U [W/m2K]	U [W/m2K]	R [ft2Fh/BTU]		Height [ft]	Width [ft]	Height [mm]	Width [mm]	Area [m2]
Non-Thermally Broken Aluminum	5G-2s	0.271	1.1943	13.7004	8.69	0.65	1%	0.984	0.656	300	200	0.06	
					7.33	0.77	10%	1.017	1.312	310	400	0.12	
					5.73	0.99	20%	2.001	0.951	610	290	0.18	
					4.74	1.20	30%	2.953	1.066	900	325	0.29	
					3.98	1.43	40%	3.937	1.247	1200	380	0.46	
					3.27	1.74	50%	4.921	1.575	1500	480	0.72	
					2.69	2.11	60%	5.906	2.034	1800	620	1.12	
					2.11	2.69	70%	6.890	2.986	2100	910	1.91	
					1.52	3.73	80%	7.874	5.906	2400	1800	4.32	
					1.38	4.11	82%	8.858	6.726	2700	2050	5.54	
					1.36	4.17	82%	10	6	3048	1829	5.57	
High Performance Aluminum	5G-2s	0.272	0.4393	2.8123	1.86	3.05	1%	0.984	0.656	300	200	0.06	
					1.60	3.54	10%	1.017	1.312	310	400	0.12	
					1.30	4.37	20%	2.001	0.951	610	290	0.18	
					1.11	5.10	30%	2.953	1.066	900	325	0.29	
					0.97	5.84	40%	3.937	1.247	1200	380	0.46	
					0.84	6.78	50%	4.921	1.575	1500	480	0.72	
					0.73	7.80	60%	5.906	2.034	1800	620	1.12	
					0.62	9.19	70%	6.890	2.986	2100	910	1.91	
					0.51	11.18	80%	7.874	5.906	2400	1800	4.32	
					0.48	11.80	82%	8.858	6.726	2700	2050	5.54	
					0.48	11.89	82%	10	6	3048	1829	5.57	
High Performance Timber Curtain Wall	5G-2s	0.272	0.7047	1.62	1.25	4.54	1%	0.984	0.656	300	200	0.06	
					1.12	5.08	10%	1.017	1.312	310	400	0.12	
					0.96	5.90	20%	2.001	0.951	610	290	0.18	
					0.85	6.64	30%	2.953	1.066	900	325	0.29	
					0.76	7.43	40%	3.937	1.247	1200	380	0.46	
					0.67	8.44	50%	4.921	1.575	1500	480	0.72	
					0.60	9.52	60%	5.906	2.034	1800	620	1.12	
					0.52	10.98	70%	6.890	2.986	2100	910	1.91	
					0.44	13.01	80%	7.874	5.906	2400	1800	4.32	
					0.42	13.59	82%	8.858	6.726	2700	2050	5.54	
					0.42	13.63	82%	10	6	3048	1829	5.57	

Appendix D1

EnergyPlus Model Parameters

ENERGYPLUS MODEL PARAMETERS

OFFICE DIMENSIONS Typical Office Dimensions

	[m]	[ft]	South-North	East-West
Floor to Floor height	3.75	12.30		
Floor to Ceiling height	2.75	9.02	z	z
Depth	4.65	15.26	y	x
Width	2.75	9.02	x	y
Floor Area	12.79	137.64		
Volume	47.95	1693.45		
Conditioned Volume	35.17	1241.86		

BUILDING ENCLOSURE

Exterior Wall: R-14

Interior walls and floors: addiabatic

Material	Thickness		k [W/mK]	C [W/m2K]	RSI [m2K/W]	R-imp [hr-ft2-F/BTU]	U-value [W/m2K]	Density [kg/m3]	Specific Heat [J/kg.K]
	[mm]	[m]							
<i>Interior</i>									
Drywall	15.9	0.0159	0.16	10.06	0.099	0.56		800	1090
Concrete Block: Limestone Aggregate: 200mm - 16.3 kg - 2 cores	200	0.2	1.13	5.65	0.177	1.00		2210	920
Insulation: Cellular polyisocyanurate (CFC-11 exp.) (gasimpermeable facers)	38	0.038	0.02	0.53	1.900	10.79		32	920
Air Space	25				0.150	0.85			
Brick - fired clay - 1760 kg/m3 - 102mm	102	0.102	0.78	7.65	0.131	0.74		1760	790
<i>Exterior</i>									
	380.9				2.457	13.95	0.407		

Complies with ASHRAE 90.1 1999

Windows Tested

Type	IGU [W/m2K]	SHGC	VT	Edge [W/m2K]	Frame [W/m2K]	
2G-1 (air, typ AL frame)	2.68	0.70	0.79	1.86	13.46	high U and high SHGC
2G-2s (Ar, Wood frame)	1.31	0.37	0.64	1.59	1.88	low U and high SHGC
2G-4uv (Ar, Wood frame)	1.33	0.25	0.41	1.59	1.88	low U and low SHGC
2G-3v (air, typ AL frame)	2.68	0.30	0.42	1.86	13.46	high U and low SHGC
2G-4uv (Ar, HP AL frame)	1.33	0.25	0.41	1.31	4.79	
3G-2s (Kr, wood frame)	0.61	0.37	0.57	1.02	1.71	low U, high SHGC
3G-5uv (Kr, wood frame)	0.56	0.19	0.43	1.02	1.71	low U, low SHGC
3G-5uv (Kr, HP AL frame)	0.56	0.19	0.43	0.67	3.43	
4G-2s (Kr, wood frame)	0.41	0.35	0.50	0.79	1.63	low U, high SHGC
4G-5uv (Kr, wood frame)	0.38	0.18	0.40	0.79	1.63	low U, low SHGC
4G-5uv (Kr, HP AL frame)	0.38	0.18	0.40	0.50	2.57	
5G-2s (Xe, wood frame)	0.27	0.33	0.45	0.70	1.62	low U, high SHGC
5G-5uv (Xe, wood frame)	0.27	0.19	0.41	0.70	1.62	low U, low SHGC
5G-5uv (Xe, HP AL frame)	0.27	0.19	0.41	0.44	2.81	

OCCUPANCY SCHEDULE

People

Occupants 1

Start	End	People	Fraction Radiant	Activity Level [W/person]	Mechanical Efficiency	Office Clothing [clo]	Air Velocity [m/s]
0	8	0	0	0	0	0.96	0.1
8	18	1	0.6	125	0 - All enrgy spent is converted to heat	0.96	0.1
18	24	0	0	0	0	0.96	0.1

Electrical Equipment

W/person 225 from EnergyStar Ratings - typical work station is 200 W idle, 10-15 W sleeping, workstation + other devices
 W/m2 17.6
 W/ft2 1.6

Schedule

Start	End	On	Power [W]	Fraction Radiant	Fraction Latent	Fraction Lost
0	8	0.1	22.5	0.3	0	0
8	18	1	225	0.3	0	0
18	24	0.1	22.5	0.3	0	0

VENTILATION

ASHRAE 62.1 STANDARD - 2004

$V_{bz} = R_p P_z + R_a A_z$

Rp	2.5 [L/s.person]	Table 6-1
Pz	1 [person]	
Ra	0.3 [L/(s.m2)]	
Az	12.8 [m2]	
Vbz	6.34 [L/s]	

Model Input

6.5 [L/s]
0.0065 [m3/s]
23.4 [m3/hr]
0.67 [ACH]

Air Leakage

0.5 ACH

Infiltration often assessed by inspection, it is a goal during design and something measured after construction
 0.25 is a relatively air-tight building, whereas most typical office buildings are around 1-2 ACH

TEMPERATURE SETPOINT

Schedule

Start	End	Heating [C]	Cooling [C]
0	6	15	30
6	20	20	24
20	24	15	30

LIGHTING

	Model	ASHRAE 90.1 - Office
Max Power [W]	184 Power = 6*28 W (T5s) + 1*16 W (desk lamp)	
W/m ²	14.4	14
W/ft ²	1.3	1.3

Schedule

Start	End	On	W
0	8	0.3	56
8	18	1	184
18	24	0.3	56

Daylighting Control

Min daylight illuminance 500 lux
 work plane height 0.762 [m] 2.5 [ft]
 Dimming: Continuous

Work Plane Location

x	y	z
[m]	[m]	[m]
2.325	1.375	0.762

Daylight Discomfort Glare

Max. Glare Index 22 this is the max glare index for comfortable glare conditions
 View Direction 90 deg cw from window (facing side wall)

HVAC

Purchased Air for heating and cooling (ideal heating and cooling LOADS only)
 (isolates mechanical efficiency)

Heating Supply Air Temperature	24 C
Cooling Supply Air Temperature	20 C
Heating Supply Air Humidity Ratio	0.00682 kg-H2O/kg-air
Cooling Supply Air Humidity Ratio	0.0109 kg-H2O/kg-air

WINDOW LOCATION

WWR	Wall Area [m2]	Window Area [m2]	Height [m]	Width [m]	Head Height [m]	Sill Height [m]	H/W
0	10.3	0.00	0.00	0.00	2.75		
0.1	10.3	1.03	1.02	1.02	2.75	1.73	1.00
0.2	10.3	2.06	1.44	1.44	2.75	1.31	1.00
0.3	10.3	3.09	1.76	1.76	2.75	0.99	1.00
0.4	10.3	4.13	1.99	2.07	2.75	0.76	0.96
0.5	10.3	5.16	1.99	2.59	2.75	0.76	0.77
0.6	10.3	6.19	2.25	2.75	2.75	0.50	0.82
0.66	10.3	6.81	2.48	2.75	2.75	0.28	0.90

STATIC SHADING DIMENSION

Projection cannot be bigger than 3.3 ft due to size limitation

WWR	Overhang [m]	Left Pro [m]	Right Pro [m]	Fin [m]	Top Projection [m]	Bottom Projection [m]
0						
0.1	0.4	0.87	0.87	1.02	1.00	1.73
0.2	0.6	0.66	0.66	1.02	1.00	1.31
0.3	0.7	0.50	0.50	1.02	1.00	0.99
0.4	0.8	0.34	0.34	1.02	1.00	0.76
0.5	0.8	0.08	0.08	1.02	1.00	0.76
0.6	0.9	0.00	0.00	1.02	1.00	0.50
0.66	0.9	0.00	0.00	1.02	1.00	0.28

SIMULATED WINDOW U-VALUES

WWR	IGU W/m2K	SHGC	VT	Non-Thermally Broken W/m2K	High Performance Aluminum W/m2K	High Performance Timber W/m2K
2G-1	2.68	0.702	0.786			
0.1				5.01		
0.2				4.35		
0.3				4.06		
0.4				3.88		
0.5				3.76		
0.6				4.11		
0.66				3.82		
2G-2s	1.305	0.37	0.639			
0.1						1.50
0.2						1.45
0.3						1.42
0.4						1.41
0.5						1.40
0.6						1.41
0.66						1.41
2G-4uv	1.334	0.253	0.413			
0.1				4.25	2.13	1.51
0.2				3.44	1.91	1.47
0.3				3.07	1.81	1.44
0.4				2.85	1.74	1.43
0.5				2.70	1.71	1.42
0.6				2.86	1.75	1.43
0.66				2.80	1.73	1.43
2G-3v	2.53	0.297	0.416			
0.1				4.93		
0.2				4.25		
0.3				3.95		
0.4				3.76		
0.5				3.65		
0.6				3.76		
0.66				3.71		
3G-2s	0.607	0.366	0.566			
0.1						0.95
0.2						0.85
0.3						0.81
0.4						0.79
0.5						0.77
0.6						0.79
0.66						0.79
3G-5uv	0.562	0.19	0.43			
0.1					1.25	0.92
0.2					1.06	0.82
0.3					0.97	0.78
0.4					0.92	0.75
0.5					0.88	0.73
0.6					0.92	0.76
0.66					0.91	0.75

4G-2s	0.406	0.351	0.502			
0.1						0.77
0.2						0.67
0.3						0.62
0.4						0.60
0.5						0.58
0.6						0.60
0.66						0.60
4G-5uv	0.376	0.184	0.397			
0.1					0.91	0.75
0.2					0.76	0.65
0.3					0.69	0.60
0.4					0.65	0.57
0.5					0.63	0.55
0.6					0.66	0.58
0.66					0.65	0.57
5G-2s	0.271	0.33	0.447			
0.1						0.67
0.2						0.56
0.3						0.51
0.4						0.48
0.5						0.46
0.6						0.49
0.66						0.48
5G-4uv	0.272	0.187	0.406			
0.1					0.89	0.67
0.2					0.72	0.56
0.3					0.64	0.51
0.4					0.60	0.48
0.5					0.56	0.46
0.6					0.60	0.49
0.66					0.59	0.48

Appendix D2

Comparison of Energy Performance of High and Low Internal Heat Gain Offices

SIMULATION RESULTS - INTERNAL HEAT GAIN AND ENERGY PERFORMANCE

Floor Area 12.7875 [m2]
 Heating System Efficiency 0.9
 Cooling System Efficiency 3

High v Low Internal Gains, CASE 1: 2G-2s

LOW INTERNAL LOADS (with daylighting and night time equipment setbacks)

Low U and High SHGC

IGU	Ucg [W/m2K]	SHGC	VT	Frame	U-edge [W/m2K]	U-frame [W/m2K]	WWR 0.1 [W/m2K]	WWR 0.2 [W/m2K]	WWR 0.3 [W/m2K]	WWR 0.4 [W/m2K]	WWR 0.5 [W/m2K]	WWR 0.6 [W/m2K]	WWR 0.66 [W/m2K]
2G-2s HP Wd	1.305	0.37	0.639	HP Wood	1.5916	1.8827	1.50	1.45	1.42	1.41	1.40	1.41	1.41

WWR	Shading	Annual Purchased Heating [kWh]	Annual Purchased Cooling [kWh]	Annual Lighting Load [kWh]	Annual Plug Load [kWh]	Total Annual Load [kWh]	Total Annual Load / Area [kWh/m2]	Peak Heating [kW]	Peak Cooling [kW]	Peak Lighting [kW]	Annual Window Energy Balance ('+' gain, '-' loss) [kWh]	Annual Heating Energy 'Metered' [kWh/m2]	Annual Cooling Energy 'Metered' [kWh/m2]	Annual Lighting Energy 'Metered' [kWh/m2]	Annual Plug Energy 'Metered' [kWh/m2]	Total Annual Energy 'Metered' [kWh/m2]	Peak Heating Energy 'Metered' [W/m2]	Peak Cooling Energy 'Metered' [W/m2]	
South																			
0	N	537.4	419.2	957.4	723.6	2637.6	206.3	0.881	0.523	0.184		46.699	10.926	74.873	56.587	189.084	76.523	13.622	
0.1	N	644.4	315.3	537.3	723.6	2220.6	173.7	0.916	0.470	0.184	142.63	55.991	8.218	42.019	56.587	162.814	79.606	12.244	
0.2	N	623.5	361.2	432.1	723.6	2140.3	167.4	0.924	0.534	0.184	299.81	54.173	9.414	33.792	56.587	153.966	80.325	13.922	
0.3	N	580.8	442.0	394.4	723.6	2140.8	167.4	0.929	0.615	0.184	453.97	50.468	11.522	30.842	56.587	149.418	80.721	16.027	
0.4	N	540.6	537.1	375.6	723.6	2177.0	170.2	0.935	0.712	0.184	599.83	46.973	14.002	29.375	56.587	146.936	81.283	18.563	
0.5	N	511.9	639.7	359.9	723.6	2235.0	174.8	0.945	0.812	0.184	737.20	44.477	16.674	28.141	56.587	145.879	82.144	21.154	
0.6	N	545.3	680.4	359.1	723.6	2308.4	180.5	0.991	0.886	0.184	720.89	47.382	17.736	28.079	56.587	149.783	86.102	23.104	
0.66	N	530.5	743.9	355.8	723.6	2353.8	184.1	0.997	0.956	0.184	793.83	46.094	19.391	27.825	56.587	149.896	86.610	24.914	
East																			
0	N	560.9	428.3	957.4	723.6	2670.3	208.8	0.895	0.535	0.184		48.740	11.166	74.873	56.587	191.365	77.784	13.941	
0.1	N	664.9	375.2	644.1	723.6	2407.8	188.3	0.938	0.525	0.184	98.54	57.769	9.781	50.368	56.587	174.505	81.501	13.685	
0.2	N	726.3	427.9	496.5	723.6	2374.3	185.7	0.972	0.585	0.184	210.66	63.109	11.153	38.825	56.587	169.674	84.457	15.253	
0.3	N	754.6	518.7	428.7	723.6	2425.6	189.7	0.999	0.721	0.184	321.55	65.564	13.522	33.525	56.587	169.197	86.807	18.801	
0.4	N	772.1	625.9	395.9	723.6	2517.5	196.9	1.024	0.868	0.184	420.49	67.090	16.315	30.958	56.587	170.950	89.005	22.622	
0.5	N	790.7	740.7	373.2	723.6	2628.2	205.5	1.051	1.028	0.184	517.12	68.704	19.308	29.183	56.587	173.781	91.296	26.791	
0.6	N	866.1	796.4	372.6	723.6	2758.7	215.7	1.108	1.159	0.184	474.04	75.259	20.760	29.136	56.587	181.741	96.251	30.223	
0.66	N	875.1	866.2	367.8	723.6	2832.6	221.5	1.122	1.264	0.184	525.98	76.037	22.579	28.761	56.587	183.963	97.516	32.954	
West																			
0	N	565.6	418.0	957.4	723.6	2664.6	208.4	0.894	0.528	0.184		49.144	10.895	74.873	56.587	191.499	77.696	13.752	
0.1	N	675.3	339.9	622.8	723.6	2361.6	184.7	0.934	0.490	0.184	79.70	58.678	8.861	48.701	56.587	172.826	81.147	12.764	
0.2	N	739.8	382.7	476.4	723.6	2322.5	181.6	0.965	0.608	0.184	171.34	64.279	9.976	37.259	56.587	168.100	83.863	15.844	
0.3	N	770.3	461.1	411.6	723.6	2366.5	185.1	0.995	0.748	0.184	261.36	66.928	12.020	32.185	56.587	167.720	86.455	19.485	
0.4	N	787.3	553.3	384.2	723.6	2448.3	191.5	1.009	0.929	0.184	339.98	68.406	14.422	30.044	56.587	169.458	87.696	24.211	
0.5	N	805.8	654.1	366.3	723.6	2549.8	199.4	1.034	1.096	0.184	416.86	70.019	17.049	28.645	56.587	172.300	89.806	28.562	
0.6	N	884.0	699.4	365.9	723.6	2672.8	209.0	1.088	1.229	0.184	359.27	76.809	18.232	28.610	56.587	180.238	94.533	32.039	
0.66	N	893.5	758.5	361.7	723.6	2737.3	214.1	1.104	1.332	0.184	399.05	77.633	19.772	28.288	56.587	182.280	95.969	34.711	
North																			
0	N	581.0	394.9	957.4	723.6	2656.9	207.8	0.901	0.513	0.184		50.487	10.293	74.873	56.587	192.239	78.275	13.366	
0.1	N	679.5	331.1	760.9	723.6	2495.1	195.1	0.943	0.486	0.184	-37.15	59.041	8.630	59.507	56.587	183.765	81.904	12.675	
0.2	N	775.9	273.1	563.4	723.6	2336.0	182.7	0.978	0.448	0.184	-59.88	67.419	7.119	44.061	56.587	175.186	84.952	11.680	
0.3	N	859.6	279.9	459.3	723.6	2322.3	181.6	1.012	0.480	0.184	-81.13	74.687	7.295	35.919	56.587	174.487	87.928	12.523	
0.4	N	921.7	309.8	410.6	723.6	2365.7	185.0	1.043	0.522	0.184	-103.22	80.090	8.076	32.106	56.587	176.858	90.595	13.605	
0.5	N	971.9	345.3	380.9	723.6	2421.7	189.4	1.074	0.565	0.184	-126.84	84.445	9.001	29.786	56.587	179.819	93.282	14.732	
0.6	N	1075.2	344.5	380.0	723.6	2523.3	197.3	1.132	0.583	0.184	-261.08	93.423	8.980	29.718	56.587	188.707	98.389	15.205	
0.66	N	1100.4	365.2	374.5	723.6	2563.7	200.5	1.149	0.607	0.184	-280.16	95.613	9.521	29.285	56.587	191.005	99.837	15.825	

HIGH INTERNAL LOADS (no daylighting and night time equipment setbacks)

Low U and High SHGC

IGU	Ucg [W/m2K]	SHGC	VT	Frame	U-edge [W/m2K]	U-frame [W/m2K]	WWR 0.1 [W/m2K]	WWR 0.2 [W/m2K]	WWR 0.3 [W/m2K]	WWR 0.4 [W/m2K]	WWR 0.5 [W/m2K]	WWR 0.6 [W/m2K]	WWR 0.66 [W/m2K]
2G-2s HP Wd	1.305	0.37	0.639	HP Wood	1.5916	1.8827	1.50	1.45	1.42	1.41	1.40	1.41	1.41

WWR	Shading	Annual Purchased Heating [kWh]	Annual Purchased Cooling [kWh]	Annual Lighting Load [kWh]	Annual Plug Load [kWh]	Total Annual Load [kWh]	Total Annual Load / Area [kWh/m2]	Peak Heating [kW]	Peak Cooling [kW]	Peak Lighting [kW]	Annual Window Energy Balance ('+' gain, '-' loss) [kWh]	Annual Heating Energy 'Metered' [kWh/m2]	Annual Cooling Energy 'Metered' [kWh/m2]	Annual Lighting Energy 'Metered' [kWh/m2]	Annual Plug Energy 'Metered' [kWh/m2]	Total Annual Energy 'Metered' [kWh/m2]	Peak Heating Energy 'Metered' [W/m2]	Peak Cooling Energy 'Metered' [W/m2]	
South																			
0	N	40.0	1359.9	1611.8	1971.0	4982.8	389.7	0.460	0.835	0.184									
0.1	N	31.6	1478.4	1611.8	1971.0	5092.9	398.3	0.472	0.854	0.184	108.80	3.478	35.449	126.048	154.135	319.110	39.992	21.754	
0.2	N	26.3	1610.2	1611.8	1971.0	5219.3	408.2	0.490	0.907	0.184	233.96	2.749	38.538	126.048	154.135	324.438	42.578	23.645	
0.3	N	22.9	1747.3	1611.8	1971.0	5353.1	418.6	0.507	0.998	0.184	359.15	2.281	41.974	126.048	154.135	327.723	44.079	26.014	
0.4	N	21.2	1888.5	1611.8	1971.0	5492.5	429.5	0.524	1.095	0.184	482.48	1.993	45.547	126.048	154.135	331.252	45.561	28.541	
0.5	N	20.1	2032.5	1611.8	1971.0	5635.4	440.7	0.542	1.210	0.184	603.94	1.841	49.227	126.048	154.135	334.908	47.064	31.534	
0.6	N	26.7	2044.8	1611.8	1971.0	5654.3	442.2	0.591	1.293	0.184	566.09	1.745	52.980	126.048	154.135	335.808	51.311	33.708	
0.66	N	26.6	2123.2	1611.8	1971.0	5732.6	448.3	0.599	1.364	0.184	628.91	2.324	53.301	126.048	154.135	337.843	52.058	35.547	
East																			
0	N	46.6	1360.0	1611.8	1971.0	4989.4	390.2	0.469	0.839	0.184		4.049	35.450	126.048	154.135	319.683	40.741	21.879	
0.1	N	55.9	1479.6	1611.8	1971.0	5118.3	400.3	0.501	0.904	0.184	67.26	4.853	38.570	126.048	154.135	323.606	43.521	23.553	
0.2	N	65.9	1608.2	1611.8	1971.0	5257.0	411.1	0.537	0.983	0.184	151.22	4.853	41.922	126.048	154.135	327.831	46.656	25.626	
0.3	N	76.7	1739.1	1611.8	1971.0	5398.6	422.2	0.575	1.130	0.184	237.51	6.664	45.334	126.048	154.135	332.181	49.958	29.467	
0.4	N	87.9	1869.8	1611.8	1971.0	5540.5	433.3	0.614	1.281	0.184	323.00	7.635	48.741	126.048	154.135	336.559	53.326	33.395	
0.5	N	99.5	2001.3	1611.8	1971.0	5683.7	444.5	0.653	1.434	0.184	408.68	8.649	52.168	126.048	154.135	341.000	56.751	37.368	
0.6	N	136.2	2026.7	1611.8	1971.0	5745.7	449.3	0.711	1.547	0.184	350.87	11.831	52.831	126.048	154.135	344.845	61.780	40.335	
0.66	N	145.2	2100.4	1611.8	1971.0	5828.4	455.8	0.730	1.635	0.184	395.18	12.612	54.752	126.048	154.135	347.547	63.408	42.617	
West																			
0	N	48.0	1346.0	1611.8	1971.0	4976.8	389.2	0.479	0.837	0.184		4.172	35.085	126.048	154.135	319.440	41.636	21.817	
0.1	N	57.5	1448.2	1611.8	1971.0	5088.6	397.9	0.518	0.864	0.184	47.64	5.000	37.750	126.048	154.135	322.932	44.999	22.509	
0.2	N	68.0	1557.3	1611.8	1971.0	5208.1	407.3	0.567	0.978	0.184	109.88	5.908	40.594	126.048	154.135	326.685	49.276	25.495	
0.3	N	79.2	1667.6	1611.8	1971.0	5329.6	416.8	0.617	1.120	0.184	174.04	6.878	43.469	126.048	154.135	330.530	53.620	29.199	
0.4	N	90.8	1777.5	1611.8	1971.0	5451.1	426.3	0.667	1.264	0.184	237.65	7.891	46.334	126.048	154.135	334.407	57.979	32.945	
0.5	N	103.4	1888.8	1611.8	1971.0	5575.1	436.0	0.716	1.414	0.184	301.51	8.987	49.235	126.048	154.135	338.405	62.212	36.863	
0.6	N	139.6	1901.9	1611.8	1971.0	5624.4	439.8	0.770	1.528	0.184	230.09	12.130	49.578	126.048	154.135	341.891	66.894	39.829	
0.66	N	148.8	1963.3	1611.8	1971.0	5694.9	445.3	0.794	1.615	0.184	261.80	12.929	51.177	126.048	154.135	344.289	69.002	42.088	
North																			
0	N	50.9	1310.3	1611.8	1971.0	4944.0	386.6	0.480	0.825	0.184		4.423	34.155	126.048	154.135	318.761	41.675	21.511	
0.1	N	69.5	1328.6	1611.8	1971.0	4981.0	389.5	0.532	0.840	0.184	-68.37	6.039	34.633	126.048	154.135	320.855	46.256	21.893	
0.2	N	89.3	1352.3	1611.8	1971.0	5024.4	392.9	0.586	0.861	0.184	-121.51	7.760	35.250	126.048	154.135	323.193	50.886	22.441	
0.3	N	110.1	1377.7	1611.8	1971.0	5070.6	396.5	0.635	0.882	0.184	-170.33	9.566	35.912	126.048	154.135	325.661	55.143	23.000	
0.4	N	131.7	1405.0	1611.8	1971.0	5119.5	400.4	0.691	0.903	0.184	-215.98	11.445	36.624	126.048	154.135	328.252	60.049	23.531	
0.5	N	152.7	1434.4	1611.8	1971.0	5169.9	404.3	0.697	0.929	0.184	-259.99	13.268	37.390	126.048	154.135	330.841	60.597	24.226	
0.6	N	207.5	1391.4	1611.8	1971.0	5181.8	405.2	0.772	0.945	0.184	-410.07	18.034	36.269	126.048	154.135	334.486	67.117	24.630	
0.66	N	224.3	1406.9	1611.8	1971.0	5214.0	407.7	0.797	0.966	0.184	-438.48	19.489	36.673	126.048	154.135	336.345	69.224	25.189	

High v Low Internal Gains, CASE 1: 5G-2s

LOW INTERNAL LOADS (daylighting and night time equipment setbacks)

IGU	Ucg [W/m2K]	SHGC	VT	Frame	U-edge [W/m2K]	U-frame [W/m2K]	WWR 0.1 [W/m2K]	WWR 0.2 [W/m2K]	WWR 0.3 [W/m2K]	WWR 0.4 [W/m2K]	WWR 0.5 [W/m2K]	WWR 0.6 [W/m2K]	WWR 0.66 [W/m2K]
5G-2s HP Wd	0.271	0.33	0.447	HP Wood	0.7047	1.62	0.67	0.56	0.51	0.48	0.46	0.49	0.48

WWR	Shading	Annual Purchased Heating [kWh]	Annual Purchased Cooling [kWh]	Annual Lighting Load [kWh]	Annual Plug Load [kWh]	Total Annual Load [kWh]	Total Annual Load / Area [kWh/m2]	Peak Heating [kW]	Peak Cooling [kW]	Peak Lighting [kW]	Annual Window Energy Balance ('+' gain, '-' loss) [kWh]	Annual Heating Energy 'Metered' [kWh/m2]	Annual Cooling Energy 'Metered' [kWh/m2]	Annual Lighting Energy 'Metered' [kWh/m2]	Annual Plug Energy 'Metered' [kWh/m2]	Total Annual Energy 'Metered' [kWh/m2]	Peak Heating Energy 'Metered' [W/m2]	Peak Cooling Energy 'Metered' [W/m2]
South																		
0	N	537.4	419.2	957.4	723.6	2637.6	206.3	0.881	0.523	0.184								
0.1	N	547.9	361.4	627.1	723.6	2260.1	176.7	0.870	0.491	0.184	223.36	46.699	10.926	74.873	56.587	189.084	76.523	13.622
0.2	N	475.3	395.9	495.6	723.6	2090.5	163.5	0.840	0.511	0.184	456.90	47.610	9.422	49.043	56.587	162.661	75.554	12.811
0.3	N	386.1	481.8	444.7	723.6	2036.2	159.2	0.816	0.586	0.184	690.04	41.301	10.321	38.758	56.587	146.967	72.986	13.330
0.4	N	303.6	591.5	420.3	723.6	2039.0	159.5	0.800	0.673	0.184	917.48	33.550	12.558	34.776	56.587	137.471	70.927	15.281
0.5	N	234.9	717.7	399.7	723.6	2075.9	162.3	0.780	0.762	0.184	1139.01	26.377	15.420	32.871	56.587	131.254	69.498	17.546
0.6	N	211.0	780.5	399.0	723.6	2114.1	165.3	0.787	0.840	0.184	1203.45	20.410	18.710	31.257	56.587	126.963	67.781	19.871
0.66	N	177.7	866.4	393.9	723.6	2161.7	169.0	0.776	0.919	0.184	1325.89	18.335	20.345	31.204	56.587	126.471	68.341	21.899
												15.443	22.585	30.806	56.587	125.420	67.433	23.950
East																		
0	N	560.9	428.3	957.4	723.6	2670.3	208.8	0.895	0.535	0.184								
0.1	N	563.3	420.4	725.3	723.6	2432.6	190.2	0.894	0.542	0.184	191.21	48.740	11.166	74.873	56.587	191.365	77.784	13.941
0.2	N	550.2	486.3	590.8	723.6	2350.9	183.8	0.892	0.569	0.184	390.32	48.950	10.958	56.716	56.587	173.210	77.683	14.129
0.3	N	520.8	588.1	513.0	723.6	2345.5	183.4	0.884	0.686	0.184	589.09	47.804	12.677	46.200	56.587	163.268	77.499	14.839
0.4	N	483.4	709.7	470.8	723.6	2387.4	186.7	0.874	0.829	0.184	776.65	45.252	15.329	40.118	56.587	157.286	76.820	17.889
0.5	N	448.0	840.0	434.1	723.6	2445.6	191.3	0.866	0.976	0.184	963.05	42.000	18.499	36.817	56.587	153.903	75.955	21.604
0.6	N	449.2	914.2	433.5	723.6	2520.4	197.1	0.880	1.083	0.184	1007.51	38.928	21.895	33.945	56.587	151.355	75.226	25.440
0.66	N	426.2	998.1	424.1	723.6	2572.0	201.1	0.872	1.178	0.184	1111.71	39.030	23.829	33.899	56.587	153.346	76.482	28.222
												37.035	26.019	33.162	56.587	152.802	75.779	30.718
West																		
0	N	565.6	418.0	957.4	723.6	2664.6	208.4	0.894	0.528	0.184								
0.1	N	568.6	383.8	706.7	723.6	2382.7	186.3	0.890	0.503	0.184	175.44	49.144	10.895	74.873	56.587	191.499	77.696	13.752
0.2	N	558.8	437.6	569.0	723.6	2289.0	179.0	0.884	0.591	0.184	356.44	49.407	10.005	55.262	56.587	171.260	77.295	13.103
0.3	N	528.6	523.5	492.5	723.6	2268.2	177.4	0.875	0.719	0.184	536.58	48.556	11.406	44.498	56.587	161.047	76.804	15.398
0.4	N	490.8	627.5	452.4	723.6	2294.3	179.4	0.869	0.849	0.184	706.27	45.934	13.645	38.511	56.587	154.676	76.004	18.745
0.5	N	456.6	745.3	419.4	723.6	2344.9	183.4	0.864	0.996	0.184	875.41	42.650	16.357	35.378	56.587	150.971	75.473	22.141
0.6	N	458.4	809.0	419.4	723.6	2410.3	188.5	0.879	1.108	0.184	906.86	39.674	19.428	32.802	56.587	148.490	75.061	25.955
0.66	N	436.0	883.9	410.6	723.6	2454.1	191.9	0.876	1.198	0.184	1000.31	39.830	21.087	32.794	56.587	150.298	76.367	28.893
												37.881	23.042	32.106	56.587	149.615	76.116	31.229
North																		
0	N	581.0	394.9	957.4	723.6	2656.9	207.8	0.901	0.513	0.184								
0.1	N	581.6	380.8	827.6	723.6	2513.6	196.6	0.901	0.506	0.184	71.41	50.487	10.293	74.873	56.587	192.239	78.275	13.366
0.2	N	579.9	364.9	698.0	723.6	2366.4	185.1	0.898	0.498	0.184	146.30	50.534	9.928	64.720	56.587	181.768	78.250	13.181
0.3	N	574.8	360.4	585.9	723.6	2244.7	175.5	0.895	0.480	0.184	220.33	50.386	9.513	54.584	56.587	171.069	78.062	12.981
0.4	N	563.7	389.7	519.6	723.6	2196.6	171.8	0.891	0.512	0.184	293.64	49.946	9.395	45.818	56.587	161.745	77.774	12.507
0.5	N	554.1	429.5	463.6	723.6	2170.8	169.8	0.889	0.547	0.184	365.91	48.981	10.159	40.630	56.587	156.357	77.387	13.334
0.6	N	568.0	439.8	462.4	723.6	2193.7	171.6	0.906	0.562	0.184	325.02	48.147	11.195	36.257	56.587	152.186	77.262	14.248
0.66	N	556.9	469.3	447.6	723.6	2197.4	171.8	0.902	0.583	0.184	360.38	49.351	11.465	36.158	56.587	153.560	78.698	14.642
												48.390	12.235	35.002	56.587	152.213	78.388	15.192

HIGH INTERNAL LOADS (no daylighting and night time equipment setbacks)

IGU	Ucg [W/m2K]	SHGC	VT	Frame	U-edge [W/m2K]	U-frame [W/m2K]	WWR 0.1 [W/m2K]	WWR 0.2 [W/m2K]	WWR 0.3 [W/m2K]	WWR 0.4 [W/m2K]	WWR 0.5 [W/m2K]	WWR 0.6 [W/m2K]	WWR 0.66 [W/m2K]
5G-2s HP Wd	0.271	0.33	0.447	HP Wood	0.7047	1.62	0.67	0.56	0.51	0.48	0.46	0.49	0.48

WWR	Shading	Annual Purchased Heating [kWh]	Annual Purchased Cooling [kWh]	Annual Lighting Load [kWh]	Annual Plug Load [kWh]	Total Annual Load [kWh]	Total Annual Load / Area [kWh/m2]	Peak Heating [kW]	Peak Cooling [kW]	Peak Lighting [kW]	Annual Window Energy Balance ('+' gain, '-' loss) [kWh]	Annual Heating Energy 'Metered' [kWh/m2]	Annual Cooling Energy 'Metered' [kWh/m2]	Annual Lighting Energy 'Metered' [kWh/m2]	Annual Plug Energy 'Metered' [kWh/m2]	Total Annual Energy 'Metered' [kWh/m2]	Peak Heating Energy 'Metered' [W/m2]	Peak Cooling Energy 'Metered' [W/m2]	
South																			
0	N	40.0	1359.9	1611.8	1971.0	4982.8	389.7	0.460	0.835	0.184		3.478	35.449	126.048	154.135	319.110	39.992	21.754	
0.1	N	18.6	1540.7	1611.8	1971.0	5142.1	402.1	0.407	0.856	0.184	225.75	1.614	40.162	126.048	154.135	321.959	35.372	22.323	
0.2	N	9.5	1751.3	1611.8	1971.0	5343.6	417.9	0.363	0.885	0.184	461.64	0.825	45.650	126.048	154.135	326.658	31.560	23.061	
0.3	N	4.4	1982.0	1611.8	1971.0	5569.3	435.5	0.316	0.974	0.184	698.03	0.385	51.665	126.048	154.135	332.232	27.418	25.380	
0.4	N	1.6	2224.0	1611.8	1971.0	5808.4	454.2	0.244	1.062	0.184	933.54	0.138	57.974	126.048	154.135	338.294	21.232	27.684	
0.5	N	0.4	2473.1	1611.8	1971.0	6056.3	473.6	0.153	1.158	0.184	1168.66	0.032	64.466	126.048	154.135	344.681	13.318	30.175	
0.6	N	0.2	2574.1	1611.8	1971.0	6157.2	481.5	0.116	1.244	0.184	1233.62	0.020	67.099	126.048	154.135	347.302	10.087	32.423	
0.66	N	0.1	2716.0	1611.8	1971.0	6299.0	492.6	0.071	1.322	0.184	1360.87	0.011	70.799	126.048	154.135	350.993	6.209	34.463	
East																			
0	N	46.6	1360.0	1611.8	1971.0	4989.4	390.2	0.469	0.839	0.184		4.049	35.450	126.048	154.135	319.683	40.741	21.879	
0.1	N	18.6	1611.8	1611.8	1971.0	5213.3	407.7	0.407	0.856	0.184	193.54	1.614	42.016	126.048	154.135	323.813	35.372	22.323	
0.2	N	24.6	1740.4	1611.8	1971.0	5347.8	418.2	0.423	0.968	0.184	395.43	2.136	45.368	126.048	154.135	327.686	36.782	25.222	
0.3	N	18.5	1943.2	1611.8	1971.0	5544.6	433.6	0.405	1.103	0.184	597.56	1.612	50.655	126.048	154.135	332.449	35.216	28.740	
0.4	N	14.0	2150.7	1611.8	1971.0	5747.5	449.5	0.387	1.244	0.184	798.58	1.219	56.062	126.048	154.135	337.464	33.627	32.416	
0.5	N	9.9	2363.1	1611.8	1971.0	5955.9	465.8	0.359	1.385	0.184	999.38	0.863	61.600	126.048	154.135	342.647	31.165	36.111	
0.6	N	10.2	2448.8	1611.8	1971.0	6041.8	472.5	0.370	1.492	0.184	1044.13	0.884	63.833	126.048	154.135	344.901	32.128	38.897	
0.66	N	8.2	2570.3	1611.8	1971.0	6161.3	481.8	0.349	1.575	0.184	1152.08	0.709	67.000	126.048	154.135	347.892	30.296	41.068	
West																			
0	N	48.0	1346.0	1611.8	1971.0	4976.8	389.2	0.479	0.837	0.184		4.172	35.085	126.048	154.135	319.440	41.636	21.817	
0.1	N	34.8	1514.1	1611.8	1971.0	5131.8	401.3	0.457	0.866	0.184	177.81	3.026	39.469	126.048	154.135	322.678	39.687	22.583	
0.2	N	26.5	1692.6	1611.8	1971.0	5301.9	414.6	0.446	0.956	0.184	361.38	2.299	44.122	126.048	154.135	326.604	38.729	24.923	
0.3	N	20.8	1877.5	1611.8	1971.0	5481.2	428.6	0.434	1.088	0.184	544.65	1.810	48.941	126.048	154.135	330.934	37.739	28.374	
0.4	N	16.9	2067.6	1611.8	1971.0	5667.3	443.2	0.423	1.224	0.184	726.94	1.465	53.896	126.048	154.135	335.544	36.734	31.916	
0.5	N	13.2	2263.2	1611.8	1971.0	5859.3	458.2	0.399	1.365	0.184	908.99	1.150	58.996	126.048	154.135	340.329	34.689	35.579	
0.6	N	13.6	2337.0	1611.8	1971.0	5933.4	464.0	0.414	1.471	0.184	941.83	1.182	60.919	126.048	154.135	342.284	35.949	38.341	
0.66	N	11.5	2448.3	1611.8	1971.0	6042.7	472.5	0.394	1.553	0.184	1038.84	1.003	63.820	126.048	154.135	345.006	34.204	40.488	
North																			
0	N	50.9	1310.3	1611.8	1971.0	4944.0	386.6	0.480	0.825	0.184		4.423	34.155	126.048	154.135	318.761	41.675	21.511	
0.1	N	41.6	1398.8	1611.8	1971.0	5023.3	392.8	0.459	0.843	0.184	73.08	3.615	36.463	126.048	154.135	320.261	39.867	21.983	
0.2	N	34.5	1490.4	1611.8	1971.0	5107.7	399.4	0.450	0.861	0.184	149.77	2.995	38.851	126.048	154.135	322.029	39.072	22.453	
0.3	N	28.7	1584.4	1611.8	1971.0	5195.9	406.3	0.440	0.882	0.184	226.14	2.491	41.300	126.048	154.135	323.974	38.253	23.002	
0.4	N	23.9	1680.3	1611.8	1971.0	5287.0	413.5	0.431	0.902	0.184	301.97	2.073	43.802	126.048	154.135	326.058	37.424	23.514	
0.5	N	19.4	1778.6	1611.8	1971.0	5380.8	420.8	0.409	0.920	0.184	377.26	1.685	46.363	126.048	154.135	328.231	35.518	23.994	
0.6	N	20.8	1782.2	1611.8	1971.0	5385.9	421.2	0.424	0.933	0.184	332.50	1.809	46.458	126.048	154.135	328.450	36.878	24.314	
0.66	N	18.3	1835.8	1611.8	1971.0	5436.9	425.2	0.405	0.953	0.184	368.41	1.589	47.853	126.048	154.135	329.625	35.172	24.853	

High v Low Internal Gains, CASE 2: 5G-2s and 5G-4uv (SHGC)

LOW INTERNAL LOADS (daylighting and night time equipment setbacks)

IGU	Ucg [W/m2K]	SHGC	VT	Frame	U-edge [W/m2K]	U-frame [W/m2K]	WWR 0.1 [W/m2K]	WWR 0.2 [W/m2K]	WWR 0.3 [W/m2K]	WWR 0.4 [W/m2K]	WWR 0.5 [W/m2K]	WWR 0.6 [W/m2K]	WWR 0.66 [W/m2K]
5G-2s HP Wd	0.271	0.33	0.447	HP Wood	0.7047	1.62	0.67	0.56	0.51	0.48	0.46	0.49	0.48

WWR	Shading	Annual Purchased Heating [kWh]	Annual Purchased Cooling [kWh]	Annual Lighting Load [kWh]	Annual Plug Load [kWh]	Total Annual Load [kWh]	Total Annual Load / Area [kWh/m2]	Peak Heating [kW]	Peak Cooling [kW]	Peak Lighting [kW]	Annual Window Energy Balance ('+' gain, '-' loss) [kWh]	Annual Heating Energy 'Metered' [kWh/m2]	Annual Cooling Energy 'Metered' [kWh/m2]	Annual Lighting Energy 'Metered' [kWh/m2]	Annual Plug Energy 'Metered' [kWh/m2]	Total Annual Energy 'Metered' [kWh/m2]	Peak Heating Energy 'Metered' [W/m2]	Peak Cooling Energy 'Metered' [W/m2]
South																		
0	N	537.4	419.2	957.4	723.6	2637.6	206.3	0.881	0.523	0.184								
0.1	N	547.9	361.4	627.1	723.6	2260.1	176.7	0.870	0.491	0.184	223.36	46.699	10.926	74.873	56.587	189.084	76.523	13.622
0.2	N	475.3	395.9	495.6	723.6	2090.5	163.5	0.840	0.511	0.184	456.90	41.301	10.321	38.758	56.587	146.967	72.986	13.330
0.3	N	386.1	481.8	444.7	723.6	2036.2	159.2	0.816	0.586	0.184	690.04	33.550	12.558	34.776	56.587	137.471	70.927	15.281
0.4	N	303.6	591.5	420.3	723.6	2039.0	159.5	0.800	0.673	0.184	917.48	26.377	15.420	32.871	56.587	131.254	69.498	17.546
0.5	N	234.9	717.7	399.7	723.6	2075.9	162.3	0.780	0.762	0.184	1139.01	20.410	18.710	31.257	56.587	126.963	67.781	19.871
0.6	N	211.0	780.5	399.0	723.6	2114.1	165.3	0.787	0.840	0.184	1203.45	18.335	20.345	31.204	56.587	126.471	68.341	21.899
0.66	N	177.7	866.4	393.9	723.6	2161.7	169.0	0.776	0.919	0.184	1325.89	15.443	22.585	30.806	56.587	125.420	67.433	23.950
East																		
0	N	560.9	428.3	957.4	723.6	2670.3	208.8	0.895	0.535	0.184								
0.1	N	563.3	420.4	725.3	723.6	2432.6	190.2	0.894	0.542	0.184	191.21	48.950	10.958	56.716	56.587	173.210	77.683	14.129
0.2	N	550.2	486.3	590.8	723.6	2350.9	183.8	0.892	0.569	0.184	390.32	47.804	12.677	46.200	56.587	163.268	77.499	14.839
0.3	N	520.8	588.1	513.0	723.6	2345.5	183.4	0.884	0.686	0.184	589.09	45.252	15.329	40.118	56.587	157.286	76.820	17.889
0.4	N	483.4	709.7	470.8	723.6	2387.4	186.7	0.874	0.829	0.184	776.65	42.000	18.499	36.817	56.587	153.903	75.955	21.604
0.5	N	448.0	840.0	434.1	723.6	2445.6	191.3	0.866	0.976	0.184	963.05	38.928	21.895	33.945	56.587	151.355	75.226	25.440
0.6	N	449.2	914.2	433.5	723.6	2520.4	197.1	0.880	1.083	0.184	1007.51	39.030	23.829	33.899	56.587	153.346	76.482	28.222
0.66	N	426.2	998.1	424.1	723.6	2572.0	201.1	0.872	1.178	0.184	1111.71	37.035	26.019	33.162	56.587	152.802	75.779	30.718
West																		
0	N	565.6	418.0	957.4	723.6	2664.6	208.4	0.894	0.528	0.184								
0.1	N	568.6	383.8	706.7	723.6	2382.7	186.3	0.890	0.503	0.184	175.44	49.407	10.005	55.262	56.587	171.260	77.295	13.103
0.2	N	558.8	437.6	569.0	723.6	2289.0	179.0	0.884	0.591	0.184	356.44	48.556	11.406	44.498	56.587	161.047	76.804	15.398
0.3	N	528.6	523.5	492.5	723.6	2268.2	177.4	0.875	0.719	0.184	536.58	45.934	13.645	38.511	56.587	154.676	76.004	18.745
0.4	N	490.8	627.5	452.4	723.6	2294.3	179.4	0.869	0.849	0.184	706.27	42.650	16.357	35.378	56.587	150.971	75.473	22.141
0.5	N	456.6	745.3	419.4	723.6	2344.9	183.4	0.864	0.996	0.184	875.41	39.674	19.428	32.802	56.587	148.490	75.061	25.955
0.6	N	458.4	809.0	419.4	723.6	2410.3	188.5	0.879	1.108	0.184	906.86	39.830	21.087	32.794	56.587	150.298	76.367	28.893
0.66	N	436.0	883.9	410.6	723.6	2454.1	191.9	0.876	1.198	0.184	1000.31	37.881	23.042	32.106	56.587	149.615	76.116	31.229
North																		
0	N	581.0	394.9	957.4	723.6	2656.9	207.8	0.901	0.513	0.184								
0.1	N	581.6	380.8	827.6	723.6	2513.6	196.6	0.901	0.506	0.184	71.41	50.534	9.928	64.720	56.587	181.768	78.250	13.181
0.2	N	579.9	364.9	698.0	723.6	2366.4	185.1	0.898	0.498	0.184	146.30	50.386	9.513	54.584	56.587	171.069	78.062	12.981
0.3	N	574.8	360.4	585.9	723.6	2244.7	175.5	0.895	0.480	0.184	220.33	49.946	9.395	45.818	56.587	161.745	77.774	12.507
0.4	N	563.7	389.7	519.6	723.6	2196.6	171.8	0.891	0.512	0.184	293.64	48.981	10.159	40.630	56.587	156.357	77.387	13.334
0.5	N	554.1	429.5	463.6	723.6	2170.8	169.8	0.889	0.547	0.184	365.91	48.147	11.195	36.257	56.587	152.186	77.262	14.248
0.6	N	568.0	439.8	462.4	723.6	2193.7	171.6	0.906	0.562	0.184	325.02	49.351	11.465	36.158	56.587	153.560	78.698	14.642
0.66	N	556.9	469.3	447.6	723.6	2197.4	171.8	0.902	0.583	0.184	360.38	48.390	12.235	35.002	56.587	152.213	78.388	15.192

LOW INTERNAL LOADS (daylighting and night time equipment setbacks)

IGU	Ucg	SHGC	VT	Frame	U-edge	U-frame	WWR 0.1	WWR 0.2	WWR 0.3	WWR 0.4	WWR 0.5	WWR 0.6	WWR 0.66
	[W/m2K]				[W/m2K]	[W/m2K]	[W/m2K]	[W/m2K]	[W/m2K]	[W/m2K]	[W/m2K]	[W/m2K]	[W/m2K]
G-4uv HP Woo	0.272	0.187	0.406	HP Wood	0.7047	1.62	0.67	0.56	0.51	0.48	0.46	0.49	0.48

WWR	Shading	Annual Purchased Heating [kWh]	Annual Purchased Cooling [kWh]	Annual Lighting Load [kWh]	Annual Plug Load [kWh]	Total Annual Load [kWh]	Total Annual Load / Area [kWh/m2]	Peak Heating [kW]	Peak Cooling [kW]	Peak Lighting [kW]	Annual Window Energy Balance ('+' gain, '-' loss) [kWh]	Annual Heating Energy 'Metered' [kWh/m2]	Annual Cooling Energy 'Metered' [kWh/m2]	Annual Lighting Energy 'Metered' [kWh/m2]	Annual Plug Energy 'Metered' [kWh/m2]	Total Annual Energy 'Metered' [kWh/m2]	Peak Heating Energy 'Metered' [W/m2]	Peak Cooling Energy 'Metered' [W/m2]	
South																			
0	N	537.4	419.2	957.4	723.6	2637.6	206.3	0.881	0.523	0.184		46.699	10.926	74.873	56.587	189.084	76.523	13.622	
0.1	N	593.1	325.9	649.8	723.6	2292.3	179.3	0.887	0.473	0.184	102.27	51.531	8.495	50.815	56.587	167.427	77.045	12.341	
0.2	N	572.3	305.1	512.1	723.6	2113.2	165.3	0.875	0.458	0.184	211.12	49.725	7.954	40.050	56.587	154.315	76.001	11.940	
0.3	N	523.7	327.4	458.7	723.6	2033.5	159.0	0.858	0.469	0.184	320.05	45.505	8.536	35.873	56.587	146.500	74.588	12.216	
0.4	N	469.0	365.1	432.5	723.6	1990.1	155.6	0.843	0.513	0.184	427.50	40.748	9.516	33.821	56.587	140.672	73.267	13.376	
0.5	N	417.2	408.5	410.5	723.6	1959.8	153.3	0.831	0.559	0.184	532.94	36.252	10.649	32.102	56.587	135.589	72.183	14.580	
0.6	N	411.8	412.9	409.7	723.6	1958.0	153.1	0.842	0.582	0.184	516.04	35.780	10.763	32.039	56.587	135.168	73.130	15.170	
0.66	N	382.3	441.6	404.5	723.6	1952.0	152.7	0.834	0.609	0.184	571.03	33.221	11.512	31.631	56.587	132.950	72.432	15.868	
East																			
0	N	560.9	428.3	957.4	723.6	2670.3	208.8	0.895	0.535	0.184		48.740	11.166	74.873	56.587	191.365	77.784	13.941	
0.1	N	585.0	372.4	742.3	723.6	2423.3	189.5	0.899	0.513	0.184	89.36	50.832	9.708	58.045	56.587	175.172	78.077	13.360	
0.2	N	595.3	378.4	613.0	723.6	2310.4	180.7	0.901	0.510	0.184	184.18	51.730	9.863	47.941	56.587	166.120	78.278	13.296	
0.3	N	588.8	411.1	535.2	723.6	2258.7	176.6	0.900	0.518	0.184	278.77	51.162	10.717	41.851	56.587	160.317	78.226	13.510	
0.4	N	569.8	460.8	491.4	723.6	2245.6	175.6	0.897	0.585	0.184	370.48	49.509	12.011	38.429	56.587	156.535	77.917	15.260	
0.5	N	550.7	516.6	453.0	723.6	2243.9	175.5	0.893	0.676	0.184	461.48	47.851	13.465	35.428	56.587	153.330	77.631	17.620	
0.6	N	566.9	536.8	452.2	723.6	2279.5	178.3	0.912	0.748	0.184	436.45	49.255	13.993	35.363	56.587	155.197	79.225	19.500	
0.66	N	553.1	574.9	441.9	723.6	2293.5	179.4	0.909	0.808	0.184	483.88	48.057	14.985	34.560	56.587	154.189	79.006	21.061	
West																			
0	N	565.6	418.0	957.4	723.6	2664.6	208.4	0.894	0.528	0.184		49.144	10.895	74.873	56.587	191.499	77.696	13.752	
0.1	N	590.3	341.6	723.8	723.6	2379.2	186.1	0.896	0.481	0.184	79.65	51.288	8.905	56.601	56.587	173.380	77.878	12.542	
0.2	N	604.8	342.5	590.4	723.6	2261.2	176.8	0.898	0.490	0.184	163.88	52.547	8.927	46.169	56.587	164.230	78.007	12.769	
0.3	N	598.2	370.6	514.6	723.6	2207.0	172.6	0.895	0.555	0.184	247.78	51.976	9.660	40.244	56.587	158.466	77.790	14.476	
0.4	N	579.4	413.7	471.7	723.6	2188.4	171.1	0.889	0.643	0.184	328.92	50.347	10.784	36.885	56.587	154.602	77.258	16.768	
0.5	N	559.3	464.0	437.2	723.6	2184.1	170.8	0.883	0.735	0.184	409.68	48.597	12.095	34.188	56.587	151.467	76.753	19.166	
0.6	N	574.8	479.1	437.0	723.6	2214.4	173.2	0.900	0.806	0.184	377.26	49.941	12.488	34.171	56.587	153.186	78.207	21.022	
0.66	N	560.9	511.7	427.1	723.6	2223.3	173.9	0.897	0.863	0.184	418.44	48.738	13.339	33.399	56.587	152.062	77.927	22.500	
North																			
0	N	581.0	394.9	957.4	723.6	2656.9	207.8	0.901	0.513	0.184		50.487	10.293	74.873	56.587	192.239	78.275	13.366	
0.1	N	591.8	360.8	839.5	723.6	2515.7	196.7	0.903	0.494	0.184	22.01	51.423	9.404	65.651	56.587	183.064	78.453	12.877	
0.2	N	600.7	329.0	726.5	723.6	2379.7	186.1	0.903	0.475	0.184	47.85	52.194	8.575	56.810	56.587	174.166	78.475	12.392	
0.3	N	606.3	297.2	617.3	723.6	2244.4	175.5	0.902	0.459	0.184	73.24	52.683	7.748	48.270	56.587	165.288	78.413	11.970	
0.4	N	606.1	296.0	550.2	723.6	2175.8	170.2	0.901	0.441	0.184	98.33	52.662	7.716	43.023	56.587	159.988	78.282	11.497	
0.5	N	608.9	303.7	490.6	723.6	2126.8	166.3	0.901	0.455	0.184	122.58	52.906	7.917	38.368	56.587	155.777	78.269	11.872	
0.6	N	634.5	294.2	489.0	723.6	2141.3	167.5	0.920	0.456	0.184	48.34	55.134	7.669	38.239	56.587	157.628	79.951	11.892	
0.66	N	629.9	304.6	473.1	723.6	2131.2	166.7	0.920	0.466	0.184	56.92	54.730	7.940	37.000	56.587	156.257	79.964	12.158	

HIGH INTERNAL LOADS (no daylighting and night time equipment setbacks)

IGU	Ucg [W/m2K]	SHGC	VT	Frame	U-edge [W/m2K]	U-frame [W/m2K]	WWR 0.1 [W/m2K]	WWR 0.2 [W/m2K]	WWR 0.3 [W/m2K]	WWR 0.4 [W/m2K]	WWR 0.5 [W/m2K]	WWR 0.6 [W/m2K]	WWR 0.66 [W/m2K]
5G-2s HP Wd	0.271	0.33	0.447	HP Wood	0.7047	1.62	0.67	0.56	0.51	0.48	0.46	0.49	0.48

WWR	Shading	Annual Purchased Heating [kWh]	Annual Purchased Cooling [kWh]	Annual Lighting Load [kWh]	Annual Plug Load [kWh]	Total Annual Load [kWh]	Total Annual Load / Area [kWh/m2]	Peak Heating [kW]	Peak Cooling [kW]	Peak Lighting [kW]	Annual Window Energy Balance ('+' gain, '-' loss) [kWh]	Annual Heating Energy 'Metered' [kWh/m2]	Annual Cooling Energy 'Metered' [kWh/m2]	Annual Lighting Energy 'Metered' [kWh/m2]	Annual Plug Energy 'Metered' [kWh/m2]	Total Annual Energy 'Metered' [kWh/m2]	Peak Heating Energy 'Metered' [W/m2]	Peak Cooling Energy 'Metered' [W/m2]	
South																			
0	N	40.0	1359.9	1611.8	1971.0	4982.8	389.7	0.460	0.835	0.184		3.478	35.449	126.048	154.135	319.110	39.992	21.754	
0.1	N	18.6	1540.7	1611.8	1971.0	5142.1	402.1	0.407	0.856	0.184	225.75	1.614	40.162	126.048	154.135	321.959	35.372	22.323	
0.2	N	9.5	1751.3	1611.8	1971.0	5343.6	417.9	0.363	0.885	0.184	461.64	0.825	45.650	126.048	154.135	326.658	31.560	23.061	
0.3	N	4.4	1982.0	1611.8	1971.0	5569.3	435.5	0.316	0.974	0.184	698.03	0.385	51.665	126.048	154.135	332.232	27.418	25.380	
0.4	N	1.6	2224.0	1611.8	1971.0	5808.4	454.2	0.244	1.062	0.184	933.54	0.138	57.974	126.048	154.135	338.294	21.232	27.684	
0.5	N	0.4	2473.1	1611.8	1971.0	6056.3	473.6	0.153	1.158	0.184	1168.66	0.032	64.466	126.048	154.135	344.681	13.318	30.175	
0.6	N	0.2	2574.1	1611.8	1971.0	6157.2	481.5	0.116	1.244	0.184	1233.62	0.020	67.099	126.048	154.135	347.302	10.087	32.423	
0.66	N	0.1	2716.0	1611.8	1971.0	6299.0	492.6	0.071	1.322	0.184	1360.87	0.011	70.799	126.048	154.135	350.993	6.209	34.463	
East																			
0	N	46.6	1360.0	1611.8	1971.0	4989.4	390.2	0.469	0.839	0.184		4.049	35.450	126.048	154.135	319.683	40.741	21.879	
0.1	N	18.6	1611.8	1611.8	1971.0	5213.3	407.7	0.407	0.856	0.184	193.54	1.614	42.016	126.048	154.135	323.813	35.372	22.323	
0.2	N	24.6	1740.4	1611.8	1971.0	5347.8	418.2	0.423	0.968	0.184	395.43	2.136	45.368	126.048	154.135	327.686	36.782	25.222	
0.3	N	18.5	1943.2	1611.8	1971.0	5544.6	433.6	0.405	1.103	0.184	597.56	1.612	50.655	126.048	154.135	332.449	35.216	28.740	
0.4	N	14.0	2150.7	1611.8	1971.0	5747.5	449.5	0.387	1.244	0.184	798.58	1.219	56.062	126.048	154.135	337.464	33.627	32.416	
0.5	N	9.9	2363.1	1611.8	1971.0	5955.9	465.8	0.359	1.385	0.184	999.38	0.863	61.600	126.048	154.135	342.647	31.165	36.111	
0.6	N	10.2	2448.8	1611.8	1971.0	6041.8	472.5	0.370	1.492	0.184	1044.13	0.884	63.833	126.048	154.135	344.901	32.128	38.897	
0.66	N	8.2	2570.3	1611.8	1971.0	6161.3	481.8	0.349	1.575	0.184	1152.08	0.709	67.000	126.048	154.135	347.892	30.296	41.068	
West																			
0	N	48.0	1346.0	1611.8	1971.0	4976.8	389.2	0.479	0.837	0.184		4.172	35.085	126.048	154.135	319.440	41.636	21.817	
0.1	N	34.8	1514.1	1611.8	1971.0	5131.8	401.3	0.457	0.866	0.184	177.81	3.026	39.469	126.048	154.135	322.678	39.687	22.583	
0.2	N	26.5	1692.6	1611.8	1971.0	5301.9	414.6	0.446	0.956	0.184	361.38	2.299	44.122	126.048	154.135	326.604	38.729	24.923	
0.3	N	20.8	1877.5	1611.8	1971.0	5481.2	428.6	0.434	1.088	0.184	544.65	1.810	48.941	126.048	154.135	330.934	37.739	28.374	
0.4	N	16.9	2067.6	1611.8	1971.0	5667.3	443.2	0.423	1.224	0.184	726.94	1.465	53.896	126.048	154.135	335.544	36.734	31.916	
0.5	N	13.2	2263.2	1611.8	1971.0	5859.3	458.2	0.399	1.365	0.184	908.99	1.150	58.996	126.048	154.135	340.329	34.689	35.579	
0.6	N	13.6	2337.0	1611.8	1971.0	5933.4	464.0	0.414	1.471	0.184	941.83	1.182	60.919	126.048	154.135	342.284	35.949	38.341	
0.66	N	11.5	2448.3	1611.8	1971.0	6042.7	472.5	0.394	1.553	0.184	1038.84	1.003	63.820	126.048	154.135	345.006	34.204	40.488	
North																			
0	N	50.9	1310.3	1611.8	1971.0	4944.0	386.6	0.480	0.825	0.184		4.423	34.155	126.048	154.135	318.761	41.675	21.511	
0.1	N	41.6	1398.8	1611.8	1971.0	5023.3	392.8	0.459	0.843	0.184	73.08	3.615	36.463	126.048	154.135	320.261	39.867	21.983	
0.2	N	34.5	1490.4	1611.8	1971.0	5107.7	399.4	0.450	0.861	0.184	149.77	2.995	38.851	126.048	154.135	322.029	39.072	22.453	
0.3	N	28.7	1584.4	1611.8	1971.0	5195.9	406.3	0.440	0.882	0.184	226.14	2.491	41.300	126.048	154.135	323.974	38.253	23.002	
0.4	N	23.9	1680.3	1611.8	1971.0	5287.0	413.5	0.431	0.902	0.184	301.97	2.073	43.802	126.048	154.135	326.058	37.424	23.514	
0.5	N	19.4	1778.6	1611.8	1971.0	5380.8	420.8	0.409	0.920	0.184	377.26	1.685	46.363	126.048	154.135	328.231	35.518	23.994	
0.6	N	20.8	1782.2	1611.8	1971.0	5385.9	421.2	0.424	0.933	0.184	332.50	1.809	46.458	126.048	154.135	328.450	36.878	24.314	
0.66	N	18.3	1835.8	1611.8	1971.0	5436.9	425.2	0.405	0.953	0.184	368.41	1.589	47.853	126.048	154.135	329.625	35.172	24.853	

HIGH INTERNAL LOADS (no daylighting and night time equipment setbacks)

IGU	Ucg [W/m2K]	SHGC	VT	Frame	U-edge [W/m2K]	U-frame [W/m2K]	WWR 0.1 [W/m2K]	WWR 0.2 [W/m2K]	WWR 0.3 [W/m2K]	WWR 0.4 [W/m2K]	WWR 0.5 [W/m2K]	WWR 0.6 [W/m2K]	WWR 0.66 [W/m2K]
5G-4uv HP AL	0.272	0.187	0.406	HP Wood	0.7047	1.62	0.67	0.56	0.51	0.48	0.46	0.49	0.48

WWR	Shading	Annual Purchased Heating [kWh]	Annual Purchased Cooling [kWh]	Annual Lighting Load [kWh]	Annual Plug Load [kWh]	Total Annual Load [kWh]	Total Annual Load / Area [kWh/m2]	Peak Heating [kW]	Peak Cooling [kW]	Peak Lighting [kW]	Annual Window Energy Balance ('+' gain, '-' loss) [kWh]	Annual Heating Energy 'Metered' [kWh/m2]	Annual Cooling Energy 'Metered' [kWh/m2]	Annual Lighting Energy 'Metered' [kWh/m2]	Annual Plug Energy 'Metered' [kWh/m2]	Total Annual Energy 'Metered' [kWh/m2]	Peak Heating Energy 'Metered' [W/m2]	Peak Cooling Energy 'Metered' [W/m2]																																																																																																																																																																																																																																																																																																																																																																																																																																																																																																																																																																																																																																																																																									
South																			0	N	40.0	1359.9	1611.8	1971.0	4982.8	389.7	0.460	0.835	0.184		3.478	35.449	126.048	154.135	319.110	39.992	21.754	0.1	N	25.8	1451.0	1611.8	1971.0	5059.6	395.7	0.438	0.845	0.184	104.87	2.243	37.823	126.048	154.135	320.249	38.033	22.016	0.2	N	16.3	1552.5	1611.8	1971.0	5151.6	402.9	0.403	0.854	0.184	216.09	1.418	40.468	126.048	154.135	322.069	34.991	22.270	0.3	N	11.1	1663.1	1611.8	1971.0	5257.0	411.1	0.378	0.864	0.184	327.41	0.965	43.351	126.048	154.135	324.499	32.879	22.511	0.4	N	7.2	1781.4	1611.8	1971.0	5371.5	420.1	0.353	0.902	0.184	438.47	0.629	46.436	126.048	154.135	327.248	30.692	23.512	0.5	N	4.6	1905.5	1611.8	1971.0	5493.0	429.6	0.326	0.951	0.184	549.16	0.399	49.672	126.048	154.135	330.253	28.287	24.794	0.6	N	4.1	1918.3	1611.8	1971.0	5505.2	430.5	0.324	0.975	0.184	527.23	0.356	50.004	126.048	154.135	330.543	28.143	25.412	0.66	N	3.0	1988.2	1611.8	1971.0	5574.1	435.9	0.300	1.002	0.184	583.56	0.262	51.827	126.048	154.135	332.272	26.107	26.129	East																			0	N	46.6	1360.0	1611.8	1971.0	4989.4	390.2	0.469	0.839	0.184		4.049	35.450	126.048	154.135	319.683	40.741	21.879	0.1	N	38.6	1459.4	1611.8	1971.0	5080.8	397.3	0.460	0.873	0.184	91.80	3.350	38.042	126.048	154.135	321.575	39.990	22.746	0.2	N	31.2	1564.7	1611.8	1971.0	5178.7	405.0	0.438	0.913	0.184	189.29	2.711	40.787	126.048	154.135	323.680	38.094	23.796	0.3	N	25.7	1672.8	1611.8	1971.0	5281.3	413.0	0.428	0.957	0.184	288.99	2.234	43.605	126.048	154.135	326.022	37.225	24.951	0.4	N	21.4	1783.3	1611.8	1971.0	5387.6	421.3	0.418	1.006	0.184	384.36	1.859	46.486	126.048	154.135	328.528	36.342	26.215	0.5	N	18.0	1896.1	1611.8	1971.0	5496.9	429.9	0.408	1.088	0.184	481.30	1.564	49.425	126.048	154.135	331.172	35.473	28.358	0.6	N	19.5	1910.7	1611.8	1971.0	5513.0	431.1	0.425	1.143	0.184	452.81	1.691	49.805	126.048	154.135	331.680	36.888	29.792	0.66	N	17.8	1973.0	1611.8	1971.0	5573.6	435.9	0.419	1.190	0.184	501.52	1.548	51.430	126.048	154.135	333.161	36.437	31.020	West																			0	N	48.0	1346.0	1611.8	1971.0	4976.8	389.2	0.479	0.837	0.184		4.172	35.085	126.048	154.135	319.440	41.636	21.817	0.1	N	39.7	1436.9	1611.8	1971.0	5059.5	395.7	0.473	0.852	0.184	82.17	3.453	37.456	126.048	154.135	321.091	41.096	22.206	0.2	N	32.4	1532.6	1611.8	1971.0	5147.8	402.6	0.453	0.866	0.184	168.97	2.818	39.949	126.048	154.135	322.951	39.397	22.568	0.3	N	27.2	1630.8	1611.8	1971.0	5240.9	409.8	0.446	0.927	0.184	255.72	2.364	42.511	126.048	154.135	325.058	38.759	24.171	0.4	N	23.0	1731.4	1611.8	1971.0	5337.3	417.4	0.439	1.004	0.184	342.09	2.002	45.134	126.048	154.135	327.319	38.109	26.183	0.5	N	19.8	1834.7	1611.8	1971.0	5437.4	425.2	0.431	1.087	0.184	428.00	1.724	47.825	126.048	154.135	329.732	37.473	28.332	0.6	N	21.3	1842.9	1611.8	1971.0	5447.1	428.0	0.449	1.145	0.184	392.05	1.853	48.039	126.048	154.135	330.075	39.011	29.844	0.66	N	19.7	1899.8	1611.8	1971.0	5502.4	430.3	0.445	1.192	0.184	434.36	1.716	49.521	126.048	154.135	331.420	38.687	31.075	North																			0	N	50.9	1310.3	1611.8	1971.0	4944.0	386.6	0.480	0.825	0.184		4.423	34.155	126.048	154.135	318.761	41.675	21.511	0.1	N	44.1	1359.8	1611.8	1971.0	4986.7	390.0	0.462	0.835	0.184	23.90	3.829	35.447	126.048	154.135	319.459	40.115	21.765	0.2	N	38.7	1410.5	1611.8	1971.0	5032.0	393.5	0.455	0.844	0.184	51.60	3.364	36.767	126.048	154.135	320.314	39.568	22.003	0.3	N	34.0	1462.3	1611.8	1971.0	5079.1	397.2	0.449	0.853	0.184	79.29	2.950	38.118	126.048	154.135	321.251	39.003	22.249	0.4	N	29.8	1515.2	1611.8	1971.0	5127.8	401.0	0.442	0.861	0.184	106.73	2.590	39.496	126.048	154.135	322.269	38.429	22.440	0.5	N	26.1	1569.2	1611.8	1971.0	5178.2	404.9	0.436	0.869	0.184	133.74	2.270	40.905	126.048	154.135	323.357	37.874	22.651	0.6	N	29.1	1542.2	1611.8	1971.0	5154.1	403.1	0.454	0.864	0.184	54.61	2.532	40.200	126.048	154.135	322.915	39.452	22.530	0.66	N	27.3	1570.0	1611.8	1971.0	5180.1	405.1	0.451	0.868	0.184	63.39	2.369	40.926	126.048	154.135	323.478	39.172	22.618
0	N	40.0	1359.9	1611.8	1971.0	4982.8	389.7	0.460	0.835	0.184		3.478	35.449	126.048	154.135	319.110	39.992	21.754	0.1	N	25.8	1451.0	1611.8	1971.0	5059.6	395.7	0.438	0.845	0.184	104.87	2.243	37.823	126.048	154.135	320.249	38.033	22.016	0.2	N	16.3	1552.5	1611.8	1971.0	5151.6	402.9	0.403	0.854	0.184	216.09	1.418	40.468	126.048	154.135	322.069	34.991	22.270	0.3	N	11.1	1663.1	1611.8	1971.0	5257.0	411.1	0.378	0.864	0.184	327.41	0.965	43.351	126.048	154.135	324.499	32.879	22.511	0.4	N	7.2	1781.4	1611.8	1971.0	5371.5	420.1	0.353	0.902	0.184	438.47	0.629	46.436	126.048	154.135	327.248	30.692	23.512	0.5	N	4.6	1905.5	1611.8	1971.0	5493.0	429.6	0.326	0.951	0.184	549.16	0.399	49.672	126.048	154.135	330.253	28.287	24.794	0.6	N	4.1	1918.3	1611.8	1971.0	5505.2	430.5	0.324	0.975	0.184	527.23	0.356	50.004	126.048	154.135	330.543	28.143	25.412	0.66	N	3.0	1988.2	1611.8	1971.0	5574.1	435.9	0.300	1.002	0.184	583.56	0.262	51.827	126.048	154.135	332.272	26.107	26.129	East																			0	N	46.6	1360.0	1611.8	1971.0	4989.4	390.2	0.469	0.839	0.184		4.049	35.450	126.048	154.135	319.683	40.741	21.879	0.1	N	38.6	1459.4	1611.8	1971.0	5080.8	397.3	0.460	0.873	0.184	91.80	3.350	38.042	126.048	154.135	321.575	39.990	22.746	0.2	N	31.2	1564.7	1611.8	1971.0	5178.7	405.0	0.438	0.913	0.184	189.29	2.711	40.787	126.048	154.135	323.680	38.094	23.796	0.3	N	25.7	1672.8	1611.8	1971.0	5281.3	413.0	0.428	0.957	0.184	288.99	2.234	43.605	126.048	154.135	326.022	37.225	24.951	0.4	N	21.4	1783.3	1611.8	1971.0	5387.6	421.3	0.418	1.006	0.184	384.36	1.859	46.486	126.048	154.135	328.528	36.342	26.215	0.5	N	18.0	1896.1	1611.8	1971.0	5496.9	429.9	0.408	1.088	0.184	481.30	1.564	49.425	126.048	154.135	331.172	35.473	28.358	0.6	N	19.5	1910.7	1611.8	1971.0	5513.0	431.1	0.425	1.143	0.184	452.81	1.691	49.805	126.048	154.135	331.680	36.888	29.792	0.66	N	17.8	1973.0	1611.8	1971.0	5573.6	435.9	0.419	1.190	0.184	501.52	1.548	51.430	126.048	154.135	333.161	36.437	31.020	West																			0	N	48.0	1346.0	1611.8	1971.0	4976.8	389.2	0.479	0.837	0.184		4.172	35.085	126.048	154.135	319.440	41.636	21.817	0.1	N	39.7	1436.9	1611.8	1971.0	5059.5	395.7	0.473	0.852	0.184	82.17	3.453	37.456	126.048	154.135	321.091	41.096	22.206	0.2	N	32.4	1532.6	1611.8	1971.0	5147.8	402.6	0.453	0.866	0.184	168.97	2.818	39.949	126.048	154.135	322.951	39.397	22.568	0.3	N	27.2	1630.8	1611.8	1971.0	5240.9	409.8	0.446	0.927	0.184	255.72	2.364	42.511	126.048	154.135	325.058	38.759	24.171	0.4	N	23.0	1731.4	1611.8	1971.0	5337.3	417.4	0.439	1.004	0.184	342.09	2.002	45.134	126.048	154.135	327.319	38.109	26.183	0.5	N	19.8	1834.7	1611.8	1971.0	5437.4	425.2	0.431	1.087	0.184	428.00	1.724	47.825	126.048	154.135	329.732	37.473	28.332	0.6	N	21.3	1842.9	1611.8	1971.0	5447.1	428.0	0.449	1.145	0.184	392.05	1.853	48.039	126.048	154.135	330.075	39.011	29.844	0.66	N	19.7	1899.8	1611.8	1971.0	5502.4	430.3	0.445	1.192	0.184	434.36	1.716	49.521	126.048	154.135	331.420	38.687	31.075	North																			0	N	50.9	1310.3	1611.8	1971.0	4944.0	386.6	0.480	0.825	0.184		4.423	34.155	126.048	154.135	318.761	41.675	21.511	0.1	N	44.1	1359.8	1611.8	1971.0	4986.7	390.0	0.462	0.835	0.184	23.90	3.829	35.447	126.048	154.135	319.459	40.115	21.765	0.2	N	38.7	1410.5	1611.8	1971.0	5032.0	393.5	0.455	0.844	0.184	51.60	3.364	36.767	126.048	154.135	320.314	39.568	22.003	0.3	N	34.0	1462.3	1611.8	1971.0	5079.1	397.2	0.449	0.853	0.184	79.29	2.950	38.118	126.048	154.135	321.251	39.003	22.249	0.4	N	29.8	1515.2	1611.8	1971.0	5127.8	401.0	0.442	0.861	0.184	106.73	2.590	39.496	126.048	154.135	322.269	38.429	22.440	0.5	N	26.1	1569.2	1611.8	1971.0	5178.2	404.9	0.436	0.869	0.184	133.74	2.270	40.905	126.048	154.135	323.357	37.874	22.651	0.6	N	29.1	1542.2	1611.8	1971.0	5154.1	403.1	0.454	0.864	0.184	54.61	2.532	40.200	126.048	154.135	322.915	39.452	22.530	0.66	N	27.3	1570.0	1611.8	1971.0	5180.1	405.1	0.451	0.868	0.184	63.39	2.369	40.926	126.048	154.135	323.478	39.172	22.618																			
0.1	N	25.8	1451.0	1611.8	1971.0	5059.6	395.7	0.438	0.845	0.184	104.87	2.243	37.823	126.048	154.135	320.249	38.033	22.016	0.2	N	16.3	1552.5	1611.8	1971.0	5151.6	402.9	0.403	0.854	0.184	216.09	1.418	40.468	126.048	154.135	322.069	34.991	22.270	0.3	N	11.1	1663.1	1611.8	1971.0	5257.0	411.1	0.378	0.864	0.184	327.41	0.965	43.351	126.048	154.135	324.499	32.879	22.511	0.4	N	7.2	1781.4	1611.8	1971.0	5371.5	420.1	0.353	0.902	0.184	438.47	0.629	46.436	126.048	154.135	327.248	30.692	23.512	0.5	N	4.6	1905.5	1611.8	1971.0	5493.0	429.6	0.326	0.951	0.184	549.16	0.399	49.672	126.048	154.135	330.253	28.287	24.794	0.6	N	4.1	1918.3	1611.8	1971.0	5505.2	430.5	0.324	0.975	0.184	527.23	0.356	50.004	126.048	154.135	330.543	28.143	25.412	0.66	N	3.0	1988.2	1611.8	1971.0	5574.1	435.9	0.300	1.002	0.184	583.56	0.262	51.827	126.048	154.135	332.272	26.107	26.129	East																			0	N	46.6	1360.0	1611.8	1971.0	4989.4	390.2	0.469	0.839	0.184		4.049	35.450	126.048	154.135	319.683	40.741	21.879	0.1	N	38.6	1459.4	1611.8	1971.0	5080.8	397.3	0.460	0.873	0.184	91.80	3.350	38.042	126.048	154.135	321.575	39.990	22.746	0.2	N	31.2	1564.7	1611.8	1971.0	5178.7	405.0	0.438	0.913	0.184	189.29	2.711	40.787	126.048	154.135	323.680	38.094	23.796	0.3	N	25.7	1672.8	1611.8	1971.0	5281.3	413.0	0.428	0.957	0.184	288.99	2.234	43.605	126.048	154.135	326.022	37.225	24.951	0.4	N	21.4	1783.3	1611.8	1971.0	5387.6	421.3	0.418	1.006	0.184	384.36	1.859	46.486	126.048	154.135	328.528	36.342	26.215	0.5	N	18.0	1896.1	1611.8	1971.0	5496.9	429.9	0.408	1.088	0.184	481.30	1.564	49.425	126.048	154.135	331.172	35.473	28.358	0.6	N	19.5	1910.7	1611.8	1971.0	5513.0	431.1	0.425	1.143	0.184	452.81	1.691	49.805	126.048	154.135	331.680	36.888	29.792	0.66	N	17.8	1973.0	1611.8	1971.0	5573.6	435.9	0.419	1.190	0.184	501.52	1.548	51.430	126.048	154.135	333.161	36.437	31.020	West																			0	N	48.0	1346.0	1611.8	1971.0	4976.8	389.2	0.479	0.837	0.184		4.172	35.085	126.048	154.135	319.440	41.636	21.817	0.1	N	39.7	1436.9	1611.8	1971.0	5059.5	395.7	0.473	0.852	0.184	82.17	3.453	37.456	126.048	154.135	321.091	41.096	22.206	0.2	N	32.4	1532.6	1611.8	1971.0	5147.8	402.6	0.453	0.866	0.184	168.97	2.818	39.949	126.048	154.135	322.951	39.397	22.568	0.3	N	27.2	1630.8	1611.8	1971.0	5240.9	409.8	0.446	0.927	0.184	255.72	2.364	42.511	126.048	154.135	325.058	38.759	24.171	0.4	N	23.0	1731.4	1611.8	1971.0	5337.3	417.4	0.439	1.004	0.184	342.09	2.002	45.134	126.048	154.135	327.319	38.109	26.183	0.5	N	19.8	1834.7	1611.8	1971.0	5437.4	425.2	0.431	1.087	0.184	428.00	1.724	47.825	126.048	154.135	329.732	37.473	28.332	0.6	N	21.3	1842.9	1611.8	1971.0	5447.1	428.0	0.449	1.145	0.184	392.05	1.853	48.039	126.048	154.135	330.075	39.011	29.844	0.66	N	19.7	1899.8	1611.8	1971.0	5502.4	430.3	0.445	1.192	0.184	434.36	1.716	49.521	126.048	154.135	331.420	38.687	31.075	North																			0	N	50.9	1310.3	1611.8	1971.0	4944.0	386.6	0.480	0.825	0.184		4.423	34.155	126.048	154.135	318.761	41.675	21.511	0.1	N	44.1	1359.8	1611.8	1971.0	4986.7	390.0	0.462	0.835	0.184	23.90	3.829	35.447	126.048	154.135	319.459	40.115	21.765	0.2	N	38.7	1410.5	1611.8	1971.0	5032.0	393.5	0.455	0.844	0.184	51.60	3.364	36.767	126.048	154.135	320.314	39.568	22.003	0.3	N	34.0	1462.3	1611.8	1971.0	5079.1	397.2	0.449	0.853	0.184	79.29	2.950	38.118	126.048	154.135	321.251	39.003	22.249	0.4	N	29.8	1515.2	1611.8	1971.0	5127.8	401.0	0.442	0.861	0.184	106.73	2.590	39.496	126.048	154.135	322.269	38.429	22.440	0.5	N	26.1	1569.2	1611.8	1971.0	5178.2	404.9	0.436	0.869	0.184	133.74	2.270	40.905	126.048	154.135	323.357	37.874	22.651	0.6	N	29.1	1542.2	1611.8	1971.0	5154.1	403.1	0.454	0.864	0.184	54.61	2.532	40.200	126.048	154.135	322.915	39.452	22.530	0.66	N	27.3	1570.0	1611.8	1971.0	5180.1	405.1	0.451	0.868	0.184	63.39	2.369	40.926	126.048	154.135	323.478	39.172	22.618																																						
0.2	N	16.3	1552.5	1611.8	1971.0	5151.6	402.9	0.403	0.854	0.184	216.09	1.418	40.468	126.048	154.135	322.069	34.991	22.270	0.3	N	11.1	1663.1	1611.8	1971.0	5257.0	411.1	0.378	0.864	0.184	327.41	0.965	43.351	126.048	154.135	324.499	32.879	22.511	0.4	N	7.2	1781.4	1611.8	1971.0	5371.5	420.1	0.353	0.902	0.184	438.47	0.629	46.436	126.048	154.135	327.248	30.692	23.512	0.5	N	4.6	1905.5	1611.8	1971.0	5493.0	429.6	0.326	0.951	0.184	549.16	0.399	49.672	126.048	154.135	330.253	28.287	24.794	0.6	N	4.1	1918.3	1611.8	1971.0	5505.2	430.5	0.324	0.975	0.184	527.23	0.356	50.004	126.048	154.135	330.543	28.143	25.412	0.66	N	3.0	1988.2	1611.8	1971.0	5574.1	435.9	0.300	1.002	0.184	583.56	0.262	51.827	126.048	154.135	332.272	26.107	26.129	East																			0	N	46.6	1360.0	1611.8	1971.0	4989.4	390.2	0.469	0.839	0.184		4.049	35.450	126.048	154.135	319.683	40.741	21.879	0.1	N	38.6	1459.4	1611.8	1971.0	5080.8	397.3	0.460	0.873	0.184	91.80	3.350	38.042	126.048	154.135	321.575	39.990	22.746	0.2	N	31.2	1564.7	1611.8	1971.0	5178.7	405.0	0.438	0.913	0.184	189.29	2.711	40.787	126.048	154.135	323.680	38.094	23.796	0.3	N	25.7	1672.8	1611.8	1971.0	5281.3	413.0	0.428	0.957	0.184	288.99	2.234	43.605	126.048	154.135	326.022	37.225	24.951	0.4	N	21.4	1783.3	1611.8	1971.0	5387.6	421.3	0.418	1.006	0.184	384.36	1.859	46.486	126.048	154.135	328.528	36.342	26.215	0.5	N	18.0	1896.1	1611.8	1971.0	5496.9	429.9	0.408	1.088	0.184	481.30	1.564	49.425	126.048	154.135	331.172	35.473	28.358	0.6	N	19.5	1910.7	1611.8	1971.0	5513.0	431.1	0.425	1.143	0.184	452.81	1.691	49.805	126.048	154.135	331.680	36.888	29.792	0.66	N	17.8	1973.0	1611.8	1971.0	5573.6	435.9	0.419	1.190	0.184	501.52	1.548	51.430	126.048	154.135	333.161	36.437	31.020	West																			0	N	48.0	1346.0	1611.8	1971.0	4976.8	389.2	0.479	0.837	0.184		4.172	35.085	126.048	154.135	319.440	41.636	21.817	0.1	N	39.7	1436.9	1611.8	1971.0	5059.5	395.7	0.473	0.852	0.184	82.17	3.453	37.456	126.048	154.135	321.091	41.096	22.206	0.2	N	32.4	1532.6	1611.8	1971.0	5147.8	402.6	0.453	0.866	0.184	168.97	2.818	39.949	126.048	154.135	322.951	39.397	22.568	0.3	N	27.2	1630.8	1611.8	1971.0	5240.9	409.8	0.446	0.927	0.184	255.72	2.364	42.511	126.048	154.135	325.058	38.759	24.171	0.4	N	23.0	1731.4	1611.8	1971.0	5337.3	417.4	0.439	1.004	0.184	342.09	2.002	45.134	126.048	154.135	327.319	38.109	26.183	0.5	N	19.8	1834.7	1611.8	1971.0	5437.4	425.2	0.431	1.087	0.184	428.00	1.724	47.825	126.048	154.135	329.732	37.473	28.332	0.6	N	21.3	1842.9	1611.8	1971.0	5447.1	428.0	0.449	1.145	0.184	392.05	1.853	48.039	126.048	154.135	330.075	39.011	29.844	0.66	N	19.7	1899.8	1611.8	1971.0	5502.4	430.3	0.445	1.192	0.184	434.36	1.716	49.521	126.048	154.135	331.420	38.687	31.075	North																			0	N	50.9	1310.3	1611.8	1971.0	4944.0	386.6	0.480	0.825	0.184		4.423	34.155	126.048	154.135	318.761	41.675	21.511	0.1	N	44.1	1359.8	1611.8	1971.0	4986.7	390.0	0.462	0.835	0.184	23.90	3.829	35.447	126.048	154.135	319.459	40.115	21.765	0.2	N	38.7	1410.5	1611.8	1971.0	5032.0	393.5	0.455	0.844	0.184	51.60	3.364	36.767	126.048	154.135	320.314	39.568	22.003	0.3	N	34.0	1462.3	1611.8	1971.0	5079.1	397.2	0.449	0.853	0.184	79.29	2.950	38.118	126.048	154.135	321.251	39.003	22.249	0.4	N	29.8	1515.2	1611.8	1971.0	5127.8	401.0	0.442	0.861	0.184	106.73	2.590	39.496	126.048	154.135	322.269	38.429	22.440	0.5	N	26.1	1569.2	1611.8	1971.0	5178.2	404.9	0.436	0.869	0.184	133.74	2.270	40.905	126.048	154.135	323.357	37.874	22.651	0.6	N	29.1	1542.2	1611.8	1971.0	5154.1	403.1	0.454	0.864	0.184	54.61	2.532	40.200	126.048	154.135	322.915	39.452	22.530	0.66	N	27.3	1570.0	1611.8	1971.0	5180.1	405.1	0.451	0.868	0.184	63.39	2.369	40.926	126.048	154.135	323.478	39.172	22.618																																																									
0.3	N	11.1	1663.1	1611.8	1971.0	5257.0	411.1	0.378	0.864	0.184	327.41	0.965	43.351	126.048	154.135	324.499	32.879	22.511	0.4	N	7.2	1781.4	1611.8	1971.0	5371.5	420.1	0.353	0.902	0.184	438.47	0.629	46.436	126.048	154.135	327.248	30.692	23.512	0.5	N	4.6	1905.5	1611.8	1971.0	5493.0	429.6	0.326	0.951	0.184	549.16	0.399	49.672	126.048	154.135	330.253	28.287	24.794	0.6	N	4.1	1918.3	1611.8	1971.0	5505.2	430.5	0.324	0.975	0.184	527.23	0.356	50.004	126.048	154.135	330.543	28.143	25.412	0.66	N	3.0	1988.2	1611.8	1971.0	5574.1	435.9	0.300	1.002	0.184	583.56	0.262	51.827	126.048	154.135	332.272	26.107	26.129	East																			0	N	46.6	1360.0	1611.8	1971.0	4989.4	390.2	0.469	0.839	0.184		4.049	35.450	126.048	154.135	319.683	40.741	21.879	0.1	N	38.6	1459.4	1611.8	1971.0	5080.8	397.3	0.460	0.873	0.184	91.80	3.350	38.042	126.048	154.135	321.575	39.990	22.746	0.2	N	31.2	1564.7	1611.8	1971.0	5178.7	405.0	0.438	0.913	0.184	189.29	2.711	40.787	126.048	154.135	323.680	38.094	23.796	0.3	N	25.7	1672.8	1611.8	1971.0	5281.3	413.0	0.428	0.957	0.184	288.99	2.234	43.605	126.048	154.135	326.022	37.225	24.951	0.4	N	21.4	1783.3	1611.8	1971.0	5387.6	421.3	0.418	1.006	0.184	384.36	1.859	46.486	126.048	154.135	328.528	36.342	26.215	0.5	N	18.0	1896.1	1611.8	1971.0	5496.9	429.9	0.408	1.088	0.184	481.30	1.564	49.425	126.048	154.135	331.172	35.473	28.358	0.6	N	19.5	1910.7	1611.8	1971.0	5513.0	431.1	0.425	1.143	0.184	452.81	1.691	49.805	126.048	154.135	331.680	36.888	29.792	0.66	N	17.8	1973.0	1611.8	1971.0	5573.6	435.9	0.419	1.190	0.184	501.52	1.548	51.430	126.048	154.135	333.161	36.437	31.020	West																			0	N	48.0	1346.0	1611.8	1971.0	4976.8	389.2	0.479	0.837	0.184		4.172	35.085	126.048	154.135	319.440	41.636	21.817	0.1	N	39.7	1436.9	1611.8	1971.0	5059.5	395.7	0.473	0.852	0.184	82.17	3.453	37.456	126.048	154.135	321.091	41.096	22.206	0.2	N	32.4	1532.6	1611.8	1971.0	5147.8	402.6	0.453	0.866	0.184	168.97	2.818	39.949	126.048	154.135	322.951	39.397	22.568	0.3	N	27.2	1630.8	1611.8	1971.0	5240.9	409.8	0.446	0.927	0.184	255.72	2.364	42.511	126.048	154.135	325.058	38.759	24.171	0.4	N	23.0	1731.4	1611.8	1971.0	5337.3	417.4	0.439	1.004	0.184	342.09	2.002	45.134	126.048	154.135	327.319	38.109	26.183	0.5	N	19.8	1834.7	1611.8	1971.0	5437.4	425.2	0.431	1.087	0.184	428.00	1.724	47.825	126.048	154.135	329.732	37.473	28.332	0.6	N	21.3	1842.9	1611.8	1971.0	5447.1	428.0	0.449	1.145	0.184	392.05	1.853	48.039	126.048	154.135	330.075	39.011	29.844	0.66	N	19.7	1899.8	1611.8	1971.0	5502.4	430.3	0.445	1.192	0.184	434.36	1.716	49.521	126.048	154.135	331.420	38.687	31.075	North																			0	N	50.9	1310.3	1611.8	1971.0	4944.0	386.6	0.480	0.825	0.184		4.423	34.155	126.048	154.135	318.761	41.675	21.511	0.1	N	44.1	1359.8	1611.8	1971.0	4986.7	390.0	0.462	0.835	0.184	23.90	3.829	35.447	126.048	154.135	319.459	40.115	21.765	0.2	N	38.7	1410.5	1611.8	1971.0	5032.0	393.5	0.455	0.844	0.184	51.60	3.364	36.767	126.048	154.135	320.314	39.568	22.003	0.3	N	34.0	1462.3	1611.8	1971.0	5079.1	397.2	0.449	0.853	0.184	79.29	2.950	38.118	126.048	154.135	321.251	39.003	22.249	0.4	N	29.8	1515.2	1611.8	1971.0	5127.8	401.0	0.442	0.861	0.184	106.73	2.590	39.496	126.048	154.135	322.269	38.429	22.440	0.5	N	26.1	1569.2	1611.8	1971.0	5178.2	404.9	0.436	0.869	0.184	133.74	2.270	40.905	126.048	154.135	323.357	37.874	22.651	0.6	N	29.1	1542.2	1611.8	1971.0	5154.1	403.1	0.454	0.864	0.184	54.61	2.532	40.200	126.048	154.135	322.915	39.452	22.530	0.66	N	27.3	1570.0	1611.8	1971.0	5180.1	405.1	0.451	0.868	0.184	63.39	2.369	40.926	126.048	154.135	323.478	39.172	22.618																																																																												
0.4	N	7.2	1781.4	1611.8	1971.0	5371.5	420.1	0.353	0.902	0.184	438.47	0.629	46.436	126.048	154.135	327.248	30.692	23.512	0.5	N	4.6	1905.5	1611.8	1971.0	5493.0	429.6	0.326	0.951	0.184	549.16	0.399	49.672	126.048	154.135	330.253	28.287	24.794	0.6	N	4.1	1918.3	1611.8	1971.0	5505.2	430.5	0.324	0.975	0.184	527.23	0.356	50.004	126.048	154.135	330.543	28.143	25.412	0.66	N	3.0	1988.2	1611.8	1971.0	5574.1	435.9	0.300	1.002	0.184	583.56	0.262	51.827	126.048	154.135	332.272	26.107	26.129	East																			0	N	46.6	1360.0	1611.8	1971.0	4989.4	390.2	0.469	0.839	0.184		4.049	35.450	126.048	154.135	319.683	40.741	21.879	0.1	N	38.6	1459.4	1611.8	1971.0	5080.8	397.3	0.460	0.873	0.184	91.80	3.350	38.042	126.048	154.135	321.575	39.990	22.746	0.2	N	31.2	1564.7	1611.8	1971.0	5178.7	405.0	0.438	0.913	0.184	189.29	2.711	40.787	126.048	154.135	323.680	38.094	23.796	0.3	N	25.7	1672.8	1611.8	1971.0	5281.3	413.0	0.428	0.957	0.184	288.99	2.234	43.605	126.048	154.135	326.022	37.225	24.951	0.4	N	21.4	1783.3	1611.8	1971.0	5387.6	421.3	0.418	1.006	0.184	384.36	1.859	46.486	126.048	154.135	328.528	36.342	26.215	0.5	N	18.0	1896.1	1611.8	1971.0	5496.9	429.9	0.408	1.088	0.184	481.30	1.564	49.425	126.048	154.135	331.172	35.473	28.358	0.6	N	19.5	1910.7	1611.8	1971.0	5513.0	431.1	0.425	1.143	0.184	452.81	1.691	49.805	126.048	154.135	331.680	36.888	29.792	0.66	N	17.8	1973.0	1611.8	1971.0	5573.6	435.9	0.419	1.190	0.184	501.52	1.548	51.430	126.048	154.135	333.161	36.437	31.020	West																			0	N	48.0	1346.0	1611.8	1971.0	4976.8	389.2	0.479	0.837	0.184		4.172	35.085	126.048	154.135	319.440	41.636	21.817	0.1	N	39.7	1436.9	1611.8	1971.0	5059.5	395.7	0.473	0.852	0.184	82.17	3.453	37.456	126.048	154.135	321.091	41.096	22.206	0.2	N	32.4	1532.6	1611.8	1971.0	5147.8	402.6	0.453	0.866	0.184	168.97	2.818	39.949	126.048	154.135	322.951	39.397	22.568	0.3	N	27.2	1630.8	1611.8	1971.0	5240.9	409.8	0.446	0.927	0.184	255.72	2.364	42.511	126.048	154.135	325.058	38.759	24.171	0.4	N	23.0	1731.4	1611.8	1971.0	5337.3	417.4	0.439	1.004	0.184	342.09	2.002	45.134	126.048	154.135	327.319	38.109	26.183	0.5	N	19.8	1834.7	1611.8	1971.0	5437.4	425.2	0.431	1.087	0.184	428.00	1.724	47.825	126.048	154.135	329.732	37.473	28.332	0.6	N	21.3	1842.9	1611.8	1971.0	5447.1	428.0	0.449	1.145	0.184	392.05	1.853	48.039	126.048	154.135	330.075	39.011	29.844	0.66	N	19.7	1899.8	1611.8	1971.0	5502.4	430.3	0.445	1.192	0.184	434.36	1.716	49.521	126.048	154.135	331.420	38.687	31.075	North																			0	N	50.9	1310.3	1611.8	1971.0	4944.0	386.6	0.480	0.825	0.184		4.423	34.155	126.048	154.135	318.761	41.675	21.511	0.1	N	44.1	1359.8	1611.8	1971.0	4986.7	390.0	0.462	0.835	0.184	23.90	3.829	35.447	126.048	154.135	319.459	40.115	21.765	0.2	N	38.7	1410.5	1611.8	1971.0	5032.0	393.5	0.455	0.844	0.184	51.60	3.364	36.767	126.048	154.135	320.314	39.568	22.003	0.3	N	34.0	1462.3	1611.8	1971.0	5079.1	397.2	0.449	0.853	0.184	79.29	2.950	38.118	126.048	154.135	321.251	39.003	22.249	0.4	N	29.8	1515.2	1611.8	1971.0	5127.8	401.0	0.442	0.861	0.184	106.73	2.590	39.496	126.048	154.135	322.269	38.429	22.440	0.5	N	26.1	1569.2	1611.8	1971.0	5178.2	404.9	0.436	0.869	0.184	133.74	2.270	40.905	126.048	154.135	323.357	37.874	22.651	0.6	N	29.1	1542.2	1611.8	1971.0	5154.1	403.1	0.454	0.864	0.184	54.61	2.532	40.200	126.048	154.135	322.915	39.452	22.530	0.66	N	27.3	1570.0	1611.8	1971.0	5180.1	405.1	0.451	0.868	0.184	63.39	2.369	40.926	126.048	154.135	323.478	39.172	22.618																																																																																															
0.5	N	4.6	1905.5	1611.8	1971.0	5493.0	429.6	0.326	0.951	0.184	549.16	0.399	49.672	126.048	154.135	330.253	28.287	24.794	0.6	N	4.1	1918.3	1611.8	1971.0	5505.2	430.5	0.324	0.975	0.184	527.23	0.356	50.004	126.048	154.135	330.543	28.143	25.412	0.66	N	3.0	1988.2	1611.8	1971.0	5574.1	435.9	0.300	1.002	0.184	583.56	0.262	51.827	126.048	154.135	332.272	26.107	26.129	East																			0	N	46.6	1360.0	1611.8	1971.0	4989.4	390.2	0.469	0.839	0.184		4.049	35.450	126.048	154.135	319.683	40.741	21.879	0.1	N	38.6	1459.4	1611.8	1971.0	5080.8	397.3	0.460	0.873	0.184	91.80	3.350	38.042	126.048	154.135	321.575	39.990	22.746	0.2	N	31.2	1564.7	1611.8	1971.0	5178.7	405.0	0.438	0.913	0.184	189.29	2.711	40.787	126.048	154.135	323.680	38.094	23.796	0.3	N	25.7	1672.8	1611.8	1971.0	5281.3	413.0	0.428	0.957	0.184	288.99	2.234	43.605	126.048	154.135	326.022	37.225	24.951	0.4	N	21.4	1783.3	1611.8	1971.0	5387.6	421.3	0.418	1.006	0.184	384.36	1.859	46.486	126.048	154.135	328.528	36.342	26.215	0.5	N	18.0	1896.1	1611.8	1971.0	5496.9	429.9	0.408	1.088	0.184	481.30	1.564	49.425	126.048	154.135	331.172	35.473	28.358	0.6	N	19.5	1910.7	1611.8	1971.0	5513.0	431.1	0.425	1.143	0.184	452.81	1.691	49.805	126.048	154.135	331.680	36.888	29.792	0.66	N	17.8	1973.0	1611.8	1971.0	5573.6	435.9	0.419	1.190	0.184	501.52	1.548	51.430	126.048	154.135	333.161	36.437	31.020	West																			0	N	48.0	1346.0	1611.8	1971.0	4976.8	389.2	0.479	0.837	0.184		4.172	35.085	126.048	154.135	319.440	41.636	21.817	0.1	N	39.7	1436.9	1611.8	1971.0	5059.5	395.7	0.473	0.852	0.184	82.17	3.453	37.456	126.048	154.135	321.091	41.096	22.206	0.2	N	32.4	1532.6	1611.8	1971.0	5147.8	402.6	0.453	0.866	0.184	168.97	2.818	39.949	126.048	154.135	322.951	39.397	22.568	0.3	N	27.2	1630.8	1611.8	1971.0	5240.9	409.8	0.446	0.927	0.184	255.72	2.364	42.511	126.048	154.135	325.058	38.759	24.171	0.4	N	23.0	1731.4	1611.8	1971.0	5337.3	417.4	0.439	1.004	0.184	342.09	2.002	45.134	126.048	154.135	327.319	38.109	26.183	0.5	N	19.8	1834.7	1611.8	1971.0	5437.4	425.2	0.431	1.087	0.184	428.00	1.724	47.825	126.048	154.135	329.732	37.473	28.332	0.6	N	21.3	1842.9	1611.8	1971.0	5447.1	428.0	0.449	1.145	0.184	392.05	1.853	48.039	126.048	154.135	330.075	39.011	29.844	0.66	N	19.7	1899.8	1611.8	1971.0	5502.4	430.3	0.445	1.192	0.184	434.36	1.716	49.521	126.048	154.135	331.420	38.687	31.075	North																			0	N	50.9	1310.3	1611.8	1971.0	4944.0	386.6	0.480	0.825	0.184		4.423	34.155	126.048	154.135	318.761	41.675	21.511	0.1	N	44.1	1359.8	1611.8	1971.0	4986.7	390.0	0.462	0.835	0.184	23.90	3.829	35.447	126.048	154.135	319.459	40.115	21.765	0.2	N	38.7	1410.5	1611.8	1971.0	5032.0	393.5	0.455	0.844	0.184	51.60	3.364	36.767	126.048	154.135	320.314	39.568	22.003	0.3	N	34.0	1462.3	1611.8	1971.0	5079.1	397.2	0.449	0.853	0.184	79.29	2.950	38.118	126.048	154.135	321.251	39.003	22.249	0.4	N	29.8	1515.2	1611.8	1971.0	5127.8	401.0	0.442	0.861	0.184	106.73	2.590	39.496	126.048	154.135	322.269	38.429	22.440	0.5	N	26.1	1569.2	1611.8	1971.0	5178.2	404.9	0.436	0.869	0.184	133.74	2.270	40.905	126.048	154.135	323.357	37.874	22.651	0.6	N	29.1	1542.2	1611.8	1971.0	5154.1	403.1	0.454	0.864	0.184	54.61	2.532	40.200	126.048	154.135	322.915	39.452	22.530	0.66	N	27.3	1570.0	1611.8	1971.0	5180.1	405.1	0.451	0.868	0.184	63.39	2.369	40.926	126.048	154.135	323.478	39.172	22.618																																																																																																																		
0.6	N	4.1	1918.3	1611.8	1971.0	5505.2	430.5	0.324	0.975	0.184	527.23	0.356	50.004	126.048	154.135	330.543	28.143	25.412	0.66	N	3.0	1988.2	1611.8	1971.0	5574.1	435.9	0.300	1.002	0.184	583.56	0.262	51.827	126.048	154.135	332.272	26.107	26.129	East																			0	N	46.6	1360.0	1611.8	1971.0	4989.4	390.2	0.469	0.839	0.184		4.049	35.450	126.048	154.135	319.683	40.741	21.879	0.1	N	38.6	1459.4	1611.8	1971.0	5080.8	397.3	0.460	0.873	0.184	91.80	3.350	38.042	126.048	154.135	321.575	39.990	22.746	0.2	N	31.2	1564.7	1611.8	1971.0	5178.7	405.0	0.438	0.913	0.184	189.29	2.711	40.787	126.048	154.135	323.680	38.094	23.796	0.3	N	25.7	1672.8	1611.8	1971.0	5281.3	413.0	0.428	0.957	0.184	288.99	2.234	43.605	126.048	154.135	326.022	37.225	24.951	0.4	N	21.4	1783.3	1611.8	1971.0	5387.6	421.3	0.418	1.006	0.184	384.36	1.859	46.486	126.048	154.135	328.528	36.342	26.215	0.5	N	18.0	1896.1	1611.8	1971.0	5496.9	429.9	0.408	1.088	0.184	481.30	1.564	49.425	126.048	154.135	331.172	35.473	28.358	0.6	N	19.5	1910.7	1611.8	1971.0	5513.0	431.1	0.425	1.143	0.184	452.81	1.691	49.805	126.048	154.135	331.680	36.888	29.792	0.66	N	17.8	1973.0	1611.8	1971.0	5573.6	435.9	0.419	1.190	0.184	501.52	1.548	51.430	126.048	154.135	333.161	36.437	31.020	West																			0	N	48.0	1346.0	1611.8	1971.0	4976.8	389.2	0.479	0.837	0.184		4.172	35.085	126.048	154.135	319.440	41.636	21.817	0.1	N	39.7	1436.9	1611.8	1971.0	5059.5	395.7	0.473	0.852	0.184	82.17	3.453	37.456	126.048	154.135	321.091	41.096	22.206	0.2	N	32.4	1532.6	1611.8	1971.0	5147.8	402.6	0.453	0.866	0.184	168.97	2.818	39.949	126.048	154.135	322.951	39.397	22.568	0.3	N	27.2	1630.8	1611.8	1971.0	5240.9	409.8	0.446	0.927	0.184	255.72	2.364	42.511	126.048	154.135	325.058	38.759	24.171	0.4	N	23.0	1731.4	1611.8	1971.0	5337.3	417.4	0.439	1.004	0.184	342.09	2.002	45.134	126.048	154.135	327.319	38.109	26.183	0.5	N	19.8	1834.7	1611.8	1971.0	5437.4	425.2	0.431	1.087	0.184	428.00	1.724	47.825	126.048	154.135	329.732	37.473	28.332	0.6	N	21.3	1842.9	1611.8	1971.0	5447.1	428.0	0.449	1.145	0.184	392.05	1.853	48.039	126.048	154.135	330.075	39.011	29.844	0.66	N	19.7	1899.8	1611.8	1971.0	5502.4	430.3	0.445	1.192	0.184	434.36	1.716	49.521	126.048	154.135	331.420	38.687	31.075	North																			0	N	50.9	1310.3	1611.8	1971.0	4944.0	386.6	0.480	0.825	0.184		4.423	34.155	126.048	154.135	318.761	41.675	21.511	0.1	N	44.1	1359.8	1611.8	1971.0	4986.7	390.0	0.462	0.835	0.184	23.90	3.829	35.447	126.048	154.135	319.459	40.115	21.765	0.2	N	38.7	1410.5	1611.8	1971.0	5032.0	393.5	0.455	0.844	0.184	51.60	3.364	36.767	126.048	154.135	320.314	39.568	22.003	0.3	N	34.0	1462.3	1611.8	1971.0	5079.1	397.2	0.449	0.853	0.184	79.29	2.950	38.118	126.048	154.135	321.251	39.003	22.249	0.4	N	29.8	1515.2	1611.8	1971.0	5127.8	401.0	0.442	0.861	0.184	106.73	2.590	39.496	126.048	154.135	322.269	38.429	22.440	0.5	N	26.1	1569.2	1611.8	1971.0	5178.2	404.9	0.436	0.869	0.184	133.74	2.270	40.905	126.048	154.135	323.357	37.874	22.651	0.6	N	29.1	1542.2	1611.8	1971.0	5154.1	403.1	0.454	0.864	0.184	54.61	2.532	40.200	126.048	154.135	322.915	39.452	22.530	0.66	N	27.3	1570.0	1611.8	1971.0	5180.1	405.1	0.451	0.868	0.184	63.39	2.369	40.926	126.048	154.135	323.478	39.172	22.618																																																																																																																																					
0.66	N	3.0	1988.2	1611.8	1971.0	5574.1	435.9	0.300	1.002	0.184	583.56	0.262	51.827	126.048	154.135	332.272	26.107	26.129	East																			0	N	46.6	1360.0	1611.8	1971.0	4989.4	390.2	0.469	0.839	0.184		4.049	35.450	126.048	154.135	319.683	40.741	21.879	0.1	N	38.6	1459.4	1611.8	1971.0	5080.8	397.3	0.460	0.873	0.184	91.80	3.350	38.042	126.048	154.135	321.575	39.990	22.746	0.2	N	31.2	1564.7	1611.8	1971.0	5178.7	405.0	0.438	0.913	0.184	189.29	2.711	40.787	126.048	154.135	323.680	38.094	23.796	0.3	N	25.7	1672.8	1611.8	1971.0	5281.3	413.0	0.428	0.957	0.184	288.99	2.234	43.605	126.048	154.135	326.022	37.225	24.951	0.4	N	21.4	1783.3	1611.8	1971.0	5387.6	421.3	0.418	1.006	0.184	384.36	1.859	46.486	126.048	154.135	328.528	36.342	26.215	0.5	N	18.0	1896.1	1611.8	1971.0	5496.9	429.9	0.408	1.088	0.184	481.30	1.564	49.425	126.048	154.135	331.172	35.473	28.358	0.6	N	19.5	1910.7	1611.8	1971.0	5513.0	431.1	0.425	1.143	0.184	452.81	1.691	49.805	126.048	154.135	331.680	36.888	29.792	0.66	N	17.8	1973.0	1611.8	1971.0	5573.6	435.9	0.419	1.190	0.184	501.52	1.548	51.430	126.048	154.135	333.161	36.437	31.020	West																			0	N	48.0	1346.0	1611.8	1971.0	4976.8	389.2	0.479	0.837	0.184		4.172	35.085	126.048	154.135	319.440	41.636	21.817	0.1	N	39.7	1436.9	1611.8	1971.0	5059.5	395.7	0.473	0.852	0.184	82.17	3.453	37.456	126.048	154.135	321.091	41.096	22.206	0.2	N	32.4	1532.6	1611.8	1971.0	5147.8	402.6	0.453	0.866	0.184	168.97	2.818	39.949	126.048	154.135	322.951	39.397	22.568	0.3	N	27.2	1630.8	1611.8	1971.0	5240.9	409.8	0.446	0.927	0.184	255.72	2.364	42.511	126.048	154.135	325.058	38.759	24.171	0.4	N	23.0	1731.4	1611.8	1971.0	5337.3	417.4	0.439	1.004	0.184	342.09	2.002	45.134	126.048	154.135	327.319	38.109	26.183	0.5	N	19.8	1834.7	1611.8	1971.0	5437.4	425.2	0.431	1.087	0.184	428.00	1.724	47.825	126.048	154.135	329.732	37.473	28.332	0.6	N	21.3	1842.9	1611.8	1971.0	5447.1	428.0	0.449	1.145	0.184	392.05	1.853	48.039	126.048	154.135	330.075	39.011	29.844	0.66	N	19.7	1899.8	1611.8	1971.0	5502.4	430.3	0.445	1.192	0.184	434.36	1.716	49.521	126.048	154.135	331.420	38.687	31.075	North																			0	N	50.9	1310.3	1611.8	1971.0	4944.0	386.6	0.480	0.825	0.184		4.423	34.155	126.048	154.135	318.761	41.675	21.511	0.1	N	44.1	1359.8	1611.8	1971.0	4986.7	390.0	0.462	0.835	0.184	23.90	3.829	35.447	126.048	154.135	319.459	40.115	21.765	0.2	N	38.7	1410.5	1611.8	1971.0	5032.0	393.5	0.455	0.844	0.184	51.60	3.364	36.767	126.048	154.135	320.314	39.568	22.003	0.3	N	34.0	1462.3	1611.8	1971.0	5079.1	397.2	0.449	0.853	0.184	79.29	2.950	38.118	126.048	154.135	321.251	39.003	22.249	0.4	N	29.8	1515.2	1611.8	1971.0	5127.8	401.0	0.442	0.861	0.184	106.73	2.590	39.496	126.048	154.135	322.269	38.429	22.440	0.5	N	26.1	1569.2	1611.8	1971.0	5178.2	404.9	0.436	0.869	0.184	133.74	2.270	40.905	126.048	154.135	323.357	37.874	22.651	0.6	N	29.1	1542.2	1611.8	1971.0	5154.1	403.1	0.454	0.864	0.184	54.61	2.532	40.200	126.048	154.135	322.915	39.452	22.530	0.66	N	27.3	1570.0	1611.8	1971.0	5180.1	405.1	0.451	0.868	0.184	63.39	2.369	40.926	126.048	154.135	323.478	39.172	22.618																																																																																																																																																								
East																			0	N	46.6	1360.0	1611.8	1971.0	4989.4	390.2	0.469	0.839	0.184		4.049	35.450	126.048	154.135	319.683	40.741	21.879	0.1	N	38.6	1459.4	1611.8	1971.0	5080.8	397.3	0.460	0.873	0.184	91.80	3.350	38.042	126.048	154.135	321.575	39.990	22.746	0.2	N	31.2	1564.7	1611.8	1971.0	5178.7	405.0	0.438	0.913	0.184	189.29	2.711	40.787	126.048	154.135	323.680	38.094	23.796	0.3	N	25.7	1672.8	1611.8	1971.0	5281.3	413.0	0.428	0.957	0.184	288.99	2.234	43.605	126.048	154.135	326.022	37.225	24.951	0.4	N	21.4	1783.3	1611.8	1971.0	5387.6	421.3	0.418	1.006	0.184	384.36	1.859	46.486	126.048	154.135	328.528	36.342	26.215	0.5	N	18.0	1896.1	1611.8	1971.0	5496.9	429.9	0.408	1.088	0.184	481.30	1.564	49.425	126.048	154.135	331.172	35.473	28.358	0.6	N	19.5	1910.7	1611.8	1971.0	5513.0	431.1	0.425	1.143	0.184	452.81	1.691	49.805	126.048	154.135	331.680	36.888	29.792	0.66	N	17.8	1973.0	1611.8	1971.0	5573.6	435.9	0.419	1.190	0.184	501.52	1.548	51.430	126.048	154.135	333.161	36.437	31.020	West																			0	N	48.0	1346.0	1611.8	1971.0	4976.8	389.2	0.479	0.837	0.184		4.172	35.085	126.048	154.135	319.440	41.636	21.817	0.1	N	39.7	1436.9	1611.8	1971.0	5059.5	395.7	0.473	0.852	0.184	82.17	3.453	37.456	126.048	154.135	321.091	41.096	22.206	0.2	N	32.4	1532.6	1611.8	1971.0	5147.8	402.6	0.453	0.866	0.184	168.97	2.818	39.949	126.048	154.135	322.951	39.397	22.568	0.3	N	27.2	1630.8	1611.8	1971.0	5240.9	409.8	0.446	0.927	0.184	255.72	2.364	42.511	126.048	154.135	325.058	38.759	24.171	0.4	N	23.0	1731.4	1611.8	1971.0	5337.3	417.4	0.439	1.004	0.184	342.09	2.002	45.134	126.048	154.135	327.319	38.109	26.183	0.5	N	19.8	1834.7	1611.8	1971.0	5437.4	425.2	0.431	1.087	0.184	428.00	1.724	47.825	126.048	154.135	329.732	37.473	28.332	0.6	N	21.3	1842.9	1611.8	1971.0	5447.1	428.0	0.449	1.145	0.184	392.05	1.853	48.039	126.048	154.135	330.075	39.011	29.844	0.66	N	19.7	1899.8	1611.8	1971.0	5502.4	430.3	0.445	1.192	0.184	434.36	1.716	49.521	126.048	154.135	331.420	38.687	31.075	North																			0	N	50.9	1310.3	1611.8	1971.0	4944.0	386.6	0.480	0.825	0.184		4.423	34.155	126.048	154.135	318.761	41.675	21.511	0.1	N	44.1	1359.8	1611.8	1971.0	4986.7	390.0	0.462	0.835	0.184	23.90	3.829	35.447	126.048	154.135	319.459	40.115	21.765	0.2	N	38.7	1410.5	1611.8	1971.0	5032.0	393.5	0.455	0.844	0.184	51.60	3.364	36.767	126.048	154.135	320.314	39.568	22.003	0.3	N	34.0	1462.3	1611.8	1971.0	5079.1	397.2	0.449	0.853	0.184	79.29	2.950	38.118	126.048	154.135	321.251	39.003	22.249	0.4	N	29.8	1515.2	1611.8	1971.0	5127.8	401.0	0.442	0.861	0.184	106.73	2.590	39.496	126.048	154.135	322.269	38.429	22.440	0.5	N	26.1	1569.2	1611.8	1971.0	5178.2	404.9	0.436	0.869	0.184	133.74	2.270	40.905	126.048	154.135	323.357	37.874	22.651	0.6	N	29.1	1542.2	1611.8	1971.0	5154.1	403.1	0.454	0.864	0.184	54.61	2.532	40.200	126.048	154.135	322.915	39.452	22.530	0.66	N	27.3	1570.0	1611.8	1971.0	5180.1	405.1	0.451	0.868	0.184	63.39	2.369	40.926	126.048	154.135	323.478	39.172	22.618																																																																																																																																																																											
0	N	46.6	1360.0	1611.8	1971.0	4989.4	390.2	0.469	0.839	0.184		4.049	35.450	126.048	154.135	319.683	40.741	21.879	0.1	N	38.6	1459.4	1611.8	1971.0	5080.8	397.3	0.460	0.873	0.184	91.80	3.350	38.042	126.048	154.135	321.575	39.990	22.746	0.2	N	31.2	1564.7	1611.8	1971.0	5178.7	405.0	0.438	0.913	0.184	189.29	2.711	40.787	126.048	154.135	323.680	38.094	23.796	0.3	N	25.7	1672.8	1611.8	1971.0	5281.3	413.0	0.428	0.957	0.184	288.99	2.234	43.605	126.048	154.135	326.022	37.225	24.951	0.4	N	21.4	1783.3	1611.8	1971.0	5387.6	421.3	0.418	1.006	0.184	384.36	1.859	46.486	126.048	154.135	328.528	36.342	26.215	0.5	N	18.0	1896.1	1611.8	1971.0	5496.9	429.9	0.408	1.088	0.184	481.30	1.564	49.425	126.048	154.135	331.172	35.473	28.358	0.6	N	19.5	1910.7	1611.8	1971.0	5513.0	431.1	0.425	1.143	0.184	452.81	1.691	49.805	126.048	154.135	331.680	36.888	29.792	0.66	N	17.8	1973.0	1611.8	1971.0	5573.6	435.9	0.419	1.190	0.184	501.52	1.548	51.430	126.048	154.135	333.161	36.437	31.020	West																			0	N	48.0	1346.0	1611.8	1971.0	4976.8	389.2	0.479	0.837	0.184		4.172	35.085	126.048	154.135	319.440	41.636	21.817	0.1	N	39.7	1436.9	1611.8	1971.0	5059.5	395.7	0.473	0.852	0.184	82.17	3.453	37.456	126.048	154.135	321.091	41.096	22.206	0.2	N	32.4	1532.6	1611.8	1971.0	5147.8	402.6	0.453	0.866	0.184	168.97	2.818	39.949	126.048	154.135	322.951	39.397	22.568	0.3	N	27.2	1630.8	1611.8	1971.0	5240.9	409.8	0.446	0.927	0.184	255.72	2.364	42.511	126.048	154.135	325.058	38.759	24.171	0.4	N	23.0	1731.4	1611.8	1971.0	5337.3	417.4	0.439	1.004	0.184	342.09	2.002	45.134	126.048	154.135	327.319	38.109	26.183	0.5	N	19.8	1834.7	1611.8	1971.0	5437.4	425.2	0.431	1.087	0.184	428.00	1.724	47.825	126.048	154.135	329.732	37.473	28.332	0.6	N	21.3	1842.9	1611.8	1971.0	5447.1	428.0	0.449	1.145	0.184	392.05	1.853	48.039	126.048	154.135	330.075	39.011	29.844	0.66	N	19.7	1899.8	1611.8	1971.0	5502.4	430.3	0.445	1.192	0.184	434.36	1.716	49.521	126.048	154.135	331.420	38.687	31.075	North																			0	N	50.9	1310.3	1611.8	1971.0	4944.0	386.6	0.480	0.825	0.184		4.423	34.155	126.048	154.135	318.761	41.675	21.511	0.1	N	44.1	1359.8	1611.8	1971.0	4986.7	390.0	0.462	0.835	0.184	23.90	3.829	35.447	126.048	154.135	319.459	40.115	21.765	0.2	N	38.7	1410.5	1611.8	1971.0	5032.0	393.5	0.455	0.844	0.184	51.60	3.364	36.767	126.048	154.135	320.314	39.568	22.003	0.3	N	34.0	1462.3	1611.8	1971.0	5079.1	397.2	0.449	0.853	0.184	79.29	2.950	38.118	126.048	154.135	321.251	39.003	22.249	0.4	N	29.8	1515.2	1611.8	1971.0	5127.8	401.0	0.442	0.861	0.184	106.73	2.590	39.496	126.048	154.135	322.269	38.429	22.440	0.5	N	26.1	1569.2	1611.8	1971.0	5178.2	404.9	0.436	0.869	0.184	133.74	2.270	40.905	126.048	154.135	323.357	37.874	22.651	0.6	N	29.1	1542.2	1611.8	1971.0	5154.1	403.1	0.454	0.864	0.184	54.61	2.532	40.200	126.048	154.135	322.915	39.452	22.530	0.66	N	27.3	1570.0	1611.8	1971.0	5180.1	405.1	0.451	0.868	0.184	63.39	2.369	40.926	126.048	154.135	323.478	39.172	22.618																																																																																																																																																																																														
0.1	N	38.6	1459.4	1611.8	1971.0	5080.8	397.3	0.460	0.873	0.184	91.80	3.350	38.042	126.048	154.135	321.575	39.990	22.746	0.2	N	31.2	1564.7	1611.8	1971.0	5178.7	405.0	0.438	0.913	0.184	189.29	2.711	40.787	126.048	154.135	323.680	38.094	23.796	0.3	N	25.7	1672.8	1611.8	1971.0	5281.3	413.0	0.428	0.957	0.184	288.99	2.234	43.605	126.048	154.135	326.022	37.225	24.951	0.4	N	21.4	1783.3	1611.8	1971.0	5387.6	421.3	0.418	1.006	0.184	384.36	1.859	46.486	126.048	154.135	328.528	36.342	26.215	0.5	N	18.0	1896.1	1611.8	1971.0	5496.9	429.9	0.408	1.088	0.184	481.30	1.564	49.425	126.048	154.135	331.172	35.473	28.358	0.6	N	19.5	1910.7	1611.8	1971.0	5513.0	431.1	0.425	1.143	0.184	452.81	1.691	49.805	126.048	154.135	331.680	36.888	29.792	0.66	N	17.8	1973.0	1611.8	1971.0	5573.6	435.9	0.419	1.190	0.184	501.52	1.548	51.430	126.048	154.135	333.161	36.437	31.020	West																			0	N	48.0	1346.0	1611.8	1971.0	4976.8	389.2	0.479	0.837	0.184		4.172	35.085	126.048	154.135	319.440	41.636	21.817	0.1	N	39.7	1436.9	1611.8	1971.0	5059.5	395.7	0.473	0.852	0.184	82.17	3.453	37.456	126.048	154.135	321.091	41.096	22.206	0.2	N	32.4	1532.6	1611.8	1971.0	5147.8	402.6	0.453	0.866	0.184	168.97	2.818	39.949	126.048	154.135	322.951	39.397	22.568	0.3	N	27.2	1630.8	1611.8	1971.0	5240.9	409.8	0.446	0.927	0.184	255.72	2.364	42.511	126.048	154.135	325.058	38.759	24.171	0.4	N	23.0	1731.4	1611.8	1971.0	5337.3	417.4	0.439	1.004	0.184	342.09	2.002	45.134	126.048	154.135	327.319	38.109	26.183	0.5	N	19.8	1834.7	1611.8	1971.0	5437.4	425.2	0.431	1.087	0.184	428.00	1.724	47.825	126.048	154.135	329.732	37.473	28.332	0.6	N	21.3	1842.9	1611.8	1971.0	5447.1	428.0	0.449	1.145	0.184	392.05	1.853	48.039	126.048	154.135	330.075	39.011	29.844	0.66	N	19.7	1899.8	1611.8	1971.0	5502.4	430.3	0.445	1.192	0.184	434.36	1.716	49.521	126.048	154.135	331.420	38.687	31.075	North																			0	N	50.9	1310.3	1611.8	1971.0	4944.0	386.6	0.480	0.825	0.184		4.423	34.155	126.048	154.135	318.761	41.675	21.511	0.1	N	44.1	1359.8	1611.8	1971.0	4986.7	390.0	0.462	0.835	0.184	23.90	3.829	35.447	126.048	154.135	319.459	40.115	21.765	0.2	N	38.7	1410.5	1611.8	1971.0	5032.0	393.5	0.455	0.844	0.184	51.60	3.364	36.767	126.048	154.135	320.314	39.568	22.003	0.3	N	34.0	1462.3	1611.8	1971.0	5079.1	397.2	0.449	0.853	0.184	79.29	2.950	38.118	126.048	154.135	321.251	39.003	22.249	0.4	N	29.8	1515.2	1611.8	1971.0	5127.8	401.0	0.442	0.861	0.184	106.73	2.590	39.496	126.048	154.135	322.269	38.429	22.440	0.5	N	26.1	1569.2	1611.8	1971.0	5178.2	404.9	0.436	0.869	0.184	133.74	2.270	40.905	126.048	154.135	323.357	37.874	22.651	0.6	N	29.1	1542.2	1611.8	1971.0	5154.1	403.1	0.454	0.864	0.184	54.61	2.532	40.200	126.048	154.135	322.915	39.452	22.530	0.66	N	27.3	1570.0	1611.8	1971.0	5180.1	405.1	0.451	0.868	0.184	63.39	2.369	40.926	126.048	154.135	323.478	39.172	22.618																																																																																																																																																																																																																	
0.2	N	31.2	1564.7	1611.8	1971.0	5178.7	405.0	0.438	0.913	0.184	189.29	2.711	40.787	126.048	154.135	323.680	38.094	23.796	0.3	N	25.7	1672.8	1611.8	1971.0	5281.3	413.0	0.428	0.957	0.184	288.99	2.234	43.605	126.048	154.135	326.022	37.225	24.951	0.4	N	21.4	1783.3	1611.8	1971.0	5387.6	421.3	0.418	1.006	0.184	384.36	1.859	46.486	126.048	154.135	328.528	36.342	26.215	0.5	N	18.0	1896.1	1611.8	1971.0	5496.9	429.9	0.408	1.088	0.184	481.30	1.564	49.425	126.048	154.135	331.172	35.473	28.358	0.6	N	19.5	1910.7	1611.8	1971.0	5513.0	431.1	0.425	1.143	0.184	452.81	1.691	49.805	126.048	154.135	331.680	36.888	29.792	0.66	N	17.8	1973.0	1611.8	1971.0	5573.6	435.9	0.419	1.190	0.184	501.52	1.548	51.430	126.048	154.135	333.161	36.437	31.020	West																			0	N	48.0	1346.0	1611.8	1971.0	4976.8	389.2	0.479	0.837	0.184		4.172	35.085	126.048	154.135	319.440	41.636	21.817	0.1	N	39.7	1436.9	1611.8	1971.0	5059.5	395.7	0.473	0.852	0.184	82.17	3.453	37.456	126.048	154.135	321.091	41.096	22.206	0.2	N	32.4	1532.6	1611.8	1971.0	5147.8	402.6	0.453	0.866	0.184	168.97	2.818	39.949	126.048	154.135	322.951	39.397	22.568	0.3	N	27.2	1630.8	1611.8	1971.0	5240.9	409.8	0.446	0.927	0.184	255.72	2.364	42.511	126.048	154.135	325.058	38.759	24.171	0.4	N	23.0	1731.4	1611.8	1971.0	5337.3	417.4	0.439	1.004	0.184	342.09	2.002	45.134	126.048	154.135	327.319	38.109	26.183	0.5	N	19.8	1834.7	1611.8	1971.0	5437.4	425.2	0.431	1.087	0.184	428.00	1.724	47.825	126.048	154.135	329.732	37.473	28.332	0.6	N	21.3	1842.9	1611.8	1971.0	5447.1	428.0	0.449	1.145	0.184	392.05	1.853	48.039	126.048	154.135	330.075	39.011	29.844	0.66	N	19.7	1899.8	1611.8	1971.0	5502.4	430.3	0.445	1.192	0.184	434.36	1.716	49.521	126.048	154.135	331.420	38.687	31.075	North																			0	N	50.9	1310.3	1611.8	1971.0	4944.0	386.6	0.480	0.825	0.184		4.423	34.155	126.048	154.135	318.761	41.675	21.511	0.1	N	44.1	1359.8	1611.8	1971.0	4986.7	390.0	0.462	0.835	0.184	23.90	3.829	35.447	126.048	154.135	319.459	40.115	21.765	0.2	N	38.7	1410.5	1611.8	1971.0	5032.0	393.5	0.455	0.844	0.184	51.60	3.364	36.767	126.048	154.135	320.314	39.568	22.003	0.3	N	34.0	1462.3	1611.8	1971.0	5079.1	397.2	0.449	0.853	0.184	79.29	2.950	38.118	126.048	154.135	321.251	39.003	22.249	0.4	N	29.8	1515.2	1611.8	1971.0	5127.8	401.0	0.442	0.861	0.184	106.73	2.590	39.496	126.048	154.135	322.269	38.429	22.440	0.5	N	26.1	1569.2	1611.8	1971.0	5178.2	404.9	0.436	0.869	0.184	133.74	2.270	40.905	126.048	154.135	323.357	37.874	22.651	0.6	N	29.1	1542.2	1611.8	1971.0	5154.1	403.1	0.454	0.864	0.184	54.61	2.532	40.200	126.048	154.135	322.915	39.452	22.530	0.66	N	27.3	1570.0	1611.8	1971.0	5180.1	405.1	0.451	0.868	0.184	63.39	2.369	40.926	126.048	154.135	323.478	39.172	22.618																																																																																																																																																																																																																																				
0.3	N	25.7	1672.8	1611.8	1971.0	5281.3	413.0	0.428	0.957	0.184	288.99	2.234	43.605	126.048	154.135	326.022	37.225	24.951	0.4	N	21.4	1783.3	1611.8	1971.0	5387.6	421.3	0.418	1.006	0.184	384.36	1.859	46.486	126.048	154.135	328.528	36.342	26.215	0.5	N	18.0	1896.1	1611.8	1971.0	5496.9	429.9	0.408	1.088	0.184	481.30	1.564	49.425	126.048	154.135	331.172	35.473	28.358	0.6	N	19.5	1910.7	1611.8	1971.0	5513.0	431.1	0.425	1.143	0.184	452.81	1.691	49.805	126.048	154.135	331.680	36.888	29.792	0.66	N	17.8	1973.0	1611.8	1971.0	5573.6	435.9	0.419	1.190	0.184	501.52	1.548	51.430	126.048	154.135	333.161	36.437	31.020	West																			0	N	48.0	1346.0	1611.8	1971.0	4976.8	389.2	0.479	0.837	0.184		4.172	35.085	126.048	154.135	319.440	41.636	21.817	0.1	N	39.7	1436.9	1611.8	1971.0	5059.5	395.7	0.473	0.852	0.184	82.17	3.453	37.456	126.048	154.135	321.091	41.096	22.206	0.2	N	32.4	1532.6	1611.8	1971.0	5147.8	402.6	0.453	0.866	0.184	168.97	2.818	39.949	126.048	154.135	322.951	39.397	22.568	0.3	N	27.2	1630.8	1611.8	1971.0	5240.9	409.8	0.446	0.927	0.184	255.72	2.364	42.511	126.048	154.135	325.058	38.759	24.171	0.4	N	23.0	1731.4	1611.8	1971.0	5337.3	417.4	0.439	1.004	0.184	342.09	2.002	45.134	126.048	154.135	327.319	38.109	26.183	0.5	N	19.8	1834.7	1611.8	1971.0	5437.4	425.2	0.431	1.087	0.184	428.00	1.724	47.825	126.048	154.135	329.732	37.473	28.332	0.6	N	21.3	1842.9	1611.8	1971.0	5447.1	428.0	0.449	1.145	0.184	392.05	1.853	48.039	126.048	154.135	330.075	39.011	29.844	0.66	N	19.7	1899.8	1611.8	1971.0	5502.4	430.3	0.445	1.192	0.184	434.36	1.716	49.521	126.048	154.135	331.420	38.687	31.075	North																			0	N	50.9	1310.3	1611.8	1971.0	4944.0	386.6	0.480	0.825	0.184		4.423	34.155	126.048	154.135	318.761	41.675	21.511	0.1	N	44.1	1359.8	1611.8	1971.0	4986.7	390.0	0.462	0.835	0.184	23.90	3.829	35.447	126.048	154.135	319.459	40.115	21.765	0.2	N	38.7	1410.5	1611.8	1971.0	5032.0	393.5	0.455	0.844	0.184	51.60	3.364	36.767	126.048	154.135	320.314	39.568	22.003	0.3	N	34.0	1462.3	1611.8	1971.0	5079.1	397.2	0.449	0.853	0.184	79.29	2.950	38.118	126.048	154.135	321.251	39.003	22.249	0.4	N	29.8	1515.2	1611.8	1971.0	5127.8	401.0	0.442	0.861	0.184	106.73	2.590	39.496	126.048	154.135	322.269	38.429	22.440	0.5	N	26.1	1569.2	1611.8	1971.0	5178.2	404.9	0.436	0.869	0.184	133.74	2.270	40.905	126.048	154.135	323.357	37.874	22.651	0.6	N	29.1	1542.2	1611.8	1971.0	5154.1	403.1	0.454	0.864	0.184	54.61	2.532	40.200	126.048	154.135	322.915	39.452	22.530	0.66	N	27.3	1570.0	1611.8	1971.0	5180.1	405.1	0.451	0.868	0.184	63.39	2.369	40.926	126.048	154.135	323.478	39.172	22.618																																																																																																																																																																																																																																																							
0.4	N	21.4	1783.3	1611.8	1971.0	5387.6	421.3	0.418	1.006	0.184	384.36	1.859	46.486	126.048	154.135	328.528	36.342	26.215	0.5	N	18.0	1896.1	1611.8	1971.0	5496.9	429.9	0.408	1.088	0.184	481.30	1.564	49.425	126.048	154.135	331.172	35.473	28.358	0.6	N	19.5	1910.7	1611.8	1971.0	5513.0	431.1	0.425	1.143	0.184	452.81	1.691	49.805	126.048	154.135	331.680	36.888	29.792	0.66	N	17.8	1973.0	1611.8	1971.0	5573.6	435.9	0.419	1.190	0.184	501.52	1.548	51.430	126.048	154.135	333.161	36.437	31.020	West																			0	N	48.0	1346.0	1611.8	1971.0	4976.8	389.2	0.479	0.837	0.184		4.172	35.085	126.048	154.135	319.440	41.636	21.817	0.1	N	39.7	1436.9	1611.8	1971.0	5059.5	395.7	0.473	0.852	0.184	82.17	3.453	37.456	126.048	154.135	321.091	41.096	22.206	0.2	N	32.4	1532.6	1611.8	1971.0	5147.8	402.6	0.453	0.866	0.184	168.97	2.818	39.949	126.048	154.135	322.951	39.397	22.568	0.3	N	27.2	1630.8	1611.8	1971.0	5240.9	409.8	0.446	0.927	0.184	255.72	2.364	42.511	126.048	154.135	325.058	38.759	24.171	0.4	N	23.0	1731.4	1611.8	1971.0	5337.3	417.4	0.439	1.004	0.184	342.09	2.002	45.134	126.048	154.135	327.319	38.109	26.183	0.5	N	19.8	1834.7	1611.8	1971.0	5437.4	425.2	0.431	1.087	0.184	428.00	1.724	47.825	126.048	154.135	329.732	37.473	28.332	0.6	N	21.3	1842.9	1611.8	1971.0	5447.1	428.0	0.449	1.145	0.184	392.05	1.853	48.039	126.048	154.135	330.075	39.011	29.844	0.66	N	19.7	1899.8	1611.8	1971.0	5502.4	430.3	0.445	1.192	0.184	434.36	1.716	49.521	126.048	154.135	331.420	38.687	31.075	North																			0	N	50.9	1310.3	1611.8	1971.0	4944.0	386.6	0.480	0.825	0.184		4.423	34.155	126.048	154.135	318.761	41.675	21.511	0.1	N	44.1	1359.8	1611.8	1971.0	4986.7	390.0	0.462	0.835	0.184	23.90	3.829	35.447	126.048	154.135	319.459	40.115	21.765	0.2	N	38.7	1410.5	1611.8	1971.0	5032.0	393.5	0.455	0.844	0.184	51.60	3.364	36.767	126.048	154.135	320.314	39.568	22.003	0.3	N	34.0	1462.3	1611.8	1971.0	5079.1	397.2	0.449	0.853	0.184	79.29	2.950	38.118	126.048	154.135	321.251	39.003	22.249	0.4	N	29.8	1515.2	1611.8	1971.0	5127.8	401.0	0.442	0.861	0.184	106.73	2.590	39.496	126.048	154.135	322.269	38.429	22.440	0.5	N	26.1	1569.2	1611.8	1971.0	5178.2	404.9	0.436	0.869	0.184	133.74	2.270	40.905	126.048	154.135	323.357	37.874	22.651	0.6	N	29.1	1542.2	1611.8	1971.0	5154.1	403.1	0.454	0.864	0.184	54.61	2.532	40.200	126.048	154.135	322.915	39.452	22.530	0.66	N	27.3	1570.0	1611.8	1971.0	5180.1	405.1	0.451	0.868	0.184	63.39	2.369	40.926	126.048	154.135	323.478	39.172	22.618																																																																																																																																																																																																																																																																										
0.5	N	18.0	1896.1	1611.8	1971.0	5496.9	429.9	0.408	1.088	0.184	481.30	1.564	49.425	126.048	154.135	331.172	35.473	28.358	0.6	N	19.5	1910.7	1611.8	1971.0	5513.0	431.1	0.425	1.143	0.184	452.81	1.691	49.805	126.048	154.135	331.680	36.888	29.792	0.66	N	17.8	1973.0	1611.8	1971.0	5573.6	435.9	0.419	1.190	0.184	501.52	1.548	51.430	126.048	154.135	333.161	36.437	31.020	West																			0	N	48.0	1346.0	1611.8	1971.0	4976.8	389.2	0.479	0.837	0.184		4.172	35.085	126.048	154.135	319.440	41.636	21.817	0.1	N	39.7	1436.9	1611.8	1971.0	5059.5	395.7	0.473	0.852	0.184	82.17	3.453	37.456	126.048	154.135	321.091	41.096	22.206	0.2	N	32.4	1532.6	1611.8	1971.0	5147.8	402.6	0.453	0.866	0.184	168.97	2.818	39.949	126.048	154.135	322.951	39.397	22.568	0.3	N	27.2	1630.8	1611.8	1971.0	5240.9	409.8	0.446	0.927	0.184	255.72	2.364	42.511	126.048	154.135	325.058	38.759	24.171	0.4	N	23.0	1731.4	1611.8	1971.0	5337.3	417.4	0.439	1.004	0.184	342.09	2.002	45.134	126.048	154.135	327.319	38.109	26.183	0.5	N	19.8	1834.7	1611.8	1971.0	5437.4	425.2	0.431	1.087	0.184	428.00	1.724	47.825	126.048	154.135	329.732	37.473	28.332	0.6	N	21.3	1842.9	1611.8	1971.0	5447.1	428.0	0.449	1.145	0.184	392.05	1.853	48.039	126.048	154.135	330.075	39.011	29.844	0.66	N	19.7	1899.8	1611.8	1971.0	5502.4	430.3	0.445	1.192	0.184	434.36	1.716	49.521	126.048	154.135	331.420	38.687	31.075	North																			0	N	50.9	1310.3	1611.8	1971.0	4944.0	386.6	0.480	0.825	0.184		4.423	34.155	126.048	154.135	318.761	41.675	21.511	0.1	N	44.1	1359.8	1611.8	1971.0	4986.7	390.0	0.462	0.835	0.184	23.90	3.829	35.447	126.048	154.135	319.459	40.115	21.765	0.2	N	38.7	1410.5	1611.8	1971.0	5032.0	393.5	0.455	0.844	0.184	51.60	3.364	36.767	126.048	154.135	320.314	39.568	22.003	0.3	N	34.0	1462.3	1611.8	1971.0	5079.1	397.2	0.449	0.853	0.184	79.29	2.950	38.118	126.048	154.135	321.251	39.003	22.249	0.4	N	29.8	1515.2	1611.8	1971.0	5127.8	401.0	0.442	0.861	0.184	106.73	2.590	39.496	126.048	154.135	322.269	38.429	22.440	0.5	N	26.1	1569.2	1611.8	1971.0	5178.2	404.9	0.436	0.869	0.184	133.74	2.270	40.905	126.048	154.135	323.357	37.874	22.651	0.6	N	29.1	1542.2	1611.8	1971.0	5154.1	403.1	0.454	0.864	0.184	54.61	2.532	40.200	126.048	154.135	322.915	39.452	22.530	0.66	N	27.3	1570.0	1611.8	1971.0	5180.1	405.1	0.451	0.868	0.184	63.39	2.369	40.926	126.048	154.135	323.478	39.172	22.618																																																																																																																																																																																																																																																																																													
0.6	N	19.5	1910.7	1611.8	1971.0	5513.0	431.1	0.425	1.143	0.184	452.81	1.691	49.805	126.048	154.135	331.680	36.888	29.792	0.66	N	17.8	1973.0	1611.8	1971.0	5573.6	435.9	0.419	1.190	0.184	501.52	1.548	51.430	126.048	154.135	333.161	36.437	31.020	West																			0	N	48.0	1346.0	1611.8	1971.0	4976.8	389.2	0.479	0.837	0.184		4.172	35.085	126.048	154.135	319.440	41.636	21.817	0.1	N	39.7	1436.9	1611.8	1971.0	5059.5	395.7	0.473	0.852	0.184	82.17	3.453	37.456	126.048	154.135	321.091	41.096	22.206	0.2	N	32.4	1532.6	1611.8	1971.0	5147.8	402.6	0.453	0.866	0.184	168.97	2.818	39.949	126.048	154.135	322.951	39.397	22.568	0.3	N	27.2	1630.8	1611.8	1971.0	5240.9	409.8	0.446	0.927	0.184	255.72	2.364	42.511	126.048	154.135	325.058	38.759	24.171	0.4	N	23.0	1731.4	1611.8	1971.0	5337.3	417.4	0.439	1.004	0.184	342.09	2.002	45.134	126.048	154.135	327.319	38.109	26.183	0.5	N	19.8	1834.7	1611.8	1971.0	5437.4	425.2	0.431	1.087	0.184	428.00	1.724	47.825	126.048	154.135	329.732	37.473	28.332	0.6	N	21.3	1842.9	1611.8	1971.0	5447.1	428.0	0.449	1.145	0.184	392.05	1.853	48.039	126.048	154.135	330.075	39.011	29.844	0.66	N	19.7	1899.8	1611.8	1971.0	5502.4	430.3	0.445	1.192	0.184	434.36	1.716	49.521	126.048	154.135	331.420	38.687	31.075	North																			0	N	50.9	1310.3	1611.8	1971.0	4944.0	386.6	0.480	0.825	0.184		4.423	34.155	126.048	154.135	318.761	41.675	21.511	0.1	N	44.1	1359.8	1611.8	1971.0	4986.7	390.0	0.462	0.835	0.184	23.90	3.829	35.447	126.048	154.135	319.459	40.115	21.765	0.2	N	38.7	1410.5	1611.8	1971.0	5032.0	393.5	0.455	0.844	0.184	51.60	3.364	36.767	126.048	154.135	320.314	39.568	22.003	0.3	N	34.0	1462.3	1611.8	1971.0	5079.1	397.2	0.449	0.853	0.184	79.29	2.950	38.118	126.048	154.135	321.251	39.003	22.249	0.4	N	29.8	1515.2	1611.8	1971.0	5127.8	401.0	0.442	0.861	0.184	106.73	2.590	39.496	126.048	154.135	322.269	38.429	22.440	0.5	N	26.1	1569.2	1611.8	1971.0	5178.2	404.9	0.436	0.869	0.184	133.74	2.270	40.905	126.048	154.135	323.357	37.874	22.651	0.6	N	29.1	1542.2	1611.8	1971.0	5154.1	403.1	0.454	0.864	0.184	54.61	2.532	40.200	126.048	154.135	322.915	39.452	22.530	0.66	N	27.3	1570.0	1611.8	1971.0	5180.1	405.1	0.451	0.868	0.184	63.39	2.369	40.926	126.048	154.135	323.478	39.172	22.618																																																																																																																																																																																																																																																																																																																
0.66	N	17.8	1973.0	1611.8	1971.0	5573.6	435.9	0.419	1.190	0.184	501.52	1.548	51.430	126.048	154.135	333.161	36.437	31.020	West																			0	N	48.0	1346.0	1611.8	1971.0	4976.8	389.2	0.479	0.837	0.184		4.172	35.085	126.048	154.135	319.440	41.636	21.817	0.1	N	39.7	1436.9	1611.8	1971.0	5059.5	395.7	0.473	0.852	0.184	82.17	3.453	37.456	126.048	154.135	321.091	41.096	22.206	0.2	N	32.4	1532.6	1611.8	1971.0	5147.8	402.6	0.453	0.866	0.184	168.97	2.818	39.949	126.048	154.135	322.951	39.397	22.568	0.3	N	27.2	1630.8	1611.8	1971.0	5240.9	409.8	0.446	0.927	0.184	255.72	2.364	42.511	126.048	154.135	325.058	38.759	24.171	0.4	N	23.0	1731.4	1611.8	1971.0	5337.3	417.4	0.439	1.004	0.184	342.09	2.002	45.134	126.048	154.135	327.319	38.109	26.183	0.5	N	19.8	1834.7	1611.8	1971.0	5437.4	425.2	0.431	1.087	0.184	428.00	1.724	47.825	126.048	154.135	329.732	37.473	28.332	0.6	N	21.3	1842.9	1611.8	1971.0	5447.1	428.0	0.449	1.145	0.184	392.05	1.853	48.039	126.048	154.135	330.075	39.011	29.844	0.66	N	19.7	1899.8	1611.8	1971.0	5502.4	430.3	0.445	1.192	0.184	434.36	1.716	49.521	126.048	154.135	331.420	38.687	31.075	North																			0	N	50.9	1310.3	1611.8	1971.0	4944.0	386.6	0.480	0.825	0.184		4.423	34.155	126.048	154.135	318.761	41.675	21.511	0.1	N	44.1	1359.8	1611.8	1971.0	4986.7	390.0	0.462	0.835	0.184	23.90	3.829	35.447	126.048	154.135	319.459	40.115	21.765	0.2	N	38.7	1410.5	1611.8	1971.0	5032.0	393.5	0.455	0.844	0.184	51.60	3.364	36.767	126.048	154.135	320.314	39.568	22.003	0.3	N	34.0	1462.3	1611.8	1971.0	5079.1	397.2	0.449	0.853	0.184	79.29	2.950	38.118	126.048	154.135	321.251	39.003	22.249	0.4	N	29.8	1515.2	1611.8	1971.0	5127.8	401.0	0.442	0.861	0.184	106.73	2.590	39.496	126.048	154.135	322.269	38.429	22.440	0.5	N	26.1	1569.2	1611.8	1971.0	5178.2	404.9	0.436	0.869	0.184	133.74	2.270	40.905	126.048	154.135	323.357	37.874	22.651	0.6	N	29.1	1542.2	1611.8	1971.0	5154.1	403.1	0.454	0.864	0.184	54.61	2.532	40.200	126.048	154.135	322.915	39.452	22.530	0.66	N	27.3	1570.0	1611.8	1971.0	5180.1	405.1	0.451	0.868	0.184	63.39	2.369	40.926	126.048	154.135	323.478	39.172	22.618																																																																																																																																																																																																																																																																																																																																			
West																			0	N	48.0	1346.0	1611.8	1971.0	4976.8	389.2	0.479	0.837	0.184		4.172	35.085	126.048	154.135	319.440	41.636	21.817	0.1	N	39.7	1436.9	1611.8	1971.0	5059.5	395.7	0.473	0.852	0.184	82.17	3.453	37.456	126.048	154.135	321.091	41.096	22.206	0.2	N	32.4	1532.6	1611.8	1971.0	5147.8	402.6	0.453	0.866	0.184	168.97	2.818	39.949	126.048	154.135	322.951	39.397	22.568	0.3	N	27.2	1630.8	1611.8	1971.0	5240.9	409.8	0.446	0.927	0.184	255.72	2.364	42.511	126.048	154.135	325.058	38.759	24.171	0.4	N	23.0	1731.4	1611.8	1971.0	5337.3	417.4	0.439	1.004	0.184	342.09	2.002	45.134	126.048	154.135	327.319	38.109	26.183	0.5	N	19.8	1834.7	1611.8	1971.0	5437.4	425.2	0.431	1.087	0.184	428.00	1.724	47.825	126.048	154.135	329.732	37.473	28.332	0.6	N	21.3	1842.9	1611.8	1971.0	5447.1	428.0	0.449	1.145	0.184	392.05	1.853	48.039	126.048	154.135	330.075	39.011	29.844	0.66	N	19.7	1899.8	1611.8	1971.0	5502.4	430.3	0.445	1.192	0.184	434.36	1.716	49.521	126.048	154.135	331.420	38.687	31.075	North																			0	N	50.9	1310.3	1611.8	1971.0	4944.0	386.6	0.480	0.825	0.184		4.423	34.155	126.048	154.135	318.761	41.675	21.511	0.1	N	44.1	1359.8	1611.8	1971.0	4986.7	390.0	0.462	0.835	0.184	23.90	3.829	35.447	126.048	154.135	319.459	40.115	21.765	0.2	N	38.7	1410.5	1611.8	1971.0	5032.0	393.5	0.455	0.844	0.184	51.60	3.364	36.767	126.048	154.135	320.314	39.568	22.003	0.3	N	34.0	1462.3	1611.8	1971.0	5079.1	397.2	0.449	0.853	0.184	79.29	2.950	38.118	126.048	154.135	321.251	39.003	22.249	0.4	N	29.8	1515.2	1611.8	1971.0	5127.8	401.0	0.442	0.861	0.184	106.73	2.590	39.496	126.048	154.135	322.269	38.429	22.440	0.5	N	26.1	1569.2	1611.8	1971.0	5178.2	404.9	0.436	0.869	0.184	133.74	2.270	40.905	126.048	154.135	323.357	37.874	22.651	0.6	N	29.1	1542.2	1611.8	1971.0	5154.1	403.1	0.454	0.864	0.184	54.61	2.532	40.200	126.048	154.135	322.915	39.452	22.530	0.66	N	27.3	1570.0	1611.8	1971.0	5180.1	405.1	0.451	0.868	0.184	63.39	2.369	40.926	126.048	154.135	323.478	39.172	22.618																																																																																																																																																																																																																																																																																																																																																						
0	N	48.0	1346.0	1611.8	1971.0	4976.8	389.2	0.479	0.837	0.184		4.172	35.085	126.048	154.135	319.440	41.636	21.817	0.1	N	39.7	1436.9	1611.8	1971.0	5059.5	395.7	0.473	0.852	0.184	82.17	3.453	37.456	126.048	154.135	321.091	41.096	22.206	0.2	N	32.4	1532.6	1611.8	1971.0	5147.8	402.6	0.453	0.866	0.184	168.97	2.818	39.949	126.048	154.135	322.951	39.397	22.568	0.3	N	27.2	1630.8	1611.8	1971.0	5240.9	409.8	0.446	0.927	0.184	255.72	2.364	42.511	126.048	154.135	325.058	38.759	24.171	0.4	N	23.0	1731.4	1611.8	1971.0	5337.3	417.4	0.439	1.004	0.184	342.09	2.002	45.134	126.048	154.135	327.319	38.109	26.183	0.5	N	19.8	1834.7	1611.8	1971.0	5437.4	425.2	0.431	1.087	0.184	428.00	1.724	47.825	126.048	154.135	329.732	37.473	28.332	0.6	N	21.3	1842.9	1611.8	1971.0	5447.1	428.0	0.449	1.145	0.184	392.05	1.853	48.039	126.048	154.135	330.075	39.011	29.844	0.66	N	19.7	1899.8	1611.8	1971.0	5502.4	430.3	0.445	1.192	0.184	434.36	1.716	49.521	126.048	154.135	331.420	38.687	31.075	North																			0	N	50.9	1310.3	1611.8	1971.0	4944.0	386.6	0.480	0.825	0.184		4.423	34.155	126.048	154.135	318.761	41.675	21.511	0.1	N	44.1	1359.8	1611.8	1971.0	4986.7	390.0	0.462	0.835	0.184	23.90	3.829	35.447	126.048	154.135	319.459	40.115	21.765	0.2	N	38.7	1410.5	1611.8	1971.0	5032.0	393.5	0.455	0.844	0.184	51.60	3.364	36.767	126.048	154.135	320.314	39.568	22.003	0.3	N	34.0	1462.3	1611.8	1971.0	5079.1	397.2	0.449	0.853	0.184	79.29	2.950	38.118	126.048	154.135	321.251	39.003	22.249	0.4	N	29.8	1515.2	1611.8	1971.0	5127.8	401.0	0.442	0.861	0.184	106.73	2.590	39.496	126.048	154.135	322.269	38.429	22.440	0.5	N	26.1	1569.2	1611.8	1971.0	5178.2	404.9	0.436	0.869	0.184	133.74	2.270	40.905	126.048	154.135	323.357	37.874	22.651	0.6	N	29.1	1542.2	1611.8	1971.0	5154.1	403.1	0.454	0.864	0.184	54.61	2.532	40.200	126.048	154.135	322.915	39.452	22.530	0.66	N	27.3	1570.0	1611.8	1971.0	5180.1	405.1	0.451	0.868	0.184	63.39	2.369	40.926	126.048	154.135	323.478	39.172	22.618																																																																																																																																																																																																																																																																																																																																																																									
0.1	N	39.7	1436.9	1611.8	1971.0	5059.5	395.7	0.473	0.852	0.184	82.17	3.453	37.456	126.048	154.135	321.091	41.096	22.206	0.2	N	32.4	1532.6	1611.8	1971.0	5147.8	402.6	0.453	0.866	0.184	168.97	2.818	39.949	126.048	154.135	322.951	39.397	22.568	0.3	N	27.2	1630.8	1611.8	1971.0	5240.9	409.8	0.446	0.927	0.184	255.72	2.364	42.511	126.048	154.135	325.058	38.759	24.171	0.4	N	23.0	1731.4	1611.8	1971.0	5337.3	417.4	0.439	1.004	0.184	342.09	2.002	45.134	126.048	154.135	327.319	38.109	26.183	0.5	N	19.8	1834.7	1611.8	1971.0	5437.4	425.2	0.431	1.087	0.184	428.00	1.724	47.825	126.048	154.135	329.732	37.473	28.332	0.6	N	21.3	1842.9	1611.8	1971.0	5447.1	428.0	0.449	1.145	0.184	392.05	1.853	48.039	126.048	154.135	330.075	39.011	29.844	0.66	N	19.7	1899.8	1611.8	1971.0	5502.4	430.3	0.445	1.192	0.184	434.36	1.716	49.521	126.048	154.135	331.420	38.687	31.075	North																			0	N	50.9	1310.3	1611.8	1971.0	4944.0	386.6	0.480	0.825	0.184		4.423	34.155	126.048	154.135	318.761	41.675	21.511	0.1	N	44.1	1359.8	1611.8	1971.0	4986.7	390.0	0.462	0.835	0.184	23.90	3.829	35.447	126.048	154.135	319.459	40.115	21.765	0.2	N	38.7	1410.5	1611.8	1971.0	5032.0	393.5	0.455	0.844	0.184	51.60	3.364	36.767	126.048	154.135	320.314	39.568	22.003	0.3	N	34.0	1462.3	1611.8	1971.0	5079.1	397.2	0.449	0.853	0.184	79.29	2.950	38.118	126.048	154.135	321.251	39.003	22.249	0.4	N	29.8	1515.2	1611.8	1971.0	5127.8	401.0	0.442	0.861	0.184	106.73	2.590	39.496	126.048	154.135	322.269	38.429	22.440	0.5	N	26.1	1569.2	1611.8	1971.0	5178.2	404.9	0.436	0.869	0.184	133.74	2.270	40.905	126.048	154.135	323.357	37.874	22.651	0.6	N	29.1	1542.2	1611.8	1971.0	5154.1	403.1	0.454	0.864	0.184	54.61	2.532	40.200	126.048	154.135	322.915	39.452	22.530	0.66	N	27.3	1570.0	1611.8	1971.0	5180.1	405.1	0.451	0.868	0.184	63.39	2.369	40.926	126.048	154.135	323.478	39.172	22.618																																																																																																																																																																																																																																																																																																																																																																																												
0.2	N	32.4	1532.6	1611.8	1971.0	5147.8	402.6	0.453	0.866	0.184	168.97	2.818	39.949	126.048	154.135	322.951	39.397	22.568	0.3	N	27.2	1630.8	1611.8	1971.0	5240.9	409.8	0.446	0.927	0.184	255.72	2.364	42.511	126.048	154.135	325.058	38.759	24.171	0.4	N	23.0	1731.4	1611.8	1971.0	5337.3	417.4	0.439	1.004	0.184	342.09	2.002	45.134	126.048	154.135	327.319	38.109	26.183	0.5	N	19.8	1834.7	1611.8	1971.0	5437.4	425.2	0.431	1.087	0.184	428.00	1.724	47.825	126.048	154.135	329.732	37.473	28.332	0.6	N	21.3	1842.9	1611.8	1971.0	5447.1	428.0	0.449	1.145	0.184	392.05	1.853	48.039	126.048	154.135	330.075	39.011	29.844	0.66	N	19.7	1899.8	1611.8	1971.0	5502.4	430.3	0.445	1.192	0.184	434.36	1.716	49.521	126.048	154.135	331.420	38.687	31.075	North																			0	N	50.9	1310.3	1611.8	1971.0	4944.0	386.6	0.480	0.825	0.184		4.423	34.155	126.048	154.135	318.761	41.675	21.511	0.1	N	44.1	1359.8	1611.8	1971.0	4986.7	390.0	0.462	0.835	0.184	23.90	3.829	35.447	126.048	154.135	319.459	40.115	21.765	0.2	N	38.7	1410.5	1611.8	1971.0	5032.0	393.5	0.455	0.844	0.184	51.60	3.364	36.767	126.048	154.135	320.314	39.568	22.003	0.3	N	34.0	1462.3	1611.8	1971.0	5079.1	397.2	0.449	0.853	0.184	79.29	2.950	38.118	126.048	154.135	321.251	39.003	22.249	0.4	N	29.8	1515.2	1611.8	1971.0	5127.8	401.0	0.442	0.861	0.184	106.73	2.590	39.496	126.048	154.135	322.269	38.429	22.440	0.5	N	26.1	1569.2	1611.8	1971.0	5178.2	404.9	0.436	0.869	0.184	133.74	2.270	40.905	126.048	154.135	323.357	37.874	22.651	0.6	N	29.1	1542.2	1611.8	1971.0	5154.1	403.1	0.454	0.864	0.184	54.61	2.532	40.200	126.048	154.135	322.915	39.452	22.530	0.66	N	27.3	1570.0	1611.8	1971.0	5180.1	405.1	0.451	0.868	0.184	63.39	2.369	40.926	126.048	154.135	323.478	39.172	22.618																																																																																																																																																																																																																																																																																																																																																																																																															
0.3	N	27.2	1630.8	1611.8	1971.0	5240.9	409.8	0.446	0.927	0.184	255.72	2.364	42.511	126.048	154.135	325.058	38.759	24.171	0.4	N	23.0	1731.4	1611.8	1971.0	5337.3	417.4	0.439	1.004	0.184	342.09	2.002	45.134	126.048	154.135	327.319	38.109	26.183	0.5	N	19.8	1834.7	1611.8	1971.0	5437.4	425.2	0.431	1.087	0.184	428.00	1.724	47.825	126.048	154.135	329.732	37.473	28.332	0.6	N	21.3	1842.9	1611.8	1971.0	5447.1	428.0	0.449	1.145	0.184	392.05	1.853	48.039	126.048	154.135	330.075	39.011	29.844	0.66	N	19.7	1899.8	1611.8	1971.0	5502.4	430.3	0.445	1.192	0.184	434.36	1.716	49.521	126.048	154.135	331.420	38.687	31.075	North																			0	N	50.9	1310.3	1611.8	1971.0	4944.0	386.6	0.480	0.825	0.184		4.423	34.155	126.048	154.135	318.761	41.675	21.511	0.1	N	44.1	1359.8	1611.8	1971.0	4986.7	390.0	0.462	0.835	0.184	23.90	3.829	35.447	126.048	154.135	319.459	40.115	21.765	0.2	N	38.7	1410.5	1611.8	1971.0	5032.0	393.5	0.455	0.844	0.184	51.60	3.364	36.767	126.048	154.135	320.314	39.568	22.003	0.3	N	34.0	1462.3	1611.8	1971.0	5079.1	397.2	0.449	0.853	0.184	79.29	2.950	38.118	126.048	154.135	321.251	39.003	22.249	0.4	N	29.8	1515.2	1611.8	1971.0	5127.8	401.0	0.442	0.861	0.184	106.73	2.590	39.496	126.048	154.135	322.269	38.429	22.440	0.5	N	26.1	1569.2	1611.8	1971.0	5178.2	404.9	0.436	0.869	0.184	133.74	2.270	40.905	126.048	154.135	323.357	37.874	22.651	0.6	N	29.1	1542.2	1611.8	1971.0	5154.1	403.1	0.454	0.864	0.184	54.61	2.532	40.200	126.048	154.135	322.915	39.452	22.530	0.66	N	27.3	1570.0	1611.8	1971.0	5180.1	405.1	0.451	0.868	0.184	63.39	2.369	40.926	126.048	154.135	323.478	39.172	22.618																																																																																																																																																																																																																																																																																																																																																																																																																																		
0.4	N	23.0	1731.4	1611.8	1971.0	5337.3	417.4	0.439	1.004	0.184	342.09	2.002	45.134	126.048	154.135	327.319	38.109	26.183	0.5	N	19.8	1834.7	1611.8	1971.0	5437.4	425.2	0.431	1.087	0.184	428.00	1.724	47.825	126.048	154.135	329.732	37.473	28.332	0.6	N	21.3	1842.9	1611.8	1971.0	5447.1	428.0	0.449	1.145	0.184	392.05	1.853	48.039	126.048	154.135	330.075	39.011	29.844	0.66	N	19.7	1899.8	1611.8	1971.0	5502.4	430.3	0.445	1.192	0.184	434.36	1.716	49.521	126.048	154.135	331.420	38.687	31.075	North																			0	N	50.9	1310.3	1611.8	1971.0	4944.0	386.6	0.480	0.825	0.184		4.423	34.155	126.048	154.135	318.761	41.675	21.511	0.1	N	44.1	1359.8	1611.8	1971.0	4986.7	390.0	0.462	0.835	0.184	23.90	3.829	35.447	126.048	154.135	319.459	40.115	21.765	0.2	N	38.7	1410.5	1611.8	1971.0	5032.0	393.5	0.455	0.844	0.184	51.60	3.364	36.767	126.048	154.135	320.314	39.568	22.003	0.3	N	34.0	1462.3	1611.8	1971.0	5079.1	397.2	0.449	0.853	0.184	79.29	2.950	38.118	126.048	154.135	321.251	39.003	22.249	0.4	N	29.8	1515.2	1611.8	1971.0	5127.8	401.0	0.442	0.861	0.184	106.73	2.590	39.496	126.048	154.135	322.269	38.429	22.440	0.5	N	26.1	1569.2	1611.8	1971.0	5178.2	404.9	0.436	0.869	0.184	133.74	2.270	40.905	126.048	154.135	323.357	37.874	22.651	0.6	N	29.1	1542.2	1611.8	1971.0	5154.1	403.1	0.454	0.864	0.184	54.61	2.532	40.200	126.048	154.135	322.915	39.452	22.530	0.66	N	27.3	1570.0	1611.8	1971.0	5180.1	405.1	0.451	0.868	0.184	63.39	2.369	40.926	126.048	154.135	323.478	39.172	22.618																																																																																																																																																																																																																																																																																																																																																																																																																																																					
0.5	N	19.8	1834.7	1611.8	1971.0	5437.4	425.2	0.431	1.087	0.184	428.00	1.724	47.825	126.048	154.135	329.732	37.473	28.332	0.6	N	21.3	1842.9	1611.8	1971.0	5447.1	428.0	0.449	1.145	0.184	392.05	1.853	48.039	126.048	154.135	330.075	39.011	29.844	0.66	N	19.7	1899.8	1611.8	1971.0	5502.4	430.3	0.445	1.192	0.184	434.36	1.716	49.521	126.048	154.135	331.420	38.687	31.075	North																			0	N	50.9	1310.3	1611.8	1971.0	4944.0	386.6	0.480	0.825	0.184		4.423	34.155	126.048	154.135	318.761	41.675	21.511	0.1	N	44.1	1359.8	1611.8	1971.0	4986.7	390.0	0.462	0.835	0.184	23.90	3.829	35.447	126.048	154.135	319.459	40.115	21.765	0.2	N	38.7	1410.5	1611.8	1971.0	5032.0	393.5	0.455	0.844	0.184	51.60	3.364	36.767	126.048	154.135	320.314	39.568	22.003	0.3	N	34.0	1462.3	1611.8	1971.0	5079.1	397.2	0.449	0.853	0.184	79.29	2.950	38.118	126.048	154.135	321.251	39.003	22.249	0.4	N	29.8	1515.2	1611.8	1971.0	5127.8	401.0	0.442	0.861	0.184	106.73	2.590	39.496	126.048	154.135	322.269	38.429	22.440	0.5	N	26.1	1569.2	1611.8	1971.0	5178.2	404.9	0.436	0.869	0.184	133.74	2.270	40.905	126.048	154.135	323.357	37.874	22.651	0.6	N	29.1	1542.2	1611.8	1971.0	5154.1	403.1	0.454	0.864	0.184	54.61	2.532	40.200	126.048	154.135	322.915	39.452	22.530	0.66	N	27.3	1570.0	1611.8	1971.0	5180.1	405.1	0.451	0.868	0.184	63.39	2.369	40.926	126.048	154.135	323.478	39.172	22.618																																																																																																																																																																																																																																																																																																																																																																																																																																																																								
0.6	N	21.3	1842.9	1611.8	1971.0	5447.1	428.0	0.449	1.145	0.184	392.05	1.853	48.039	126.048	154.135	330.075	39.011	29.844	0.66	N	19.7	1899.8	1611.8	1971.0	5502.4	430.3	0.445	1.192	0.184	434.36	1.716	49.521	126.048	154.135	331.420	38.687	31.075	North																			0	N	50.9	1310.3	1611.8	1971.0	4944.0	386.6	0.480	0.825	0.184		4.423	34.155	126.048	154.135	318.761	41.675	21.511	0.1	N	44.1	1359.8	1611.8	1971.0	4986.7	390.0	0.462	0.835	0.184	23.90	3.829	35.447	126.048	154.135	319.459	40.115	21.765	0.2	N	38.7	1410.5	1611.8	1971.0	5032.0	393.5	0.455	0.844	0.184	51.60	3.364	36.767	126.048	154.135	320.314	39.568	22.003	0.3	N	34.0	1462.3	1611.8	1971.0	5079.1	397.2	0.449	0.853	0.184	79.29	2.950	38.118	126.048	154.135	321.251	39.003	22.249	0.4	N	29.8	1515.2	1611.8	1971.0	5127.8	401.0	0.442	0.861	0.184	106.73	2.590	39.496	126.048	154.135	322.269	38.429	22.440	0.5	N	26.1	1569.2	1611.8	1971.0	5178.2	404.9	0.436	0.869	0.184	133.74	2.270	40.905	126.048	154.135	323.357	37.874	22.651	0.6	N	29.1	1542.2	1611.8	1971.0	5154.1	403.1	0.454	0.864	0.184	54.61	2.532	40.200	126.048	154.135	322.915	39.452	22.530	0.66	N	27.3	1570.0	1611.8	1971.0	5180.1	405.1	0.451	0.868	0.184	63.39	2.369	40.926	126.048	154.135	323.478	39.172	22.618																																																																																																																																																																																																																																																																																																																																																																																																																																																																																											
0.66	N	19.7	1899.8	1611.8	1971.0	5502.4	430.3	0.445	1.192	0.184	434.36	1.716	49.521	126.048	154.135	331.420	38.687	31.075	North																			0	N	50.9	1310.3	1611.8	1971.0	4944.0	386.6	0.480	0.825	0.184		4.423	34.155	126.048	154.135	318.761	41.675	21.511	0.1	N	44.1	1359.8	1611.8	1971.0	4986.7	390.0	0.462	0.835	0.184	23.90	3.829	35.447	126.048	154.135	319.459	40.115	21.765	0.2	N	38.7	1410.5	1611.8	1971.0	5032.0	393.5	0.455	0.844	0.184	51.60	3.364	36.767	126.048	154.135	320.314	39.568	22.003	0.3	N	34.0	1462.3	1611.8	1971.0	5079.1	397.2	0.449	0.853	0.184	79.29	2.950	38.118	126.048	154.135	321.251	39.003	22.249	0.4	N	29.8	1515.2	1611.8	1971.0	5127.8	401.0	0.442	0.861	0.184	106.73	2.590	39.496	126.048	154.135	322.269	38.429	22.440	0.5	N	26.1	1569.2	1611.8	1971.0	5178.2	404.9	0.436	0.869	0.184	133.74	2.270	40.905	126.048	154.135	323.357	37.874	22.651	0.6	N	29.1	1542.2	1611.8	1971.0	5154.1	403.1	0.454	0.864	0.184	54.61	2.532	40.200	126.048	154.135	322.915	39.452	22.530	0.66	N	27.3	1570.0	1611.8	1971.0	5180.1	405.1	0.451	0.868	0.184	63.39	2.369	40.926	126.048	154.135	323.478	39.172	22.618																																																																																																																																																																																																																																																																																																																																																																																																																																																																																																														
North																			0	N	50.9	1310.3	1611.8	1971.0	4944.0	386.6	0.480	0.825	0.184		4.423	34.155	126.048	154.135	318.761	41.675	21.511	0.1	N	44.1	1359.8	1611.8	1971.0	4986.7	390.0	0.462	0.835	0.184	23.90	3.829	35.447	126.048	154.135	319.459	40.115	21.765	0.2	N	38.7	1410.5	1611.8	1971.0	5032.0	393.5	0.455	0.844	0.184	51.60	3.364	36.767	126.048	154.135	320.314	39.568	22.003	0.3	N	34.0	1462.3	1611.8	1971.0	5079.1	397.2	0.449	0.853	0.184	79.29	2.950	38.118	126.048	154.135	321.251	39.003	22.249	0.4	N	29.8	1515.2	1611.8	1971.0	5127.8	401.0	0.442	0.861	0.184	106.73	2.590	39.496	126.048	154.135	322.269	38.429	22.440	0.5	N	26.1	1569.2	1611.8	1971.0	5178.2	404.9	0.436	0.869	0.184	133.74	2.270	40.905	126.048	154.135	323.357	37.874	22.651	0.6	N	29.1	1542.2	1611.8	1971.0	5154.1	403.1	0.454	0.864	0.184	54.61	2.532	40.200	126.048	154.135	322.915	39.452	22.530	0.66	N	27.3	1570.0	1611.8	1971.0	5180.1	405.1	0.451	0.868	0.184	63.39	2.369	40.926	126.048	154.135	323.478	39.172	22.618																																																																																																																																																																																																																																																																																																																																																																																																																																																																																																																																	
0	N	50.9	1310.3	1611.8	1971.0	4944.0	386.6	0.480	0.825	0.184		4.423	34.155	126.048	154.135	318.761	41.675	21.511	0.1	N	44.1	1359.8	1611.8	1971.0	4986.7	390.0	0.462	0.835	0.184	23.90	3.829	35.447	126.048	154.135	319.459	40.115	21.765	0.2	N	38.7	1410.5	1611.8	1971.0	5032.0	393.5	0.455	0.844	0.184	51.60	3.364	36.767	126.048	154.135	320.314	39.568	22.003	0.3	N	34.0	1462.3	1611.8	1971.0	5079.1	397.2	0.449	0.853	0.184	79.29	2.950	38.118	126.048	154.135	321.251	39.003	22.249	0.4	N	29.8	1515.2	1611.8	1971.0	5127.8	401.0	0.442	0.861	0.184	106.73	2.590	39.496	126.048	154.135	322.269	38.429	22.440	0.5	N	26.1	1569.2	1611.8	1971.0	5178.2	404.9	0.436	0.869	0.184	133.74	2.270	40.905	126.048	154.135	323.357	37.874	22.651	0.6	N	29.1	1542.2	1611.8	1971.0	5154.1	403.1	0.454	0.864	0.184	54.61	2.532	40.200	126.048	154.135	322.915	39.452	22.530	0.66	N	27.3	1570.0	1611.8	1971.0	5180.1	405.1	0.451	0.868	0.184	63.39	2.369	40.926	126.048	154.135	323.478	39.172	22.618																																																																																																																																																																																																																																																																																																																																																																																																																																																																																																																																																				
0.1	N	44.1	1359.8	1611.8	1971.0	4986.7	390.0	0.462	0.835	0.184	23.90	3.829	35.447	126.048	154.135	319.459	40.115	21.765	0.2	N	38.7	1410.5	1611.8	1971.0	5032.0	393.5	0.455	0.844	0.184	51.60	3.364	36.767	126.048	154.135	320.314	39.568	22.003	0.3	N	34.0	1462.3	1611.8	1971.0	5079.1	397.2	0.449	0.853	0.184	79.29	2.950	38.118	126.048	154.135	321.251	39.003	22.249	0.4	N	29.8	1515.2	1611.8	1971.0	5127.8	401.0	0.442	0.861	0.184	106.73	2.590	39.496	126.048	154.135	322.269	38.429	22.440	0.5	N	26.1	1569.2	1611.8	1971.0	5178.2	404.9	0.436	0.869	0.184	133.74	2.270	40.905	126.048	154.135	323.357	37.874	22.651	0.6	N	29.1	1542.2	1611.8	1971.0	5154.1	403.1	0.454	0.864	0.184	54.61	2.532	40.200	126.048	154.135	322.915	39.452	22.530	0.66	N	27.3	1570.0	1611.8	1971.0	5180.1	405.1	0.451	0.868	0.184	63.39	2.369	40.926	126.048	154.135	323.478	39.172	22.618																																																																																																																																																																																																																																																																																																																																																																																																																																																																																																																																																																							
0.2	N	38.7	1410.5	1611.8	1971.0	5032.0	393.5	0.455	0.844	0.184	51.60	3.364	36.767	126.048	154.135	320.314	39.568	22.003	0.3	N	34.0	1462.3	1611.8	1971.0	5079.1	397.2	0.449	0.853	0.184	79.29	2.950	38.118	126.048	154.135	321.251	39.003	22.249	0.4	N	29.8	1515.2	1611.8	1971.0	5127.8	401.0	0.442	0.861	0.184	106.73	2.590	39.496	126.048	154.135	322.269	38.429	22.440	0.5	N	26.1	1569.2	1611.8	1971.0	5178.2	404.9	0.436	0.869	0.184	133.74	2.270	40.905	126.048	154.135	323.357	37.874	22.651	0.6	N	29.1	1542.2	1611.8	1971.0	5154.1	403.1	0.454	0.864	0.184	54.61	2.532	40.200	126.048	154.135	322.915	39.452	22.530	0.66	N	27.3	1570.0	1611.8	1971.0	5180.1	405.1	0.451	0.868	0.184	63.39	2.369	40.926	126.048	154.135	323.478	39.172	22.618																																																																																																																																																																																																																																																																																																																																																																																																																																																																																																																																																																																										
0.3	N	34.0	1462.3	1611.8	1971.0	5079.1	397.2	0.449	0.853	0.184	79.29	2.950	38.118	126.048	154.135	321.251	39.003	22.249	0.4	N	29.8	1515.2	1611.8	1971.0	5127.8	401.0	0.442	0.861	0.184	106.73	2.590	39.496	126.048	154.135	322.269	38.429	22.440	0.5	N	26.1	1569.2	1611.8	1971.0	5178.2	404.9	0.436	0.869	0.184	133.74	2.270	40.905	126.048	154.135	323.357	37.874	22.651	0.6	N	29.1	1542.2	1611.8	1971.0	5154.1	403.1	0.454	0.864	0.184	54.61	2.532	40.200	126.048	154.135	322.915	39.452	22.530	0.66	N	27.3	1570.0	1611.8	1971.0	5180.1	405.1	0.451	0.868	0.184	63.39	2.369	40.926	126.048	154.135	323.478	39.172	22.618																																																																																																																																																																																																																																																																																																																																																																																																																																																																																																																																																																																																													
0.4	N	29.8	1515.2	1611.8	1971.0	5127.8	401.0	0.442	0.861	0.184	106.73	2.590	39.496	126.048	154.135	322.269	38.429	22.440	0.5	N	26.1	1569.2	1611.8	1971.0	5178.2	404.9	0.436	0.869	0.184	133.74	2.270	40.905	126.048	154.135	323.357	37.874	22.651	0.6	N	29.1	1542.2	1611.8	1971.0	5154.1	403.1	0.454	0.864	0.184	54.61	2.532	40.200	126.048	154.135	322.915	39.452	22.530	0.66	N	27.3	1570.0	1611.8	1971.0	5180.1	405.1	0.451	0.868	0.184	63.39	2.369	40.926	126.048	154.135	323.478	39.172	22.618																																																																																																																																																																																																																																																																																																																																																																																																																																																																																																																																																																																																																																
0.5	N	26.1	1569.2	1611.8	1971.0	5178.2	404.9	0.436	0.869	0.184	133.74	2.270	40.905	126.048	154.135	323.357	37.874	22.651	0.6	N	29.1	1542.2	1611.8	1971.0	5154.1	403.1	0.454	0.864	0.184	54.61	2.532	40.200	126.048	154.135	322.915	39.452	22.530	0.66	N	27.3	1570.0	1611.8	1971.0	5180.1	405.1	0.451	0.868	0.184	63.39	2.369	40.926	126.048	154.135	323.478	39.172	22.618																																																																																																																																																																																																																																																																																																																																																																																																																																																																																																																																																																																																																																																			
0.6	N	29.1	1542.2	1611.8	1971.0	5154.1	403.1	0.454	0.864	0.184	54.61	2.532	40.200	126.048	154.135	322.915	39.452	22.530	0.66	N	27.3	1570.0	1611.8	1971.0	5180.1	405.1	0.451	0.868	0.184	63.39	2.369	40.926	126.048	154.135	323.478	39.172	22.618																																																																																																																																																																																																																																																																																																																																																																																																																																																																																																																																																																																																																																																																						
0.66	N	27.3	1570.0	1611.8	1971.0	5180.1	405.1	0.451	0.868	0.184	63.39	2.369	40.926	126.048	154.135	323.478	39.172	22.618																																																																																																																																																																																																																																																																																																																																																																																																																																																																																																																																																																																																																																																																																									

Appendix D3

Comparison of Window U-value and Solar Heat Gain Coefficient on Energy Performance

SIMULATION RESULTS - WINDOW U-VALUE vs SHGC AND ENERGY PERFORMANCE

Floor Area 12.7875 [m2]
 Heating System Efficiency 0.9
 Cooling System Efficiency 3

CASE 1 (Varying SHGC)

2G-1 AL v 2G-3v AL

High U and High SHGC

IGU	U _{cg} [W/m ² K]	SHGC	VT	Frame	U-edge [W/m ² K]	U-frame [W/m ² K]	WWR 0.1 [W/m ² K]	WWR 0.2 [W/m ² K]	WWR 0.3 [W/m ² K]	WWR 0.4 [W/m ² K]	WWR 0.5 [W/m ² K]	WWR 0.6 [W/m ² K]	WWR 0.66 [W/m ² K]
2G-1 AL	2.68	0.702	0.786	AL	1.8608	13.4626	5.01	4.35	4.06	3.88	3.76	3.87	3.82

WWR	Shading	Annual Purchased Heating [kWh]	Annual Purchased Cooling [kWh]	Annual Lighting Load [kWh]	Annual Plug Load [kWh]	Total Annual Load [kWh]	Total Annual Load / Area [kWh/m ²]	Peak Heating [kW]	Peak Cooling [kW]	Peak Lighting [kW]	Annual Window Energy Balance ('+' gain, '-' loss) [kWh]	Annual Heating Energy 'Metered' [kWh/m ²]	Annual Cooling Energy 'Metered' [kWh/m ²]	Annual Lighting Energy 'Metered' [kWh/m ²]	Annual Plug Energy 'Metered' [kWh/m ²]	Total Annual Energy 'Metered' [kWh/m ²]	Peak Heating Energy 'Metered' [W/m ²]	Peak Cooling Energy 'Metered' [W/m ²]	
South																			
0	N	537.4	419.2	957.4	723.6	2637.6	206.3	0.881	0.523	0.184									
0.1	N	732.6	324.5	521.7	723.6	2302.5	180.1	0.976	0.496	0.184	52.77	67.404	10.150	40.801	56.587	174.942	89.802	15.520	
0.2	N	625.8	486.0	406.0	723.6	2241.3	175.3	0.960	0.672	0.184	474.65	57.573	15.202	31.746	56.587	161.108	88.346	21.023	
0.3	N	582.8	650.2	373.3	723.6	2329.9	182.2	0.991	0.848	0.184	720.23	53.622	20.337	29.192	56.587	159.738	91.199	26.512	
0.4	N	567.8	830.2	357.3	723.6	2478.8	193.8	1.038	1.050	0.184	934.16	52.236	25.969	27.938	56.587	162.730	95.513	32.830	
0.5	N	581.4	1021.0	343.5	723.6	2669.6	208.8	1.072	1.267	0.184	1117.77	53.492	31.938	26.866	56.587	168.883	98.628	39.619	
0.6	N	687.6	1091.6	343.0	723.6	2845.8	222.5	1.171	1.407	0.184	994.20	63.261	34.146	26.819	56.587	180.813	107.710	44.026	
0.66	N	690.3	1204.0	340.3	723.6	2958.1	231.3	1.192	1.532	0.184	1093.62	63.511	37.660	26.609	56.587	184.367	109.632	47.911	
East																			
0	N	560.9	428.3	957.4	723.6	2670.3	208.8	0.895	0.535	0.184									
0.1	N	745.1	443.9	596.7	723.6	2509.3	196.2	0.987	0.584	0.184	139.84	68.550	13.887	46.662	56.587	185.685	90.845	18.273	
0.2	N	846.3	597.6	451.9	723.6	2619.3	204.8	1.053	0.823	0.184	319.38	77.861	18.692	35.336	56.587	188.475	96.894	25.744	
0.3	N	915.6	796.8	393.2	723.6	2829.2	221.2	1.111	1.108	0.184	494.63	84.237	24.924	30.747	56.587	196.494	102.247	34.669	
0.4	N	986.7	984.8	369.4	723.6	3064.5	239.6	1.166	1.402	0.184	615.93	90.781	30.805	28.887	56.587	207.059	107.311	43.868	
0.5	N	1062.6	1175.9	352.2	723.6	3314.3	259.6	1.225	1.699	0.184	728.53	97.758	36.782	27.543	56.587	218.670	112.740	53.149	
0.6	N	1239.1	1267.4	351.7	723.6	3581.8	280.1	1.337	1.906	0.184	566.95	113.999	39.646	27.503	56.587	237.735	122.964	59.614	
0.66	N	1277.7	1382.0	348.1	723.6	3731.4	291.8	1.368	2.074	0.184	630.60	117.551	43.229	27.219	56.587	244.586	125.861	64.871	
West																			
0	N	565.6	418.0	957.4	723.6	2664.6	208.4	0.894	0.528	0.184									
0.1	N	758.7	398.4	576.0	723.6	2456.8	192.1	0.980	0.589	0.184	105.01	69.802	12.463	45.046	56.587	183.898	90.128	18.431	
0.2	N	865.7	526.4	433.4	723.6	2549.0	199.3	1.038	0.852	0.184	245.72	79.643	16.465	33.890	56.587	186.583	95.497	26.647	
0.3	N	938.2	694.8	380.5	723.6	2737.0	214.0	1.097	1.134	0.184	380.55	86.316	21.733	29.754	56.587	194.389	100.896	35.470	
0.4	N	1006.3	848.5	361.7	723.6	2940.0	229.9	1.163	1.399	0.184	467.04	92.582	26.540	28.283	56.587	203.992	106.961	43.754	
0.5	N	1085.8	1014.2	348.1	723.6	3171.7	248.0	1.230	1.686	0.184	546.88	99.899	31.724	27.221	56.587	215.431	113.141	52.744	
0.6	N	1273.5	1090.1	347.6	723.6	3434.8	268.6	1.314	1.889	0.184	356.08	117.164	34.100	27.180	56.587	235.031	120.869	59.102	
0.66	N	1314.5	1186.2	344.1	723.6	3568.3	279.0	1.346	2.053	0.184	398.63	120.932	37.105	26.907	56.587	241.531	123.837	64.214	
North																			
0	N	581.0	394.9	957.4	723.6	2656.9	207.8	0.901	0.513	0.184									
0.1	N	787.9	323.7	705.7	723.6	2540.9	198.7	0.994	0.500	0.184	-115.98	72.487	10.125	55.190	56.587	194.389	91.426	15.632	
0.2	N	978.0	301.2	496.6	723.6	2499.4	195.5	1.068	0.516	0.184	-184.46	89.976	9.420	38.837	56.587	194.820	98.235	16.133	
0.3	N	1134.9	345.6	408.0	723.6	2612.1	204.3	1.136	0.590	0.184	-250.33	104.414	10.811	31.906	56.587	203.718	104.553	18.440	
0.4	N	1258.1	404.7	377.6	723.6	2764.0	216.2	1.199	0.667	0.184	-318.19	115.746	12.661	29.528	56.587	214.521	110.289	20.864	
0.5	N	1378.2	464.5	357.2	723.6	2923.5	228.6	1.262	0.744	0.184	-391.30	126.797	14.531	27.930	56.587	225.845	116.062	23.282	
0.6	N	1605.3	472.4	356.3	723.6	3157.6	246.9	1.373	0.787	0.184	-684.41	147.693	14.776	27.860	56.587	246.915	126.336	24.627	
0.66	N	1671.2	504.5	352.4	723.6	3251.7	254.3	1.407	0.829	0.184	-736.76	153.754	15.781	27.557	56.587	253.678	129.471	25.922	
Average																			
0	N	561.3	415.1	957.4	723.6	2657.4	207.8	0.893	0.524	0.184									
0.1	N	756.1	372.6	600.0	723.6	2452.4	191.8	0.984	0.542	0.184	45.41	51.636	12.984	46.925	56.587	184.728	90.550	16.964	
0.2	N	828.9	477.8	447.0	723.6	2477.3	193.7	1.030	0.716	0.184	213.82	76.263	14.945	34.952	56.587	182.747	94.743	22.387	
0.3	N	892.9	621.8	388.7	723.6	2627.1	205.4	1.084	0.920	0.184	336.27	82.147	19.451	30.400	56.587	188.585	99.724	28.773	
0.4	N	954.7	767.0	366.5	723.6	2811.9	219.9	1.141	1.129	0.184	424.74	87.837	23.994	28.659	56.587	197.075	105.018	35.329	
0.5	N	1027.0	918.9	350.3	723.6	3019.8	236.1	1.197	1.349	0.184	500.47	94.487	28.744	27.390	56.587	207.207	110.143	42.198	
0.6	N	1201.4	980.4	349.6	723.6	3255.0	254.5	1.299	1.497	0.184	308.21	110.529	30.667	27.341	56.587	225.124	119.470	46.842	
0.66	N	1238.4	1069.2	346.2	723.6	3377.4	264.1	1.328	1.622	0.184	346.52	113.937	33.444	27.073	56.587	231.040	122.200	50.729	

CASE 1 (Varying SHGC)

High U and Low SHGC

IGU	Ucg	SHGC	VT	Frame	U-edge	U-frame	WWR 0.1	WWR 0.2	WWR 0.3	WWR 0.4	WWR 0.5	WWR 0.6	WWR 0.66
	[W/m2K]				[W/m2K]	[W/m2K]	[W/m2K]	[W/m2K]	[W/m2K]	[W/m2K]	[W/m2K]	[W/m2K]	[W/m2K]
2G-3v AL	2.53	0.297	0.416	AL	1.8608	13.4626	4.93	4.25	3.95	3.76	3.65	3.76	3.71

WWR	Shading	Annual Purchased Heating [kWh]	Annual Purchased Cooling [kWh]	Annual Lighting Load [kWh]	Annual Plug Load [kWh]	Total Annual Load [kWh]	Total Annual Load / Area [kWh/m2]	Peak Heating [kW]	Peak Cooling [kW]	Peak Lighting [kW]	Annual Window Energy Balance ('+' gain, '-' loss) [kWh]	Annual Heating Energy 'Metered' [kWh/m2]	Annual Cooling Energy 'Metered' [kWh/m2]	Annual Lighting Energy 'Metered' [kWh/m2]	Annual Plug Energy 'Metered' [kWh/m2]	Total Annual Energy 'Metered' [kWh/m2]	Peak Heating Energy 'Metered' [W/m2]	Peak Cooling Energy 'Metered' [W/m2]																																																																																																																																																																																																																																																																																																																																																																																																																																																																																																																																																																																																																																																																																																																																																																																																																																																																				
South																			0	N	537.4	419.2	957.4	723.6	2637.6	206.3	0.881	0.523	0.184		49.446	13.111	74.873	56.587	194.016	81.024	16.347	0.1	N	753.6	318.1	633.4	723.6	2428.8	189.9	0.976	0.499	0.184	-78.22	69.334	9.951	49.536	56.587	185.408	89.798	15.598	0.2	N	863.9	307.9	500.0	723.6	2395.3	187.3	1.038	0.521	0.184	-110.09	79.477	9.632	39.097	56.587	184.793	95.486	16.303	0.3	N	943.2	336.4	448.7	723.6	2452.0	191.7	1.093	0.586	0.184	-137.11	86.780	10.522	35.092	56.587	188.982	100.563	18.341	0.4	N	1016.5	375.5	423.7	723.6	2539.2	198.6	1.156	0.655	0.184	-168.55	93.515	11.746	33.130	56.587	194.979	106.333	20.496	0.5	N	1098.0	417.3	402.6	723.6	2641.4	206.6	1.212	0.727	0.184	-208.76	101.015	13.053	31.483	56.587	202.137	111.535	22.735	0.6	N	1286.4	418.0	401.4	723.6	2829.4	221.3	1.324	0.775	0.184	-466.93	118.350	13.075	31.392	56.587	219.404	121.772	24.239	0.66	N	1327.1	443.0	396.4	723.6	2890.1	226.0	1.355	0.815	0.184	-495.51	122.091	13.858	30.998	56.587	223.533	124.634	25.505	East																			0	N	560.9	428.3	957.4	723.6	2670.3	208.8	0.895	0.535	0.184		51.607	13.399	74.873	56.587	196.465	82.359	16.729	0.1	N	765.0	368.4	730.8	723.6	2587.8	202.4	0.993	0.543	0.184	-113.16	70.383	11.522	57.153	56.587	195.645	91.316	16.979	0.2	N	930.0	380.6	598.3	723.6	2632.5	205.9	1.070	0.570	0.184	-180.86	85.565	11.905	46.785	56.587	200.842	98.468	17.844	0.3	N	1072.4	417.8	520.6	723.6	2734.5	213.8	1.140	0.687	0.184	-241.58	98.666	13.070	40.711	56.587	209.033	104.874	21.492	0.4	N	1204.2	464.3	477.5	723.6	2869.6	224.4	1.205	0.809	0.184	-313.65	110.784	14.523	37.345	56.587	219.238	110.861	25.299	0.5	N	1338.6	515.2	440.0	723.6	3017.5	236.0	1.270	0.933	0.184	-387.36	123.157	16.117	34.410	56.587	230.271	116.865	29.197	0.6	N	1566.9	527.3	438.8	723.6	3256.6	254.7	1.386	1.028	0.184	-668.14	144.157	16.495	34.311	56.587	251.550	127.511	32.142	0.66	N	1635.9	560.5	428.8	723.6	3348.9	261.9	1.422	1.103	0.184	-714.28	150.509	17.534	33.533	56.587	258.162	130.799	34.493	West																			0	N	565.6	418.0	957.4	723.6	2664.6	208.4	0.894	0.528	0.184		52.035	13.075	74.873	56.587	196.569	82.266	16.502	0.1	N	778.5	332.9	712.4	723.6	2547.4	199.2	0.989	0.507	0.184	-137.93	71.620	10.414	55.708	56.587	194.329	90.990	15.853	0.2	N	955.9	337.2	576.3	723.6	2593.0	202.8	1.065	0.581	0.184	-229.18	87.945	10.549	45.065	56.587	200.145	97.984	18.177	0.3	N	1106.7	366.6	500.0	723.6	2696.9	210.9	1.132	0.698	0.184	-312.57	101.814	11.468	39.101	56.587	208.969	104.149	21.829	0.4	N	1243.8	403.5	458.4	723.6	2829.4	221.3	1.195	0.821	0.184	-404.96	114.433	12.622	35.851	56.587	219.492	109.905	25.687	0.5	N	1385.2	449.3	424.6	723.6	2982.7	233.3	1.260	0.952	0.184	-497.92	127.439	14.054	33.208	56.587	231.287	115.877	29.786	0.6	N	1626.7	459.3	423.9	723.6	3233.4	252.9	1.374	1.060	0.184	-796.48	149.657	14.367	33.147	56.587	253.758	126.420	33.152	0.66	N	1699.9	487.5	414.6	723.6	3325.6	260.1	1.408	1.144	0.184	-854.03	156.392	15.248	32.425	56.587	260.652	129.513	35.801	North																			0	N	581.0	394.9	957.4	723.6	2656.9	207.8	0.901	0.513	0.184		53.457	12.352	74.873	56.587	197.267	82.879	16.039	0.1	N	790.5	328.1	831.9	723.6	2674.1	209.1	0.997	0.501	0.184	-242.79	72.724	10.264	65.056	56.587	204.631	91.763	15.677	0.2	N	980.8	276.3	708.8	723.6	2689.5	210.3	1.074	0.488	0.184	-433.10	90.236	8.643	55.433	56.587	210.898	98.833	15.269	0.3	N	1166.9	238.3	597.0	723.6	2725.8	213.2	1.145	0.472	0.184	-607.23	107.353	7.455	46.686	56.587	218.080	105.370	14.757	0.4	N	1345.2	232.3	529.3	723.6	2830.4	221.3	1.213	0.500	0.184	-774.63	123.762	7.265	41.392	56.587	229.006	111.559	15.631	0.5	N	1527.8	234.1	471.4	723.6	2956.9	231.2	1.282	0.531	0.184	-942.27	140.561	7.323	36.866	56.587	241.336	117.966	16.823	0.6	N	1797.5	220.3	469.0	723.6	3210.4	251.1	1.397	0.547	0.184	-1291.85	165.375	6.890	36.678	56.587	265.529	128.550	17.103	0.66	N	1894.3	225.8	454.4	723.6	3298.1	257.9	1.434	0.565	0.184	-1392.77	174.281	7.063	35.535	56.587	273.466	131.932	17.688	Average																			0	N	561.3	415.1	957.4	723.6	2657.4	207.8	0.893	0.524	0.184		51.636	12.984	74.873	56.587	196.079	82.132	16.404	0.1	N	771.9	336.9	727.1	723.6	2559.5	200.2	0.989	0.512	0.184	-143.02	71.015	10.538	56.863	56.587	195.003	90.967	16.027	0.2	N	932.7	325.5	595.8	723.6	2577.6	201.6	1.062	0.540	0.184	-238.31	85.806	10.182	46.595	56.587	199.169	97.693	16.898	0.3	N	1072.3	339.8	516.6	723.6	2652.3	207.4	1.128	0.611	0.184	-324.62	98.653	10.629	40.397	56.587	206.266	103.739	19.105	0.4	N	1202.4	368.9	472.2	723.6	2767.1	216.4	1.192	0.696	0.184	-415.45	110.624	11.539	36.930	56.587	215.679	109.665	21.778	0.5	N	1337.4	404.0	434.7	723.6	2899.7	226.8	1.256	0.786	0.184	-509.08	123.043	12.637	33.992	56.587	226.258	115.561	24.585	0.6	N	1569.4	406.2	433.3	723.6	3132.5	245.0	1.370	0.852	0.184	-805.85	144.385	12.707	33.882	56.587	247.560	126.063	26.659	0.66	N	1639.3	429.2	423.6	723.6	3215.7	251.5	1.405	0.907	0.184	-864.15	150.819	13.426	33.123	56.587	253.953	129.219	28.372
0	N	537.4	419.2	957.4	723.6	2637.6	206.3	0.881	0.523	0.184		49.446	13.111	74.873	56.587	194.016	81.024	16.347	0.1	N	753.6	318.1	633.4	723.6	2428.8	189.9	0.976	0.499	0.184	-78.22	69.334	9.951	49.536	56.587	185.408	89.798	15.598	0.2	N	863.9	307.9	500.0	723.6	2395.3	187.3	1.038	0.521	0.184	-110.09	79.477	9.632	39.097	56.587	184.793	95.486	16.303	0.3	N	943.2	336.4	448.7	723.6	2452.0	191.7	1.093	0.586	0.184	-137.11	86.780	10.522	35.092	56.587	188.982	100.563	18.341	0.4	N	1016.5	375.5	423.7	723.6	2539.2	198.6	1.156	0.655	0.184	-168.55	93.515	11.746	33.130	56.587	194.979	106.333	20.496	0.5	N	1098.0	417.3	402.6	723.6	2641.4	206.6	1.212	0.727	0.184	-208.76	101.015	13.053	31.483	56.587	202.137	111.535	22.735	0.6	N	1286.4	418.0	401.4	723.6	2829.4	221.3	1.324	0.775	0.184	-466.93	118.350	13.075	31.392	56.587	219.404	121.772	24.239	0.66	N	1327.1	443.0	396.4	723.6	2890.1	226.0	1.355	0.815	0.184	-495.51	122.091	13.858	30.998	56.587	223.533	124.634	25.505	East																			0	N	560.9	428.3	957.4	723.6	2670.3	208.8	0.895	0.535	0.184		51.607	13.399	74.873	56.587	196.465	82.359	16.729	0.1	N	765.0	368.4	730.8	723.6	2587.8	202.4	0.993	0.543	0.184	-113.16	70.383	11.522	57.153	56.587	195.645	91.316	16.979	0.2	N	930.0	380.6	598.3	723.6	2632.5	205.9	1.070	0.570	0.184	-180.86	85.565	11.905	46.785	56.587	200.842	98.468	17.844	0.3	N	1072.4	417.8	520.6	723.6	2734.5	213.8	1.140	0.687	0.184	-241.58	98.666	13.070	40.711	56.587	209.033	104.874	21.492	0.4	N	1204.2	464.3	477.5	723.6	2869.6	224.4	1.205	0.809	0.184	-313.65	110.784	14.523	37.345	56.587	219.238	110.861	25.299	0.5	N	1338.6	515.2	440.0	723.6	3017.5	236.0	1.270	0.933	0.184	-387.36	123.157	16.117	34.410	56.587	230.271	116.865	29.197	0.6	N	1566.9	527.3	438.8	723.6	3256.6	254.7	1.386	1.028	0.184	-668.14	144.157	16.495	34.311	56.587	251.550	127.511	32.142	0.66	N	1635.9	560.5	428.8	723.6	3348.9	261.9	1.422	1.103	0.184	-714.28	150.509	17.534	33.533	56.587	258.162	130.799	34.493	West																			0	N	565.6	418.0	957.4	723.6	2664.6	208.4	0.894	0.528	0.184		52.035	13.075	74.873	56.587	196.569	82.266	16.502	0.1	N	778.5	332.9	712.4	723.6	2547.4	199.2	0.989	0.507	0.184	-137.93	71.620	10.414	55.708	56.587	194.329	90.990	15.853	0.2	N	955.9	337.2	576.3	723.6	2593.0	202.8	1.065	0.581	0.184	-229.18	87.945	10.549	45.065	56.587	200.145	97.984	18.177	0.3	N	1106.7	366.6	500.0	723.6	2696.9	210.9	1.132	0.698	0.184	-312.57	101.814	11.468	39.101	56.587	208.969	104.149	21.829	0.4	N	1243.8	403.5	458.4	723.6	2829.4	221.3	1.195	0.821	0.184	-404.96	114.433	12.622	35.851	56.587	219.492	109.905	25.687	0.5	N	1385.2	449.3	424.6	723.6	2982.7	233.3	1.260	0.952	0.184	-497.92	127.439	14.054	33.208	56.587	231.287	115.877	29.786	0.6	N	1626.7	459.3	423.9	723.6	3233.4	252.9	1.374	1.060	0.184	-796.48	149.657	14.367	33.147	56.587	253.758	126.420	33.152	0.66	N	1699.9	487.5	414.6	723.6	3325.6	260.1	1.408	1.144	0.184	-854.03	156.392	15.248	32.425	56.587	260.652	129.513	35.801	North																			0	N	581.0	394.9	957.4	723.6	2656.9	207.8	0.901	0.513	0.184		53.457	12.352	74.873	56.587	197.267	82.879	16.039	0.1	N	790.5	328.1	831.9	723.6	2674.1	209.1	0.997	0.501	0.184	-242.79	72.724	10.264	65.056	56.587	204.631	91.763	15.677	0.2	N	980.8	276.3	708.8	723.6	2689.5	210.3	1.074	0.488	0.184	-433.10	90.236	8.643	55.433	56.587	210.898	98.833	15.269	0.3	N	1166.9	238.3	597.0	723.6	2725.8	213.2	1.145	0.472	0.184	-607.23	107.353	7.455	46.686	56.587	218.080	105.370	14.757	0.4	N	1345.2	232.3	529.3	723.6	2830.4	221.3	1.213	0.500	0.184	-774.63	123.762	7.265	41.392	56.587	229.006	111.559	15.631	0.5	N	1527.8	234.1	471.4	723.6	2956.9	231.2	1.282	0.531	0.184	-942.27	140.561	7.323	36.866	56.587	241.336	117.966	16.823	0.6	N	1797.5	220.3	469.0	723.6	3210.4	251.1	1.397	0.547	0.184	-1291.85	165.375	6.890	36.678	56.587	265.529	128.550	17.103	0.66	N	1894.3	225.8	454.4	723.6	3298.1	257.9	1.434	0.565	0.184	-1392.77	174.281	7.063	35.535	56.587	273.466	131.932	17.688	Average																			0	N	561.3	415.1	957.4	723.6	2657.4	207.8	0.893	0.524	0.184		51.636	12.984	74.873	56.587	196.079	82.132	16.404	0.1	N	771.9	336.9	727.1	723.6	2559.5	200.2	0.989	0.512	0.184	-143.02	71.015	10.538	56.863	56.587	195.003	90.967	16.027	0.2	N	932.7	325.5	595.8	723.6	2577.6	201.6	1.062	0.540	0.184	-238.31	85.806	10.182	46.595	56.587	199.169	97.693	16.898	0.3	N	1072.3	339.8	516.6	723.6	2652.3	207.4	1.128	0.611	0.184	-324.62	98.653	10.629	40.397	56.587	206.266	103.739	19.105	0.4	N	1202.4	368.9	472.2	723.6	2767.1	216.4	1.192	0.696	0.184	-415.45	110.624	11.539	36.930	56.587	215.679	109.665	21.778	0.5	N	1337.4	404.0	434.7	723.6	2899.7	226.8	1.256	0.786	0.184	-509.08	123.043	12.637	33.992	56.587	226.258	115.561	24.585	0.6	N	1569.4	406.2	433.3	723.6	3132.5	245.0	1.370	0.852	0.184	-805.85	144.385	12.707	33.882	56.587	247.560	126.063	26.659	0.66	N	1639.3	429.2	423.6	723.6	3215.7	251.5	1.405	0.907	0.184	-864.15	150.819	13.426	33.123	56.587	253.953	129.219	28.372																			
0.1	N	753.6	318.1	633.4	723.6	2428.8	189.9	0.976	0.499	0.184	-78.22	69.334	9.951	49.536	56.587	185.408	89.798	15.598	0.2	N	863.9	307.9	500.0	723.6	2395.3	187.3	1.038	0.521	0.184	-110.09	79.477	9.632	39.097	56.587	184.793	95.486	16.303	0.3	N	943.2	336.4	448.7	723.6	2452.0	191.7	1.093	0.586	0.184	-137.11	86.780	10.522	35.092	56.587	188.982	100.563	18.341	0.4	N	1016.5	375.5	423.7	723.6	2539.2	198.6	1.156	0.655	0.184	-168.55	93.515	11.746	33.130	56.587	194.979	106.333	20.496	0.5	N	1098.0	417.3	402.6	723.6	2641.4	206.6	1.212	0.727	0.184	-208.76	101.015	13.053	31.483	56.587	202.137	111.535	22.735	0.6	N	1286.4	418.0	401.4	723.6	2829.4	221.3	1.324	0.775	0.184	-466.93	118.350	13.075	31.392	56.587	219.404	121.772	24.239	0.66	N	1327.1	443.0	396.4	723.6	2890.1	226.0	1.355	0.815	0.184	-495.51	122.091	13.858	30.998	56.587	223.533	124.634	25.505	East																			0	N	560.9	428.3	957.4	723.6	2670.3	208.8	0.895	0.535	0.184		51.607	13.399	74.873	56.587	196.465	82.359	16.729	0.1	N	765.0	368.4	730.8	723.6	2587.8	202.4	0.993	0.543	0.184	-113.16	70.383	11.522	57.153	56.587	195.645	91.316	16.979	0.2	N	930.0	380.6	598.3	723.6	2632.5	205.9	1.070	0.570	0.184	-180.86	85.565	11.905	46.785	56.587	200.842	98.468	17.844	0.3	N	1072.4	417.8	520.6	723.6	2734.5	213.8	1.140	0.687	0.184	-241.58	98.666	13.070	40.711	56.587	209.033	104.874	21.492	0.4	N	1204.2	464.3	477.5	723.6	2869.6	224.4	1.205	0.809	0.184	-313.65	110.784	14.523	37.345	56.587	219.238	110.861	25.299	0.5	N	1338.6	515.2	440.0	723.6	3017.5	236.0	1.270	0.933	0.184	-387.36	123.157	16.117	34.410	56.587	230.271	116.865	29.197	0.6	N	1566.9	527.3	438.8	723.6	3256.6	254.7	1.386	1.028	0.184	-668.14	144.157	16.495	34.311	56.587	251.550	127.511	32.142	0.66	N	1635.9	560.5	428.8	723.6	3348.9	261.9	1.422	1.103	0.184	-714.28	150.509	17.534	33.533	56.587	258.162	130.799	34.493	West																			0	N	565.6	418.0	957.4	723.6	2664.6	208.4	0.894	0.528	0.184		52.035	13.075	74.873	56.587	196.569	82.266	16.502	0.1	N	778.5	332.9	712.4	723.6	2547.4	199.2	0.989	0.507	0.184	-137.93	71.620	10.414	55.708	56.587	194.329	90.990	15.853	0.2	N	955.9	337.2	576.3	723.6	2593.0	202.8	1.065	0.581	0.184	-229.18	87.945	10.549	45.065	56.587	200.145	97.984	18.177	0.3	N	1106.7	366.6	500.0	723.6	2696.9	210.9	1.132	0.698	0.184	-312.57	101.814	11.468	39.101	56.587	208.969	104.149	21.829	0.4	N	1243.8	403.5	458.4	723.6	2829.4	221.3	1.195	0.821	0.184	-404.96	114.433	12.622	35.851	56.587	219.492	109.905	25.687	0.5	N	1385.2	449.3	424.6	723.6	2982.7	233.3	1.260	0.952	0.184	-497.92	127.439	14.054	33.208	56.587	231.287	115.877	29.786	0.6	N	1626.7	459.3	423.9	723.6	3233.4	252.9	1.374	1.060	0.184	-796.48	149.657	14.367	33.147	56.587	253.758	126.420	33.152	0.66	N	1699.9	487.5	414.6	723.6	3325.6	260.1	1.408	1.144	0.184	-854.03	156.392	15.248	32.425	56.587	260.652	129.513	35.801	North																			0	N	581.0	394.9	957.4	723.6	2656.9	207.8	0.901	0.513	0.184		53.457	12.352	74.873	56.587	197.267	82.879	16.039	0.1	N	790.5	328.1	831.9	723.6	2674.1	209.1	0.997	0.501	0.184	-242.79	72.724	10.264	65.056	56.587	204.631	91.763	15.677	0.2	N	980.8	276.3	708.8	723.6	2689.5	210.3	1.074	0.488	0.184	-433.10	90.236	8.643	55.433	56.587	210.898	98.833	15.269	0.3	N	1166.9	238.3	597.0	723.6	2725.8	213.2	1.145	0.472	0.184	-607.23	107.353	7.455	46.686	56.587	218.080	105.370	14.757	0.4	N	1345.2	232.3	529.3	723.6	2830.4	221.3	1.213	0.500	0.184	-774.63	123.762	7.265	41.392	56.587	229.006	111.559	15.631	0.5	N	1527.8	234.1	471.4	723.6	2956.9	231.2	1.282	0.531	0.184	-942.27	140.561	7.323	36.866	56.587	241.336	117.966	16.823	0.6	N	1797.5	220.3	469.0	723.6	3210.4	251.1	1.397	0.547	0.184	-1291.85	165.375	6.890	36.678	56.587	265.529	128.550	17.103	0.66	N	1894.3	225.8	454.4	723.6	3298.1	257.9	1.434	0.565	0.184	-1392.77	174.281	7.063	35.535	56.587	273.466	131.932	17.688	Average																			0	N	561.3	415.1	957.4	723.6	2657.4	207.8	0.893	0.524	0.184		51.636	12.984	74.873	56.587	196.079	82.132	16.404	0.1	N	771.9	336.9	727.1	723.6	2559.5	200.2	0.989	0.512	0.184	-143.02	71.015	10.538	56.863	56.587	195.003	90.967	16.027	0.2	N	932.7	325.5	595.8	723.6	2577.6	201.6	1.062	0.540	0.184	-238.31	85.806	10.182	46.595	56.587	199.169	97.693	16.898	0.3	N	1072.3	339.8	516.6	723.6	2652.3	207.4	1.128	0.611	0.184	-324.62	98.653	10.629	40.397	56.587	206.266	103.739	19.105	0.4	N	1202.4	368.9	472.2	723.6	2767.1	216.4	1.192	0.696	0.184	-415.45	110.624	11.539	36.930	56.587	215.679	109.665	21.778	0.5	N	1337.4	404.0	434.7	723.6	2899.7	226.8	1.256	0.786	0.184	-509.08	123.043	12.637	33.992	56.587	226.258	115.561	24.585	0.6	N	1569.4	406.2	433.3	723.6	3132.5	245.0	1.370	0.852	0.184	-805.85	144.385	12.707	33.882	56.587	247.560	126.063	26.659	0.66	N	1639.3	429.2	423.6	723.6	3215.7	251.5	1.405	0.907	0.184	-864.15	150.819	13.426	33.123	56.587	253.953	129.219	28.372																																						
0.2	N	863.9	307.9	500.0	723.6	2395.3	187.3	1.038	0.521	0.184	-110.09	79.477	9.632	39.097	56.587	184.793	95.486	16.303	0.3	N	943.2	336.4	448.7	723.6	2452.0	191.7	1.093	0.586	0.184	-137.11	86.780	10.522	35.092	56.587	188.982	100.563	18.341	0.4	N	1016.5	375.5	423.7	723.6	2539.2	198.6	1.156	0.655	0.184	-168.55	93.515	11.746	33.130	56.587	194.979	106.333	20.496	0.5	N	1098.0	417.3	402.6	723.6	2641.4	206.6	1.212	0.727	0.184	-208.76	101.015	13.053	31.483	56.587	202.137	111.535	22.735	0.6	N	1286.4	418.0	401.4	723.6	2829.4	221.3	1.324	0.775	0.184	-466.93	118.350	13.075	31.392	56.587	219.404	121.772	24.239	0.66	N	1327.1	443.0	396.4	723.6	2890.1	226.0	1.355	0.815	0.184	-495.51	122.091	13.858	30.998	56.587	223.533	124.634	25.505	East																			0	N	560.9	428.3	957.4	723.6	2670.3	208.8	0.895	0.535	0.184		51.607	13.399	74.873	56.587	196.465	82.359	16.729	0.1	N	765.0	368.4	730.8	723.6	2587.8	202.4	0.993	0.543	0.184	-113.16	70.383	11.522	57.153	56.587	195.645	91.316	16.979	0.2	N	930.0	380.6	598.3	723.6	2632.5	205.9	1.070	0.570	0.184	-180.86	85.565	11.905	46.785	56.587	200.842	98.468	17.844	0.3	N	1072.4	417.8	520.6	723.6	2734.5	213.8	1.140	0.687	0.184	-241.58	98.666	13.070	40.711	56.587	209.033	104.874	21.492	0.4	N	1204.2	464.3	477.5	723.6	2869.6	224.4	1.205	0.809	0.184	-313.65	110.784	14.523	37.345	56.587	219.238	110.861	25.299	0.5	N	1338.6	515.2	440.0	723.6	3017.5	236.0	1.270	0.933	0.184	-387.36	123.157	16.117	34.410	56.587	230.271	116.865	29.197	0.6	N	1566.9	527.3	438.8	723.6	3256.6	254.7	1.386	1.028	0.184	-668.14	144.157	16.495	34.311	56.587	251.550	127.511	32.142	0.66	N	1635.9	560.5	428.8	723.6	3348.9	261.9	1.422	1.103	0.184	-714.28	150.509	17.534	33.533	56.587	258.162	130.799	34.493	West																			0	N	565.6	418.0	957.4	723.6	2664.6	208.4	0.894	0.528	0.184		52.035	13.075	74.873	56.587	196.569	82.266	16.502	0.1	N	778.5	332.9	712.4	723.6	2547.4	199.2	0.989	0.507	0.184	-137.93	71.620	10.414	55.708	56.587	194.329	90.990	15.853	0.2	N	955.9	337.2	576.3	723.6	2593.0	202.8	1.065	0.581	0.184	-229.18	87.945	10.549	45.065	56.587	200.145	97.984	18.177	0.3	N	1106.7	366.6	500.0	723.6	2696.9	210.9	1.132	0.698	0.184	-312.57	101.814	11.468	39.101	56.587	208.969	104.149	21.829	0.4	N	1243.8	403.5	458.4	723.6	2829.4	221.3	1.195	0.821	0.184	-404.96	114.433	12.622	35.851	56.587	219.492	109.905	25.687	0.5	N	1385.2	449.3	424.6	723.6	2982.7	233.3	1.260	0.952	0.184	-497.92	127.439	14.054	33.208	56.587	231.287	115.877	29.786	0.6	N	1626.7	459.3	423.9	723.6	3233.4	252.9	1.374	1.060	0.184	-796.48	149.657	14.367	33.147	56.587	253.758	126.420	33.152	0.66	N	1699.9	487.5	414.6	723.6	3325.6	260.1	1.408	1.144	0.184	-854.03	156.392	15.248	32.425	56.587	260.652	129.513	35.801	North																			0	N	581.0	394.9	957.4	723.6	2656.9	207.8	0.901	0.513	0.184		53.457	12.352	74.873	56.587	197.267	82.879	16.039	0.1	N	790.5	328.1	831.9	723.6	2674.1	209.1	0.997	0.501	0.184	-242.79	72.724	10.264	65.056	56.587	204.631	91.763	15.677	0.2	N	980.8	276.3	708.8	723.6	2689.5	210.3	1.074	0.488	0.184	-433.10	90.236	8.643	55.433	56.587	210.898	98.833	15.269	0.3	N	1166.9	238.3	597.0	723.6	2725.8	213.2	1.145	0.472	0.184	-607.23	107.353	7.455	46.686	56.587	218.080	105.370	14.757	0.4	N	1345.2	232.3	529.3	723.6	2830.4	221.3	1.213	0.500	0.184	-774.63	123.762	7.265	41.392	56.587	229.006	111.559	15.631	0.5	N	1527.8	234.1	471.4	723.6	2956.9	231.2	1.282	0.531	0.184	-942.27	140.561	7.323	36.866	56.587	241.336	117.966	16.823	0.6	N	1797.5	220.3	469.0	723.6	3210.4	251.1	1.397	0.547	0.184	-1291.85	165.375	6.890	36.678	56.587	265.529	128.550	17.103	0.66	N	1894.3	225.8	454.4	723.6	3298.1	257.9	1.434	0.565	0.184	-1392.77	174.281	7.063	35.535	56.587	273.466	131.932	17.688	Average																			0	N	561.3	415.1	957.4	723.6	2657.4	207.8	0.893	0.524	0.184		51.636	12.984	74.873	56.587	196.079	82.132	16.404	0.1	N	771.9	336.9	727.1	723.6	2559.5	200.2	0.989	0.512	0.184	-143.02	71.015	10.538	56.863	56.587	195.003	90.967	16.027	0.2	N	932.7	325.5	595.8	723.6	2577.6	201.6	1.062	0.540	0.184	-238.31	85.806	10.182	46.595	56.587	199.169	97.693	16.898	0.3	N	1072.3	339.8	516.6	723.6	2652.3	207.4	1.128	0.611	0.184	-324.62	98.653	10.629	40.397	56.587	206.266	103.739	19.105	0.4	N	1202.4	368.9	472.2	723.6	2767.1	216.4	1.192	0.696	0.184	-415.45	110.624	11.539	36.930	56.587	215.679	109.665	21.778	0.5	N	1337.4	404.0	434.7	723.6	2899.7	226.8	1.256	0.786	0.184	-509.08	123.043	12.637	33.992	56.587	226.258	115.561	24.585	0.6	N	1569.4	406.2	433.3	723.6	3132.5	245.0	1.370	0.852	0.184	-805.85	144.385	12.707	33.882	56.587	247.560	126.063	26.659	0.66	N	1639.3	429.2	423.6	723.6	3215.7	251.5	1.405	0.907	0.184	-864.15	150.819	13.426	33.123	56.587	253.953	129.219	28.372																																																									
0.3	N	943.2	336.4	448.7	723.6	2452.0	191.7	1.093	0.586	0.184	-137.11	86.780	10.522	35.092	56.587	188.982	100.563	18.341	0.4	N	1016.5	375.5	423.7	723.6	2539.2	198.6	1.156	0.655	0.184	-168.55	93.515	11.746	33.130	56.587	194.979	106.333	20.496	0.5	N	1098.0	417.3	402.6	723.6	2641.4	206.6	1.212	0.727	0.184	-208.76	101.015	13.053	31.483	56.587	202.137	111.535	22.735	0.6	N	1286.4	418.0	401.4	723.6	2829.4	221.3	1.324	0.775	0.184	-466.93	118.350	13.075	31.392	56.587	219.404	121.772	24.239	0.66	N	1327.1	443.0	396.4	723.6	2890.1	226.0	1.355	0.815	0.184	-495.51	122.091	13.858	30.998	56.587	223.533	124.634	25.505	East																			0	N	560.9	428.3	957.4	723.6	2670.3	208.8	0.895	0.535	0.184		51.607	13.399	74.873	56.587	196.465	82.359	16.729	0.1	N	765.0	368.4	730.8	723.6	2587.8	202.4	0.993	0.543	0.184	-113.16	70.383	11.522	57.153	56.587	195.645	91.316	16.979	0.2	N	930.0	380.6	598.3	723.6	2632.5	205.9	1.070	0.570	0.184	-180.86	85.565	11.905	46.785	56.587	200.842	98.468	17.844	0.3	N	1072.4	417.8	520.6	723.6	2734.5	213.8	1.140	0.687	0.184	-241.58	98.666	13.070	40.711	56.587	209.033	104.874	21.492	0.4	N	1204.2	464.3	477.5	723.6	2869.6	224.4	1.205	0.809	0.184	-313.65	110.784	14.523	37.345	56.587	219.238	110.861	25.299	0.5	N	1338.6	515.2	440.0	723.6	3017.5	236.0	1.270	0.933	0.184	-387.36	123.157	16.117	34.410	56.587	230.271	116.865	29.197	0.6	N	1566.9	527.3	438.8	723.6	3256.6	254.7	1.386	1.028	0.184	-668.14	144.157	16.495	34.311	56.587	251.550	127.511	32.142	0.66	N	1635.9	560.5	428.8	723.6	3348.9	261.9	1.422	1.103	0.184	-714.28	150.509	17.534	33.533	56.587	258.162	130.799	34.493	West																			0	N	565.6	418.0	957.4	723.6	2664.6	208.4	0.894	0.528	0.184		52.035	13.075	74.873	56.587	196.569	82.266	16.502	0.1	N	778.5	332.9	712.4	723.6	2547.4	199.2	0.989	0.507	0.184	-137.93	71.620	10.414	55.708	56.587	194.329	90.990	15.853	0.2	N	955.9	337.2	576.3	723.6	2593.0	202.8	1.065	0.581	0.184	-229.18	87.945	10.549	45.065	56.587	200.145	97.984	18.177	0.3	N	1106.7	366.6	500.0	723.6	2696.9	210.9	1.132	0.698	0.184	-312.57	101.814	11.468	39.101	56.587	208.969	104.149	21.829	0.4	N	1243.8	403.5	458.4	723.6	2829.4	221.3	1.195	0.821	0.184	-404.96	114.433	12.622	35.851	56.587	219.492	109.905	25.687	0.5	N	1385.2	449.3	424.6	723.6	2982.7	233.3	1.260	0.952	0.184	-497.92	127.439	14.054	33.208	56.587	231.287	115.877	29.786	0.6	N	1626.7	459.3	423.9	723.6	3233.4	252.9	1.374	1.060	0.184	-796.48	149.657	14.367	33.147	56.587	253.758	126.420	33.152	0.66	N	1699.9	487.5	414.6	723.6	3325.6	260.1	1.408	1.144	0.184	-854.03	156.392	15.248	32.425	56.587	260.652	129.513	35.801	North																			0	N	581.0	394.9	957.4	723.6	2656.9	207.8	0.901	0.513	0.184		53.457	12.352	74.873	56.587	197.267	82.879	16.039	0.1	N	790.5	328.1	831.9	723.6	2674.1	209.1	0.997	0.501	0.184	-242.79	72.724	10.264	65.056	56.587	204.631	91.763	15.677	0.2	N	980.8	276.3	708.8	723.6	2689.5	210.3	1.074	0.488	0.184	-433.10	90.236	8.643	55.433	56.587	210.898	98.833	15.269	0.3	N	1166.9	238.3	597.0	723.6	2725.8	213.2	1.145	0.472	0.184	-607.23	107.353	7.455	46.686	56.587	218.080	105.370	14.757	0.4	N	1345.2	232.3	529.3	723.6	2830.4	221.3	1.213	0.500	0.184	-774.63	123.762	7.265	41.392	56.587	229.006	111.559	15.631	0.5	N	1527.8	234.1	471.4	723.6	2956.9	231.2	1.282	0.531	0.184	-942.27	140.561	7.323	36.866	56.587	241.336	117.966	16.823	0.6	N	1797.5	220.3	469.0	723.6	3210.4	251.1	1.397	0.547	0.184	-1291.85	165.375	6.890	36.678	56.587	265.529	128.550	17.103	0.66	N	1894.3	225.8	454.4	723.6	3298.1	257.9	1.434	0.565	0.184	-1392.77	174.281	7.063	35.535	56.587	273.466	131.932	17.688	Average																			0	N	561.3	415.1	957.4	723.6	2657.4	207.8	0.893	0.524	0.184		51.636	12.984	74.873	56.587	196.079	82.132	16.404	0.1	N	771.9	336.9	727.1	723.6	2559.5	200.2	0.989	0.512	0.184	-143.02	71.015	10.538	56.863	56.587	195.003	90.967	16.027	0.2	N	932.7	325.5	595.8	723.6	2577.6	201.6	1.062	0.540	0.184	-238.31	85.806	10.182	46.595	56.587	199.169	97.693	16.898	0.3	N	1072.3	339.8	516.6	723.6	2652.3	207.4	1.128	0.611	0.184	-324.62	98.653	10.629	40.397	56.587	206.266	103.739	19.105	0.4	N	1202.4	368.9	472.2	723.6	2767.1	216.4	1.192	0.696	0.184	-415.45	110.624	11.539	36.930	56.587	215.679	109.665	21.778	0.5	N	1337.4	404.0	434.7	723.6	2899.7	226.8	1.256	0.786	0.184	-509.08	123.043	12.637	33.992	56.587	226.258	115.561	24.585	0.6	N	1569.4	406.2	433.3	723.6	3132.5	245.0	1.370	0.852	0.184	-805.85	144.385	12.707	33.882	56.587	247.560	126.063	26.659	0.66	N	1639.3	429.2	423.6	723.6	3215.7	251.5	1.405	0.907	0.184	-864.15	150.819	13.426	33.123	56.587	253.953	129.219	28.372																																																																												
0.4	N	1016.5	375.5	423.7	723.6	2539.2	198.6	1.156	0.655	0.184	-168.55	93.515	11.746	33.130	56.587	194.979	106.333	20.496	0.5	N	1098.0	417.3	402.6	723.6	2641.4	206.6	1.212	0.727	0.184	-208.76	101.015	13.053	31.483	56.587	202.137	111.535	22.735	0.6	N	1286.4	418.0	401.4	723.6	2829.4	221.3	1.324	0.775	0.184	-466.93	118.350	13.075	31.392	56.587	219.404	121.772	24.239	0.66	N	1327.1	443.0	396.4	723.6	2890.1	226.0	1.355	0.815	0.184	-495.51	122.091	13.858	30.998	56.587	223.533	124.634	25.505	East																			0	N	560.9	428.3	957.4	723.6	2670.3	208.8	0.895	0.535	0.184		51.607	13.399	74.873	56.587	196.465	82.359	16.729	0.1	N	765.0	368.4	730.8	723.6	2587.8	202.4	0.993	0.543	0.184	-113.16	70.383	11.522	57.153	56.587	195.645	91.316	16.979	0.2	N	930.0	380.6	598.3	723.6	2632.5	205.9	1.070	0.570	0.184	-180.86	85.565	11.905	46.785	56.587	200.842	98.468	17.844	0.3	N	1072.4	417.8	520.6	723.6	2734.5	213.8	1.140	0.687	0.184	-241.58	98.666	13.070	40.711	56.587	209.033	104.874	21.492	0.4	N	1204.2	464.3	477.5	723.6	2869.6	224.4	1.205	0.809	0.184	-313.65	110.784	14.523	37.345	56.587	219.238	110.861	25.299	0.5	N	1338.6	515.2	440.0	723.6	3017.5	236.0	1.270	0.933	0.184	-387.36	123.157	16.117	34.410	56.587	230.271	116.865	29.197	0.6	N	1566.9	527.3	438.8	723.6	3256.6	254.7	1.386	1.028	0.184	-668.14	144.157	16.495	34.311	56.587	251.550	127.511	32.142	0.66	N	1635.9	560.5	428.8	723.6	3348.9	261.9	1.422	1.103	0.184	-714.28	150.509	17.534	33.533	56.587	258.162	130.799	34.493	West																			0	N	565.6	418.0	957.4	723.6	2664.6	208.4	0.894	0.528	0.184		52.035	13.075	74.873	56.587	196.569	82.266	16.502	0.1	N	778.5	332.9	712.4	723.6	2547.4	199.2	0.989	0.507	0.184	-137.93	71.620	10.414	55.708	56.587	194.329	90.990	15.853	0.2	N	955.9	337.2	576.3	723.6	2593.0	202.8	1.065	0.581	0.184	-229.18	87.945	10.549	45.065	56.587	200.145	97.984	18.177	0.3	N	1106.7	366.6	500.0	723.6	2696.9	210.9	1.132	0.698	0.184	-312.57	101.814	11.468	39.101	56.587	208.969	104.149	21.829	0.4	N	1243.8	403.5	458.4	723.6	2829.4	221.3	1.195	0.821	0.184	-404.96	114.433	12.622	35.851	56.587	219.492	109.905	25.687	0.5	N	1385.2	449.3	424.6	723.6	2982.7	233.3	1.260	0.952	0.184	-497.92	127.439	14.054	33.208	56.587	231.287	115.877	29.786	0.6	N	1626.7	459.3	423.9	723.6	3233.4	252.9	1.374	1.060	0.184	-796.48	149.657	14.367	33.147	56.587	253.758	126.420	33.152	0.66	N	1699.9	487.5	414.6	723.6	3325.6	260.1	1.408	1.144	0.184	-854.03	156.392	15.248	32.425	56.587	260.652	129.513	35.801	North																			0	N	581.0	394.9	957.4	723.6	2656.9	207.8	0.901	0.513	0.184		53.457	12.352	74.873	56.587	197.267	82.879	16.039	0.1	N	790.5	328.1	831.9	723.6	2674.1	209.1	0.997	0.501	0.184	-242.79	72.724	10.264	65.056	56.587	204.631	91.763	15.677	0.2	N	980.8	276.3	708.8	723.6	2689.5	210.3	1.074	0.488	0.184	-433.10	90.236	8.643	55.433	56.587	210.898	98.833	15.269	0.3	N	1166.9	238.3	597.0	723.6	2725.8	213.2	1.145	0.472	0.184	-607.23	107.353	7.455	46.686	56.587	218.080	105.370	14.757	0.4	N	1345.2	232.3	529.3	723.6	2830.4	221.3	1.213	0.500	0.184	-774.63	123.762	7.265	41.392	56.587	229.006	111.559	15.631	0.5	N	1527.8	234.1	471.4	723.6	2956.9	231.2	1.282	0.531	0.184	-942.27	140.561	7.323	36.866	56.587	241.336	117.966	16.823	0.6	N	1797.5	220.3	469.0	723.6	3210.4	251.1	1.397	0.547	0.184	-1291.85	165.375	6.890	36.678	56.587	265.529	128.550	17.103	0.66	N	1894.3	225.8	454.4	723.6	3298.1	257.9	1.434	0.565	0.184	-1392.77	174.281	7.063	35.535	56.587	273.466	131.932	17.688	Average																			0	N	561.3	415.1	957.4	723.6	2657.4	207.8	0.893	0.524	0.184		51.636	12.984	74.873	56.587	196.079	82.132	16.404	0.1	N	771.9	336.9	727.1	723.6	2559.5	200.2	0.989	0.512	0.184	-143.02	71.015	10.538	56.863	56.587	195.003	90.967	16.027	0.2	N	932.7	325.5	595.8	723.6	2577.6	201.6	1.062	0.540	0.184	-238.31	85.806	10.182	46.595	56.587	199.169	97.693	16.898	0.3	N	1072.3	339.8	516.6	723.6	2652.3	207.4	1.128	0.611	0.184	-324.62	98.653	10.629	40.397	56.587	206.266	103.739	19.105	0.4	N	1202.4	368.9	472.2	723.6	2767.1	216.4	1.192	0.696	0.184	-415.45	110.624	11.539	36.930	56.587	215.679	109.665	21.778	0.5	N	1337.4	404.0	434.7	723.6	2899.7	226.8	1.256	0.786	0.184	-509.08	123.043	12.637	33.992	56.587	226.258	115.561	24.585	0.6	N	1569.4	406.2	433.3	723.6	3132.5	245.0	1.370	0.852	0.184	-805.85	144.385	12.707	33.882	56.587	247.560	126.063	26.659	0.66	N	1639.3	429.2	423.6	723.6	3215.7	251.5	1.405	0.907	0.184	-864.15	150.819	13.426	33.123	56.587	253.953	129.219	28.372																																																																																															
0.5	N	1098.0	417.3	402.6	723.6	2641.4	206.6	1.212	0.727	0.184	-208.76	101.015	13.053	31.483	56.587	202.137	111.535	22.735	0.6	N	1286.4	418.0	401.4	723.6	2829.4	221.3	1.324	0.775	0.184	-466.93	118.350	13.075	31.392	56.587	219.404	121.772	24.239	0.66	N	1327.1	443.0	396.4	723.6	2890.1	226.0	1.355	0.815	0.184	-495.51	122.091	13.858	30.998	56.587	223.533	124.634	25.505	East																			0	N	560.9	428.3	957.4	723.6	2670.3	208.8	0.895	0.535	0.184		51.607	13.399	74.873	56.587	196.465	82.359	16.729	0.1	N	765.0	368.4	730.8	723.6	2587.8	202.4	0.993	0.543	0.184	-113.16	70.383	11.522	57.153	56.587	195.645	91.316	16.979	0.2	N	930.0	380.6	598.3	723.6	2632.5	205.9	1.070	0.570	0.184	-180.86	85.565	11.905	46.785	56.587	200.842	98.468	17.844	0.3	N	1072.4	417.8	520.6	723.6	2734.5	213.8	1.140	0.687	0.184	-241.58	98.666	13.070	40.711	56.587	209.033	104.874	21.492	0.4	N	1204.2	464.3	477.5	723.6	2869.6	224.4	1.205	0.809	0.184	-313.65	110.784	14.523	37.345	56.587	219.238	110.861	25.299	0.5	N	1338.6	515.2	440.0	723.6	3017.5	236.0	1.270	0.933	0.184	-387.36	123.157	16.117	34.410	56.587	230.271	116.865	29.197	0.6	N	1566.9	527.3	438.8	723.6	3256.6	254.7	1.386	1.028	0.184	-668.14	144.157	16.495	34.311	56.587	251.550	127.511	32.142	0.66	N	1635.9	560.5	428.8	723.6	3348.9	261.9	1.422	1.103	0.184	-714.28	150.509	17.534	33.533	56.587	258.162	130.799	34.493	West																			0	N	565.6	418.0	957.4	723.6	2664.6	208.4	0.894	0.528	0.184		52.035	13.075	74.873	56.587	196.569	82.266	16.502	0.1	N	778.5	332.9	712.4	723.6	2547.4	199.2	0.989	0.507	0.184	-137.93	71.620	10.414	55.708	56.587	194.329	90.990	15.853	0.2	N	955.9	337.2	576.3	723.6	2593.0	202.8	1.065	0.581	0.184	-229.18	87.945	10.549	45.065	56.587	200.145	97.984	18.177	0.3	N	1106.7	366.6	500.0	723.6	2696.9	210.9	1.132	0.698	0.184	-312.57	101.814	11.468	39.101	56.587	208.969	104.149	21.829	0.4	N	1243.8	403.5	458.4	723.6	2829.4	221.3	1.195	0.821	0.184	-404.96	114.433	12.622	35.851	56.587	219.492	109.905	25.687	0.5	N	1385.2	449.3	424.6	723.6	2982.7	233.3	1.260	0.952	0.184	-497.92	127.439	14.054	33.208	56.587	231.287	115.877	29.786	0.6	N	1626.7	459.3	423.9	723.6	3233.4	252.9	1.374	1.060	0.184	-796.48	149.657	14.367	33.147	56.587	253.758	126.420	33.152	0.66	N	1699.9	487.5	414.6	723.6	3325.6	260.1	1.408	1.144	0.184	-854.03	156.392	15.248	32.425	56.587	260.652	129.513	35.801	North																			0	N	581.0	394.9	957.4	723.6	2656.9	207.8	0.901	0.513	0.184		53.457	12.352	74.873	56.587	197.267	82.879	16.039	0.1	N	790.5	328.1	831.9	723.6	2674.1	209.1	0.997	0.501	0.184	-242.79	72.724	10.264	65.056	56.587	204.631	91.763	15.677	0.2	N	980.8	276.3	708.8	723.6	2689.5	210.3	1.074	0.488	0.184	-433.10	90.236	8.643	55.433	56.587	210.898	98.833	15.269	0.3	N	1166.9	238.3	597.0	723.6	2725.8	213.2	1.145	0.472	0.184	-607.23	107.353	7.455	46.686	56.587	218.080	105.370	14.757	0.4	N	1345.2	232.3	529.3	723.6	2830.4	221.3	1.213	0.500	0.184	-774.63	123.762	7.265	41.392	56.587	229.006	111.559	15.631	0.5	N	1527.8	234.1	471.4	723.6	2956.9	231.2	1.282	0.531	0.184	-942.27	140.561	7.323	36.866	56.587	241.336	117.966	16.823	0.6	N	1797.5	220.3	469.0	723.6	3210.4	251.1	1.397	0.547	0.184	-1291.85	165.375	6.890	36.678	56.587	265.529	128.550	17.103	0.66	N	1894.3	225.8	454.4	723.6	3298.1	257.9	1.434	0.565	0.184	-1392.77	174.281	7.063	35.535	56.587	273.466	131.932	17.688	Average																			0	N	561.3	415.1	957.4	723.6	2657.4	207.8	0.893	0.524	0.184		51.636	12.984	74.873	56.587	196.079	82.132	16.404	0.1	N	771.9	336.9	727.1	723.6	2559.5	200.2	0.989	0.512	0.184	-143.02	71.015	10.538	56.863	56.587	195.003	90.967	16.027	0.2	N	932.7	325.5	595.8	723.6	2577.6	201.6	1.062	0.540	0.184	-238.31	85.806	10.182	46.595	56.587	199.169	97.693	16.898	0.3	N	1072.3	339.8	516.6	723.6	2652.3	207.4	1.128	0.611	0.184	-324.62	98.653	10.629	40.397	56.587	206.266	103.739	19.105	0.4	N	1202.4	368.9	472.2	723.6	2767.1	216.4	1.192	0.696	0.184	-415.45	110.624	11.539	36.930	56.587	215.679	109.665	21.778	0.5	N	1337.4	404.0	434.7	723.6	2899.7	226.8	1.256	0.786	0.184	-509.08	123.043	12.637	33.992	56.587	226.258	115.561	24.585	0.6	N	1569.4	406.2	433.3	723.6	3132.5	245.0	1.370	0.852	0.184	-805.85	144.385	12.707	33.882	56.587	247.560	126.063	26.659	0.66	N	1639.3	429.2	423.6	723.6	3215.7	251.5	1.405	0.907	0.184	-864.15	150.819	13.426	33.123	56.587	253.953	129.219	28.372																																																																																																																		
0.6	N	1286.4	418.0	401.4	723.6	2829.4	221.3	1.324	0.775	0.184	-466.93	118.350	13.075	31.392	56.587	219.404	121.772	24.239	0.66	N	1327.1	443.0	396.4	723.6	2890.1	226.0	1.355	0.815	0.184	-495.51	122.091	13.858	30.998	56.587	223.533	124.634	25.505	East																			0	N	560.9	428.3	957.4	723.6	2670.3	208.8	0.895	0.535	0.184		51.607	13.399	74.873	56.587	196.465	82.359	16.729	0.1	N	765.0	368.4	730.8	723.6	2587.8	202.4	0.993	0.543	0.184	-113.16	70.383	11.522	57.153	56.587	195.645	91.316	16.979	0.2	N	930.0	380.6	598.3	723.6	2632.5	205.9	1.070	0.570	0.184	-180.86	85.565	11.905	46.785	56.587	200.842	98.468	17.844	0.3	N	1072.4	417.8	520.6	723.6	2734.5	213.8	1.140	0.687	0.184	-241.58	98.666	13.070	40.711	56.587	209.033	104.874	21.492	0.4	N	1204.2	464.3	477.5	723.6	2869.6	224.4	1.205	0.809	0.184	-313.65	110.784	14.523	37.345	56.587	219.238	110.861	25.299	0.5	N	1338.6	515.2	440.0	723.6	3017.5	236.0	1.270	0.933	0.184	-387.36	123.157	16.117	34.410	56.587	230.271	116.865	29.197	0.6	N	1566.9	527.3	438.8	723.6	3256.6	254.7	1.386	1.028	0.184	-668.14	144.157	16.495	34.311	56.587	251.550	127.511	32.142	0.66	N	1635.9	560.5	428.8	723.6	3348.9	261.9	1.422	1.103	0.184	-714.28	150.509	17.534	33.533	56.587	258.162	130.799	34.493	West																			0	N	565.6	418.0	957.4	723.6	2664.6	208.4	0.894	0.528	0.184		52.035	13.075	74.873	56.587	196.569	82.266	16.502	0.1	N	778.5	332.9	712.4	723.6	2547.4	199.2	0.989	0.507	0.184	-137.93	71.620	10.414	55.708	56.587	194.329	90.990	15.853	0.2	N	955.9	337.2	576.3	723.6	2593.0	202.8	1.065	0.581	0.184	-229.18	87.945	10.549	45.065	56.587	200.145	97.984	18.177	0.3	N	1106.7	366.6	500.0	723.6	2696.9	210.9	1.132	0.698	0.184	-312.57	101.814	11.468	39.101	56.587	208.969	104.149	21.829	0.4	N	1243.8	403.5	458.4	723.6	2829.4	221.3	1.195	0.821	0.184	-404.96	114.433	12.622	35.851	56.587	219.492	109.905	25.687	0.5	N	1385.2	449.3	424.6	723.6	2982.7	233.3	1.260	0.952	0.184	-497.92	127.439	14.054	33.208	56.587	231.287	115.877	29.786	0.6	N	1626.7	459.3	423.9	723.6	3233.4	252.9	1.374	1.060	0.184	-796.48	149.657	14.367	33.147	56.587	253.758	126.420	33.152	0.66	N	1699.9	487.5	414.6	723.6	3325.6	260.1	1.408	1.144	0.184	-854.03	156.392	15.248	32.425	56.587	260.652	129.513	35.801	North																			0	N	581.0	394.9	957.4	723.6	2656.9	207.8	0.901	0.513	0.184		53.457	12.352	74.873	56.587	197.267	82.879	16.039	0.1	N	790.5	328.1	831.9	723.6	2674.1	209.1	0.997	0.501	0.184	-242.79	72.724	10.264	65.056	56.587	204.631	91.763	15.677	0.2	N	980.8	276.3	708.8	723.6	2689.5	210.3	1.074	0.488	0.184	-433.10	90.236	8.643	55.433	56.587	210.898	98.833	15.269	0.3	N	1166.9	238.3	597.0	723.6	2725.8	213.2	1.145	0.472	0.184	-607.23	107.353	7.455	46.686	56.587	218.080	105.370	14.757	0.4	N	1345.2	232.3	529.3	723.6	2830.4	221.3	1.213	0.500	0.184	-774.63	123.762	7.265	41.392	56.587	229.006	111.559	15.631	0.5	N	1527.8	234.1	471.4	723.6	2956.9	231.2	1.282	0.531	0.184	-942.27	140.561	7.323	36.866	56.587	241.336	117.966	16.823	0.6	N	1797.5	220.3	469.0	723.6	3210.4	251.1	1.397	0.547	0.184	-1291.85	165.375	6.890	36.678	56.587	265.529	128.550	17.103	0.66	N	1894.3	225.8	454.4	723.6	3298.1	257.9	1.434	0.565	0.184	-1392.77	174.281	7.063	35.535	56.587	273.466	131.932	17.688	Average																			0	N	561.3	415.1	957.4	723.6	2657.4	207.8	0.893	0.524	0.184		51.636	12.984	74.873	56.587	196.079	82.132	16.404	0.1	N	771.9	336.9	727.1	723.6	2559.5	200.2	0.989	0.512	0.184	-143.02	71.015	10.538	56.863	56.587	195.003	90.967	16.027	0.2	N	932.7	325.5	595.8	723.6	2577.6	201.6	1.062	0.540	0.184	-238.31	85.806	10.182	46.595	56.587	199.169	97.693	16.898	0.3	N	1072.3	339.8	516.6	723.6	2652.3	207.4	1.128	0.611	0.184	-324.62	98.653	10.629	40.397	56.587	206.266	103.739	19.105	0.4	N	1202.4	368.9	472.2	723.6	2767.1	216.4	1.192	0.696	0.184	-415.45	110.624	11.539	36.930	56.587	215.679	109.665	21.778	0.5	N	1337.4	404.0	434.7	723.6	2899.7	226.8	1.256	0.786	0.184	-509.08	123.043	12.637	33.992	56.587	226.258	115.561	24.585	0.6	N	1569.4	406.2	433.3	723.6	3132.5	245.0	1.370	0.852	0.184	-805.85	144.385	12.707	33.882	56.587	247.560	126.063	26.659	0.66	N	1639.3	429.2	423.6	723.6	3215.7	251.5	1.405	0.907	0.184	-864.15	150.819	13.426	33.123	56.587	253.953	129.219	28.372																																																																																																																																					
0.66	N	1327.1	443.0	396.4	723.6	2890.1	226.0	1.355	0.815	0.184	-495.51	122.091	13.858	30.998	56.587	223.533	124.634	25.505	East																			0	N	560.9	428.3	957.4	723.6	2670.3	208.8	0.895	0.535	0.184		51.607	13.399	74.873	56.587	196.465	82.359	16.729	0.1	N	765.0	368.4	730.8	723.6	2587.8	202.4	0.993	0.543	0.184	-113.16	70.383	11.522	57.153	56.587	195.645	91.316	16.979	0.2	N	930.0	380.6	598.3	723.6	2632.5	205.9	1.070	0.570	0.184	-180.86	85.565	11.905	46.785	56.587	200.842	98.468	17.844	0.3	N	1072.4	417.8	520.6	723.6	2734.5	213.8	1.140	0.687	0.184	-241.58	98.666	13.070	40.711	56.587	209.033	104.874	21.492	0.4	N	1204.2	464.3	477.5	723.6	2869.6	224.4	1.205	0.809	0.184	-313.65	110.784	14.523	37.345	56.587	219.238	110.861	25.299	0.5	N	1338.6	515.2	440.0	723.6	3017.5	236.0	1.270	0.933	0.184	-387.36	123.157	16.117	34.410	56.587	230.271	116.865	29.197	0.6	N	1566.9	527.3	438.8	723.6	3256.6	254.7	1.386	1.028	0.184	-668.14	144.157	16.495	34.311	56.587	251.550	127.511	32.142	0.66	N	1635.9	560.5	428.8	723.6	3348.9	261.9	1.422	1.103	0.184	-714.28	150.509	17.534	33.533	56.587	258.162	130.799	34.493	West																			0	N	565.6	418.0	957.4	723.6	2664.6	208.4	0.894	0.528	0.184		52.035	13.075	74.873	56.587	196.569	82.266	16.502	0.1	N	778.5	332.9	712.4	723.6	2547.4	199.2	0.989	0.507	0.184	-137.93	71.620	10.414	55.708	56.587	194.329	90.990	15.853	0.2	N	955.9	337.2	576.3	723.6	2593.0	202.8	1.065	0.581	0.184	-229.18	87.945	10.549	45.065	56.587	200.145	97.984	18.177	0.3	N	1106.7	366.6	500.0	723.6	2696.9	210.9	1.132	0.698	0.184	-312.57	101.814	11.468	39.101	56.587	208.969	104.149	21.829	0.4	N	1243.8	403.5	458.4	723.6	2829.4	221.3	1.195	0.821	0.184	-404.96	114.433	12.622	35.851	56.587	219.492	109.905	25.687	0.5	N	1385.2	449.3	424.6	723.6	2982.7	233.3	1.260	0.952	0.184	-497.92	127.439	14.054	33.208	56.587	231.287	115.877	29.786	0.6	N	1626.7	459.3	423.9	723.6	3233.4	252.9	1.374	1.060	0.184	-796.48	149.657	14.367	33.147	56.587	253.758	126.420	33.152	0.66	N	1699.9	487.5	414.6	723.6	3325.6	260.1	1.408	1.144	0.184	-854.03	156.392	15.248	32.425	56.587	260.652	129.513	35.801	North																			0	N	581.0	394.9	957.4	723.6	2656.9	207.8	0.901	0.513	0.184		53.457	12.352	74.873	56.587	197.267	82.879	16.039	0.1	N	790.5	328.1	831.9	723.6	2674.1	209.1	0.997	0.501	0.184	-242.79	72.724	10.264	65.056	56.587	204.631	91.763	15.677	0.2	N	980.8	276.3	708.8	723.6	2689.5	210.3	1.074	0.488	0.184	-433.10	90.236	8.643	55.433	56.587	210.898	98.833	15.269	0.3	N	1166.9	238.3	597.0	723.6	2725.8	213.2	1.145	0.472	0.184	-607.23	107.353	7.455	46.686	56.587	218.080	105.370	14.757	0.4	N	1345.2	232.3	529.3	723.6	2830.4	221.3	1.213	0.500	0.184	-774.63	123.762	7.265	41.392	56.587	229.006	111.559	15.631	0.5	N	1527.8	234.1	471.4	723.6	2956.9	231.2	1.282	0.531	0.184	-942.27	140.561	7.323	36.866	56.587	241.336	117.966	16.823	0.6	N	1797.5	220.3	469.0	723.6	3210.4	251.1	1.397	0.547	0.184	-1291.85	165.375	6.890	36.678	56.587	265.529	128.550	17.103	0.66	N	1894.3	225.8	454.4	723.6	3298.1	257.9	1.434	0.565	0.184	-1392.77	174.281	7.063	35.535	56.587	273.466	131.932	17.688	Average																			0	N	561.3	415.1	957.4	723.6	2657.4	207.8	0.893	0.524	0.184		51.636	12.984	74.873	56.587	196.079	82.132	16.404	0.1	N	771.9	336.9	727.1	723.6	2559.5	200.2	0.989	0.512	0.184	-143.02	71.015	10.538	56.863	56.587	195.003	90.967	16.027	0.2	N	932.7	325.5	595.8	723.6	2577.6	201.6	1.062	0.540	0.184	-238.31	85.806	10.182	46.595	56.587	199.169	97.693	16.898	0.3	N	1072.3	339.8	516.6	723.6	2652.3	207.4	1.128	0.611	0.184	-324.62	98.653	10.629	40.397	56.587	206.266	103.739	19.105	0.4	N	1202.4	368.9	472.2	723.6	2767.1	216.4	1.192	0.696	0.184	-415.45	110.624	11.539	36.930	56.587	215.679	109.665	21.778	0.5	N	1337.4	404.0	434.7	723.6	2899.7	226.8	1.256	0.786	0.184	-509.08	123.043	12.637	33.992	56.587	226.258	115.561	24.585	0.6	N	1569.4	406.2	433.3	723.6	3132.5	245.0	1.370	0.852	0.184	-805.85	144.385	12.707	33.882	56.587	247.560	126.063	26.659	0.66	N	1639.3	429.2	423.6	723.6	3215.7	251.5	1.405	0.907	0.184	-864.15	150.819	13.426	33.123	56.587	253.953	129.219	28.372																																																																																																																																																								
East																			0	N	560.9	428.3	957.4	723.6	2670.3	208.8	0.895	0.535	0.184		51.607	13.399	74.873	56.587	196.465	82.359	16.729	0.1	N	765.0	368.4	730.8	723.6	2587.8	202.4	0.993	0.543	0.184	-113.16	70.383	11.522	57.153	56.587	195.645	91.316	16.979	0.2	N	930.0	380.6	598.3	723.6	2632.5	205.9	1.070	0.570	0.184	-180.86	85.565	11.905	46.785	56.587	200.842	98.468	17.844	0.3	N	1072.4	417.8	520.6	723.6	2734.5	213.8	1.140	0.687	0.184	-241.58	98.666	13.070	40.711	56.587	209.033	104.874	21.492	0.4	N	1204.2	464.3	477.5	723.6	2869.6	224.4	1.205	0.809	0.184	-313.65	110.784	14.523	37.345	56.587	219.238	110.861	25.299	0.5	N	1338.6	515.2	440.0	723.6	3017.5	236.0	1.270	0.933	0.184	-387.36	123.157	16.117	34.410	56.587	230.271	116.865	29.197	0.6	N	1566.9	527.3	438.8	723.6	3256.6	254.7	1.386	1.028	0.184	-668.14	144.157	16.495	34.311	56.587	251.550	127.511	32.142	0.66	N	1635.9	560.5	428.8	723.6	3348.9	261.9	1.422	1.103	0.184	-714.28	150.509	17.534	33.533	56.587	258.162	130.799	34.493	West																			0	N	565.6	418.0	957.4	723.6	2664.6	208.4	0.894	0.528	0.184		52.035	13.075	74.873	56.587	196.569	82.266	16.502	0.1	N	778.5	332.9	712.4	723.6	2547.4	199.2	0.989	0.507	0.184	-137.93	71.620	10.414	55.708	56.587	194.329	90.990	15.853	0.2	N	955.9	337.2	576.3	723.6	2593.0	202.8	1.065	0.581	0.184	-229.18	87.945	10.549	45.065	56.587	200.145	97.984	18.177	0.3	N	1106.7	366.6	500.0	723.6	2696.9	210.9	1.132	0.698	0.184	-312.57	101.814	11.468	39.101	56.587	208.969	104.149	21.829	0.4	N	1243.8	403.5	458.4	723.6	2829.4	221.3	1.195	0.821	0.184	-404.96	114.433	12.622	35.851	56.587	219.492	109.905	25.687	0.5	N	1385.2	449.3	424.6	723.6	2982.7	233.3	1.260	0.952	0.184	-497.92	127.439	14.054	33.208	56.587	231.287	115.877	29.786	0.6	N	1626.7	459.3	423.9	723.6	3233.4	252.9	1.374	1.060	0.184	-796.48	149.657	14.367	33.147	56.587	253.758	126.420	33.152	0.66	N	1699.9	487.5	414.6	723.6	3325.6	260.1	1.408	1.144	0.184	-854.03	156.392	15.248	32.425	56.587	260.652	129.513	35.801	North																			0	N	581.0	394.9	957.4	723.6	2656.9	207.8	0.901	0.513	0.184		53.457	12.352	74.873	56.587	197.267	82.879	16.039	0.1	N	790.5	328.1	831.9	723.6	2674.1	209.1	0.997	0.501	0.184	-242.79	72.724	10.264	65.056	56.587	204.631	91.763	15.677	0.2	N	980.8	276.3	708.8	723.6	2689.5	210.3	1.074	0.488	0.184	-433.10	90.236	8.643	55.433	56.587	210.898	98.833	15.269	0.3	N	1166.9	238.3	597.0	723.6	2725.8	213.2	1.145	0.472	0.184	-607.23	107.353	7.455	46.686	56.587	218.080	105.370	14.757	0.4	N	1345.2	232.3	529.3	723.6	2830.4	221.3	1.213	0.500	0.184	-774.63	123.762	7.265	41.392	56.587	229.006	111.559	15.631	0.5	N	1527.8	234.1	471.4	723.6	2956.9	231.2	1.282	0.531	0.184	-942.27	140.561	7.323	36.866	56.587	241.336	117.966	16.823	0.6	N	1797.5	220.3	469.0	723.6	3210.4	251.1	1.397	0.547	0.184	-1291.85	165.375	6.890	36.678	56.587	265.529	128.550	17.103	0.66	N	1894.3	225.8	454.4	723.6	3298.1	257.9	1.434	0.565	0.184	-1392.77	174.281	7.063	35.535	56.587	273.466	131.932	17.688	Average																			0	N	561.3	415.1	957.4	723.6	2657.4	207.8	0.893	0.524	0.184		51.636	12.984	74.873	56.587	196.079	82.132	16.404	0.1	N	771.9	336.9	727.1	723.6	2559.5	200.2	0.989	0.512	0.184	-143.02	71.015	10.538	56.863	56.587	195.003	90.967	16.027	0.2	N	932.7	325.5	595.8	723.6	2577.6	201.6	1.062	0.540	0.184	-238.31	85.806	10.182	46.595	56.587	199.169	97.693	16.898	0.3	N	1072.3	339.8	516.6	723.6	2652.3	207.4	1.128	0.611	0.184	-324.62	98.653	10.629	40.397	56.587	206.266	103.739	19.105	0.4	N	1202.4	368.9	472.2	723.6	2767.1	216.4	1.192	0.696	0.184	-415.45	110.624	11.539	36.930	56.587	215.679	109.665	21.778	0.5	N	1337.4	404.0	434.7	723.6	2899.7	226.8	1.256	0.786	0.184	-509.08	123.043	12.637	33.992	56.587	226.258	115.561	24.585	0.6	N	1569.4	406.2	433.3	723.6	3132.5	245.0	1.370	0.852	0.184	-805.85	144.385	12.707	33.882	56.587	247.560	126.063	26.659	0.66	N	1639.3	429.2	423.6	723.6	3215.7	251.5	1.405	0.907	0.184	-864.15	150.819	13.426	33.123	56.587	253.953	129.219	28.372																																																																																																																																																																											
0	N	560.9	428.3	957.4	723.6	2670.3	208.8	0.895	0.535	0.184		51.607	13.399	74.873	56.587	196.465	82.359	16.729	0.1	N	765.0	368.4	730.8	723.6	2587.8	202.4	0.993	0.543	0.184	-113.16	70.383	11.522	57.153	56.587	195.645	91.316	16.979	0.2	N	930.0	380.6	598.3	723.6	2632.5	205.9	1.070	0.570	0.184	-180.86	85.565	11.905	46.785	56.587	200.842	98.468	17.844	0.3	N	1072.4	417.8	520.6	723.6	2734.5	213.8	1.140	0.687	0.184	-241.58	98.666	13.070	40.711	56.587	209.033	104.874	21.492	0.4	N	1204.2	464.3	477.5	723.6	2869.6	224.4	1.205	0.809	0.184	-313.65	110.784	14.523	37.345	56.587	219.238	110.861	25.299	0.5	N	1338.6	515.2	440.0	723.6	3017.5	236.0	1.270	0.933	0.184	-387.36	123.157	16.117	34.410	56.587	230.271	116.865	29.197	0.6	N	1566.9	527.3	438.8	723.6	3256.6	254.7	1.386	1.028	0.184	-668.14	144.157	16.495	34.311	56.587	251.550	127.511	32.142	0.66	N	1635.9	560.5	428.8	723.6	3348.9	261.9	1.422	1.103	0.184	-714.28	150.509	17.534	33.533	56.587	258.162	130.799	34.493	West																			0	N	565.6	418.0	957.4	723.6	2664.6	208.4	0.894	0.528	0.184		52.035	13.075	74.873	56.587	196.569	82.266	16.502	0.1	N	778.5	332.9	712.4	723.6	2547.4	199.2	0.989	0.507	0.184	-137.93	71.620	10.414	55.708	56.587	194.329	90.990	15.853	0.2	N	955.9	337.2	576.3	723.6	2593.0	202.8	1.065	0.581	0.184	-229.18	87.945	10.549	45.065	56.587	200.145	97.984	18.177	0.3	N	1106.7	366.6	500.0	723.6	2696.9	210.9	1.132	0.698	0.184	-312.57	101.814	11.468	39.101	56.587	208.969	104.149	21.829	0.4	N	1243.8	403.5	458.4	723.6	2829.4	221.3	1.195	0.821	0.184	-404.96	114.433	12.622	35.851	56.587	219.492	109.905	25.687	0.5	N	1385.2	449.3	424.6	723.6	2982.7	233.3	1.260	0.952	0.184	-497.92	127.439	14.054	33.208	56.587	231.287	115.877	29.786	0.6	N	1626.7	459.3	423.9	723.6	3233.4	252.9	1.374	1.060	0.184	-796.48	149.657	14.367	33.147	56.587	253.758	126.420	33.152	0.66	N	1699.9	487.5	414.6	723.6	3325.6	260.1	1.408	1.144	0.184	-854.03	156.392	15.248	32.425	56.587	260.652	129.513	35.801	North																			0	N	581.0	394.9	957.4	723.6	2656.9	207.8	0.901	0.513	0.184		53.457	12.352	74.873	56.587	197.267	82.879	16.039	0.1	N	790.5	328.1	831.9	723.6	2674.1	209.1	0.997	0.501	0.184	-242.79	72.724	10.264	65.056	56.587	204.631	91.763	15.677	0.2	N	980.8	276.3	708.8	723.6	2689.5	210.3	1.074	0.488	0.184	-433.10	90.236	8.643	55.433	56.587	210.898	98.833	15.269	0.3	N	1166.9	238.3	597.0	723.6	2725.8	213.2	1.145	0.472	0.184	-607.23	107.353	7.455	46.686	56.587	218.080	105.370	14.757	0.4	N	1345.2	232.3	529.3	723.6	2830.4	221.3	1.213	0.500	0.184	-774.63	123.762	7.265	41.392	56.587	229.006	111.559	15.631	0.5	N	1527.8	234.1	471.4	723.6	2956.9	231.2	1.282	0.531	0.184	-942.27	140.561	7.323	36.866	56.587	241.336	117.966	16.823	0.6	N	1797.5	220.3	469.0	723.6	3210.4	251.1	1.397	0.547	0.184	-1291.85	165.375	6.890	36.678	56.587	265.529	128.550	17.103	0.66	N	1894.3	225.8	454.4	723.6	3298.1	257.9	1.434	0.565	0.184	-1392.77	174.281	7.063	35.535	56.587	273.466	131.932	17.688	Average																			0	N	561.3	415.1	957.4	723.6	2657.4	207.8	0.893	0.524	0.184		51.636	12.984	74.873	56.587	196.079	82.132	16.404	0.1	N	771.9	336.9	727.1	723.6	2559.5	200.2	0.989	0.512	0.184	-143.02	71.015	10.538	56.863	56.587	195.003	90.967	16.027	0.2	N	932.7	325.5	595.8	723.6	2577.6	201.6	1.062	0.540	0.184	-238.31	85.806	10.182	46.595	56.587	199.169	97.693	16.898	0.3	N	1072.3	339.8	516.6	723.6	2652.3	207.4	1.128	0.611	0.184	-324.62	98.653	10.629	40.397	56.587	206.266	103.739	19.105	0.4	N	1202.4	368.9	472.2	723.6	2767.1	216.4	1.192	0.696	0.184	-415.45	110.624	11.539	36.930	56.587	215.679	109.665	21.778	0.5	N	1337.4	404.0	434.7	723.6	2899.7	226.8	1.256	0.786	0.184	-509.08	123.043	12.637	33.992	56.587	226.258	115.561	24.585	0.6	N	1569.4	406.2	433.3	723.6	3132.5	245.0	1.370	0.852	0.184	-805.85	144.385	12.707	33.882	56.587	247.560	126.063	26.659	0.66	N	1639.3	429.2	423.6	723.6	3215.7	251.5	1.405	0.907	0.184	-864.15	150.819	13.426	33.123	56.587	253.953	129.219	28.372																																																																																																																																																																																														
0.1	N	765.0	368.4	730.8	723.6	2587.8	202.4	0.993	0.543	0.184	-113.16	70.383	11.522	57.153	56.587	195.645	91.316	16.979	0.2	N	930.0	380.6	598.3	723.6	2632.5	205.9	1.070	0.570	0.184	-180.86	85.565	11.905	46.785	56.587	200.842	98.468	17.844	0.3	N	1072.4	417.8	520.6	723.6	2734.5	213.8	1.140	0.687	0.184	-241.58	98.666	13.070	40.711	56.587	209.033	104.874	21.492	0.4	N	1204.2	464.3	477.5	723.6	2869.6	224.4	1.205	0.809	0.184	-313.65	110.784	14.523	37.345	56.587	219.238	110.861	25.299	0.5	N	1338.6	515.2	440.0	723.6	3017.5	236.0	1.270	0.933	0.184	-387.36	123.157	16.117	34.410	56.587	230.271	116.865	29.197	0.6	N	1566.9	527.3	438.8	723.6	3256.6	254.7	1.386	1.028	0.184	-668.14	144.157	16.495	34.311	56.587	251.550	127.511	32.142	0.66	N	1635.9	560.5	428.8	723.6	3348.9	261.9	1.422	1.103	0.184	-714.28	150.509	17.534	33.533	56.587	258.162	130.799	34.493	West																			0	N	565.6	418.0	957.4	723.6	2664.6	208.4	0.894	0.528	0.184		52.035	13.075	74.873	56.587	196.569	82.266	16.502	0.1	N	778.5	332.9	712.4	723.6	2547.4	199.2	0.989	0.507	0.184	-137.93	71.620	10.414	55.708	56.587	194.329	90.990	15.853	0.2	N	955.9	337.2	576.3	723.6	2593.0	202.8	1.065	0.581	0.184	-229.18	87.945	10.549	45.065	56.587	200.145	97.984	18.177	0.3	N	1106.7	366.6	500.0	723.6	2696.9	210.9	1.132	0.698	0.184	-312.57	101.814	11.468	39.101	56.587	208.969	104.149	21.829	0.4	N	1243.8	403.5	458.4	723.6	2829.4	221.3	1.195	0.821	0.184	-404.96	114.433	12.622	35.851	56.587	219.492	109.905	25.687	0.5	N	1385.2	449.3	424.6	723.6	2982.7	233.3	1.260	0.952	0.184	-497.92	127.439	14.054	33.208	56.587	231.287	115.877	29.786	0.6	N	1626.7	459.3	423.9	723.6	3233.4	252.9	1.374	1.060	0.184	-796.48	149.657	14.367	33.147	56.587	253.758	126.420	33.152	0.66	N	1699.9	487.5	414.6	723.6	3325.6	260.1	1.408	1.144	0.184	-854.03	156.392	15.248	32.425	56.587	260.652	129.513	35.801	North																			0	N	581.0	394.9	957.4	723.6	2656.9	207.8	0.901	0.513	0.184		53.457	12.352	74.873	56.587	197.267	82.879	16.039	0.1	N	790.5	328.1	831.9	723.6	2674.1	209.1	0.997	0.501	0.184	-242.79	72.724	10.264	65.056	56.587	204.631	91.763	15.677	0.2	N	980.8	276.3	708.8	723.6	2689.5	210.3	1.074	0.488	0.184	-433.10	90.236	8.643	55.433	56.587	210.898	98.833	15.269	0.3	N	1166.9	238.3	597.0	723.6	2725.8	213.2	1.145	0.472	0.184	-607.23	107.353	7.455	46.686	56.587	218.080	105.370	14.757	0.4	N	1345.2	232.3	529.3	723.6	2830.4	221.3	1.213	0.500	0.184	-774.63	123.762	7.265	41.392	56.587	229.006	111.559	15.631	0.5	N	1527.8	234.1	471.4	723.6	2956.9	231.2	1.282	0.531	0.184	-942.27	140.561	7.323	36.866	56.587	241.336	117.966	16.823	0.6	N	1797.5	220.3	469.0	723.6	3210.4	251.1	1.397	0.547	0.184	-1291.85	165.375	6.890	36.678	56.587	265.529	128.550	17.103	0.66	N	1894.3	225.8	454.4	723.6	3298.1	257.9	1.434	0.565	0.184	-1392.77	174.281	7.063	35.535	56.587	273.466	131.932	17.688	Average																			0	N	561.3	415.1	957.4	723.6	2657.4	207.8	0.893	0.524	0.184		51.636	12.984	74.873	56.587	196.079	82.132	16.404	0.1	N	771.9	336.9	727.1	723.6	2559.5	200.2	0.989	0.512	0.184	-143.02	71.015	10.538	56.863	56.587	195.003	90.967	16.027	0.2	N	932.7	325.5	595.8	723.6	2577.6	201.6	1.062	0.540	0.184	-238.31	85.806	10.182	46.595	56.587	199.169	97.693	16.898	0.3	N	1072.3	339.8	516.6	723.6	2652.3	207.4	1.128	0.611	0.184	-324.62	98.653	10.629	40.397	56.587	206.266	103.739	19.105	0.4	N	1202.4	368.9	472.2	723.6	2767.1	216.4	1.192	0.696	0.184	-415.45	110.624	11.539	36.930	56.587	215.679	109.665	21.778	0.5	N	1337.4	404.0	434.7	723.6	2899.7	226.8	1.256	0.786	0.184	-509.08	123.043	12.637	33.992	56.587	226.258	115.561	24.585	0.6	N	1569.4	406.2	433.3	723.6	3132.5	245.0	1.370	0.852	0.184	-805.85	144.385	12.707	33.882	56.587	247.560	126.063	26.659	0.66	N	1639.3	429.2	423.6	723.6	3215.7	251.5	1.405	0.907	0.184	-864.15	150.819	13.426	33.123	56.587	253.953	129.219	28.372																																																																																																																																																																																																																	
0.2	N	930.0	380.6	598.3	723.6	2632.5	205.9	1.070	0.570	0.184	-180.86	85.565	11.905	46.785	56.587	200.842	98.468	17.844	0.3	N	1072.4	417.8	520.6	723.6	2734.5	213.8	1.140	0.687	0.184	-241.58	98.666	13.070	40.711	56.587	209.033	104.874	21.492	0.4	N	1204.2	464.3	477.5	723.6	2869.6	224.4	1.205	0.809	0.184	-313.65	110.784	14.523	37.345	56.587	219.238	110.861	25.299	0.5	N	1338.6	515.2	440.0	723.6	3017.5	236.0	1.270	0.933	0.184	-387.36	123.157	16.117	34.410	56.587	230.271	116.865	29.197	0.6	N	1566.9	527.3	438.8	723.6	3256.6	254.7	1.386	1.028	0.184	-668.14	144.157	16.495	34.311	56.587	251.550	127.511	32.142	0.66	N	1635.9	560.5	428.8	723.6	3348.9	261.9	1.422	1.103	0.184	-714.28	150.509	17.534	33.533	56.587	258.162	130.799	34.493	West																			0	N	565.6	418.0	957.4	723.6	2664.6	208.4	0.894	0.528	0.184		52.035	13.075	74.873	56.587	196.569	82.266	16.502	0.1	N	778.5	332.9	712.4	723.6	2547.4	199.2	0.989	0.507	0.184	-137.93	71.620	10.414	55.708	56.587	194.329	90.990	15.853	0.2	N	955.9	337.2	576.3	723.6	2593.0	202.8	1.065	0.581	0.184	-229.18	87.945	10.549	45.065	56.587	200.145	97.984	18.177	0.3	N	1106.7	366.6	500.0	723.6	2696.9	210.9	1.132	0.698	0.184	-312.57	101.814	11.468	39.101	56.587	208.969	104.149	21.829	0.4	N	1243.8	403.5	458.4	723.6	2829.4	221.3	1.195	0.821	0.184	-404.96	114.433	12.622	35.851	56.587	219.492	109.905	25.687	0.5	N	1385.2	449.3	424.6	723.6	2982.7	233.3	1.260	0.952	0.184	-497.92	127.439	14.054	33.208	56.587	231.287	115.877	29.786	0.6	N	1626.7	459.3	423.9	723.6	3233.4	252.9	1.374	1.060	0.184	-796.48	149.657	14.367	33.147	56.587	253.758	126.420	33.152	0.66	N	1699.9	487.5	414.6	723.6	3325.6	260.1	1.408	1.144	0.184	-854.03	156.392	15.248	32.425	56.587	260.652	129.513	35.801	North																			0	N	581.0	394.9	957.4	723.6	2656.9	207.8	0.901	0.513	0.184		53.457	12.352	74.873	56.587	197.267	82.879	16.039	0.1	N	790.5	328.1	831.9	723.6	2674.1	209.1	0.997	0.501	0.184	-242.79	72.724	10.264	65.056	56.587	204.631	91.763	15.677	0.2	N	980.8	276.3	708.8	723.6	2689.5	210.3	1.074	0.488	0.184	-433.10	90.236	8.643	55.433	56.587	210.898	98.833	15.269	0.3	N	1166.9	238.3	597.0	723.6	2725.8	213.2	1.145	0.472	0.184	-607.23	107.353	7.455	46.686	56.587	218.080	105.370	14.757	0.4	N	1345.2	232.3	529.3	723.6	2830.4	221.3	1.213	0.500	0.184	-774.63	123.762	7.265	41.392	56.587	229.006	111.559	15.631	0.5	N	1527.8	234.1	471.4	723.6	2956.9	231.2	1.282	0.531	0.184	-942.27	140.561	7.323	36.866	56.587	241.336	117.966	16.823	0.6	N	1797.5	220.3	469.0	723.6	3210.4	251.1	1.397	0.547	0.184	-1291.85	165.375	6.890	36.678	56.587	265.529	128.550	17.103	0.66	N	1894.3	225.8	454.4	723.6	3298.1	257.9	1.434	0.565	0.184	-1392.77	174.281	7.063	35.535	56.587	273.466	131.932	17.688	Average																			0	N	561.3	415.1	957.4	723.6	2657.4	207.8	0.893	0.524	0.184		51.636	12.984	74.873	56.587	196.079	82.132	16.404	0.1	N	771.9	336.9	727.1	723.6	2559.5	200.2	0.989	0.512	0.184	-143.02	71.015	10.538	56.863	56.587	195.003	90.967	16.027	0.2	N	932.7	325.5	595.8	723.6	2577.6	201.6	1.062	0.540	0.184	-238.31	85.806	10.182	46.595	56.587	199.169	97.693	16.898	0.3	N	1072.3	339.8	516.6	723.6	2652.3	207.4	1.128	0.611	0.184	-324.62	98.653	10.629	40.397	56.587	206.266	103.739	19.105	0.4	N	1202.4	368.9	472.2	723.6	2767.1	216.4	1.192	0.696	0.184	-415.45	110.624	11.539	36.930	56.587	215.679	109.665	21.778	0.5	N	1337.4	404.0	434.7	723.6	2899.7	226.8	1.256	0.786	0.184	-509.08	123.043	12.637	33.992	56.587	226.258	115.561	24.585	0.6	N	1569.4	406.2	433.3	723.6	3132.5	245.0	1.370	0.852	0.184	-805.85	144.385	12.707	33.882	56.587	247.560	126.063	26.659	0.66	N	1639.3	429.2	423.6	723.6	3215.7	251.5	1.405	0.907	0.184	-864.15	150.819	13.426	33.123	56.587	253.953	129.219	28.372																																																																																																																																																																																																																																				
0.3	N	1072.4	417.8	520.6	723.6	2734.5	213.8	1.140	0.687	0.184	-241.58	98.666	13.070	40.711	56.587	209.033	104.874	21.492	0.4	N	1204.2	464.3	477.5	723.6	2869.6	224.4	1.205	0.809	0.184	-313.65	110.784	14.523	37.345	56.587	219.238	110.861	25.299	0.5	N	1338.6	515.2	440.0	723.6	3017.5	236.0	1.270	0.933	0.184	-387.36	123.157	16.117	34.410	56.587	230.271	116.865	29.197	0.6	N	1566.9	527.3	438.8	723.6	3256.6	254.7	1.386	1.028	0.184	-668.14	144.157	16.495	34.311	56.587	251.550	127.511	32.142	0.66	N	1635.9	560.5	428.8	723.6	3348.9	261.9	1.422	1.103	0.184	-714.28	150.509	17.534	33.533	56.587	258.162	130.799	34.493	West																			0	N	565.6	418.0	957.4	723.6	2664.6	208.4	0.894	0.528	0.184		52.035	13.075	74.873	56.587	196.569	82.266	16.502	0.1	N	778.5	332.9	712.4	723.6	2547.4	199.2	0.989	0.507	0.184	-137.93	71.620	10.414	55.708	56.587	194.329	90.990	15.853	0.2	N	955.9	337.2	576.3	723.6	2593.0	202.8	1.065	0.581	0.184	-229.18	87.945	10.549	45.065	56.587	200.145	97.984	18.177	0.3	N	1106.7	366.6	500.0	723.6	2696.9	210.9	1.132	0.698	0.184	-312.57	101.814	11.468	39.101	56.587	208.969	104.149	21.829	0.4	N	1243.8	403.5	458.4	723.6	2829.4	221.3	1.195	0.821	0.184	-404.96	114.433	12.622	35.851	56.587	219.492	109.905	25.687	0.5	N	1385.2	449.3	424.6	723.6	2982.7	233.3	1.260	0.952	0.184	-497.92	127.439	14.054	33.208	56.587	231.287	115.877	29.786	0.6	N	1626.7	459.3	423.9	723.6	3233.4	252.9	1.374	1.060	0.184	-796.48	149.657	14.367	33.147	56.587	253.758	126.420	33.152	0.66	N	1699.9	487.5	414.6	723.6	3325.6	260.1	1.408	1.144	0.184	-854.03	156.392	15.248	32.425	56.587	260.652	129.513	35.801	North																			0	N	581.0	394.9	957.4	723.6	2656.9	207.8	0.901	0.513	0.184		53.457	12.352	74.873	56.587	197.267	82.879	16.039	0.1	N	790.5	328.1	831.9	723.6	2674.1	209.1	0.997	0.501	0.184	-242.79	72.724	10.264	65.056	56.587	204.631	91.763	15.677	0.2	N	980.8	276.3	708.8	723.6	2689.5	210.3	1.074	0.488	0.184	-433.10	90.236	8.643	55.433	56.587	210.898	98.833	15.269	0.3	N	1166.9	238.3	597.0	723.6	2725.8	213.2	1.145	0.472	0.184	-607.23	107.353	7.455	46.686	56.587	218.080	105.370	14.757	0.4	N	1345.2	232.3	529.3	723.6	2830.4	221.3	1.213	0.500	0.184	-774.63	123.762	7.265	41.392	56.587	229.006	111.559	15.631	0.5	N	1527.8	234.1	471.4	723.6	2956.9	231.2	1.282	0.531	0.184	-942.27	140.561	7.323	36.866	56.587	241.336	117.966	16.823	0.6	N	1797.5	220.3	469.0	723.6	3210.4	251.1	1.397	0.547	0.184	-1291.85	165.375	6.890	36.678	56.587	265.529	128.550	17.103	0.66	N	1894.3	225.8	454.4	723.6	3298.1	257.9	1.434	0.565	0.184	-1392.77	174.281	7.063	35.535	56.587	273.466	131.932	17.688	Average																			0	N	561.3	415.1	957.4	723.6	2657.4	207.8	0.893	0.524	0.184		51.636	12.984	74.873	56.587	196.079	82.132	16.404	0.1	N	771.9	336.9	727.1	723.6	2559.5	200.2	0.989	0.512	0.184	-143.02	71.015	10.538	56.863	56.587	195.003	90.967	16.027	0.2	N	932.7	325.5	595.8	723.6	2577.6	201.6	1.062	0.540	0.184	-238.31	85.806	10.182	46.595	56.587	199.169	97.693	16.898	0.3	N	1072.3	339.8	516.6	723.6	2652.3	207.4	1.128	0.611	0.184	-324.62	98.653	10.629	40.397	56.587	206.266	103.739	19.105	0.4	N	1202.4	368.9	472.2	723.6	2767.1	216.4	1.192	0.696	0.184	-415.45	110.624	11.539	36.930	56.587	215.679	109.665	21.778	0.5	N	1337.4	404.0	434.7	723.6	2899.7	226.8	1.256	0.786	0.184	-509.08	123.043	12.637	33.992	56.587	226.258	115.561	24.585	0.6	N	1569.4	406.2	433.3	723.6	3132.5	245.0	1.370	0.852	0.184	-805.85	144.385	12.707	33.882	56.587	247.560	126.063	26.659	0.66	N	1639.3	429.2	423.6	723.6	3215.7	251.5	1.405	0.907	0.184	-864.15	150.819	13.426	33.123	56.587	253.953	129.219	28.372																																																																																																																																																																																																																																																							
0.4	N	1204.2	464.3	477.5	723.6	2869.6	224.4	1.205	0.809	0.184	-313.65	110.784	14.523	37.345	56.587	219.238	110.861	25.299	0.5	N	1338.6	515.2	440.0	723.6	3017.5	236.0	1.270	0.933	0.184	-387.36	123.157	16.117	34.410	56.587	230.271	116.865	29.197	0.6	N	1566.9	527.3	438.8	723.6	3256.6	254.7	1.386	1.028	0.184	-668.14	144.157	16.495	34.311	56.587	251.550	127.511	32.142	0.66	N	1635.9	560.5	428.8	723.6	3348.9	261.9	1.422	1.103	0.184	-714.28	150.509	17.534	33.533	56.587	258.162	130.799	34.493	West																			0	N	565.6	418.0	957.4	723.6	2664.6	208.4	0.894	0.528	0.184		52.035	13.075	74.873	56.587	196.569	82.266	16.502	0.1	N	778.5	332.9	712.4	723.6	2547.4	199.2	0.989	0.507	0.184	-137.93	71.620	10.414	55.708	56.587	194.329	90.990	15.853	0.2	N	955.9	337.2	576.3	723.6	2593.0	202.8	1.065	0.581	0.184	-229.18	87.945	10.549	45.065	56.587	200.145	97.984	18.177	0.3	N	1106.7	366.6	500.0	723.6	2696.9	210.9	1.132	0.698	0.184	-312.57	101.814	11.468	39.101	56.587	208.969	104.149	21.829	0.4	N	1243.8	403.5	458.4	723.6	2829.4	221.3	1.195	0.821	0.184	-404.96	114.433	12.622	35.851	56.587	219.492	109.905	25.687	0.5	N	1385.2	449.3	424.6	723.6	2982.7	233.3	1.260	0.952	0.184	-497.92	127.439	14.054	33.208	56.587	231.287	115.877	29.786	0.6	N	1626.7	459.3	423.9	723.6	3233.4	252.9	1.374	1.060	0.184	-796.48	149.657	14.367	33.147	56.587	253.758	126.420	33.152	0.66	N	1699.9	487.5	414.6	723.6	3325.6	260.1	1.408	1.144	0.184	-854.03	156.392	15.248	32.425	56.587	260.652	129.513	35.801	North																			0	N	581.0	394.9	957.4	723.6	2656.9	207.8	0.901	0.513	0.184		53.457	12.352	74.873	56.587	197.267	82.879	16.039	0.1	N	790.5	328.1	831.9	723.6	2674.1	209.1	0.997	0.501	0.184	-242.79	72.724	10.264	65.056	56.587	204.631	91.763	15.677	0.2	N	980.8	276.3	708.8	723.6	2689.5	210.3	1.074	0.488	0.184	-433.10	90.236	8.643	55.433	56.587	210.898	98.833	15.269	0.3	N	1166.9	238.3	597.0	723.6	2725.8	213.2	1.145	0.472	0.184	-607.23	107.353	7.455	46.686	56.587	218.080	105.370	14.757	0.4	N	1345.2	232.3	529.3	723.6	2830.4	221.3	1.213	0.500	0.184	-774.63	123.762	7.265	41.392	56.587	229.006	111.559	15.631	0.5	N	1527.8	234.1	471.4	723.6	2956.9	231.2	1.282	0.531	0.184	-942.27	140.561	7.323	36.866	56.587	241.336	117.966	16.823	0.6	N	1797.5	220.3	469.0	723.6	3210.4	251.1	1.397	0.547	0.184	-1291.85	165.375	6.890	36.678	56.587	265.529	128.550	17.103	0.66	N	1894.3	225.8	454.4	723.6	3298.1	257.9	1.434	0.565	0.184	-1392.77	174.281	7.063	35.535	56.587	273.466	131.932	17.688	Average																			0	N	561.3	415.1	957.4	723.6	2657.4	207.8	0.893	0.524	0.184		51.636	12.984	74.873	56.587	196.079	82.132	16.404	0.1	N	771.9	336.9	727.1	723.6	2559.5	200.2	0.989	0.512	0.184	-143.02	71.015	10.538	56.863	56.587	195.003	90.967	16.027	0.2	N	932.7	325.5	595.8	723.6	2577.6	201.6	1.062	0.540	0.184	-238.31	85.806	10.182	46.595	56.587	199.169	97.693	16.898	0.3	N	1072.3	339.8	516.6	723.6	2652.3	207.4	1.128	0.611	0.184	-324.62	98.653	10.629	40.397	56.587	206.266	103.739	19.105	0.4	N	1202.4	368.9	472.2	723.6	2767.1	216.4	1.192	0.696	0.184	-415.45	110.624	11.539	36.930	56.587	215.679	109.665	21.778	0.5	N	1337.4	404.0	434.7	723.6	2899.7	226.8	1.256	0.786	0.184	-509.08	123.043	12.637	33.992	56.587	226.258	115.561	24.585	0.6	N	1569.4	406.2	433.3	723.6	3132.5	245.0	1.370	0.852	0.184	-805.85	144.385	12.707	33.882	56.587	247.560	126.063	26.659	0.66	N	1639.3	429.2	423.6	723.6	3215.7	251.5	1.405	0.907	0.184	-864.15	150.819	13.426	33.123	56.587	253.953	129.219	28.372																																																																																																																																																																																																																																																																										
0.5	N	1338.6	515.2	440.0	723.6	3017.5	236.0	1.270	0.933	0.184	-387.36	123.157	16.117	34.410	56.587	230.271	116.865	29.197	0.6	N	1566.9	527.3	438.8	723.6	3256.6	254.7	1.386	1.028	0.184	-668.14	144.157	16.495	34.311	56.587	251.550	127.511	32.142	0.66	N	1635.9	560.5	428.8	723.6	3348.9	261.9	1.422	1.103	0.184	-714.28	150.509	17.534	33.533	56.587	258.162	130.799	34.493	West																			0	N	565.6	418.0	957.4	723.6	2664.6	208.4	0.894	0.528	0.184		52.035	13.075	74.873	56.587	196.569	82.266	16.502	0.1	N	778.5	332.9	712.4	723.6	2547.4	199.2	0.989	0.507	0.184	-137.93	71.620	10.414	55.708	56.587	194.329	90.990	15.853	0.2	N	955.9	337.2	576.3	723.6	2593.0	202.8	1.065	0.581	0.184	-229.18	87.945	10.549	45.065	56.587	200.145	97.984	18.177	0.3	N	1106.7	366.6	500.0	723.6	2696.9	210.9	1.132	0.698	0.184	-312.57	101.814	11.468	39.101	56.587	208.969	104.149	21.829	0.4	N	1243.8	403.5	458.4	723.6	2829.4	221.3	1.195	0.821	0.184	-404.96	114.433	12.622	35.851	56.587	219.492	109.905	25.687	0.5	N	1385.2	449.3	424.6	723.6	2982.7	233.3	1.260	0.952	0.184	-497.92	127.439	14.054	33.208	56.587	231.287	115.877	29.786	0.6	N	1626.7	459.3	423.9	723.6	3233.4	252.9	1.374	1.060	0.184	-796.48	149.657	14.367	33.147	56.587	253.758	126.420	33.152	0.66	N	1699.9	487.5	414.6	723.6	3325.6	260.1	1.408	1.144	0.184	-854.03	156.392	15.248	32.425	56.587	260.652	129.513	35.801	North																			0	N	581.0	394.9	957.4	723.6	2656.9	207.8	0.901	0.513	0.184		53.457	12.352	74.873	56.587	197.267	82.879	16.039	0.1	N	790.5	328.1	831.9	723.6	2674.1	209.1	0.997	0.501	0.184	-242.79	72.724	10.264	65.056	56.587	204.631	91.763	15.677	0.2	N	980.8	276.3	708.8	723.6	2689.5	210.3	1.074	0.488	0.184	-433.10	90.236	8.643	55.433	56.587	210.898	98.833	15.269	0.3	N	1166.9	238.3	597.0	723.6	2725.8	213.2	1.145	0.472	0.184	-607.23	107.353	7.455	46.686	56.587	218.080	105.370	14.757	0.4	N	1345.2	232.3	529.3	723.6	2830.4	221.3	1.213	0.500	0.184	-774.63	123.762	7.265	41.392	56.587	229.006	111.559	15.631	0.5	N	1527.8	234.1	471.4	723.6	2956.9	231.2	1.282	0.531	0.184	-942.27	140.561	7.323	36.866	56.587	241.336	117.966	16.823	0.6	N	1797.5	220.3	469.0	723.6	3210.4	251.1	1.397	0.547	0.184	-1291.85	165.375	6.890	36.678	56.587	265.529	128.550	17.103	0.66	N	1894.3	225.8	454.4	723.6	3298.1	257.9	1.434	0.565	0.184	-1392.77	174.281	7.063	35.535	56.587	273.466	131.932	17.688	Average																			0	N	561.3	415.1	957.4	723.6	2657.4	207.8	0.893	0.524	0.184		51.636	12.984	74.873	56.587	196.079	82.132	16.404	0.1	N	771.9	336.9	727.1	723.6	2559.5	200.2	0.989	0.512	0.184	-143.02	71.015	10.538	56.863	56.587	195.003	90.967	16.027	0.2	N	932.7	325.5	595.8	723.6	2577.6	201.6	1.062	0.540	0.184	-238.31	85.806	10.182	46.595	56.587	199.169	97.693	16.898	0.3	N	1072.3	339.8	516.6	723.6	2652.3	207.4	1.128	0.611	0.184	-324.62	98.653	10.629	40.397	56.587	206.266	103.739	19.105	0.4	N	1202.4	368.9	472.2	723.6	2767.1	216.4	1.192	0.696	0.184	-415.45	110.624	11.539	36.930	56.587	215.679	109.665	21.778	0.5	N	1337.4	404.0	434.7	723.6	2899.7	226.8	1.256	0.786	0.184	-509.08	123.043	12.637	33.992	56.587	226.258	115.561	24.585	0.6	N	1569.4	406.2	433.3	723.6	3132.5	245.0	1.370	0.852	0.184	-805.85	144.385	12.707	33.882	56.587	247.560	126.063	26.659	0.66	N	1639.3	429.2	423.6	723.6	3215.7	251.5	1.405	0.907	0.184	-864.15	150.819	13.426	33.123	56.587	253.953	129.219	28.372																																																																																																																																																																																																																																																																																													
0.6	N	1566.9	527.3	438.8	723.6	3256.6	254.7	1.386	1.028	0.184	-668.14	144.157	16.495	34.311	56.587	251.550	127.511	32.142	0.66	N	1635.9	560.5	428.8	723.6	3348.9	261.9	1.422	1.103	0.184	-714.28	150.509	17.534	33.533	56.587	258.162	130.799	34.493	West																			0	N	565.6	418.0	957.4	723.6	2664.6	208.4	0.894	0.528	0.184		52.035	13.075	74.873	56.587	196.569	82.266	16.502	0.1	N	778.5	332.9	712.4	723.6	2547.4	199.2	0.989	0.507	0.184	-137.93	71.620	10.414	55.708	56.587	194.329	90.990	15.853	0.2	N	955.9	337.2	576.3	723.6	2593.0	202.8	1.065	0.581	0.184	-229.18	87.945	10.549	45.065	56.587	200.145	97.984	18.177	0.3	N	1106.7	366.6	500.0	723.6	2696.9	210.9	1.132	0.698	0.184	-312.57	101.814	11.468	39.101	56.587	208.969	104.149	21.829	0.4	N	1243.8	403.5	458.4	723.6	2829.4	221.3	1.195	0.821	0.184	-404.96	114.433	12.622	35.851	56.587	219.492	109.905	25.687	0.5	N	1385.2	449.3	424.6	723.6	2982.7	233.3	1.260	0.952	0.184	-497.92	127.439	14.054	33.208	56.587	231.287	115.877	29.786	0.6	N	1626.7	459.3	423.9	723.6	3233.4	252.9	1.374	1.060	0.184	-796.48	149.657	14.367	33.147	56.587	253.758	126.420	33.152	0.66	N	1699.9	487.5	414.6	723.6	3325.6	260.1	1.408	1.144	0.184	-854.03	156.392	15.248	32.425	56.587	260.652	129.513	35.801	North																			0	N	581.0	394.9	957.4	723.6	2656.9	207.8	0.901	0.513	0.184		53.457	12.352	74.873	56.587	197.267	82.879	16.039	0.1	N	790.5	328.1	831.9	723.6	2674.1	209.1	0.997	0.501	0.184	-242.79	72.724	10.264	65.056	56.587	204.631	91.763	15.677	0.2	N	980.8	276.3	708.8	723.6	2689.5	210.3	1.074	0.488	0.184	-433.10	90.236	8.643	55.433	56.587	210.898	98.833	15.269	0.3	N	1166.9	238.3	597.0	723.6	2725.8	213.2	1.145	0.472	0.184	-607.23	107.353	7.455	46.686	56.587	218.080	105.370	14.757	0.4	N	1345.2	232.3	529.3	723.6	2830.4	221.3	1.213	0.500	0.184	-774.63	123.762	7.265	41.392	56.587	229.006	111.559	15.631	0.5	N	1527.8	234.1	471.4	723.6	2956.9	231.2	1.282	0.531	0.184	-942.27	140.561	7.323	36.866	56.587	241.336	117.966	16.823	0.6	N	1797.5	220.3	469.0	723.6	3210.4	251.1	1.397	0.547	0.184	-1291.85	165.375	6.890	36.678	56.587	265.529	128.550	17.103	0.66	N	1894.3	225.8	454.4	723.6	3298.1	257.9	1.434	0.565	0.184	-1392.77	174.281	7.063	35.535	56.587	273.466	131.932	17.688	Average																			0	N	561.3	415.1	957.4	723.6	2657.4	207.8	0.893	0.524	0.184		51.636	12.984	74.873	56.587	196.079	82.132	16.404	0.1	N	771.9	336.9	727.1	723.6	2559.5	200.2	0.989	0.512	0.184	-143.02	71.015	10.538	56.863	56.587	195.003	90.967	16.027	0.2	N	932.7	325.5	595.8	723.6	2577.6	201.6	1.062	0.540	0.184	-238.31	85.806	10.182	46.595	56.587	199.169	97.693	16.898	0.3	N	1072.3	339.8	516.6	723.6	2652.3	207.4	1.128	0.611	0.184	-324.62	98.653	10.629	40.397	56.587	206.266	103.739	19.105	0.4	N	1202.4	368.9	472.2	723.6	2767.1	216.4	1.192	0.696	0.184	-415.45	110.624	11.539	36.930	56.587	215.679	109.665	21.778	0.5	N	1337.4	404.0	434.7	723.6	2899.7	226.8	1.256	0.786	0.184	-509.08	123.043	12.637	33.992	56.587	226.258	115.561	24.585	0.6	N	1569.4	406.2	433.3	723.6	3132.5	245.0	1.370	0.852	0.184	-805.85	144.385	12.707	33.882	56.587	247.560	126.063	26.659	0.66	N	1639.3	429.2	423.6	723.6	3215.7	251.5	1.405	0.907	0.184	-864.15	150.819	13.426	33.123	56.587	253.953	129.219	28.372																																																																																																																																																																																																																																																																																																																
0.66	N	1635.9	560.5	428.8	723.6	3348.9	261.9	1.422	1.103	0.184	-714.28	150.509	17.534	33.533	56.587	258.162	130.799	34.493	West																			0	N	565.6	418.0	957.4	723.6	2664.6	208.4	0.894	0.528	0.184		52.035	13.075	74.873	56.587	196.569	82.266	16.502	0.1	N	778.5	332.9	712.4	723.6	2547.4	199.2	0.989	0.507	0.184	-137.93	71.620	10.414	55.708	56.587	194.329	90.990	15.853	0.2	N	955.9	337.2	576.3	723.6	2593.0	202.8	1.065	0.581	0.184	-229.18	87.945	10.549	45.065	56.587	200.145	97.984	18.177	0.3	N	1106.7	366.6	500.0	723.6	2696.9	210.9	1.132	0.698	0.184	-312.57	101.814	11.468	39.101	56.587	208.969	104.149	21.829	0.4	N	1243.8	403.5	458.4	723.6	2829.4	221.3	1.195	0.821	0.184	-404.96	114.433	12.622	35.851	56.587	219.492	109.905	25.687	0.5	N	1385.2	449.3	424.6	723.6	2982.7	233.3	1.260	0.952	0.184	-497.92	127.439	14.054	33.208	56.587	231.287	115.877	29.786	0.6	N	1626.7	459.3	423.9	723.6	3233.4	252.9	1.374	1.060	0.184	-796.48	149.657	14.367	33.147	56.587	253.758	126.420	33.152	0.66	N	1699.9	487.5	414.6	723.6	3325.6	260.1	1.408	1.144	0.184	-854.03	156.392	15.248	32.425	56.587	260.652	129.513	35.801	North																			0	N	581.0	394.9	957.4	723.6	2656.9	207.8	0.901	0.513	0.184		53.457	12.352	74.873	56.587	197.267	82.879	16.039	0.1	N	790.5	328.1	831.9	723.6	2674.1	209.1	0.997	0.501	0.184	-242.79	72.724	10.264	65.056	56.587	204.631	91.763	15.677	0.2	N	980.8	276.3	708.8	723.6	2689.5	210.3	1.074	0.488	0.184	-433.10	90.236	8.643	55.433	56.587	210.898	98.833	15.269	0.3	N	1166.9	238.3	597.0	723.6	2725.8	213.2	1.145	0.472	0.184	-607.23	107.353	7.455	46.686	56.587	218.080	105.370	14.757	0.4	N	1345.2	232.3	529.3	723.6	2830.4	221.3	1.213	0.500	0.184	-774.63	123.762	7.265	41.392	56.587	229.006	111.559	15.631	0.5	N	1527.8	234.1	471.4	723.6	2956.9	231.2	1.282	0.531	0.184	-942.27	140.561	7.323	36.866	56.587	241.336	117.966	16.823	0.6	N	1797.5	220.3	469.0	723.6	3210.4	251.1	1.397	0.547	0.184	-1291.85	165.375	6.890	36.678	56.587	265.529	128.550	17.103	0.66	N	1894.3	225.8	454.4	723.6	3298.1	257.9	1.434	0.565	0.184	-1392.77	174.281	7.063	35.535	56.587	273.466	131.932	17.688	Average																			0	N	561.3	415.1	957.4	723.6	2657.4	207.8	0.893	0.524	0.184		51.636	12.984	74.873	56.587	196.079	82.132	16.404	0.1	N	771.9	336.9	727.1	723.6	2559.5	200.2	0.989	0.512	0.184	-143.02	71.015	10.538	56.863	56.587	195.003	90.967	16.027	0.2	N	932.7	325.5	595.8	723.6	2577.6	201.6	1.062	0.540	0.184	-238.31	85.806	10.182	46.595	56.587	199.169	97.693	16.898	0.3	N	1072.3	339.8	516.6	723.6	2652.3	207.4	1.128	0.611	0.184	-324.62	98.653	10.629	40.397	56.587	206.266	103.739	19.105	0.4	N	1202.4	368.9	472.2	723.6	2767.1	216.4	1.192	0.696	0.184	-415.45	110.624	11.539	36.930	56.587	215.679	109.665	21.778	0.5	N	1337.4	404.0	434.7	723.6	2899.7	226.8	1.256	0.786	0.184	-509.08	123.043	12.637	33.992	56.587	226.258	115.561	24.585	0.6	N	1569.4	406.2	433.3	723.6	3132.5	245.0	1.370	0.852	0.184	-805.85	144.385	12.707	33.882	56.587	247.560	126.063	26.659	0.66	N	1639.3	429.2	423.6	723.6	3215.7	251.5	1.405	0.907	0.184	-864.15	150.819	13.426	33.123	56.587	253.953	129.219	28.372																																																																																																																																																																																																																																																																																																																																			
West																			0	N	565.6	418.0	957.4	723.6	2664.6	208.4	0.894	0.528	0.184		52.035	13.075	74.873	56.587	196.569	82.266	16.502	0.1	N	778.5	332.9	712.4	723.6	2547.4	199.2	0.989	0.507	0.184	-137.93	71.620	10.414	55.708	56.587	194.329	90.990	15.853	0.2	N	955.9	337.2	576.3	723.6	2593.0	202.8	1.065	0.581	0.184	-229.18	87.945	10.549	45.065	56.587	200.145	97.984	18.177	0.3	N	1106.7	366.6	500.0	723.6	2696.9	210.9	1.132	0.698	0.184	-312.57	101.814	11.468	39.101	56.587	208.969	104.149	21.829	0.4	N	1243.8	403.5	458.4	723.6	2829.4	221.3	1.195	0.821	0.184	-404.96	114.433	12.622	35.851	56.587	219.492	109.905	25.687	0.5	N	1385.2	449.3	424.6	723.6	2982.7	233.3	1.260	0.952	0.184	-497.92	127.439	14.054	33.208	56.587	231.287	115.877	29.786	0.6	N	1626.7	459.3	423.9	723.6	3233.4	252.9	1.374	1.060	0.184	-796.48	149.657	14.367	33.147	56.587	253.758	126.420	33.152	0.66	N	1699.9	487.5	414.6	723.6	3325.6	260.1	1.408	1.144	0.184	-854.03	156.392	15.248	32.425	56.587	260.652	129.513	35.801	North																			0	N	581.0	394.9	957.4	723.6	2656.9	207.8	0.901	0.513	0.184		53.457	12.352	74.873	56.587	197.267	82.879	16.039	0.1	N	790.5	328.1	831.9	723.6	2674.1	209.1	0.997	0.501	0.184	-242.79	72.724	10.264	65.056	56.587	204.631	91.763	15.677	0.2	N	980.8	276.3	708.8	723.6	2689.5	210.3	1.074	0.488	0.184	-433.10	90.236	8.643	55.433	56.587	210.898	98.833	15.269	0.3	N	1166.9	238.3	597.0	723.6	2725.8	213.2	1.145	0.472	0.184	-607.23	107.353	7.455	46.686	56.587	218.080	105.370	14.757	0.4	N	1345.2	232.3	529.3	723.6	2830.4	221.3	1.213	0.500	0.184	-774.63	123.762	7.265	41.392	56.587	229.006	111.559	15.631	0.5	N	1527.8	234.1	471.4	723.6	2956.9	231.2	1.282	0.531	0.184	-942.27	140.561	7.323	36.866	56.587	241.336	117.966	16.823	0.6	N	1797.5	220.3	469.0	723.6	3210.4	251.1	1.397	0.547	0.184	-1291.85	165.375	6.890	36.678	56.587	265.529	128.550	17.103	0.66	N	1894.3	225.8	454.4	723.6	3298.1	257.9	1.434	0.565	0.184	-1392.77	174.281	7.063	35.535	56.587	273.466	131.932	17.688	Average																			0	N	561.3	415.1	957.4	723.6	2657.4	207.8	0.893	0.524	0.184		51.636	12.984	74.873	56.587	196.079	82.132	16.404	0.1	N	771.9	336.9	727.1	723.6	2559.5	200.2	0.989	0.512	0.184	-143.02	71.015	10.538	56.863	56.587	195.003	90.967	16.027	0.2	N	932.7	325.5	595.8	723.6	2577.6	201.6	1.062	0.540	0.184	-238.31	85.806	10.182	46.595	56.587	199.169	97.693	16.898	0.3	N	1072.3	339.8	516.6	723.6	2652.3	207.4	1.128	0.611	0.184	-324.62	98.653	10.629	40.397	56.587	206.266	103.739	19.105	0.4	N	1202.4	368.9	472.2	723.6	2767.1	216.4	1.192	0.696	0.184	-415.45	110.624	11.539	36.930	56.587	215.679	109.665	21.778	0.5	N	1337.4	404.0	434.7	723.6	2899.7	226.8	1.256	0.786	0.184	-509.08	123.043	12.637	33.992	56.587	226.258	115.561	24.585	0.6	N	1569.4	406.2	433.3	723.6	3132.5	245.0	1.370	0.852	0.184	-805.85	144.385	12.707	33.882	56.587	247.560	126.063	26.659	0.66	N	1639.3	429.2	423.6	723.6	3215.7	251.5	1.405	0.907	0.184	-864.15	150.819	13.426	33.123	56.587	253.953	129.219	28.372																																																																																																																																																																																																																																																																																																																																																						
0	N	565.6	418.0	957.4	723.6	2664.6	208.4	0.894	0.528	0.184		52.035	13.075	74.873	56.587	196.569	82.266	16.502	0.1	N	778.5	332.9	712.4	723.6	2547.4	199.2	0.989	0.507	0.184	-137.93	71.620	10.414	55.708	56.587	194.329	90.990	15.853	0.2	N	955.9	337.2	576.3	723.6	2593.0	202.8	1.065	0.581	0.184	-229.18	87.945	10.549	45.065	56.587	200.145	97.984	18.177	0.3	N	1106.7	366.6	500.0	723.6	2696.9	210.9	1.132	0.698	0.184	-312.57	101.814	11.468	39.101	56.587	208.969	104.149	21.829	0.4	N	1243.8	403.5	458.4	723.6	2829.4	221.3	1.195	0.821	0.184	-404.96	114.433	12.622	35.851	56.587	219.492	109.905	25.687	0.5	N	1385.2	449.3	424.6	723.6	2982.7	233.3	1.260	0.952	0.184	-497.92	127.439	14.054	33.208	56.587	231.287	115.877	29.786	0.6	N	1626.7	459.3	423.9	723.6	3233.4	252.9	1.374	1.060	0.184	-796.48	149.657	14.367	33.147	56.587	253.758	126.420	33.152	0.66	N	1699.9	487.5	414.6	723.6	3325.6	260.1	1.408	1.144	0.184	-854.03	156.392	15.248	32.425	56.587	260.652	129.513	35.801	North																			0	N	581.0	394.9	957.4	723.6	2656.9	207.8	0.901	0.513	0.184		53.457	12.352	74.873	56.587	197.267	82.879	16.039	0.1	N	790.5	328.1	831.9	723.6	2674.1	209.1	0.997	0.501	0.184	-242.79	72.724	10.264	65.056	56.587	204.631	91.763	15.677	0.2	N	980.8	276.3	708.8	723.6	2689.5	210.3	1.074	0.488	0.184	-433.10	90.236	8.643	55.433	56.587	210.898	98.833	15.269	0.3	N	1166.9	238.3	597.0	723.6	2725.8	213.2	1.145	0.472	0.184	-607.23	107.353	7.455	46.686	56.587	218.080	105.370	14.757	0.4	N	1345.2	232.3	529.3	723.6	2830.4	221.3	1.213	0.500	0.184	-774.63	123.762	7.265	41.392	56.587	229.006	111.559	15.631	0.5	N	1527.8	234.1	471.4	723.6	2956.9	231.2	1.282	0.531	0.184	-942.27	140.561	7.323	36.866	56.587	241.336	117.966	16.823	0.6	N	1797.5	220.3	469.0	723.6	3210.4	251.1	1.397	0.547	0.184	-1291.85	165.375	6.890	36.678	56.587	265.529	128.550	17.103	0.66	N	1894.3	225.8	454.4	723.6	3298.1	257.9	1.434	0.565	0.184	-1392.77	174.281	7.063	35.535	56.587	273.466	131.932	17.688	Average																			0	N	561.3	415.1	957.4	723.6	2657.4	207.8	0.893	0.524	0.184		51.636	12.984	74.873	56.587	196.079	82.132	16.404	0.1	N	771.9	336.9	727.1	723.6	2559.5	200.2	0.989	0.512	0.184	-143.02	71.015	10.538	56.863	56.587	195.003	90.967	16.027	0.2	N	932.7	325.5	595.8	723.6	2577.6	201.6	1.062	0.540	0.184	-238.31	85.806	10.182	46.595	56.587	199.169	97.693	16.898	0.3	N	1072.3	339.8	516.6	723.6	2652.3	207.4	1.128	0.611	0.184	-324.62	98.653	10.629	40.397	56.587	206.266	103.739	19.105	0.4	N	1202.4	368.9	472.2	723.6	2767.1	216.4	1.192	0.696	0.184	-415.45	110.624	11.539	36.930	56.587	215.679	109.665	21.778	0.5	N	1337.4	404.0	434.7	723.6	2899.7	226.8	1.256	0.786	0.184	-509.08	123.043	12.637	33.992	56.587	226.258	115.561	24.585	0.6	N	1569.4	406.2	433.3	723.6	3132.5	245.0	1.370	0.852	0.184	-805.85	144.385	12.707	33.882	56.587	247.560	126.063	26.659	0.66	N	1639.3	429.2	423.6	723.6	3215.7	251.5	1.405	0.907	0.184	-864.15	150.819	13.426	33.123	56.587	253.953	129.219	28.372																																																																																																																																																																																																																																																																																																																																																																									
0.1	N	778.5	332.9	712.4	723.6	2547.4	199.2	0.989	0.507	0.184	-137.93	71.620	10.414	55.708	56.587	194.329	90.990	15.853	0.2	N	955.9	337.2	576.3	723.6	2593.0	202.8	1.065	0.581	0.184	-229.18	87.945	10.549	45.065	56.587	200.145	97.984	18.177	0.3	N	1106.7	366.6	500.0	723.6	2696.9	210.9	1.132	0.698	0.184	-312.57	101.814	11.468	39.101	56.587	208.969	104.149	21.829	0.4	N	1243.8	403.5	458.4	723.6	2829.4	221.3	1.195	0.821	0.184	-404.96	114.433	12.622	35.851	56.587	219.492	109.905	25.687	0.5	N	1385.2	449.3	424.6	723.6	2982.7	233.3	1.260	0.952	0.184	-497.92	127.439	14.054	33.208	56.587	231.287	115.877	29.786	0.6	N	1626.7	459.3	423.9	723.6	3233.4	252.9	1.374	1.060	0.184	-796.48	149.657	14.367	33.147	56.587	253.758	126.420	33.152	0.66	N	1699.9	487.5	414.6	723.6	3325.6	260.1	1.408	1.144	0.184	-854.03	156.392	15.248	32.425	56.587	260.652	129.513	35.801	North																			0	N	581.0	394.9	957.4	723.6	2656.9	207.8	0.901	0.513	0.184		53.457	12.352	74.873	56.587	197.267	82.879	16.039	0.1	N	790.5	328.1	831.9	723.6	2674.1	209.1	0.997	0.501	0.184	-242.79	72.724	10.264	65.056	56.587	204.631	91.763	15.677	0.2	N	980.8	276.3	708.8	723.6	2689.5	210.3	1.074	0.488	0.184	-433.10	90.236	8.643	55.433	56.587	210.898	98.833	15.269	0.3	N	1166.9	238.3	597.0	723.6	2725.8	213.2	1.145	0.472	0.184	-607.23	107.353	7.455	46.686	56.587	218.080	105.370	14.757	0.4	N	1345.2	232.3	529.3	723.6	2830.4	221.3	1.213	0.500	0.184	-774.63	123.762	7.265	41.392	56.587	229.006	111.559	15.631	0.5	N	1527.8	234.1	471.4	723.6	2956.9	231.2	1.282	0.531	0.184	-942.27	140.561	7.323	36.866	56.587	241.336	117.966	16.823	0.6	N	1797.5	220.3	469.0	723.6	3210.4	251.1	1.397	0.547	0.184	-1291.85	165.375	6.890	36.678	56.587	265.529	128.550	17.103	0.66	N	1894.3	225.8	454.4	723.6	3298.1	257.9	1.434	0.565	0.184	-1392.77	174.281	7.063	35.535	56.587	273.466	131.932	17.688	Average																			0	N	561.3	415.1	957.4	723.6	2657.4	207.8	0.893	0.524	0.184		51.636	12.984	74.873	56.587	196.079	82.132	16.404	0.1	N	771.9	336.9	727.1	723.6	2559.5	200.2	0.989	0.512	0.184	-143.02	71.015	10.538	56.863	56.587	195.003	90.967	16.027	0.2	N	932.7	325.5	595.8	723.6	2577.6	201.6	1.062	0.540	0.184	-238.31	85.806	10.182	46.595	56.587	199.169	97.693	16.898	0.3	N	1072.3	339.8	516.6	723.6	2652.3	207.4	1.128	0.611	0.184	-324.62	98.653	10.629	40.397	56.587	206.266	103.739	19.105	0.4	N	1202.4	368.9	472.2	723.6	2767.1	216.4	1.192	0.696	0.184	-415.45	110.624	11.539	36.930	56.587	215.679	109.665	21.778	0.5	N	1337.4	404.0	434.7	723.6	2899.7	226.8	1.256	0.786	0.184	-509.08	123.043	12.637	33.992	56.587	226.258	115.561	24.585	0.6	N	1569.4	406.2	433.3	723.6	3132.5	245.0	1.370	0.852	0.184	-805.85	144.385	12.707	33.882	56.587	247.560	126.063	26.659	0.66	N	1639.3	429.2	423.6	723.6	3215.7	251.5	1.405	0.907	0.184	-864.15	150.819	13.426	33.123	56.587	253.953	129.219	28.372																																																																																																																																																																																																																																																																																																																																																																																												
0.2	N	955.9	337.2	576.3	723.6	2593.0	202.8	1.065	0.581	0.184	-229.18	87.945	10.549	45.065	56.587	200.145	97.984	18.177	0.3	N	1106.7	366.6	500.0	723.6	2696.9	210.9	1.132	0.698	0.184	-312.57	101.814	11.468	39.101	56.587	208.969	104.149	21.829	0.4	N	1243.8	403.5	458.4	723.6	2829.4	221.3	1.195	0.821	0.184	-404.96	114.433	12.622	35.851	56.587	219.492	109.905	25.687	0.5	N	1385.2	449.3	424.6	723.6	2982.7	233.3	1.260	0.952	0.184	-497.92	127.439	14.054	33.208	56.587	231.287	115.877	29.786	0.6	N	1626.7	459.3	423.9	723.6	3233.4	252.9	1.374	1.060	0.184	-796.48	149.657	14.367	33.147	56.587	253.758	126.420	33.152	0.66	N	1699.9	487.5	414.6	723.6	3325.6	260.1	1.408	1.144	0.184	-854.03	156.392	15.248	32.425	56.587	260.652	129.513	35.801	North																			0	N	581.0	394.9	957.4	723.6	2656.9	207.8	0.901	0.513	0.184		53.457	12.352	74.873	56.587	197.267	82.879	16.039	0.1	N	790.5	328.1	831.9	723.6	2674.1	209.1	0.997	0.501	0.184	-242.79	72.724	10.264	65.056	56.587	204.631	91.763	15.677	0.2	N	980.8	276.3	708.8	723.6	2689.5	210.3	1.074	0.488	0.184	-433.10	90.236	8.643	55.433	56.587	210.898	98.833	15.269	0.3	N	1166.9	238.3	597.0	723.6	2725.8	213.2	1.145	0.472	0.184	-607.23	107.353	7.455	46.686	56.587	218.080	105.370	14.757	0.4	N	1345.2	232.3	529.3	723.6	2830.4	221.3	1.213	0.500	0.184	-774.63	123.762	7.265	41.392	56.587	229.006	111.559	15.631	0.5	N	1527.8	234.1	471.4	723.6	2956.9	231.2	1.282	0.531	0.184	-942.27	140.561	7.323	36.866	56.587	241.336	117.966	16.823	0.6	N	1797.5	220.3	469.0	723.6	3210.4	251.1	1.397	0.547	0.184	-1291.85	165.375	6.890	36.678	56.587	265.529	128.550	17.103	0.66	N	1894.3	225.8	454.4	723.6	3298.1	257.9	1.434	0.565	0.184	-1392.77	174.281	7.063	35.535	56.587	273.466	131.932	17.688	Average																			0	N	561.3	415.1	957.4	723.6	2657.4	207.8	0.893	0.524	0.184		51.636	12.984	74.873	56.587	196.079	82.132	16.404	0.1	N	771.9	336.9	727.1	723.6	2559.5	200.2	0.989	0.512	0.184	-143.02	71.015	10.538	56.863	56.587	195.003	90.967	16.027	0.2	N	932.7	325.5	595.8	723.6	2577.6	201.6	1.062	0.540	0.184	-238.31	85.806	10.182	46.595	56.587	199.169	97.693	16.898	0.3	N	1072.3	339.8	516.6	723.6	2652.3	207.4	1.128	0.611	0.184	-324.62	98.653	10.629	40.397	56.587	206.266	103.739	19.105	0.4	N	1202.4	368.9	472.2	723.6	2767.1	216.4	1.192	0.696	0.184	-415.45	110.624	11.539	36.930	56.587	215.679	109.665	21.778	0.5	N	1337.4	404.0	434.7	723.6	2899.7	226.8	1.256	0.786	0.184	-509.08	123.043	12.637	33.992	56.587	226.258	115.561	24.585	0.6	N	1569.4	406.2	433.3	723.6	3132.5	245.0	1.370	0.852	0.184	-805.85	144.385	12.707	33.882	56.587	247.560	126.063	26.659	0.66	N	1639.3	429.2	423.6	723.6	3215.7	251.5	1.405	0.907	0.184	-864.15	150.819	13.426	33.123	56.587	253.953	129.219	28.372																																																																																																																																																																																																																																																																																																																																																																																																															
0.3	N	1106.7	366.6	500.0	723.6	2696.9	210.9	1.132	0.698	0.184	-312.57	101.814	11.468	39.101	56.587	208.969	104.149	21.829	0.4	N	1243.8	403.5	458.4	723.6	2829.4	221.3	1.195	0.821	0.184	-404.96	114.433	12.622	35.851	56.587	219.492	109.905	25.687	0.5	N	1385.2	449.3	424.6	723.6	2982.7	233.3	1.260	0.952	0.184	-497.92	127.439	14.054	33.208	56.587	231.287	115.877	29.786	0.6	N	1626.7	459.3	423.9	723.6	3233.4	252.9	1.374	1.060	0.184	-796.48	149.657	14.367	33.147	56.587	253.758	126.420	33.152	0.66	N	1699.9	487.5	414.6	723.6	3325.6	260.1	1.408	1.144	0.184	-854.03	156.392	15.248	32.425	56.587	260.652	129.513	35.801	North																			0	N	581.0	394.9	957.4	723.6	2656.9	207.8	0.901	0.513	0.184		53.457	12.352	74.873	56.587	197.267	82.879	16.039	0.1	N	790.5	328.1	831.9	723.6	2674.1	209.1	0.997	0.501	0.184	-242.79	72.724	10.264	65.056	56.587	204.631	91.763	15.677	0.2	N	980.8	276.3	708.8	723.6	2689.5	210.3	1.074	0.488	0.184	-433.10	90.236	8.643	55.433	56.587	210.898	98.833	15.269	0.3	N	1166.9	238.3	597.0	723.6	2725.8	213.2	1.145	0.472	0.184	-607.23	107.353	7.455	46.686	56.587	218.080	105.370	14.757	0.4	N	1345.2	232.3	529.3	723.6	2830.4	221.3	1.213	0.500	0.184	-774.63	123.762	7.265	41.392	56.587	229.006	111.559	15.631	0.5	N	1527.8	234.1	471.4	723.6	2956.9	231.2	1.282	0.531	0.184	-942.27	140.561	7.323	36.866	56.587	241.336	117.966	16.823	0.6	N	1797.5	220.3	469.0	723.6	3210.4	251.1	1.397	0.547	0.184	-1291.85	165.375	6.890	36.678	56.587	265.529	128.550	17.103	0.66	N	1894.3	225.8	454.4	723.6	3298.1	257.9	1.434	0.565	0.184	-1392.77	174.281	7.063	35.535	56.587	273.466	131.932	17.688	Average																			0	N	561.3	415.1	957.4	723.6	2657.4	207.8	0.893	0.524	0.184		51.636	12.984	74.873	56.587	196.079	82.132	16.404	0.1	N	771.9	336.9	727.1	723.6	2559.5	200.2	0.989	0.512	0.184	-143.02	71.015	10.538	56.863	56.587	195.003	90.967	16.027	0.2	N	932.7	325.5	595.8	723.6	2577.6	201.6	1.062	0.540	0.184	-238.31	85.806	10.182	46.595	56.587	199.169	97.693	16.898	0.3	N	1072.3	339.8	516.6	723.6	2652.3	207.4	1.128	0.611	0.184	-324.62	98.653	10.629	40.397	56.587	206.266	103.739	19.105	0.4	N	1202.4	368.9	472.2	723.6	2767.1	216.4	1.192	0.696	0.184	-415.45	110.624	11.539	36.930	56.587	215.679	109.665	21.778	0.5	N	1337.4	404.0	434.7	723.6	2899.7	226.8	1.256	0.786	0.184	-509.08	123.043	12.637	33.992	56.587	226.258	115.561	24.585	0.6	N	1569.4	406.2	433.3	723.6	3132.5	245.0	1.370	0.852	0.184	-805.85	144.385	12.707	33.882	56.587	247.560	126.063	26.659	0.66	N	1639.3	429.2	423.6	723.6	3215.7	251.5	1.405	0.907	0.184	-864.15	150.819	13.426	33.123	56.587	253.953	129.219	28.372																																																																																																																																																																																																																																																																																																																																																																																																																																		
0.4	N	1243.8	403.5	458.4	723.6	2829.4	221.3	1.195	0.821	0.184	-404.96	114.433	12.622	35.851	56.587	219.492	109.905	25.687	0.5	N	1385.2	449.3	424.6	723.6	2982.7	233.3	1.260	0.952	0.184	-497.92	127.439	14.054	33.208	56.587	231.287	115.877	29.786	0.6	N	1626.7	459.3	423.9	723.6	3233.4	252.9	1.374	1.060	0.184	-796.48	149.657	14.367	33.147	56.587	253.758	126.420	33.152	0.66	N	1699.9	487.5	414.6	723.6	3325.6	260.1	1.408	1.144	0.184	-854.03	156.392	15.248	32.425	56.587	260.652	129.513	35.801	North																			0	N	581.0	394.9	957.4	723.6	2656.9	207.8	0.901	0.513	0.184		53.457	12.352	74.873	56.587	197.267	82.879	16.039	0.1	N	790.5	328.1	831.9	723.6	2674.1	209.1	0.997	0.501	0.184	-242.79	72.724	10.264	65.056	56.587	204.631	91.763	15.677	0.2	N	980.8	276.3	708.8	723.6	2689.5	210.3	1.074	0.488	0.184	-433.10	90.236	8.643	55.433	56.587	210.898	98.833	15.269	0.3	N	1166.9	238.3	597.0	723.6	2725.8	213.2	1.145	0.472	0.184	-607.23	107.353	7.455	46.686	56.587	218.080	105.370	14.757	0.4	N	1345.2	232.3	529.3	723.6	2830.4	221.3	1.213	0.500	0.184	-774.63	123.762	7.265	41.392	56.587	229.006	111.559	15.631	0.5	N	1527.8	234.1	471.4	723.6	2956.9	231.2	1.282	0.531	0.184	-942.27	140.561	7.323	36.866	56.587	241.336	117.966	16.823	0.6	N	1797.5	220.3	469.0	723.6	3210.4	251.1	1.397	0.547	0.184	-1291.85	165.375	6.890	36.678	56.587	265.529	128.550	17.103	0.66	N	1894.3	225.8	454.4	723.6	3298.1	257.9	1.434	0.565	0.184	-1392.77	174.281	7.063	35.535	56.587	273.466	131.932	17.688	Average																			0	N	561.3	415.1	957.4	723.6	2657.4	207.8	0.893	0.524	0.184		51.636	12.984	74.873	56.587	196.079	82.132	16.404	0.1	N	771.9	336.9	727.1	723.6	2559.5	200.2	0.989	0.512	0.184	-143.02	71.015	10.538	56.863	56.587	195.003	90.967	16.027	0.2	N	932.7	325.5	595.8	723.6	2577.6	201.6	1.062	0.540	0.184	-238.31	85.806	10.182	46.595	56.587	199.169	97.693	16.898	0.3	N	1072.3	339.8	516.6	723.6	2652.3	207.4	1.128	0.611	0.184	-324.62	98.653	10.629	40.397	56.587	206.266	103.739	19.105	0.4	N	1202.4	368.9	472.2	723.6	2767.1	216.4	1.192	0.696	0.184	-415.45	110.624	11.539	36.930	56.587	215.679	109.665	21.778	0.5	N	1337.4	404.0	434.7	723.6	2899.7	226.8	1.256	0.786	0.184	-509.08	123.043	12.637	33.992	56.587	226.258	115.561	24.585	0.6	N	1569.4	406.2	433.3	723.6	3132.5	245.0	1.370	0.852	0.184	-805.85	144.385	12.707	33.882	56.587	247.560	126.063	26.659	0.66	N	1639.3	429.2	423.6	723.6	3215.7	251.5	1.405	0.907	0.184	-864.15	150.819	13.426	33.123	56.587	253.953	129.219	28.372																																																																																																																																																																																																																																																																																																																																																																																																																																																					
0.5	N	1385.2	449.3	424.6	723.6	2982.7	233.3	1.260	0.952	0.184	-497.92	127.439	14.054	33.208	56.587	231.287	115.877	29.786	0.6	N	1626.7	459.3	423.9	723.6	3233.4	252.9	1.374	1.060	0.184	-796.48	149.657	14.367	33.147	56.587	253.758	126.420	33.152	0.66	N	1699.9	487.5	414.6	723.6	3325.6	260.1	1.408	1.144	0.184	-854.03	156.392	15.248	32.425	56.587	260.652	129.513	35.801	North																			0	N	581.0	394.9	957.4	723.6	2656.9	207.8	0.901	0.513	0.184		53.457	12.352	74.873	56.587	197.267	82.879	16.039	0.1	N	790.5	328.1	831.9	723.6	2674.1	209.1	0.997	0.501	0.184	-242.79	72.724	10.264	65.056	56.587	204.631	91.763	15.677	0.2	N	980.8	276.3	708.8	723.6	2689.5	210.3	1.074	0.488	0.184	-433.10	90.236	8.643	55.433	56.587	210.898	98.833	15.269	0.3	N	1166.9	238.3	597.0	723.6	2725.8	213.2	1.145	0.472	0.184	-607.23	107.353	7.455	46.686	56.587	218.080	105.370	14.757	0.4	N	1345.2	232.3	529.3	723.6	2830.4	221.3	1.213	0.500	0.184	-774.63	123.762	7.265	41.392	56.587	229.006	111.559	15.631	0.5	N	1527.8	234.1	471.4	723.6	2956.9	231.2	1.282	0.531	0.184	-942.27	140.561	7.323	36.866	56.587	241.336	117.966	16.823	0.6	N	1797.5	220.3	469.0	723.6	3210.4	251.1	1.397	0.547	0.184	-1291.85	165.375	6.890	36.678	56.587	265.529	128.550	17.103	0.66	N	1894.3	225.8	454.4	723.6	3298.1	257.9	1.434	0.565	0.184	-1392.77	174.281	7.063	35.535	56.587	273.466	131.932	17.688	Average																			0	N	561.3	415.1	957.4	723.6	2657.4	207.8	0.893	0.524	0.184		51.636	12.984	74.873	56.587	196.079	82.132	16.404	0.1	N	771.9	336.9	727.1	723.6	2559.5	200.2	0.989	0.512	0.184	-143.02	71.015	10.538	56.863	56.587	195.003	90.967	16.027	0.2	N	932.7	325.5	595.8	723.6	2577.6	201.6	1.062	0.540	0.184	-238.31	85.806	10.182	46.595	56.587	199.169	97.693	16.898	0.3	N	1072.3	339.8	516.6	723.6	2652.3	207.4	1.128	0.611	0.184	-324.62	98.653	10.629	40.397	56.587	206.266	103.739	19.105	0.4	N	1202.4	368.9	472.2	723.6	2767.1	216.4	1.192	0.696	0.184	-415.45	110.624	11.539	36.930	56.587	215.679	109.665	21.778	0.5	N	1337.4	404.0	434.7	723.6	2899.7	226.8	1.256	0.786	0.184	-509.08	123.043	12.637	33.992	56.587	226.258	115.561	24.585	0.6	N	1569.4	406.2	433.3	723.6	3132.5	245.0	1.370	0.852	0.184	-805.85	144.385	12.707	33.882	56.587	247.560	126.063	26.659	0.66	N	1639.3	429.2	423.6	723.6	3215.7	251.5	1.405	0.907	0.184	-864.15	150.819	13.426	33.123	56.587	253.953	129.219	28.372																																																																																																																																																																																																																																																																																																																																																																																																																																																																								
0.6	N	1626.7	459.3	423.9	723.6	3233.4	252.9	1.374	1.060	0.184	-796.48	149.657	14.367	33.147	56.587	253.758	126.420	33.152	0.66	N	1699.9	487.5	414.6	723.6	3325.6	260.1	1.408	1.144	0.184	-854.03	156.392	15.248	32.425	56.587	260.652	129.513	35.801	North																			0	N	581.0	394.9	957.4	723.6	2656.9	207.8	0.901	0.513	0.184		53.457	12.352	74.873	56.587	197.267	82.879	16.039	0.1	N	790.5	328.1	831.9	723.6	2674.1	209.1	0.997	0.501	0.184	-242.79	72.724	10.264	65.056	56.587	204.631	91.763	15.677	0.2	N	980.8	276.3	708.8	723.6	2689.5	210.3	1.074	0.488	0.184	-433.10	90.236	8.643	55.433	56.587	210.898	98.833	15.269	0.3	N	1166.9	238.3	597.0	723.6	2725.8	213.2	1.145	0.472	0.184	-607.23	107.353	7.455	46.686	56.587	218.080	105.370	14.757	0.4	N	1345.2	232.3	529.3	723.6	2830.4	221.3	1.213	0.500	0.184	-774.63	123.762	7.265	41.392	56.587	229.006	111.559	15.631	0.5	N	1527.8	234.1	471.4	723.6	2956.9	231.2	1.282	0.531	0.184	-942.27	140.561	7.323	36.866	56.587	241.336	117.966	16.823	0.6	N	1797.5	220.3	469.0	723.6	3210.4	251.1	1.397	0.547	0.184	-1291.85	165.375	6.890	36.678	56.587	265.529	128.550	17.103	0.66	N	1894.3	225.8	454.4	723.6	3298.1	257.9	1.434	0.565	0.184	-1392.77	174.281	7.063	35.535	56.587	273.466	131.932	17.688	Average																			0	N	561.3	415.1	957.4	723.6	2657.4	207.8	0.893	0.524	0.184		51.636	12.984	74.873	56.587	196.079	82.132	16.404	0.1	N	771.9	336.9	727.1	723.6	2559.5	200.2	0.989	0.512	0.184	-143.02	71.015	10.538	56.863	56.587	195.003	90.967	16.027	0.2	N	932.7	325.5	595.8	723.6	2577.6	201.6	1.062	0.540	0.184	-238.31	85.806	10.182	46.595	56.587	199.169	97.693	16.898	0.3	N	1072.3	339.8	516.6	723.6	2652.3	207.4	1.128	0.611	0.184	-324.62	98.653	10.629	40.397	56.587	206.266	103.739	19.105	0.4	N	1202.4	368.9	472.2	723.6	2767.1	216.4	1.192	0.696	0.184	-415.45	110.624	11.539	36.930	56.587	215.679	109.665	21.778	0.5	N	1337.4	404.0	434.7	723.6	2899.7	226.8	1.256	0.786	0.184	-509.08	123.043	12.637	33.992	56.587	226.258	115.561	24.585	0.6	N	1569.4	406.2	433.3	723.6	3132.5	245.0	1.370	0.852	0.184	-805.85	144.385	12.707	33.882	56.587	247.560	126.063	26.659	0.66	N	1639.3	429.2	423.6	723.6	3215.7	251.5	1.405	0.907	0.184	-864.15	150.819	13.426	33.123	56.587	253.953	129.219	28.372																																																																																																																																																																																																																																																																																																																																																																																																																																																																																											
0.66	N	1699.9	487.5	414.6	723.6	3325.6	260.1	1.408	1.144	0.184	-854.03	156.392	15.248	32.425	56.587	260.652	129.513	35.801	North																			0	N	581.0	394.9	957.4	723.6	2656.9	207.8	0.901	0.513	0.184		53.457	12.352	74.873	56.587	197.267	82.879	16.039	0.1	N	790.5	328.1	831.9	723.6	2674.1	209.1	0.997	0.501	0.184	-242.79	72.724	10.264	65.056	56.587	204.631	91.763	15.677	0.2	N	980.8	276.3	708.8	723.6	2689.5	210.3	1.074	0.488	0.184	-433.10	90.236	8.643	55.433	56.587	210.898	98.833	15.269	0.3	N	1166.9	238.3	597.0	723.6	2725.8	213.2	1.145	0.472	0.184	-607.23	107.353	7.455	46.686	56.587	218.080	105.370	14.757	0.4	N	1345.2	232.3	529.3	723.6	2830.4	221.3	1.213	0.500	0.184	-774.63	123.762	7.265	41.392	56.587	229.006	111.559	15.631	0.5	N	1527.8	234.1	471.4	723.6	2956.9	231.2	1.282	0.531	0.184	-942.27	140.561	7.323	36.866	56.587	241.336	117.966	16.823	0.6	N	1797.5	220.3	469.0	723.6	3210.4	251.1	1.397	0.547	0.184	-1291.85	165.375	6.890	36.678	56.587	265.529	128.550	17.103	0.66	N	1894.3	225.8	454.4	723.6	3298.1	257.9	1.434	0.565	0.184	-1392.77	174.281	7.063	35.535	56.587	273.466	131.932	17.688	Average																			0	N	561.3	415.1	957.4	723.6	2657.4	207.8	0.893	0.524	0.184		51.636	12.984	74.873	56.587	196.079	82.132	16.404	0.1	N	771.9	336.9	727.1	723.6	2559.5	200.2	0.989	0.512	0.184	-143.02	71.015	10.538	56.863	56.587	195.003	90.967	16.027	0.2	N	932.7	325.5	595.8	723.6	2577.6	201.6	1.062	0.540	0.184	-238.31	85.806	10.182	46.595	56.587	199.169	97.693	16.898	0.3	N	1072.3	339.8	516.6	723.6	2652.3	207.4	1.128	0.611	0.184	-324.62	98.653	10.629	40.397	56.587	206.266	103.739	19.105	0.4	N	1202.4	368.9	472.2	723.6	2767.1	216.4	1.192	0.696	0.184	-415.45	110.624	11.539	36.930	56.587	215.679	109.665	21.778	0.5	N	1337.4	404.0	434.7	723.6	2899.7	226.8	1.256	0.786	0.184	-509.08	123.043	12.637	33.992	56.587	226.258	115.561	24.585	0.6	N	1569.4	406.2	433.3	723.6	3132.5	245.0	1.370	0.852	0.184	-805.85	144.385	12.707	33.882	56.587	247.560	126.063	26.659	0.66	N	1639.3	429.2	423.6	723.6	3215.7	251.5	1.405	0.907	0.184	-864.15	150.819	13.426	33.123	56.587	253.953	129.219	28.372																																																																																																																																																																																																																																																																																																																																																																																																																																																																																																														
North																			0	N	581.0	394.9	957.4	723.6	2656.9	207.8	0.901	0.513	0.184		53.457	12.352	74.873	56.587	197.267	82.879	16.039	0.1	N	790.5	328.1	831.9	723.6	2674.1	209.1	0.997	0.501	0.184	-242.79	72.724	10.264	65.056	56.587	204.631	91.763	15.677	0.2	N	980.8	276.3	708.8	723.6	2689.5	210.3	1.074	0.488	0.184	-433.10	90.236	8.643	55.433	56.587	210.898	98.833	15.269	0.3	N	1166.9	238.3	597.0	723.6	2725.8	213.2	1.145	0.472	0.184	-607.23	107.353	7.455	46.686	56.587	218.080	105.370	14.757	0.4	N	1345.2	232.3	529.3	723.6	2830.4	221.3	1.213	0.500	0.184	-774.63	123.762	7.265	41.392	56.587	229.006	111.559	15.631	0.5	N	1527.8	234.1	471.4	723.6	2956.9	231.2	1.282	0.531	0.184	-942.27	140.561	7.323	36.866	56.587	241.336	117.966	16.823	0.6	N	1797.5	220.3	469.0	723.6	3210.4	251.1	1.397	0.547	0.184	-1291.85	165.375	6.890	36.678	56.587	265.529	128.550	17.103	0.66	N	1894.3	225.8	454.4	723.6	3298.1	257.9	1.434	0.565	0.184	-1392.77	174.281	7.063	35.535	56.587	273.466	131.932	17.688	Average																			0	N	561.3	415.1	957.4	723.6	2657.4	207.8	0.893	0.524	0.184		51.636	12.984	74.873	56.587	196.079	82.132	16.404	0.1	N	771.9	336.9	727.1	723.6	2559.5	200.2	0.989	0.512	0.184	-143.02	71.015	10.538	56.863	56.587	195.003	90.967	16.027	0.2	N	932.7	325.5	595.8	723.6	2577.6	201.6	1.062	0.540	0.184	-238.31	85.806	10.182	46.595	56.587	199.169	97.693	16.898	0.3	N	1072.3	339.8	516.6	723.6	2652.3	207.4	1.128	0.611	0.184	-324.62	98.653	10.629	40.397	56.587	206.266	103.739	19.105	0.4	N	1202.4	368.9	472.2	723.6	2767.1	216.4	1.192	0.696	0.184	-415.45	110.624	11.539	36.930	56.587	215.679	109.665	21.778	0.5	N	1337.4	404.0	434.7	723.6	2899.7	226.8	1.256	0.786	0.184	-509.08	123.043	12.637	33.992	56.587	226.258	115.561	24.585	0.6	N	1569.4	406.2	433.3	723.6	3132.5	245.0	1.370	0.852	0.184	-805.85	144.385	12.707	33.882	56.587	247.560	126.063	26.659	0.66	N	1639.3	429.2	423.6	723.6	3215.7	251.5	1.405	0.907	0.184	-864.15	150.819	13.426	33.123	56.587	253.953	129.219	28.372																																																																																																																																																																																																																																																																																																																																																																																																																																																																																																																																	
0	N	581.0	394.9	957.4	723.6	2656.9	207.8	0.901	0.513	0.184		53.457	12.352	74.873	56.587	197.267	82.879	16.039	0.1	N	790.5	328.1	831.9	723.6	2674.1	209.1	0.997	0.501	0.184	-242.79	72.724	10.264	65.056	56.587	204.631	91.763	15.677	0.2	N	980.8	276.3	708.8	723.6	2689.5	210.3	1.074	0.488	0.184	-433.10	90.236	8.643	55.433	56.587	210.898	98.833	15.269	0.3	N	1166.9	238.3	597.0	723.6	2725.8	213.2	1.145	0.472	0.184	-607.23	107.353	7.455	46.686	56.587	218.080	105.370	14.757	0.4	N	1345.2	232.3	529.3	723.6	2830.4	221.3	1.213	0.500	0.184	-774.63	123.762	7.265	41.392	56.587	229.006	111.559	15.631	0.5	N	1527.8	234.1	471.4	723.6	2956.9	231.2	1.282	0.531	0.184	-942.27	140.561	7.323	36.866	56.587	241.336	117.966	16.823	0.6	N	1797.5	220.3	469.0	723.6	3210.4	251.1	1.397	0.547	0.184	-1291.85	165.375	6.890	36.678	56.587	265.529	128.550	17.103	0.66	N	1894.3	225.8	454.4	723.6	3298.1	257.9	1.434	0.565	0.184	-1392.77	174.281	7.063	35.535	56.587	273.466	131.932	17.688	Average																			0	N	561.3	415.1	957.4	723.6	2657.4	207.8	0.893	0.524	0.184		51.636	12.984	74.873	56.587	196.079	82.132	16.404	0.1	N	771.9	336.9	727.1	723.6	2559.5	200.2	0.989	0.512	0.184	-143.02	71.015	10.538	56.863	56.587	195.003	90.967	16.027	0.2	N	932.7	325.5	595.8	723.6	2577.6	201.6	1.062	0.540	0.184	-238.31	85.806	10.182	46.595	56.587	199.169	97.693	16.898	0.3	N	1072.3	339.8	516.6	723.6	2652.3	207.4	1.128	0.611	0.184	-324.62	98.653	10.629	40.397	56.587	206.266	103.739	19.105	0.4	N	1202.4	368.9	472.2	723.6	2767.1	216.4	1.192	0.696	0.184	-415.45	110.624	11.539	36.930	56.587	215.679	109.665	21.778	0.5	N	1337.4	404.0	434.7	723.6	2899.7	226.8	1.256	0.786	0.184	-509.08	123.043	12.637	33.992	56.587	226.258	115.561	24.585	0.6	N	1569.4	406.2	433.3	723.6	3132.5	245.0	1.370	0.852	0.184	-805.85	144.385	12.707	33.882	56.587	247.560	126.063	26.659	0.66	N	1639.3	429.2	423.6	723.6	3215.7	251.5	1.405	0.907	0.184	-864.15	150.819	13.426	33.123	56.587	253.953	129.219	28.372																																																																																																																																																																																																																																																																																																																																																																																																																																																																																																																																																				
0.1	N	790.5	328.1	831.9	723.6	2674.1	209.1	0.997	0.501	0.184	-242.79	72.724	10.264	65.056	56.587	204.631	91.763	15.677	0.2	N	980.8	276.3	708.8	723.6	2689.5	210.3	1.074	0.488	0.184	-433.10	90.236	8.643	55.433	56.587	210.898	98.833	15.269	0.3	N	1166.9	238.3	597.0	723.6	2725.8	213.2	1.145	0.472	0.184	-607.23	107.353	7.455	46.686	56.587	218.080	105.370	14.757	0.4	N	1345.2	232.3	529.3	723.6	2830.4	221.3	1.213	0.500	0.184	-774.63	123.762	7.265	41.392	56.587	229.006	111.559	15.631	0.5	N	1527.8	234.1	471.4	723.6	2956.9	231.2	1.282	0.531	0.184	-942.27	140.561	7.323	36.866	56.587	241.336	117.966	16.823	0.6	N	1797.5	220.3	469.0	723.6	3210.4	251.1	1.397	0.547	0.184	-1291.85	165.375	6.890	36.678	56.587	265.529	128.550	17.103	0.66	N	1894.3	225.8	454.4	723.6	3298.1	257.9	1.434	0.565	0.184	-1392.77	174.281	7.063	35.535	56.587	273.466	131.932	17.688	Average																			0	N	561.3	415.1	957.4	723.6	2657.4	207.8	0.893	0.524	0.184		51.636	12.984	74.873	56.587	196.079	82.132	16.404	0.1	N	771.9	336.9	727.1	723.6	2559.5	200.2	0.989	0.512	0.184	-143.02	71.015	10.538	56.863	56.587	195.003	90.967	16.027	0.2	N	932.7	325.5	595.8	723.6	2577.6	201.6	1.062	0.540	0.184	-238.31	85.806	10.182	46.595	56.587	199.169	97.693	16.898	0.3	N	1072.3	339.8	516.6	723.6	2652.3	207.4	1.128	0.611	0.184	-324.62	98.653	10.629	40.397	56.587	206.266	103.739	19.105	0.4	N	1202.4	368.9	472.2	723.6	2767.1	216.4	1.192	0.696	0.184	-415.45	110.624	11.539	36.930	56.587	215.679	109.665	21.778	0.5	N	1337.4	404.0	434.7	723.6	2899.7	226.8	1.256	0.786	0.184	-509.08	123.043	12.637	33.992	56.587	226.258	115.561	24.585	0.6	N	1569.4	406.2	433.3	723.6	3132.5	245.0	1.370	0.852	0.184	-805.85	144.385	12.707	33.882	56.587	247.560	126.063	26.659	0.66	N	1639.3	429.2	423.6	723.6	3215.7	251.5	1.405	0.907	0.184	-864.15	150.819	13.426	33.123	56.587	253.953	129.219	28.372																																																																																																																																																																																																																																																																																																																																																																																																																																																																																																																																																																							
0.2	N	980.8	276.3	708.8	723.6	2689.5	210.3	1.074	0.488	0.184	-433.10	90.236	8.643	55.433	56.587	210.898	98.833	15.269	0.3	N	1166.9	238.3	597.0	723.6	2725.8	213.2	1.145	0.472	0.184	-607.23	107.353	7.455	46.686	56.587	218.080	105.370	14.757	0.4	N	1345.2	232.3	529.3	723.6	2830.4	221.3	1.213	0.500	0.184	-774.63	123.762	7.265	41.392	56.587	229.006	111.559	15.631	0.5	N	1527.8	234.1	471.4	723.6	2956.9	231.2	1.282	0.531	0.184	-942.27	140.561	7.323	36.866	56.587	241.336	117.966	16.823	0.6	N	1797.5	220.3	469.0	723.6	3210.4	251.1	1.397	0.547	0.184	-1291.85	165.375	6.890	36.678	56.587	265.529	128.550	17.103	0.66	N	1894.3	225.8	454.4	723.6	3298.1	257.9	1.434	0.565	0.184	-1392.77	174.281	7.063	35.535	56.587	273.466	131.932	17.688	Average																			0	N	561.3	415.1	957.4	723.6	2657.4	207.8	0.893	0.524	0.184		51.636	12.984	74.873	56.587	196.079	82.132	16.404	0.1	N	771.9	336.9	727.1	723.6	2559.5	200.2	0.989	0.512	0.184	-143.02	71.015	10.538	56.863	56.587	195.003	90.967	16.027	0.2	N	932.7	325.5	595.8	723.6	2577.6	201.6	1.062	0.540	0.184	-238.31	85.806	10.182	46.595	56.587	199.169	97.693	16.898	0.3	N	1072.3	339.8	516.6	723.6	2652.3	207.4	1.128	0.611	0.184	-324.62	98.653	10.629	40.397	56.587	206.266	103.739	19.105	0.4	N	1202.4	368.9	472.2	723.6	2767.1	216.4	1.192	0.696	0.184	-415.45	110.624	11.539	36.930	56.587	215.679	109.665	21.778	0.5	N	1337.4	404.0	434.7	723.6	2899.7	226.8	1.256	0.786	0.184	-509.08	123.043	12.637	33.992	56.587	226.258	115.561	24.585	0.6	N	1569.4	406.2	433.3	723.6	3132.5	245.0	1.370	0.852	0.184	-805.85	144.385	12.707	33.882	56.587	247.560	126.063	26.659	0.66	N	1639.3	429.2	423.6	723.6	3215.7	251.5	1.405	0.907	0.184	-864.15	150.819	13.426	33.123	56.587	253.953	129.219	28.372																																																																																																																																																																																																																																																																																																																																																																																																																																																																																																																																																																																										
0.3	N	1166.9	238.3	597.0	723.6	2725.8	213.2	1.145	0.472	0.184	-607.23	107.353	7.455	46.686	56.587	218.080	105.370	14.757	0.4	N	1345.2	232.3	529.3	723.6	2830.4	221.3	1.213	0.500	0.184	-774.63	123.762	7.265	41.392	56.587	229.006	111.559	15.631	0.5	N	1527.8	234.1	471.4	723.6	2956.9	231.2	1.282	0.531	0.184	-942.27	140.561	7.323	36.866	56.587	241.336	117.966	16.823	0.6	N	1797.5	220.3	469.0	723.6	3210.4	251.1	1.397	0.547	0.184	-1291.85	165.375	6.890	36.678	56.587	265.529	128.550	17.103	0.66	N	1894.3	225.8	454.4	723.6	3298.1	257.9	1.434	0.565	0.184	-1392.77	174.281	7.063	35.535	56.587	273.466	131.932	17.688	Average																			0	N	561.3	415.1	957.4	723.6	2657.4	207.8	0.893	0.524	0.184		51.636	12.984	74.873	56.587	196.079	82.132	16.404	0.1	N	771.9	336.9	727.1	723.6	2559.5	200.2	0.989	0.512	0.184	-143.02	71.015	10.538	56.863	56.587	195.003	90.967	16.027	0.2	N	932.7	325.5	595.8	723.6	2577.6	201.6	1.062	0.540	0.184	-238.31	85.806	10.182	46.595	56.587	199.169	97.693	16.898	0.3	N	1072.3	339.8	516.6	723.6	2652.3	207.4	1.128	0.611	0.184	-324.62	98.653	10.629	40.397	56.587	206.266	103.739	19.105	0.4	N	1202.4	368.9	472.2	723.6	2767.1	216.4	1.192	0.696	0.184	-415.45	110.624	11.539	36.930	56.587	215.679	109.665	21.778	0.5	N	1337.4	404.0	434.7	723.6	2899.7	226.8	1.256	0.786	0.184	-509.08	123.043	12.637	33.992	56.587	226.258	115.561	24.585	0.6	N	1569.4	406.2	433.3	723.6	3132.5	245.0	1.370	0.852	0.184	-805.85	144.385	12.707	33.882	56.587	247.560	126.063	26.659	0.66	N	1639.3	429.2	423.6	723.6	3215.7	251.5	1.405	0.907	0.184	-864.15	150.819	13.426	33.123	56.587	253.953	129.219	28.372																																																																																																																																																																																																																																																																																																																																																																																																																																																																																																																																																																																																													
0.4	N	1345.2	232.3	529.3	723.6	2830.4	221.3	1.213	0.500	0.184	-774.63	123.762	7.265	41.392	56.587	229.006	111.559	15.631	0.5	N	1527.8	234.1	471.4	723.6	2956.9	231.2	1.282	0.531	0.184	-942.27	140.561	7.323	36.866	56.587	241.336	117.966	16.823	0.6	N	1797.5	220.3	469.0	723.6	3210.4	251.1	1.397	0.547	0.184	-1291.85	165.375	6.890	36.678	56.587	265.529	128.550	17.103	0.66	N	1894.3	225.8	454.4	723.6	3298.1	257.9	1.434	0.565	0.184	-1392.77	174.281	7.063	35.535	56.587	273.466	131.932	17.688	Average																			0	N	561.3	415.1	957.4	723.6	2657.4	207.8	0.893	0.524	0.184		51.636	12.984	74.873	56.587	196.079	82.132	16.404	0.1	N	771.9	336.9	727.1	723.6	2559.5	200.2	0.989	0.512	0.184	-143.02	71.015	10.538	56.863	56.587	195.003	90.967	16.027	0.2	N	932.7	325.5	595.8	723.6	2577.6	201.6	1.062	0.540	0.184	-238.31	85.806	10.182	46.595	56.587	199.169	97.693	16.898	0.3	N	1072.3	339.8	516.6	723.6	2652.3	207.4	1.128	0.611	0.184	-324.62	98.653	10.629	40.397	56.587	206.266	103.739	19.105	0.4	N	1202.4	368.9	472.2	723.6	2767.1	216.4	1.192	0.696	0.184	-415.45	110.624	11.539	36.930	56.587	215.679	109.665	21.778	0.5	N	1337.4	404.0	434.7	723.6	2899.7	226.8	1.256	0.786	0.184	-509.08	123.043	12.637	33.992	56.587	226.258	115.561	24.585	0.6	N	1569.4	406.2	433.3	723.6	3132.5	245.0	1.370	0.852	0.184	-805.85	144.385	12.707	33.882	56.587	247.560	126.063	26.659	0.66	N	1639.3	429.2	423.6	723.6	3215.7	251.5	1.405	0.907	0.184	-864.15	150.819	13.426	33.123	56.587	253.953	129.219	28.372																																																																																																																																																																																																																																																																																																																																																																																																																																																																																																																																																																																																																																
0.5	N	1527.8	234.1	471.4	723.6	2956.9	231.2	1.282	0.531	0.184	-942.27	140.561	7.323	36.866	56.587	241.336	117.966	16.823	0.6	N	1797.5	220.3	469.0	723.6	3210.4	251.1	1.397	0.547	0.184	-1291.85	165.375	6.890	36.678	56.587	265.529	128.550	17.103	0.66	N	1894.3	225.8	454.4	723.6	3298.1	257.9	1.434	0.565	0.184	-1392.77	174.281	7.063	35.535	56.587	273.466	131.932	17.688	Average																			0	N	561.3	415.1	957.4	723.6	2657.4	207.8	0.893	0.524	0.184		51.636	12.984	74.873	56.587	196.079	82.132	16.404	0.1	N	771.9	336.9	727.1	723.6	2559.5	200.2	0.989	0.512	0.184	-143.02	71.015	10.538	56.863	56.587	195.003	90.967	16.027	0.2	N	932.7	325.5	595.8	723.6	2577.6	201.6	1.062	0.540	0.184	-238.31	85.806	10.182	46.595	56.587	199.169	97.693	16.898	0.3	N	1072.3	339.8	516.6	723.6	2652.3	207.4	1.128	0.611	0.184	-324.62	98.653	10.629	40.397	56.587	206.266	103.739	19.105	0.4	N	1202.4	368.9	472.2	723.6	2767.1	216.4	1.192	0.696	0.184	-415.45	110.624	11.539	36.930	56.587	215.679	109.665	21.778	0.5	N	1337.4	404.0	434.7	723.6	2899.7	226.8	1.256	0.786	0.184	-509.08	123.043	12.637	33.992	56.587	226.258	115.561	24.585	0.6	N	1569.4	406.2	433.3	723.6	3132.5	245.0	1.370	0.852	0.184	-805.85	144.385	12.707	33.882	56.587	247.560	126.063	26.659	0.66	N	1639.3	429.2	423.6	723.6	3215.7	251.5	1.405	0.907	0.184	-864.15	150.819	13.426	33.123	56.587	253.953	129.219	28.372																																																																																																																																																																																																																																																																																																																																																																																																																																																																																																																																																																																																																																																			
0.6	N	1797.5	220.3	469.0	723.6	3210.4	251.1	1.397	0.547	0.184	-1291.85	165.375	6.890	36.678	56.587	265.529	128.550	17.103	0.66	N	1894.3	225.8	454.4	723.6	3298.1	257.9	1.434	0.565	0.184	-1392.77	174.281	7.063	35.535	56.587	273.466	131.932	17.688	Average																			0	N	561.3	415.1	957.4	723.6	2657.4	207.8	0.893	0.524	0.184		51.636	12.984	74.873	56.587	196.079	82.132	16.404	0.1	N	771.9	336.9	727.1	723.6	2559.5	200.2	0.989	0.512	0.184	-143.02	71.015	10.538	56.863	56.587	195.003	90.967	16.027	0.2	N	932.7	325.5	595.8	723.6	2577.6	201.6	1.062	0.540	0.184	-238.31	85.806	10.182	46.595	56.587	199.169	97.693	16.898	0.3	N	1072.3	339.8	516.6	723.6	2652.3	207.4	1.128	0.611	0.184	-324.62	98.653	10.629	40.397	56.587	206.266	103.739	19.105	0.4	N	1202.4	368.9	472.2	723.6	2767.1	216.4	1.192	0.696	0.184	-415.45	110.624	11.539	36.930	56.587	215.679	109.665	21.778	0.5	N	1337.4	404.0	434.7	723.6	2899.7	226.8	1.256	0.786	0.184	-509.08	123.043	12.637	33.992	56.587	226.258	115.561	24.585	0.6	N	1569.4	406.2	433.3	723.6	3132.5	245.0	1.370	0.852	0.184	-805.85	144.385	12.707	33.882	56.587	247.560	126.063	26.659	0.66	N	1639.3	429.2	423.6	723.6	3215.7	251.5	1.405	0.907	0.184	-864.15	150.819	13.426	33.123	56.587	253.953	129.219	28.372																																																																																																																																																																																																																																																																																																																																																																																																																																																																																																																																																																																																																																																																						
0.66	N	1894.3	225.8	454.4	723.6	3298.1	257.9	1.434	0.565	0.184	-1392.77	174.281	7.063	35.535	56.587	273.466	131.932	17.688	Average																			0	N	561.3	415.1	957.4	723.6	2657.4	207.8	0.893	0.524	0.184		51.636	12.984	74.873	56.587	196.079	82.132	16.404	0.1	N	771.9	336.9	727.1	723.6	2559.5	200.2	0.989	0.512	0.184	-143.02	71.015	10.538	56.863	56.587	195.003	90.967	16.027	0.2	N	932.7	325.5	595.8	723.6	2577.6	201.6	1.062	0.540	0.184	-238.31	85.806	10.182	46.595	56.587	199.169	97.693	16.898	0.3	N	1072.3	339.8	516.6	723.6	2652.3	207.4	1.128	0.611	0.184	-324.62	98.653	10.629	40.397	56.587	206.266	103.739	19.105	0.4	N	1202.4	368.9	472.2	723.6	2767.1	216.4	1.192	0.696	0.184	-415.45	110.624	11.539	36.930	56.587	215.679	109.665	21.778	0.5	N	1337.4	404.0	434.7	723.6	2899.7	226.8	1.256	0.786	0.184	-509.08	123.043	12.637	33.992	56.587	226.258	115.561	24.585	0.6	N	1569.4	406.2	433.3	723.6	3132.5	245.0	1.370	0.852	0.184	-805.85	144.385	12.707	33.882	56.587	247.560	126.063	26.659	0.66	N	1639.3	429.2	423.6	723.6	3215.7	251.5	1.405	0.907	0.184	-864.15	150.819	13.426	33.123	56.587	253.953	129.219	28.372																																																																																																																																																																																																																																																																																																																																																																																																																																																																																																																																																																																																																																																																																									
Average																			0	N	561.3	415.1	957.4	723.6	2657.4	207.8	0.893	0.524	0.184		51.636	12.984	74.873	56.587	196.079	82.132	16.404	0.1	N	771.9	336.9	727.1	723.6	2559.5	200.2	0.989	0.512	0.184	-143.02	71.015	10.538	56.863	56.587	195.003	90.967	16.027	0.2	N	932.7	325.5	595.8	723.6	2577.6	201.6	1.062	0.540	0.184	-238.31	85.806	10.182	46.595	56.587	199.169	97.693	16.898	0.3	N	1072.3	339.8	516.6	723.6	2652.3	207.4	1.128	0.611	0.184	-324.62	98.653	10.629	40.397	56.587	206.266	103.739	19.105	0.4	N	1202.4	368.9	472.2	723.6	2767.1	216.4	1.192	0.696	0.184	-415.45	110.624	11.539	36.930	56.587	215.679	109.665	21.778	0.5	N	1337.4	404.0	434.7	723.6	2899.7	226.8	1.256	0.786	0.184	-509.08	123.043	12.637	33.992	56.587	226.258	115.561	24.585	0.6	N	1569.4	406.2	433.3	723.6	3132.5	245.0	1.370	0.852	0.184	-805.85	144.385	12.707	33.882	56.587	247.560	126.063	26.659	0.66	N	1639.3	429.2	423.6	723.6	3215.7	251.5	1.405	0.907	0.184	-864.15	150.819	13.426	33.123	56.587	253.953	129.219	28.372																																																																																																																																																																																																																																																																																																																																																																																																																																																																																																																																																																																																																																																																																																												
0	N	561.3	415.1	957.4	723.6	2657.4	207.8	0.893	0.524	0.184		51.636	12.984	74.873	56.587	196.079	82.132	16.404	0.1	N	771.9	336.9	727.1	723.6	2559.5	200.2	0.989	0.512	0.184	-143.02	71.015	10.538	56.863	56.587	195.003	90.967	16.027	0.2	N	932.7	325.5	595.8	723.6	2577.6	201.6	1.062	0.540	0.184	-238.31	85.806	10.182	46.595	56.587	199.169	97.693	16.898	0.3	N	1072.3	339.8	516.6	723.6	2652.3	207.4	1.128	0.611	0.184	-324.62	98.653	10.629	40.397	56.587	206.266	103.739	19.105	0.4	N	1202.4	368.9	472.2	723.6	2767.1	216.4	1.192	0.696	0.184	-415.45	110.624	11.539	36.930	56.587	215.679	109.665	21.778	0.5	N	1337.4	404.0	434.7	723.6	2899.7	226.8	1.256	0.786	0.184	-509.08	123.043	12.637	33.992	56.587	226.258	115.561	24.585	0.6	N	1569.4	406.2	433.3	723.6	3132.5	245.0	1.370	0.852	0.184	-805.85	144.385	12.707	33.882	56.587	247.560	126.063	26.659	0.66	N	1639.3	429.2	423.6	723.6	3215.7	251.5	1.405	0.907	0.184	-864.15	150.819	13.426	33.123	56.587	253.953	129.219	28.372																																																																																																																																																																																																																																																																																																																																																																																																																																																																																																																																																																																																																																																																																																																															
0.1	N	771.9	336.9	727.1	723.6	2559.5	200.2	0.989	0.512	0.184	-143.02	71.015	10.538	56.863	56.587	195.003	90.967	16.027	0.2	N	932.7	325.5	595.8	723.6	2577.6	201.6	1.062	0.540	0.184	-238.31	85.806	10.182	46.595	56.587	199.169	97.693	16.898	0.3	N	1072.3	339.8	516.6	723.6	2652.3	207.4	1.128	0.611	0.184	-324.62	98.653	10.629	40.397	56.587	206.266	103.739	19.105	0.4	N	1202.4	368.9	472.2	723.6	2767.1	216.4	1.192	0.696	0.184	-415.45	110.624	11.539	36.930	56.587	215.679	109.665	21.778	0.5	N	1337.4	404.0	434.7	723.6	2899.7	226.8	1.256	0.786	0.184	-509.08	123.043	12.637	33.992	56.587	226.258	115.561	24.585	0.6	N	1569.4	406.2	433.3	723.6	3132.5	245.0	1.370	0.852	0.184	-805.85	144.385	12.707	33.882	56.587	247.560	126.063	26.659	0.66	N	1639.3	429.2	423.6	723.6	3215.7	251.5	1.405	0.907	0.184	-864.15	150.819	13.426	33.123	56.587	253.953	129.219	28.372																																																																																																																																																																																																																																																																																																																																																																																																																																																																																																																																																																																																																																																																																																																																																		
0.2	N	932.7	325.5	595.8	723.6	2577.6	201.6	1.062	0.540	0.184	-238.31	85.806	10.182	46.595	56.587	199.169	97.693	16.898	0.3	N	1072.3	339.8	516.6	723.6	2652.3	207.4	1.128	0.611	0.184	-324.62	98.653	10.629	40.397	56.587	206.266	103.739	19.105	0.4	N	1202.4	368.9	472.2	723.6	2767.1	216.4	1.192	0.696	0.184	-415.45	110.624	11.539	36.930	56.587	215.679	109.665	21.778	0.5	N	1337.4	404.0	434.7	723.6	2899.7	226.8	1.256	0.786	0.184	-509.08	123.043	12.637	33.992	56.587	226.258	115.561	24.585	0.6	N	1569.4	406.2	433.3	723.6	3132.5	245.0	1.370	0.852	0.184	-805.85	144.385	12.707	33.882	56.587	247.560	126.063	26.659	0.66	N	1639.3	429.2	423.6	723.6	3215.7	251.5	1.405	0.907	0.184	-864.15	150.819	13.426	33.123	56.587	253.953	129.219	28.372																																																																																																																																																																																																																																																																																																																																																																																																																																																																																																																																																																																																																																																																																																																																																																					
0.3	N	1072.3	339.8	516.6	723.6	2652.3	207.4	1.128	0.611	0.184	-324.62	98.653	10.629	40.397	56.587	206.266	103.739	19.105	0.4	N	1202.4	368.9	472.2	723.6	2767.1	216.4	1.192	0.696	0.184	-415.45	110.624	11.539	36.930	56.587	215.679	109.665	21.778	0.5	N	1337.4	404.0	434.7	723.6	2899.7	226.8	1.256	0.786	0.184	-509.08	123.043	12.637	33.992	56.587	226.258	115.561	24.585	0.6	N	1569.4	406.2	433.3	723.6	3132.5	245.0	1.370	0.852	0.184	-805.85	144.385	12.707	33.882	56.587	247.560	126.063	26.659	0.66	N	1639.3	429.2	423.6	723.6	3215.7	251.5	1.405	0.907	0.184	-864.15	150.819	13.426	33.123	56.587	253.953	129.219	28.372																																																																																																																																																																																																																																																																																																																																																																																																																																																																																																																																																																																																																																																																																																																																																																																								
0.4	N	1202.4	368.9	472.2	723.6	2767.1	216.4	1.192	0.696	0.184	-415.45	110.624	11.539	36.930	56.587	215.679	109.665	21.778	0.5	N	1337.4	404.0	434.7	723.6	2899.7	226.8	1.256	0.786	0.184	-509.08	123.043	12.637	33.992	56.587	226.258	115.561	24.585	0.6	N	1569.4	406.2	433.3	723.6	3132.5	245.0	1.370	0.852	0.184	-805.85	144.385	12.707	33.882	56.587	247.560	126.063	26.659	0.66	N	1639.3	429.2	423.6	723.6	3215.7	251.5	1.405	0.907	0.184	-864.15	150.819	13.426	33.123	56.587	253.953	129.219	28.372																																																																																																																																																																																																																																																																																																																																																																																																																																																																																																																																																																																																																																																																																																																																																																																																											
0.5	N	1337.4	404.0	434.7	723.6	2899.7	226.8	1.256	0.786	0.184	-509.08	123.043	12.637	33.992	56.587	226.258	115.561	24.585	0.6	N	1569.4	406.2	433.3	723.6	3132.5	245.0	1.370	0.852	0.184	-805.85	144.385	12.707	33.882	56.587	247.560	126.063	26.659	0.66	N	1639.3	429.2	423.6	723.6	3215.7	251.5	1.405	0.907	0.184	-864.15	150.819	13.426	33.123	56.587	253.953	129.219	28.372																																																																																																																																																																																																																																																																																																																																																																																																																																																																																																																																																																																																																																																																																																																																																																																																																														
0.6	N	1569.4	406.2	433.3	723.6	3132.5	245.0	1.370	0.852	0.184	-805.85	144.385	12.707	33.882	56.587	247.560	126.063	26.659	0.66	N	1639.3	429.2	423.6	723.6	3215.7	251.5	1.405	0.907	0.184	-864.15	150.819	13.426	33.123	56.587	253.953	129.219	28.372																																																																																																																																																																																																																																																																																																																																																																																																																																																																																																																																																																																																																																																																																																																																																																																																																																																	
0.66	N	1639.3	429.2	423.6	723.6	3215.7	251.5	1.405	0.907	0.184	-864.15	150.819	13.426	33.123	56.587	253.953	129.219	28.372																																																																																																																																																																																																																																																																																																																																																																																																																																																																																																																																																																																																																																																																																																																																																																																																																																																																				

CASE 1 (Varying SHGC)

2G-2s v 2G-4uv

Low U and High SHGC

IGU	Ucg	SHGC	VT	Frame	U-edge	U-frame	WWR 0.1	WWR 0.2	WWR 0.3	WWR 0.4	WWR 0.5	WWR 0.6	WWR 0.66
	[W/m2K]				[W/m2K]	[W/m2K]	[W/m2K]	[W/m2K]	[W/m2K]	[W/m2K]	[W/m2K]	[W/m2K]	[W/m2K]
2G-2s HP Wd	1.305	0.37	0.639	HP Wood	1.5916	1.8827	1.50	1.45	1.42	1.41	1.40	1.41	1.41

WWR	Shading	Annual Purchased Heating [kWh]	Annual Purchased Cooling [kWh]	Annual Lighting Load [kWh]	Annual Plug Load [kWh]	Total Annual Load [kWh]	Total Annual Load / Area [kWh/m2]	Peak Heating [kW]	Peak Cooling [kW]	Peak Lighting [kW]	Annual Window Energy Balance ('+' gain, '-' loss) [kWh]	Annual Heating Energy 'Metered' [kWh/m2]	Annual Cooling Energy 'Metered' [kWh/m2]	Annual Lighting Energy 'Metered' [kWh/m2]	Annual Plug Energy 'Metered' [kWh/m2]	Total Annual Energy 'Metered' [kWh/m2]	Peak Heating Energy 'Metered' [W/m2]	Peak Cooling Energy 'Metered' [W/m2]	
South	0	N	537.4	419.2	957.4	723.6	2637.6	206.3	0.881	0.523	0.184		49.446	13.111	74.873	56.587	194.016	81.024	16.347
	0.1	N	644.4	315.3	537.3	723.6	2220.6	173.7	0.916	0.470	0.184	142.63	59.285	9.861	42.019	56.587	167.751	84.289	14.693
	0.2	N	623.5	361.2	432.1	723.6	2140.3	167.4	0.924	0.534	0.184	299.81	57.359	11.297	33.792	56.587	159.035	85.050	16.706
	0.3	N	580.8	442.0	394.4	723.6	2140.8	167.4	0.929	0.615	0.184	453.97	53.437	13.826	30.842	56.587	154.692	85.469	19.232
	0.4	N	540.6	537.1	375.6	723.6	2177.0	170.2	0.935	0.712	0.184	599.83	49.736	16.802	29.375	56.587	152.499	86.064	22.276
	0.5	N	511.9	639.7	359.9	723.6	2235.0	174.8	0.945	0.812	0.184	737.20	47.093	20.009	28.141	56.587	151.830	86.976	25.385
	0.6	N	545.3	680.4	359.1	723.6	2308.4	180.5	0.991	0.886	0.184	720.89	50.169	21.283	28.079	56.587	156.117	91.167	27.725
	0.66	N	530.5	743.9	355.8	723.6	2353.8	184.1	0.997	0.956	0.184	793.83	48.806	23.269	27.825	56.587	156.486	91.705	29.897
East	0	N	560.9	428.3	957.4	723.6	2670.3	208.8	0.895	0.535	0.184		51.607	13.399	74.873	56.587	196.465	82.359	16.729
	0.1	N	664.9	375.2	644.1	723.6	2407.8	188.3	0.938	0.525	0.184	98.54	61.167	11.737	50.368	56.587	179.859	86.295	16.422
	0.2	N	726.3	427.9	496.5	723.6	2374.3	185.7	0.972	0.585	0.184	210.66	66.822	13.384	38.825	56.587	175.617	89.425	18.304
	0.3	N	754.6	518.7	428.7	723.6	2425.6	189.7	0.999	0.721	0.184	321.55	69.421	16.226	33.525	56.587	175.758	91.913	22.561
	0.4	N	772.1	625.9	395.9	723.6	2517.5	196.9	1.024	0.868	0.184	420.49	71.037	19.579	30.958	56.587	178.159	94.241	27.147
	0.5	N	790.7	740.7	373.2	723.6	2628.2	205.5	1.051	1.028	0.184	517.12	72.746	23.169	29.183	56.587	181.684	96.666	32.149
	0.6	N	866.1	796.4	372.6	723.6	2758.7	215.7	1.108	1.159	0.184	474.04	79.686	24.912	29.136	56.587	190.320	101.913	36.267
	0.66	N	875.1	866.2	367.8	723.6	2832.6	221.5	1.122	1.264	0.184	525.98	80.509	27.094	28.761	56.587	192.951	103.252	39.545
West	0	N	565.6	418.0	957.4	723.6	2664.6	208.4	0.894	0.528	0.184		52.035	13.075	74.873	56.587	196.569	82.266	16.502
	0.1	N	675.3	339.9	622.8	723.6	2361.6	184.7	0.934	0.490	0.184	79.70	62.129	10.633	48.701	56.587	178.050	85.921	15.317
	0.2	N	739.8	382.7	476.4	723.6	2322.5	181.6	0.965	0.608	0.184	171.34	68.060	11.972	37.259	56.587	173.877	88.796	19.013
	0.3	N	770.3	461.1	411.6	723.6	2366.5	185.1	0.995	0.748	0.184	261.36	70.865	14.424	32.185	56.587	174.061	91.540	23.382
	0.4	N	787.3	553.3	384.2	723.6	2448.3	191.5	1.009	0.929	0.184	339.98	72.429	17.306	30.044	56.587	176.366	92.854	29.054
	0.5	N	805.8	654.1	366.3	723.6	2549.8	199.4	1.034	1.096	0.184	416.86	74.138	20.459	28.645	56.587	179.829	95.088	34.274
	0.6	N	884.0	699.4	365.9	723.6	2672.8	209.0	1.088	1.229	0.184	359.27	81.327	21.878	28.610	56.587	188.402	100.094	38.446
	0.66	N	893.5	758.5	361.7	723.6	2737.3	214.1	1.104	1.332	0.184	399.05	82.199	23.727	28.288	56.587	190.801	101.614	41.653
North	0	N	581.0	394.9	957.4	723.6	2656.9	207.8	0.901	0.513	0.184		53.457	12.352	74.873	56.587	197.267	82.879	16.039
	0.1	N	679.5	331.1	760.9	723.6	2495.1	195.1	0.943	0.486	0.184	-37.15	62.514	10.356	59.507	56.587	188.964	86.721	15.210
	0.2	N	775.9	273.1	563.4	723.6	2336.0	182.7	0.978	0.448	0.184	-59.88	71.385	8.543	44.061	56.587	180.575	89.949	14.016
	0.3	N	859.6	279.9	459.3	723.6	2322.3	181.6	1.012	0.480	0.184	-81.13	79.080	8.754	35.919	56.587	180.340	93.101	15.028
	0.4	N	921.7	309.8	410.6	723.6	2365.7	185.0	1.043	0.522	0.184	-103.22	84.801	9.691	32.106	56.587	183.184	95.924	16.326
	0.5	N	971.9	345.3	380.9	723.6	2421.7	189.4	1.074	0.565	0.184	-126.84	89.413	10.802	29.786	56.587	186.587	98.770	17.879
	0.6	N	1075.2	344.5	380.0	723.6	2523.3	197.3	1.132	0.583	0.184	-261.08	98.918	10.776	29.718	56.587	195.998	104.176	18.246
	0.66	N	1100.4	365.2	374.5	723.6	2563.7	200.5	1.149	0.607	0.184	-280.16	101.237	11.425	29.285	56.587	198.533	105.709	18.990
Average	0	N	561.3	415.1	957.4	723.6	2657.4	207.8	0.893	0.524	0.184		51.636	12.984	74.873	56.587	196.079	82.132	16.404
	0.1	N	666.0	340.4	641.3	723.6	2371.3	185.4	0.933	0.493	0.184	70.93	61.274	10.647	50.149	56.587	178.656	85.807	15.410
	0.2	N	716.4	361.2	492.1	723.6	2293.3	179.3	0.960	0.544	0.184	155.48	65.906	11.299	38.484	56.587	172.276	88.305	17.010
	0.3	N	741.3	425.4	423.5	723.6	2313.8	180.9	0.984	0.641	0.184	238.94	68.201	13.308	33.118	56.587	171.212	90.506	20.051
	0.4	N	755.4	506.5	391.6	723.6	2377.1	185.9	1.003	0.758	0.184	314.27	69.501	15.845	30.621	56.587	172.552	92.271	23.701
	0.5	N	770.1	594.9	370.1	723.6	2458.7	192.3	1.026	0.875	0.184	386.09	70.847	18.610	28.939	56.587	174.983	94.375	27.372
	0.6	N	842.6	630.2	369.4	723.6	2565.8	200.6	1.080	0.965	0.184	323.28	77.525	19.712	28.886	56.587	182.710	99.338	30.171
	0.66	N	849.9	683.4	365.0	723.6	2621.9	205.0	1.093	1.040	0.184	359.68	78.188	21.379	28.540	56.587	184.693	100.570	32.521

CASE 1 (Varying SHGC)

Low U and Low SHGC

IGU	Ucg [W/m2K]	SHGC	VT	Frame	U-edge [W/m2K]	U-frame [W/m2K]	WWR 0.1 [W/m2K]	WWR 0.2 [W/m2K]	WWR 0.3 [W/m2K]	WWR 0.4 [W/m2K]	WWR 0.5 [W/m2K]	WWR 0.6 [W/m2K]	WWR 0.66 [W/m2K]
2G-4uv HP Wd	1.334	0.253	0.413	HP Wood	1.5916	1.8827	1.51	1.47	1.44	1.43	1.42	1.43	1.43

WWR	Shading	Annual Purchased Heating [kWh]	Annual Purchased Cooling [kWh]	Annual Lighting Load [kWh]	Annual Plug Load [kWh]	Total Annual Load [kWh]	Total Annual Load / Area [kWh/m2]	Peak Heating [kW]	Peak Cooling [kW]	Peak Lighting [kW]	Annual Window Energy Balance ('+' gain, '-' loss) [kWh]	Annual Heating Energy 'Metered' [kWh/m2]	Annual Cooling Energy 'Metered' [kWh/m2]	Annual Lighting Energy 'Metered' [kWh/m2]	Annual Plug Energy 'Metered' [kWh/m2]	Total Annual Energy 'Metered' [kWh/m2]	Peak Heating Energy 'Metered' [W/m2]	Peak Cooling Energy 'Metered' [W/m2]
South																		
0	N	537.4	419.2	957.4	723.6	2637.6	206.3	0.881	0.523	0.184		49.446	13.111	74.873	56.587	194.016	81.024	16.347
0.1	N	644.6	334.3	635.3	723.6	2337.8	182.8	0.921	0.489	0.184	67.46	59.301	10.456	49.685	56.587	176.029	84.717	15.288
0.2	N	665.3	333.7	501.5	723.6	2224.0	173.9	0.940	0.498	0.184	150.30	61.206	10.437	39.214	56.587	167.444	86.480	15.572
0.3	N	658.0	374.6	450.2	723.6	2206.4	172.5	0.954	0.553	0.184	232.26	60.536	11.719	35.203	56.587	164.044	87.798	17.285
0.4	N	644.6	428.2	425.1	723.6	2221.5	173.7	0.977	0.611	0.184	307.63	59.302	13.395	33.241	56.587	162.525	89.887	19.116
0.5	N	639.6	486.1	404.0	723.6	2253.2	176.2	0.992	0.676	0.184	375.67	58.840	15.205	31.591	56.587	162.222	91.251	21.156
0.6	N	696.2	498.0	403.1	723.6	2320.9	181.5	1.043	0.716	0.184	310.77	64.055	15.577	31.520	56.587	167.738	95.946	22.412
0.66	N	691.6	533.3	398.1	723.6	2346.6	183.5	1.051	0.756	0.184	346.29	63.629	16.681	31.132	56.587	168.028	96.667	23.656
East																		
0	N	560.9	428.3	957.4	723.6	2670.3	208.8	0.895	0.535	0.184		51.607	13.399	74.873	56.587	196.465	82.359	16.729
0.1	N	650.2	383.2	732.3	723.6	2489.3	194.7	0.937	0.533	0.184	36.83	59.817	11.988	57.264	56.587	185.655	86.233	16.680
0.2	N	719.7	405.6	600.3	723.6	2449.1	191.5	0.973	0.551	0.184	87.67	66.215	12.686	46.943	56.587	182.430	89.560	17.228
0.3	N	768.9	454.0	522.8	723.6	2469.2	193.1	1.005	0.626	0.184	138.77	70.741	14.201	40.881	56.587	182.409	92.425	19.591
0.4	N	805.8	514.0	479.9	723.6	2523.2	197.3	1.033	0.730	0.184	177.81	74.133	16.077	37.529	56.587	184.326	95.049	22.830
0.5	N	845.6	579.0	442.2	723.6	2590.4	202.6	1.063	0.836	0.184	215.52	77.794	18.113	34.582	56.587	187.075	97.765	26.159
0.6	N	937.1	604.2	441.1	723.6	2706.0	211.6	1.122	0.914	0.184	130.09	86.215	18.898	34.495	56.587	196.195	103.258	28.587
0.66	N	956.3	646.6	431.2	723.6	2757.6	215.6	1.139	0.980	0.184	149.80	87.980	20.225	33.719	56.587	198.509	104.766	30.669
West																		
0	N	565.6	418.0	957.4	723.6	2664.6	208.4	0.894	0.528	0.184		52.035	13.075	74.873	56.587	196.569	82.266	16.502
0.1	N	658.1	348.8	713.8	723.6	2444.2	191.1	0.934	0.497	0.184	19.97	60.543	10.910	55.819	56.587	183.859	85.936	15.552
0.2	N	734.3	362.6	578.1	723.6	2398.6	187.6	0.969	0.541	0.184	52.96	67.555	11.342	45.211	56.587	180.696	89.116	16.927
0.3	N	786.4	402.3	502.1	723.6	2414.4	188.8	0.999	0.638	0.184	86.21	72.354	12.584	39.261	56.587	180.786	91.865	19.966
0.4	N	824.2	451.3	460.7	723.6	2459.8	192.4	1.023	0.741	0.184	108.71	75.827	14.117	36.030	56.587	182.561	94.098	23.190
0.5	N	865.4	508.3	427.0	723.6	2524.3	197.4	1.051	0.856	0.184	130.42	79.617	15.899	33.394	56.587	185.496	96.711	26.789
0.6	N	960.9	527.4	426.4	723.6	2638.3	206.3	1.109	0.947	0.184	32.42	88.402	16.497	33.346	56.587	194.831	102.045	29.635
0.66	N	981.4	562.8	417.2	723.6	2685.0	210.0	1.124	1.019	0.184	42.15	90.288	17.606	32.625	56.587	197.106	103.443	31.872
North																		
0	N	581.0	394.9	957.4	723.6	2656.9	207.8	0.901	0.513	0.184		53.457	12.352	74.873	56.587	197.267	82.879	16.039
0.1	N	668.4	353.6	832.9	723.6	2578.5	201.6	0.943	0.500	0.184	-68.98	61.495	11.060	65.133	56.587	194.274	86.731	15.650
0.2	N	749.8	315.9	711.4	723.6	2500.8	195.6	0.978	0.487	0.184	-123.86	68.984	9.883	55.633	56.587	191.086	89.981	15.245
0.3	N	827.8	285.4	599.8	723.6	2436.5	190.5	1.011	0.465	0.184	-174.89	76.156	8.926	46.903	56.587	188.572	93.015	14.531
0.4	N	899.0	286.0	532.6	723.6	2441.2	190.9	1.043	0.486	0.184	-224.70	82.706	8.946	41.649	56.587	189.888	95.936	15.203
0.5	N	971.1	295.0	474.6	723.6	2464.3	192.7	1.077	0.514	0.184	-275.13	89.344	9.227	37.116	56.587	192.273	99.112	16.071
0.6	N	1087.2	284.4	472.4	723.6	2567.6	200.8	1.138	0.523	0.184	-428.84	100.025	8.897	36.944	56.587	202.452	104.721	16.356
0.66	N	1124.2	294.5	457.7	723.6	2600.1	203.3	1.157	0.539	0.184	-462.44	103.432	9.213	35.796	56.587	205.028	106.403	16.876
Average																		
0	N	561.3	415.1	957.4	723.6	2657.4	207.8	0.893	0.524	0.184		51.636	12.984	74.873	56.587	196.079	82.132	16.404
0.1	N	655.3	355.0	728.6	723.6	2462.4	192.6	0.934	0.505	0.184	13.82	60.289	11.103	56.975	56.587	184.954	85.904	15.793
0.2	N	717.3	354.4	597.8	723.6	2393.1	187.1	0.965	0.519	0.184	41.77	65.990	11.087	46.750	56.587	180.414	88.784	16.243
0.3	N	760.3	379.1	518.7	723.6	2381.6	186.2	0.992	0.570	0.184	70.59	69.947	11.858	40.562	56.587	178.953	91.276	17.843
0.4	N	793.4	419.9	474.6	723.6	2411.4	188.6	1.019	0.642	0.184	92.36	72.992	13.134	37.112	56.587	179.825	93.742	20.085
0.5	N	830.4	467.1	437.0	723.6	2458.0	192.2	1.046	0.721	0.184	111.62	76.399	14.611	34.171	56.587	181.766	96.210	22.544
0.6	N	920.4	478.5	435.8	723.6	2558.2	200.1	1.103	0.775	0.184	11.11	84.674	14.967	34.076	56.587	190.304	101.492	24.247
0.66	N	938.4	509.3	426.1	723.6	2597.3	203.1	1.118	0.824	0.184	18.95	86.332	15.931	33.318	56.587	192.168	102.820	25.768

CASE 2 (Varying IGU and Window U-value, similar SHGC)

5G-2s Wood v 2G-2s Wood

Low U and High SHGC

IGU	Ucg [W/m2K]	SHGC	VT	Frame	U-edge [W/m2K]	U-frame [W/m2K]	WWR 0.1 [W/m2K]	WWR 0.2 [W/m2K]	WWR 0.3 [W/m2K]	WWR 0.4 [W/m2K]	WWR 0.5 [W/m2K]	WWR 0.6 [W/m2K]	WWR 0.66 [W/m2K]
2G-2s HP Wd	1.305	0.37	0.639	HP Wood	1.5916	1.8827	1.50	1.45	1.42	1.41	1.40	1.41	1.41

WWR	Shading	Annual Purchased Heating [kWh]	Annual Purchased Cooling [kWh]	Annual Lighting Load [kWh]	Annual Plug Load [kWh]	Total Annual Load [kWh]	Total Annual Load / Area [kWh/m2]	Peak Heating [kW]	Peak Cooling [kW]	Peak Lighting [kW]	Annual Window Energy Balance ('+' gain, '-' loss) [kWh]	Annual Heating Energy 'Metered' [kWh/m2]	Annual Cooling Energy 'Metered' [kWh/m2]	Annual Lighting Energy 'Metered' [kWh/m2]	Annual Plug Energy 'Metered' [kWh/m2]	Total Annual Energy 'Metered' [kWh/m2]	Peak Heating Energy 'Metered' [W/m2]	Peak Cooling Energy 'Metered' [W/m2]	
South	0	N	537.4	419.2	957.4	723.6	2637.6	206.3	0.881	0.523	0.184		49.446	13.111	74.873	56.587	194.016	81.024	16.347
	0.1	N	644.4	315.3	537.3	723.6	2220.6	173.7	0.916	0.470	0.184	142.63	59.285	9.861	42.019	56.587	167.751	84.289	14.693
	0.2	N	623.5	361.2	432.1	723.6	2140.3	167.4	0.924	0.534	0.184	299.81	57.359	11.297	33.792	56.587	159.035	85.050	16.706
	0.3	N	580.8	442.0	394.4	723.6	2140.8	167.4	0.929	0.615	0.184	453.97	53.437	13.826	30.842	56.587	154.692	85.469	19.232
	0.4	N	540.6	537.1	375.6	723.6	2177.0	170.2	0.935	0.712	0.184	599.83	49.736	16.802	29.375	56.587	152.499	86.064	22.276
	0.5	N	511.9	639.7	359.9	723.6	2235.0	174.8	0.945	0.812	0.184	737.20	47.093	20.009	28.141	56.587	151.830	86.976	25.385
	0.6	N	545.3	680.4	359.1	723.6	2308.4	180.5	0.991	0.886	0.184	720.89	50.169	21.283	28.079	56.587	156.117	91.167	27.725
	0.66	N	530.5	743.9	355.8	723.6	2353.8	184.1	0.997	0.956	0.184	793.83	48.806	23.269	27.825	56.587	156.486	91.705	29.897
East	0	N	560.9	428.3	957.4	723.6	2670.3	208.8	0.895	0.535	0.184		51.607	13.399	74.873	56.587	196.465	82.359	16.729
	0.1	N	664.9	375.2	644.1	723.6	2407.8	188.3	0.938	0.525	0.184	98.54	61.167	11.737	50.368	56.587	179.859	86.295	16.422
	0.2	N	726.3	427.9	496.5	723.6	2374.3	185.7	0.972	0.585	0.184	210.66	66.822	13.384	38.825	56.587	175.617	89.425	18.304
	0.3	N	754.6	518.7	428.7	723.6	2425.6	189.7	0.999	0.721	0.184	321.55	69.421	16.226	33.525	56.587	175.758	91.913	22.561
	0.4	N	772.1	625.9	395.9	723.6	2517.5	196.9	1.024	0.868	0.184	420.49	71.037	19.579	30.958	56.587	178.159	94.241	27.147
	0.5	N	790.7	740.7	373.2	723.6	2628.2	205.5	1.051	1.028	0.184	517.12	72.746	23.169	29.183	56.587	181.684	96.666	32.149
	0.6	N	866.1	796.4	372.6	723.6	2758.7	215.7	1.108	1.159	0.184	474.04	79.686	24.912	29.136	56.587	190.320	101.913	36.267
	0.66	N	875.1	866.2	367.8	723.6	2832.6	221.5	1.122	1.264	0.184	525.98	80.509	27.094	28.761	56.587	192.951	103.252	39.545
West	0	N	565.6	418.0	957.4	723.6	2664.6	208.4	0.894	0.528	0.184		52.035	13.075	74.873	56.587	196.569	82.266	16.502
	0.1	N	675.3	339.9	622.8	723.6	2361.6	184.7	0.934	0.490	0.184	79.70	62.129	10.633	48.701	56.587	178.050	85.921	15.317
	0.2	N	739.8	382.7	476.4	723.6	2322.5	181.6	0.965	0.608	0.184	171.34	68.060	11.972	37.259	56.587	173.877	88.796	19.013
	0.3	N	770.3	461.1	411.6	723.6	2366.5	185.1	0.995	0.748	0.184	261.36	70.865	14.424	32.185	56.587	174.061	91.540	23.382
	0.4	N	787.3	553.3	384.2	723.6	2448.3	191.5	1.009	0.929	0.184	339.98	72.429	17.306	30.044	56.587	176.366	92.854	29.054
	0.5	N	805.8	654.1	366.3	723.6	2549.8	199.4	1.034	1.096	0.184	416.86	74.138	20.459	28.645	56.587	179.829	95.088	34.274
	0.6	N	884.0	699.4	365.9	723.6	2672.8	209.0	1.088	1.229	0.184	359.27	81.327	21.878	28.610	56.587	188.402	100.094	38.446
	0.66	N	893.5	758.5	361.7	723.6	2737.3	214.1	1.104	1.332	0.184	399.05	82.199	23.727	28.288	56.587	190.801	101.614	41.653
North	0	N	581.0	394.9	957.4	723.6	2656.9	207.8	0.901	0.513	0.184		53.457	12.352	74.873	56.587	197.267	82.879	16.039
	0.1	N	679.5	331.1	760.9	723.6	2495.1	195.1	0.943	0.486	0.184	-37.15	62.514	10.356	59.507	56.587	188.964	86.721	15.210
	0.2	N	775.9	273.1	563.4	723.6	2336.0	182.7	0.978	0.448	0.184	-59.88	71.385	8.543	44.061	56.587	180.575	89.949	14.016
	0.3	N	859.6	279.9	459.3	723.6	2322.3	181.6	1.012	0.480	0.184	-81.13	79.080	8.754	35.919	56.587	180.340	93.101	15.028
	0.4	N	921.7	309.8	410.6	723.6	2365.7	185.0	1.043	0.522	0.184	-103.22	84.801	9.691	32.106	56.587	183.184	95.924	16.326
	0.5	N	971.9	345.3	380.9	723.6	2421.7	189.4	1.074	0.565	0.184	-126.84	89.413	10.802	29.786	56.587	186.587	98.770	17.879
	0.6	N	1075.2	344.5	380.0	723.6	2523.3	197.3	1.132	0.583	0.184	-261.08	98.918	10.776	29.718	56.587	195.998	104.176	18.246
	0.66	N	1100.4	365.2	374.5	723.6	2563.7	200.5	1.149	0.607	0.184	-280.16	101.237	11.425	29.285	56.587	198.533	105.709	18.990
Average	0	N	561.3	415.1	957.4	723.6	2657.4	207.8	0.893	0.524	0.184		51.636	12.984	74.873	56.587	196.079	82.132	16.404
	0.1	N	666.0	340.4	641.3	723.6	2371.3	185.4	0.933	0.493	0.184	70.93	61.274	10.647	50.149	56.587	178.656	85.807	15.410
	0.2	N	716.4	361.2	492.1	723.6	2293.3	179.3	0.960	0.544	0.184	155.48	65.906	11.299	38.484	56.587	172.276	88.305	17.010
	0.3	N	741.3	425.4	423.5	723.6	2313.8	180.9	0.984	0.641	0.184	238.94	68.201	13.308	33.118	56.587	171.212	90.506	20.051
	0.4	N	755.4	506.5	391.6	723.6	2377.1	185.9	1.003	0.758	0.184	314.27	69.501	15.845	30.621	56.587	172.552	92.271	23.701
	0.5	N	770.1	594.9	370.1	723.6	2458.7	192.3	1.026	0.875	0.184	386.09	70.847	18.610	28.939	56.587	174.983	94.375	27.372
	0.6	N	842.6	630.2	369.4	723.6	2565.8	200.6	1.080	0.965	0.184	323.28	77.525	19.712	28.886	56.587	182.710	99.338	30.171
	0.66	N	849.9	683.4	365.0	723.6	2621.9	205.0	1.093	1.040	0.184	359.68	78.188	21.379	28.540	56.587	184.693	100.570	32.521

CASE 2 (Varying IGU and Window U-value, similar SHGC)

Low U and High SHGC

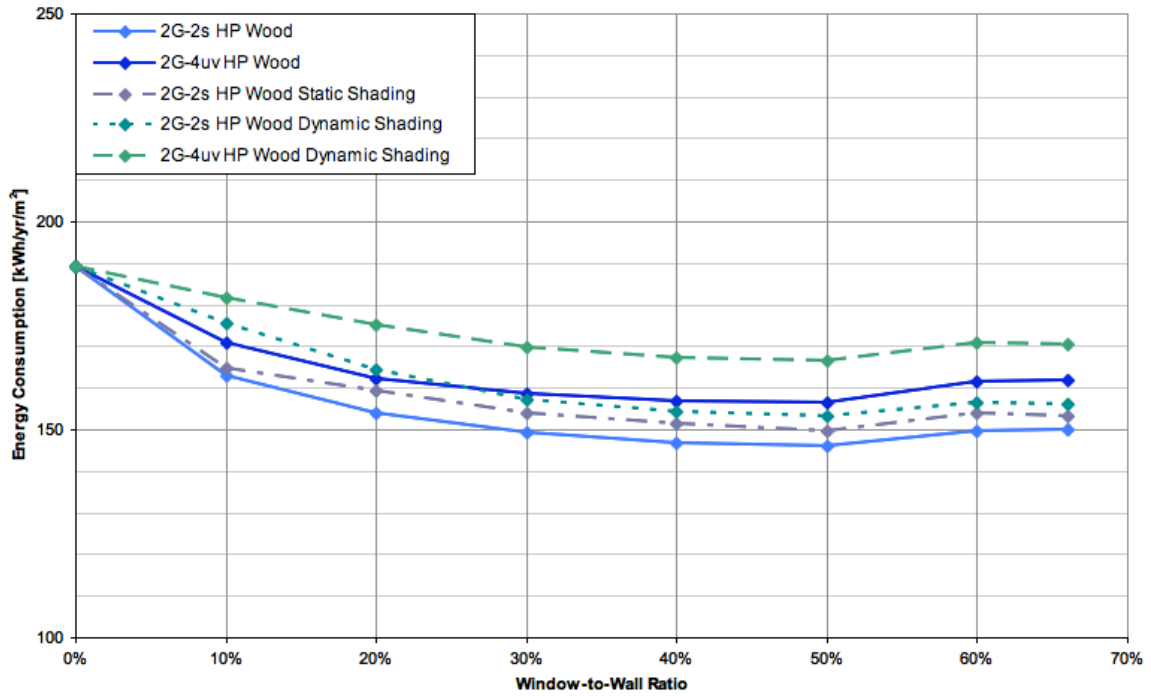
IGU	Ucg [W/m2K]	SHGC	VT	Frame	U-edge [W/m2K]	U-frame [W/m2K]	WWR 0.1 [W/m2K]	WWR 0.2 [W/m2K]	WWR 0.3 [W/m2K]	WWR 0.4 [W/m2K]	WWR 0.5 [W/m2K]	WWR 0.6 [W/m2K]	WWR 0.66 [W/m2K]
5G-2s HP Wd	0.271	0.33	0.447	HP Wood	0.7047	1.62	0.67	0.56	0.51	0.48	0.46	0.49	0.48

WWR	Shading	Annual Purchased Heating [kWh]	Annual Purchased Cooling [kWh]	Annual Lighting Load [kWh]	Annual Plug Load [kWh]	Total Annual Load [kWh]	Total Annual Load / Area [kWh/m2]	Peak Heating [kW]	Peak Cooling [kW]	Peak Lighting [kW]	Annual Window Energy Balance ('+' gain, '-' loss) [kWh]	Annual Heating Energy 'Metered' [kWh/m2]	Annual Cooling Energy 'Metered' [kWh/m2]	Annual Lighting Energy 'Metered' [kWh/m2]	Annual Plug Energy 'Metered' [kWh/m2]	Total Annual Energy 'Metered' [kWh/m2]	Peak Heating Energy 'Metered' [W/m2]	Peak Cooling Energy 'Metered' [W/m2]
South																		
0	N	537.4	419.2	957.4	723.6	2637.6	206.3	0.881	0.523	0.184	223.36	49.446	13.111	74.873	56.587	194.016	81.024	16.347
0.1	N	547.9	361.4	627.1	723.6	2260.1	176.7	0.870	0.491	0.184	223.36	50.410	11.306	49.043	56.587	167.346	79.999	15.373
0.2	N	475.3	395.9	495.6	723.6	2090.5	163.5	0.840	0.511	0.184	456.90	43.731	12.385	38.758	56.587	151.460	77.279	15.995
0.3	N	386.1	481.8	444.7	723.6	2036.2	159.2	0.816	0.586	0.184	690.04	35.524	15.070	34.776	56.587	141.956	75.099	18.337
0.4	N	303.6	591.5	420.3	723.6	2039.0	159.5	0.800	0.673	0.184	917.48	27.929	18.504	32.871	56.587	135.890	73.587	21.055
0.5	N	234.9	717.7	399.7	723.6	2075.9	162.3	0.780	0.762	0.184	1139.01	21.610	22.451	31.257	56.587	131.906	71.768	23.845
0.6	N	211.0	780.5	399.0	723.6	2114.1	165.3	0.787	0.840	0.184	1203.45	19.413	24.414	31.204	56.587	131.618	72.361	26.279
0.66	N	177.7	866.4	393.9	723.6	2161.7	169.0	0.776	0.919	0.184	1325.89	16.351	27.102	30.806	56.587	130.845	71.399	28.740
East																		
0	N	560.9	428.3	957.4	723.6	2670.3	208.8	0.895	0.535	0.184	191.21	51.607	13.399	74.873	56.587	196.465	82.359	16.729
0.1	N	563.3	420.4	725.3	723.6	2432.6	190.2	0.894	0.542	0.184	390.32	51.829	13.150	56.716	56.587	178.281	82.253	16.955
0.2	N	550.2	486.3	590.8	723.6	2350.9	183.8	0.892	0.569	0.184	589.09	50.616	15.212	46.200	56.587	168.615	82.058	17.807
0.3	N	520.8	588.1	513.0	723.6	2345.5	183.4	0.884	0.686	0.184	776.65	47.914	18.395	40.118	56.587	163.013	81.339	21.467
0.4	N	483.4	709.7	470.8	723.6	2387.4	186.7	0.874	0.829	0.184	963.05	44.471	22.198	36.817	56.587	160.073	80.423	25.925
0.5	N	448.0	840.0	434.1	723.6	2445.6	191.3	0.866	0.976	0.184	1007.51	41.218	26.274	33.945	56.587	158.024	79.651	30.528
0.6	N	449.2	914.2	433.5	723.6	2520.4	197.1	0.880	1.083	0.184	1111.71	41.326	28.595	33.899	56.587	160.407	80.981	33.867
0.66	N	426.2	998.1	424.1	723.6	2572.0	201.1	0.872	1.178	0.184	1111.71	39.213	31.222	33.162	56.587	160.184	80.236	36.862
West																		
0	N	565.6	418.0	957.4	723.6	2664.6	208.4	0.894	0.528	0.184	175.44	52.035	13.075	74.873	56.587	196.569	82.266	16.502
0.1	N	568.6	383.8	706.7	723.6	2382.7	186.3	0.890	0.503	0.184	356.44	52.313	12.006	55.262	56.587	176.167	81.842	15.723
0.2	N	558.8	437.6	569.0	723.6	2289.0	179.0	0.884	0.591	0.184	536.58	51.412	13.687	44.498	56.587	166.185	81.322	18.478
0.3	N	528.6	523.5	492.5	723.6	2268.2	177.4	0.875	0.719	0.184	706.27	48.636	16.374	38.511	56.587	160.107	80.475	22.494
0.4	N	490.8	627.5	452.4	723.6	2294.3	179.4	0.869	0.849	0.184	875.41	45.158	19.628	35.378	56.587	156.752	79.913	26.570
0.5	N	456.6	745.3	419.4	723.6	2344.9	183.4	0.864	0.996	0.184	906.86	42.007	23.314	32.802	56.587	154.709	79.476	31.147
0.6	N	458.4	809.0	419.4	723.6	2410.3	188.5	0.879	1.108	0.184	1000.31	42.173	25.305	32.794	56.587	156.859	80.859	34.672
0.66	N	436.0	883.9	410.6	723.6	2454.1	191.9	0.876	1.198	0.184	1000.31	40.109	27.650	32.106	56.587	156.452	80.593	37.475
North																		
0	N	581.0	394.9	957.4	723.6	2656.9	207.8	0.901	0.513	0.184	71.41	53.457	12.352	74.873	56.587	197.267	82.879	16.039
0.1	N	581.6	380.8	827.6	723.6	2513.6	196.6	0.901	0.506	0.184	146.30	53.507	11.913	64.720	56.587	186.726	82.853	15.817
0.2	N	579.9	364.9	698.0	723.6	2366.4	185.1	0.898	0.498	0.184	220.33	53.350	11.415	54.584	56.587	175.936	82.654	15.578
0.3	N	574.8	360.4	585.9	723.6	2244.7	175.5	0.895	0.480	0.184	293.64	52.884	11.274	45.818	56.587	166.562	82.349	15.009
0.4	N	563.7	389.7	519.6	723.6	2196.6	171.8	0.891	0.512	0.184	365.91	51.862	12.191	40.630	56.587	161.270	81.939	16.001
0.5	N	554.1	429.5	463.6	723.6	2170.8	169.8	0.889	0.547	0.184	325.02	50.979	13.434	36.257	56.587	157.257	81.806	17.098
0.6	N	568.0	439.8	462.4	723.6	2193.7	171.6	0.906	0.562	0.184	360.38	52.254	13.757	36.158	56.587	158.756	83.328	17.570
0.66	N	556.9	469.3	447.6	723.6	2197.4	171.8	0.902	0.583	0.184	360.38	51.237	14.681	35.002	56.587	157.506	83.000	18.231
Average																		
0	N	561.3	415.1	957.4	723.6	2657.4	207.8	0.893	0.524	0.184	165.36	51.636	12.984	74.873	56.587	196.079	82.132	16.404
0.1	N	565.4	386.6	721.7	723.6	2397.3	187.5	0.888	0.510	0.184	337.49	52.015	12.094	56.435	56.587	177.130	81.737	15.967
0.2	N	541.0	421.2	588.4	723.6	2274.2	177.8	0.879	0.542	0.184	509.01	49.777	13.175	46.010	56.587	165.549	80.828	16.964
0.3	N	502.6	488.4	509.0	723.6	2223.6	173.9	0.868	0.618	0.184	673.51	46.240	15.278	39.806	56.587	157.910	79.816	19.327
0.4	N	460.4	579.6	465.8	723.6	2229.4	174.3	0.858	0.716	0.184	835.84	42.355	18.130	36.424	56.587	153.496	78.965	22.388
0.5	N	423.4	683.1	429.2	723.6	2259.3	176.7	0.850	0.820	0.184	860.71	38.954	21.368	33.565	56.587	150.474	78.175	25.655
0.6	N	421.6	735.9	428.6	723.6	2309.7	180.6	0.863	0.898	0.184	949.57	38.792	23.018	33.514	56.587	151.910	79.382	28.097
0.66	N	399.2	804.5	419.0	723.6	2346.3	183.5	0.857	0.970	0.184	949.57	36.728	25.164	32.769	56.587	151.247	78.807	30.327

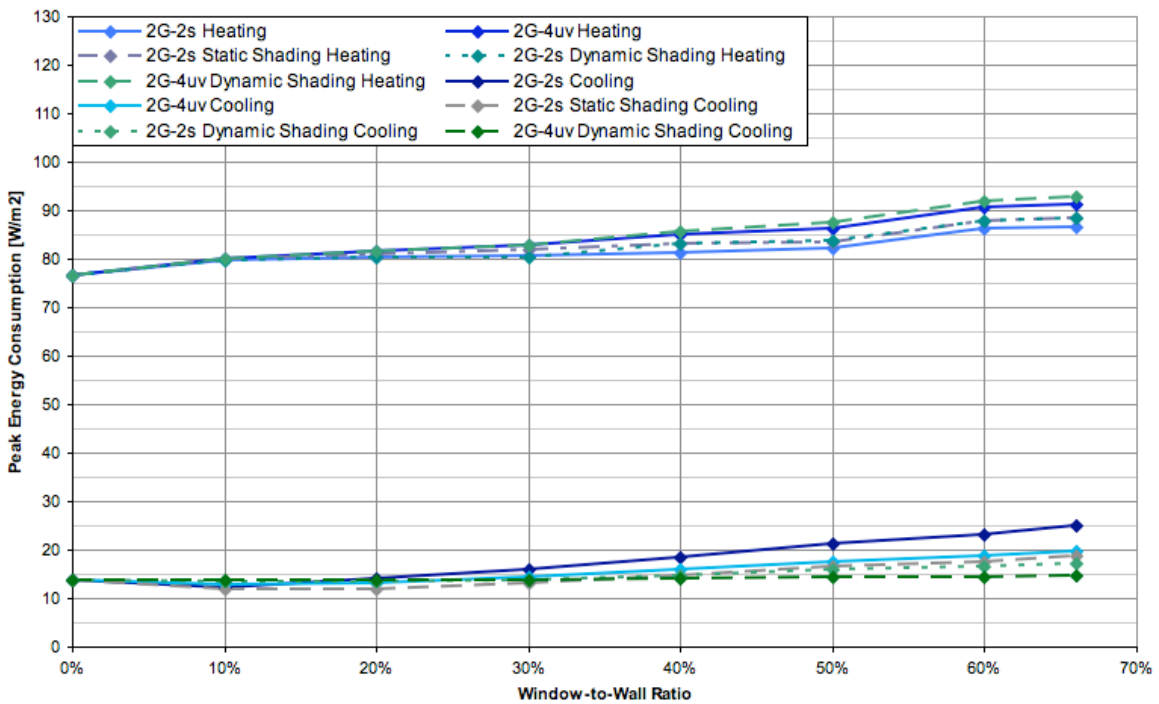
Appendix D4

Energy Performance of Unshaded and Shaded Offices

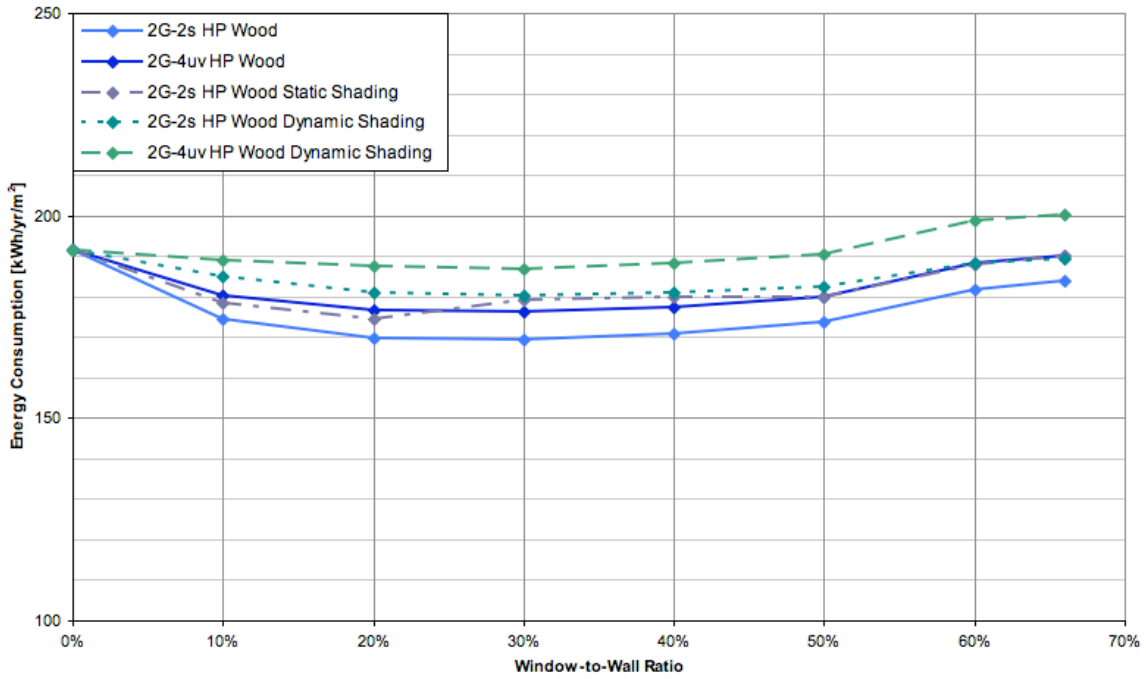
**High Performance Wood Double Glazed, Low-E, Ar,
(2G-2s: SHGC = 0.37, VT = 0.64) (2G-4uv: SHGC = 0.25, VT = 0.41)
Annual Energy Consumption, South facing**



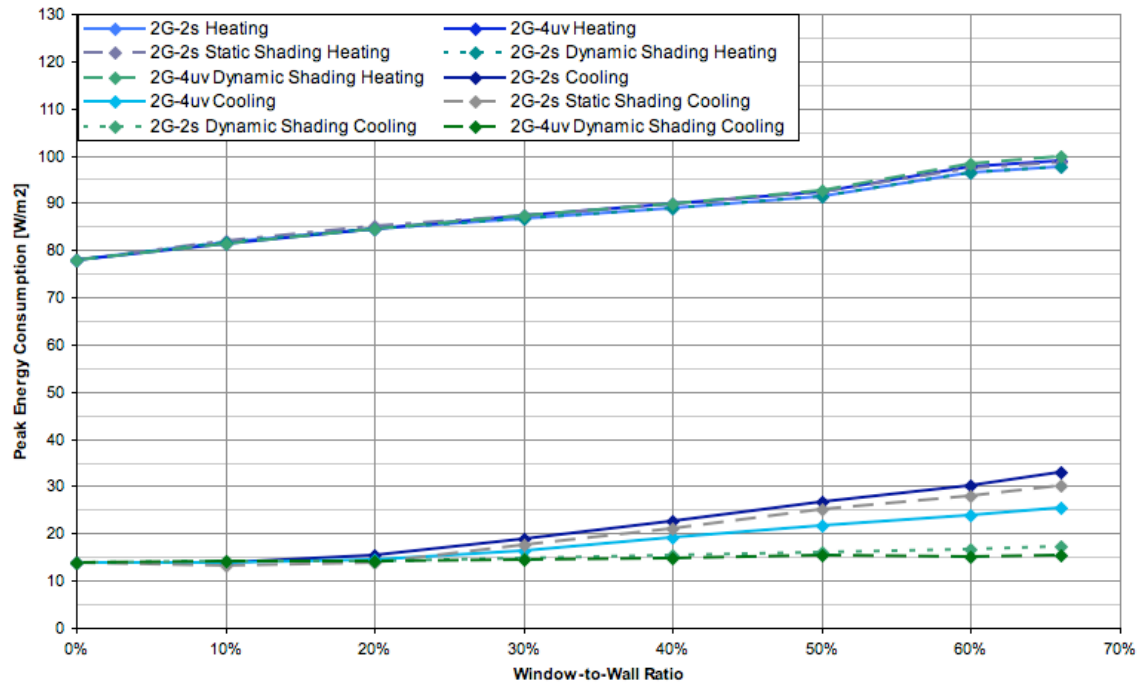
**High Performance Wood Double Glazed, Low-E, Ar,
(2G-2s: SHGC = 0.37, VT = 0.64) (2G-4uv: SHGC = 0.25, VT = 0.41)
Peak Energy Consumption, South facing**



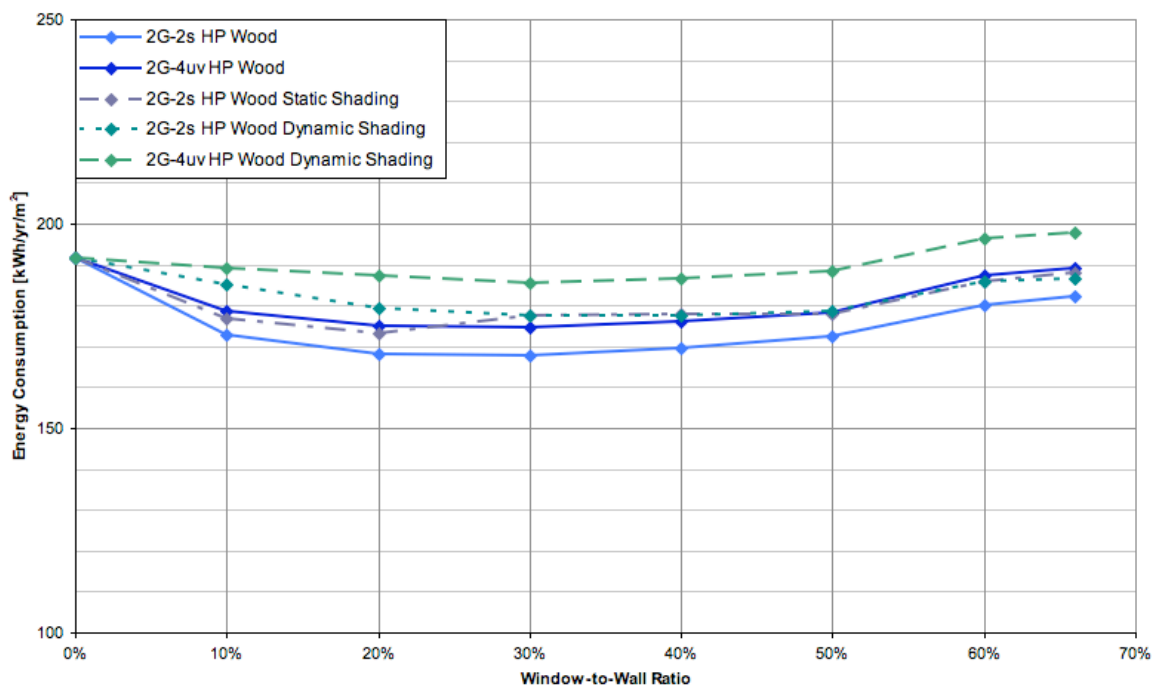
**High Performance Wood Double Glazed, Low-E, Ar,
(2G-2s: SHGC = 0.37, VT = 0.64) (2G-4uv: SHGC = 0.25, VT = 0.41)
Annual Energy Consumption, East facing**



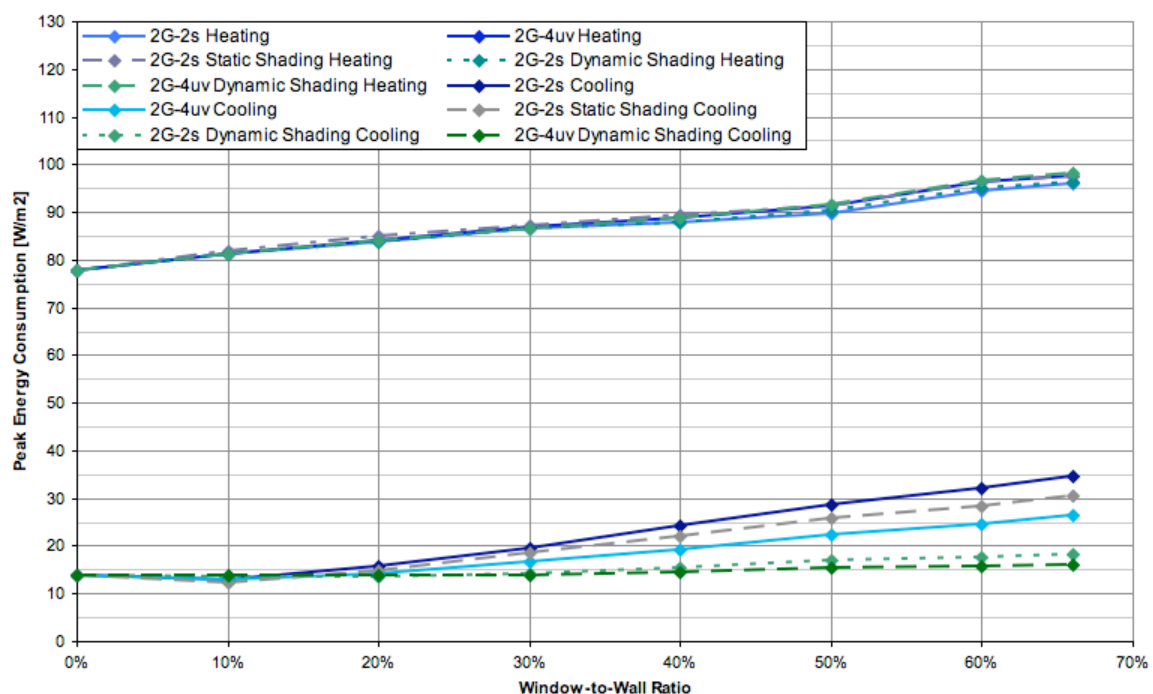
**High Performance Wood Double Glazed, Low-E, Ar,
(2G-2s: SHGC = 0.37, VT = 0.64) (2G-4uv: SHGC = 0.25, VT = 0.41)
Peak Energy Consumption, East facing**



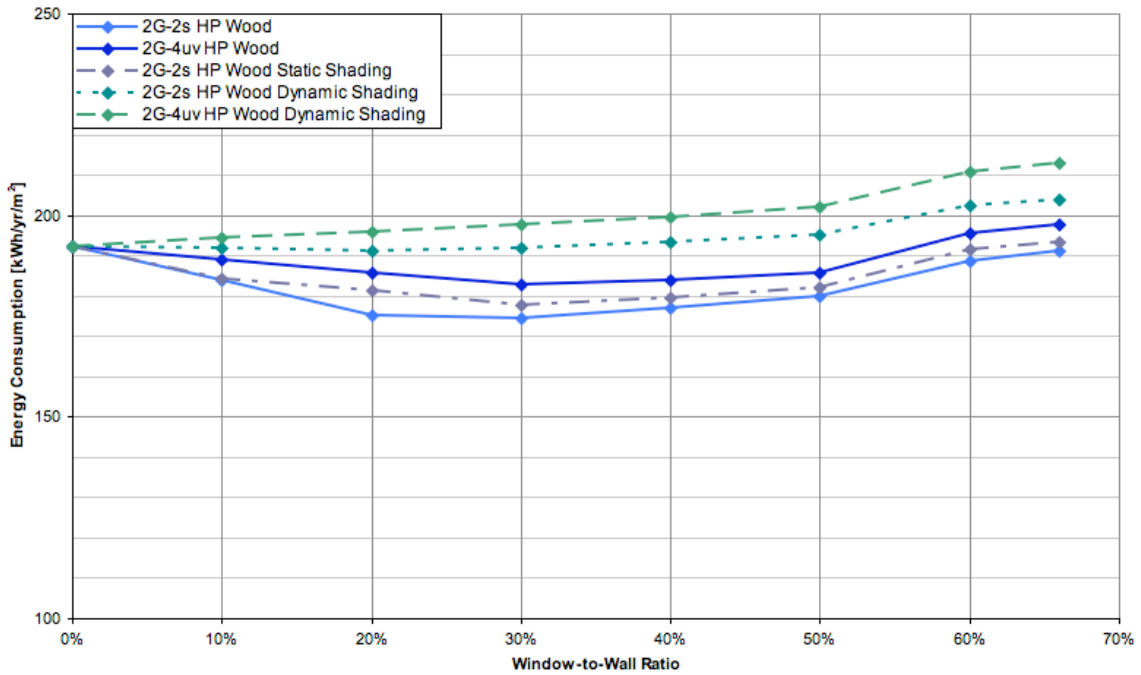
High Performance Wood Double Glazed, Low-E, Ar,
 (2G-2s: SHGC = 0.37, VT = 0.64) (2G-4uv: SHGC = 0.25, VT = 0.41)
 Annual Energy Consumption, West facing



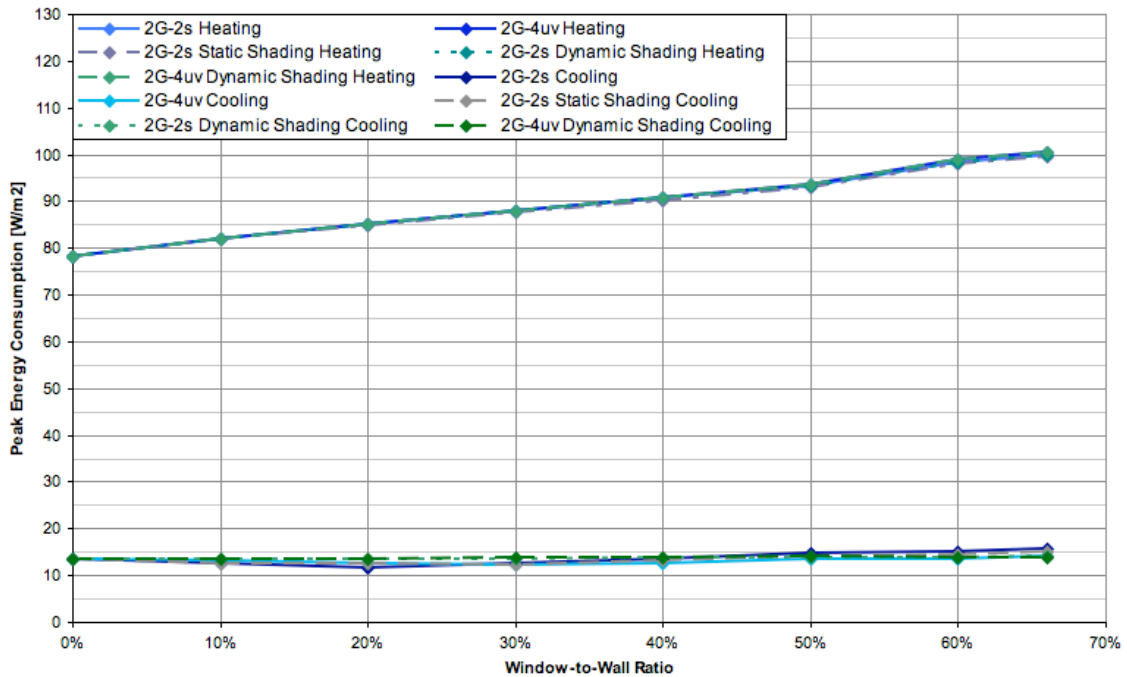
High Performance Wood Double Glazed, Low-E, Ar,
 (2G-2s: SHGC = 0.37, VT = 0.64) (2G-4uv: SHGC = 0.25, VT = 0.41)
 Peak Energy Consumption, West facing



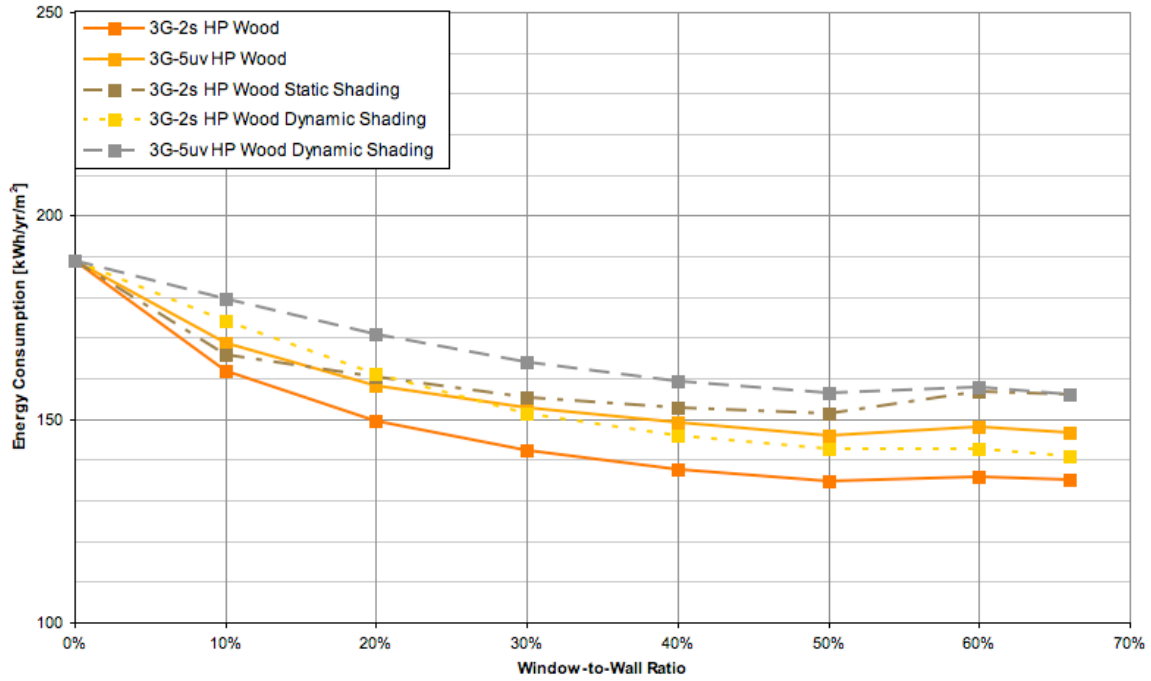
**High Performance Wood Double Glazed, Low-E, Ar,
 (2G-2s: SHGC = 0.37, VT = 0.64) (2G-4uv: SHGC = 0.25, VT = 0.41)
 Annual Energy Consumption, North facing**



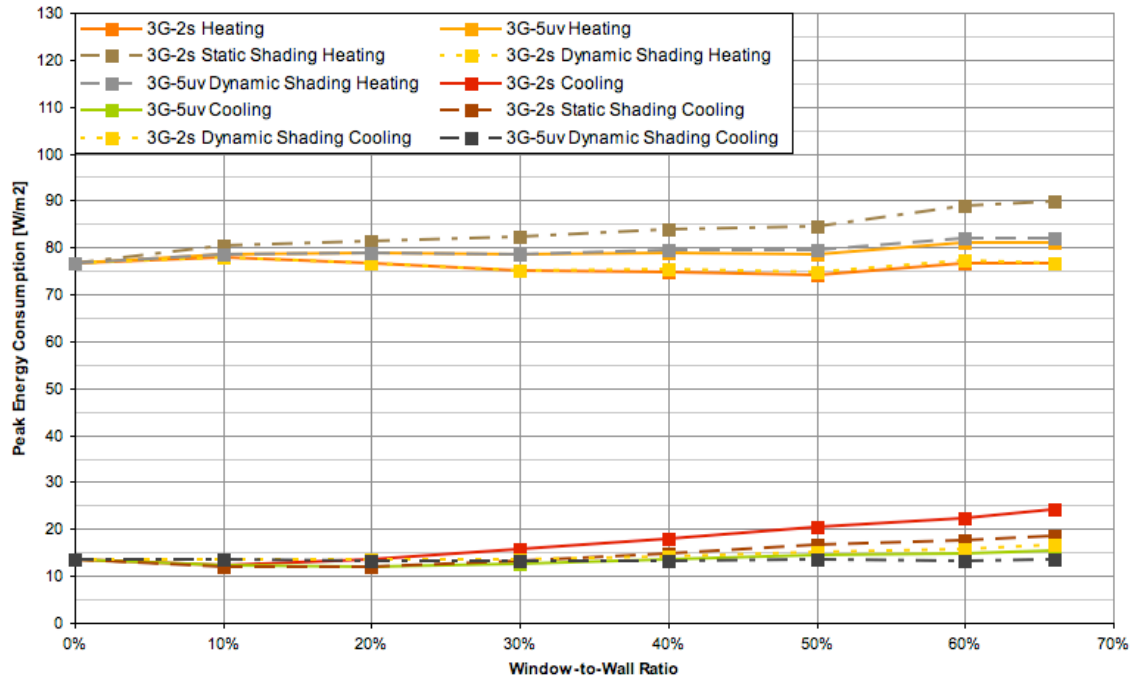
**High Performance Wood Double Glazed, Low-E, Ar,
 (2G-2s: SHGC = 0.37, VT = 0.64) (2G-4uv: SHGC = 0.25, VT = 0.41)
 Peak Energy Consumption, North facing**



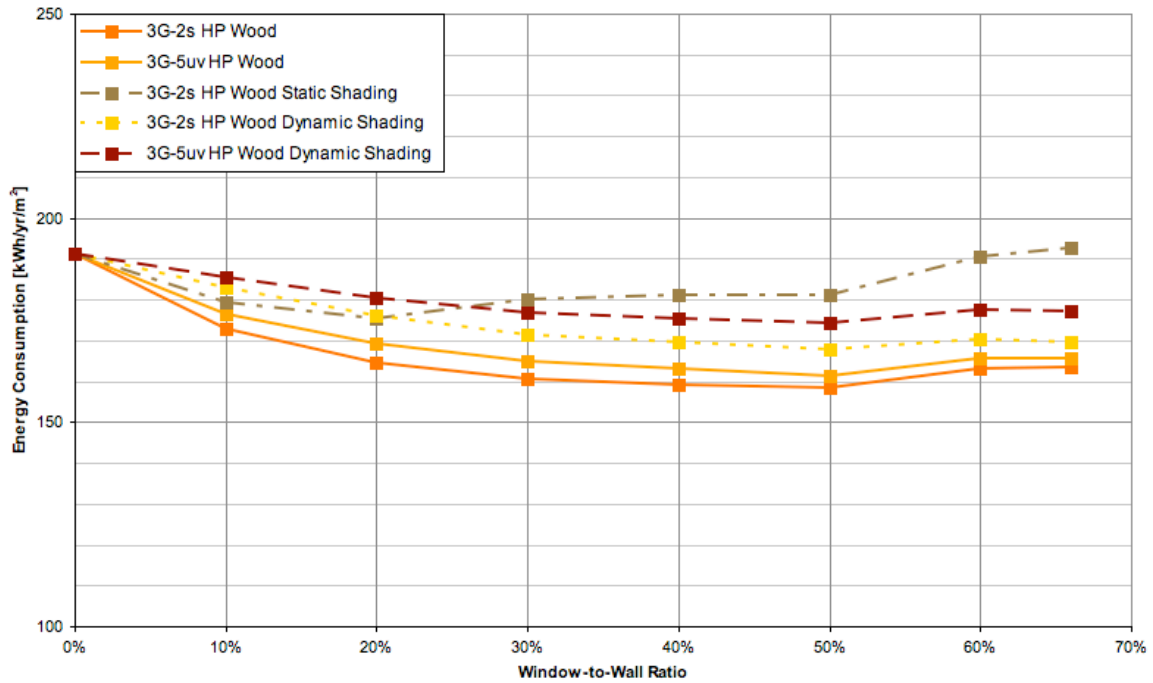
**High Performance Wood Triple Glazed, Low-E, Kr,
 (3G-2s: SHGC = 0.37, VT = 0.57) (3G-5uv: SHGC = 0.19, VT = 0.43)
 Annual Energy Consumption, South facing**



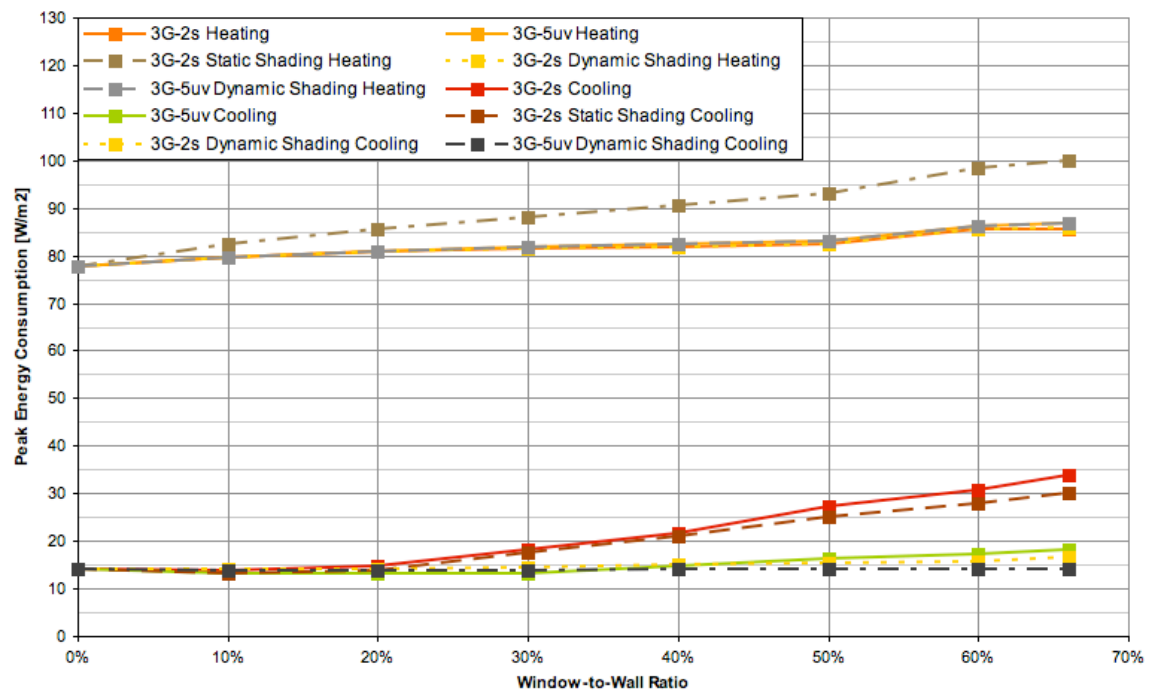
**High Performance Wood Triple Glazed, Low-E, Kr,
 (3G-2s: SHGC = 0.37, VT = 0.57) (3G-5uv: SHGC = 0.19, VT = 0.43)
 Peak Energy Consumption, South facing**



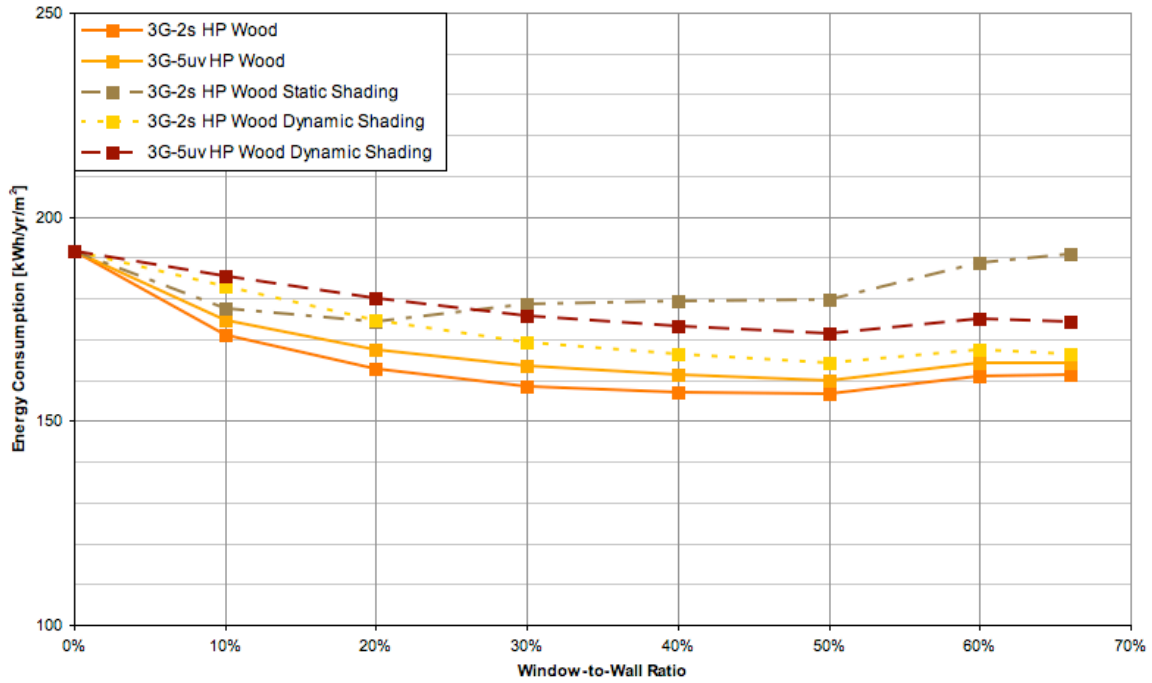
High Performance Wood Triple Glazed, Low-E, Kr,
 (3G-2s: SHGC = 0.37, VT = 0.57) (3G-5uv: SHGC = 0.19, VT = 0.43)
 Annual Energy Consumption, East facing



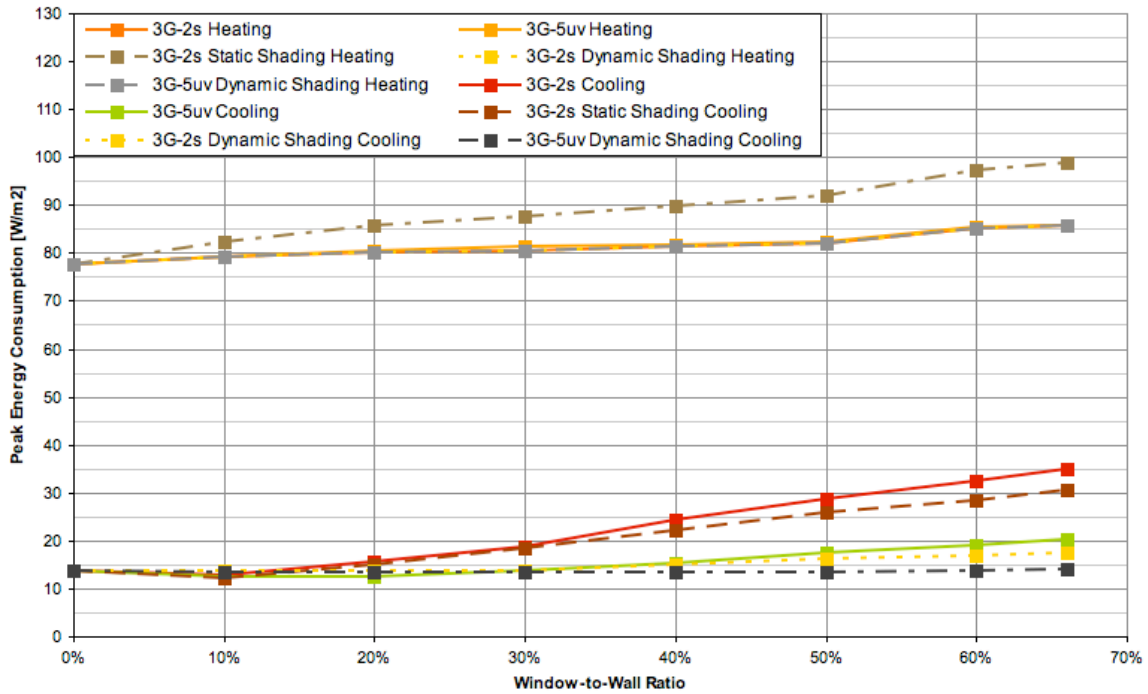
High Performance Wood Triple Glazed, Low-E, Kr,
 (3G-2s: SHGC = 0.37, VT = 0.57) (3G-5uv: SHGC = 0.19, VT = 0.43)
 Peak Energy Consumption, East facing



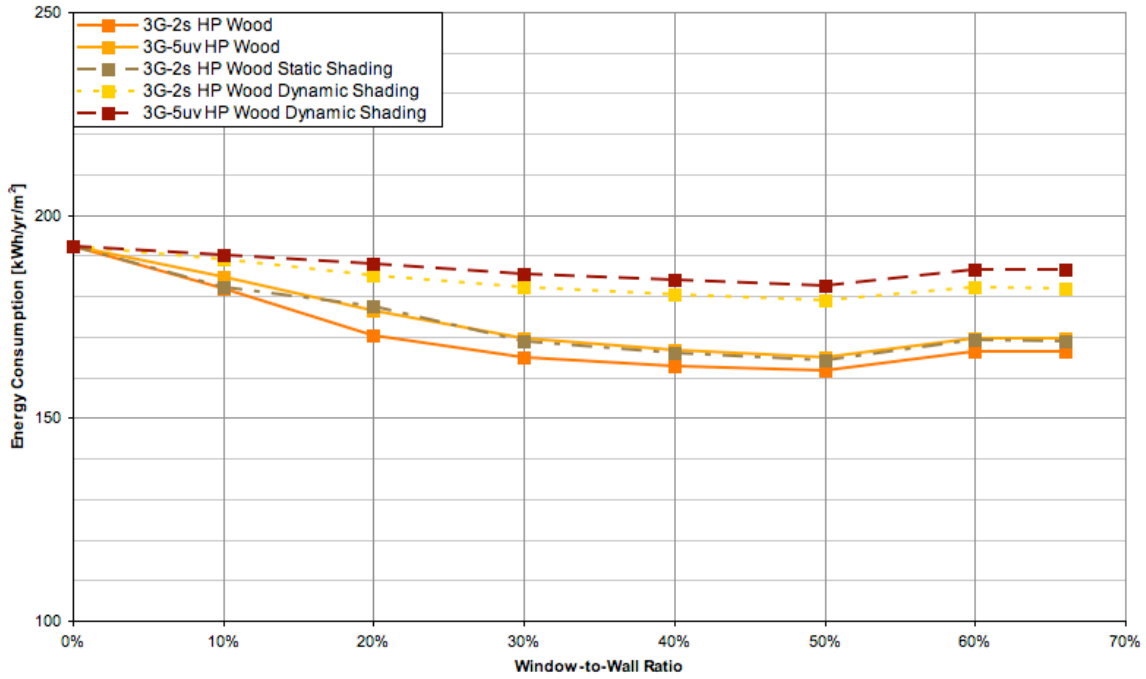
High Performance Wood Triple Glazed, Low-E, Kr,
 (3G-2s: SHGC = 0.37, VT = 0.57) (3G-5uv: SHGC = 0.19, VT = 0.43)
 Annual Energy Consumption, West facing



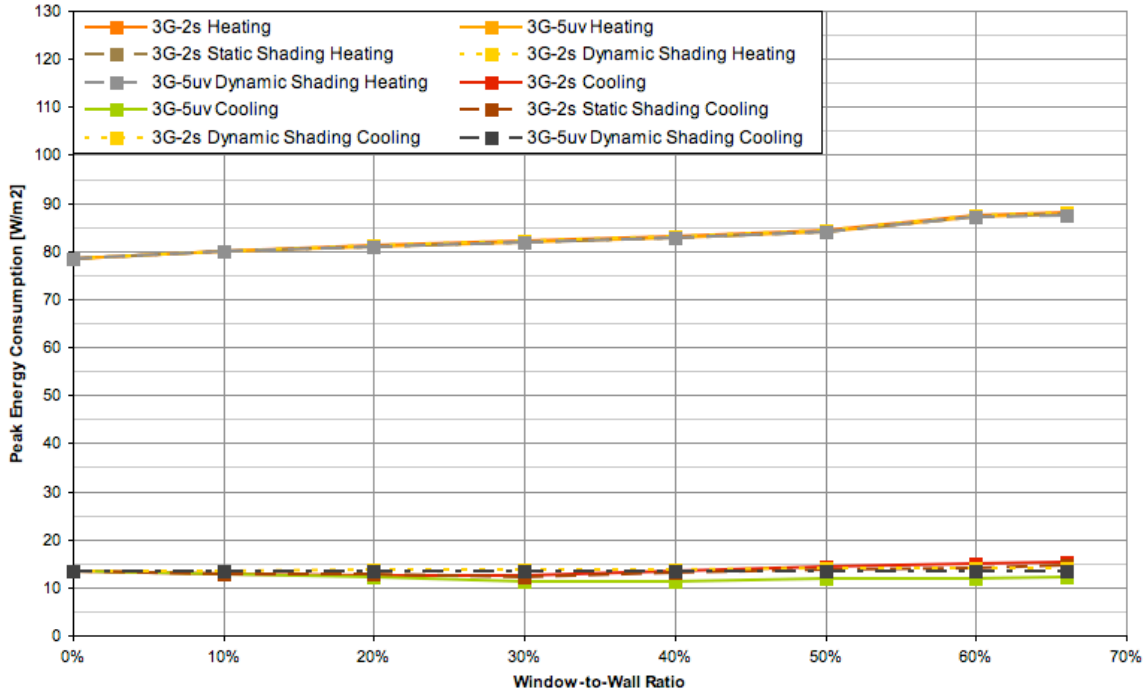
High Performance Wood Triple Glazed, Low-E, Kr,
 (3G-2s: SHGC = 0.37, VT = 0.57) (3G-5uv: SHGC = 0.19, VT = 0.43)
 Peak Energy Consumption, West facing



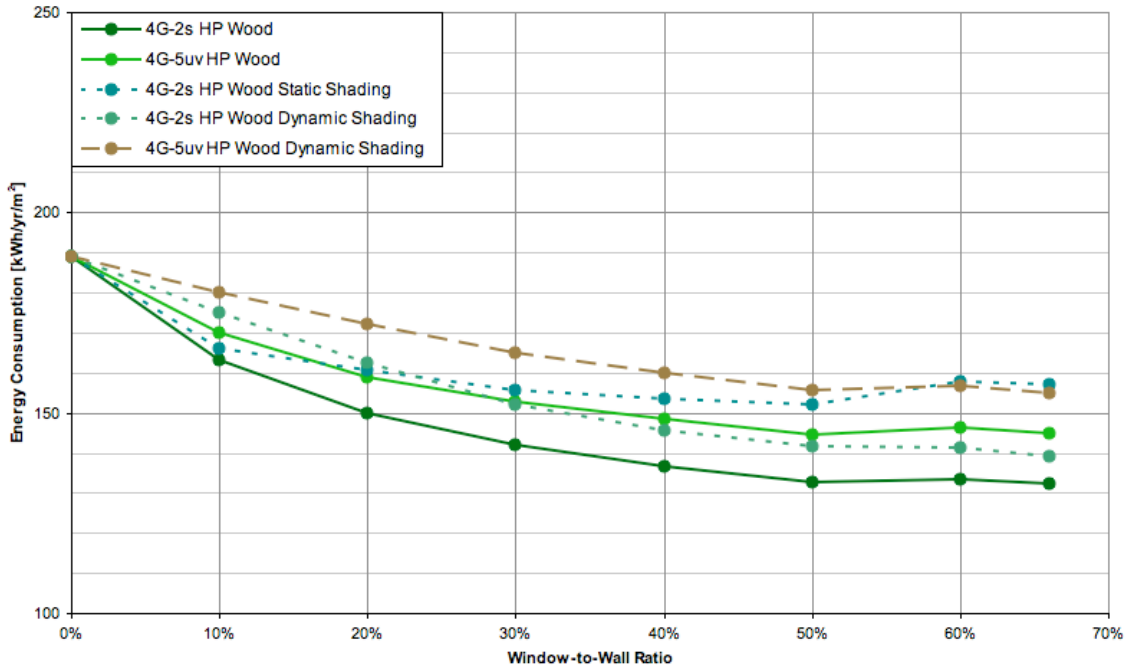
High Performance Wood Triple Glazed, Low-E, Kr,
 (3G-2s: SHGC = 0.37, VT = 0.57) (3G-5uv: SHGC = 0.19, VT = 0.43)
 Annual Energy Consumption, North facing



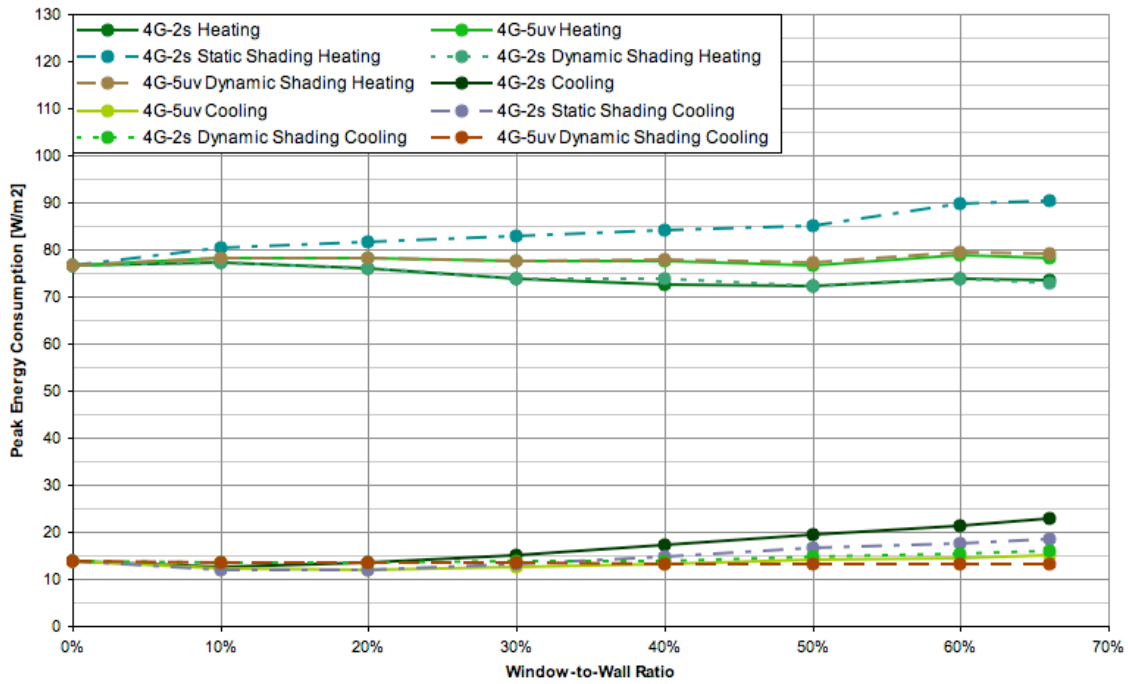
High Performance Wood Triple Glazed, Low-E, Kr,
 (3G-2s: SHGC = 0.37, VT = 0.57) (3G-5uv: SHGC = 0.19, VT = 0.43)
 Peak Energy Consumption, North facing



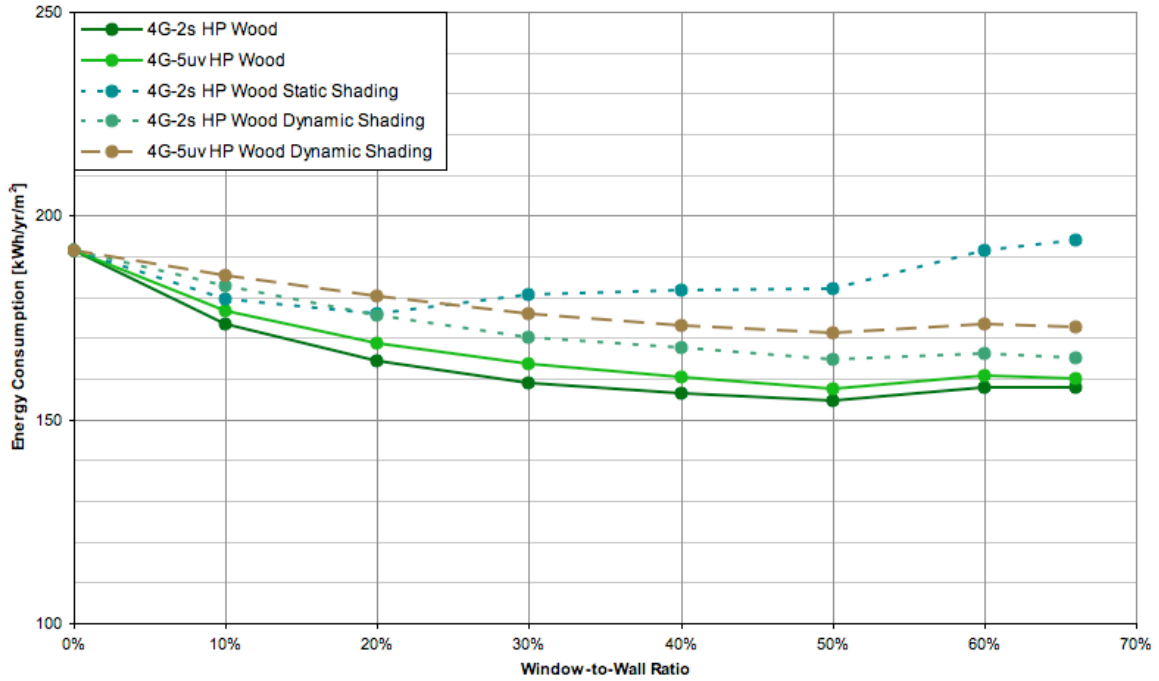
High Performance Wood Quad Glazed, Low-E, Kr,
 (4G-2s: SHGC = 0.35, VT = 0.50) (4G-5uv: SHGC = 0.18, VT = 0.40)
 Annual Energy Consumption, South facing



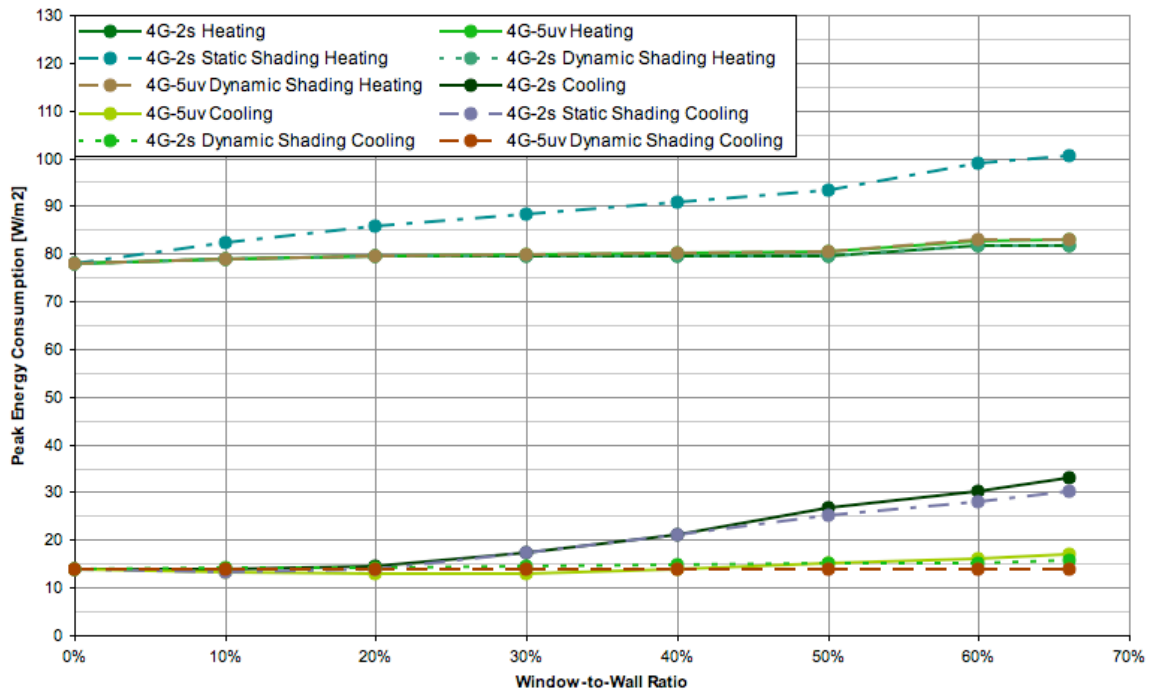
High Performance Wood Quad Glazed, Low-E, Kr,
 (4G-2s: SHGC = 0.35, VT = 0.50) (4G-5uv: SHGC = 0.18, VT = 0.40)
 Peak Energy Consumption, South facing



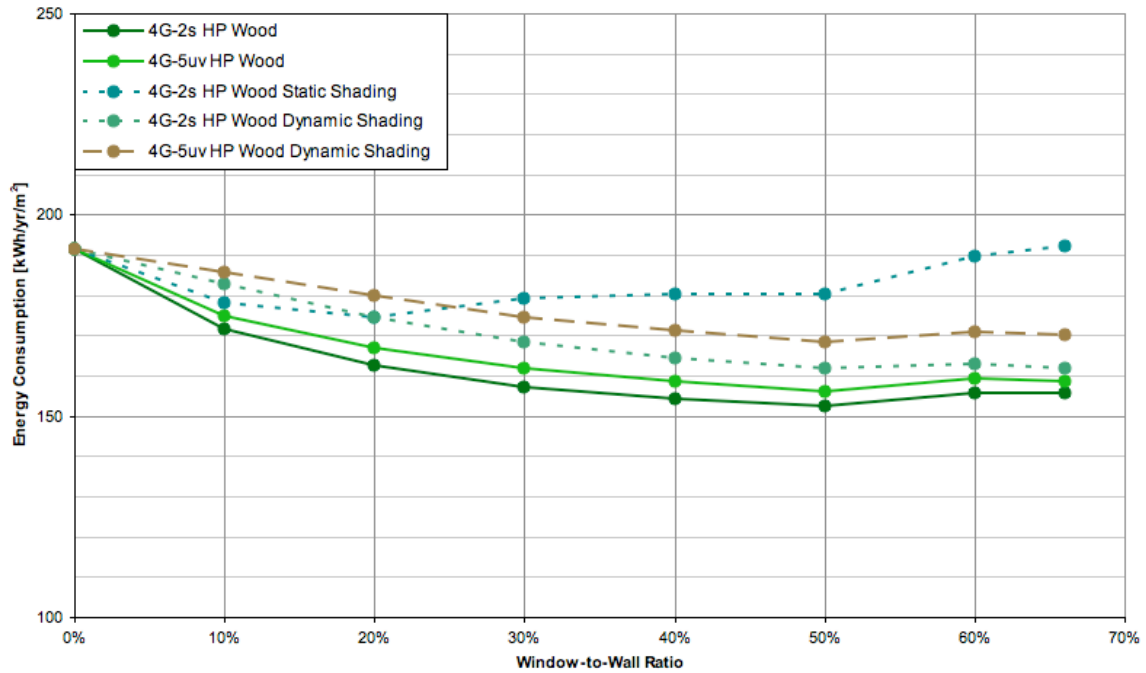
High Performance Wood Quad Glazed, Low-E, Kr,
 (4G-2s: SHGC = 0.35, VT = 0.50) (4G-5uv: SHGC = 0.18, VT = 0.40)
 Annual Energy Consumption, East facing



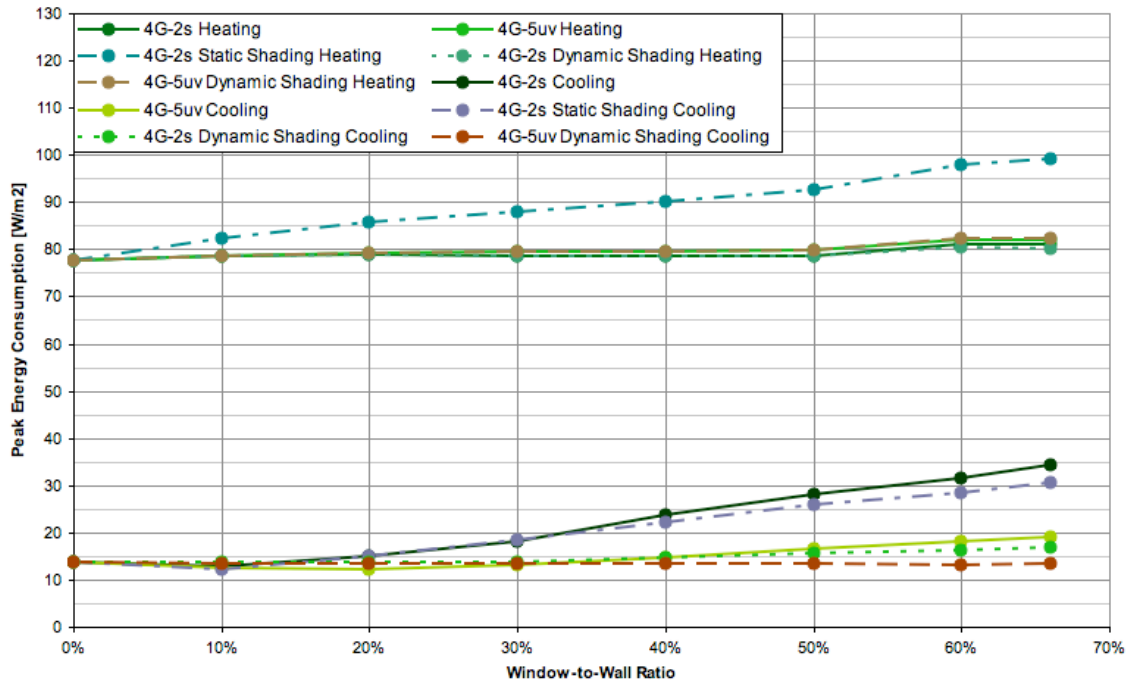
High Performance Wood Quad Glazed, Low-E, Kr,
 (4G-2s: SHGC = 0.35, VT = 0.50) (4G-5uv: SHGC = 0.18, VT = 0.40)
 Peak Energy Consumption, East facing



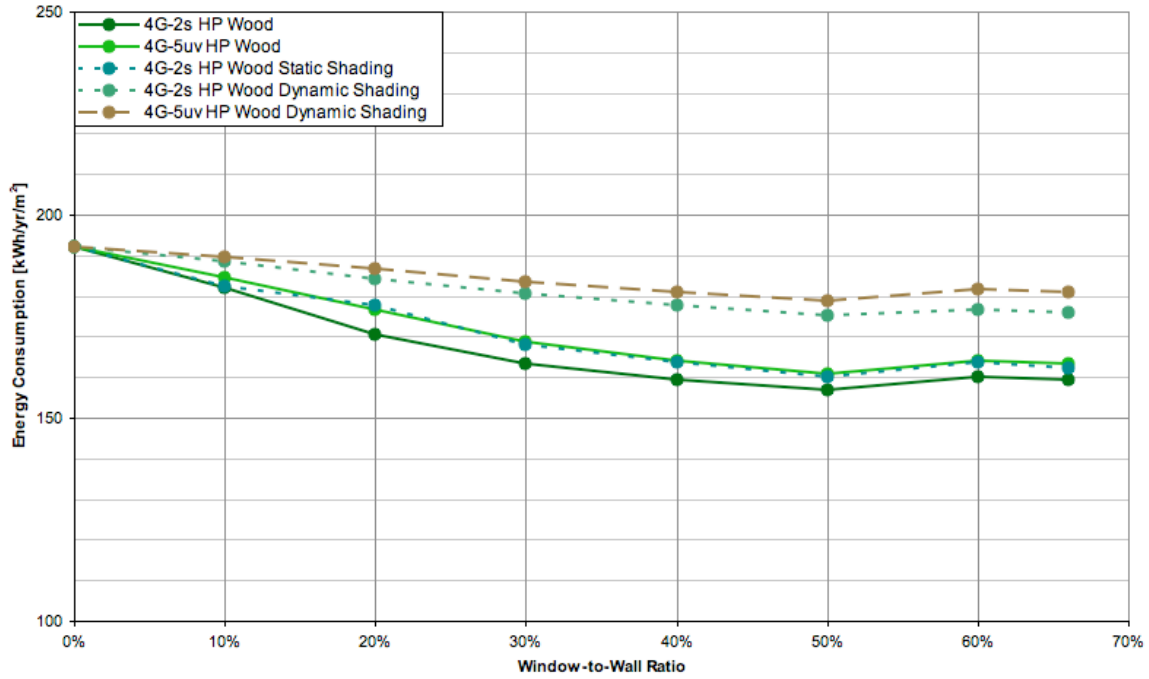
High Performance Wood Quad Glazed, Low-E, Kr,
 (4G-2s: SHGC = 0.35, VT = 0.50) (4G-5uv: SHGC = 0.18, VT = 0.40)
 Annual Energy Consumption, West facing



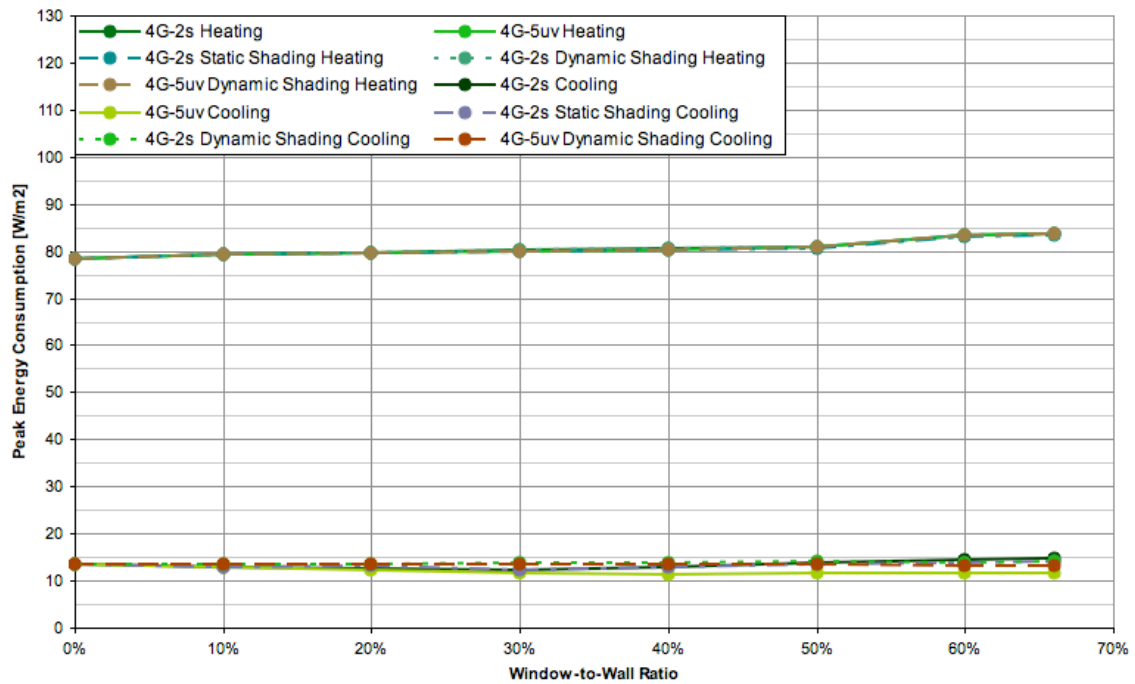
High Performance Wood Quad Glazed, Low-E, Kr,
 (4G-2s: SHGC = 0.35, VT = 0.50) (4G-5uv: SHGC = 0.18, VT = 0.40)
 Peak Energy Consumption, West facing



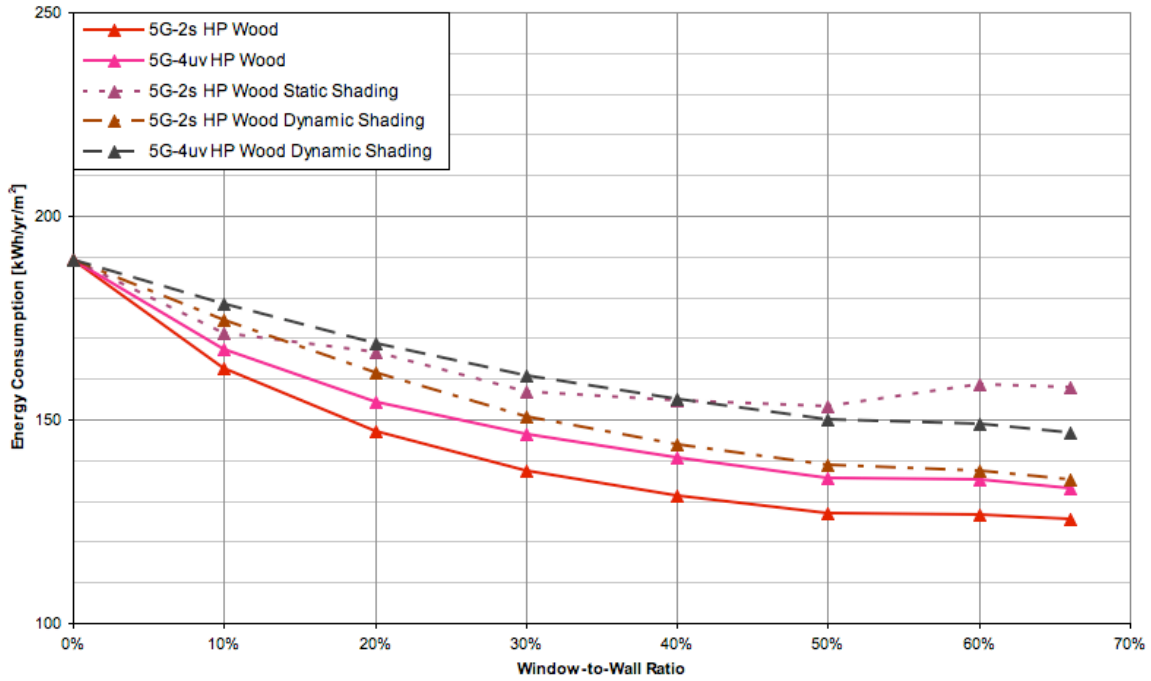
High Performance Wood Quad Glazed, Low-E, Kr,
 (4G-2s: SHGC = 0.35, VT = 0.50) (4G-5uv: SHGC = 0.18, VT = 0.40)
 Annual Energy Consumption, North facing



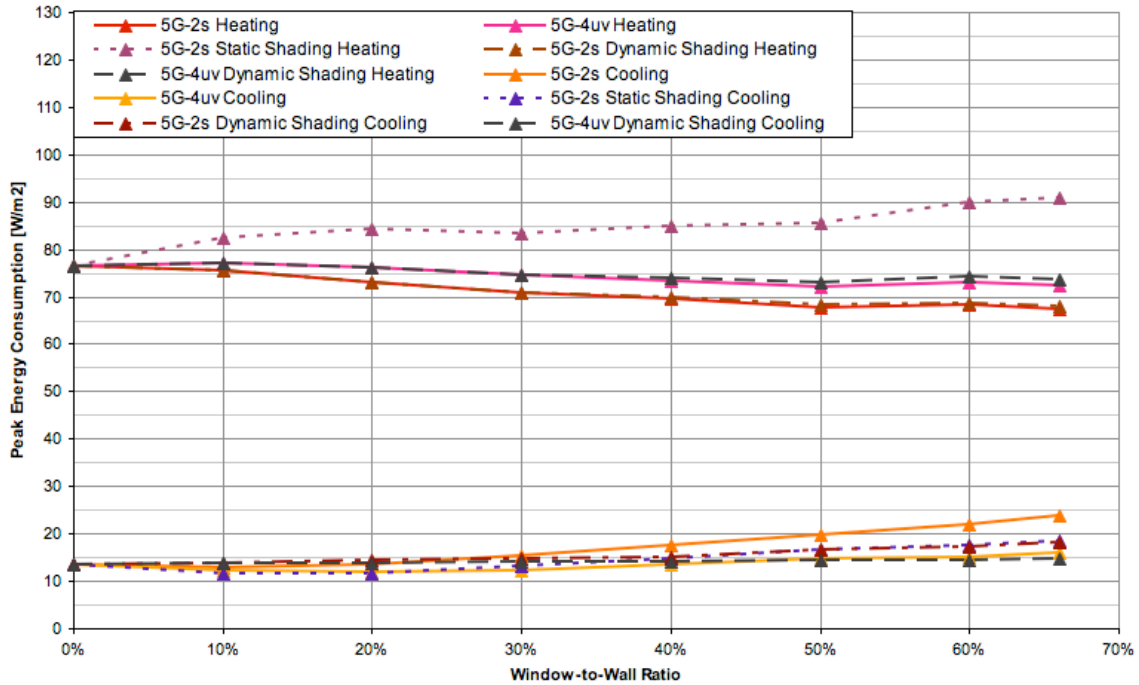
High Performance Wood Quad Glazed, Low-E, Kr,
 (4G-2s: SHGC = 0.35, VT = 0.50) (4G-5uv: SHGC = 0.18, VT = 0.40)
 Peak Energy Consumption, North facing



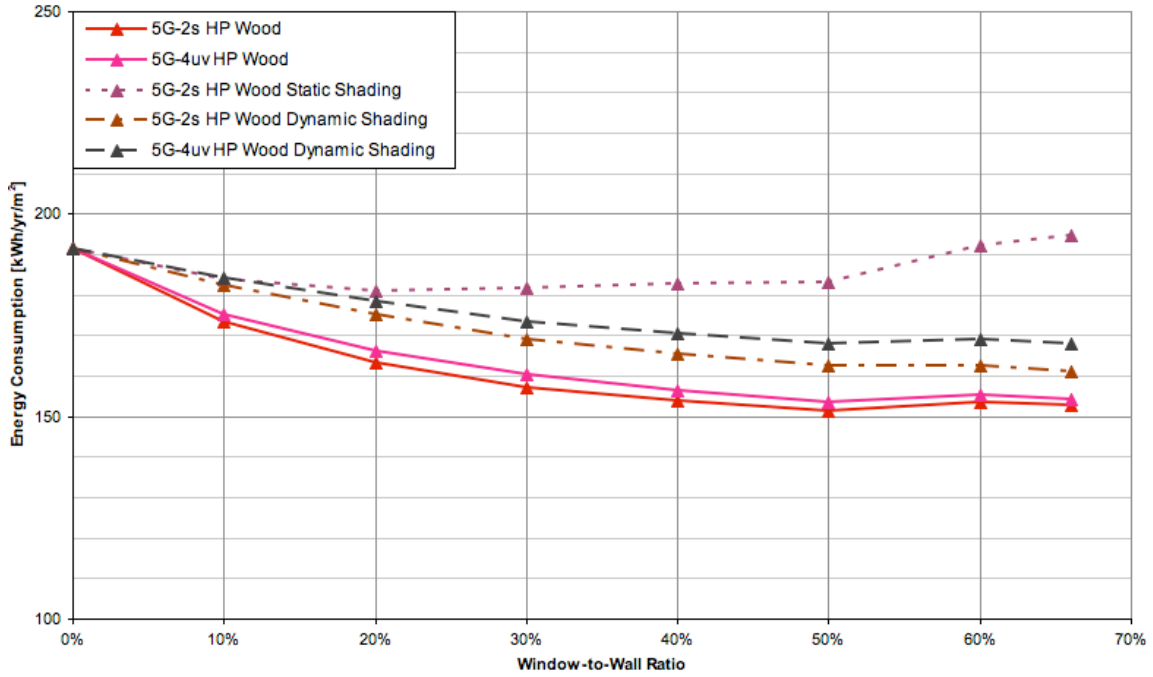
**High Performance Wood Quint Glazed, Low-E, Xe,
 (5G-2s: SHGC = 0.33, VT = 0.45) (5G-4uv: SHGC = 0.19, VT = 0.41)
 Annual Energy Consumption, South facing**



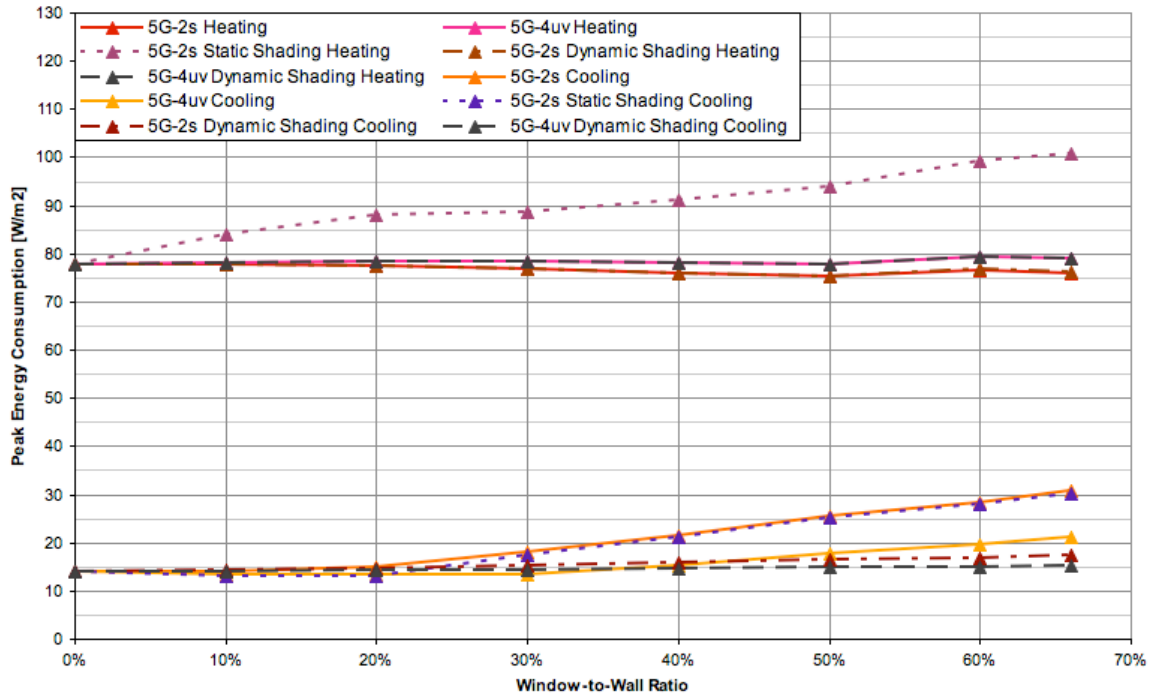
**High Performance Wood Quint Glazed, Low-E, Xe,
 (5G-2s: SHGC = 0.33, VT = 0.45) (5G-4uv: SHGC = 0.19, VT = 0.41)
 Peak Energy Consumption, South facing**



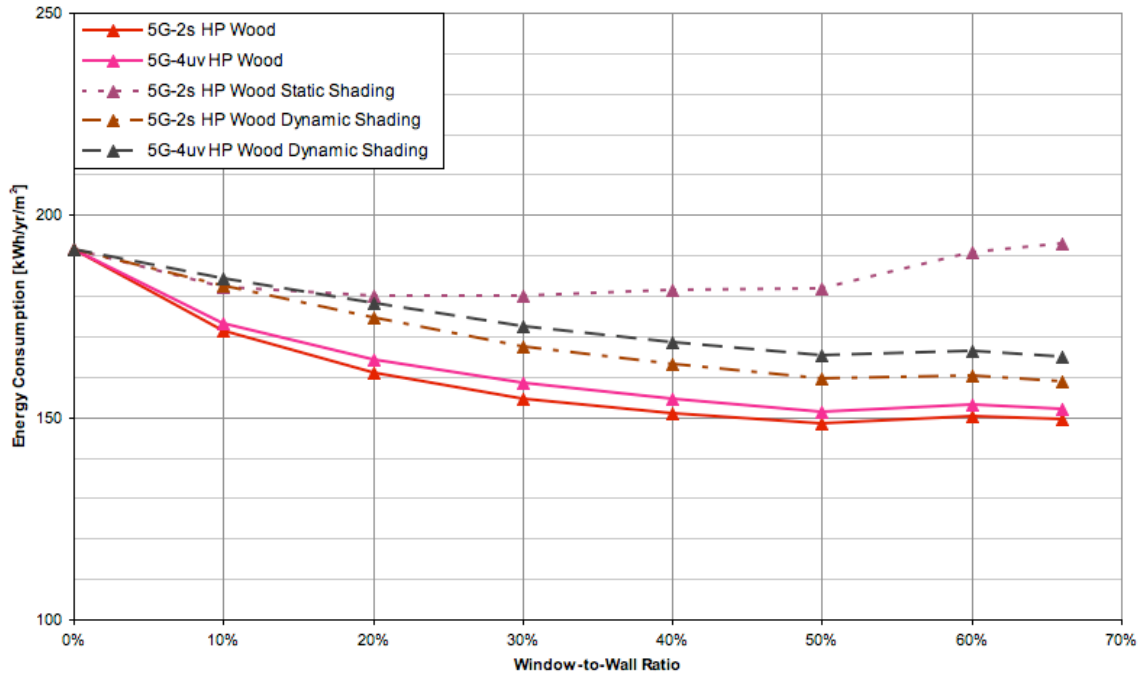
High Performance Wood Quint Glazed, Low-E, Xe,
 (5G-2s: SHGC = 0.33, VT = 0.45) (5G-4uv: SHGC = 0.19, VT = 0.41)
 Annual Energy Consumption, East facing



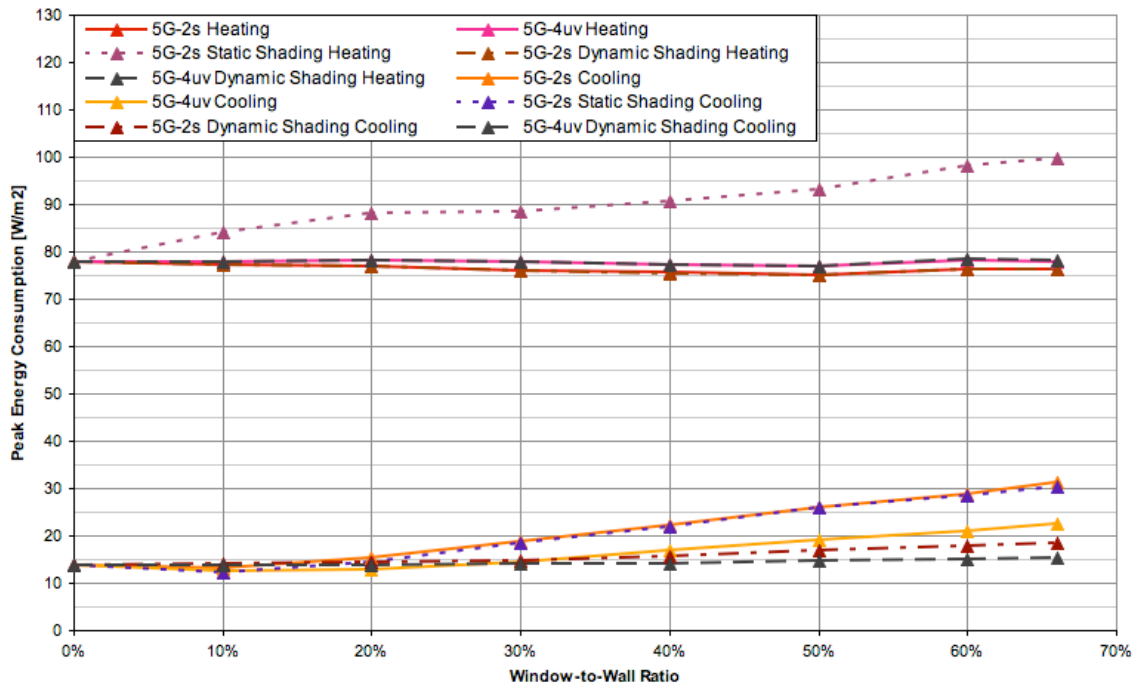
High Performance Wood Quint Glazed, Low-E, Xe,
 (5G-2s: SHGC = 0.33, VT = 0.45) (5G-4uv: SHGC = 0.19, VT = 0.41)
 Peak Energy Consumption, East facing



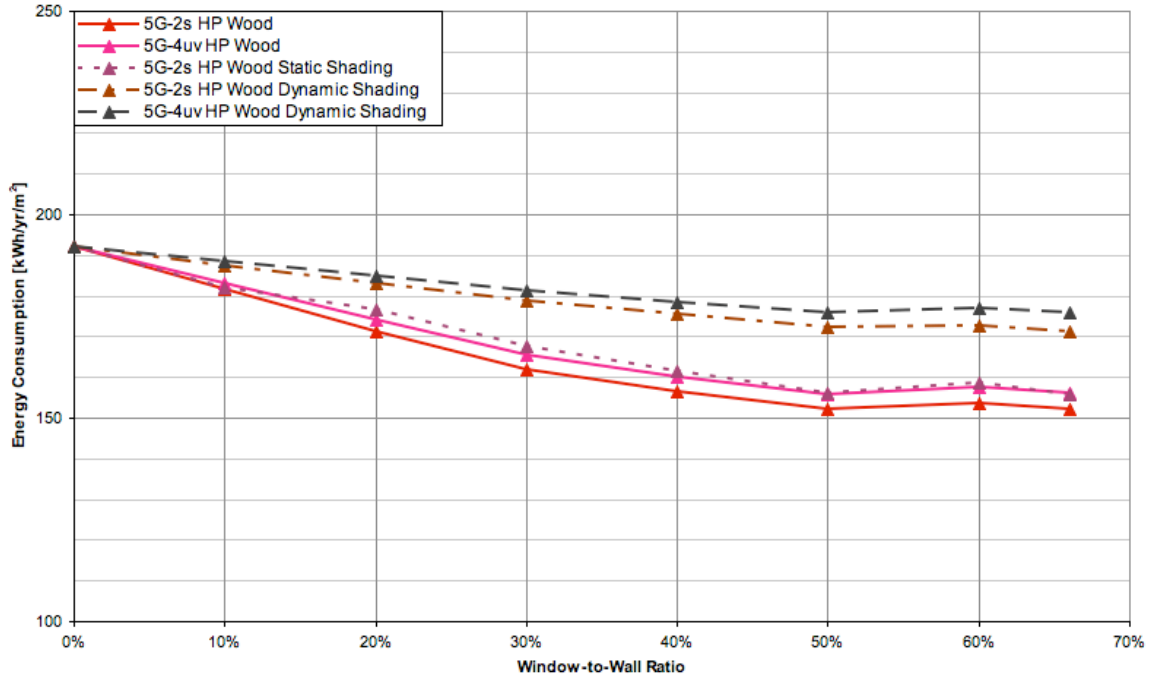
High Performance Wood Quint Glazed, Low-E, Xe,
 (5G-2s: SHGC = 0.33, VT = 0.45) (5G-4uv: SHGC = 0.19, VT = 0.41)
 Annual Energy Consumption, West facing



High Performance Wood Quint Glazed, Low-E, Xe,
 (5G-2s: SHGC = 0.33, VT = 0.45) (5G-4uv: SHGC = 0.19, VT = 0.41)
 Peak Energy Consumption, West facing



High Performance Wood Quint Glazed, Low-E, Xe,
 (5G-2s: SHGC = 0.33, VT = 0.45) (5G-4uv: SHGC = 0.19, VT = 0.41)
 Annual Energy Consumption, North facing



High Performance Wood Quint Glazed, Low-E, Xe,
 (5G-2s: SHGC = 0.33, VT = 0.45) (5G-4uv: SHGC = 0.19, VT = 0.41)
 Peak Energy Consumption, North facing

